Technical Report Documentation Page

1. Report No.	2. Government Accession No.	3. Recipient's Catalog No.
FHWA/TX-07/0-4751-1 Vol. 1		

4. Title and Subtitle	5. Report Date
IMPACT OF LRFD SPECIFICATIONS ON DESIGN OF TEXAS BRIDGES VOLUME 1: PARAMETRIC STUDY	September 2006 Published: December 2006
	6. Performing Organization Code
7. Author(s) Mary Beth D. Hueste, Mohammed Safi Uddin Adil, Mohsin Adnan, and Peter B. Keating	8. Performing Organization Report No. Report 0-4751-1 Vol. 1
9. Performing Organization Name and Address Texas Transportation Institute The Texas A&M University System College Station, Texas 77843-3135	10. Work Unit No. (TRAIS) 11. Contract or Grant No. Project 0-4751
12. Sponsoring Agency Name and Address Texas Department of Transportation Research and Technology Implementation Office P. O. Box 5080 Austin, Texas 78763-5080	13. Type of Report and Period Covered Technical Report: September 2003-August 2005 14. Sponsoring Agency Code

15. Supplementary Notes
Project performed in cooperation with the Texas Department of Transportation and the Federal Highway Administration.
Project Title: Impact of LRFD Specifications on the Design of Texas Bridges
URL: http://tti.tamu.edu/documents/0-4751-1-V1.pdf

16. Abstract
The Texas Department of Transportation (TxDOT) is currently designing highway bridge structures using the American Association of State Highway and Transportation Officials (AASHTO) *Standard Specifications for Highway Bridges*, and it is expected that the agency will transition to the use of the *AASHTO LRFD Bridge Design Specifications* before 2007. This is a two-volume report that documents the findings of a TxDOT-sponsored research project to evaluate the impact of the Load and Resistance Factor (LRFD) Specifications on the design of typical Texas bridges as compared to the Standard Specifications. The objectives of this portion of the project are to evaluate the current LRFD Specifications to assess the calibration of the code with respect to typical Texas prestressed bridge girders, to perform a critical review of the major changes when transitioning to LRFD design, and to recommend guidelines to assist TxDOT in implementing the LRFD Specifications.

A parametric study for AASHTO Type IV, Type C, and Texas U54 girders was conducted using span length, girder spacing, and strand diameter as the major parameters that are varied. Based on the results obtained from the parametric study, two critical areas were identified where significant changes in design results were observed when comparing Standard and LRFD designs. The critical areas are the transverse shear requirements and interface shear requirements, and these are further investigated. In addition, limitations in the LRFD Specifications, such as those for the percentage of debonded strands and use of the LRFD live load distribution factor formulas, were identified as restrictions that would impact TxDOT bridge girder designs, and these issues are further assessed. The results of the parametric study, along with critical design issues that were identified and related recommendations, are summarized in Volume 1 of this report. Detailed design examples for an AASHTO Type IV girder and a Texas U54 girder using both the AASHTO Standard Specifications and AASHTO LRFD Specifications were also developed and compared. Volume 2 of this report contains these examples.

17. Key Words	18. Distribution Statement
Prestressed Concrete, LRFD, Design, Bridge Girders, U54 Girder, Type IV Girder, Type C Girder, Parametric Study	No restrictions. This document is available to the public through NTIS: National Technical Information Service Springfield, Virginia 22161 http://www.ntis.gov

19. Security Classif.(of this report)	20. Security Classif.(of this page)	21. No. of Pages	22. Price
Unclassified	Unclassified	390	

Form DOT F 1700.7 **(8-72)** **Reproduction of completed page authorized**

IMPACT OF LRFD SPECIFICATIONS ON DESIGN OF TEXAS BRIDGES
VOLUME 1: PARAMETRIC STUDY

by

Mary Beth D. Hueste, P.E.
Associate Research Engineer
Texas Transportation Institute

Mohammed Safi Uddin Adil
Graduate Research Assistant
Texas Transportation Institute

Mohsin Adnan
Graduate Research Assistant
Texas Transportation Institute

and

Peter B. Keating
Associate Research Engineer
Texas Transportation Institute

Report 0-4751-1
Project 0-4751
Project Title: Impact of LRFD Specifications on the Design of Texas Bridges

Performed in Cooperation with the
Texas Department of Transportation
and the
Federal Highway Administration

September 2006
Published: December 2006

TEXAS TRANSPORTATION INSTITUTE
The Texas A&M University System
College Station, Texas 77843-3135

DISCLAIMER

The contents of this report reflect the views of the authors, who are responsible for the facts and the accuracy of the data presented herein. The contents do not necessarily reflect the official view or policies of the Federal Highway Administration (FHWA) or the Texas Department of Transportation (TxDOT). While every effort has been made to ensure the accuracy of the information provided in this report, this material is not intended to be a substitute for the actual codes and specifications for the design of prestressed bridge girders. This report does not constitute a standard, specification, or regulation; and is not intended for constructing, bidding, or permit purposes. The engineer in charge was Mary Beth D. Hueste, P.E. (TX 89660).

ACKNOWLEDGMENTS

This research was conducted at Texas A&M University (TAMU) and was supported by TxDOT and FHWA through the Texas Transportation Institute (TTI) as part of Project 0-4751, "Impact of LRFD Specifications on the Design of Texas Bridges." The authors are grateful to the individuals who were involved with this project and provided invaluable assistance, including Rachel Ruperto (TxDOT, Research Project Director), David Hohmann (Research Project Coordinator), Gregg Freeby (TxDOT), John Holt (TxDOT), Mark Steves (TxDOT), John Vogel (TxDOT), and Dennis Mertz (University of Delaware).

TABLE OF CONTENTS

LIST OF FIGURES

Page

LIST OF TABLES

Page

1. INTRODUCTION

1.1 BACKGROUND AND PROBLEM STATEMENT

Bridge structures constructed across the nation not only require the desired safety reserve, but also consistency and uniformity in the level of safety. This uniformity is made possible using improved design techniques based on probabilistic theories. One such technique is reliability based design, which accounts for the inherent variability of the loads and resistance to provide an acceptable and uniform level of safety in the design of structures.

The American Association of State Highway and Transportation Officials (AASHTO) first introduced the *Standard Specifications for Highway Bridges* in 1931 and since then these specifications have been updated through 17 editions, with the latest edition being published in 2002 (AASHTO 2002). The *AASHTO Standard Specifications for Highway Bridges* were based on the Allowable Stress Design (ASD) philosophy until 1970, after which the Load Factor Design (LFD) philosophy was incorporated in the specifications. In ASD, the allowable stresses are considered to be a fraction of a given structural member's load carrying capacity and the calculated design stresses are restricted to be less than or equal to those allowable stresses. The possibility of several loads acting simultaneously on the structure is specified through different load combinations, but variation in likelihood of those load combinations and loads themselves is not recognized in ASD. LFD was introduced to take into account the variability of loads by using different multipliers for dead, live, wind, and other loads to a limited extent (i.e., statistical variability of design parameters was not taken into account). These methodologies provide the desirable level of safety for bridge designs, but do not ensure uniformity in the level of safety for various bridge types and configurations (Nowak 1995).

AASHTO's National Cooperative Highway Research Program (NCHRP) initiated Project 12-33 in July of 1988 to develop Load and Resistance Factor Design (LRFD) specifications for bridges. The project included the development of load models, resistance models, and a reliability analysis procedure for a wide variety of typical bridges in the United States. To calibrate this code, a reliability index related to the probability of exceeding a particular limit state was used as a measure of structural safety. About 200 representative bridges were chosen from various geographical regions of the United States based on current and future trends in bridge designs, rather than choosing from existing bridges only. Reliability indices were calculated using an iterative procedure for these bridges, which were designed according to the Standard Specifications (AASHTO 1992). In order to ensure an adequate level of reliability for calibration of the LRFD Specifications, the performance of all the representative bridges was evaluated and a corresponding target reliability index was chosen to provide a minimum, consistent, and uniform safety margin for all structures. The load and resistance factors were then calculated so that the structural reliability is close to the target reliability index (Nowak 1995). AASHTO introduced the *AASHTO Load and Resistance Factor Design (LRFD) Bridge Design Specifications* in 1994 (AASHTO 1994).

The *AASHTO LRFD Bridge Design Specifications* (AASHTO 2004) are intended to replace the latest edition of the *AASHTO Standard Specifications for Highway Bridges* (AASHTO 2002), which will not continue to be updated except for corrections. The Federal Highway Association (FHWA) has mandated that this transition be completed by State Departments of Transportation (DOTs) by 2007. The design philosophy adopted in the *AASHTO LRFD Bridge Design Specifications* provides a common framework for the design of structures made of steel, concrete, and other materials.

Many state DOTs within the United States (U.S.) have already implemented the AASHTO LRFD Specifications for their bridge designs, and the remaining states are transitioning from the Standard Specifications to the LRFD Specifications. Because many bridge engineers are not completely familiar with reliability based design and the new design methodologies adopted in the LRFD Specifications, the transition to LRFD based design can take time.

This study is part of the Texas Department of Transportation (TxDOT) project 0-4751 “Impact of AASHTO LRFD Specifications on the Design of Texas Bridges.” TxDOT is currently using the *AASHTO Standard Specifications for Highway Bridges* with slight modifications for designing prestressed concrete bridges. However, TxDOT is planning to replace the AASHTO Standard Specifications with the AASHTO LRFD Specifications for design of Texas bridges. This study will provide useful information to aid in this transition, including guidelines and detailed design examples. The impact of using the LRFD Specifications on the design of prestressed concrete bridge girders for various limit states is evaluated using a detailed parametric study. Issues pertaining to the design and the areas where major differences occur are identified, and guidelines addressing these issues are suggested for adoption and implementation by TxDOT. This study is aimed toward helping bridge engineers understand and implement AASHTO LRFD bridge design for prestressed concrete bridges, specifically Type C, AASHTO Type IV, and Texas U54 girder bridges.

1.2 OBJECTIVES AND SCOPE

The main purpose of this research study is to develop guidelines to help TxDOT adopt and implement the *AASHTO LRFD Bridge Design Specifications*. The objectives of this study are as follows.

1. Identify major differences between the AASHTO Standard and LRFD Specifications.
2. Generate detailed design examples based on the AASHTO Standard and LRFD Specifications as a reference for bridge engineers to follow for step-by-step design and to highlight major differences in the designs.
3. Evaluate the simplifying assumptions made by TxDOT for bridge design for their applicability when using the AASHTO LRFD Specifications.
4. Conduct a parametric study based on parameters representative of Texas bridges to investigate the impact of the AASHTO LRFD Specifications on the design as compared to the AASHTO Standard Specifications. The impact of the AASHTO LRFD Specifications on different design limit states is quantified.
5. Identify the areas where major differences occur in the design, and develop guidelines on these critical design issues to help in implementation of the LRFD Specifications.

This study focuses on Type C, AASHTO Type IV, and Texas U54 prestressed concrete bridge girders, which are widely used in the state of Texas and other states.

1.3 RESEARCH PLAN

The following five major tasks were performed to accomplish the objectives of this research study.

Task 1: Literature Review

The researchers reviewed in detail the previous studies related to the development and implementation of the AASHTO LRFD Bridge Design Specifications. The literature review discusses the studies related to the development of dead load, live load, dynamic load models, distribution factors, and calibration of the LRFD Specifications. The studies that form the basis of new methodologies employed in the LRFD Specifications for transverse and interface shear designs are also reviewed. The past research evaluating the impact of the AASHTO LRFD Bridge Design Specifications on bridge design as compared to the AASHTO Standard Specifications is also included. The observations made from the review of the relevant literature are summarized in Chapter 2.

Task 2: Development of Detailed Design Examples

Researchers developed detailed design examples for an AASHTO Type IV girder bridge and a Texas U54 girder bridge using the *AASHTO Standard Specifications for Highway Bridges, 17th edition* (2002) and the *AASHTO LRFD Bridge Design Specifications, 3rd edition* (2004). Both girder types were selected for detailed design comparison as they are widely used by TxDOT. Type C girder bridges are also used in many cases, but the design process does not differ significantly from that of AASHTO Type IV girder bridges. The detailed examples are included in Volume 2 of this report. The detailed design examples highlight major differences in the AASHTO Standard and LRFD design methodologies. These examples are aimed to be comprehensive and easy to follow in order to provide a useful reference for bridge engineers.

Task 3: Review of TxDOT Design Criteria for Bridge Design

Simplifying assumptions made by TxDOT in bridge design were evaluated for their applicability when using the AASHTO LRFD Specifications. The simplifications considered for evaluation include the assumption of the modular ratio between slab and beam concrete to be unity throughout the design. In addition, the practice of not updating the modular ratio for calculating actual prestress losses, flexural strength limit state checks, and deflection calculations was assessed. The impact of these simplifications in LRFD design were conveyed to TxDOT during this project and, based on their input, design procedures were finalized. The modifications in the designs or deviations from the LRFD Specifications to simplify the design are clearly stated and their limitations are illustrated.

Task 4: Parametric Study

A parametric study was conducted to perform an in-depth analysis of the differences between designs using the current Standard and LRFD Specifications (AASHTO 2002, 2004). The focus of this study was Type C, Type IV, and Texas U54 prestressed girder bridges. The main parameters for this study were girder spacing, span length, concrete strengths at release and at service, skew angle, and strand diameter. The researches chose the values for these parameters in collaboration with TxDOT to ensure that they are representative of the typical bridges in Texas. The concrete strengths at service and at release were limited to values commonly available from Texas precasters. The spans and girder spacing are dictated by TxDOT practice. Typically in TxDOT designs, all girders in the bridge are designed as interior girders. Following this practice, only interior girders were considered for this parametric study.

Prestress losses were calculated using TxDOT's methodology for Standard designs and using the AASHTO LRFD Specifications for LRFD designs. Concrete strengths at service and at release were optimized following an iteration process used by TxDOT. The flexural strength was evaluated based on the actual concrete strength when determining the transformed effective slab width. The transverse reinforcement is based on the demand of both transverse and interface shears. The results of the parametric study were verified using TxDOT's bridge design software PSTRS14 (TxDOT 2004) results. The results are presented in tabular and graphical formats to highlight the major differences in the designs using the Standard and LRFD Specifications.

Task 5: Identification of Critical Design Issues and Further Study

Several areas requiring further study were identified based on the detailed design examples and the results of the parametric study. Transverse shear design was identified because considerable changes took place when the AASHTO LRFD Specifications adopted a significantly different methodology for shear design. The shear design in the Standard Specifications is based on a constant 45-degree truss analogy for shear, whereas the LRFD Specifications use a variable truss analogy based on Modified Compression Field Theory (MCFT) for its shear provisions. A second area identified for further study is the interface shear design for which the LRFD Specifications give new formulas based on recent results from studies in this area.

Detailed study on the background of interface and transverse shear was conducted. Additional guidelines for these design issues are provided so that smooth transitioning to the AASHTO LRFD Specifications is made possible. Recent studies in the respective areas were reviewed and the findings are noted. The impact of the new provisions on the interface shear design was studied and recommendations are provided. Areas relevant to Texas U beams include the validation of AASHTO LRFD live load distribution factors formulas (especially for wider girder spacings and span lengths longer than 140 ft.) and the LRFD debonding provisions. The debonding provisions of the LRFD Specifications are more restrictive than those in the TxDOT Bridge Design Manual guidelines (TxDOT 2001), leading to a limitation in the span capability of Texas U54 girders. Further investigation into the basis for the LRFD debonding limits was conducted as part of this study. A grillage analogy model for Texas U54 beams was developed to study the validity of the LRFD live load distribution factor formulas beyond the span length limit. Two cases were evaluated using the grillage analysis method to determine the applicability of the LRFD live load distribution factors.

1.4 OUTLINE

Chapter 1 provides an introduction to this research project. Chapter 2 includes the documentation of the literature review. Chapter 3 highlights the design methodology and TxDOT practices and describes the parametric study and design examples. Chapters 4, 5, and 6 present the results of the parametric study conducted for AASHTO Type IV, Type C, and Texas U54 girders, respectively. Chapter 7 presents the background on critical design issues and related findings. Chapter 8 outlines the summary of the project, along with conclusions and recommendations for future research. Additional details of this study have been documented by Adil (2005) and Adnan (2005).

2. LITERATURE REVIEW

2.1 GENERAL

This section consists of a review and synthesis of the available literature to document the research relevant to the development of the *AASHTO LRFD Bridge Design Specifications* (AASHTO 2004). This includes studies related to the development of load models for bridge design, formulation of load distribution factors (DFs), and development of resistance models for prestressed concrete girder bridge design, along with background on reliability theory. Significant design changes in the LRFD Specifications are also reviewed and a comparison of the LRFD and Standard Specifications is provided. The literature review is carried out with special emphasis on the issues relevant to precast, pretensioned concrete Type C, AASHTO Type IV, and Texas U54 girder bridges. The following sections summarize the findings from the literature.

2.2 CODE CALIBRATION AND APPLICATION OF RELIABILITY THEORY

2.2.1 Introduction

The main portions of the *AASHTO Standard Specifications for Highway Bridges* (AASHTO 2002) were written about 60 years ago, and there have been many changes and adjustments at different times that have resulted in gaps and inconsistencies (Nowak 1995). Moreover, the Standard Specifications do not provide for a consistent and uniform safety level for various groups of bridges. To overcome these shortcomings, rewriting the specifications based on the state-of-the-art knowledge about various branches of bridge engineering was required. As a result, a new generation of bridge design specifications, based on structural reliability theory, has been developed, including the Ontario Highway Bridge Design Code (OHBDC), the AASHTO LRFD Specifications (AASHTO 2004), and the Eurocode.

The major tool in the development of the LRFD Specifications is a reliability analysis procedure that maximizes structural safety within the economic constraints. To design structures to a predefined target reliability level and to provide a consistent margin of safety for a variety of bridge structure types, the theory of probability and statistics is used to derive the load and resistance factors. The greater the safety margin, the smaller is the risk of failure of the structural system. However, a higher safety level will increase initial investment cost in terms of design and construction. In contrast, the probability of failure decreases with a higher safety level. Thus, selection of the desired level of safety margin is a trade-off between economy and safety.

2.2.2 Calibration Procedure

The calibration procedure for the LRFD Specifications was developed by Nowak et al. (1987) and was described by Nowak (1995, 1999). The LRFD Specifications are calibrated to provide the same target safety level as that of previous bridge designs with satisfactory performance (Nowak 1999). The major calibration steps were as follows: (1) selection of representative bridges, (2) establishment of a statistical database for load and resistance parameters, (3) development of load and resistance models, (4) calculation of reliability indices for selected bridges, (5) selection of a target reliability index, and (6) calculation of load and resistance factors (Nowak 1995). These steps are briefly outlined below.

About 200 representative bridges were chosen from various geographical regions of the United States based on current and future trends in bridge designs instead of choosing very old bridges. Reliability indices were calculated using an iterative procedure for these bridges, which were designed according to the Standard Specifications (AASHTO 1992). To ensure an adequate level of reliability for calibration of the LRFD Specifications, the performance of all representative bridges was evaluated and a corresponding target reliability index was chosen to provide a minimum, consistent, and uniform safety margin for all structures. The load and resistance factors for the LRFD Specifications were calculated so that the resulting designs have a reliability index close to the target value (Nowak 1995).

2.2.3 Probabilistic Load Models

Load components can include dead load, live load (static and dynamic), environmental forces (wind, earthquake, temperature, water pressure, ice pressure), and special forces (collision and emergency braking forces) (Nowak 1995). These load components are further divided into subcomponents. The load models are developed using the available statistical data, surveys, and other observations. Load components were treated as normal random variables, and their variation was described by the cumulative distribution function (CDF), mean value or bias factor (ratio of mean-to-nominal value), and coefficient of variation (ratio of standard deviation to mean, COV). The relationship among various load parameters was described in terms of the coefficients of correlation. Several load combinations were also considered.

The self-weight of permanent structural or non-structural components under the action of gravity forces was termed as dead load. Due to the variation between subcomponents, the dead load was further categorized into weight of factory-made elements, cast-in-place concrete members, wearing surface, and miscellaneous items (e.g., railing, luminaries) (Nowak 1999, Nowak and Szerszen 1996). Bias factors were taken as used by Nowak (1999), while the coefficients of variation were taken as recommended by Ellingwood et al. (1980). The thickness of the asphalt surface was modeled on the basis of statistical data available from the Ontario Ministry of Transportation (MTO) and reported by Nowak and Zhou (1985). The statistical parameters for dead load used for calibration are summarized in Table 2.1.

Table 2.1. Statistical Parameters of Dead Load (adapted from Nowak and Szerszen 1996).

Component	Bias Factor	Coefficient of Variation
Factory-made members, D1	1.03	0.08
Cast-in-place members, D2	1.05	0.10
Asphalt, D3	3.5 in.	0.25
Miscellaneous, D4	1.03-1.05	0.08-0.10

2.2.4 Probabilistic Resistance Models

The determination of resistance parameters was critical to the development of the AASHTO LRFD Specifications. To quantify the safety reserve for resistance using reliability theory, accurate prediction of the load-carrying capacity of structural components is critical. The bridge capacity depends on the resistance of its components and connections. The resistance of a component, R, is assumed to be a lognormal random variable that is primarily dependent on material strength, and dimensions. Uncertainty in this case is caused by three major factors, namely, material properties M, fabrication (dimensions) F, and analysis approximations P. Material uncertainty is caused by the variation in the material strength, modulus of elasticity, cracking stress, and chemical composition. Fabrication uncertainty is the result of variations in geometry, dimensions, and section modulus. Analysis uncertainty exists due to approximation in the methods of analysis and idealized stress strain distribution models (Nowak et al. 1994).

Material and fabrication uncertainties were combined by Nowak et al. (1994) into one single variable *MF*. The statistical parameters for the professional factor *P* are taken from the available literature (Nowak et al. 1994). The statistical parameters for the mechanical properties of concrete and prestressing steel were taken from available test data (Ellingwood et al. 1980) for use in the simulations.

Statistical parameters, including the bias factor and coefficient of variation, are critical to the reliability methods used. In the absence of an extensive experimental database, the Monte Carlo simulation technique was used to calculate these parameters for bending and shear capacity. The flexural capacity of prestressed concrete AASHTO type girders was established by the strain incremental approach, and moment-curvature relationships were developed. The technique was used to simulate moment-curvature curves corresponding to spans of 40, 60, and 80 ft. for AASHTO Type II, III, and IV prestressed concrete girders. The shear resistance was also calculated using Monte Carlo simulation (Nowak 1995).

The resistance of a component, *R*, and the mean value of *R* are computed as follows.

$$R = R_n MFP \tag{2.1}$$

$$m_R = R_n m_M m_F m_P \tag{2.2}$$

where, m_R, m_M, m_F, and m_P are the means of *R*, *M*, *F*, and *P* respectively. The coefficient of variation of *R*, V_R, may be approximated as:

$$V_R \approx \sqrt{V_M^2 + V_F^2 + V_P^2} \tag{2.3}$$

The final calculated statistical parameters for resistance of prestressed concrete bridges are shown in Table 2.2.

Table 2.2. Statistical Parameters for Resistance of Prestressed Concrete Bridges (adapted from Nowak et al. 1994).

Limit State	*FM*		*P*		*R*	
	Bias	COV	Bias	COV	Bias	COV
Moment	1.04	0.04	1.01	0.06	1.05	0.075
Shear	1.07	0.08	1.075	0.1	1.15	0.13

Nowak (1994) found the resistance factors for prestressed concrete girders. The load factors from the LRFD Specifications were used and the target reliability index was set to 3.5.

Using trial and error, resistance factors (ϕ) were calculated. The resistance factor for prestressed concrete girders was determined to be 1.00 for moment and 0.85 for shear. These resistance factors, when used in conjunction with the LRFD specified load factors, yield a uniform safety level for a wide range of span lengths.

2.2.5 Reliability Analysis of Prestressed Concrete Girder Bridges

As resistance is a product of parameters M, F, and P, therefore, Nowak (1995) assumed that the cumulative distribution function of R is lognormal. The CDF of the load is treated as a normal distribution function because Q is a sum of the components of dead, live, and dynamic load. Very often structural safety is related to the limit states. If $R - Q > 0$, the structure is expected to fail. The probability of failure, P_F, can be defined as:

$$P_F = Prob(R - Q < 0) \tag{2.4}$$

Generally, a limit state function can include many variables (e.g., material properties, structural geometry and dimensions, analysis techniques, etc.), which makes the direct calculation of P_F very complex. Therefore, it is convenient to measure the structural safety in terms of a reliability index. The reliability index, β, defined as a function of P_F, is:

$$\beta = -\Phi^{-1}(P_F) \tag{2.5}$$

where:

Φ^{-1} = Inverse standard normal distribution function

As an example, a normal random variable having a reliability index of 3.5 has a probability of failure of 0.0233 percent. For the cases where the R and Q are best treated using dissimilar distribution functions, iterative methods such as the Rackwitz-Fiessler method can be used to determine the value of β (Nowak 1999, Rackwitz and Fiessler 1978).

Nowak and Saraf (1996) discuss the selection of an optimum target safety level for bridges for various limit states. The optimum safety level depends on several factors such as consequences of failure and cost of safety. Increasing the safety of any structure is desirable, but this increases the cost of construction and requires that the safety of a structure be restricted to a certain level in order to render a safe and economic design. Figure 2.1 shows the relationship between the cost of failure and the reliability index β. The increase in the reliability index, β_T

reduces the cost of failure (C_F) and the probability of failure (P_F), and increases the cost of investment (C_I). The total cost (C_T) is the sum of cost of failure and the cost of investment.

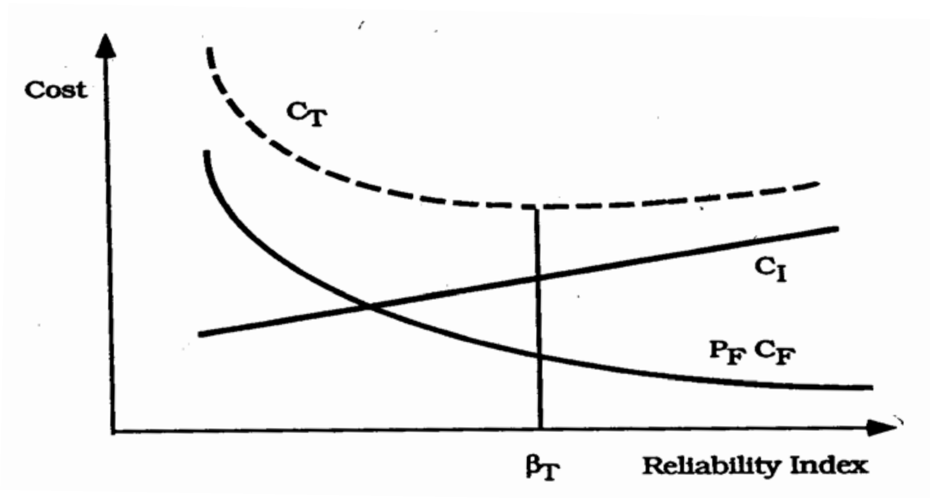

Figure 2.1. Cost vs. Reliability Index and Optimum Safety Level (Nowak and Saraf 1996).

Reliability indices were calculated for bridges designed according to the AASHTO Standard Specifications, which gave a considerable variation in β values. Nowak (1999) assumed that the safety level corresponding to 60 ft. span, 6 ft. spacing, and simple span moment is considered acceptable. Therefore, target reliability index was set equal to 3.5, which is the average β value, considering all the girder types for the aforementioned span and spacing. In general, the target reliability can change for different scenarios depending upon the acceptability of the consequences of potential failure and the cost of increasing safety. The use of the calculated load and resistance factors provide a consistent and uniform reliability of design, as shown by the comparison of Standard and LRFD designs in Figures 2.2 and 2.3.

Nowak and Saraf (1996) designed each structural component to satisfy ultimate, serviceability, and fatigue limit states. They considered the ultimate limit state to be reached upon loss of flexural strength, shear strength, stability, or onset of rupture. The serviceability limit state was assumed to be related to cracking, deflection, and vibration. Analysis of selected bridges and idealized structures without any over-design was performed and the level of safety in the existing bridges was calculated. It was observed that most of the structures are over-designed for serviceability and ultimate limit states. A study on existing bridges designed using Standard

Specifications was carried out and a target safety index was then proposed by Nowak and Saraf (1996).

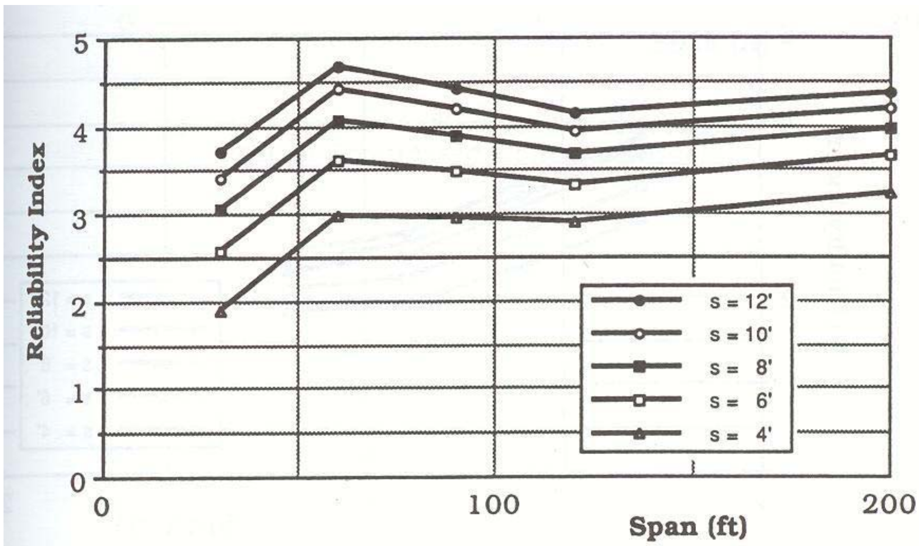

Figure 2.2. Reliability Indices for AASHTO Standard Specifications, Simple Span Moments in Prestressed Concrete Girders (Nowak 1999).

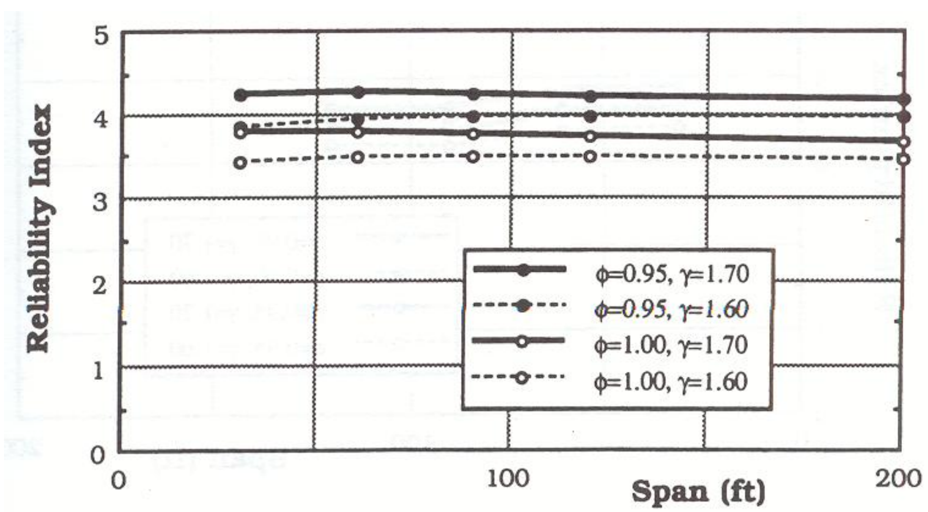

Figure 2.3. Reliability Indices for LRFD Specifications, Simple Span Moments in Prestressed Concrete Girders (Nowak 1999).

The analysis of a number of design cases indicates that unlike other structures, prestressed concrete girders are typically not governed by ultimate limit state. The number of prestressing strands is generally governed by the allowable tension stress at the final load stage. For the serviceability limit state, the β value is 1.0 for the tension stress limit and 3.0 for the compression stress limit, whereas, for ultimate limit state the β value is 3.5. Lower β values for the serviceability limit state indicate the lesser severity of consequences as compared to ultimate limit states.

The ultimate limit states and the corresponding reliability indices represent component reliability rather than system, as observed by Tabsh and Nowak (1991). The LRFD Specifications were developed using the target reliability index for a structural component as β_T=3.5. Tabsh and Nowak (1991) proposed that the target reliability index for structural components be taken as β_T=3.5 and for structural system as β_T=5.5 for ultimate limit states and β_T=1.0 for serviceability limit states.

2.2.6 Future Trends and Challenges

Perhaps the most important issue facing code writers, as well as researchers and engineers involved in safety evaluation of new and existing bridges, is the selection of target reliability levels. Currently, only the strength limit state is calibrated, while other limit states such as service, fatigue and fracture, and extreme event limit states should also be calibrated based on structural reliability theory. In general, future research will be geared toward resolving the issues like time-dependent reliability models, deterioration models and bridge reliability, bridge load and resistance reliability models, nonlinear reliability analysis of bridge structures, reliability of a bridge as a link in transportation network systems, and lifetime reliability.

2.3 LOAD MODELS

2.3.1 General

The development of load and load combination models had an important role in the development of the reliability-based LRFD Specifications. Extensive research studies by Nowak (1987, 1991, 1993c, 1993d 1995, 1999) and Kulicki (1994) were focused on the development of load models representative of the truck loads on highway bridges in the United States. Load models are based on available data from truck surveys, material tests, and component testing.

2.3.2 Dead Load Models

The gravity loads due to self-weight of the structural and nonstructural components of a bridge contribute to the dead load. Depending on the degree of variation, the dead load components are divided into four categories: weight of factory-made components, weight of cast-in-place concrete members, weight of wearing surface and miscellaneous weights (railings, curbs, luminaries, signs, conduits, pipes, etc.) each having different bias factor (ratio of mean to nominal values) and coefficient of variation. Bias factors and coefficients of variation for each dead load category were based on material and component test data, and these values were summarized in Table 2.1.

2.3.3 Live Load Models

2.3.3.1 General

Several studies have been undertaken to model the live load on U.S. highway bridges to reflect actual truck traffic in the coming years and its effects on bridges as accurately as possible. The uncertainty in the live load model is caused by unpredictability of the future trends with regard to configuration of axles and weights. The NCHRP 12-33 project was developed to determine appropriate models for bridge live loads, and its results were incorporated into the LRFD Specifications (Nowak 1993a, 1999). Knowledge of the statistical models including distribution of loads, rate of occurrence, time variation, and correlation with other load components is needed to model the loads accurately. A 75-year extrapolation of the traffic on U.S. bridges was done. Moments and shears were then calculated for these loads and it was found that the shears and moments caused by the heaviest vehicles range from 1.5 to 1.8 times the design moment provided by the Standard Specifications. Possible truck positions were considered with varying degrees of correlation between them in order to arrive at the maximum moments and shears due to actual traffic loading.

2.3.3.2 Live Load Model

A live load model for highway bridges was developed by Nowak and Hong (1991) from the truck survey data and weigh-in-motion (WIM) measurements carried out by different state departments of transportation, mostly from the former source. A procedure for the calculation of live load moments and shears for highway girder bridges was proposed by Nowak and Hong (1991). In this formulation the load components are treated as random variables, and load combinations of dead load, live load, and dynamic load were considered. The findings by Nowak and Hong suggest that a single truck causes maximum moment and shear for single-lane bridges with spans up to 100 ft., and two trucks following behind each other control for longer spans. For two-lane bridges, the maximum values are obtained for two trucks side by side with fully correlated trucks.

Nowak (1995) calibrated the LRFD Specifications using a probability-based approach. About 200 bridges were selected in this study, and for each bridge, load effects and load-carrying capacities were calculated for various components. Live load models were developed using WIM data that included the effects of presence of multiple trucks on the bridge in one and in adjacent lanes. A reduction factor for multilane bridges was also calculated for wider bridges. Numerical models were developed for simulation of dynamic bridge behavior for single trucks and two trucks, side by side, due to inadequate field data.

Kulicki (1994) discussed the development of the vehicular live load model, HL-93, adopted by the AASHTO LRFD Specifications. This study considered 22 representative vehicles from a report released by the National Transportation Research Board. This report reviewed the vehicle configurations allowed by various states as exceptions to the allowable weight limits. The bending moment ratio (i.e., ratio between exclusion vehicle and 1989 AASHTO live load moments) varied from 0.9 to 1.8 with respect to various spans, which called for a new live load model that can represent the exclusion vehicles adequately. Therefore, five candidate notional loads were selected for the development of a new live load model for the AASHTO LRFD Specifications:

(1) a single vehicle weighing a total of 57 tons with a fixed wheel base, axle spacing, and weights;

(2) a design family, HL-93, having of a combination of a design tandem or design HS-20 truck with a uniform load of 0.64 kips per running foot of the lane;

(3) HS-25 truck load followed and preceded by a uniform load of 0.48 kips per running foot of the lane, with the uniformly distributed load broken for the HS vehicle;

(4) a family of three loads consisting of a tandem, a four-axle single unit, with a tridem rear combination, and a 3-S-3 axle configuration taken together with a uniform load, preceding and following that axle grouping; and

(5) an equivalent uniform load in kips per foot of the lane required to produce the same force effect as that produced by the envelope of the exclusion vehicles.

The equivalent uniform load option was eliminated due to the possibility of a complex equation required to represent such a load. A comparison of four remaining possible live load models was performed for various combinations of moments and shears in simply supported beams and continuous beams. The HL-93 live load model proved to be the best combination to represent the exclusion vehicles. Moreover, the results showed that this live load model was independent of the span length, and a single live load factor will suffice to represent all the force effects.

2.3.4 Dynamic Load Models

Hwang and Nowak (1991) presented a dynamic load model for bridges in the U.S. based on simulations and consideration of field effects to find the statistical parameters for the dynamic load effect. An equivalent static load effect was considered for the dynamic load effect. The factors affecting the dynamic load are road surface roughness, bridge dynamics, and vehicle dynamics. Modal equations for bridges were modeled using analytical methods. The dynamic load allowance for the bridges was calculated using different truck types. The mean dynamic load was determined to be equal to 0.10 and 0.15 of the mean live load for one truck and two trucks, respectively. However, the dynamic load is specified as 0.33 of the live load in the LRFD Specifications.

2.3.5 Joint Effect of Dead, Live, and Dynamic Loads

Nowak (1993b) modeled the joint effect of dead, live, and dynamic loads by considering the maximum 75-year combination of these loads using their individual statistical parameters. The live load was assumed to be a product of static live load and the live load analysis factor, P, having mean value of 1.0 and coefficient of variation of 0.12. The statistical parameters of the combination of dead load, live load, and dynamic load depend on various factors such as span length and number of lanes. For a single lane, the coefficient of variation was found to be 0.19 for most of the spans and 0.205 for very short spans. For two-lane bridges, the coefficient of variation was found to be 0.18 for most spans and 0.19 for very short spans.

2.3.6 Earthquake Load Model

Earthquake loading is challenging to model because of its high uncertainty and variation with time. Earthquake load can be represented as a function of ground acceleration, which is highly site specific, along with parameters specific to the structural system and structural component. Earthquake loading is presented by Nowak (1999) as a product of three variables representing variation in ground acceleration, uncertainty in transition from load (ground acceleration) to load effect in a component (moment, shear, and axial forces), and uncertainty due to approximations in structural analysis. The LRFD Specifications present the design values of the return period for an earthquake and its magnitude in the form of contour maps, based on probabilistic analysis.

The AASHTO Standard Specifications present the earthquake load as a function of the acceleration coefficient as obtained from contour maps, site effect coefficients that approximate the effect of the soil profile type, and importance classification allotted to all bridges having an acceleration coefficient greater than 0.29 for seismic performance categorization. The LRFD Specifications specify the earthquake load in a similar manner as that of the Standard Specifications, but it introduces three categories of importance: critical bridges, essential bridges, and other bridges that are used to modify the load and resistance factors. The return period is assumed to be 475 years for essential and other bridges and 2500 years for critical bridges.

2.3.7 Scour Effect Model

Scour, although not considered as a load, can cause a significant effect on bridge performance due to load distribution, and it is a major cause of bridge failure in the U.S. (Nowak 1999). Scour can be considered as an extreme event in bridge design. The three types of scour are long-term channel degradation (scour across the entire waterway breadth), contraction scour (scour caused due to the constriction of the stream caused by bridge approach embankments), and local scour (severe erosion around piers and abutments).

2.3.8 Vessel Collision Model

Vessel collision is another extreme load that is very difficult to model due to its time varying effects. A time varying product of three variables representing variation in the vessel collision force, variation due to transition from vessel collision to load effect in a component, and variation due to approximations in structural analysis can be used to statistically represent the vessel collision effect. The vessel impact force depends on type, displacement tonnage and speed of vessels, and other site-specific factors such as waterway characteristics and geometry, vessel and/or barge configurations, and bridge type and geometry. Any one of the three different procedures to determine the vessel collision force provided in the AASHTO Guide Specifications and Commentary for Vessel Collision Design of Highway Bridges can be used. The LRFD Specifications use different return periods with different importance classifications with three levels of statistical complexity. Vessel collision force is based on a return period of 1000 years for essential and other bridges, whereas for critical bridges the return period is 10,000 years (Nowak 1999).

2.3.9 Load Combination Models

A load combination is the effect of simultaneous occurrence of two or more load components and is a random variable that can be represented by a probability distribution function (PDF) for statistical analysis. The PDFs for critical load combinations should be generated and calibrated to achieve a consistent risk level, but this is not possible in most cases due to numerical difficulties. Reliability analysis is the best alternative to find the critical load combination, where load and resistance factors are selected such that the reliability of the structure is at a predefined target safety level.

The design values for load combinations in the AASHTO Standard Specifications are based on engineering judgment and past experience, whereas the design values for factored load combinations in the LRFD Specifications are based on a statistical approach to attain a uniform reliability index of 3.5. The LRFD Specifications are calibrated for basic load combinations only, due to the lack of a statistical database of correlation of extreme load events.

2.3.10 Load Factors

Nowak (1999) recommended load factors that, when used with specified resistance factors, yield uniform safety levels for bridges that are close to the target reliability index. For the dead loads due to factory-made members and cast-in-place members, the load factor was 1.25. For asphalt-wearing surface weight, the load factor was calculated as 1.5 and the negative dead load can be obtained by multiplying the dead load by 0.85 – 0.90. The live load factor was given as 1.6 for Average Daily Truck Traffic (ADTT) =1000, and for ADTT=5000, the load factor is calculated as 1.70. The following combinations were suggested by Nowak (1999).

$$1.25\,D + 1.50\,D_A + 1.70(L+I) \tag{2.6}$$

$$1.25\,D + 1.50\,D_A + 1.40\,W \tag{2.7}$$

$$-0.85\,D - 0.50\,D_A + 1.40\,W \tag{2.8}$$

$$1.25\,D + 1.50\,D_A + 1.35(L+I) + 0.45\,W \tag{2.9}$$

$$1.25\,D + 1.50\,D_A + \gamma_L\,(L+I) + 1.00\,E \tag{2.10}$$

where:

D = Dead load of structural components and non-structural attachments

D_A = Dead load of asphalt wearing surface

L = Live load

I = Dynamic load

W = Wind load

E = Earthquake load

γ_L = 0.25 – 0.50 for ADTT = 5000

= 0.10 – 0.20 for ADTT = 1000

= 0 for ADTT = 100

2.4 LOAD DISTRIBUTION FACTORS

2.4.1 Introduction

The lateral distribution of vehicular live load has a significant impact on quantifying the demand on highway bridges. One of the major changes encountered by bridge engineers in the LRFD Specifications is in the load DFs, which are based on a detailed parametric study and recommendations by Zokaie et al. (1991). Despite the universal agreement about the superiority of the LRFD Specifications (AASHTO 2004) live load DFs over Standard Specifications (AASHTO 2002) live load DFs, the former still lack accuracy. This is primarily due to overlooking various structural and non-structural components of a typical bridge, as found by Chen and Aswad (1996), Barr et al. (2001), and Eamon and Nowak (2002), among others.

2.4.2 Differences between Standard and LRFD Load Distribution Factors

In general, the bridge design community has been using the empirical relations for live load distribution as recommended by the AASHTO Standard Specifications, with only minor changes since 1931, and recent additions to these specifications have included improved load DFs for particular types of superstructures based on tests and/or mathematical analyses (Zokaie et al. 1991). The AASHTO Standard Specifications give very simple expressions for live load

DFs for girder bridges in an *S*/*D* format, where *S* is the girder spacing in feet and *D* is 5.5 for a bridge constructed with a concrete deck on prestressed concrete girders carrying two or more lanes of traffic. The effects of various parameters such as skew, continuity, and deck stiffness were ignored in this expression and it was found to be accurate for a few selected bridge geometries and was inaccurate once the geometry was changed. Hence, development of a formula for a broad range of beam and slab bridges, including prestressed concrete bridges was needed. Much research was carried out using finite element analysis, grillage analysis, and field tests to arrive at more accurate expressions for DFs. The DFs proposed by LRFD consider the effects of different parameters such as skew, deck stiffness, and span length. The LRFD Specifications also provide correction factors for skewed bridges to be applied to the DFs.

2.4.3 Development of LRFD Distribution Factors

Zokaie et al. (1991) conducted a study to provide the basis for the current AASHTO LRFD live load DFs. In 1994, the AASHTO LRFD Specifications (AASHTO 1994) introduced a comprehensive set of live load DF formulas that resulted from the NCHRP 12-26 project, entitled "Distribution of Live Loads on Highway Bridges" (Zokaie 2000). Although these formulas are also approximate, they consistently give conservative results, with better accuracy, for a wide range of bridge types and bridge geometric parameters when compared to the other formulas available in the literature (Zokaie et al. 1991). The procedures followed by Zokaie et al. (1991) are summarized below.

2.4.3.1 History and Objectives

In 1994, the AASHTO LRFD Specifications (AASHTO 1994) introduced a comprehensive set of live load DF formulas that resulted from the NCHRP 12-26 project, entitled "Distribution of Live Loads on Highway Bridges" (Zokaie 2000). The NCHRP 12-26 project was initiated in 1985 to improve the accuracy of the *S*/*D* formulas of the Standard Specifications and to develop comprehensive specifications for distribution of wheel loads on highway bridges (Zokaie et al. 1991 and Zokaie 2000). The resulting recommendations from this project were adopted by AASHTO as the guide specifications for lateral distribution of vehicular live loads on highway bridges in 1994. With the advent of the first edition of the LRFD Specifications (AASHTO 1994), the formulas that were developed for the Standard Specifications needed to be modified to take into account the changes in vehicular live load model and multiple presence factors (Zokaie 2000). Thus, the formulas were recalibrated and incorporated in the LRFD Specifications (AASHTO 1994). The objectives of this project were to evaluate the available methods for live load distribution, develop additional formulas to improve the accuracy of existing methods, and to provide guidelines for the selection of the most efficient refined analysis methods.

2.4.3.2 Procedure

Several hundred bridges were selected from the National Bridge Inventory File (NBIF) to create a representative database of all the bridges in the United States (Zokaie 2000). The focus of this project was on typical bridge types such as beam-slab bridges, box girder bridges, slab bridges, multi-box beam bridges, and spread box beam bridges. The database basically included the details required to build the analytical model of a particular bridge required to carry out a finite-element or grillage analysis of bridge superstructure. In particular, several parameters such as bridge type, span length, edge-to-edge width, curb-to-curb width, skew angle, number of girders, girder depth, slab thickness, overhang, year built, girder moment of inertia, girder area, and girder eccentricity (distance between the centroids of the girder and the slab) were extracted from the bridge plans obtained from various state departments of transportation. Among other bridge types, the database included 55 spread box beam bridges. The statistical analysis of the database parameters was performed with the help of histogram and scattergram plots to identify the range and variation of each parameter, and the degree of correlation among several parameters. According to Zokaie (2000), the parameters were by and large not found to be correlated to each other.

For each bridge type, three different levels of analyses were considered. The most accurate level of analysis, Level Three, included the detailed three-dimensional (3D) modeling of the bridge superstructure, and finite element modeling was recommended for this level of accuracy. Level Two included graphical methods, nomographs, influence surfaces, or simplified computer programs. The grillage analysis method, which has the comparable level of accuracy, was considered to be in the Level Two analysis category. Level One analysis methods include the empirical formulas developed as the result of experimental or analytical studies, which generate approximate results and are simple in their application. To identify the most accurate available computer program for a particular bridge type, test data from field and laboratory experiments were compiled and analytical models developed in the Level Three computer programs. Analytical models were analyzed and results were compared with experimental results. The programs that produced the most accurate results were identified for particular bridge types and considered as the basis for the evaluation of Level Two and Level One methods. A computer program, GENDEK5A, was selected for the development of finite element models because this program can model the bridge system more accurately, and it generated accurate results as compared with field test results from many prototype bridges.

A parametric sensitivity study was performed to identify the important parameters that affect the lateral distribution of live loads. A finite element model was developed using the mean values of all the parameters except the one under consideration, which was varied from minimum to maximum to recognize its affects on the DFs under HS-20 truck loading. After examining the results, span length, girder spacing, and beam depth were considered key parameters for spread box beams. Since the HS-20 truck gage length is constant at 6 ft., it was not considered in the sensitivity study but it may have a considerable affect on live load DFs if varied. A smaller gage width will result in larger DFs and vice versa. Although this study is based on the AASHTO HS family of trucks, a limited parametric study showed that truck weight and axle configuration does not significantly affect the live load distribution.

According to Zokaie (2000) the development of the simplified formulas for the AASHTO LRFD DFs was based on certain assumptions. It was assumed that there was no correlation between parameters considered to be included in the formula. It was also assumed that the effect of each parameter can be modeled by an exponential function of the form ax^b, where x is the value of the given parameter and constants a and b are determined to represent the degree of variation of the DF. For the selected set of key parameters for a particular bridge type, the following general form of the exponential formulas was devised.

$$g = (a)(S)^{b1}(L)^{b2}(d)^{b3}(.......)^{b4} \tag{2.11}$$

where a is a scale factor; g is the distribution factor; S, L, d are selected parameters; and $b1$, $b2$, $b3$, $b4$ are exponents of each parameter. The exponents of each parameter were selected to make the exponential curve fit the simulated variation between the particular parameter and the DF. Different values of DFs (g) were calculated for different values of a particular parameter in the formula, say S, while keeping all other parameters the same as for the average bridge. The resulting formulas are then,

$$\begin{aligned} g_1 &= (a)(S_1)^{b1}(L)^{b2}(d)^{b3}(.......)^{b4} \\ g_2 &= (a)(S_2)^{b1}(L)^{b2}(d)^{b3}(.......)^{b4} \\ &. \quad . \quad . \quad . \quad . \quad . \\ &. \quad . \quad . \quad . \quad . \quad . \\ g_n &= (a)(S_n)^{b1}(L)^{b2}(d)^{b3}(.......)^{b4} \end{aligned} \tag{2.12}$$

For the first two equations,

$$\left(\frac{g_1}{g_2}\right) = \left(\frac{S_1}{S_2}\right)^{b1} \tag{2.13}$$

or $$b1 = \frac{\ln\left(\frac{g_1}{g_2}\right)}{\ln\left(\frac{S_1}{S_2}\right)} \tag{2.14}$$

So, for n equations there are (n-1) different *b1* values. If all *b1* values are generally close to each other, then an exponential curve based on the average of all *b1* values was used to model the variation in the DFs. The value of scale factor a was determined from the average bridge by the following equation,

$$a = \frac{g_{avg}}{\left((S_{avg})^{b1}(L_{avg})^{b2}(d_{avg})^{b3}(.......)^{b4}\right)} \tag{2.15}$$

This entire procedure was repeated for all other parameters in the similar manner.

The process of developing simplified formulas was based on certain assumptions. Parameters that did not affect the load distribution in a significant way were ignored altogether. To gain confidence in the accuracy of the developed formulas and to compare their relative accuracy level with other proposed formulas, their verification and evaluation was a very important step. Therefore, the bridges in the database were analyzed by a Level Three accurate method, best suited to a particular class of bridges as determined earlier. Mean, minimum, maximum and standard deviations were determined and compared for all the formulas and the accurate method. A low standard deviation was considered to be indicative of relatively higher accuracy level for a particular formula. The trends in the accuracy of the formula with respect to the Level Three accurate method were analyzed with the help of statistical data so obtained. To optimize the level of accuracy of the developed formulas, the researchers minimized the standard deviation and ensured that it was kept lower than that obtained from the AASHTO Standard formulas. The formulas were made as simple as possible while maintaining the desired level of accuracy.

The database of results was used to identify the key parameters affecting the DFs for a given bridge (Zokaie 2000). The results showed that the parameters are not correlated. After significant testing, Zokaie (2000) determined that girder spacing, span length, girder stiffness, and slab thickness control the DFs for a given bridge. The effects of these parameters were studied and Zokaie (2000) arrived at simplified base formulas, provided in Figure 2.4, that represent the effects of different parameters on girder DFs and yield conservative results.

Further extensions to the base formulas were made by Zokaie (2000) to account for various factors such as presence of edge girder, continuity, and skew effect. Correction factors to adjust the base formulas were proposed. The formulas that appear in the LRFD Specifications are slightly different from those developed from this study. Changes were made to account for the new live load required in the LRFD Specifications, which is different from the HS-20 trucks used for this study. A simple program called LDFAC (Zokaie et al. 1993) was developed to assist engineers in finding out the applicable DFs for a given bridge. Zokaie et al. (1991) recommend the use of accurate analysis if the geometry of the bridge is different from those considered in the study, and they also give a set of recommendations for such analysis.

TABLE 7. AASHTO-LRFD Formulas for Moment/Shear Distribution (g) to Interior Girders

Bridge type (1)	Bridge designed for one traffic lane (2)	Bridge designed for two or more traffic lanes (3)	Range of applicability (4)
(a) Moment			
Beam and slab	$0.12 + 2\left(\frac{S}{14f}\right)^{0.4}\left(\frac{S}{L}\right)^{0.3}\left(\frac{K_g}{Lt_s^3}\right)^{0.1}$	$0.15 + \left(\frac{S}{9.5f}\right)^{0.6}\left(\frac{S}{L}\right)^{0.2}\left(\frac{K_g}{Lt_s^3}\right)^{0.1}$	$3.5f \le S \le 16f$ $20f \le L \le 240f$ $N_b \ge 4$
Concrete box girders	$\left(3.5 + \frac{S}{1.8f}\right)\left(\frac{f}{L}\right)^{0.35}\left(\frac{1}{N_c}\right)^{0.45}$	$2\left(\frac{13}{N_c}\right)^{0.3} + \left(\frac{S}{5.8f}\right)\left(\frac{f}{L}\right)^{0.25}$	$7f \le S \le 13f$ $60f \le L \le 240f$ $3 \le N_c$ if $N_c > 8$ use $N_c = 8$
Slab	$\frac{2f + \sqrt{L_1 W_1}}{4}$	$3.5f + 0.06\sqrt{L_1 W_1}$	$8f \le L \le 70f$ $12f \le W \le 100f$
Spread box beams	$2\left(\frac{S}{3f}\right)^{0.35}\left[\left(\frac{S}{L}\right)\left(\frac{d}{L}\right)\right]^{0.25}$	$2\left(\frac{S}{6.3f}\right)^{0.6}\left[\left(\frac{S}{L}\right)\left(\frac{d}{L}\right)\right]^{0.125}$	$6f \le S \le 11.5f$ $20f \le L \le 140f$ $1.5f \le d \le 5.4f$ $N_b \ge 3$
Multibox beam decks	$1.2k\left(\frac{b}{L}\right)^{0.5}\left(\frac{I}{J}\right)^{0.25}$ $k = 2.5(N_b)^{-0.2} \ge 1.5$	$2k\left(\frac{b}{25.4f}\right)^{0.6}\left(\frac{b}{L}\right)^{0.2}\left(\frac{I}{J}\right)^{0.06}$ $k = 2.5(N_b)^{-0.2} \ge 1.5$	$3f \le b \le 5f$ $20f \le L \le 120f$ $2.92f \le b \le 5f$ $5 \le N_b \le 20$
(b) Shear			
Beam and slab (slab on girder)	$2\left(0.36 + \frac{S}{25f}\right)$	$0.4 + \frac{S}{6f} - 2\left(\frac{S}{35f}\right)^{2.0}$	$3.5f \le S \le 16f$ $20f \le L \le 200f$ $0.375f \le t_s \le 12.0f$ $0.48f^4 \le K_g \le 337f$ $N_b \ge 4$
Concrete box girder	$2\left(\frac{S}{9.5f}\right)^{0.6}\left(\frac{d}{L}\right)^{0.1}$	$2\left(\frac{S}{7.3f}\right)^{0.9}\left(\frac{d}{L}\right)^{0.1}$	$7f \le S \le 13f$ $60f \le L \le 240f$ $3 \le N_c$
Spread box beams	$2\left(\frac{S}{10f}\right)^{0.6}\left(\frac{d}{L}\right)^{0.1}$ for $S \ge 11.5'$ use lever rule	$2\left(\frac{S}{7.4f}\right)^{0.8}\left(\frac{d}{L}\right)^{0.1}$	$6f \le S \le 11.5f$ $20f \le L \le 135.5f$ $N_b \ge 3$
Multibox beams	$2\left(\frac{S}{10.83L}\right)^{0.15}\left(\frac{I}{J}\right)^{0.05}$	$2\left(\frac{b}{13f}\right)^{0.4}\left(\frac{b}{L}\right)^{0.1}\left(\frac{I}{J}\right)^{0.05}$	$3f \le b \le 5f$ $20f \le L \le 105f$ $5 \le N_b \le 20$ $1.2f^4 \le J \le 29.5f^4$ $1.92f^4 \le I \le 29.5f^4$

Note: f = 304.8 mm (1.0 ft)

Figure 2.4. Proposed Distribution Factors (Zokaie 2000).

2.4.3.3 Limitations

The AASHTO LRFD Specifications formulas were calibrated against a database of real bridges. This database was characterized by particular ranges of span lengths, girder spacings, girder depths, and over-hang widths. These formulas produce results that are generally within 5 percent of the results of finite element deck analysis results and are most accurate when applied to bridges within the scope of the calibration database (Zokaie 2000). The effects of edge stiffening elements were ignored in this study. Some special cases where these formulas were recommended to be applied by using engineering judgment are non-prismatic girders, varying skew and span lengths in continuous bridges, different girder spacings, varying girder widths, and large curvatures.

2.4.4 Subsequent Research Studies

To determine the suitability and applicability of the new proposed formulas to their particular bridges, several departments of transportation and independent researchers carried out studies. The Illinois (IDOT), California (Caltrans), and Tennessee (TDOT) departments of transportation sponsored research aimed at either simplifying and revamping the live load distribution criteria to suit their typical bridge construction practices or to justify their previous practices of live load distribution (Tobias et al. 2004, Song et al. 2003, Huo et al. 2004). Some recommendations made in these research studies are summarized in Section 2.5 and are not discussed below to avoid repetition.

2.4.4.1 Song et al. (2003)

Song et al. (2003) found that limitations on the use of the LRFD (AASHTO 1998) live load DF formulas place severe restrictions on the routine designs of bridges in California, as box-girder bridges outside of these limits are frequently constructed. These restrictions include: constant deck width, parallel beams with approximately equal stiffness, span length-to-width ratio greater than 2.5, and angular change of less than 12 degrees in plan for a torsionally stiff closed section. They performed a grillage analysis for multicellular box girders typical of California bridges with aspect ratios from 0.93 to 3.28, an angular change in curvature from 5.7 to 34.4 degrees, and with nonparallel girders or a non-prismatic cross-section. They concluded that, in general, these formulas can be used for the box girder bridges within the scope considered in their parametric study. The plan aspect ratio limit was concluded to be unwarranted because as the plan aspect ratio becomes smaller than the 2.5 limit, the general trend indicates that the LRFD Specifications formula becomes increasingly conservative. Furthermore, it was found that the DF from the refined analysis does not vary significantly with the different radii of curvature or angular change between the bents. The authors finally concluded that because of the small set of bridges used in this study, results presented should not be construed to imply an overall conservatism of the LRFD formulas; further study of the limits with a more extensive parameter range is warranted.

2.4.4.2 *Huo et al. (2004)*

Huo et al. (2004) carefully examined Henry's method, which is a simplified live load distribution method used by the Tennessee Department of Transportation since 1963, and proposed modifications to the original method. They introduced the method as simple and flexible in application, which can treat both interior and exterior beams in a bridge. The method requires only basic bridge information including the width of the bridge, the number of traffic lanes, and the number of beams. It was concluded that the results of Henry's method were in reasonable agreement with the values from the LRFD Specifications (AASHTO 1998), the Standard Specifications (AASHTO 1996), and finite element analysis. Effects of four key parameters including span length, beam spacing, slab thickness, and beam stiffness were documented, and for all these parameters Henry's method was found to be in very good agreement with the LRFD and the Standard Specifications. Particularly, the DF values from the LRFD Specifications were found to have a better correlation with Henry's method.

2.4.4.3 *Kocsis (2004)*

Kocsis (2004) evaluated the AASHTO Standard Specifications line loads (curbs, sidewalks, barriers, and railings) and live load DFs. The author discussed the computer program SECAN (Semi-continuum Method of Analysis for Bridges) and made suggestions for obtaining more accurate DFs for line loads, AASHTO live loads, and non-AASHTO live loads. The author raised the question as to how line loads should be accurately distributed to bridge girders. He further noted that the wearing surface, being spread over almost the entire deck, can be distributed equally to all girders; but for curbs, sidewalks, barriers, and railings, it would be expected that the girder nearest the load would take the largest portion of the load. For a particular case of a 175 ft. simple span five steel girder bridge with a total weight of sidewalk and railing to be 635 lb/ft, he showed that AASHTO Standard uniform distribution of sidewalk and railing yielded 254 lb/ft per girder as compared to analysis performed by the computer program SECAN, which yielded the actual load taken by the exterior girder to be 632 lb/ft. His calculations showed that the actual share of the sidewalk and railing loads carried by the outer girders is substantially more than given by the AASHTO method of dividing the load equally among all the girders. Moreover, he recommends the use of SECAN for line load DFs and the use of the LRFD (AASHTO 1994) formulas for live load distribution.

2.4.4.4 Tobias et al. (2004)

The study conducted by Tobias et al. (2004) targeted typical bridges in Illinois' inventory, such as concrete deck-on-steel stringer construction and concrete deck-on-precast prestressed I-beams. Moreover, they considered simply supported and continuous bridges, which had span lengths ranging between 20 ft. to 120 ft. with 10 ft. increments. The transverse beam spacing varied from 3.5 ft. to 10 ft. with 0.5 ft. increments. The continuous structures had two spans of equal lengths. The stringers were of constant depths and section moduli throughout each span. The studied structures were designed efficiently (i.e., the ratios of actual section moduli to required were all close to unity). No curved or skewed structures were included in the study and interior beams were assumed to govern the design. Only the factored design moments and shears were compared because of the dissimilar nature of the two design philosophies (LFD and LRFD). For all considered simple spans and continuous spans, LRFD design moments ranged between 22 percent larger to 7 percent smaller than those computed using LFD. For mid-range spans (50 – 90 ft.) with common Illinois transverse spacings (5.5 – 7.5 ft.), the average increase in design moment over LFD was 3 to 4 percent. LRFD design shears ranged between 41 percent larger to 3 percent smaller. For mid-range spans (50 – 90 ft.) with common Illinois transverse spacings (5.5 –7.5 ft.), the average increase in design shears over LFD was about 20 percent. In general, the disparity between predicted shears using LRFD and LFD was found to be more profound for shear than for moment. The authors described the pile analogy method provision for calculation of live load DF for exterior beams in bridges with diaphragms or cross-frames to be a very conservative approach. The ratio of longitudinal to transverse stiffness parameter (K_g/Lt^3) in the live load DF formula is said to have insignificant affect on the final calculation of bending moment or shear and was set equal to 1.10 for prestressed I-beam shapes and 1.15 for standard Illinois bulb-tee shapes. They recommended that the exterior beam overhang cantilever span is such that the interior beam governs primary superstructure design in Illinois for typical bridges; and that these bridges be designed for two or more lane loadings, except for fatigue and stud design where a single lane loading should be checked.

2.4.4.5 Chen and Aswad (1996)

Chen and Aswad (1996) reviewed the LRFD live load distribution formulas for modern prestressed concrete I-girder and spread box girder bridges with larger span-to-depth ratios, and compared LRFD's results with those obtained by the finite element analysis method. They pointed out certain shortcomings in the methodology followed by Zokaie et al. (1991). The "average bridge" and the database of bridges was not representative of future bridges that are characterized by larger span-to-depth ratios and higher concrete strengths. As an example, they said that Zokaie et al. (1991) considered the average bridge span length to be 65.5 ft., which was well below the expected average span of future bridges and, thus, a more rigorous analysis is required to take into account this increase in average span. The effect of diaphragms was not considered in the original study; therefore, the rigid diaphragm model required by interim LRFD (AASHTO 1994) provisions in Section 4.6.2.2.2d produces over-conservative results. They observed that for spread box girders, finite element analysis method produced smaller DFs by 6 to 12 percent for both interior and exterior girders. But, in the two cases where the aforementioned LRFD (AASHTO 1994) provision of rigid diaphragm model was controlling, the LRFD DFs were conservative by 30 percent for the cases considered (e.g., 0.785 and 0.9 by LRFD as compared to 0.548 and 0.661 by finite element analysis). The assumption of a rigid diaphragm model for exterior girders is no longer applicable to spread box beams in the latest LRFD Specifications (AASHTO 2004).

The authors also indicated that the average I-beam span length of 48 ft. considered by Zokaie et al. (1991) for arriving at the DFs is rather short for I-beam bridges, which are more likely to be 80 to 90 ft. long. The finite element analysis showed the DFs given by the LRFD Specifications to be conservative by at least 18 percent for interior girders and 4 to 12 percent for exterior girders. If the DFs from Chen and Aswad's analysis are used instead of the LRFD DFs, the required concrete release strength can be reduced or the span length can be increased by 4 to 5 percent for the same section.

2.4.4.6 Eamon and Nowak (2002)

Eamon and Nowak (2002) studied the effects of edge-stiffening elements (barriers, sidewalks, and other secondary elements including diaphragms) on the resistance and load distribution characteristics of composite steel and prestressed concrete bridge girders. They found that steel girder bridges tend to benefit more from secondary elements in terms of load distribution than generally stiffer prestressed concrete bridge girders. For the finite element analysis in the elastic range, they found that diaphragms reduce the maximum girder moment by up to 13 percent (4 percent on average); barriers up to 32 percent (10 percent on average); sidewalks up to 35 percent (20 percent on average); combinations of barriers and sidewalks from 9 to 34 percent; combinations of barriers and diaphragms from 11 to 25 percent; and combinations of barriers, sidewalks, and diaphragms from 17 to 42 percent. In general, for the elastic finite element analysis case, neglecting barriers and diaphragms together lead to discrepancies ranging from 10 to 35 percent, while neglecting barriers, sidewalks, and diaphragms gave discrepancies ranging from 25 to 55 percent. Finally, they concluded that in the elastic range, secondary elements affect the longitudinal and transverse position and magnitude of maximum girder moment and can have results in a 10 to 40 percent decrease in girder DF for typical cases. Similarly, for the inelastic finite element analysis case, girder DFs can undergo an additional decrease of 5 to 20 percent. Moreover, they observed that ignoring the secondary element effect can produce varying levels of reliability for girder bridges designed as per LRFD Specifications (AASHTO 1998).

2.4.4.7 Khaloo and Mirzabozorg (2003)

Khaloo and Mirzabozorg (2003) conducted a study to assess the effect of skew and internal diaphragms on the live load distribution characteristics of simply supported bridges consisting of five I-section concrete girders. Their study confirmed that the Standard Specifications DFs (AASHTO 1996) are very conservative when compared with the load DFs obtained by finite element analysis. The scope of their study was defined by the key parameters of girder spacings (1.8, 2.4, and 2.7 m), span lengths (25, 30, and 35 m), skew angles (0, 30, 45, and 60 degrees), and different arrangements and spacings of internal diaphragms. The authors proposed some modifications to relationships originally proposed by Khaleel and Itani (1990) for load DF calculations for decks with internal diaphragms perpendicular to the longitudinal girders. Those relationships lower the conservatism in the load DFs provided by the Standard Specifications (AASHTO 1996). The authors concluded that the arrangement of internal diaphragms has a great effect on the load distribution pattern. They showed that even in bridges with zero skew without internal diaphragms, the load DFs of the aforementioned Standard Specifications are very conservative. This difference between the Standard Specifications and finite element analysis increases with the increment in skew angle, especially in decks with internal diaphragms perpendicular to the longitudinal girders.

2.4.4.8 *Khaloo and Mirzabozorg (2003)*

A study by Khaloo and Mirzabozorg (2003) also confirmed the conservatism of the LRFD DFs. Their research evaluated the effects due to bridge skew and addition of transverse diaphragms on the load DFs using finite-element models. The parameters of the study were girder spacing (1.8 – 2.7 m), span length (25 – 35 m), skew angle (0 – 60 degrees), and different arrangements of internal transverse diaphragms. Bridge models with three spans of 25, 30, and 35 m, varying the girder spacing as 1.8, 2.4, and 2.7 m were considered. The models were loaded with an HS-20 truck according to the AASHTO Standard Specifications. The results of the study indicated that the skew has the greatest effect on the load DF. The load DFs for skew bridges were found to be always less than that of right bridges (with no skew). In all the cases the load DFs of the LRFD Specifications were found to be conservative and in some cases over-conservative.

2.4.4.9 *Barr et al. (2001)*

Barr et al. (2001) studied the effects of lifts (haunches), intermediate and end diaphragms, continuity, skew angle, and load type (truck and lane) on the live load distribution in a continuous high-performance prestressed concrete girder bridge, designed by the Washington Department of Transportation (WSDOT). The bridge had five W74MG girders and was skewed at 40 degrees with three span lengths of 24.4 m, 41.7 m, and 24.4 m. A finely meshed (6000 nodes) finite element model was evaluated with the results of field measurements of the bridge, and the discrepancy in the maximum moments in each girder in the analytical model as compared to the actual field measurements was found to be within 6 percent, with the results from the analytical model always on the conservative side. In their study, the difference between a rigorous finite element model, which most closely represented the actual bridge, and the LRFD Specifications (AASHTO 1998) was up to 28 percent. For comparison, a finite element model similar to that considered in developing the LRFD live load DFs (i.e., without lifts, diaphragms, and continuity) gave values that were 6 percent smaller than the LRFD DFs (AASHTO 1998), which matches the 5 percent value anticipated by Zokaie et al. (1991). It was observed in their study that the presence of lifts and end diaphragms were the major factors that significantly reduce the DF values. They concluded that in comparison to code DF values, the live load DF by the finite element method would, if used, either reduce the required concrete release strength by 6.9 MPa or could allow for increasing the live load by 39 percent.

2.4.5 Effect of Various Parameters

2.4.5.1 Effect of Edge Stiffening Elements

Based on a limited sensitivity study, Chen and Aswad (1996) found that exterior girders could carry more than 50 percent of parapet and/or noise wall loads and that the number of girders was a dominant variable when considering the distribution of these loads. Eamon and Nowak (2002) found that barriers and sidewalks or their combinations are more effective for closely spaced girders and longer spans. They also found that steel girder bridges tend to benefit more from edge stiffening elements in terms of load distribution than generally stiffer prestressed concrete bridge girders. They observed that: 1) the addition of the edge-stiffening elements tends to shift the location of maximum moment away from the edge and closer to the center girder, and 2) for bridges with longer spans and fewer girders, the edge-stiffening elements have the least affect on the maximum moment position. Eamon and Nowak (2002) also found that barriers decrease all girders deflections, but this decrease is more for exterior girders as compared to interior ones. Moreover, they noticed that the large shifts in the neutral axis upward at the edges of the bridge are indicative of the effectiveness of the addition of sidewalk and barrier or their combination. They also found that edge stiffening element effect is dependent upon bridge geometry (i.e., span length, bridge width, and girder spacing), stiffness of secondary elements relative to that of girders or deck slab, and sidewalk width. Kocsis (2004) noted that the wearing surface can be distributed equally to all girders; but for curbs, sidewalks, barriers, and railings, it would be expected that the girder nearest the load should take the largest portion of the load.

2.4.5.2 Effect of Diaphragms

Eamon and Nowak (2002) found that diaphragms tend to make the girder deflections uniform among interior and exterior girders. They noted that the addition of stiffer midspan diaphragms shifts the longitudinal position of maximum moment away from midspan closer to the second truck axle and that stiffer girders are not as much affected by this longitudinal shift as more flexible ones. They observed that diaphragms have a little effect on shifting the neutral axis of the bridge superstructure. Khaloo and Mirzabozorg (2003) concluded that in order to achieve the maximum efficiency for the presence of internal diaphragms, they should be placed perpendicular to the longitudinal girders, and the load distribution is negligibly affected by the spacing between internal diaphragms that are perpendicular to the longitudinal girders. As per findings of Barr et al. (2001), the end diaphragms affect the load distribution significantly in comparison to intermediate diaphragms. They found that at high skew angles (≥ 30-degrees) the intermediate diaphragms were slightly beneficial, while introducing the end diaphragms decreased the DFs, and this effect increased with increasing skew (e.g., for exterior girders, the decrease was up to 6 percent for zero skew to 23 percent for a 60-degree skew angle).

2.4.5.3 Effect of Skew Angle

Khaloo and Mirzabozorg (2003) found the skew angle to be the most influential factor on the load distribution and the load DF is always less for skewed bridges as compared to those of no skew. They observed that comparing the results of finite element analysis with those of the Standard Specifications (AASHTO 1996), the load distribution decreases by 24 percent and 26.5 percent for exterior and interior girders, respectively, for a skew angle of 60-degrees. However, for skew angles less than 30-degrees this reduction is insignificant, with the Standard Specifications always conservative. They further observed that for all girders, the effect of skew angle on the load DF decreases when span length increases. According to the findings of Barr et al. (2001), generally interior girders were more affected by skew than were exterior girders.

2.4.5.4 Effect of Lifts

According to Barr et al. (2001), the lift slightly increases the composite girder stiffness; and at the same time it significantly increases the transverse bending stiffness of the deck by adding to the effective depth of the deck slab. This change makes the live load distribution more uniform and decreases the live load DF due to increased transverse to longitudinal stiffness, especially at higher skew angles. In their investigation, they found that the addition of lifts reduced the DFs by 17 percent for exterior girders and by 11 percent for interior girders.

2.4.5.5 Effect of Continuity and Other Parameters

Barr et al. (2001) found that in their model the exterior girders in a continuous span model had higher DFs as compared to a simply supported model. Their findings are consistent with those of Zokaie et al. (1991). They further determined that continuity decreased the DF for a low skew angle and increased the DF only for skews greater than 40 degrees. Barr et al. (2001) also observed that the type of loading does affect the distribution of load, as the lane load DF was found to be 10 percent lower than the truck load distribution.

2.5 REFINED ANALYSIS METHODS

2.5.1 General

Bridge superstructure analysis is the fundamental step in the design process of any bridge structure. Generally, a bridge superstructure is structurally continuous in two dimensions of the plane of the deck slab, and the resulting distribution of the applied load into shear, flexural, and torsional stresses in two dimensions is considerably more complex as compared to those in one-dimensional continuous beams. A closed form solution of the mathematical model, which describes the structural behavior of a bridge superstructure, is seldom possible. Several approximate methods of analysis have evolved. Depending upon the objectives of analysis, several simplified or refined analysis procedures such as grillage analogy, finite strip, orthotropic plate, folded plate, finite difference, finite element, and series or harmonic methods have been used to analyze the bridge superstructures subjected to various loading conditions. The LRFD Specifications (AASHTO 2004) explicitly allow the use of the aforementioned analysis methods and all those methods that satisfy the requirements of equilibrium, and compatibility, and utilize constitutive relationships for the structural materials.

Transverse distribution of the vehicular live load to individual bridge girders has been studied for many years. The AASHTO LRFD Specifications provide simplified live load DF formulas, which were developed by Zokaie et al. (1991) based on more detailed analysis methods including the grillage analogy and finite element analysis methods. Puckett (2001) analyzed all of the 352 bridges in the original bridge database, used by Zokaie et al. (1991), using the finite strip method and validated the accuracy of these formulas for interior beams. Several other research endeavors have independently studied the validity and accuracy of the AASHTO LRFD simplified live load DF formulas and in general, all of them have used either the finite element method or the grillage analogy method toward that objective. In this section, the application of the grillage analogy and the finite element method are reviewed in the context of lateral distribution of vehicular live loads.

2.5.2 Grillage Analogy Method

Before the advent of the finite element analysis method, the grillage analogy method was a popular method for bridge deck analysis because it is easily comprehensible, computationally efficient, and produces reliably accurate results. According to Hambly and Pennells (1975) and Hambly (1991), the grillage analogy method has been applied to several types of slab bridges (e.g., composite voided and composite solid, solid and voided), slab-on-girder and box girder bridges (e.g., twin cell, multiple cell with vertical and sloping webs, spread box). In addition, skew, curvature, continuity, edge stiffening, deep haunches over supports, isolated supports and varying section properties can also be modeled without difficulty (Hambly and Pennells 1975, Jaeger and Bakht 1982).

The grillage analogy is a simplified analysis procedure in which the bridge superstructure system is represented by transverse and longitudinal grid members and the longitudinal and transverse force systems interact at the nodal points. The bending and torsional stiffness characteristics of the bridge superstructure are distributed uniformly among the grillage members. The longitudinal stiffnesses are distributed to the members in the longitudinal direction, and transverse stiffnesses are distributed to the members in the transverse direction. Hambly (1991) puts the fundamental principle of the grillage analogy method very concisely as:

> "Ideally the beam stiffnesses should be such that when prototype slab [bridge] and equivalent grillage are subjected to identical loads, the two structures should deflect identically and the moments, shear forces and torsions in any grillage beam should equal the resultants of stresses on the cross-section of the part of the slab [bridge] the beam represents."

The closeness of the response of a grillage model to that of an actual structure depends upon the degree of appreciation of the structural behavior exercised by the design engineer. There are no fixed rules to determine the appropriate arrangement and cross-sectional properties and support conditions of the grillage members. However, based on past experience, successful implementation, and engineering judgment, many researchers have given valuable guidelines for the application of the grillage analogy method to various bridge types (Hambly 1991, Bakht and Jaeger 1985, O'Brien and Keogh 1999, Cusens and Pama 1975, Hambly and Pennells 1975, Cheung et al. 1982, Jaeger and Bakht 1982, and Zokaie et al. 1991). More recently, Song et al. (2003), Schwarz and Laman (2001), and Aswad and Chen (1994) successfully used the grillage analogy method for analysis of prestressed concrete girder bridges. In particular, Schwarz et al. (2001) has compared the response results from grillage analogy models to experimental evaluations of a number of bridges and concluded that the numerical grillage model prediction of transverse distribution of live loads closely agrees with those of experimentally measured results of actual bridges.

Generally, a cellular bridge deck is continuous in three dimensions and is characterized by smooth progression of the stresses along the length, breadth, and thickness of the entire superstructure. On the contrary, the stresses in the grillage tend to change abruptly and are centered on the nodal locations as shown in Figure 2.5. A particular response force system develops in a box girder bridge under the action of applied loads. This force system, as shown in Figure 2.6, includes longitudinal bending stresses, and longitudinal bending shear flow, transverse bending stresses, torsional stresses, and distortional action due to interaction of torsion and transverse shear. Grillage modeling of cellular bridge decks can be done by a shear flexible grillage. In a shear flexible grillage the transverse members are given a reduced shear area, so that they can experience a shear distortion equal to the actual transverse distortion of the cells in the bridge deck. It is very crucial to incorporate the effects of shear lag, actual position of neutral axis, equivalent shear area, and bending and torsional stiffnesses. Due to a high level of interaction between bending and torsion at the skew supports, the torsional stiffness should be carefully calculated. Eby et al. (1973) discuss various theoretical and approximate approaches to evaluate the St. Venant's torsional stiffness constant for the non-circular cross-sections. The Poisson effect is not significant and is generally neglected in a grillage analysis, but it can be included when desired (Jaeger and Bakht 1982). These guidelines and the grillage modeling approach followed in this research study are covered in more detail in Chapter 7.

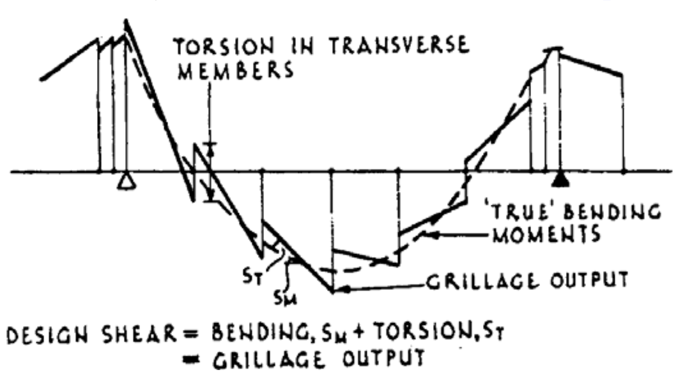

Figure 2.5. Grillage Bending Moment Diagram for Longitudinal Member (Hambly and Pennells 1975).

Zokaie et al. (1991) summarized the advantages of the grillage analogy method in comparison to other simplified methods of analysis in their final comment as:

> "Also grillage analysis presents a good alternative to other simplified bridge deck analysis methods, and will generally produce more accurate results. Grillage analogy may be used to model most common bridge types and each bridge type requires special modeling techniques. … A major advantage of plane grid analysis is that shear and moment values for girders are directly obtained and integration of stresses is not needed. Loads normally need to be applied at nodal points, and it is recommended that simple beam distribution be used to distribute wheel loads to individual nodes. If the model is generated according to Appendix G recommendations and the loads are placed in their correct locations, the results will be close to those of detailed finite element analysis."

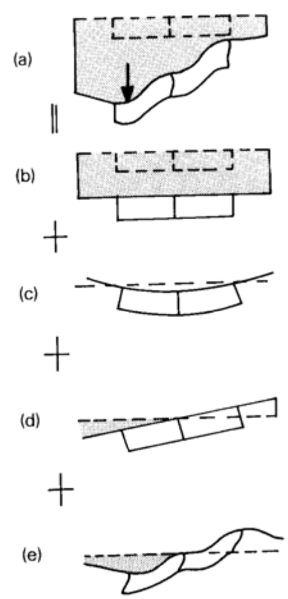

Figure 2.6. Principle Modes of Deformation (a) Total, (b) Longitudinal Bending, (c) Transverse Bending, (d) Torsion, (e) Distortion (Hambly 1991).

2.5.3 Finite Element Analysis

2.5.3.1 General

The finite element method (FEM) is the most versatile analysis technique available at present in which a complicated structure is analyzed by dividing the continuum into a number of small finite elements, which are connected at discrete nodal joints. This method of analysis is relatively computationally expensive and requires greater analysis time, and modeling and post processing of output data is often times very cumbersome. Adequate theoretical and working knowledge of FEM and classical structural mechanics is a pre-requisite for any sound finite element analysis. Finite element analysis has been used in many research studies to evaluate the live load distribution characteristics of all types of bridge superstructures. Zokaie et al. (1991), Schwarz et al. (2001), Barr et al. (2001), Khaloo and Mirzabozorg (2003), Chen and Aswad (1996), and Eamon and Nowak (2002) have evaluated the load distribution characteristics of prestressed I-girder bridge superstructures. Song et al. (2003) have used FEM to calibrate the grillage analogy model. Chen and Aswad (1996) applied the FEM to analyze the spread box girder bridges. Zokaie et al. (1991) analyzed multicellular and spread box girder bridges with the FEM. General guidelines for the application of the FEM to the analysis of bridge superstructures have been recommended by the LRFD Specifications (AASHTO 2004) and several research studies in the past. Those guidelines and other relevant information are summarized in the following paragraphs.

2.5.3.2 Type of Analysis

Almost all the research studies analyzed the prestressed bridge superstructures by linear and elastic analysis (i.e., small deflection theory and elastic and homogeneous material). Eamon and Nowak (2002) applied the FEM to analyze the structure in both the elastic and inelastic range.

2.5.3.3 Element Aspect Ratio

The LRFD Specifications allow a maximum aspect ratio of 5.0 for FEM analysis. Chen and Aswad (1996) and Barr et al. (2001) have maintained the ratio of length to width of shell elements at two or less.

2.5.3.4 Mesh Refinement

Eamon and Nowak (2002) have used simplified and detailed FEM models in their study. The simplified models contained 2900 to 9300 nodes; 1700 to 6200 elements; and 8500 to 30,000 degrees of freedom. The detailed FEM models contained 20,000 to 39,000 nodes; 12,000 to 22,000 elements; and 62,000 to 120,000 degrees of freedom. Barr et al. (2001) used 6000 nodes to model the deck slab, and the entire model contained 12,000 nodes. It is of particular interest that Eamon and Nowak (2002) had a finer mesh at the midspan region as compared to the quarter or end span regions.

2.5.3.5 Selection of Element Type

2.5.3.5.1 Plate or Shell Elements. Zokaie et al. (1991) used eight-node quadrilateral plate elements, with four integration points to model the spread box prestressed girder bridges. They further recommended that plate elements have at least five degrees of freedom (DOF) per node (i.e., three displacements and two in-plane bending rotations). The quadratic element shape functions were used to accurately model the parabolic variation of the shear stress in the girder web. According to O'Brien and Keogh (1999), the transverse distortional behavior makes cellular bridge decks different from other forms and this distortional behavior is affected by deck depth, the stiffness of individual webs and flanges (i.e., slenderness ratio) and the extent of transverse bracing (i.e., diaphragms) to the cells. They further suggest that the use of the plate element will not only allow modeling the distortional action, but also take into account the varying neutral axis depth.

Hambly (1991) recommends that a three-dimensional plate model of a cellular bridge deck must have six DOFs at each node (i.e. three displacements, two in-plane bending rotations, and one out-of-plane bending rotation). Hambly (1991) noted that at every intersection of plates lying in different planes there is an interaction between the in-plane forces of one plate and the out-of-plane forces of the other, and vice versa. Therefore, it is necessary to use an element that can distort under plane stress and plate bending. Other analytical studies that used shell elements include those by Barr et al. (2001), Chen and Aswad (1996), and Khaloo and Mirzabozorg (2003).

2.5.3.5.2 Beam Elements. A beam element is a typical 3D line element with six DOFs per node. Beam elements are used to model diaphragms, bridge girders (such as I-sections or box sections), and rigid links (used to model the eccentricity of girder centroid to deck slab centroid). Eamon and Nowak (2002) and Khaloo and Mirzobozorg (2003) have used beam elements to model girder and diaphragms in their simplified finite element models. Chen and Aswad (1996), Zokaie et al. (1991), and Barr et al. (2001) used beam elements to model the bridge girders and rigid links.

2.5.3.5.3 Solid Elements. Hambly (1991) notes that solid elements are seldom used to model the bridge decks because generally these structures correspond to thin plate behavior. Eamon and Nowak (2002) demonstrated successful implementation of an eight-node hexahedron solid element, with three DOFs (i.e., three displacements) at each node, to model a prestressed I-girder bridge. These solid elements were used to model the deck slab and the girder webs and flanges in a detailed finite element model. It should be noted that the mesh density was finer than that used on their simplified model.

2.5.3.6 Relative Eccentricity of Beam and Deck Slab

The LRFD Specifications (AASHTO 2004) recommend maintaining the relative vertical distances between the elements representing the beam and slab of the actual bridge. The LRFD Specifications also allow placing the longitudinal or transverse beam elements at the mid-thickness of plate elements, only when the equivalent element properties account for the eccentricity. Eamon and Nowak (2002) have demonstrated that using the equivalent element properties method to account for the girder slab eccentricity also yields acceptable results. Chen and Aswad (1996), Barr et al. (2001), Zokaie (2000), and Khaloo and Mirzabozorg (2003) have represented the eccentricity by using rigid link elements (beam elements with very large stiffness).

2.5.3.7 Post-Processing of Results

FEM analysis typically provides results in the form of stresses at the integration points. Zokaie et al. (1991) caution against programs providing stresses at the nodes, because stresses at the nodal locations are produced by some form of extrapolation that can be unreliable, and results should only be used with extreme care. They recommend that the stress output at the integration points should be integrated over the plate width to obtain the force results. Further details of calculating the bending moment and shear forces for a bridge girder can be found in their report. Chen and Aswad (1996) discuss a simplified method to calculate the composite girder moments by using the moment formula from simple beam theory as follows.

$$M_c = S_{bc} f_b \tag{2.16}$$

where:

M_c = Composite girder moment

S_{bc} = Composite section modulus referenced to the bottom fiber of the girder

f_b = Stress at the centerline of the bottom girder flange

2.6 IMPACT OF AASHTO LRFD SPECIFICATIONS ON DESIGN

2.6.1 General

A number of studies have been carried out to assess the impact of the LRFD Specifications on bridge design. Hueste and Cuadros (2003) presented a detailed comparison between the LRFD and Standard Specifications. A study by Shahawy and Batchelor (1996) suggests that the shear provisions of the AASHTO Standard Specifications (1989) are more accurate as compared to those in the LRFD Specifications (1994). Detailed studies by Zokaie et al. (2003) and Richard and Schmeckpeper (2002) suggest that LRFD designs are more conservative and require higher prestress or reinforcement as compared to designs using the Standard Specifications because of various factors.

2.6.2 Significant Changes

The AASHTO Standard Specifications are based on the Allowable Stress Design and LFD philosophies, whereas the LRFD Specifications have a probability-based limit state philosophy. Some of the significant differences between the two specifications are listed below.

The Standard Specifications express the impact factor as a fraction of live load and a function of span length as $I = 50/(L+125)$, where I is the impact factor and L is the length of the span in feet. Therefore for a span of 100 ft. the value of I is 0.22. The LRFD Specifications give a constant value of impact factor depending on the components and limit state under consideration. For instance, the impact factor for girder design for limit states other than the fatigue and fracture limit states comes out to be 0.33 (33 percent increase in the truck load only).

The LRFD Specifications allow the use of refined analysis for the determination of live load DFs whereas the Standard Specifications give simple expressions for the live load distribution to exterior and interior girders. For common bridge types, the LRFD Specifications include an approximate method, based on parametric analyses of selected bridge geometries. This method can be used only if the bridge geometry falls within the limits of the parametric analysis for which the DF equations are based. The LRFD Specifications specify reduction factors for application to live load moment and shear to account for the skew of the bridge. The skew factor for moment decreases the moment DF for interior and exterior girders for certain angles. The skew factor for shear increases the shear DF for the interior and exterior girders at the obtuse corners of the skewed bridge. The overhang distance is limited as per Articles 4.6.2.2.1 and 4.6.2.2.2 of the LRFD Specifications.

The LRFD Specifications provide three different options for the estimation of time-dependent prestress losses. The options are lump-sum estimates, refined estimates, and exact estimates using the time-step method. Expressions are provided for the lump-sum estimate of the time-dependent prestress losses for different type of bridges. The lump-sum time dependent losses are based on the compressive strength of concrete and the partial prestressing ratio. The Standard Specifications provide the option of the lump-sum method and refined method for the estimation of time-dependent losses. The lump-sum estimates are given as specific values for two different values of concrete strength at service.

The load and resistance factors for limit states other than the strength limit states were selected to provide designs that are consistent with the Standard Specifications. The calibration of the LRFD Specifications was focused on the ultimate limit states, but it is not readily applicable to other design considerations traditionally evaluated using service loads, such as stress limits, deflections, and fatigue. This difference accounts for the establishment of the Service III limit state for prestressed concrete structures in the LRFD Specifications, which evaluates the tensile stress in the structure, with the objective of crack control in prestressed concrete members. The check for compressive stress in the prestressed concrete girder (Service I limit state) uses a live load factor of 1.0, while the tensile stress check (Service III limit state) uses a live load factor of 0.8. The Standard Specifications specify the Group I loading for service limit states with a load factor of 1.0. In general, a larger number of limit states must be accounted for in design using the LRFD Specifications, and the extreme load cases such as collision forces must be included if their occurrence is possible in the design life of the bridge.

2.6.3 Research Studies

2.6.3.1 Shahawy and Batchelor (1996)

Shahawy and Batchelor (1996) compared the shear provisions in the AASHTO Standard Specifications (1989) and LRFD Specifications using laboratory tests on AASHTO Type II prestressed concrete girders. The Standard Specifications are based on a constant 45-degree truss analogy for shear, whereas the LRFD Specifications adopted a variable truss analogy based on the modified compression field theory for its shear provisions. Twenty full-scale prestressed concrete girders were tested with variable spans, amounts of shear reinforcement, shear spans, and strand diameters. Three of the girders were tested without any shear reinforcement to determine the contribution of the concrete to the shear strength, V_c.

Shahawy and Batchelor (1996) found that the AASHTO Standard Specifications gave a good estimate of the shear strength of the girders and are conservative regardless of the shear reinforcement ratio, whereas the LRFD Specifications overestimate the shear strength of girders having high reinforcement ratios. The shear provisions of the AASHTO Standard Specifications were found to agree with the test results in almost all the cases. For a/d ratios less than 1.5, the LRFD Specifications (1994) overestimate the shear strength; while for a/d more than 2.0, they underestimate the shear strength. The predictions of the AASHTO Standard Specifications for V_c were also found to be better than that of LRFD, with both being conservative as compared to test results. The overall results for shear indicate that the AASHTO Standard Specifications (1989) better estimate the actual shear strength of girders as compared to the LRFD Specifications (1994).

2.6.3.2 Richard and Schmeckpeper (2002)

Richard et al. (2002) compared the design of an AASHTO Type III girder bridge using the AASHTO Standard Specifications for Bridges, 16th Edition, and the AASHTO LRFD Bridge Design Specifications. The authors found the bridge design to be the same in most respects irrespective of the specifications used. The most significant changes observed were in the shear design where the skew factor and reinforcement requirements for the LRFD Specifications led to increased concrete strength and reinforcement. An increase in reinforcement in the deck overhang and wing wall was also observed by the authors, due to an increased collision force. The design of bridges using the LRFD Specifications was found to be more calculation-intensive and complex. The design experience and conclusions were limited to a single-span AASHTO Type III girder bridge.

The LRFD Specifications allow the distribution of permanent loads to be distributed uniformly among the beams and/or stringers (LRFD Art. 4.6.2.2.1), which is a significant change from the Standard Specifications practice where the dead loads due to parapets, sidewalks, and railings are applied only to the exterior girder. An increase in non-composite dead load by nine percent and decrease in composite dead load by 50 percent on the exterior girder, with a decrease in non-composite dead load by 4 percent and an increase in composite dead load by 97 percent on the interior girder were observed when LRFD Specifications were followed, as compared to the Standard Specifications. The Standard Specifications required the bridge to be designed for HS-25 loading, which is 125 percent of the AASHTO HS-20 truck load or a design lane load comprising an 800 plf distributed load plus 22.5 kip or 32.5 kip point load for flexure and shear design, respectively. The LRFD Specifications adopted the HL-93 live load model for bridge design, which consists of a 36 ton design truck or design tandem and a 640 plf design lane load. The shear and bending moment after load distribution for both load cases were found to be roughly comparable.

Richard and Schmeckpeper (2002) found that LRFD design requires the same number of prestressing strands as that of Standard design, but a higher concrete strength was required. This could be explained as an effect of changes in live loads, load DFs, impact factors, skew factors, and prestressing losses. The required shear reinforcement increased substantially for the LRFD design as a result of an increase in the live load DF for shear and a constant skew factor.

2.6.3.3 Zokaie et al. (2003)

Zokaie et al. (2003) reviewed the impact of the LRFD Specifications on the design of post-tensioned concrete box girder bridges and highlighted the changes in the specifications that lead to the requirement of higher post-tensioning. The change in design live load was found to be one of the factors. The “Dual Truck” loading in the LRFD Specifications increases the negative moment at interior supports, which require additional negative reinforcement. The major changes in the load DFs influenced the design. The load factors for different limit states are different in the LRFD Specifications as compared to the fixed load factors in the Standard Specifications. However, the allowable stresses are almost the same in both specifications. The prestress loss equations are slightly changed in the LRFD Specifications and are more conservative as compared to Standard ones. Zokaie et al. (2003) carried out a detailed design for two different cases and found that self-weight is nearly the same irrespective of the specifications used; however, the LRFD live load was much larger than for the LFD design. The LRFD impact factor was higher, but the load DF for moment was reduced. The Service III limit state used to check the tensile stresses in the bottom fiber governed in both cases. An additional 13 percent post-tensioning was required for the LRFD design. Zokaie et al. (2003) did not consider shear in the design comparison.

2.7 DEBONDING OF PRESTRESSING STRANDS

2.7.1 General Background

The purpose of the partial debonding of strands, also known as blanketing or jacketing, is to decrease the applied prestressing force to the end regions of girders by preventing bond between some of the strands and the concrete. Debonding is used to control the excessive tensile stresses that occur in the top fibers of the end regions. Debonding is an alternative to harping of strands where the stresses in the extreme fiber at the end regions are brought within allowable limits by varying the strand eccentricity at the beam ends. Harping of strands can be dangerous to workers, relatively expensive, and difficult to achieve, especially in the case of a beam with inclined webs such as Texas U-beams.

Adequate anchorage of reinforcement is crucial to the integrity of all reinforced and prestressed concrete structures. The anchorage behavior of fully bonded strands can be significantly different than that of partially debonded strands. Based on past experimental research studies, the LRFD and Standard Specifications (AASHTO 2004, 2002) and the TxDOT Bridge Design Manual (TxDOT 2001) have recommended different guidelines regarding debonding of strands.

The Standard Specifications (AASHTO 2002) require doubling the development length when the strands are partially debonded. The LRFD Specifications, among other restrictions related to strand debonding, limit the debonding percentage of strands to 40 percent per row and 25 percent per section. When these LRFD Specifications are compared to debonding percentage limits of 75 percent per row per section in the TxDOT Bridge Design Manual (TxDOT 2001), they can be very restrictive and can seriously limit the span capability. The reason for such restrictive debonding percentages is stated in the LRFD Art. C5.11.4.3 as the reduction in shear capacity of a beam section due to the reduction in horizontal prestressing force and the increase in the requirement of development length when strands are debonded.

2.7.2 Debonding Requirements

The provisions of the Standard and LRFD Specifications (AASHTO 2002, 2004) and the TxDOT Bridge Design Manual are discussed in the following sections.

2.7.2.1 Debonding Percentage Limit

The Standard Specifications do not limit the debonding percentage. The LRFD Specifications in Article 5.11.4.3 limit the debonding percentage of strands to 40 percent per horizontal row and 25 percent per section. Debonding termination is allowed at any section, if and only if, it is done for less than 40 percent of the total debonded strands or four strands, whichever is greater. The LRFD Specifications in Commentary 5.11.4.3, however, allow the consideration of successful past practices regarding debonding and further instruct to perform a thorough investigation of shear resistance of the sections in the debonded regions. The LRFD Specifications refer to the conclusions drawn in research by Shahawy and Batchelor (1992) and Shahawy et al. (1993) that shear resistance is primarily influenced by the anchored strength of the strands in the end zones of the prestressed concrete beams. The TxDOT Bridge Design Manual allows the debonding of strands as long as it satisfies the limit of 75 percent per row per section.

2.7.2.2 Debonding Length

The Standard Specifications do not specify any limit on the allowable debonding length of the debonded strands. The LRFD Specifications allow the strands to be debonded to any length as long as the total resistance developed at any section satisfies all the limit states. The TxDOT Bridge Design Manual specifies the maximum debonding length as the lesser of the following:

1. half-span length minus the maximum development length as specified in the Standard Specifications (AASHTO 1996, Article 9.28),
2. 0.2 times the span length, or
3. 15 ft.

2.7.2.3 Development Length for Debonded Strands

The Standard Specifications (Article 9.28.3) require the development length to be doubled when tension at service load is allowed in the precompressed tensile zone for the region where one or more strands are debonded. The first term is the transfer length and the second term is the flexural bond length.

$$l_d = \left(f_{ps} - \frac{2}{3} f_{pe} \right) d_b = \left(\frac{f_{pe}}{3} \right) d_b + \left(f_{ps} - f_{pe} \right) d_b \qquad (2.17)$$

The LRFD Specifications mention a general expression of development length in Article 5.11.4.2 for bonded and debonded strands, which is given as follows.

$$l_d \geq \kappa \left(f_{ps} - \frac{2}{3} f_{pe} \right) d_b \qquad (2.18)$$

where:

l_d = Development length, in.
d_b = Strand diameter, in.
κ = 1.6 for bonded strands and 2.0 for debonded strands in cases where tension exists in the precompressed tensile zones, ksi
f_{pe} = Effective prestress prior to the application of the load, ksi
f_{ps} = Average stress in prestressed strands at the time for which the nominal resistance of the member is required, ksi

2.7.2.4 Transfer Length

The Standard Specifications recommend a transfer length of $0.5d_b$, while the LRFD Specifications recommend a transfer length of $0.6d_b$ in Articles 9.20.2.4 and 5.11.4.1, respectively.

2.7.3 Research on Debonding

2.7.3.1 General

Most research studies that compared the behavior of beams with debonded strands to beams with fully bonded strands, also studied transfer and development length. The following summary presents research findings related to the effect of debonding of strands in prestressed beams, with special emphasis on the effect of debonding on the beam shear capacity.

2.7.3.2 Barnes, Burns, and Kreger (1999)

Barnes et al. (1999) measured the development and transfer length for 0.6 in. diameter prestressing strands, placed with center-to-center spacing of 2 in. More specifically, this study was conducted to study the effect of concrete strength, surface conditions of the strands, and debonding of strands on the anchorage behavior of pretensioned concrete flexural members.

A total of 36 AASHTO Type I (TxDOT Type A) I-beams were tested. These beams were designed to satisfy ACI 318-99 and the Standard Specifications' (AASHTO 1996) allowable stress limits and to represent the worst case behavior by achieving the ultimate strand elongation values of at least 3.5 percent. A cast-in-place deck slab was added to the beams to provide a large compressive top flange, and its size was determined by strain compatibility analysis so as to ensure the total elongation of 3.5 percent in the bottom row of strands at flexural failure. Beams with a span length of 40 ft. were used for the fully bonded strands series, and beams of span lengths of 54 ft. were used for debonded strands series. Concrete with a final strength ranging from 5 to 15 ksi and initial strength ranging from 4 to 9 ksi was used in the beams. Strands were debonded with percentages of 50, 60, and 75 percent. The debonding patterns were selected with a purpose of violating several requirements of LRFD Article 5.11.4.3 (AASHTO 1998). For example, all the specimens were debonded with percentages exceeding the 25 percent per section and 40 percent per row limit; in a few specimens the debonded strands were not symmetrically distributed, and in several specimens the exterior strands in the horizontal rows were debonded. The shear reinforcement was provided on the basis of conservative estimate of expected shear force, which was in excess of TxDOT standard design practice for AASHTO Type I beams. The shear reinforcement provided satisfied the provisions of the Standard and LRFD Specifications (AASHTO 1996, 1998).

The results of experiments performed to evaluate the strand transfer length showed that the use of staggered debonding of strands can effectively reduce the intensity of concrete stresses in the end regions of beams. The experiments performed to evaluate the development length required to prevent the general bond slip failure showed that the development length exhibits an increasing trend with an increasing number of debonded strands and debonding length. The location of the transfer length in relation to the load effects is influenced by the debonded length of the strands.

The cracking resistance of each transfer length region was determined by the amount and configuration of debonding. It was observed by the researchers that the presence and opening of a crack within or closer to the transfer length of strands than approximately $20d_b$ initiated the general bond slip in every group of strands in the debonded specimens. When the cracks are prevented to occur within the transfer length or adjacent to the transfer length and the strands are embedded for a length greater than or equal to the development length of fully bonded strands, no general bond slip should occur. This observation was true for cases where 75 percent of strands were debonded. The researchers concluded, "Up to 75 percent of strands may be debonded as long as cracking is prevented in or near the transfer length and the ACI and the AASHTO (1998) rules for terminating the tensile reinforcement are applied to the bonded length of prestressing strands."

All specimens failed in pure flexural, flexural with slip, and bond failure mechanisms. The influence of horizontal web reinforcement was explored to a very limited extent as part of this study. Where present, the horizontal web reinforcement slightly improved the performance and reduced the crack width. The authors concluded that due to the presence of excess shear reinforcement, the specimens could not exhibit premature shear failure due to loss of bond, and the horizontal reinforcement did not have a chance to yield significant improvements in strength.

2.7.3.3 Shahawy et al. (1993)

The main objective of this study was to develop design formulas for transfer and development length. However, it was also intended to establish shear design criteria so that optimal use of web shear reinforcement and debonding of strands can be assured for prestressed concrete beams. Additional objectives were to study the effects of debonding of prestressing strands on the shear strength of beams, to determine the effect of prestressed compressive action on the overall behavior of the beams, and to determine the minimum fatigue load below which fatigue need not be considered.

The experimental program was performed with 33 AASHTO Type II prestressed concrete girders. The primary variables considered were debonding percentage, web shear reinforcement ratio, beam end details, and size of the strands. The initial length, initial ultimate flexural strength, initial concrete compressive strength at transfer, and 28 day final concrete compressive strength of all the girders was constant at 41 ft., 2100 kip-ft., 4 ksi, and 6 ksi, respectively. This study considered 270 ksi, low-relaxation strands with diameters of 0.5 in. and 0.5 in. special with maximum debonding length of 5.5 ft., and strands with 0.6 in. diameters with maximum debonding length of 4.5 ft. The choice of debonding percentages was limited to 0, 25, or 50 percent. The amount of shear reinforcement varied from minimum shear reinforcement required to three times of what is required by the Standard Specifications (AASHTO 1992) for the design dead and live loads. The results of the part of the study related to the debonding of strands were also published by Shahawy et al. (1992).

All girders tested in this program failed beyond their ultimate design moment, M_u, and ultimate shear, V_u, with the exception of the girders that were under-designed for shear (ranging from zero to half of the nominal shear capacity required by the AASHTO Standard Specifications 1992). The researchers did not make any recommendation regarding the limits for critical percentage of debonding. Only four of the specimens with a 0.6 in. strand diameter, having 25 and 50 percent debonded strands and the nominal shear reinforcement as required by the Standard Specifications (AASHTO 1992), underwent shear and bond failure.

2.7.3.4 Abdalla, Ramirez, and Lee (1993)

The main objective of this experimental research was to study and compare the flexural and shear behavior of simply supported pretensioned beams with debonded and fully bonded strands. Adequacy of strand anchorage, and ACI (1989) and AASHTO (1992) provisions regarding development length of prestressing strands were also investigated.

Five specimen sets consisting of two beams each, one beam with strands debonded and the other one with fully bonded strands, were tested to failure under a single monotonic concentrated load. Four specimen sets consisted of AASHTO Type I girders and one specimen consisted of Indiana state type box girders. All beams were cast with a deck slab on top. All beams had a 17.5 ft. span, except for one beam specimen that had a span length of 24 ft. This experiment considered both stress-relieved and low-relaxation Grade 270, uncoated seven-wire 0.5 in. diameter strands. The initial and final concrete compressive strengths for the beam were 4000 and 6000 psi, respectively. Non-prestressed reinforcement, used in the beams and deck slab, consisted of standard deformed Grade 60 #6 bars, while the stirrup reinforcement consisted of deformed Grade 60 #3 double legged bars spaced at 4 in. center to center. The entire debonding scheme was symmetrical with the exterior strand on each side of every specimen always debonded except for the box beam. Debonding percentages were either 50 percent or 67 percent and it was ensured that debonded strands lie in a region where shear failure was likely to occur. It is also mentioned that all the beams were designed to ensure that shear failure would not occur. Therefore, none of the beams reached the predicted shear capacity.

It was concluded that based on ACI/AASHTO debonding of strands, the flexure-shear cracking capacity of the pretensioned beams is reduced when compared with those beams with fully bonded strands only. The failure loads were lower in the beams with debonded strands as compared to failure loads of beams with fully bonded strands, and the deflections were relatively larger in the beams with debonded strands. Moreover, it was observed that flexure-shear cracking occurred at the debonding points. The researchers concluded that by increasing the debonding percentage, the degree of conservatism reduced. So, they made the recommendation to limit the debonding to 67 percent of the strands in a section, although they did not consider the limit on debonding percentage of strands in a row necessary. In addition, they recommended that the debonding be staggered to reduce stress concentrations.

2.7.3.5 Russell and Burns (1993)

This research project had two objectives: to determine the transfer length and the development length for both 0.5 in. and 0.6 in. prestressing strands, and to develop design guidelines for the use of debonded strands in pretensioned concrete.

Altogether, 10 tests were performed on six specimens. Each beam contained eight 0.5 in. strands, four of which were debonded. Four beams were 40 ft. in length with the debonded length equal to 78 in. The other two beams were 27.5 ft. in length with a debonded length equal to 36 in. All of the beams had identical cross-sections that were similar to AASHTO I-beams. Shear reinforcement was spaced at 6 in. for all specimens without any variation. No special confining steel or anchorage details were provided for the debonded strands. Debonding of strands was symmetrically distributed in the cross-section with debonding percentages of 50 percent or less when the strand cut off was staggered.

The variables considered in the study were the length of debonding (36 in. or 78 in.), the type of debonding cutoff (staggered or concurrent), and the embedment length (84 in. or 150 in.). Debonded lengths were selected to test embedment lengths between 1.0 and 2.0 times the basic development length given in AASHTO Equation 9-32. The embedment lengths were chosen for each test so that the results from the complete test series would span the probable failure modes. The percentage of debonding and shear reinforcement was not considered as a variable.

In all the tests it was clearly shown that cracking was the primary source of bond or anchorage failure, not vice versa. The entire test program was aimed at validating the prediction model that states, “If cracks propagate through the anchorage zone of a strand, or immediately next to the transfer zone, then failure of the strand anchorage is imminent.” This prediction model successfully corroborated test results for pretensioned beams with debonded strands as well as beams where all of the strands are fully bonded at the end of the member. Some exceptions to this model were noticed, where the strands have slipped very small distances prior to flexural failure, without anchorage failure. The tests have shown that beams with staggered debonding performed better than beams with concurrent debonding. The recommendations from this study related to debonded strands are as follows.

- Debonded strands should be staggered.
- Termination points should be evenly distributed throughout the debond/transfer zone.
- Debonding should be terminated as gravity moments reduce stresses from pretensioning to within the allowable stresses.
- No more than 33 percent of the strands should be debonded and at least 6 percent of the total prestressing force should be included in the top flange of the pretensioned beam.

It was found that by using two top strands into the design of pretensioned girders, the number and the length of debonded strands can be significantly reduced. It was concluded that the flexural and web-shear cracking in the transfer zone region caused the slip of debonded strands and consequently, the bond failure. However, the bond failure did not take place when there was no crack in the debond/transfer zone region.

2.7.3.6 Krishnamurthy (1971)

The primary objective of this study was to investigate the effect of debonding of strands on the shear behavior of pretensioned concrete I-beams. All beams were 2.9 m long with effective span length (i.e., the distance between the supports) of 2.75 m, loaded with two-point loading, and had constant shear span of 0.5 m. The debonding length was also constant at 0.6 m. Moreover, prestressing force at the mid-section of beams, shear span-to-depth ratio, and the concrete strength were kept constant for all specimens.

All beam specimens tested failed suddenly in shear with a diagonal crack developing in the shear span region. It was observed that shear resistance of the section increased by increasing the number of debonded strands in the upper flange, and it decreased when the number of debonded strands was increased in the bottom flange of the beam. Debonding percentages used in different specimens were selected as 25 and 50 percent per row and 12.5, 25, 37.5, and 50 percent per section. In all beams with debonded strands, the diagonal crack initiated at the support and extended near the load point. No recommendation was made for the allowable debonding percentages.

2.7.3.7 Summary

Krishnamurthy (1971) observed that shear resistance of the section increased by increasing the number of debonded strands in the upper flange, and it decreased when the number of debonded strands was increased in the bottom flange of the beam. All the aforementioned studies in this section recommended the use of a staggered debonded strand pattern and confirmed that beams can fail due to loss of anchorage, before reaching ultimate capacities, if cracks propagate through the transfer length region. Abadalla et al. (1993) recommended debonding the strands to no more than 67 percent, while Barnes et al. (1999) recommended 75 percent of strands can be debonded provided that crack propagation is prevented through the transfer length region and the AASHTO (1998) rules for terminating the tensile reinforcement are followed. The study by Shahawy et al. (1993) showed that some beam specimens with debonded strands failed in shear. Based on input from TxDOT engineers, it became evident that the TxDOT Bridge Design Manual (TxDOT 2001) limits of maximum percentage of debonded strands and maximum debonded length were developed by Crawford and Ralls, when box beams were added to the TxDOT prestressed girder design program, PSTRS14 (TxDOT 2004).

2.8 RESEARCH NEEDS

The findings in previous studies are limited to the bridge types considered, and may vary by changing the bridge geometry, girder type and spacing, span length, and other parameters. The main purpose of this research study is to develop guidelines to help TxDOT adopt and implement the *AASHTO LRFD Bridge Design Specifications*. There is a need for a detailed study to determine the effect of LRFD Specifications on bridge design by changing various parameters, such as span length and spacing between the girders. The prestressed concrete bridges typical to Texas, including the I-shaped Type C and the AASHTO Type IV girders and the open box Texas U beams, are considered in this project. Designs using the Standard and

LRFD Specifications are compared, and specific areas where the LRFD designs differ are investigated further.

3. DESIGN PARAMETERS AND METHODOLOGY

3.1 GENERAL

A parametric study was conducted for Type C, AASHTO Type IV, and Texas U54 single-span, interior prestressed concrete bridge girders. Designs based on the AASHTO Standard Specifications (2002) were compared to parallel designs based on the AASHTO LRFD Specifications (2004) using the same parameters. The main focus of the parametric study was to evaluate the impact of the AASHTO LRFD Specifications on various design results including maximum span length, required number of strands, required concrete strengths at release and at service, and the ultimate flexural and shear limit states.

The following sections describe the girder sections and their properties and discuss the design methodology. The design of prestressed concrete girders essentially includes the service load design, ultimate flexural strength design, and shear design. The differences in each of the design procedures specified by the AASHTO Standard and LRFD Specifications are outlined. In addition, assumptions made in the analysis and design are discussed. The results from the parametric study are provided in Chapters 4, 5, and 6.

3.2 SUMMARY OF DESIGN PARAMETERS

3.2.1 Girder Sections

Three girder sections were considered in this study: Type C, AASHTO Type IV, and Texas U54 girders. The AASHTO Type IV girder was introduced in 1968. Since then it has been one of the most economical shapes for prestressed concrete bridges. This girder type is used widely in Texas and in other states. The AASHTO Type IV girder can be used for bridges spanning up to 130 ft. with normal concrete strengths, and it is considered to be tough and stable. The girder is 54 in. deep with an I-shaped cross-section. The top flange is 20 in. wide and the web thickness is 8 in. The fillets are provided between the web and the flanges to ensure a uniform transition of the cross-section. The girder can hold a maximum of 102 strands. Both straight and harped strand patterns are allowed for this girder type. Figure 3.1 shows the details of the AASHTO Type IV girder cross-section. The non-composite section properties for the Type IV girder section are provided in Table 3.1.

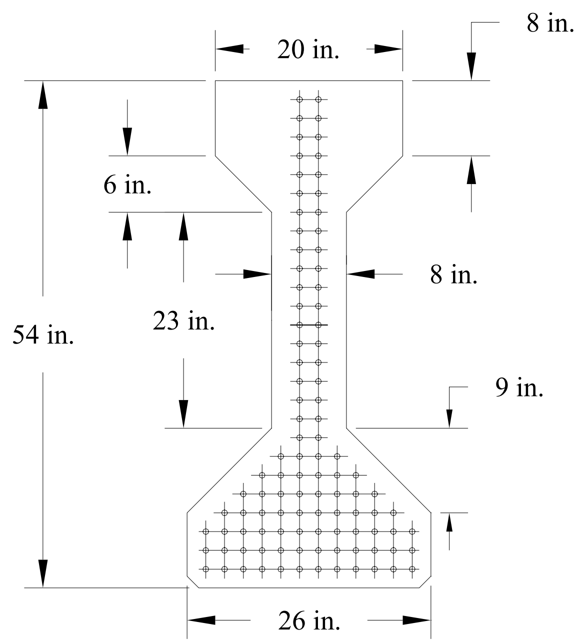

Figure 3.1. Section Geometry and Strand Pattern of AASHTO Type IV Girder (Adapted from TxDOT 2001).

Table 3.1. Non-Composite Section Properties for Type IV and Type C Girders.

Girder Type	y_t (in.)	y_b (in.)	Area (in.^{2})	I (in.^{4})
Type IV	29.25	24.75	788.4	260,403
Type C	22.91	17.09	494.9	82,602

where:

I = Moment of inertia about centroid of non-composite precast girder, in.^{4}

y_b = Distance from centroid to extreme bottom fiber of non-composite precast girder, in.

y_t = Distance from centroid to the extreme top fiber of non-composite precast girder, in.

Type C girders are typically used in Texas for bridges spanning in the range of 40 to 90 ft. with normal concrete strengths. This is one of the earliest I-shaped girder sections, first developed in 1957. It has been modified slightly since then to handle longer spans. The total depth of the girder is 40 in. with a 14 in. top flange and 7 in. thick web. The top flange is 6 in. thick and the bottom flange is 7 in. thick. The fillets are provided between the web and the flanges to ensure uniform transition of the cross-section. The larger bottom flange allows an increased number of strands. The girder can hold a maximum of 74 strands. Both straight and harped strand patterns are allowed for this girder. Figure 3.2 shows the dimensions and configuration of the Type C girder cross-section. The non-composite section properties for the Type C girder section are provided in Table 3.1.

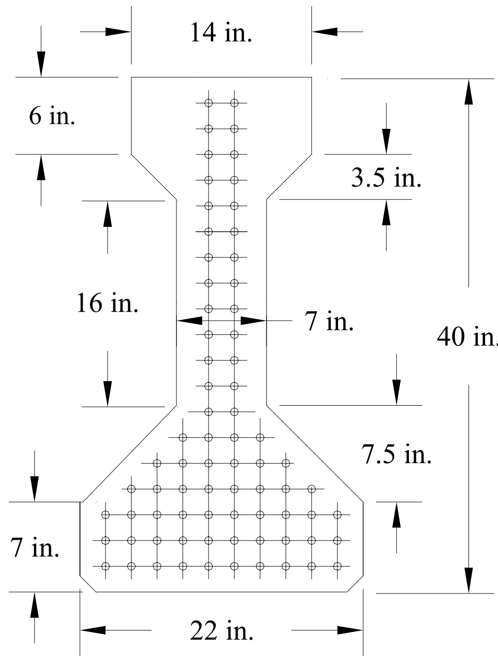

Figure 3.2. Section Geometry and Strand Pattern of Type C Girder (Adapted from TxDOT 2001).

The development of the precast, prestressed Texas U beam, which is an open-top trapezoidal section, began in the late 1980s (Ralls et al. 1993). The main purpose of developing U beams was not to replace the widely used AASHTO Type IV and Texas Type C beams, but rather to provide an aesthetically pleasing, efficient cross-section that is economically more viable with ease of construction (TxDOT 2001). Two U beam sections, U40 and U54, were developed for use as prestressed concrete bridge girders, where '40' and '54' signify the non-composite depth in inches of the two girders, respectively. Figure 3.3 shows the U54 beam cross-section and a pre-determined pattern for the arrangement of strands. The major section dimensions are outlined in Table 3.2. According to Appendix A in the TxDOT Bridge Design Manual (TxDOT 2001), for a normal strength concrete, 0.5 in. strand diameter, and miscellaneous other design constraints as mentioned in the manual, a maximum span length of 130 ft. is achievable for a maximum girder spacing of 9.75 ft. using Texas U54 girders.

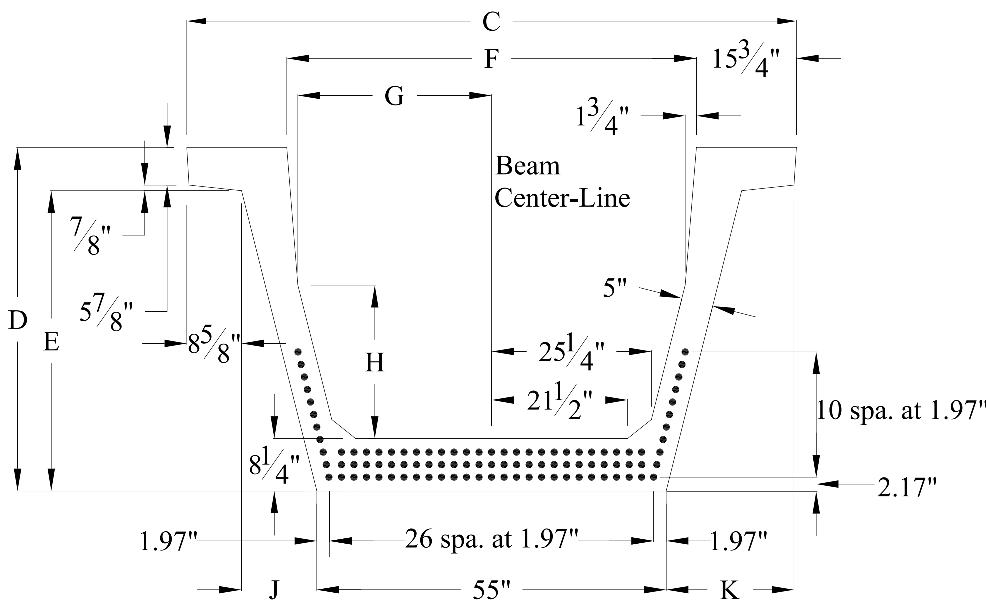

Figure 3.3. Section Geometry and Strand Pattern of Texas U54 Girder (Adapted from TxDOT 2001).

Table 3.2. Section Properties of Texas U54 Beams (Adapted from TxDOT 2001).

C	D	E	F	G	H	J	K	Y_t	Y_b	Area	I	Weight
in.	in.	in.	in.	in.	in.	in.	in.	in.	in.	in.^{2}	in.^{4}	plf
96	54	47.25	64.5	30.5	24.125	11.875	20.5	31.58	22.36	1120	403,020	1,167

3.2.2 Outline of Parametric Study

The parametric study and design values were outlined based on input from TxDOT. The design parameters that were varied for the parametric study are outlined in Table 3.3. In addition, various design parameters that were kept constant for a particular specification are outlined in Table 3.4. Span lengths, as given in Table 3.3, are considered to be the distances between faces of the abutment backwalls or centerlines of the interior bents. The skew angles were varied for LRFD designs to investigate the impact of the skew, which is introduced through the skew reduction factors for live load moments and skew correction factors for live load shears. The skew does not affect the designs based on AASHTO Standard Specifications, as the DFs for live load are independent of the skew.

Table 3.3. Design Parameters for Parametric Study.

Parameter	Description / Selected Values
Design Codes	AASHTO Standard Specifications, 17th Edition (2002) AASHTO LRFD Specifications, 3rd Edition (2004)
Girder Spacing (ft.)	6'-0", 8'-0", and 8'-8" (Type IV and Type C) 8'-6", 10'-0", 11'-6", 14'-0" and 16'-8" (U54)
Spans	40 ft. to maximum span at 10 ft. intervals (Type C) 90 ft. to maximum span at 10 ft. intervals (Type IV and U54)
Strand Diameter (in.)	0.5 and 0.6
Concrete Strength at Release, f'_{ci}	Varied from 4000 to 6750 psi for design with optimum number of strands
Concrete Strength at Service, f'_c	Varied from 5000 to 8500 psi for design with optimum number of strands (f'_c may be increased up to 8750 psi for optimization on longer spans)
Skew Angle	0, 15, 30, and 60 degrees

3.3 DETAILED DESIGN EXAMPLES

Two sets of parallel detailed design examples were developed to illustrate the application of the AASHTO Standard Specifications for Highway Bridges, 17th edition (2002), and AASHTO LRFD Bridge Design Specifications, 3rd edition (2004), for design of typical precast, pretensioned girders in Texas. The examples allow a more detailed comparison of the Standard and LRFD Specifications and are intended to serve as a reference for bridge engineers and to assist in the transition from prestressed girder designs using the AASHTO Standard Specifications to designs using the AASHTO LRFD Specifications.

The detailed examples were developed for an AASHTO Type IV girder bridge and a Texas U54 girder bridge. The cross-sections of the two bridge types are shown in Figures 3.4 and 3.5. The detailed design examples for Type IV girder bridges are found in Appendices A.1 and A.2 for the Standard and LRFD Specifications, respectively. The examples for the U54 girder bridges are found in Appendices B.1 and B.2 for the Standard and LRFD Specifications, respectively.

Table 3.4. Additional Design Variables.

Category	Specification	Description	Value
Prestressing Strands	Standard	Ultimate Strength, f_s'	270 ksi – low-relaxation
		Jacking Stress Limit, f_{si}	$0.75\ f_s'$
		Yield Strength, f_y	$0.9\ f_s'$
		Modulus of Elasticity, E_s	28,000 ksi
	LRFD	Ultimate Strength, f_{pu}	270 ksi – low-relaxation
		Jacking Stress Limit, f_{pj}	$0.75\ f_{pu}$
		Yield Strength, f_{py}	$0.9\ f_{pu}$
		Modulus of Elasticity, E_p	28,500 ksi
Concrete-Precast	Standard and LRFD	Unit Weight, w_c	150 pcf
		Modulus of Elasticity, E_c	$33\ w_c^{1.5}\sqrt{f_c'}$ (f_c' precast)
Concrete-CIP Slab	Standard and LRFD	Slab Thickness, t_s	8 in.
		Unit Weight, w_c	150 pcf
		Modulus of Elasticity, E_{cip}	$33\ w_c^{1.5}\sqrt{f_c'}$ (f_c' CIP)
		Specified Compressive Strength (f_c')	4000 psi
		Modular Ratio, n	E_{cip}/E_c
Other	Standard and LRFD	Relative Humidity	60%
		Non-Composite Dead Loads	1.5" asphalt wearing surface (Unit weight of 140 pcf) U54 Girders: Two interior diaphragms of 3 kips each, located at 10 ft. on either side of the beam midspan
		Composite Dead Loads	T501 type rails (326 plf)
		Harping in AASHTO Type IV & Type C Girders	An allowable harping pattern consistent with TxDOT practices will be selected to limit the initial stresses to the required values.
		Debonding Length & Percentage in U54 Girders	$L \leq 100$ ft.: the lesser of 0.2 L or 15 ft. 100 ft. < L <120 ft.: 0.15 L $L \geq 120$ ft.: 18 ft. No more than 75% of strands debonded per row per section

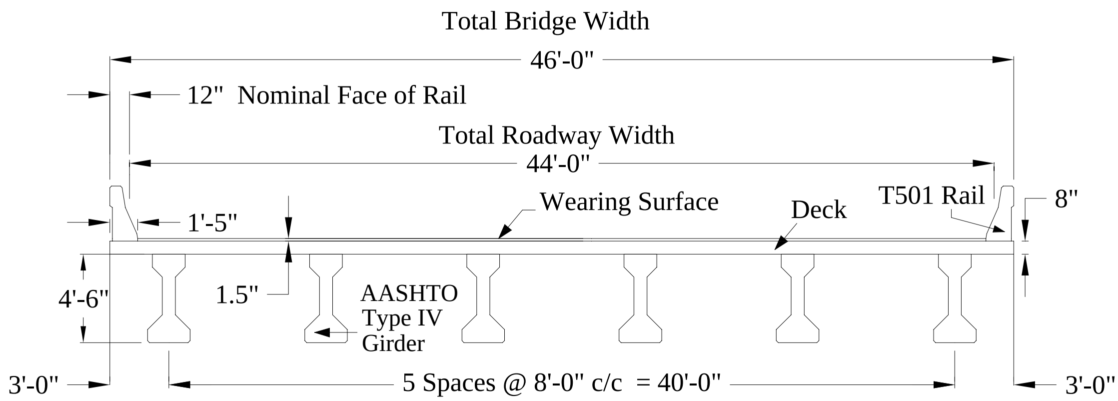

Figure 3.4. Cross-Section of Type IV Girder Bridge.

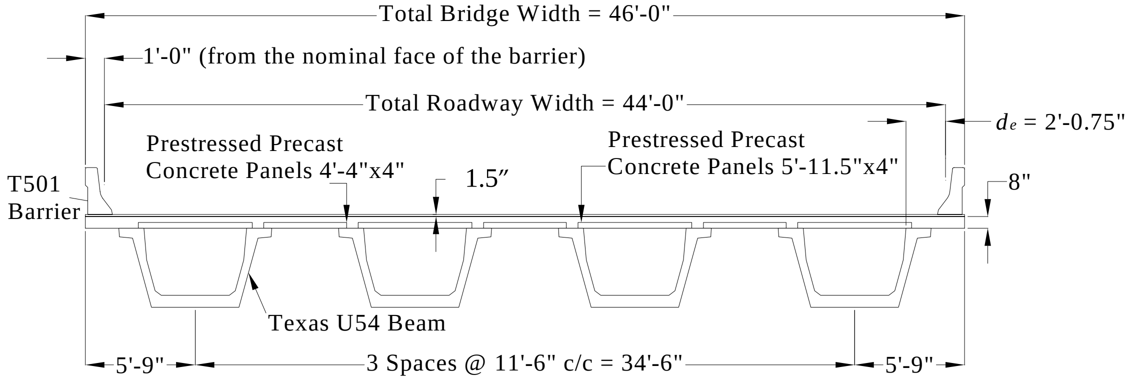

Figure 3.5. Cross-Section of U54 Girder Bridge.

The detailed design examples developed follow the same procedures for load and response calculations, prestress loss calculations, and limit state design described in this chapter. The parameters outlined in Table 3.5 were selected for the detailed design examples based on TxDOT input. Additional parameters followed the values presented in Tables 3.2 and 3.3.

Table 3.5. Design Parameters for Detailed Design Examples.

Parameter	Description / Selected Values
Design Codes	AASHTO Standard Specifications, 17th Edition (2002) AASHTO LRFD Specifications, 3rd Edition (2004)
Girder Spacing (ft.)	8'-0" (Type IV) 11'-6" (U54)
Spans	110 ft.
Strand Diameter (in.)	0.5
Skew Angle	0 degrees

3.4 DESIGN SPECIFICATIONS AND METHODOLOGY

3.4.1 Load and Resistance Factors

In the Standard Specifications, pretensioned concrete bridge girders are designed to satisfy the ASD and LFD philosophies. To satisfy ASD, the pretensioned concrete bridge girders must stay within allowable initial flexural stress limits at release, as well as final flexural stress limits at service load conditions. To satisfy LFD, the ultimate flexural and shear capacity of the section is checked. The Standard Specifications give several load combination groups and require that the structure be able to resist the load combination in each applicable load group corresponding to ASD and LFD. The general design equation is of the following form,

$$\phi R_n \geq Group(N) = \gamma \sum \left[\beta_i L_i \right] \tag{3.1}$$

where:

ϕ = Resistance factor

R_n = Nominal resistance

N = Group number

γ = Load factor

β_I = Coefficient that varies with type of load and depends on load group and design method

L_i = Force effect

In the AASHTO LRFD Specifications, the load and resistance factors are chosen more systematically based on reliability theory and on the statistical variation of the load and resistance. Moreover, additional factors are introduced in the general design equation to account for ductility, redundancy, and operational importance. The general design equation that is required to be satisfied for all limit states is as follows.

$$\phi R_n \geq Q = \sum\left[\eta_i \gamma_i Q_i\right] \tag{3.2}$$

where:

γ_i = Statistical load factor applied to the force effects

Q_i = Force effect

η_i = $\eta_D\ \eta_R\ \eta_I$ is the load modification factor

η_D = Ductility factor

η_R = Redundancy factor

η_I = Operational importance factor

3.4.2 Limit States and Load Combinations

Significantly different load combinations are specified by the LRFD Specifications as compared to the Standard Specifications. The major difference occurred due to the different methodologies followed by the two codes. The AASHTO LRFD Specifications specifies Service III and Fatigue load combinations for prestressed concrete members in addition to the Service I and Strength I load combinations. Service III load combination is exclusively applicable to prestressed concrete members to check tensile stresses at the bottom fiber of the girder. The objective of this load combination is to prevent cracking of prestressed concrete members. The Fatigue load combination is used to check the fatigue of prestressing strands due to repetitive vehicular live load. Extreme events, such as earthquake loads and vehicle collision loads are not accounted for in this parametric study. The wind load is also not considered as this does not govern the design of bridges in Texas.

The applicable load combinations including dead, superimposed, and live loads specified by AASHTO Standard Table 3.22.1A are outlined as follows.

For service load design (Group I):

$$Q = 1.00D + 1.00(L+I) \tag{3.3}$$

For load factor design (Group I):

$$Q = 1.3[1.00D + 1.67(L+I)] \tag{3.4}$$

where:

Q = Factored load effect

D = Dead load effect

L = Live load effect

I = Impact load effect

The load combinations specified by AASHTO LRFD Table 3.4.1-1 are outlined as follows.

Service I – checks compressive stresses in prestressed concrete components:

$$Q = 1.00(DC + DW) + 1.00(LL + IM) \tag{3.5}$$

where:

Q = Total load effect

DC = Self-weight of girder and attachment (slab and barrier) load effect

DW = Wearing surface load effect

LL = Live load effect

IM = Dynamic load effect

Service III – checks tensile stresses in prestressed concrete components:

$$Q = 1.00(DC + DW) + 0.80(LL + IM) \tag{3.6}$$

Strength I – checks ultimate strength:

$$\text{Maximum } Q = 1.25(DC) + 1.50(DW) + 1.75(LL + IM) \tag{3.7}$$

$$\text{Minimum } Q = 0.90(DC) + 0.65(DW) + 1.75(LL + IM) \tag{3.8}$$

For simple span bridges, the maximum load factors produce maximum effects. However, minimum load factors are used for dead load (DC) and wearing surface load (DW) when dead load and wearing surface stresses are opposite to those of the live load. For the present study involving simply supported bridge girders, only the maximum load combination is applicable.

Fatigue – checks stress range in strands:

$$Q = 0.75(LL + IM) \tag{3.9}$$

3.4.3 Allowable Stress Limits

Table 3.6 summarizes the allowable stress limits for the Standard and LRFD Specifications. The LRFD Specifications give the allowable stress limits in units of *ksi* as compared to *psi* in the Standard Specifications and, thus, the coefficients are different. Moreover, the tensile stress limit at the initial loading stage at transfer and the compressive stress limit at the intermediate loading stage at service slightly increased from the Standard to the LRFD Specifications.

Table 3.6. Summary of Allowable Stress Limits.

Stage of Loading	Type of Stress	Allowable Stress Limits		
		LRFD		Standard
		f'_c or f'_{ci} (ksi)	f'_c or f'_{ci} (psi)	f'_c or f'_{ci} (psi)
Initial Loading Stage at Transfer	Compressive	$0.6f'_{ci}$	$0.6f'_{ci}$	$0.6f'_{ci}$
	Tensile	$0.24\sqrt{f'_{ci}}$ [1]	$7.59\sqrt{f'_{ci}}$ [1]	$7.5\sqrt{f'_{ci}}$ [2]
Intermediate Loading Stage at Service	Compressive	$0.45f'_c$	$0.45f'_c$	$0.4f'_c$
	Tensile	$0.19\sqrt{f'_c}$	$6\sqrt{f'_c}$	$6\sqrt{f'_c}$
Final Loading Stage at Service	Compression: Case I[3]	$0.6\phi_\omega f'_c$	$0.6\phi_\omega f'_c$	$0.6f'_c$
	Compression: Case II[3]	$0.4f'_c$	$0.4f'_c$	$0.4f'_c$
	Tensile	$0.19\sqrt{f'_c}$	$6\sqrt{f'_c}$	$6\sqrt{f'_c}$

Notes:

1. LRFD Specifications allow this larger tensile stress limit when additional bonded reinforcement is provided to resist the total tensile force in the concrete when the tensile stress exceeds $0.0948\sqrt{f'_{ci}}$, or 0.2 ksi, whichever is smaller.
2. Standard Specifications allow this larger tensile stress limit when additional bonded reinforcement is provided to resist the total tensile force in the concrete when the tensile stress exceeds $3\sqrt{f'_{ci}}$, or 200 psi, whichever is smaller.
3. Case (I): For all load combinations.
   Case (II): For live load + 0.5 × (effective pretension force + dead loads)

The LRFD Specifications introduced a reduction factor, ϕ_ω, for the compressive stress limit at the final load stage to account for the fact that the unconfined concrete of the compression sides of the box girders are expected to creep to failure at a stress far lower than the nominal strength of the concrete. This reduction factor is taken equal to 1.0 when the web or flange slenderness ratio, calculated according to the LRFD Art. 5.7.4.7.1, is less than or equal to 15. When either the web or flange slenderness ratio is greater than 15, the provisions of the LRFD Art. 5.7.4.7.2 are used to calculate the value for the reduction factor, ϕ_ω. For a trapezoidal box section such as the composite Texas U54 beam, which has variable thickness across the flanges and webs, the LRFD Specifications outline a general guideline to determine the approximate slenderness ratios for webs and flanges. The slenderness ratio for any web or flange portion of Texas U54 beam is less than 15, which gives the value of the reduction factor, ϕ_ω equal to 1.0. The maximum slenderness ratio of 9.2 occurs in the webs of the U54 beam.

3.4.4 Dead Load and Superimposed Dead Load

The dead and superimposed dead loads considered in the design are girder self-weight, slab weight, and barrier and asphalt wearing surface loads. The superimposed dead load on the non-composite section is due to the slab weight. The tributary width for calculating the slab load is taken as the center–to–center spacing between the adjacent girders. The load due to the barrier and asphalt wearing surface are accounted for as composite loads (loads occurring after the onset of composite action between the deck slab and the precast girder section). The superimposed dead loads on the composite section are the weight of the barrier and the asphalt wearing surface weight. The two interior diaphragms of the Texas U54 beam are considered to be a three kip load each with a maximum average thickness of 13 in. Each of the interior diaphragms is considered to be located as close as 10 ft. from midspan of the beam.

The Standard Specifications allow the superimposed dead loads on the composite section to be distributed equally among all the girders for all cases. The LRFD Specifications allow the equal distribution of the composite superimposed dead loads (permanent loads) only when the following conditions specified by LRFD Article 4.6.2.2.1 are satisfied:

- width of deck is constant;
- number of girders (N_b) is not less than four;
- girders are parallel and have approximately the same stiffness;
- the roadway part of the overhang, $d_e \leq 3.0$ ft.;
- curvature in plan is less than 3 degrees for 3 or 4 girders and less than 4 degrees for 5 or more girders; and
- cross-section of the bridge is consistent with one of the crosssections given in LRFD Table 4.6.2.2.1-1.

If the above conditions are not satisfied, then refined analysis is required to determine the actual load on each girder. Grillage analysis and finite element analysis are recommended by the LRFD Specifications as appropriate refined analysis methods.

In the above criteria, the edge distance parameter, d_e, takes into account the closeness of a truck wheel line to the exterior girder. The edge girder is more sensitive to the truck wheel line placement than any other factor, as reported by Zokaie (2000). The LRFD Specifications define d_e as the distance from the exterior web of exterior beam to the interior edge of curb or traffic barrier. The value of d_e is important because it limits the use of the LRFD live load DF formulas and it is also used to determine the correction factor to determine the live load distribution for the exterior girder. For calculating d_e for inclined webs, as in the case of the Texas U54 beam, the LRFD Specifications and the research references (Zokaie et al.1991, Zokaie 2000) do not provide guidance to calculate the exact value of d_e. Thus, in this study the d_e value is considered to be the average distance between the curb and exterior inclined web of the U54 beam, as shown in the Figure 3.6.

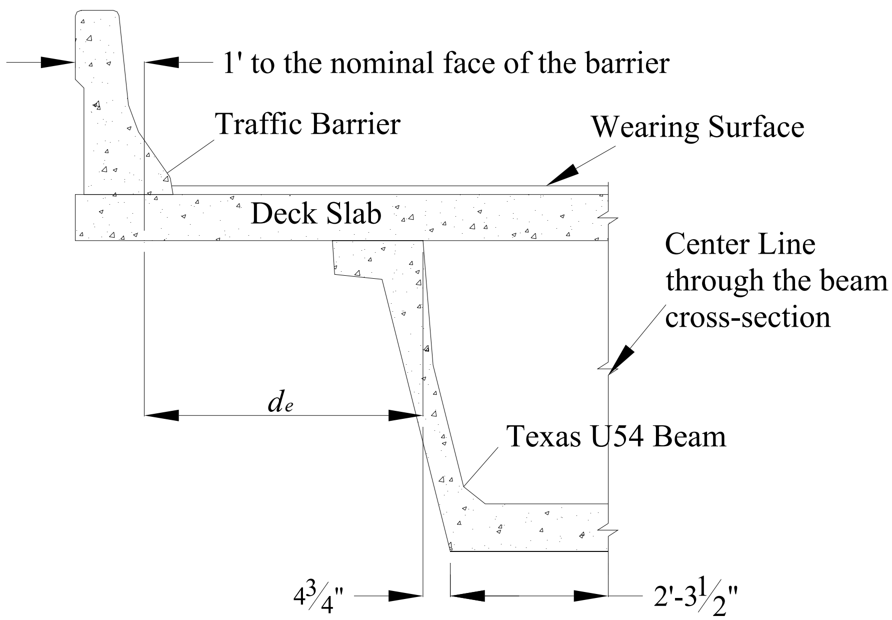

Figure 3.6. Definition of d_e (for this study).

Initially, the total roadway width (TRW) was considered to be a constant of 46 ft. For this value of TRW, certain spacings used for the parametric study of precast, prestressed Texas U54 beams were found to violate the LRFD Specifications provisions for applicability of live load DFs and uniform distribution of permanent dead loads. The spacings and summary of the parameters in violation are stated in Table 3.7.

According to the TxDOT Bridge Design Manual (TxDOT 2001) the standard bridge overhang is 6 ft. 9 in. for Texas U beams. Overhang is defined as the distance between the centerline of the exterior U54 beam to the edge of deck slab. For the 10 ft. and 14 ft. spacings, the overhang is restricted to 6 ft. 9 in., rather than the value determined for a 46 ft. TRW.

Referring to Figure 3.6, d_e is calculated to be 3 ft. 0.75 in., which is reasonably close to the limiting value of $d_e \leq 3$ ft. The resulting TRW is 42 ft. for these spacings.

Table 3.7. Spacings – Reasons of Invalidation.

Spacings	LRFD Restrictions Violated	LRFD Restrictions
10 ft.	Actual $d_e = 4.31$ ft.	$0 < d_e \leq 3$ ft.[2]
14 ft.	Actual $d_e = 5.31$ ft. Actual $N_b = 3$	$0 < d_e \leq 3$ ft.[2] $0 < d_e \leq 4.5$ ft.[1] $N_b \geq 4$ [2]
16.67 ft.	Actual $N_b = 3$	$N_b \geq 4$ [2]

1. This restriction is related to the LRFD Live Load DF formulas.
2. This restriction is related to the general set of limitations described in this section.

Among other restrictions, the LRFD Specifications allow for uniform distribution of permanent dead loads (such as rail, sidewalks, and wearing surface) if $N_b \geq 4$, where N_b is the number of beams in a bridge cross-section. Kocsis (2004) shows that, in general, a larger portion of the rail and sidewalk load is taken by exterior girders for cases when $N_b < 4$. The implication of distributing the dead load of railing and sidewalk uniformly among all the beams for the case where $N_b = 3$ is that the exterior girder may be designed unconservatively, if the same design is used for the exterior and interior girders. The justification of using the spacings with $N_b = 3$, is that as per TxDOT standard practices (TxDOT 2001), two-thirds of the railing load is distributed to the exterior girder and one-third is distributed to the interior girder.

Finally, the bending moment (M) and shear force (V) due to dead loads and superimposed dead loads at any section having a distance x from the support, are calculated using the following equations.

$$M = 0.5wx\,(L - x) \tag{3.10}$$

$$V = w(0.5L - x) \tag{3.11}$$

where:

w = Uniform load, k/ft.

L = Design span length, ft.

3.4.5 Live Load

3.4.5.1 Live Load Model

There is a significant change in the live load specified by the LRFD Specifications as compared to the Standard Specifications. The Standard Specifications specify the live load to be taken as one of the following, whichever produces maximum stresses at the section considered.

1. HS 20-44 truck consisting of one front axle weighing 8 kips and two rear axles weighing 32 kips each. The truck details are shown in Figure 3.7.
2. HS 20-44 lane loading consisting of 0.64 klf distributed load and a point load traversing the span having a magnitude of 18 kips for moment and 26 kips for shear. The details are shown in Figure 3.8.
3. Tandem loading consisting of two 24 kip axles spaced 4 ft. apart.

The live load model used in the Standard Specifications did not prove adequate because its accuracy varied with the span length (Kulicki 1994). The LRFD Specifications specify a new live load model. The live load is to be taken as one of the following, whichever yields maximum stresses at the section considered.

1. HL-93: This is a combination of an HS 20-44 truck consisting of one front axle weighing 8 kips and two rear axles weighing 32 kips each with a 0.64 klf uniformly distributed lane load.
2. Combination of a tandem loading consisting of two 25-kip axles spaced 4 ft. apart with a 0.64 klf distributed lane load.

This new live load model more accurately represents the truck traffic on national highways and was developed to give a consistent margin of safety for a wide range of spans (Kulicki 1994).

3.4.5.2 Undistributed Live Load Shear and Moment

The maximum bending moments and shear forces are calculated from load placement schemes shown in Figure 3.9. The undistributed shear force (V) and bending moment (M) due to HS 20-44 truck load, HS 20-44 lane load, and tandem load on a per-lane-basis are calculated using the following equations prescribed by the PCI Design Manual (PCI 2003).

Maximum bending moment due to HS 20-44 truck load.

For $x/L = 0 - 0.333$:

$$M = \frac{72(x)[(L - x) - 9.33]}{L} \tag{3.12}$$

For $x/L = 0.333 - 0.50$:

$$M = \frac{72(x)[(L - x) - 4.67]}{L} - 112 \tag{3.13}$$

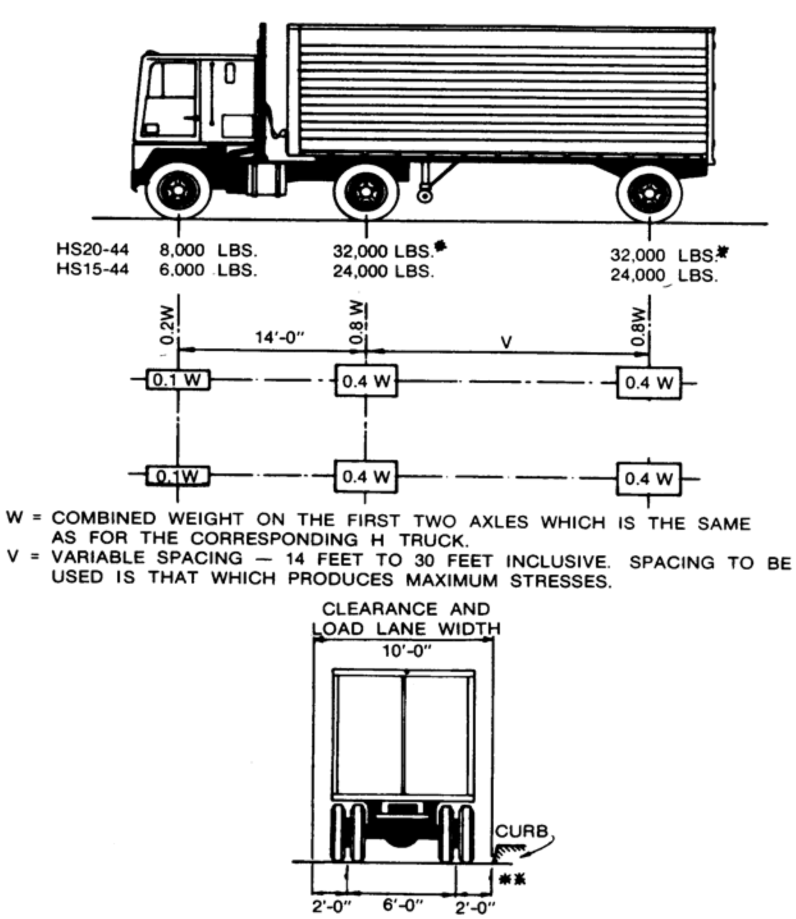

Figure 3.7. HS 20-44 Truck Configuration (AASHTO Standard Specifications 2002).

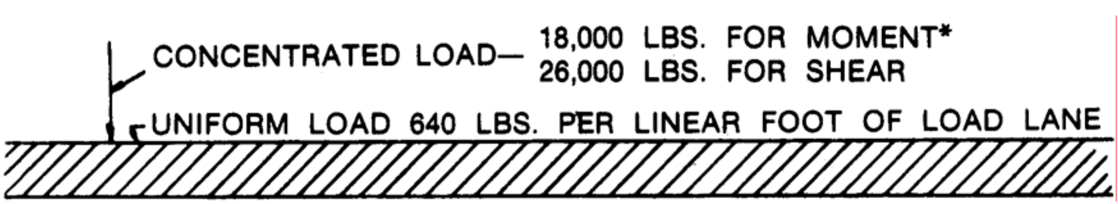

Figure 3.8. HS 20-44 Lane Loading (AASHTO Standard Specifications 2002).

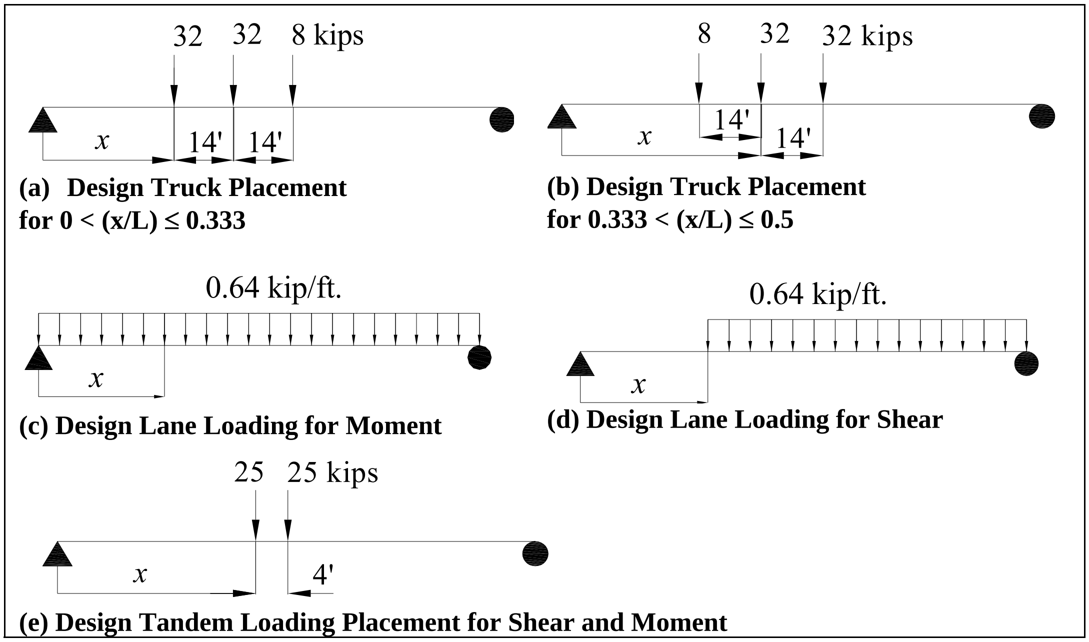

Figure 3.9. Placement of Design Live Loads for a Simply Supported Beam.

Maximum shear force due to HS 20-44 truck load.

For $x/L = 0 – 0.50$:

$$V = \frac{72[(L - x) - 9.33]}{L} \tag{3.14}$$

Maximum bending moment due to HS 20-44 lane loading.

$$M = \frac{P(x)(L - x)}{L} + 0.5(w)(x)(L - x) \tag{3.15}$$

Maximum shear force due to HS 20-44 lane load.

$$V = \frac{Q(L - x)}{L} + (w)(\frac{L}{2} - x) \tag{3.16}$$

Maximum bending moment due to AASHTO LRFD lane load.

$$M = 0.5(w)(x)(L-x) \tag{3.17}$$

Maximum shear force due to AASHTO LRFD lane load.

$$V = \frac{0.32(L - x)^2}{L} \quad \text{for } x \le 0.5L \tag{3.18}$$

Maximum bending moment due to tandem load.

$$M = \frac{T(x)[(L - x) - 2]}{L} \tag{3.19}$$

Maximum shear force due to tandem load.

$$V = \frac{T[(L - x) - 2]}{L} \tag{3.20}$$

where:

M = Live load moment, k-ft.

V = Live load shear, kips

x = Distance from the support to the section at which bending moment or shear force is calculated, ft.

L = Design span length, ft.

P = Concentrated load for moment = 18 kips

Q = Concentrated load for shear = 26 kips

W = Uniform load per linear foot of load lane = 0.64 klf

T = Tandem load, 48 kips for AASHTO Standard and 50 kips for AASHTO LRFD design.

3.4.5.3 Fatigue Load

The AASHTO LRFD Specifications require that the fatigue in the prestressing strands be checked except in certain cases. This limit state is not provided in the AASHTO Standard Specifications. The fatigue load for calculating the fatigue stress is given by LRFD Article 3.6.1.4 as a single HS 20-44 truck load with constant spacing of 30 ft. between the 32 kip rear axles. The maximum undistributed bending moment (M) due to the fatigue truck load on a per-lane-basis is calculated using the following equations provided by the PCI Design Manual (PCI 2003).

For $x/L = 0 – 0.241$:

$$M = \frac{72(x)[(L - x) - 18.22]}{L} \tag{3.21}$$

For $x/L = 0.241 – 0.50$:

$$M = \frac{72(x)[(L - x) - 11.78]}{L} - 112 \tag{3.22}$$

where:

x = Distance from the support to the section at which bending moment or shear force is calculated, ft.

L = Design span length, ft.

Note that LRFD Article 5.5.3 specifies that the check for fatigue of the prestressing strands is not necessary for fully prestressed components that are designed to have extreme fiber tensile stress due to Service III limit state within the specified limit of $0.19\sqrt{f_c'}$ (same as $6\sqrt{f_c'\text{ (psi)}}$). In the parametric study, the girders are designed to always satisfy this specified limit and so the fatigue limit state check is not required.

3.4.5.4 Impact Factor

The AASHTO Standard and LRFD Specifications require the effect of dynamic (impact) loading to be considered. The dynamic load is expressed as a percentage of live load. AASHTO Standard Article 3.8.2.1 specifies the following expression to determine the impact load factor.

$$I = \frac{50}{L+125} \leq 30\% \tag{3.23}$$

where:

I = Impact factor

L = Design span length, ft.

AASHTO LRFD Article 3.6.2 specifies the dynamic load to be taken as 33 percent of the live load for all limit states except the fatigue limit state for which the impact factor is specified as 15 percent of the fatigue load moment. The impact factor for the Standard Specifications is applicable to truck, lane, and tandem loads; however, the LRFD Specifications do not require the lane loading to be increased for dynamic effects.

3.4.5.5 Live Load Distribution Factors

The live load moments and shear forces including the dynamic load (impact load) effect are distributed to the individual girders using distribution factors (DFs). The Standard Specifications live load DF formulas are of the form *S*/*D*, where, *S* is the girder spacing and *D* is 11 for prestressed concrete girders.

The Standard Specifications only consider girder spacing for the DFs for I-shaped girders. The effects of other critical parameters such as slab stiffness, girder stiffness, and span length are ignored. The Standard Specifications formulas were found to give valid results for typical bridge geometries (i.e., girder spacing of 6 ft. and span length of 60 ft.), but lose accuracy when the bridge parameters are varied (Zokaie 2000). For this reason, major changes have occurred in the way live load DFs are calculated in the LRFD Specifications. More complex formulas are provided that depend on the location (interior or exterior) of the girder, limit state (bending moment, shear force, or fatigue), and type of bridge superstructure. To make live load DFs more accurate for a wider range of bridge geometries and types, additional parameters such as bridge type, span length, girder depth, girder location, transverse and longitudinal stiffness, and skew were taken into account. For skewed bridges, the LRFD Specifications require that the DFs for moment be reduced and the shear DFs be corrected for skew. LRFD Tables 4.6.2.2.2 and 4.6.2.2.3 specify the DFs for moment and shear for I-shaped girder sections.

The use of these approximate DFs is allowed for prestressed concrete girders having an I-shaped cross-section with composite slab, if the conditions outlined below are satisfied. For bridge configurations not satisfying the limits below, refined analysis is required to estimate the moment and shear DFs.

1. width of deck is constant;
2. number of girders (N_b) is not less than four (Lever rule can be used for three girders);
3. girders are parallel and of approximately the same stiffness;
4. the roadway part of the overhang, $d_e \leq 3.0$ ft.;
5. curvature in plan is less than 3 degrees for 3 or 4 girders and less than 4 degrees for 5 or more girders ;
6. cross-section of the bridge is consistent with one of the cross-sections given in LRFD Table 4.6.2.2.1-1;
7. $3.5 \leq S \leq 16$ where S is the girder spacing, ft.;
8. $4.5 \leq t_s \leq 12$ where t_s is the slab thickness, in.;
9. $20 \leq L \leq 240$ where L is the span length, ft.; and
10. $10{,}000 \leq K_g \leq 7{,}000{,}000$, in.^{4}

where:

$$K_g = n\,(I + Ae_g^2)$$

n = Modular ratio between the girder and slab concrete = E_c/E_{cip}

E_{cip}= Modulus of elasticity of cast-in-place slab concrete, ksi

E_c = Modulus of elasticity of precast girder concrete, ksi

I = Moment of inertia of the girder section, in.^{4}

A = Area of the girder cross-section, in.^{2}

e_g = Distance between the centroids of the girder and the slab, in.

The DFs shall be taken as the greater of the two cases when two design lanes are loaded and one design lane is loaded. The approximate live load moment DFs (*DFM*) and the live load shear DFs (*DFV*) for an interior I-shaped girder cross-section with a composite slab (type k) is given by AASHTO LRFD Tables 4.6.2.2.2 and 4.6.2.2.3 as follows.

For two or more lanes loaded:

$$DFM = 0.075 + \left(\frac{S}{9.5}\right)^{0.6}\left(\frac{S}{L}\right)^{0.2}\left(\frac{K_g}{12.0Lt_s^{\,3}}\right)^{0.1} \tag{3.24}$$

For one design lane loaded:

$$DFM = 0.06 + \left(\frac{S}{14}\right)^{0.4}\left(\frac{S}{L}\right)^{0.3}\left(\frac{K_g}{12.0Lt_s^{\,3}}\right)^{0.1} \tag{3.25}$$

For two or more lanes loaded:

$$DFV = 0.2 + \left(\frac{S}{12}\right) - \left(\frac{S}{35}\right)^{2} \tag{3.26}$$

For one design lane loaded:

$$DFV = 0.36 + \left(\frac{S}{25.0}\right) \tag{3.27}$$

where:

DFM = DF for moment

DFV = DF for shear

S = Girder spacing, ft.

L = Design span length, ft.

t_s = Thickness of slab, in.

K_g = Longitudinal stiffness parameter, in.^{4} = $n\,(I + Ae_g^{\,2})$

n = Modular ratio between the girder and slab concrete

I = Moment of inertia of the girder section, in.^{3}

A = Area of the girder cross-section, in.^{2}

e_g = Distance between the centroids of the girder and the slab, in.

The TxDOT Bridge Design Manual (TxDOT 2001) also recommends a DF of $S/11$ for TxDOT U54 beams. In the Standard Specifications (AASHTO 2002), the live load DF formula for interior girders consisting of a concrete deck on spread box beams (similar to Texas U54 beams), originally developed by Mortarjemi and Vanhorn (1969), is as follows.

$$DFM_{interior} = \frac{2N_L}{N_B} + k\frac{S}{L} \quad (3.28)$$

where:

N_L = Number of design traffic lanes
N_B = Number of beams ($4 \le N_B \le 10$)
S = Beam spacing, ft. ($6.57 \le N_B \le 11.0$)
L = Span length, ft.
K = $0.07W - N_L(0.10N_L - 0.26) - 0.2N_B - 0.12$
W = Roadway width between curbs, ft. ($32 \le W \le 66$)

In the LRFD Specifications, the bridge type corresponding to the TxDOT U54 beam comes under the category of type c, which is concrete deck on concrete spread box beams. The live load DF formulas for precast, prestressed box beams are given in Table 3.8. These formulas are valid within their range of applicability. The general limitations on the use of all LRFD live load DF formulas, as stated in the LRFD Art. 4.6.2.2, are the same as discussed for uniform distribution of permanent dead loads. In addition, some general restrictions, such as span curvature to be less than 12 degrees and girders to be parallel and prismatic, are also imposed on the use of these formulas.

The DF for fatigue load moment is to be taken as:

$$DFM_f = \frac{DFM \text{ (single lane loaded)}}{m} \quad (3.29)$$

where:

DFM_f = DF for fatigue load moment

M = Multiple presence factor taken as 1.2

Table 3.8. LRFD Live Load DFs for Concrete Deck on Concrete Spread Box Beams.

Category	DF Formulas	Range of Applicability
Live Load Distribution per Lane for Moment in Interior Beams	One Design Lane Loaded: $\left(\frac{S}{3.0}\right)^{0.35}\left(\frac{Sd}{12.0L^2}\right)^{0.25}$ Two or More Design Lanes Loaded: $\left(\frac{S}{6.3}\right)^{0.6}\left(\frac{Sd}{12.0L^2}\right)^{0.125}$	$6.0 \le S \le 18.0$ $20 \le L \le 140$ $18 \le d \le 65$ $N_b \ge 3$
	Use Lever Rule	$S > 18.0$
Live Load Distribution per Lane for Moment in Exterior Longitudinal Beams	One Design Lane Loaded: Lever Rule Two or More Design Lanes Loaded: $g = e \times g_{interior}$ $e = 0.97 + \frac{d_e}{28.5}$	$0 \le d_e \le 4.5$ $6.0 \le S \le 18.0$
	Use Lever Rule	$S > 18.0$
Live Load Distribution per Lane for Shear in Interior Beams	One Design Lane Loaded: $\left(\frac{S}{10}\right)^{0.6}\left(\frac{d}{12.0L}\right)^{0.1}$ Two or More Design Lanes Loaded: $\left(\frac{S}{7.4}\right)^{0.8}\left(\frac{d}{12.0L}\right)^{0.1}$	$6.0 \le S \le 18.0$ $20 \le L \le 140$ $18 \le d \le 65$ $N_b \ge 3$
	Use Lever Rule	$S > 18.0$
Live Load Distribution per Lane for Shear in Exterior Beams	One Design Lane Loaded: Lever Rule Two or More Design Lanes Loaded: $g = e \times g_{interior}$ $e = 0.8 + \frac{d_e}{10}$	$0 \le d_e \le 4.5$
	Use Lever Rule	$S > 18.0$

where:

S = Beam spacing, ft.
L = Span length, ft.
D = Girder depth, in.
N_b = Number of beams.
d = Distance from exterior web of exterior beam to the interior edge of curb or traffic barrier, in.

The live load moment DFs shall be reduced for skew using the skew reduction formula specified by AASHTO LRFD Article 4.6.2.2.2e. The skew reduction formula is applicable to any number of design lanes loaded. The skew reduction formula for prestressed concrete I-shaped (type k) girders can be used when the following conditions are satisfied.

1. $30° \leq \theta \leq 60°$ where θ is the skew angle, if $\theta > 60°$, use $\theta = 60°$;
2. $3.5 \leq S \leq 16$ where S is the girder spacing, ft.;
3. $20 \leq L \leq 240$ where L is the span length, ft.; and
4. Number of girders (N_b) is not less than four.

3.4.5.6 Distributed Live Load Shear Force and Bending Moment

The governing live load for the designs based on the AASHTO Standard Specifications is determined based on undistributed live load moments. The shear force at the critical section and bending moment at the midspan of the girder due to the governing live load, including the impact load, is calculated using the following formulas.

$$M_{LL+I} = (M)\,(DF)\,(1+I) \tag{3.30}$$

$$V_{LL+I} = (V)\,(DF)\,(1+I) \tag{3.31}$$

where:

M_{LL+I} = Distributed governing live load moment including impact loading, k-ft.

V_{LL+I} = Distributed governing live load shear including impact loading, kips

M = Governing live load bending moment per lane, k-ft.

V = Governing live load shear force per lane, kips

DF = DF specified by the Standard Specifications

I = Impact factor specified by the Standard Specifications

For the designs based on LRFD Specifications, the shear force at the critical section and bending moment at midspan is calculated for the governing (HS 20-44 truck or tandem) load and lane load separately. The governing load is based on undistributed tandem and truck load moments. The effect of dynamic loading is included only for the truck or tandem loading and not for lane loading. The formulas used in the design are as follows.

$$M_{LT} = (M_T)(DFM)(1+IM) \tag{3.32}$$

$$V_{LT} = (V_T)(DFV)(1+IM) \tag{3.33}$$

$$M_{LL} = (M_L)(DFM) \tag{3.34}$$

$$V_{LL} = (V_L)(DFV) \tag{3.35}$$

$$M_{LL+I} = M_{LT} + M_{LL} \tag{3.36}$$

$$V_{LL+I} = V_{LT} + V_{LL} \quad (3.37)$$

$$M_f = (M_{fatigue})(DFM_f)(1+IM_f) \quad (3.38)$$

where:

M_{LL+I} = Distributed moment due to live load including dynamic load effect, k-ft.

V_{LL+I} = Distributed shear due to live load including dynamic load effect, kips

M_{LT} = Distributed moment due to governing (truck or tandem) load including dynamic load effect, k-ft.

M_T = Bending moment per lane due to governing (truck or tandem) load, k-ft.

V_{LT} = Distributed shear due to governing (truck or tandem) load including dynamic load effect, kips

V_T = Shear force per lane due to governing (truck or tandem) load, kips

M_{LL} = Distributed moment due to lane load, k-ft.

M_L = Bending moment per lane due to lane load, k-ft.

V_{LL} = Distributed shear due to lane load, kips

V_L = Shear force per lane due to lane load, kips

M_f = Distributed moment due to fatigue load including dynamic load effect, k-ft.

$M_{fatigue}$ = Bending moment per lane due to fatigue load, k-ft.

DFM = Moment DF specified by LRFD Specifications

DFV = Shear DF specified by LRFD Specifications

IM = Impact factor specified by LRFD Specifications

DFM_f = Moment DF for fatigue loading

IM_f = Impact factor for fatigue limit state

3.4.5.7 Dynamic Load Allowance Factor

The dynamic load allowance (*IM*) is an increment to be applied to the static lane load to account for wheel load impact from moving vehicles. The LRFD Specifications give a dynamic load allowance factor for all limit states as 33 percent, except 15 percent for the fatigue and fracture limit state and 75 percent for design of deck joints. The Standard Specifications use the following formula to calculate the impact factor, *I*,

$$I = \frac{50}{L+125} \leq 30\% \quad (3.39)$$

where L is the span length in ft.

The new *IM* factor can substantially increase the live load moments for LRFD designs as compared to designs based on the Standard Specifications, especially for longer spans (e.g., a 48.5 percent increase for a 100 ft. span and a 75 percent increase for a 140 ft. span).

3.4.6 Member Properties

3.4.6.1 Section Properties

The non-composite section properties for the precast girders were provided in Section 3.2. The composite section properties depend on the effective flange width of the girder. Standard Article 9.8.3.2 specifies the effective flange width of an interior girder to be the least of the following:

1. one-fourth of the span length of the girder,
2. 6 × (slab thickness on each side of the effective web width) + effective web width, or
3. one-half the clear distance on each side of the effective web width plus the effective web width.

The effective web width used in conditions (2) and (3) is specified by Standard Article 9.8.3.1, as the lesser of the following:

1. 6 × (flange thickness on either side of web) + web thickness + fillets, and
2. width of the top flange.

The LRFD Specifications specify a slightly modified approach for the calculation of effective flange width of interior girders. LRFD Article 4.6.2.6.1 specifies the effective flange width for an interior girder to be the least of the following:

1. one-fourth of the effective span length,
2. 12 × (average slab thickness) + greater of web thickness or one-half the girder top flange width, or
3. the average spacing of adjacent girders.

The LRFD Specifications do not require the calculation of the effective web width and instead use the greater of the actual web thickness and one-half of the girder top flange width in condition (2).

Once the effective flange width is established, the transformed flange width and flange area is calculated as:

Transformed flange width = n × (effective flange width) (3.40)

Transformed flange area = $n \times$ (effective flange width) $\times t_s$ (3.41)

where:

n = Modular ratio between slab and girder concrete = E_{cip}/E_c

t_s = Thickness of the slab, in.

E_{cip} = Modulus of elasticity of cast-in-place slab concrete, ksi

E_c = Modulus of elasticity of precast girder concrete, ksi

Composite section properties of the Texas U54 composite section are calculated based on the effective flange width of the deck slab associated with each girder section. According to Hambly (1991), "The effective flange width is the width of a hypothetical flange that compresses uniformly across its width by the same amount as the loaded edge of the real flange under the same edge shear forces." The Standard Specifications do not give any specific guidelines regarding the calculation of the effective flange width for open box sections, such as the Texas U54 beam. So, for both the LRFD and Standard Specifications, each web of the Texas U54 beam is considered an individual supporting element according to the LRFD Specifications commentary C4.6.2.6.1. Each supporting element is then considered to be similar to a wide flanged I-beam, and the provisions for the effective flange width in the Standard Art. 9.8.3 (AASHTO 2002) and LRFD Art. 4.6.2.6.1 (AASHTO 2004), stated above, are applied to the individual webs of the Texas U54 beam.

TxDOT recommends using the modular ratio as 1 because the concrete strengths are unknown at the beginning of the design process and are optimized during the design. This recommendation was followed for the service load design in this study. For shear and deflection calculations the actual modular ratio based on the selected optimized precast concrete strength is used in this study. For these calculations the composite section properties are evaluated using the transformed flange width and precast section properties. The flexural strength calculations are based on the selected optimized precast concrete strength, the actual slab concrete strength, and the actual slab and girder dimensions.

3.4.6.2 Transfer and Development Lengths

The transfer length of prestressing strands is determined as $50d_b$ in the Standard Specifications, as compared to the LRFD Specifications where the transfer length is increased to $60d_b$. The development length is determined by Eq. 3.42 for the Standard Specifications and by Eq. 3.43 for the LRFD Specifications. Standard Article 9.28.3 requires the development length, calculated by the Eq. 3.42, to be doubled when tension at service load is allowed in the precompressed tensile zone for the region where one or more strands are debonded.

$$l_d = \left(f_{su}^* - \frac{2}{3} f_{se} \right) D \tag{3.42}$$

$$l_d = \kappa \left(f_{ps} - \frac{2}{3} f_{pe} \right) d_b \tag{3.43}$$

where:

f_{su}^* or f_{ps}	=	Average stress in prestressing steel for the ultimate conditions, ksi
f_{se} or f_{pe}	=	Effective stress in prestressing steel after all losses, ksi
κ	=	Modification factor taken as 1.6 for precast, prestressed beams
D or d_b	=	Diameter of prestressing strands, in.

3.4.6.3 Design Span Length, Hold-Down Point, and Debonding

The design span length is the center-to-center distance between bearings. This length is obtained by deducting the distance between the centerlines of the bearing pad and the pier from the total span length (center-to-center distance between the piers). Figures 3.10 and 3.11 illustrate the details at the girder end at a conventional support.

The stresses at the ends of the Type IV and Type C girders are reduced by harping some of the strands. The hold-down point for harped strands in the I-girders is specified by the TxDOT Bridge Design Manual (TxDOT 2001) to be the greater of 5 ft. and 0.05 times the span length, on either side of the midspan.

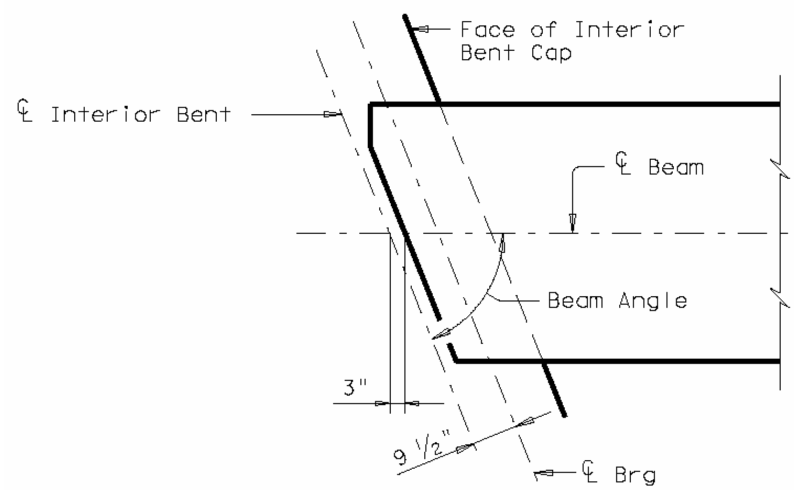

Figure 3.10. Girder End Detail for Texas U54 Beams (TxDOT 2001).

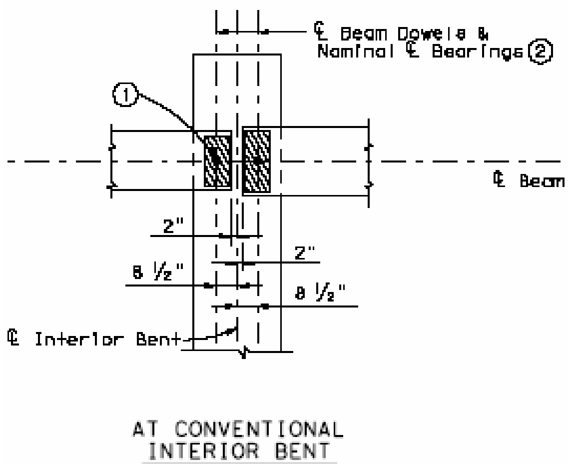

Figure 3.11. Girder End Details for I-Girders (TxDOT 2001).

The stresses at the ends of the U54 girders are reduced by debonding the prestressing strands. The Standard Specifications do not limit the debonding percentage. However, LRFD Article 5.11.4.3 limits the debonding of strands to 40 percent per horizontal row and 25 percent per section. Debonding termination is allowed at any section, if and only if, it is done for less than 40 percent of the total debonded strands or four strands, whichever is greater. The LRFD Specifications in Commentary 5.11.4.3, however, allow the consideration of successful past practices regarding debonding and further instruct to perform a thorough investigation of shear resistance of the sections in the debonded regions. The Standard Specifications do not specify any limit on the allowable debonding length. The LRFD Specifications allow the strands to be debonded to any length as long as the total resistance developed at any section satisfies all the limit states.

To be consistent with TxDOT design procedures, the debonding of strands for U54 girders was carried out in accordance with the procedure followed in the TxDOT bridge design software PSTRS14 (TxDOT 2004). Two strands are debonded at a time at each section located at uniform increments of 3 ft. along the span length, beginning at the end of the girder. The debonding is started at the end of the girder because, due to relatively higher initial stresses at the end, a greater number of strands are required to be debonded. The debonding requirement, in terms of number of strands, reduces as the section moves away from the end of the girder. To make the most efficient use of debonding, due to greater eccentricities in the lower rows, the debonding at each section begins at the bottom-most row and goes up. Debonding at a particular section will continue until the initial stresses are within the allowable stress limits or until a debonding limit is reached. When the debonding limit is reached, the initial concrete strength is increased and the design cycles to convergence.

As per the TxDOT Bridge Design Manual (TxDOT 2001) and LRFD Article 5.11.4.3, the limits of debonding for partially debonded strands are described as follows:

1. Maximum percentage of debonded strands per row:
    - TxDOT Bridge Design Manual (TxDOT 2001) recommends a maximum percentage of debonded strands per row should not exceed 75 percent.
    - AASHTO LRFD recommends a maximum percentage of debonded strands per row should not exceed 40 percent.
2. Maximum percentage of debonded strands per section:
    - TxDOT Bridge Design Manual (TxDOT 2001) recommends a maximum percentage of debonded strands per section should not exceed 75 percent.
    - AASHTO LRFD recommends a maximum percentage of debonded strands per section should not exceed 25 percent.
3. LRFD Specifications recommend that not more than 40 percent of the debonded strands or four strands, whichever is greater, shall have debonding terminated at any section.
4. Maximum length of debonding:
    - According to the TxDOT Bridge Design Manual (TxDOT 2001), the maximum debonding length should be chosen to be the lesser of the following:

- 15 ft.,
- 0.2 times the span length, or
- half the span length minus the maximum development length as specified in AASHTO LRFD Art. 5.11.4.2 and Art. 5.11.4.3 for LRFD designs and as specified in the 1996 AASHTO Standard Specifications for Highway Bridges, Section 9.28 for the Standard designs.

- An additional requirement for the LRFD designs was followed, which states that the length of debonding of any strand shall be such that all limit states are satisfied with the consideration of total developed resistance at any section being investigated.

5. An additional requirement for the LRFD designs was followed, which states:
   - Debonded strands shall be symmetrically distributed about the centerline of the member.
   - Debonded lengths of pairs of strands that are symmetrically positioned about the centerline of the member shall be equal.

   Exterior strands in each horizontal row shall be fully bonded.

3.4.6.4 Critical Section for Shear

The critical section for shear is specified by the AASHTO Standard Specifications as the distance $h/2$ from the face of the support, where h is the depth of the composite section. However, as the support dimensions are not specified in this study, the critical section is measured from the centerline of bearing, which yields a conservative estimate of the design shear force.

The LRFD Specifications require the critical section for shear to be calculated based on the parameter θ evaluated in the shear design section. The initial estimate for the location of the critical section for shear is taken as the distance equal to $h/2$ plus one-half the bearing pad width, from the girder end, where h is the depth of the composite section. The critical section is then refined based on an iterative process that determines the final values of the parameters θ and β.

3.5 PRESTRESS LOSSES

3.5.1 General

When computing the stresses at service, the prestressed force is reduced from the initial force at transfer to account for losses that occur over time. Prestress losses can be categorized as immediate losses and time-dependent losses. The prestress loss due to initial steel relaxation and elastic shortening are grouped into immediate losses. The prestress loss due to concrete creep, concrete shrinkage, and steel relaxation after transfer are grouped into time-dependent losses. There is an uncertainty in the prestress loss over time as it depends on many factors that cannot be calibrated accurately. Previous research has led to empirical formulas to predict the loss of prestress that are fairly accurate. A more accurate estimate of the prestress losses can be made using the time-step method. The AASHTO Standard and LRFD Specifications recommend the use of more accurate methods, like the time-step method, for exceptionally long spans or for unusual designs. However, for the parametric study the time-step method was not used as the spans were fairly standard.

The AASHTO Standard Specifications provide two options to estimate the loss of prestress. The first option is the lump-sum estimate of the total loss of prestress provided by AASHTO Standard Table 9.16.2.2. The second option is to use a detailed method for estimation of prestress losses that is believed to yield a more accurate estimate of losses in prestress as compared to the lump-sum estimate. The detailed method is used in the parametric study to estimate the prestress losses. The AASHTO Standard Article 9.16.2 gives the empirical formulas for the detailed estimation of prestress losses as outlined in the following sections. These formulas are applicable when normal weight concrete and 250 ksi or 270 ksi low-relaxation strands are used.

The AASHTO LRFD Specifications contain empirical formulas to determine the instantaneous losses. For time-dependent losses, two different options are provided. The first option is to use a lump-sum estimate of time-dependent losses given by AASHTO LRFD Article 5.9.5.3. The second option is to use refined estimates of time-dependent losses given by AASHTO LRFD Article 5.9.5.4. The refined estimates outlined in the following sections are used for the parametric study as they are more accurate than the lump-sum estimate. The refined estimates are not applicable for prestressed concrete girders exceeding a span length of 250 ft. or made using concrete other than normal weight concrete.

3.5.2 Instantaneous Losses

Instantaneous losses include the loss of prestress due to elastic shortening and initial relaxation of steel. However, the Standard Specifications do not provide an estimate of the initial steel relaxation. Rather, only the formula for the estimation of total steel relaxation is provided. Thus, for estimating the instantaneous prestress loss for the Standard designs, half the total prestress loss due to steel relaxation is considered as the instantaneous loss and the other half as the time-dependent loss. This method is recommended by the TxDOT Bridge Design Manual (TxDOT 2001).

The instantaneous prestress loss is given by the following expression.

$$\Delta f_{pi} = (ES + \frac{1}{2} CR_s) \tag{3.44}$$

The percent instantaneous loss is calculated using the following expression.

$$\% \, \Delta f_{pi} = \frac{100(ES + \frac{1}{2} CR_s)}{0.75 f_s'} \tag{3.45}$$

where:

Δf_{pi} = Instantaneous prestress loss, ksi

ES = Prestress loss due to elastic shortening, ksi

CR_S = Prestress loss due to steel relaxation, ksi

f_s' = Ultimate strength of prestressing strands, ksi

The LRFD Specifications provide the following expression to estimate the instantaneous loss of prestress.

$$\Delta f_{pi} = (\Delta f_{pES} + \Delta f_{pR1}) \tag{3.46}$$

The percent instantaneous loss is calculated using the following expression.

$$\% \Delta f_{pi} = \frac{100(\Delta f_{pES} + \Delta f_{pR1})}{f_{pj}} \tag{3.47}$$

where:

Δf_{pES} = Prestress loss due to elastic shortening, ksi

Δf_{pR1} = Prestress loss due to steel relaxation at transfer, ksi

f_{pj} = Jacking stress in prestressing strands, ksi

3.5.3 Time-Dependent Losses

Time-dependent prestress losses include those due to concrete creep, concrete shrinkage, and steel relaxation after transfer. The time-dependent loss for the Standard designs is calculated using the following expression.

$$\text{Time Dependent Loss} = SH + CR_C + 0.5(CR_S) \tag{3.48}$$

where:

SH = Prestress loss due to concrete shrinkage, ksi

CR_C = Prestress loss due to concrete creep, ksi

CR_S = Prestress loss due to steel relaxation, ksi

The following expression is used to estimate the time-dependent losses for designs based on the LRFD Specifications.

$$\text{Time Dependent Loss} = \Delta f_{pSR} + \Delta f_{pCR} + \Delta f_{pR2} \tag{3.49}$$

where:

Δf_{pSR} = Prestress loss due to concrete shrinkage, ksi

Δf_{pCR} = Prestress loss due to concrete creep, ksi

Δf_{pR2} = Prestress loss due to steel relaxation after transfer, ksi

3.5.4 Total Prestress Loss

The total loss and percent total loss of prestress is calculated using the following expressions.

For designs based on the Standard Specifications:

$$\Delta f_{pT} = ES + SH + CR_C + CR_S \tag{3.50}$$

$$\%\ \Delta f_{pT} = \frac{100(ES + SH + CR_c + CR_s)}{0.75 f_s'} \tag{3.51}$$

For designs based on the LRFD Specifications:

$$\Delta f_{pT} = \Delta f_{pES} + \Delta f_{pSR} + \Delta f_{pCR} + \Delta f_{pR1} + \Delta f_{pR2} \tag{3.52}$$

$$\%\Delta f_{pT} = \frac{100(\Delta f_{pES} + \Delta f_{pSR} + \Delta f_{pCR} + \Delta f_{pR1} + \Delta f_{pR2})}{f_{pj}} \tag{3.53}$$

where:

Δf_{pT} = Total prestress loss, ksi

f_{pj} = Jacking stress in prestressing strands, ksi

3.5.5 Elastic Shortening

The AASHTO Standard Specifications specify the following expression to estimate the prestress loss in pretensioned members due to elastic shortening (*ES*).

$$ES = \frac{E_s}{E_{ci}} f_{cir} \tag{3.54}$$

where:

E_s = Modulus of elasticity of prestressing strands, ksi

E_{ci} = Modulus of elasticity of girder concrete at transfer, ksi = $33{,}000(w_c)^{3/2}\sqrt{f'_{ci}}$

w_c = Unit weight of girder concrete, kcf

f'_{ci} = Girder concrete strength at transfer, ksi

f_{cir} = Average concrete stress at the center-of-gravity of the pretensioning steel due to pretensioning force and dead load of girder immediately after transfer,

= $\frac{P_{si}}{A} + \frac{P_{si}e_c^2}{I} - \frac{(M_g)e_c}{I}$

P_{si} = Pretensioning force after allowing for the initial prestress losses, kips

M_g = Unfactored bending moment due to girder self-weight, k-in.

e_c = Eccentricity of the prestressing strands at the midspan, in.

A = Area of cross-section of the girder, in.^{2}

I = Moment of inertia of the girder section, in.^{4}

The AASHTO LRFD Specifications specify a similar expression to determine the loss in prestress due to elastic shortening (Δf_{pES}).

$$\Delta f_{pES} = \frac{E_p}{E_{ci}} f_{cgp} \tag{3.55}$$

where:

E_p = Modulus of elasticity of prestressing reinforcement, ksi

E_{ci} = Modulus of elasticity of girder concrete at release, ksi

= $33{,}000(w_c)^{3/2}\sqrt{f'_{ci}}$

w_c = Unit weight of girder concrete, kcf

f'_{ci} = Girder concrete strength at transfer, ksi

f_{cgp} = Sum of concrete stresses at the center-of-gravity of the prestressing steel due to prestressing force at transfer and self-weight of the member at sections of maximum moment, ksi

$$= \frac{P_i}{A} + \frac{P_i e_c^2}{I} - \frac{(M_g)e_c}{I}$$

P_i = Pretension force after allowing for the initial prestress losses, kips

M_g = Unfactored bending moment due to girder self-weight, k-in.

e_c = Eccentricity of the prestressing strand group at the midspan, in.

A = Area of girder cross-section, in.^{2}

I = Moment of inertia of the girder section, in.^{4}

3.5.6 Steel Relaxation

The AASHTO Standard Specifications provide the following expression to estimate the loss of prestress due to steel relaxation (CR_S).

$$CR_S = 5000 - 0.10\, ES - 0.05(SH + CR_C) \tag{3.56}$$

where:

ES = Prestress loss due to elastic shortening, ksi

SH = Prestress loss due to concrete shrinkage, ksi

CR_C = Prestress loss due to concrete creep, ksi

The AASHTO LRFD Specifications provide the following expressions to estimate the prestress losses due to relaxation of steel.

At transfer – low-relaxation strands initially stressed in excess of $0.5f_{pu}$:

$$\Delta f_{pR1} = \frac{\log(24.0t)}{40}\left[\frac{f_{pj}}{f_{py}} - 0.55\right] f_{pj} \tag{3.57}$$

where:

Δf_{pR1}= Prestress loss due to steel relaxation at transfer, ksi

t = Time estimated in days from stressing to transfer [taken as 1 day for this study consistent with the TxDOT bridge design software PSTRS14 (TxDOT 2004)]

f_{pj} = Initial stress in tendon at the end of stressing, ksi

f_{py} = Specified yield strength of prestressing steel, ksi

After transfer – for low-relaxation strands:

$$\Delta f_{pR2} = 0.3\ [20.0 - 0.4\ \Delta f_{pES} - 0.2(\Delta f_{pSR} + \Delta f_{pCR})] \qquad (3.58)$$

where:

Δf_{pR2} = Prestress loss due to steel relaxation after transfer, ksi

Δf_{pES} = Prestress loss due to elastic shortening, ksi

Δf_{pSR} = Prestress loss due to concrete shrinkage, ksi

Δf_{pCR} = Prestress loss due to concrete creep, ksi

3.5.7 Concrete Creep

The Standard Specifications provide the following expression to estimate the prestress loss due to concrete creep (CR_C):

$$CR_C = 12\, f_{cir} - 7\, f_{cds} \qquad (3.59)$$

where:

f_{cir} = Average concrete stress at the center-of-gravity of the pretensioning steel due to pretensioning force and dead load of girder immediately after transfer, ksi

f_{cds} = Concrete stress at the center-of-gravity of pretensioning steel due to all dead loads except the dead load present at the time the pretensioning force is applied, ksi

$$= \frac{M_S e_c}{I} + \frac{M_{SDL}(y_{bc} - y_{bs})}{I_c}$$

M_S = Moment due to slab weight, k-in.

M_{SDL} = Superimposed dead load moment, k-in.

e_c = Eccentricity of the strand at the midspan, in.

y_{bc} = Distance from the centroid of the composite section to extreme bottom fiber of the precast girder, in.

y_{bs} = Distance from center-of-gravity of the strands at midspan to the bottom of the girder, in.

I = Moment of inertia of the non-composite section, in.^{4}

I_c = Moment of inertia of composite section, in.^{4}

The LRFD Specifications provide a similar expression as Standard Specifications to estimate the loss of prestress due to creep of concrete (Δf_{pCR}).

$$\Delta f_{pCR} = 12 f_{cgp} - 7 \Delta f_{cdp} \geq 0 \quad (3.60)$$

where:

f_{cgp} = Sum of concrete stresses at the center-of-gravity of the prestressing steel due to prestressing force at transfer and self-weight of the member at sections of maximum moment, ksi

Δf_{cdp} = Change in concrete stresses at the center-of-gravity of the prestressing steel due to permanent loads except the dead load present at the time the prestress force is applied calculated at the same section as f_{cgp}, ksi

$$= \frac{M_S e_c}{I} + \frac{M_{SDL}(y_{bc} - y_{bs})}{I_c}$$

The additional variables are defined above.

3.5.8 Concrete Shrinkage

The Standard Specifications provide the following expression to estimate the loss in prestressing force due to concrete shrinkage (SH).

$$SH = 17{,}000 - 150\ RH \quad (3.61)$$

where:

RH = Mean annual ambient relative humidity in percent, taken as 60 percent for this parametric study

The LRFD Specifications specify a similar expression to estimate the loss of prestress due to concrete shrinkage (Δf_{pSR}).

$$\Delta f_{pSR} = 17 - 0.15\ H \quad (3.62)$$

where:

H = Mean annual ambient relative humidity in percent, taken as 60 percent for this parametric study

3.5.9 Final Estimate of Required Prestress and Concrete Strengths

The TxDOT methodology is used to optimize the number of strands and the concrete strengths at release and service in this study. This methodology involves several iterations of updating the prestressing strands and concrete strengths to satisfy the allowable stress limits. The step-by-step methodology is described as follows.

1. An initial estimate of concrete strength is taken as 4000 psi at release and 5000 psi at service. The prestress losses are calculated for the estimated preliminary number of strands using the estimated concrete strengths.
2. The calculation of prestress loss due to elastic shortening depends on the initial prestressing force. As the initial loss is unknown at the beginning of the prestress loss calculation process, an initial loss of 8 percent is assumed. Based on this assumption, the prestress loss due to elastic shortening, concrete creep, concrete shrinkage, and steel relaxation at transfer and at service are calculated.

The initial loss percentage is computed. If the initial loss percentage is different from 8 percent, a second iteration is made using the obtained initial loss percentage from the previous iteration. The process is repeated until the initial loss percent converges to 0.1 percent of the previous iteration. The effective prestress at transfer and at service are calculated using the following expressions.

For Standard Specifications:

$$f_{si} = 0.75\, f_s' - \Delta f_{pi} \tag{3.63}$$

$$f_{se} = 0.75\, f_s' - \Delta f_{pT} \tag{3.64}$$

where:

f_{si} = Effective initial prestress, ksi

f_{se} = Effective final prestress, ksi

f_s' = Ultimate strength of prestressing strands, ksi

Δf_{pi} = Instantaneous prestress losses, ksi

Δf_{pT} = Total prestress losses, ksi

For LRFD Specifications:

$$f_{pi} = f_{pj} - \Delta f_{pi} \tag{3.65}$$

$$f_{pe} = f_{pj} - \Delta f_{pT} \tag{3.66}$$

where:

f_{pi} = Effective initial prestress, ksi

f_{pe} = Effective final prestress, ksi

f_{pj} = Jacking stress in prestressing strands, ksi

The total effective prestressing force is calculated by multiplying the calculated effective prestress per strand, area of strand, and the number of strands. The concrete stress at the bottom fiber of the girder due to the effective prestressing force is calculated. If this stress is found to be less than the required prestress, the number of strands is incremented by two in each step until the required prestress is achieved. The initial bottom fiber stress at the hold-down points is calculated and using the allowable stress limit at this section, the required concrete strength at release is determined. The number of strands and concrete strength at release is used to determine the prestress losses for the next trial. The effective prestress after the losses at transfer and at service are then calculated.

The initial concrete stresses at the top and bottom fibers at the girder end, transfer length section, and hold-down points are determined using the effective prestress at transfer. The final concrete stresses at the top and bottom fibers at the midspan section are determined using the applied loads and effective prestress at service. The initial tensile stress at the top fiber at the girder end is minimized by harping the web strands at the girder end. The web strands are incrementally raised as a unit by 2 in. for each step. The steps are repeated until the top fiber stress satisfies the allowable stress limit or the centroid of the topmost row of the harped strands is at a distance of 2 in. from the top fiber of the girder. If the latter case is applicable, the concrete strength at release is updated based on the governing stress.

The expressions used for the determination of stresses at each location are outlined in the following section. The concrete stress at each location is compared with the allowable stresses and, if necessary, the corresponding concrete strength is updated. This process is repeated until the concrete strengths at release and at service converge within 10 psi of the values calculated in the previous iteration. The governing concrete strength at release and at service is established using the greatest required concrete strengths. The program terminates if the required concrete strength at release or service exceeds predefined maximum values for Standard girder designs.

3.6 FLEXURAL DESIGN FOR SERVICE LIMITS

3.6.1 General

The service limit state design of prestressed concrete load-carrying members typically governs the flexural design. However, the strength limit state needs to be checked to ensure safety at ultimate load conditions. The LRFD and Standard Specifications (AASHTO 2004,

2002) provide allowable compressive and tensile stress limits for three loading stages, as provided in Table 3.6. Furthermore, the LRFD Specifications specify various subcategories of service limit states and only Service I and Service III are found to be relevant to the scope of this study. Compression in prestressed concrete is evaluated through the Service I limit state and tension in the prestressed concrete superstructures is evaluated through the Service III limit state with the objective of crack control. The difference, pertaining to this study, between these two limit states is that Service I uses a load factor of 1.0 for all permanent dead loads and live load plus impact, while Service III uses a load factor of 1.0 for all permanent dead loads and a load factor of 0.8 for live load plus impact.

This section describes the equations that are used to compute the compressive and tensile stresses caused due to the applied loading for both specifications. These equations are derived on the basis of simple statical analysis of prestressed concrete bridge girder, using the uncracked section properties and assuming the beam to be homogeneous and elastic.

3.6.2 Preliminary Service Load Stress Check

The tensile stress at the bottom fiber of the girder at midspan due to external loading is evaluated using the Service I limit state load combination for the Standard Specifications and the Service III limit state for the LRFD Specifications. This limit state often controls the service load design of prestressed concrete members and is used for the preliminary design. The formulas used are as follows, with the construction considered to be unshored.

For the Standard Specifications:

$$f_b = \frac{M_g + M_S}{S_b} + \frac{M_{SDL} + M_{LL+I}}{S_{bc}} \tag{3.67}$$

where:

f_b = Concrete stress at the bottom fiber of the girder due to applied loads, ksi

M_g = Unfactored bending moment due to girder self-weight, k-in.

M_S = Unfactored bending moment due to slab weight, k-in.

M_{SDL} = Unfactored bending moment due to superimposed dead loads (barrier and asphalt wearing surface), k-in.

M_{LL+I} = Distributed bending moment due to live load including impact, k-in.

S_b = Section modulus referenced to the extreme bottom fiber of the non-composite precast girder, in.^{3}

S_{bc} = Composite section modulus referenced to the extreme bottom fiber of the precast girder, in.^{3}

For the LRFD Specifications:

$$f_b = \frac{M_g + M_S}{S_b} + \frac{M_{SDL} + (0.8)(M_{LT} + M_{LL})}{S_{bc}} \tag{3.68}$$

where:

M_{LT} = Distributed bending moment due to governing (truck or tandem) load including impact load, k-in.

M_{LL} = Distributed bending moment due to lane load, k-in.

The additional variables were defined above.

3.6.3 Preliminary Estimate of Required Prestress

The preliminary estimate of the required prestress is made once the maximum tensile stress due to service loads at the bottom fiber of the girder is calculated. The difference between the maximum tensile stress and the allowable tensile stress at the bottom fiber gives the required stress due to prestressing. Assuming the total prestress losses of 20 percent and the eccentricity of the strands at the midspan equal to the distance from the centroid of the girder to the bottom fiber, an estimate of the required number of strands is made. For this number of strands the actual midspan eccentricity and bottom fiber stress due to prestressing is calculated. The number of strands is incremented by two in each trial until the final bottom fiber stress satisfies the allowable stress limits. The strands are placed as low as possible on the grid shown in Figures 3.1 and 3.2, and each row is filled before proceeding to the next higher row (TxDOT 2005). The bottom fiber stress at the midspan due to the prestressing force is calculated using the following formula.

$$f_{bp} = \frac{P_{se}}{A} + \frac{P_{se}\, e_c}{S_b} \tag{3.69}$$

where:

f_{bp} = Concrete stress at the bottom fiber of the girder due to prestressing, ksi

P_{se} = Effective pretension force after all losses, kips

A = Girder cross-sectional area, in.^{2}

e_c = Eccentricity of strand group at the midspan, in.

S_b = Section modulus referenced to the extreme bottom fiber of the non-composite precast girder, in.^{3}

3.6.4 Check for Concrete Stresses

3.6.4.1 General

The expressions used to calculate the concrete stress at different sections are outlined in the following subsections. These expressions utilize the notation for the LRFD Specifications. The same expressions are used for calculating the stresses for designs following the Standard Specifications with the corresponding notation. The calculated concrete stress is compared with the corresponding allowable stress limit provided in Table 4.4.

3.6.4.2 Concrete Stress at Transfer

The concrete stress at transfer at different locations along the girder length is determined using the following expressions.

At girder ends – top fiber:

$$f_{ti} = \frac{P_i}{A} - \frac{P_i e_e}{S_t} \tag{3.70}$$

At girder ends – bottom fiber:

$$f_{bi} = \frac{P_i}{A} + \frac{P_i e_e}{S_b} \tag{3.71}$$

At transfer length section – top fiber:

$$f_{ti} = \frac{P_i}{A} - \frac{P_i e_t}{S_t} + \frac{M_g}{S_t} \tag{3.72}$$

At transfer length section – bottom fiber:

$$f_{bi} = \frac{P_i}{A} + \frac{P_i e_t}{S_b} - \frac{M_g}{S_b} \tag{3.73}$$

At hold-down points – top fiber:

$$f_{ti} = \frac{P_i}{A} - \frac{P_i e_c}{S_t} + \frac{M_g}{S_t} \tag{3.74}$$

At hold-down points – bottom fiber:

$$f_{bi} = \frac{P_i}{A} + \frac{P_i\, e_c}{S_b} - \frac{M_g}{S_b} \qquad (3.75)$$

At midspan – top fiber:

$$f_{ti} = \frac{P_i}{A} - \frac{P_i\, e_c}{S_t} + \frac{M_g}{S_t} \qquad (3.76)$$

At midspan – bottom fiber:

$$f_{bi} = \frac{P_i}{A} + \frac{P_i\, e_c}{S_b} - \frac{M_g}{S_b} \qquad (3.77)$$

where:

f_{ti} = Initial concrete stress at the top fiber of the girder, ksi

f_{bi} = Initial concrete stress at the bottom fiber of the girder, ksi

P_i = Pretension force after allowing for the initial losses, kips

M_g = Unfactored bending moment due to girder self-weight at the location under consideration, k-in.

e_c = Eccentricity of the strands at the midspan and hold-down point, in.

e_e = Eccentricity of the strands at the girder ends, in.

e_t = Eccentricity of the strands at the transfer length section, in.

A = Area of girder cross-section, in.^{2}

S_b = Section modulus referenced to the extreme bottom fiber of the non-composite precast girder, in.^{3}

S_t = Section modulus referenced to the extreme top fiber of the non-composite precast girder, in.^{3}

3.6.4.3 Concrete Stress at Intermediate Stage

The concrete stress at the midspan for the intermediate load stage is determined using the following expressions.

$$f_t = \frac{P_{se}}{A} - \frac{P_{se}\, e_c}{S_t} + \frac{M_g + M_S}{S_t} + \frac{M_{SDL}}{S_{tg}} \qquad (3.78)$$

$$f_b = \frac{P_{se}}{A} + \frac{P_{se}\, e_c}{S_b} - \frac{M_g + M_S}{S_b} - \frac{M_{SDL}}{S_{bc}} \qquad (3.79)$$

where:

f_t = Concrete stress at the top fiber of the girder, ksi

f_b = Concrete stress at the bottom fiber of the girder, ksi

P_{se} = Effective pretension force after all losses, kips

M_S = Bending moment due to slab weight, k-in.

M_{SDL} = Bending moment due to superimposed dead load, k-in.

S_{tg} = Composite section modulus referenced to the extreme top fiber of the precast girder, in.^{3}

S_{bc} = Composite section modulus referenced to the extreme bottom fiber of the precast girder, in.^{3}

The additional variables are the same as defined above.

3.6.4.4 Concrete Stresses at Service

The concrete stress at service at the midspan for different load combinations is determined using the following expressions. For the Standard Specifications, the stresses for the following cases of the Service I load combination were investigated.

Concrete stress at the top fiber of the girder under:

Case (I) – Live load + 0.5 × (pretensioning force + dead loads)

$$f_t = \frac{M_{LL+I}}{S_{tg}} + 0.5\left(\frac{P_{se}}{A} - \frac{P_{se}\,e_c}{S_t} + \frac{M_g + M_S}{S_t} + \frac{M_{SDL}}{S_{tg}}\right) \tag{3.80}$$

Case (II) – Service loads

$$f_t = \frac{P_{se}}{A} - \frac{P_{se}\,e_c}{S_t} + \frac{M_g + M_S}{S_t} + \frac{M_{SDL} + M_{LL+I}}{S_{tg}} \tag{3.81}$$

Concrete stresses at bottom fiber of the girder under service loads:

$$f_b = \frac{P_{se}}{A} + \frac{P_{se}\,e_c}{S_b} - \frac{M_g + M_S}{S_b} - \frac{M_{SDL} + M_{LL+I}}{S_{bc}} \tag{3.82}$$

where:

M_{LL+I} = Moment due to live load including impact at the midspan, k-in.

The additional variables are the same as defined for Equation 4.76.

For the LRFD Specifications, the stresses for the Service I and Service III load: combinations were investigated.

Service I – Concrete stresses at the top fiber of the girder under:

Case (I) – 0.5 × (effective prestress force + permanent loads) + transient loads

$$f_t = 0.5\left(\frac{P_{pe}}{A} - \frac{P_{pe}\, e_c}{S_t} + \frac{M_g + M_S}{S_t} + \frac{M_{SDL}}{S_{tg}}\right) + \frac{M_{LL} + M_{LT}}{S_{tg}} \qquad (3.83)$$

Case (II) – Permanent and transient loads

$$f_t = \frac{P_{pe}}{A} - \frac{P_{pe}\, e_c}{S_t} + \frac{M_g + M_S}{S_t} + \frac{M_{SDL}}{S_{tg}} + \frac{M_{LL} + M_{LT}}{S_{tg}} \qquad (3.84)$$

Service III – Concrete stresses at the bottom fiber of the girder:

$$f_b = \frac{P_{pe}}{A} + \frac{P_{pe}\, e_c}{S_b} - \frac{M_g + M_S}{S_b} - \frac{M_{SDL} + 0.8(M_{LT} + M_{LL})}{S_{bc}} \qquad (3.85)$$

where:

P_{pe} = Effective pretension force after all losses, kips

M_{LT} = Bending moment due to truck load including impact, at the section, k-in.

M_{LL} = Bending moment due to lane load at the section, k-in.

3.7 FLEXURAL STRENGTH LIMIT STATE

3.7.1 General

The flexural strength limit state design requires the reduced nominal moment capacity of the member to be greater than the factored ultimate design moment, expressed as follows.

$$\phi M_n \geq M_u \qquad (3.86)$$

where:

M_u = Factored ultimate moment at a section, k-ft.

M_n = Nominal moment strength of a section, k-ft.

ϕ = Resistance factor = 1.0 for flexure and tension of prestressed concrete members

The total bending moment for the ultimate limit state according to AASHTO Standard Specifications given by the Group I factored load combination is as follows.

$$M_u = 1.3[M_g + M_S + M_{SDL} + 1.67(M_{LL+I})] \qquad (3.87)$$

where:

M_g = Unfactored bending moment due to girder self-weight, k-ft.

M_S = Unfactored bending moment due to slab weight, k-ft.

M_{SDL} = Unfactored bending moment due to superimposed dead (barrier and asphalt wearing surface) load, k-ft.

M_{LL+I} = Bending moment due to live load including impact, k-ft.

The total ultimate bending moment for Strength I limit state, according to the AASHTO LRFD Specifications is as follows.

$$M_u = 1.25(DC) + 1.5(DW) + 1.75(LL + IM) \tag{3.88}$$

where:

DC = Bending moment due to all dead loads except wearing surface, k-ft.

DW = Bending moment due to wearing surface load, k-ft.

$LL+IM$ = Bending moment due to live load and impact, k-ft.

The flexural strength limit state design reduces to a check as the number of prestressing strands and the concrete strengths are already established from the service load design. For the case when the flexural limit state is not satisfied, the number of strands is incremented by two, and the service load stresses are checked and concrete strengths are updated if required. This process is carried out until the flexural limit state is satisfied. However, for prestressed concrete members, service load design almost always governs, and the designs satisfying service load criteria usually satisfy the flexural limit state.

3.7.2 Assumptions for Flexural Strength

The AASHTO Standard and LRFD Specifications use different approaches for the calculation of the nominal moment capacity of prestressed concrete girders. The two specifications essentially follow the force and equilibrium formulations with slight modifications. Because the depth of neutral axis and the effective prestress are inter-related, modifications in the force equilibrium formulations are required. The Standard Specifications use an empirical formulation of effective prestress, and the depth of neutral axis is calculated using this value.

The LRFD Specifications use the ultimate strength of the prestressing strands to establish the depth of neutral axis based upon which the effective prestress is calculated. The differences in the methodologies followed by the Standard and LRFD Specifications are outlined in this section. The methodology used in the parametric study for designs based on Standard and LRFD Specifications is also presented. The Standard and LRFD Specifications also allow the use of strut and tie model to determine the design moment strength of the prestressed concrete girders. However, this approach is not considered for the parametric study.

The AASHTO Standard and LRFD Specifications provide the formula for the nominal moment resistance of prestressed concrete girders assuming:

1. the members are uncracked,
2. the maximum usable strain in unconfined concrete at extreme compression fiber is not greater than 0.003,
3. the tensile strength of concrete is neglected,
4. a rectangular stress distribution in the concrete compression zone,
5. a linear variation of strain over the section depth, and
6. the section is transformed based on actual concrete strengths of the slab and the girder.

In the parametric study, the last assumption is not used. A more accurate estimate of the compression contribution of each element (cast-in-place slab, girder flange and girder web) was evaluated for flanged section behavior. This requires the Standard and LRFD specifications expressions to be modified. The modified expressions are provided in the following section.

The Standard and LRFD Specifications define rectangular and flanged section behavior in different ways. The Standard Specifications Article 9.17.2 specifies that rectangular or flanged sections, having prestressing steel only can be considered to behave like rectangular sections if the depth of equivalent rectangular stress block, a, is less than the thickness of the compression flange (slab). The LRFD Specifications consider the section to behave like a rectangular section if the depth of neutral axis, c, lies within the flange (slab). As per LRFD C5.7.3.2.2 (AASHTO 2004), there is an inconsistency in the Standard Specifications' equations for T-sections, which becomes evident when, at first, a rectangular section behavior is assumed and it is found that $c > h_f$, while $a = \beta_1 c < h_f$. When c is recalculated using the expressions for T-section behavior, it can come out to be smaller than h_f or even negative. In order to overcome this deficiency, β_1 is included in the LRFD equations for calculating the nominal flexural strength for the case of T-section behavior.

3.7.3 Equivalent Rectangular Stress Block

The stress distribution in the compression concrete is approximated with an equivalent rectangular stress distribution of intensity $0.85 f'_c$ over a zone bounded by the edges of the cross-section and a straight line located parallel to the neutral axis at a distance $a = \beta_1 c$, where β_1 is the stress block factor. The value of β_1 is 0.85 for concrete strengths less than 4.0 ksi and is reduced at a rate of 0.05 for each 1.0 ksi of strength in excess of 4.0 ksi, but is not taken less than 0.65. For flanged section behavior, the concrete strengths are different for the flange (slab) and the web (girder), which brings an inconsistency in the calculation of the parameter β_1 if the section is not transformed. The LRFD Specifications Article 5.7.2.2 provides three different options to evaluate β_1 when the cross-section behaves as a flanged section:

1. use the β_1 value of the slab for composite design,
2. use the actual values of β_1 for each section, or
3. use the average value of β_1 given by the following expression.

$$\beta_{1avg} = \frac{\Sigma(f'_c A_{cc} \beta_1)}{\Sigma(f'_c A_{cc})} \tag{3.89}$$

where:

β_1 = Stress block factor

f'_c = Concrete strength at service, ksi

A_{cc} = Area of concrete element in compression with the corresponding concrete strength, in.^{2}

The average value of β_1 given by the above equation was used for the parametric study for designs based on the LRFD Specifications to determine the depth of neutral axis when the section behaved as a flanged section. The β_1 for the slab concrete is used in the evaluation of effective prestress for the Standard designs.

3.7.4 Effective Stress in Prestressing Steel

The AASHTO Standard Specifications provide the following empirical relation to estimate the average stress in the bonded prestressing steel at ultimate load. The expression is applicable when the effective prestress after losses is not less than $0.5 f'_s$.

$$f_{su}^{*} = f_s' \left(1 - \frac{\gamma^*}{\beta_1} \rho^* \frac{f_s'}{f_c'} \right) \tag{3.90}$$

where:

f_{su}* = Average stress in pretensioning steel at ultimate load, ksi

γ^* = Factor for type of prestressing steel, taken as 0.28 for low-relaxation strand

β_1 = Stress block factor

ρ^* = Ratio of prestressing steel = $\dfrac{A_s^*}{bd}$

A_s^* = Area of pretensioned reinforcement, in.^{2}

b = Effective flange width, in.

d = Distance from top of slab to centroid of prestressing strands, in.

f_s' = Ultimate strength of prestressing strands, ksi

f_c' = Concrete strength at service (taken as f_c' of slab to be conservative), ksi

The LRFD Specifications specify the following expression to estimate the stress in prestressing steel at ultimate conditions. This expression is applicable when the effective prestress after losses, f_{pe}, is not less than 0.5 f_{pu}, where f_{pu} is the ultimate strength of the prestressing strands.

$$f_{ps} = f_{pu} \left(1 - k \frac{c}{d_p} \right) \tag{3.91}$$

where:

f_{ps} = Average stress in prestressing steel, ksi

f_{pu} = Specified tensile strength of prestressing steel, ksi

k = $2\left(1.04 - \dfrac{f_{py}}{f_{pu}} \right)$ = 0.28 for low-relaxation strands

c = Distance between neutral axis and the compressive face, in.

d_p = Distance from extreme compression fiber to the centroid of the prestressing tendons, in.

3.7.5 Depth of Neutral Axis and Nominal Moment for I-Girders

The provisions of the AASHTO Standard and LRFD Specifications for calculating the depth of neutral axis and the nominal moment resistance of the I-shaped girder sections are outlined below. The methodology used in the parametric study is also described.

3.7.5.1 Standard Specifications

The flexural behavior of the section at ultimate conditions is classified as rectangular or flanged based on the depth of equivalent rectangular stress block. The Standard Specifications specify that if the depth of equivalent rectangular stress block, *a*, is less than the thickness of the compression flange (slab), the section behavior shall be considered as rectangular. The corresponding relationship is given below. Figure 3.12 illustrates the rectangular section behavior of the composite section and the appropriate stress distribution.

$$a = \frac{A_s^* f_{su}^*}{0.85 f'_{cs} b} \leq t \tag{3.92}$$

where:

a = Depth of equivalent stress block, in.

A_s^* = Area of pretensioned reinforcement, in.^{2}

f_{su}^* = Average stress in pretensioning steel at ultimate load, ksi

b = Effective flange width (denoted as b_{eff} in Figure 3.12), in.

f'_{cs} = Flange (slab) concrete compressive strength at service, ksi

t = Depth of compression flange (slab), in.

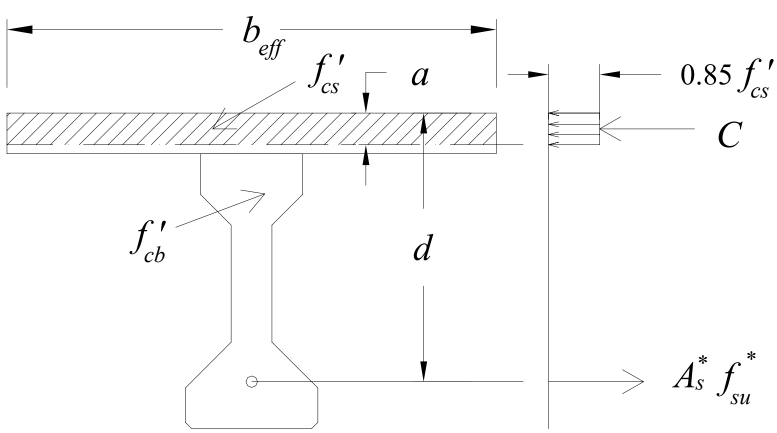

Figure 3.12. Rectangular Section Behavior – Standard Notation.

The above expression can be verified by simple mechanics, and it is valid for the parametric study. The depth of neutral axis, c, is calculated as $c = a/\beta_1$, where β_1 is calculated using the slab concrete compressive strength. The design flexural moment strength for rectangular section behavior can be evaluated using the following expression.

$$\phi M_n = \phi (A_s^*)(f_{su}^*)(d)\left(1 - 0.6\frac{\rho^* f_{su}^*}{f'_{cs}}\right) \tag{3.93}$$

where:

ϕ = Strength reduction factor specified as 1.0 for prestressed concrete members.

M_n = Nominal moment strength at the section, k-ft.

Additional variables are the same as defined earlier.

If the condition in Equation 3.92 is not satisfied, the section shall be checked for the flanged section behavior provided by the following expression.

$$\frac{A_{sr} f_{su}^*}{0.85 f'_{cs} b'} > t \tag{3.94}$$

where:

A_{sr} = $A_s^* - A_{sf}$ (in.^{2})

A_s^* = Area of pretensioned reinforcement, in.^{2}

A_{sf} = Steel area required to develop the ultimate compressive strength of the overhanging portions of the flange, in.^{2}

A_{sf} = $0.85\, f'_{cs}\, (b-b')t / f_{su}^*$

b' = Width of the web, in.

f_{su}^* = Average stress in pretensioning steel at ultimate load, ksi

b = Effective flange width (denoted as b_{eff} in Figure 3.12), in.

f'_{cs} = Flange (slab) concrete strength at service, ksi

t = Depth of compression flange (slab), in.

The design flexural strength of the flanged section is determined as follows.

$$\phi M_n = \phi\left\{A_{sr}\, f_{su}^* d\left(1\text{-}0.6\frac{A_{sr} f_{su}^*}{b' d f'_{cs}}\right) + 0.85 f'_{cs}(b - b')t(d - 0.5t)\right\} \tag{3.95}$$

The above expressions are based on the following assumptions:

1. The section is transformed and the concrete strengths of the transformed slab and the girder are equal. (This assumption is not considered for the parametric study to establish a more accurate estimate of the design flexural moment resistance.)
2. The thickness of the web is constant. (This assumption is also not valid for the parametric study as the neutral axis might fall in the flange of the girder, the fillet portion, or the web.)

Considering the stated reasons, formulas for determining the depth of neutral axis and the design flexural strength of the section are developed for Standard designs in the parametric study for two different cases, as outlined below.

Case I considers the lower portion of the equivalent rectangular stress block lies in the flange of the girder as shown in Figure 3.13. From this figure, the following values may be computed.

$$C_1 = 0.85\, f'_{cs}\, b_{eff}\, t \tag{3.96}$$

$$C_2 = 0.85\, f'_{cb}\, b_f\, (a - t) \tag{3.97}$$

$$T = A_s{*}f_{su}{*} \tag{3.98}$$

From equilibrium,

$$T = C_1 + C_2 \tag{3.99}$$

$$a = \frac{A_s^* f_{su}^* - 0.85 f'_{cs} b_{eff} t + 0.85 f'_{cb} b_f t}{0.85 f'_{cb} b_f} \leq (t + t_f) \tag{3.100}$$

Taking moments about C_1, the nominal design flexural strength is the following.

$$\phi M_n = \phi\, [T(d - 0.5t) - C_2(0.5a)] \tag{3.101}$$

where:

T = Tensile force in the prestressing strands, kips

C_1 = Compression force in the slab, kips

C_2 = Compression force in the girder flange, kips

f'_{cs} = Flange (slab) concrete strength at service, ksi

f'_{cb} = Girder concrete strength at service, ksi

b_{eff} = Effective flange (slab) width, in.

b_f = Flange width of the girder, in.

t = Thickness of the deck slab, in.

Case II considers the lower portion of the equivalent rectangular stress block lies in the web of the girder as shown in Figure 3.14. The contribution of the fillet area is neglected for simplicity.

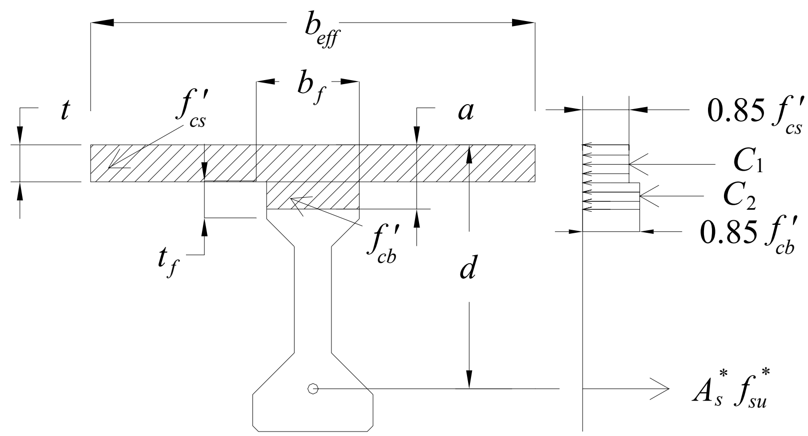

Figure 3.13. Rectangular Stress Block lies in the Girder Flange.

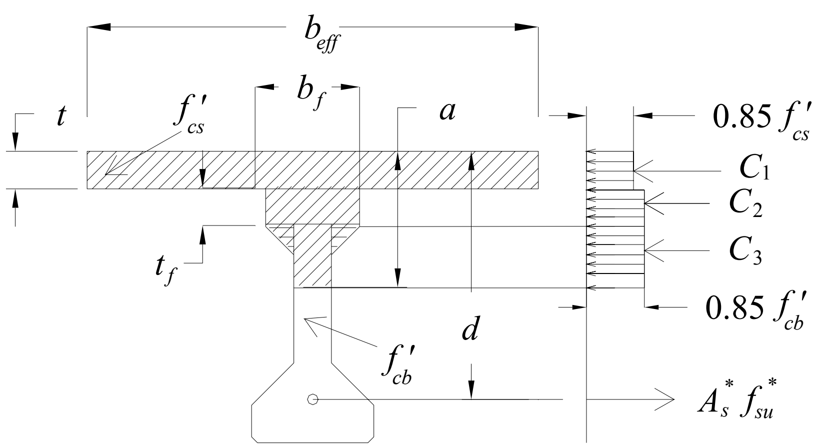

Figure 3.14. Rectangular Stress Block in the Girder Web.

From Figure 3.14, the following values may be computed.

$$C_1 = 0.85\ f'_{cs}\ b_{eff}\ t \tag{3.102}$$

$$C_2 = 0.85\ f'_{cb}\ b_f\ t_f \tag{3.103}$$

$$C_3 = 0.85\ f'_{cb}\ b'\ (a - t_f - t) \tag{3.104}$$

$$T = A_s{}^* f_{su}{}^* \tag{3.105}$$

Applying equilibrium,

$$T = C_1 + C_2 + C_3 \tag{3.106}$$

$$a = \frac{A_s^* f_{su}^* - 0.85f'_{cs}b_{eff}t - 0.85f'_{cb}b_f t_f + 0.85f'_{cb}b't_f + 0.85f'_{cb}b't}{0.85f'_{cb}b'} \tag{3.107}$$

Taking moments about C_1, the nominal design flexural strength is the following.

$$\phi M_n = \phi\,[T(d - 0.5t) - C_2(0.5t + 0.5t_f) - C_3(0.5a + 0.5t_f] \tag{3.108}$$

where:

T = Tensile force in the prestressing strands, kips

C_1 = Compression force in the slab, kips

C_2 = Compression force in the girder flange, kips

C_3 = Compression force in the girder web, kips

t_f = Thickness of girder flange, in.

b' = Girder web width, in.

The impact of ignoring the small fillet area on the design nominal flexural strength was investigated (Adil 2005). It was found that the depth of neutral axis is changed significantly when the fillet portion is ignored. However, the inclusion of the fillet portion does not have a significant contribution to the design flexural strength. If the fillet portion is considered, the expression for the nominal moment strength calculation becomes much more complex than is reasonable in practice. Therefore, the fillet portion is ignored in the parametric study without any significant loss in accuracy in computing the nominal moment strength.

3.7.5.2 LRFD Specifications

The LRFD Specifications assume a section to behave as a flanged section if the neutral axis lies within the web. However, while using this assumption an inconsistency is found when the neutral axis lies within the web (i.e., $c > h_f$) but the depth of the equivalent rectangular stress block is less than the flange thickness, h_f ($a = \beta_1 c < h_f$). When the depth of the neutral axis, c is recomputed based on the ACI 318 (ACI Comm. 318, 2002) approach, the value of c, within the web width is observed to be smaller than h_f and even negative. This inconsistency occurs because the factor β_1 is applied only to the web but not to the flange portion. The LRFD Specifications recommend applying the factor β_1 for both the flange and the web portion of the girder when the section behaves as a flanged section. Figure 3.15 illustrates this case, and Figure 3.16 compares the depth of the neutral axis based on the ACI approach and proposed LRFD approach.

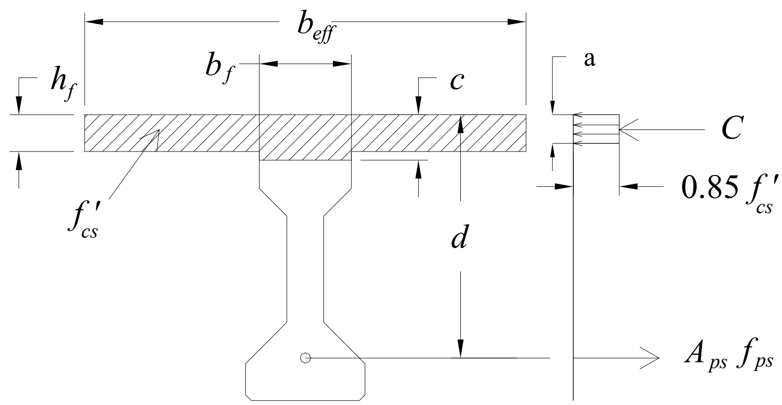

Figure 3.15. Neutral Axis Lies in the Girder Flange and the Stress Block is in the Slab.

Using either approach does not affect the value of the nominal flexural resistance significantly, but there is a significant effect on the depth of neutral axis, c. The provisions for limits for ductility requirement are based on c/d_e value, and there is a significant affect on these provisions when the proposed AASHTO LRFD Specifications approach is used. LRFD Specifications Article 5.7.3 specifies the following expressions to determine the depth of neutral axis and the design flexural moment strength.

Rectangular section behavior is assumed first to determine the depth of neutral axis, as illustrated in Figure 3.17.

$$c = \frac{A_{ps} f_{pu}}{0.85 f'_{cs} \beta_1 b + k A_{ps} \dfrac{f_{pu}}{d_p}} < h_f \tag{3.109}$$

where:

- c = Distance between neutral axis and the compressive face, in.
- A_{ps} = Area of prestressing steel, in.^{2}
- f'_{cs} = Compressive strength of slab concrete at service, ksi
- β_1 = Stress factor of compression block (computed for f'_{cs})
- b = Effective width of compression flange, in.
- f_{pu} = Specified tensile strength of prestressing steel, ksi

$k \quad = \quad 2\left(1.04 - \dfrac{f_{py}}{f_{pu}}\right) = 0.28$ for low-relaxation strand.

$d_p \quad =$ Distance from extreme compression fiber to the centroid of the prestressing tendons, in.

$h_f \quad =$ Depth of compression flange, in.

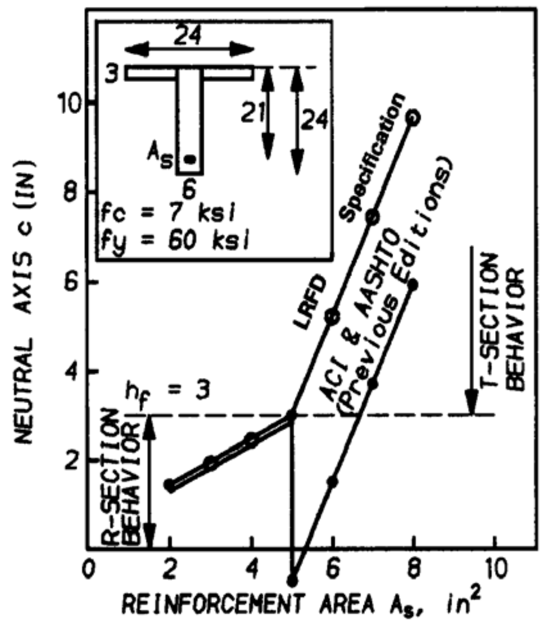

Figure 3.16. Neutral Axis Depth using ACI Approach and Proposed AASHTO LRFD Approach (AASHTO LRFD Specifications 2004).

If the condition in the above expression is satisfied, the nominal flexural resistance of the rectangular section is given as:

$$M_n = A_{ps} f_{ps}\left(d_p - \frac{a}{2}\right) \tag{3.110}$$

where:

$M_n =$ Nominal flexural moment resistance, k-ft.

$f_{ps} =$ Average stress in prestressing steel at nominal conditions, ksi

$d_p =$ Distance from extreme compression fiber to the centroid of the prestressing tendons, in.

$a = \beta_1 c$

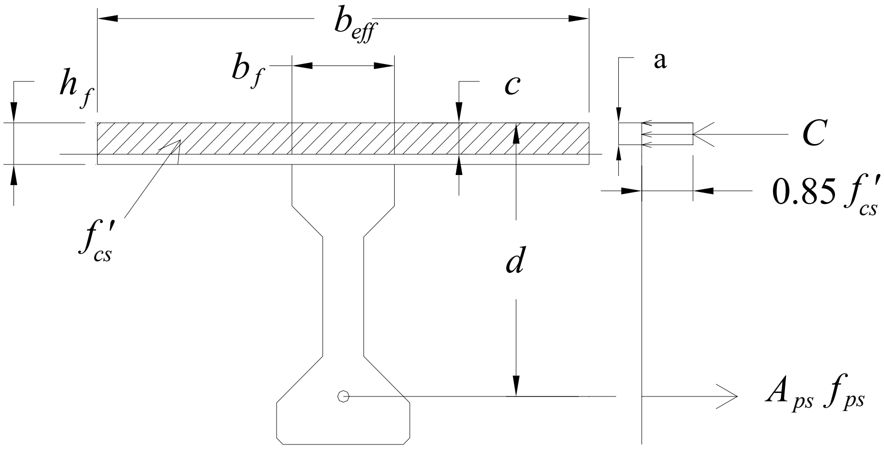

Figure 3.17. Rectangular Section Behavior – LRFD Notation.

If the section is found to behave like a flanged section, the depth of the neutral axis is found using the following expression.

$$c = \frac{A_{ps} f_{pu} - 0.85 f'_{cb} \beta_{1avg} (b - b_w) h_f}{0.85 f'_{cs} \beta_{1avg} b_w + k A_{ps} \dfrac{f_{pu}}{d_p}} \tag{3.111}$$

where:

f'_{cb} = Compressive strength of girder concrete at service, ksi

β_{1avg} = Stress block factor

b_w = Width of the web, in.

The additional variables are the same as defined above.

The nominal flexural moment resistance for a flanged section is given by the following expression.

$$M_n = A_{ps} f_{ps} \left(d_p - \frac{a}{2} \right) + 0.85\, f'_c\, (b - b_w)\, \beta_{1avg} h_f\, (0.5a - 0.5h_f) \tag{3.112}$$

The above equations are based on the following assumptions.

1. The section is transformed and the concrete strengths of the transformed slab and the girder are equal. (This assumption is not considered for the parametric study to establish a more accurate estimate of the design flexural moment resistance.)

2. The thickness of the web is constant. (This assumption is also not valid for the parametric study for I-shaped sections because the neutral axis might fall in the flange of the girder, the fillet portion, or the web.)

Considering the above stated reasons, formulas for determining the depth of the neutral axis and the design flexural strength of the section are developed for different cases in the parametric study, as outlined below.

Case I considers the neutral axis lies in the flange of the girder, as shown in Figure 3.18. Using the AASHTO LRFD approach to multiply the flange compression force with the stress block factor, β_1, gives the following expressions.

$$C_1 = 0.85\, f'_{cs}\, \beta_{1avg} b_{eff} h_f \tag{3.113}$$

$$C_2 = 0.85\, f'_{cb}\, b_f\, \beta_{1avg}(c - h_f) \tag{3.114}$$

$$T = A_{ps} f_{ps} \tag{3.115}$$

$$T = A_{ps}\, f_{pu}\left(1 - k\frac{c}{d_p}\right) \tag{3.116}$$

Applying equilibrium and solving for the neutral axis depth gives the following.

$$T = C_1 + C_2 \tag{3.117}$$

$$c = \frac{A_{ps} f_{pu} - 0.85 h_f \beta_{1avg}\left(f'_{cs} b_{eff} - f'_{cb} b_f\right)}{0.85 f'_{cb} \beta_{1avg} b_f + k A_{ps}\dfrac{f_{pu}}{d_p}} \le h_f + t_f \tag{3.118}$$

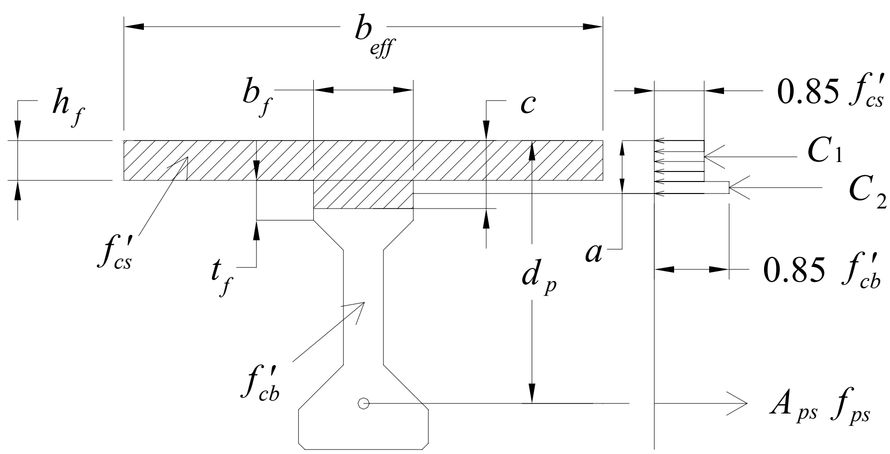

Figure 3.18. Neutral Axis lies in the Girder Flange.

Taking moments about C_1, the reduced nominal flexural moment strength at the section is as follows.

$$\phi M_n = \phi [T(d_p - 0.5h_f) - C_2(0.5a)] \tag{3.119}$$

where:

T = Tensile force in the prestressing strands, kips

C_1 = Compression force in the slab, kips

C_2 = Compression force in the girder flange within stress block depth, kips

f'_{cs} = Flange (slab) concrete strength at service, ksi

f'_{cb} = Girder concrete strength at service, ksi

b_{eff} = Effective flange width, in.

b_f = Girder flange width, in.

h_f = Thickness of slab, in.

β_{1avg} = Stress block factor

Case II considers the neutral axis lies in the fillet portion of the girder as shown in Figure 3.19. This case was ignored for Standard designs as the fillet portion does not affect the design moment resistance significantly. However, it was found that ignoring the fillet contribution changes the depth of the neutral axis significantly. As the ductility limits for the LRFD Specifications are based on the depth of the neutral axis, the fillet contribution for estimating the neutral axis depth cannot be ignored. However, for nominal moment calculations, the fillet contribution is ignored for simplicity and because it has little effect on the flexural capacity.

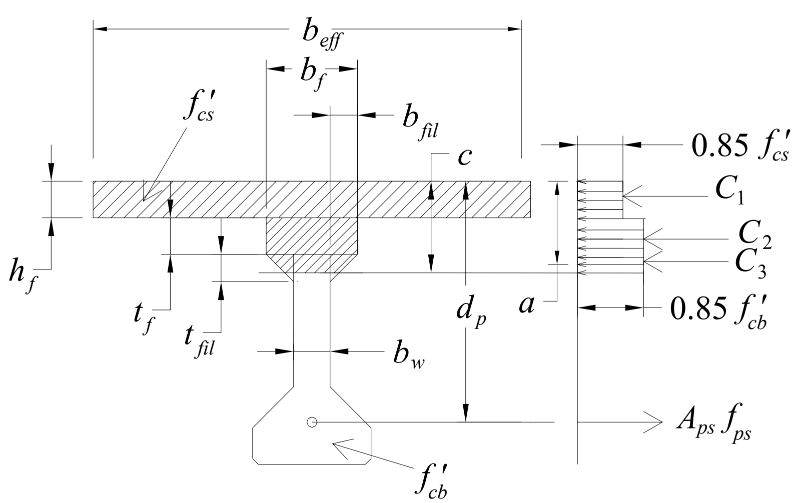

Figure 3.19. Neutral Axis lies in the Fillet Portion of the Girder.

Using the LRFD approach to multiply the flange compression with the factor β_{1avg} gives the following expressions.

$$C_1 = 0.85\, f'_{cs}\, \beta_{1avg} b_{eff} h_f \tag{3.120}$$

$$C_2 = 0.85\, f'_{cb}\, \beta_{1avg} b_f\, t_f \tag{3.121}$$

when $c \leq h_f + t_f + t_{fil}$:

$$C_3 = 0.85\, f'_{cb}\, \beta_{1avg}(c - h_f - t_f)\left\{ b_w + b_{fil} + b_{fil} \frac{\left[t_{fil} - \beta_{1avg}(c - h_f - t_f) \right]}{t_{fil}} \right\} \tag{3.122}$$

$$T = A_{ps} f_{ps} \tag{3.123}$$

$$T = A_{ps}\, f_{pu} \left(1 - k \frac{c}{d_p} \right) \tag{3.124}$$

Applying the equilibrium gives the following expression.

$$T = C_1 + C_2 + C_3 \tag{3.125}$$

Imposing the equilibrium condition in the above equation results in a quadratic equation in c, which can then be determined. For the moment resistance calculation, the fillet contribution is neglected. The Equation 3.122 is modified to the following.

$$C_3 = 0.85\, f'_{cb}\, \beta_{1avg}\,(c - h_f - t_f)\, b_w \tag{3.126}$$

Taking moments about C_1, the design flexural strength at the section can be given as:

$$\phi M_n = \phi\,[T\,(d_p - 0.5h_f) - C_2\,(0.5h_f + 0.5t_f) - C_3\,(0.5a + 0.5t_f] \tag{3.127}$$

where:

T = Tensile force in the prestressing strands, kips

C_1 = Compression force in the slab, kips

C_2 = Compression force in the girder flange, kips

C_3 = Compression force in the girder web within the stress block depth, kips

f'_{cs} = Flange (slab) concrete strength at service, ksi

f'_{cb} = Girder concrete strength at service, ksi

b_{eff} = Effective flange width, in.

b_f = Flange width of the girder, in.

h_f = Thickness of the slab, in.

t_{fil} = Thickness of the girder fillet, in.

b_{fil} = Girder fillet width, in.

β_{1avg} = Stress block factor

Case III considers the neutral axis lies in the web portion of the girder as shown in Figure 3.20. Using the LRFD Specifications approach to multiply the flange compression with the factor β_{1avg} gives the following expressions.

$$C_1 = 0.85\, f'_{cs}\, \beta_{1avg}\, b_{eff}\, h_f \tag{3.128}$$

$$C_2 = 0.85\, f'_{cb}\, \beta_{1avg}\, b_f\, t_f \tag{3.129}$$

$$C_3 = 0.85\, f'_{cb}\, \beta_{1avg}\, t_{fil}\, (b_w + b_{fil}) \tag{3.130}$$

$$C_4 = 0.85\, f'_{cb}\, \beta_{1avg}\, (c - h_f - t_f - t_{fil}) b_w \tag{3.131}$$

$$T = A_{ps} f_{ps} \tag{3.132}$$

$$T = A_{ps}\, f_{pu} \left(1 - k \frac{c}{d_p} \right) \tag{3.133}$$

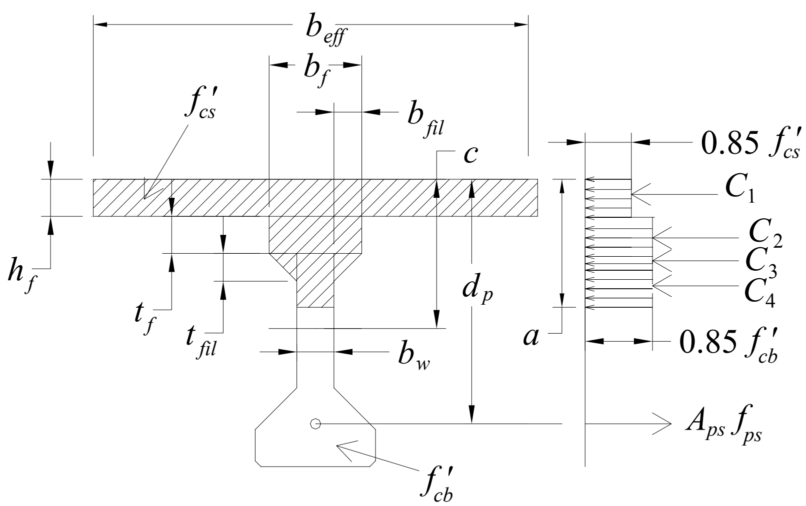

Figure 3.20. Neutral Axis Lies in the Web Portion of the Girder.

Applying the equilibrium condition gives the following expression.

$$T = C_1 + C_2 + C_3 + C_4 \tag{3.134}$$

$$c = \frac{A_{ps} f_{pu} - 0.85 h_f \beta_{1avg} (f'_{cs} b_{eff} - f'_{cb} b_w) - 0.85 f'_{cb} \beta_{1avg} t_f (b_f - b_w) - 0.85 f'_{cb} \beta_{1avg} t_{fil} b_{fil}}{0.85 f'_{cb} \beta_{1avg} b_w + k A_{ps} \dfrac{f_{pu}}{d_p}} \tag{3.135}$$

Taking moments about C_1, the reduced nominal flexural strength at the section can be given as:

$$\phi M_n = \phi \left[T (d_p - 0.5h_f) - C_2 (0.5h_f + 0.5t_f) - C_3 \left\{ \frac{t_{fil}}{3} \left[\frac{3b_w + 2b_{fil}}{2b_w + 2b_{fil}} \right] + t_f + 0.5h_f \right\} - C_4 (0.5a + 0.5t_f + 0.5t_{fil}) \right] \tag{3.136}$$

where:

C_3 = Compression force in the fillet and the web between fillets, kips

C_4 = Compression force in the web portion (excluding web portion between the fillets) under the stress block, kips

t_{fil} = Thickness of girder fillet, in.

b_{fil} = Girder fillet width, in.

b_w = Girder web width, in.

β_{1avg} = Stress block factor

3.7.6 Depth of Neutral Axis and Nominal Moment Resistance for U54 Girders

As a part of this study, three equations were derived to calculate the nominal flexural strength of the Texas U54 beam based on the conditions of equilibrium and strain compatibility. One of the equations is for the case when the neutral axis falls within the deck slab, and the other two equations are for the case when the neutral axis falls within the depth of the Texas U54 beam. These three locations of the neutral axis are shown in Figure 3.21. As noted for Type C and Type IV girders, the term β_1 is included in the equations according to the LRFD C5.7.3.2.2. For the U54 girders, the same equations were used for both the Standard and LRFD Specifications.

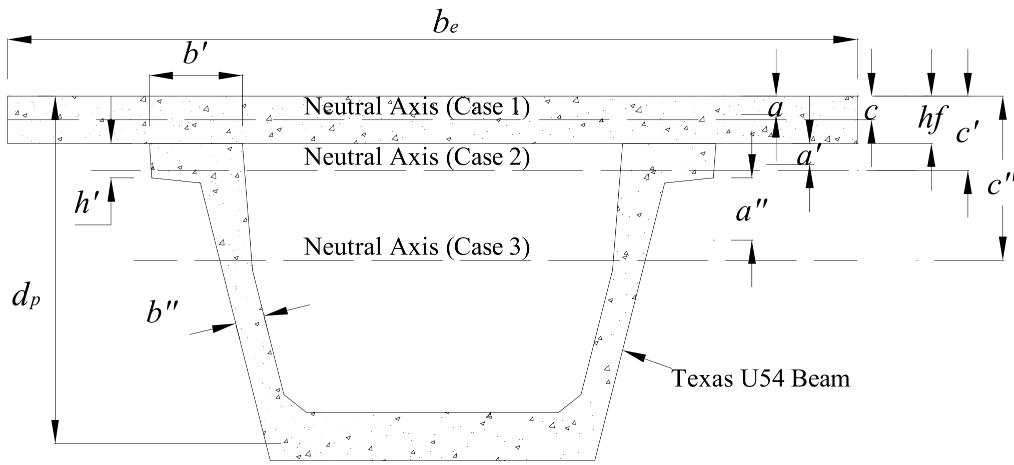

Figure 3.21. Neutral Axis Location.

3.7.6.1 Rectangular Section Behavior (Case 1)

Rectangular section behavior occurs when the neutral axis falls within the thickness of the deck slab. The reduced nominal moment strength of Texas U54 beams can be found using the following equations.

$$c = \frac{A_{ps} f_{ps}}{0.85 f'_{cs} b_e \beta_{1s} + \dfrac{k}{d_p} A_{ps} f_{ps}} \tag{3.137}$$

$$\phi M_n = \phi \left[A_{ps} f_{ps} \left(d_p - \frac{a}{2} \right) \right] \tag{3.138}$$

where:

β_{1s} = Stress block factor, β_1, for the deck slab based on f'_{cs}

b_e = Effective flange width, in.

ϕ = Resistance factor = 1.0 for flexural limit state for prestressed members

A_{ps} = Area of prestressing tendons, in.^{2}

M_n = Nominal moment strength at ultimate conditions, k-in.

a = Depth of the equivalent stress block = $c\,\beta_{1s}$, in.

3.7.6.2 Neutral Axis Falls within the U54 Flanges (Case 2)

T-section behavior occurs when the neutral axis falls within the depth of the precast U54 beam section. Due to the difference in the concrete compressive strengths at the interface of the CIP deck slab and the precast U54 beam, a stress discontinuity is introduced by considering different equivalent stress blocks for the deck slab and the U54 beam. LRFD Articles 5.7.2.2 and C5.7.2.2 recommend three different ways to account for the stress block factor, β_1, which bears a different value for the deck slab than the U54 beam because of their different concrete compressive strengths. In this study, the stress block factor for slab, β_{1s}, is calculated corresponding to f'_{cs} and the stress block factor for the U54 beam, β_{1b}, is calculated corresponding to f'_{cb}.

When the neutral axis lies within the U54 beam flange thickness, h', the following equations are used to calculate the nominal flexural strength at the ultimate conditions. This situation corresponds to Case 2 as shown in Figure 3.21.

$$c' = \frac{\left[A_{ps} f_{ps} - 0.85 h_f \left(f'_{cs} b_e \bar{\beta}_{1s} - f'_{cb} b' \frac{\beta_{1b}}{\beta_{1s}} \right) \right]}{0.85 f'_{cb} b' \beta_{1b} + \frac{k}{d_p} A_{ps} f_{ps}} \tag{3.139}$$

$$\phi M_n = \phi \left[A_{ps} f_{ps} \left(d_p - \left(h_f + \frac{a'}{2} \right) \right) + 0.85 f'_{cs} b_e \bar{\beta}_{1s} \left(\frac{h_f + a'}{2} \right) \right] \tag{3.140}$$

where:

c' = Distance between neutral axis (Case 2) and extreme compression fiber, in.

β_{1b} = Stress block factor, β_1, for the U54 section based on f'_{cb}

$\bar{\beta}_{1s}$ = Same value as β_{1s}. The bar on top of β signifies that the term $\bar{\beta}_{1s}$ is included in the original equation derived based on principles of equilibrium and strain compatibility to account for the inconsistency as per LRFD C5.7.3.2.2.

b' = Effective flange width, in.

h_f = Flange thickness, in.

a' = Depth of the equivalent stress block of the compression area in the U54 beam flanges only = $\left(c - \frac{h_f}{\beta_{1s}}\right)\beta_{1b}$, in.

3.7.6.3 Neutral Axis Falls within the U54 Beam Web (Case 3)

When the neutral axis lies within the U54 beam web, the following equations are developed to calculate the nominal flexural strength at the ultimate conditions. This situation corresponds to Case 3 as shown in Figure 3.21.

$$c'' = \frac{\left[A_{ps}f_{ps} - \left[0.85h_f\left(f'_{cs}b_e\overline{\beta}_{1s} - f'_{cb}b'\frac{\beta_{1b}}{\beta_{1s}}\right) + 0.85f'_{cb}h'\left(b'\overline{\beta}_{1b} - b''\frac{\beta_{1b}}{\beta_{1s}}\right)\right]\right]}{0.85f'_{cb}b''\beta_{1b} + \frac{k}{d_p}A_{ps}f_{ps}} \quad (3.141)$$

$$\phi M_n = \phi\left[A_{ps}f_{ps}\left(d_p - \left(h_f + h' + \frac{a''}{2}\right)\right) + 0.85f'_{cs}b_e\overline{\beta}_{1s}\left(\frac{h_f + a''}{2} + h'\right) + 0.85f'_{cb}b'\overline{\beta}_{1b}\left(\frac{h' + a''}{2}\right)\right] \quad (3.142)$$

where:

c'' = Distance between the neutral axis (Case 3) and the extreme compression fiber, in.

b'' = Combined width of the webs of the U54 section, in.

$\overline{\beta}_{1b}$ = Same value as β_{1b}. The bar on top of β signifies that the term $\overline{\beta}_{1b}$ is included in the original equation derived based on principle of equilibrium and strain compatibility to account for the inconsistency as per LRFD C5.7.3.2.2.

h' = U54 flange thickness, in.

a'' = Depth of the equivalent stress block of the compression area in the U54 beam web only = $\left(c - \frac{h_f}{\beta_{1s}} - \frac{h'}{\beta_{1b}}\right)\beta_{1b}$, in.

3.7.7 Reinforcement Limits

3.7.7.1 Maximum Steel Reinforcement

The AASHTO Standard Specifications require that the maximum prestressing steel be limited to ensure yielding of steel when ultimate capacity is reached. The Standard Specifications Article 9.18.1 specifies the limits of reinforcement as follows.

Reinforcement index for rectangular sections:

$$\frac{\rho^* f_{su}^*}{f_c'} < 0.36\beta_1 \tag{3.143}$$

Reinforcement index for flanged sections:

$$\frac{A_{sr} f_{su}^*}{b' d f_c'} < 0.36\beta_1 \tag{3.144}$$

If the above maximum reinforcement limits are not satisfied, the Standard Specifications recommend the design flexural moment strength of the girder to be limited as follows.

For rectangular sections:

$$\phi M_n = \phi\ [(0.36\beta_1 - 0.08\beta_1^2) f_c'\ b\ d^2] \tag{3.145}$$

For flanged sections:

$$\phi M_n = \phi\ [(0.36\beta_1 - 0.08\beta_1^2) f_c'\ b\ d^2 + 0.85 f_c'(b - b')\ t\ (d\text{-}0.5t)] \tag{3.146}$$

where:

ρ^* = Ratio of prestressing reinforcement $= \frac{A_s^*}{bd}$

A_s^* = Area of prestressing reinforcement, in.^{2}

b = Effective flange width, in.

d = Distance from extreme compression fiber to centroid of prestressing force, in.

f_{su}^* = Average stress in prestressing steel at ultimate load, ksi

f_c' = Compressive strength of slab concrete at service, ksi

β_1 = Stress block factor

A_{sr} = Steel area required to develop the compressive strength of the overhanging portions of the slab, in.^{2}

ϕ = Resistance factor specified as 1.0 for flexure of prestressed concrete member

M_n = Nominal moment strength at the section, k-in.

b' = Width of web of a flanged member, in.

t = Average thickness of the flange, in.

The above flexural moment strength limit provided by the Standard Specifications for flanged section behavior is based on the transformed section. However, for the parametric study a transformed section was not considered because refined equations were developed for computation of moment strength of the flanged sections. Hence, a conservative estimate of the design flexural strength can be made by using the concrete strength of the slab for the entire flanged section, as the concrete strength of slab is less than the girder concrete strength. This method is used in the parametric study.

LRFD Specifications Article 5.7.3.3.1 specifies the maximum total amount of prestressed and non-prestressed reinforcement to be limited such that:

$$\frac{c}{d_e} \leq 0.42 \tag{3.147}$$

where:

c = Distance from the extreme compression fiber to the neutral axis, in.

d_e = Corresponding effective depth from the extreme compression fiber to the centroid of the tensile force in the tensile reinforcement, in.

$$= \frac{A_{ps} f_{ps} d_p + A_s f_y d_s}{A_{ps} f_{ps} + A_s f_y} \tag{3.148}$$

The parametric study only considers fully prestressed sections, for which the effective depth d_e reduces to d_p. In case the above limit is not satisfied, the following equations are provided in the LRFD Specifications to limit the flexural resistance of the girder section.

For rectangular sections:

$$M_n = [(0.36\beta_{1avg} - 0.08\beta_{1avg}^2) f'_c \, b \, d_e^2] \tag{3.149}$$

For flanged sections:

$$M_n = [(0.36\beta_{1avg} - 0.08\beta_{1avg}^2) f'_c \, b_w \, d_e^2 + 0.85\beta_{1avg} f'_c (b\text{-}b_w) \, h_f \, (d_e\text{-}0.5h_f)] \tag{3.150}$$

where:

M_n = Nominal moment strength at the section, k-ft.

b = Effective flange width, in.

f'_c = Compressive strength of slab concrete at service, ksi

β_{1avg} = Stress block factor

b_w = Width of web of a flanged member, in.

h_f = Compression flange depth, in.

Additional variables are the same as defined above.

The flexural moment strength limit provided by the LRFD Specifications for flanged section behavior is based on the transformed section. However, for the parametric study, transformed section was not considered. Hence, a conservative estimate of the design flexural strength can be made by using the concrete strength of the slab. This method is used in the parametric study.

3.7.7.2 Minimum Steel Reinforcement

The Standard Specifications Article 9.18.2 requires the minimum amount of prestressed and non-prestressed reinforcement to be adequate to develop an ultimate moment at the critical section of at least 1.2 times the cracking moment, M_{cr}^{*}.

$$\phi M_n \geq 1.2\ M_{cr}^{*} \tag{3.151}$$

where:

M_n = Nominal flexural moment strength, k-in.

M_{cr}^{*} = Cracking moment, k-in.

$$= (f_r + f_{pe})\, S_c - M_{d/nc}\left(\frac{S_c}{S_b} - 1\right) \tag{3.152}$$

f_r = Modulus of rupture, psi

= $7.5\sqrt{f_c'}$ for normal weight concrete

f_c' = Compressive strength of girder concrete at service, psi

f_{pe} = Compressive stress in concrete due to effective prestress force at extreme fiber of section where tensile stress is caused by externally applied loads, ksi

$$= \frac{P_{se}}{A} + \frac{P_{se} e_c}{S_b}$$

P_{se} = Effective prestress force after losses, kips

A = Area of cross-section, in.^{2}

e_c = Eccentricity of prestressing strands at midspan, in.

S_b = Section modulus of non-composite section referenced to the extreme fiber where tensile stress is caused by externally applied loads, in.^{3}

S_c = Section modulus of composite section referenced to the extreme fiber where tensile stress is caused by externally applied loads, in.^{3}

$M_{d/nc}$ = Non-composite dead load moment at midspan due to self-weight of girder and weight of slab, k-in.

The above limit is waived at the sections where the area of prestressed and non-prestressed reinforcement provided is at least one-third greater than that required by analysis based on the loading combinations.

The LRFD Specifications Article 5.7.3.3.2 specifies the minimum amount of prestressed and non-prestressed tensile reinforcement such that a factored flexural resistance, M_r, is at least equal to:

- 1.2 times the cracking moment, M_{cr}, determined on the basis of elastic stress distribution and the modulus of rupture, f_r, of the concrete, and
- 1.33 times the factored moment required by the applicable strength load combination.

The cracking moment is given by the following formula.

$$M_{cr} = (f_r + f_{cpe})\, S_c - M_{dnc}\left(\frac{S_c}{S_{nc}} - 1\right) \geq S_c f_r \tag{3.153}$$

where:

M_{cr} = Cracking moment, k-in.

f_{cpe} = Compressive stress in concrete due to effective prestress forces at extreme fiber of section where tensile stress is caused by externally applied loads, ksi

= $\dfrac{P_{pe}}{A} + \dfrac{P_{pe}e_c}{S_b}$

P_{pe} = Effective prestress force after losses, kips

e_c = Eccentricity of prestressing strands at midspan, in.

M_{dnc} = Total unfactored non-composite dead load moment, k-in.

S_{nc} = Section modulus referenced to the extreme fiber of the non-composite section where tensile stress is caused by externally applied loads, in.^{3}

S_c = Section modulus referenced to the extreme fiber of the composite section where tensile stress is caused by externally applied loads, in.^{3}

f_r = Rupture modulus specified as $0.24\sqrt{f'_c}$ for normal-weight concrete, ksi

f'_c = Compressive strength of girder concrete at service, ksi

3.8 TRANSVERSE SHEAR DESIGN

3.8.1 General

The AASHTO Standard and LRFD Specifications require that prestressed concrete flexural members be reinforced for shear and diagonal tension stresses. However, the two specifications follow different methodologies to determine the design shear strength of a member. The Standard Specifications use a constant 45-degree truss analogy to predict shear behavior where concrete in compression acts as struts and tension steel acts as ties. The LRFD Specifications use a variable angle truss analogy with modified compression strength of concrete popularly known as "Modified Compression Field Theory (MCFT)." MCFT is a rational method based on equilibrium, compatibility, and constitutive relationships and is a unified approach applicable to both prestressed and non-prestressed concrete members. It also accounts for the tension in the longitudinal reinforcement due to shear and the stress transfer across cracks.

For the transverse shear design approach using MCFT, the angle of the diagonal compressive stress is considered to be a variable that is determined in an iterative manner. In contrast, the Standard Specifications consider the diagonal compressive stress angle as constant at 45 degrees. This change is significant for prestressed concrete members because the angle of inclination of the diagonal compressive stress is typically 20 to 40 degrees due to the effect of the prestressing force (PCI 2003).

Another difference in the two approaches is in the determination of the critical section for shear. In the MCFT, the critical section for shear design is determined using an iterative process. In the Standard Specifications, the critical section is constant at a pre-determined section corresponding to the 45-degree angle assumed for the diagonal compressive stress.

3.8.2 Standard Specifications

The following section outlines the shear design procedures specified by the Standard Specifications Article 9.20. Shear reinforcement is not necessary if the following condition is met.

$$V_u < \frac{\phi V_c}{2} \tag{3.154}$$

where:

V_u = Factored shear force at the section, kips =

= $1.3(V_d + 1.67\ V_{LL+I})$ for this study

V_d = Shear force at the section due to dead loads, kips

V_{LL+I} = Shear force at the section due to live load including impact load, kips

V_c = Nominal shear strength provided by the concrete, taken as the lesser of V_{ci} (see Equation 3.156) and V_{cw} (see Equation 3.157), kips

ϕ = Strength reduction factor, specified as 0.9 for shear of prestressed concrete members

If the condition in the above equation is not satisfied, the member shall be designed such that:

$$V_u \leq \phi\,(V_c + V_s) \tag{3.155}$$

where:

V_s = Nominal shear strength provided by the web reinforcement, kips

The shear design in the parametric study is carried out at the critical section for shear. The critical section is specified as $h_c/2$ from the face of the support, where h_c is the depth of the composite section. However, as the support dimensions are unknown in this study the critical section is calculated from the centerline of the bearing support, which yields a slightly conservative estimate of the required web reinforcement. The concrete contribution, V_c, is taken as the force required to produce shear cracking. The Standard Specifications require that V_c be taken as the lesser of V_{ci} or V_{cw}, which are the shear forces that produce flexural-shear cracking and web-shear cracking, respectively.

$$V_{ci} = 0.6\sqrt{f_c'}\,b'd + V_d + \frac{V_i\,M_{cr}}{M_{max}} \geq 1.7\,\sqrt{f_c'}\,b'd \tag{3.156}$$

$$V_{cw} = (3.5\,\sqrt{f_c'} + 0.3\,f_{pc})\,b'd + V_p \tag{3.157}$$

where:

V_{ci} = Nominal shear strength provided by concrete when diagonal cracking results from combined shear and moment, kips

V_{cw} = Nominal shear strength provided by concrete when diagonal cracking results from excessive principal tensile stress in the web, kips

f_c' = Compressive strength of girder concrete at service, ksi

b' = Width of the web of a flanged member, in.

d = Distance from extreme compressive fiber to centroid of pretensioned reinforcement, but not less than $0.8h_c$, in.

h_c = Depth of composite section, in.

V_d = Shear force at the section due to dead loads, kips

V_i = Factored shear force at the section due to externally applied loads occurring simultaneously with M_{max}, kips

= $V_{mu} - V_d$

V_{mu} = Factored shear force occurring simultaneously with M_u, conservatively taken as maximum shear force at the section, kips

M_{cr} = Moment causing flexural cracking of section due to external loads, k-in.

$$= \left(6\sqrt{f_c'} + f_{pe} - f_d\right)\frac{I}{Y_t}$$

f_{pe} = Compressive stress in concrete due to effective pretension force at extreme fiber of section where tensile stress is caused by external loads, i.e., bottom fiber of the girder in present case, ksi

$$= \frac{P_{se}}{A} + \frac{P_{se}e_x}{S_b}$$

f_{pc} = Compressive stress in concrete at centroid of the cross-section resisting externally applied loads, ksi

$$= \frac{P_{se}}{A} - \frac{P_{se}e_x(y_{bcomp} - y_b)}{I} + \frac{M_D(y_{bcomp} - y_b)}{I}$$

P_{se} = Effective prestress force after all losses. If the section at a distance $h_c/2$ from the face of the support is closer to the girder end than the transfer length (50 strand diameters) the prestressing force is assumed to vary linearly from 0 at the end to maximum at the transfer length section, kips

e_x = Eccentricity of the strands at the section considered, in.

A = Area of girder cross-section, in.^{2}

S_b = Section modulus referenced to the extreme bottom fiber of the non-composite section, in.^{3}

f_d = Stress due to unfactored dead load, at extreme fiber of section where tensile stress is caused by externally applied loads, ksi

$$= \left[\frac{M_g + M_S}{S_b} + \frac{M_{SDL}}{S_{bc}}\right]$$

M_g = Unfactored bending moment due to girder self-weight, k-in.

M_S = Unfactored bending moment due to slab weight, k-in.

M_{SDL} = Unfactored superimposed dead load moment, k-in.

S_{bc} = Composite section modulus referenced to the extreme bottom fiber of the precast girder, in.^{3}

M_{max} = Maximum factored moment at the section due to externally applied loads, k-in.

= $M_u - M_d$

M_u = Factored bending moment at the section, k-in.

= $1.3(M_d + 1.67\, M_{LL+I})$

M_d = Bending moment at section due to unfactored dead loads, k-in.

M_{LL+I}= Bending moment at section due to live load including impact load, k-in.

I = Moment of inertia of the girder cross-section, in.^{4}

y_{bcomp}= Lesser of y_{bc} and the distance from bottom fiber of the girder to the junction of the web and top flange, in.

y_{bc} = Distance from the centroid of the composite section to the extreme bottom fiber of the precast girder, in.

y_b = Distance from the centroid to the extreme bottom fiber of the non-composite precast girder, in.

M_D = Moment due to unfactored non-composite dead loads at the critical section, k-in.

V_p = Vertical component of prestress force for harped strands, kips

= $P_{se} \sin\Psi$

Ψ = Angle of the harped tendons to the horizontal, radians

The area of the web reinforcement shall be provided such that the condition in Equation 3.149 is satisfied. The nominal shear strength provided by steel reinforcement, V_s, is calculated using the following expression.

$$V_s = \frac{A_v f_y d}{s} < 8\sqrt{f'_c}\, b'd \tag{3.158}$$

The minimum area of web reinforcement is limited to the following value.

$$A_{v\,min} = \frac{50b's}{f_y} \tag{3.159}$$

where:

A_v = Area of web reinforcement, in.^{2}

b' = Width of web of a flanged member, in.

f'_c = Compressive strength of girder concrete at service, ksi

s = Spacing of web reinforcement, in.

f_y = Yield strength of web reinforcement, ksi

d = Distance from extreme compressive fiber to centroid of pretensioned reinforcement, but not less than $0.8h_c$, in.

h_c = depth of composite section, in.

The spacing of the web reinforcement shall not exceed $0.75h_c$ or 24 in. If V_s exceeds $4\sqrt{f'_c}\,b'\,d$ the maximum spacing shall be reduced by one-half.

3.8.3 LRFD Specifications

The LRFD Specifications use the Modified Compression Field Theory for the shear design provisions. The MCFT takes into account different factors such as strain condition of the section and shear stress in the concrete to predict the shear strength of the section. The shear strength of concrete is approximated based on a parameter β. The critical section for shear is calculated based on the angle of inclination of the diagonal compressive stress, θ. If the values of these parameters are taken as θ = 45 degrees and β = 2, the theory will yield the results similar to the 45-degree truss analogy method employed in the Standard Specifications. The LRFD Specifications require that transverse reinforcement is provided at sections with the following condition.

$$V_u > 0.5\,\phi\,(V_c + V_p) \tag{3.160}$$

where:

V_u = Factored shear force at the section, kips

= $1.25(DC) + 1.5(DW) + 1.75(LL + IM)$ for this study

DC = Shear force at the section due to dead loads except wearing surface weight, kips

DW	=	Shear force at the section due to wearing surface weight, kips
$LL+IM$	=	Shear force at the section due to live load including impact, kips
V_c	=	Nominal shear strength provided by concrete, kips
ϕ	=	Strength reduction factor specified as 0.9 for shear of prestressed concrete members.
V_p	=	Component of prestressing force in the direction of shear force, kips

The AASHTO LRFD Specifications specify the critical section for shear near the supports as the larger value of $0.5d_v\cot\theta$ or d_v, measured from the face of the support, where:

d_v	=	Effective shear depth, in.
	=	Distance between resultants of tensile and compressive forces, (d_e - a/2), but not less than the greater of ($0.9d_e$) or ($0.72h$), in.
d_e	=	Corresponding effective depth from the extreme compression fiber to the centroid of the tensile force in the tensile reinforcement, in.
a	=	Depth of compression block, in.
h	=	Depth of composite section, in.
θ	=	Angle of inclination of diagonal compressive stresses (slope of compression field). The value of θ is unknown and is assumed to be 23 degrees at the beginning of design, and iterations are made until it converges to a particular value.

The nominal shear resistance at a section is the lesser of the following two values:

$$V_n = (V_c + V_s + V_p) \text{ and} \tag{3.161}$$

$$V_n = 0.25\ f_c'\ b_v d_v + V_p \tag{3.162}$$

Shear resistance provided by the concrete, V_c, is given as:

$$V_c = 0.0316\ \beta \sqrt{f_c'} b_v d_v \tag{3.163}$$

Shear resistance provided by transverse steel reinforcement, V_s, is given as:

$$V_s = \frac{A_v f_y d_v (\cot\theta + \cot\alpha) \sin\alpha}{s} \tag{3.164}$$

where:

d_v = Effective shear depth, in.

b_v = Girder web width, in.

f'_c = Girder concrete strength at service, ksi

V_p = Component of prestressing force in the direction of shear force, kips

β = Factor indicating ability of diagonally cracked concrete to transfer tension

θ = Angle of inclination of diagonal compressive stresses (slope of compression field), radians

A_v = Area of shear reinforcement within a distance s, in.^{2}

s = Spacing of stirrups, in.

f_y = Yield strength of shear reinforcement, ksi

α = Angle of inclination of transverse reinforcement to longitudinal axis, taken as 90° for vertical stirrups

The values of β *and* θ depend on the shear stress in the concrete, υ_u, and the longitudinal strain, ε_x, of the section. The shear stress in the concrete is given as:

$$\upsilon_u = \frac{V_u - \phi V_p}{\phi b_v d_v} \tag{3.165}$$

where:

υ_u = Shear stress in concrete, ksi

V_u = Factored shear force at the section, kips

ϕ = Resistance factor, specified as 0.9 for prestressed concrete members

V_p = Component of prestressing force in the direction of shear force, kips

b_v = Girder web width, in.

d_v = Effective shear depth, in.

For the sections containing at least the minimum transverse reinforcement the longitudinal strain, ε_x, is determined as follows.

$$\varepsilon_x = \frac{\dfrac{M_u}{d_v} + 0.5N_u + 0.5(V_u - V_p)\cot\theta - A_{ps} f_{po}}{2(E_p A_{ps})} \leq 0.001 \tag{3.166}$$

For the sections containing less than minimum transverse reinforcement the longitudinal strain, ε_x, is found using the following expression.

$$\varepsilon_x = \frac{\dfrac{M_u}{d_v} + 0.5N_u + 0.5(V_u - V_p)\cot\theta - A_{ps} f_{po}}{E_p A_{ps}} \leq 0.002 \tag{3.167}$$

If the value of ε_x is negative, the longitudinal strain is:

$$\varepsilon_x = \frac{\dfrac{M_u}{d_v} + 0.5N_u + 0.5(V_u - V_p)\cot\theta - A_{ps} f_{po}}{2(E_c A_c + E_p A_{ps})} \tag{3.168}$$

where:

V_u = Applied factored shear force at the specified section, kips

M_u = Applied factored moment at the specified section > $V_u d_v$, k-in.

N_u = Applied factored normal force at the specified section, kips

A_c = Area of the concrete on the flexural tension side of the member, in.^{2}

A_{ps} = Area of prestressing steel on the flexural side of the member, in.^{2}

f_{po} = Parameter taken as modulus of elasticity of prestressing tendons multiplied by the locked-in difference in strain between the prestressing tendons and the surrounding concrete (ksi). LRFD Article C5.8.3.4.2 recommends that for pretensioned members, f_{po} be taken as the stress in strands when the concrete is cast around them, which is approximately 0.7 f_{pu}, ksi

f_{pu} = Ultimate strength of prestressing strands, ksi

V_p = Vertical component of prestress force for harped strands, kips

For the sections containing less than minimum transverse reinforcement, the crack spacing parameter s_{xe} is required to determine the parameters β and θ. The crack spacing parameter, s_{xe}, is calculated as follows.

$$s_{xe} = s_x \frac{1.38}{a_g + 0.63} \leq 80 \text{ in.} \tag{3.169}$$

where:

a_g = Maximum aggregate size, in.

s_x = Lesser of either d_v or the maximum distance between layers of longitudinal crack control reinforcement, in.

The parameters β and θ are calculated by interpolating for the determined values of υ_u and ε_x from the tables provided in the LRFD Specifications.

The maximum spacing, *s,* of transverse reinforcement is limited by the LRFD Specifications as follows:

if $v_u < 0.125\, f_c'$:

$$s \leq 0.8 d_v \leq 24.0 \text{ in.} \tag{3.170}$$

or if $v_u \geq 0.125\, f_c'$:

$$s \leq 0.4 d_v \leq 12.0 \text{ in.} \tag{3.171}$$

where:

s = Center-to-center spacing of shear reinforcement, in.

v_u = Shear stress in the concrete, ksi

d_v = Effective shear depth, in.

The minimum area of transverse reinforcement is given as:

$$A_v \geq 0.0316 \sqrt{f_c'}\, \frac{b_v s}{f_y} \tag{3.172}$$

where:

A_v = Area of transverse shear reinforcement within spacing s, in.^{2}

f_c' = Girder concrete strength at service, ksi

b_v = Girder web width, in.

f_y = Yield strength of shear reinforcement, ksi

s = Center-to-center spacing of shear reinforcement, in.

The LRFD Specifications require that at each section the tensile capacity of the longitudinal reinforcement on the flexural tension side of the member must satisfy the following expression. This condition is checked at the critical section for shear in the parametric study.

$$A_s f_y + A_{ps} f_{ps} \geq \frac{M_u}{d_v \phi_f} + 0.5 \frac{N_u}{\phi_c} + \left(\frac{V_u}{\phi_v} - 0.5 V_s - V_p \right) \cot \theta \tag{3.173}$$

where:

A_s = Area of non-prestressed reinforcement on the flexural side of the member, in.^{2}

A_{ps} = Area of prestressing steel on the flexural side of the member, in.^{2}

f_y = Yield strength of non-prestressed reinforcement, ksi

f_{ps} = Effective stress in the prestressing steel, ksi

M_u = Applied factored moment at the specified section > $V_u\, d_v$, k-in.

N_u = Applied factored normal force at the specified section, kips

V_u = Applied factored shear force at the specified section, kips

V_s = Nominal shear strength provided by the web reinforcement, kips

V_p = Component of prestressing force in the direction of shear force, kips

d_v = Effective shear depth, in.

θ = Angle of inclination of diagonal compressive stresses (slope of compression field), radians

ϕ_f = Resistance factor for flexure, specified as 1.0 for prestressed concrete members

ϕ_c = Resistance factor for axial force, specified as 0.75 for compression and 1.0 for tension in prestressed concrete members

ϕ_v = Resistance factor for shear, specified as 0.9 for prestressed concrete members

3.9 INTERFACE SHEAR DESIGN

3.9.1 Standard Specifications

AASHTO Standard Specifications Article 9.20.4 specifies the requirements for horizontal shear design. The Standard Specifications also allow the use of refined methods for the interface shear design that are in agreement with comprehensive test results. The provisions of Article 9.20.4, outlined in this section, are used for the parametric study.

The horizontal shear design must satisfy the following expression.

$$V_u \leq \phi\, V_{nh} \tag{3.174}$$

where:

V_u = Factored shear force at the section, kips

ϕ = Resistance factor specified as 0.90 for shear in prestressed concrete members

V_{nh} = Nominal horizontal shear strength at the section, kips

The critical section for horizontal shear is at a distance of $h_c/2$ from the centerline of the support where h_c is the depth of the composite section (in.). The nominal horizontal shear strength must be calculated based on one of the following cases.

Case (a): Contact surface is clean, free of laitance, and intentionally roughened.

$$V_{nh} = 80\ b_v d \tag{3.175}$$

Case (b): Minimum ties are used, contact surface is clean, free of laitance, but not intentionally roughened.

$$V_{nh} = 80\ b_v d \tag{3.176}$$

Case (c): Minimum ties are used, contact surface is clean, free of laitance, and intentionally roughened to a full amplitude of ¼ in.

$$V_{nh} = 350\ b_v d \tag{3.177}$$

Case (d): For each percent of tie reinforcement crossing the contact surface in excess of the minimum requirement, V_{nh} may be increased by:

$$\frac{160 f_y}{40{,}000} b_v d \tag{3.178}$$

where:

b_v = Width of cross-section at the contact surface being investigated for horizontal shear, in.

d = Distance from extreme compressive fiber to centroid of prestressing force, in.

f_y = Yield strength of steel reinforcement, ksi

Minimum area of horizontal shear reinforcement shall be:

$$A_{vh} = 50 \frac{b_v s}{f_y} \tag{3.179}$$

where:

A_{vh} = Area of interface shear reinforcement, in.^{2}

s = Center-to-center spacing of interface shear reinforcement, in.

The spacing of tie reinforcement, s, shall not exceed four times the least web width of the girder nor 24 in.

3.9.2 LRFD Specifications

The interface shear design in the LRFD Specifications is based on shear friction theory and is significantly different from that of the Standard Specifications. This method assumes a discontinuity along the shear plane, and the relative displacement is considered to be resisted by cohesion and friction, maintained by the shear friction reinforcement crossing the crack.

The LRFD provisions for interface shear design are outlined as follows. For the strength limit state, the horizontal shear at a section shall be calculated using the following expression.

$$V_h = \frac{V_u}{d_e} \tag{3.180}$$

where:

V_h = Horizontal shear per unit length of the girder, kips

V_u = Factored shear force at specified section due to superimposed dead and live loads, kips

d_e = Distance between resultants of tensile and compressive forces, in.

= $(d_v - a/2)$

d_v = Distance between centroid of tension steel and top compression fiber, in.

a = Depth of equivalent stress block, in.

$$V_{n\,reqd} = V_h / \phi \tag{3.181}$$

where:

$V_{n\,reqd}$ = Required nominal shear strength at the interface plane, kips

ϕ = Resistance factor specified as 0.90 for shear in prestressed concrete members

The nominal shear resistance of the interface plane V_n is:

$$V_n = c\, A_{cv} + \mu\, [A_{vf} f_y + P_c] \tag{3.182}$$

where:

c = Cohesion factor

μ = Friction factor

A_{cv} = Area of concrete engaged in shear transfer, in.^{2}

A_{vf} = Area of shear reinforcement crossing the shear plane, in.^{2}

P_c = Permanent net compressive force normal to the shear plane, kips

f_y = Yield strength of shear reinforcement, ksi

The nominal shear resistance, V_n, shall not be greater than the lesser of the following two values.

$$V_n \leq 0.2 f_c' A_{cv} \tag{3.183}$$

$$V_n \leq 0.8 A_{cv} \tag{3.184}$$

where:

f'_c = The lower compressive strength at service of the two elements at the interface, ksi

For concrete placed against clean, hardened concrete and free of laitance, with the surface intentionally roughened to an amplitude of 0.25 in.:

c = 0.100 ksi

μ = 1.0λ

For concrete placed against clean, hardened concrete and free of laitance, but not intentionally roughened:

c = 0.075 ksi

μ = 0.6λ

λ = 1.0 for normal-weight concrete

The minimum interface shear reinforcement is determined as follows.

$$A_{vf} \geq (0.05 b_v)/f_y \tag{3.185}$$

The above minimum shear reinforcement requirement may be waived if $V_n/A_{cv} < 0.100$ ksi.

3.10 EVALUATION OF MODULAR RATIO

The Texas Department of Transportation specifies design recommendations for bridge engineers in *TxDOT Bridge Design Manual* (TxDOT 2001). This manual is primarily aimed to bring consistency in the design of bridges in Texas. The manual gives specific recommendations for design where the Standard Specifications give options to the designers. The manual also includes simplifications for bridge design. The manual is based on *Standard Specifications for Highway Bridges* except for a few sections that are based on previous studies and practices. In general, the approaches recommended by TxDOT are followed in this study to ensure consistency in the design approach. However, one exception is in the updating of the modular ratio between the slab and girder concrete as explained below.

The TxDOT design methodology for prestressed concrete bridges is to assume the concrete strengths at release and at service at the beginning of bridge girder design. Typically the concrete strength at release, f'_{ci}, is taken as 4000 psi and the concrete strength at service, f'_c, is assumed to be 5000 psi. The concrete strengths are optimized and selected during the design process as described in previous sections of this chapter. As the actual concrete strengths are not known at the beginning of the design process, the modular ratio between the slab and girder concrete (n) is chosen as unity. This modular ratio needs to be updated once the actual concrete strengths are selected. However, the TxDOT Bridge Manual allows for the use of modular ratio as unity throughout the design. The effect of haunch on the composite properties of the girder is not taken into account for bridges designed using TxDOT methodology. It is assumed that the haunch effect neutralizes the impact of the assumption of modular ratio being unity, and will not affect the girder designs based on Standard Specifications significantly. This simplification is also followed by the TxDOT Bridge Design Program PSTRS14 (TxDOT 2004).

The live load moment and shear distribution factors specified by the Standard Specifications do not depend on the modular ratio between slab and girder concrete. The live load moment DFs specified by the LRFD Specifications, however, involve a term K_g that depends on the modular ratio. The assumption of modular ratio as unity thus needs to be evaluated for the design based on LRFD Specifications. The impact of assuming the modular ratio as unity is evaluated in this study, when designs are based on the Standard and LRFD Specifications. However, the haunch effect is ignored, as the actual dimensions of the haunch are not provided for this study. The evaluation of the impact of not updating the modular ratio is carried out for Type IV girder with skew of 0 degrees. The skew is not a factor for this evaluation as the modular ratio has no impact on skew correction factors.

The methodology discussed in this chapter was used with slight modifications. The design was first carried out assuming a modular ratio of unity. Once the concrete strengths were obtained, the actual modular ratio was evaluated and the design was conducted using this value. The refined optimized concrete strengths were thus obtained. The modular ratio is again calculated using the refined concrete strengths. The analysis is conducted again until the difference in the modular ratios is less than 0.05. Once the modular ratio converges within this limit, the camber, and the flexure and shear design limit states are evaluated. The design results thus obtained were compared with the ones evaluated in the parametric study.

The impact of not updating the modular ratio on various design parameters was evaluated for the distribution factors, number of strands, required concrete strengths, and additional design parameters. In general, it was found that updating the modular ratio had only a small effect on the design parameters and this only occurs for a few cases (Adil 2005). The live load moment DFs specified by the LRFD Specifications were found to be decreasing in the range of 1 percent to 3 percent. The live load shear DFs specified by the LRFD Specifications are not dependent on modular ratio, thus no difference was observed. The required number of strands increased slightly for longer spans as a result of the changed composite properties. The required concrete strengths at release and at service increased in a few cases when the modular ratio is updated; however, the increase is negligible. The increase in the required concrete strengths is due to the increase in the number of strands, which increases the stresses in the girder, and leads to higher required concrete strengths. For cases where the number of strands and concrete strength changed, there were resulting changes in the nominal moment strength, shear strength, and camber.

4. PARAMETRIC STUDY - AASHTO TYPE IV GIRDERS

4.1 INTRODUCTION

A parametric study was conducted for AASHTO Type IV prestressed concrete bridge girders. A number of cases were considered based on the parameters summarized in Table 4.1. The procedure outlined in Chapter 3 was employed to evaluate the impact of the AASHTO LRFD Specifications on the design of AASHTO Type IV bridge girders. The results obtained from the design program for designs based on both the Standard and LRFD Specifications were validated using TxDOT's PRSTRS14 (TxDOT 2004) bridge design software. TxDOT's procedures were used for optimizing the number of strands and concrete strengths. This chapter provides a summary of results of the parametric study for AASHTO Type IV bridge girders. The impact of the LRFD Specifications, as compared to the Standard Specifications, on various design results is discussed.

Table 4.1. Design Parameters for Type IV Girders.

Parameter	**Description / Selected Values**
Design Codes	AASHTO Standard Specifications, 17th Edition (2002) AASHTO LRFD Specifications, 3rd Edition (2004)
Girder Spacing (ft.)	6'-0", 8'-0", and 8'-8"
Spans	90 ft. to maximum span at 10 ft. intervals
Strand Diameter (in.)	0.5 and 0.6
Concrete Strength at Release, f'_{ci}	Varied from 4000 to 6750 psi for design with optimum number of strands
Concrete Strength at Service, f'_c	Varied from 5000 to 8500 psi for design with optimum number of strands (f'_c may be increased up to 8750 psi for optimization on longer spans)
Skew Angle	0, 15, 30, and 60 degrees

The requirements for service load limit state design, flexural strength limit state design, transverse shear design, and interface shear design are evaluated in the parametric study.

The following sections provide a summary of differences observed in parallel designs based on the Standard and LRFD Specifications. This includes differences occurring in the undistributed and distributed live load moments, the distribution factors, the number of strands required, and required concrete strengths at release and at service. The differences observed in the design for the flexural and shear strength limit states are provided in the following sections. The effect on camber is also evaluated and summarized.

4.2 LIVE LOAD MOMENTS AND SHEARS

4.2.1 General

The Standard Specifications stipulate the live load to be taken as an HS-20 truck load, tandem load, or lane load; whichever produces the maximum effect at the section considered. The LRFD Specifications specify a different live load model, HL-93, which is a combination of the HS-20 truck and lane load, or tandem load and lane load, whichever produces maximum effect at the section of interest. The live load governing the moments and shears at the sections of interest for the cases considered in the parametric study was determined and are summarized below. The undistributed live load moments at midspan and shears at critical section were calculated for each case and the differences are presented in this section.

There is a significant difference in the formulas for the distribution and impact factors specified by the Standard and the LRFD Specifications. The impact factors are applicable to truck, lane, and tandem loadings for designs based on Standard Specifications, whereas the LRFD Specifications do not require the lane load to be increased for the impact loading. The effect of the LRFD Specifications on the distribution and impact factors is evaluated and the results are summarized. The combined effect of the undistributed moments and shears and the distribution and impact factors on the distributed live load moments and shears was determined. The differences observed in the distributed live load moments at midspan and shears at the critical sections are presented below.

4.2.2 Governing Live Load for Moments and Shears

The researchers investigated the live load producing the maximum moment at midspan and maximum shears at the critical section for shear. The critical section for shear in the designs based on Standard Specifications is taken as $h/2$, where h is the depth of the composite section. For designs based on the LRFD Specifications, the critical section is calculated using an iterative process given by the specifications. The governing live loads are summarized in Tables 4.2 and

4.3. These tables also summarize the design cases considered using an AASHTO Type IV girder, along with the corresponding maximum span lengths. It was observed that for Standard designs, the HS-20 truck loading always governs the moments at midspan and shears at critical sections, except for the 136 ft. span case. For designs based on LRFD Specifications, the combination of truck and lane loading governs for all the cases.

4.2.3 Undistributed Live Load Moments and Shears

The difference in the live loads specified by the Standard and the LRFD Specifications affects the undistributed live load moments and shears. Skew and strand diameter have no effect on the undistributed live load moments or shears. Therefore, results for cases with no skew angle and a strand diameter of 0.5 in. are compared in Table 4.4. The undistributed live load moments are observed to increase in the range of 48 to 65 percent for a 6 ft. girder spacing when live loads based on LRFD Specifications are used as compared to the Standard Specifications. This increase was in the range of 48 to 61 percent for an 8 ft. girder spacing, and 48 to 56 percent for an 8.67 ft. girder spacing.

A significant increase was observed in the undistributed shears at the critical section. The increase was found to be in the range of 35 to 54 percent for a 6 ft. girder spacing when the LRFD Specifications are used as compared to the Standard Specifications. This increase was found to be in the range of 35 to 50 percent for an 8 ft. girder spacing and 35 to 45 percent for an 8.67 ft. girder spacing. This increase can be attributed to the change in live load and also the shifting of critical section. The critical section for shear is specified by the Standard Specifications as $h/2$, where h is the depth of composite section. The LRFD Specifications require the critical section to be calculated using an iterative process as discussed in Chapter 3. The difference between the undistributed moments and shears based on the Standard and LRFD Specifications is found to increase with an increase in span length.

Table 4.2. Governing Live Load Moments at Midspan and Shears at Critical Section for Standard Specifications (Type IV Girder).

Strand Diameter (in.)	Girder Spacing (ft.)	Span (ft.)	Governing Live Load for Moment	Governing Live Load for Shear
0.5	6	90	Truck Loading	Truck Loading
		100		
		110		
		120		
		130		
		136		Lane Loading
	8	90	Truck Loading	Truck Loading
		100		
		110		
		120		
		124		
	8.67	90	Truck Loading	Truck Loading
		100		
		110		
		119		
0.6	6	90	Truck Loading	Truck Loading
		100		
		110		
		120		
		130		
		131		
	8	90	Truck Loading	Truck Loading
		100		
		110		
		119		
	8.67	90	Truck Loading	Truck Loading
		100		
		110		
		115		

Table 4.3. Governing Live Load Moments at Midspan and Shears at Critical Section for LRFD Specifications (Type IV Girder, Skew = 0°).

Strand Diameter (in.)	Girder Spacing (ft.)	Span (ft.)	Governing Live Load for Moment	Governing Live Load for Shear
0.5	6	90	Truck+Lane Loading	Truck+Lane Loading
		100		
		110		
		120		
		130		
		133		
	8	90	Truck+Lane Loading	Truck+Lane Loading
		100		
		110		
		120		
	8.67	90	Truck+Lane Loading	Truck+Lane Loading
		100		
		110		
		116		
0.6	6	90	Truck+Lane Loading	Truck+Lane Loading
		100		
		110		
		120		
		126		
	8	90	Truck+Lane Loading	Truck+Lane Loading
		100		
		110		
		116		
	8.67	90	Truck+Lane Loading	Truck+Lane Loading
		100		
		110		
		113		

Table 4.4. Undistributed Midspan Live Load Moments and Shears at Critical Section (Type IV Girder, Skew = 0°, Strand Diameter = 0.5 in.).

Girder Spacing (ft.)	Span (ft.)	Undistributed Moment (k-ft.)			Undistributed Shear (kips)		
		Standard	LRFD	Difference k-ft. (%)	Standard	LRFD	Difference kips (%)
6	90	1315.2	1943.0	627.8 (47.7)	62.3	83.7	21.4 (34.4)
	100	1494.4	2271.9	777.5 (52.0)	63.3	88.2	24.9 (39.3)
	110	1674.4	2617.6	943.2 (56.3)	64.1	92.6	28.5 (44.4)
	120	1854.4	2979.3	1125.0 (60.7)	64.8	96.6	31.9 (49.2)
	130	2034.4	3357.1	1322.7 (65.0)	65.3	100.5	35.2 (53.9)
	133	-	3473.5	-	-	102.5	-
	136	2142.4	-	-	66.9	-	-
8	90	1315.2	1943.0	627.8 (47.7)	62.3	84.0	21.7 (34.8)
	100	1494.4	2271.9	777.5 (52.0)	63.3	88.6	25.3 (40.0)
	110	1674.4	2617.6	943.2 (56.3)	64.1	92.6	28.5 (44.4)
	120	1854.4	2979.3	1125.0 (60.7)	64.8	96.9	32.2 (49.7)
	124	1926.4	-	-	65.0	-	-
8.67	90	1315.2	1943.0	627.8 (47.7)	62.3	84.1	21.8 (34.9)
	100	1494.4	2271.9	777.5 (52.0)	63.3	88.7	25.4 (40.1)
	110	1674.4	2617.6	943.2 (56.3)	64.1	92.6	28.5 (44.5)
	116	-	2832.7	-	-	95.4	-
	119	1836.4	-	-	64.7	-	-

4.2.4 Impact Factors

The AASHTO Standard and LRFD Specifications require that live load moments and shears be increased for impact or dynamic loading. The Standard Specifications specify impact factors that decrease with an increase in span length, whereas the LRFD Specifications specify a constant value of dynamic loading as 33 percent of the undistributed live load moment or shear. The LRFD Specifications specify the impact loading to be 15 percent of the undistributed live load fatigue moment used to check the fatigue limit state required by the LRFD Specifications. The LRFD Specifications do not require the lane load moments and shears to be increased for impact loading.

A summary of impact factors and the percent difference relative to the Standard values is provided in Table 4.5. The skew angle and strand diameter do not affect the impact factor, hence only the cases with zero skew angle and 0.5 in. strand diameter are presented.

Table 4.5. Live Load Impact Factors
(Type IV Girder, Skew = 0°, Strand Diameter = 0.5 in.).

Girder Spacing (ft.)	Span (ft.)	Impact Factor		Difference (%)
		Standard	LRFD	
6	90	0.23	0.33	41.9
	100	0.22	0.33	48.5
	110	0.21	0.33	55.1
	120	0.20	0.33	61.7
	130	0.20	0.33	68.3
	133	-	0.33	-
	136	0.19	-	-
8	90	0.23	0.33	41.9
	100	0.22	0.33	48.5
	110	0.21	0.33	55.1
	120	0.20	0.33	61.7
	124	0.20	-	-
8.67	90	0.23	0.33	41.9
	100	0.22	0.33	48.5
	110	0.21	0.33	55.1
	116	-	0.33	-
	119	0.20	-	-

It was observed that the LRFD Specifications provide a larger estimate of dynamic loading as compared to the Standard Specifications. This difference increases with increasing span length. The increase in the impact factor is in the range of 42 to 68 percent of the impact factors specified by Standard Specifications. This essentially increases the distributed live load moments for the designs based on LRFD Specifications as compared to the Standard Specifications. Figure 4.1 illustrates the effect of the LRFD Specifications on the dynamic load (impact) factors for a 6 ft. girder spacing. The same trend was observed for girder spacings of 8 ft. and 8.67 ft.

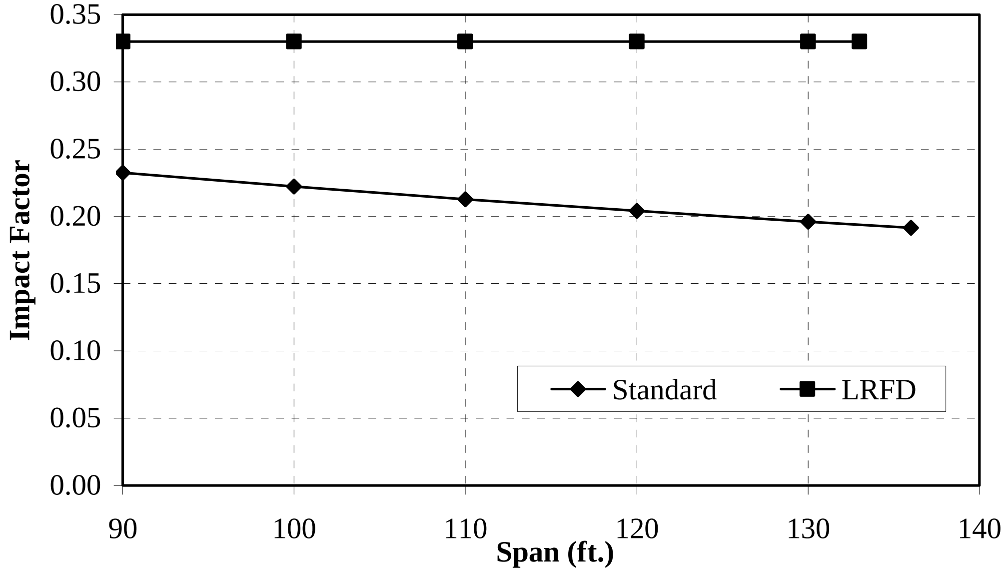

Figure 4.1. Comparison of Impact Factors (Type IV Girder, Girder Spacing = 6 ft., Skew = 0°, Strand Diameter = 0.5 in.).

4.2.5 Live Load Distribution Factors

The live load moments and shears, including the dynamic (impact) load effect are distributed to the individual girders. The Standard Specifications provide a simple formula for moment distribution factor (DF) as *S*/11 for prestressed concrete girder bridges, where *S* is the girder spacing in ft. The same DF is used for the distribution of live load shear to the girders. The LRFD Specifications provide more complex formulas for the distribution of live load moments and shears to individual girders. The effects of beam and slab stiffness are incorporated into these formulas. The LRFD Specifications require the DFs for moment to be reduced and DFs for shear to be corrected for skewed bridges. Table 4.6 compares the live load moment DFs for the Standard and LRFD Specifications.

Table 4.6. Live Load Moment Distribution Factors (DFM)
(Type IV Girder, Strand Diameter = 0.5 in.).

Girder Spacing (ft.)	Span (ft.)	STD DFM	LRFD							
			Skew = 0°		Skew = 15°		Skew = 30°		Skew = 60°	
			DFM	Diff. %	DFM	Diff. %	DFM	Diff. %	DFM	Diff. %
6	90	0.545	0.552	1.1	0.552	1.1	0.533	-2.3	0.453	-16.9
	100		0.537	-1.6	0.537	-1.6	0.520	-4.7	0.448	-17.8
	110		0.523	-4.0	0.523	-4.0	0.508	-6.9	0.443	-18.7
	120		0.512	-6.2	0.512	-6.2	0.498	-8.8	0.439	-19.6
	130		0.501	-8.1	0.501	-8.1	0.488	-10.5	0.434	-20.5
	133		0.498	-	0.498	-	0.486	-	-	-
	135		-	-	-	-	-	-	0.431	-
	136		-	-	-	-	-	-	-	-
8	90	0.727	0.675	-7.2	0.675	-7.2	0.648	-10.9	0.536	-26.3
	100		0.656	-9.8	0.656	-9.8	0.632	-13.1	0.532	-26.9
	110		0.639	-12.1	0.639	-12.1	0.618	-15.1	0.527	-27.6
	120		0.625	-14.1	0.625	-14.1	0.605	-16.8	0.522	-28.3
	124		-	-	-	-	-	-	-	-
	125		-	-	-	-	-	-	0.519	-
8.67	90	0.788	0.715	-9.3	0.715	-9.3	0.685	-13.0	0.562	-28.7
	100		0.695	-11.9	0.695	-11.9	0.668	-15.2	0.557	-29.3
	110		0.677	-14.1	0.677	-14.1	0.653	-17.1	0.553	-29.9
	116		0.667	-	0.667	-	-	-	-	-
	117		-	-	-	-	0.643	-	-	-
	119		-	-	-	-	-	-	-	-
	120		-	-	-	-	-	-	0.548	-
	121		-	-	-	-	-	-	0.547	-

It was observed that the live load moment DFs given by the LRFD Specifications are typically smaller as compared to those for the Standard Specifications. The difference increases with an increase in span length. The moment DFs increase with an increase in girder spacing for both the AASHTO Standard and LRFD Specifications, and the difference between the DFs increased for larger girder spacings. The LRFD live load moment DFs are the same for 0- and 15-degree skews, but there is a significant change when the skew angles are 30 and 60 degrees. It was observed that an increase in skew angles beyond 30 degrees decreases the moment DFs significantly for AASHTO Type IV girder bridges. The maximum difference between the Standard and LRFD DFs was found to be 8 percent for 6 ft. girder spacing, and 14 percent for 8 ft. and 8.67 ft. girder spacing for a 0-degree skew. This difference increased to 21 percent for 6 ft., 28 percent for 8 ft., and 30 percent for 8.67 ft. girder spacing for a skew angle of 60 degrees. Figure 4.2 shows the effect of girder spacing and span length on the moment DFs for each skew angle (0, 15, 30, and 60 degrees). Figure 4.3 shows the effect of skew on the moment DFs for 6 ft., 8 ft., and 8.67 ft. girder spacing.

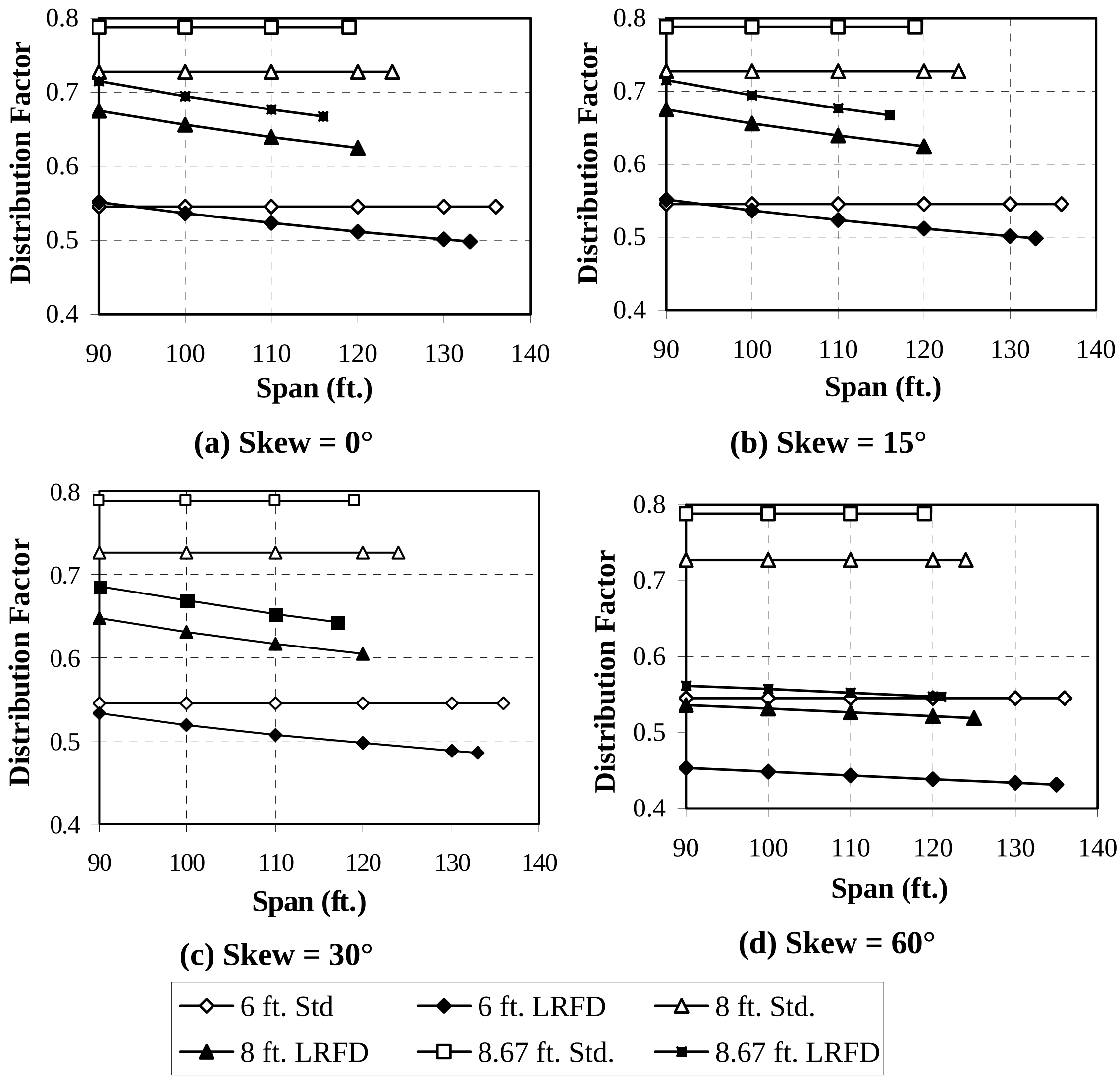

Figure 4.2. Comparison of Live Load Moment DFs by Skew Angle (Type IV Girder, Strand Dia. = 0.5 in.).

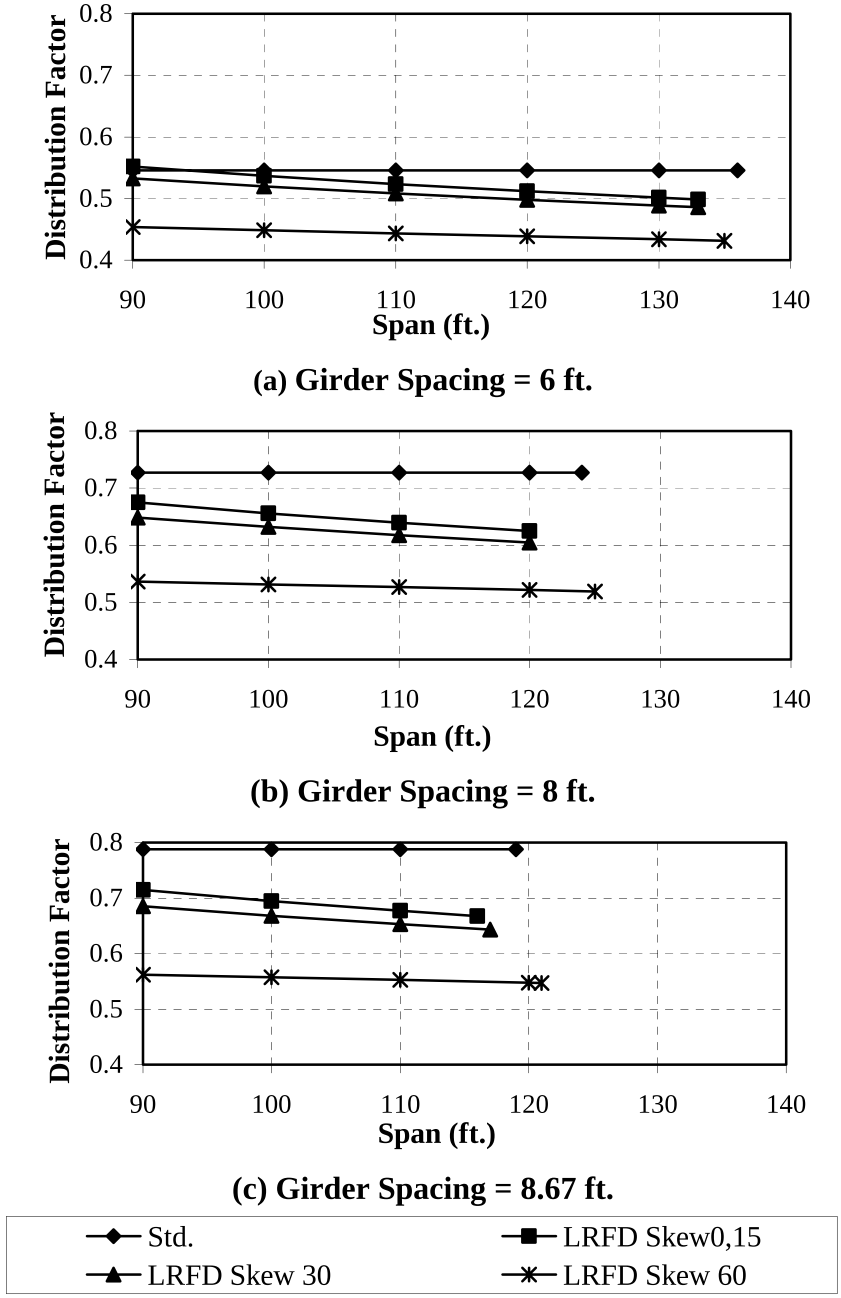

Figure 4.3. Live Load Moment DFs by Girder Spacing (Type IV Girder, Strand Dia. = 0.5 in.).

Table 4.7 and Figure 4.4 provide a summary of shear DFs for the parametric study with AASHTO Type IV girders. The strand diameter does not affect the DFs for shear. The LRFD live load shear DFs are larger than the Standard values. The DFs increase with an increase in girder spacing for both specifications, and the LRFD DFs approach Standard DFs as the girder spacing is increased. The span length and skew angle have no impact on the Standard shear DFs. The maximum difference in the shear DFs was 61 percent for 6 ft. spacing, 46 percent for 8 ft. spacing, and 42 percent for the 8.67 ft. spacing.

Table 4.7. Live Load Shear DFs (DFV) (Type IV Girder, Strand Diameter = 0.5 in.).

Girder Spacing (ft.)	Span (ft.)	STD DFV	LRFD							
			Skew = 0°		Skew = 15°		Skew = 30°		Skew = 60°	
			DFV	Diff. %	DFV	Diff. %	DFV	Diff. %	DFV	Diff. %
6	90	0.545	0.671	22.9	0.699	28.2	0.733	34.3	0.857	57.1
	100		0.671	22.9	0.700	28.4	0.735	34.7	0.863	58.3
	110		0.671	22.9	0.701	28.6	0.737	35.1	0.869	59.3
	120		0.671	22.9	0.702	28.7	0.738	35.4	0.874	60.3
	130		0.671	22.9	0.703	28.9	0.740	35.7	0.879	61.2
	133		0.671	-	0.703	-	0.741	-	-	-
	135		-	-	-	-	-	-	0.882	-
	136		-	-	-	-	-	-	-	-
8	90	0.727	0.814	12.0	0.849	16.8	0.890	22.4	1.041	43.1
	100		0.814	12.0	0.851	17.0	0.892	22.7	1.048	44.1
	110		0.814	12.0	0.852	17.1	0.895	23.0	1.055	45.1
	120		0.814	12.0	0.853	17.2	0.897	23.3	1.062	46.0
	124		-	-	-	-	-	-	-	-
	125		-	-	-	-	-	-	1.065	-
8.67	90	0.788	0.861	9.3	0.898	14.0	0.941	19.4	1.101	39.6
	100		0.861	9.3	0.899	14.1	0.944	19.7	1.108	40.6
	110		0.861	9.3	0.901	14.3	0.946	20.0	1.116	41.6
	116		0.861	-	0.901	-	-	-	-	-
	117		-	-	-	-	0.948	-	-	-
	119		-	-	-	-	-	-	-	-
	120		-	-	-	-	-	-	1.123	-
	121		-	-	-	-	-	-	1.123	-

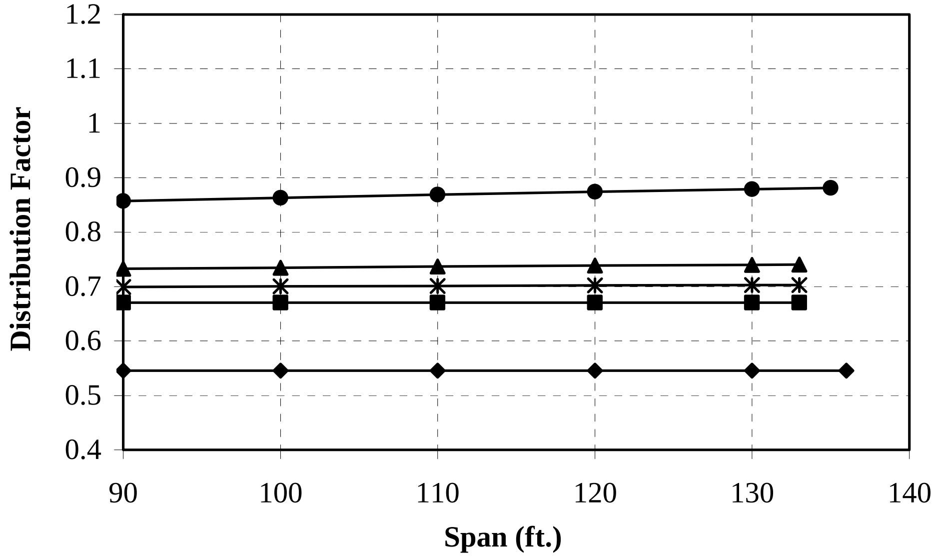

(a) Girder Spacing = 6 ft.

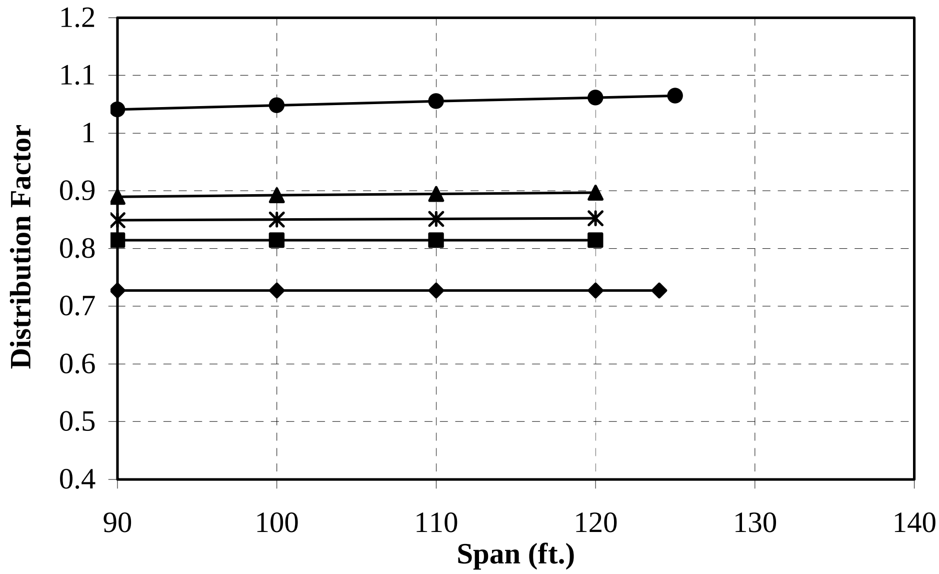

(b) Girder Spacing = 8 ft.

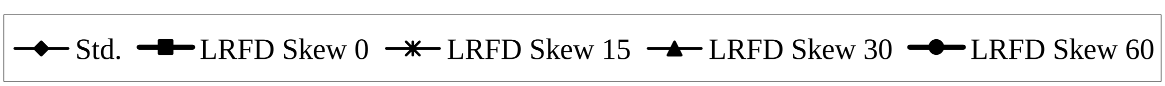

Figure 4.4. Live Load Shear DFs (Type IV Girder, Strand Dia. = 0.5 in.).

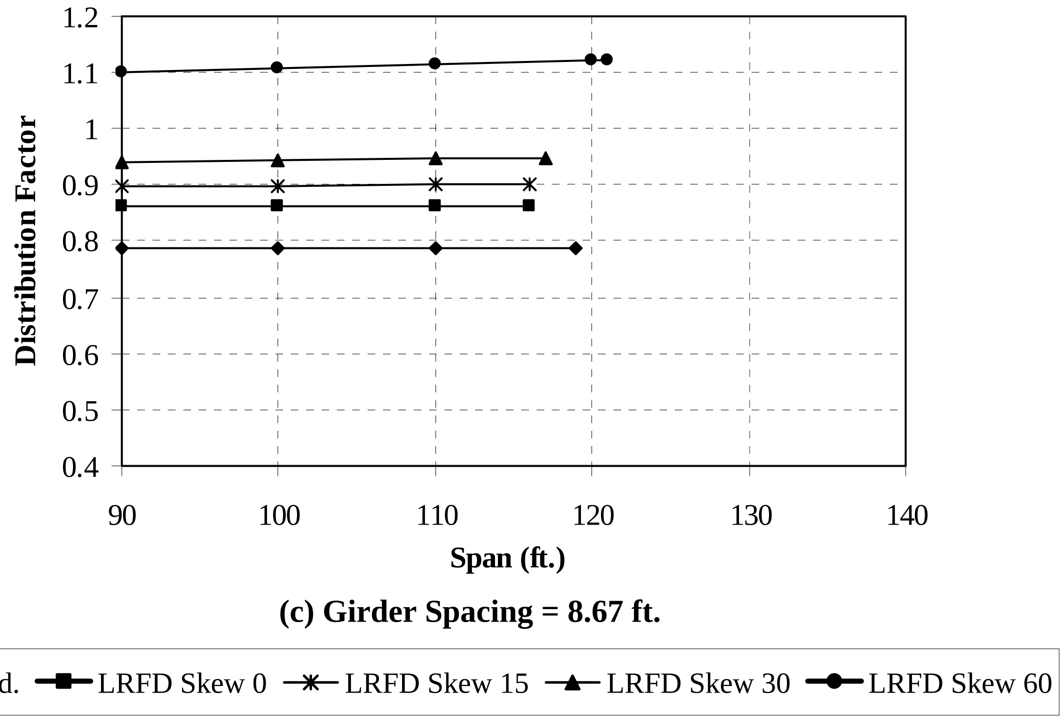

(c) Girder Spacing = 8.67 ft.

Figure 4.4. Live Load Shear DFs (Type IV Girder, Strand Dia. = 0.5 in.) (Cont.).

4.2.6 Distributed Live Load Moments and Shears

The combined effect of the impact and distribution factors on the live load moment and shears is presented in this section. The distributed live load moments are compared in Table 4.8. The distributed live load moments are the same for 0- and 15-degree skew angles for the LRFD Specifications because the distribution factors for these two skews are identical. The LRFD distributed live load moments were found to be significantly larger, increasing in the range of 48 to 52 percent for 6 ft. girder spacing and 0-degree skew. As the girder spacing increases, the difference between the distributed live load moments decreases. The LRFD moments were found to be in the range of 36 to 38 percent larger for 8 ft. spacing and 33 to 38 percent larger for 8.67 ft. girder spacing for 0-degree skew.

An increase in skew angle for 30 degrees and beyond resulted in a decrease in DFs. The increase in the LRFD live load moments relative to the Standard values was found to be in the range of 22 to 32 percent for 6 ft. girder spacing when the skew angle was 60 degrees. This increase reduces to 8 to 15 percent and 4 to 9 percent for 8 ft. and 8.67 ft. girder spacing, respectively. As the span length increases, the difference between the live load moments becomes larger.

Table 4.8. Distributed Midspan Live Load Moments (LL Mom.) (Type IV Girder, Strand Dia. = 0.5 in.).

Girder Spacing (ft.)	Span (ft.)	STD LL Mom. (k-ft.)	LRFD							
			Skew 0°		Skew 15°		Skew 30°		Skew 60°	
			LL Mom. (k-ft.)	Diff. %	LL Mom. (k-ft.)	Diff. %	LL Mom. (k-ft.)	Diff. %	LL Mom. (k-ft.)	Diff. %
6	90	885.4	1310.7	48.0	1310.7	48.0	1265.8	43.0	1077.3	21.7
	100	997.4	1483.8	48.8	1483.8	48.8	1436.8	44.1	1239.9	24.3
	110	1108.8	1659.4	49.7	1659.4	49.7	1610.5	45.3	1405.7	26.8
	120	1219.1	1837.8	50.7	1837.8	50.7	1787.2	46.6	1574.8	29.2
	130	1328.5	2019.3	52.0	2019.3	52.0	1966.9	48.1	1747.3	31.5
	133	-	2074.3	-	2074.3	-	2021.5	-	-	-
	135	-	-	-	-	-	-	-	1834.9	-
	136	1393.7	-	-	-	-	-	-	-	-
8	90	1180.5	1603.8	35.9	1603.8	35.9	1540.3	30.5	1273.9	7.9
	100	1329.9	1814.1	36.4	1814.1	36.4	1747.8	31.4	1469.7	10.5
	110	1478.4	2027.3	37.1	2027.3	37.1	1958.4	32.5	1669.4	12.9
	120	1625.5	2243.7	38.0	2243.7	38.0	2172.3	33.6	1872.9	15.2
	124	1683.9	-	-	-	-	-	-	-	-
	125	-	-	-	-	-	-	-	1976.2	-
8.67	90	1279.3	1698.5	32.8	1698.5	32.8	1628.5	27.3	1334.9	4.3
	100	1441.2	1920.9	33.3	1920.9	33.3	1847.8	28.2	1541.3	6.9
	110	1602.2	2146.2	34.0	2146.2	34.0	2070.3	29.2	1751.7	9.3
	116	-	2283.0	-	2283.0	-	-	-	-	-
	117	-	-	-	-	-	2228.1	-	-	-
	119	1745.7	-	-	-	-	-	-	-	-
	120	-	-	-	-	-	-	-	1966.3	-
	121	-	-	-	-	-	-	-	1988.0	-

The distributed shear force at the critical section due to live load was found to increase significantly when the LRFD Specifications are used. The increase in the shear force can be attributed to the increase in the undistributed shear force due to the HL-93 loading and the increase in distribution factors. The shear force at the critical section for the LRFD Specifications was found to increase in the range of 124 to 160 percent for 6 ft. girder spacing as compared to the Standard Specifications. The increase was found to range from 104 to 129 percent for 8 ft. and 99 to 115 percent for 8.67 ft. girder spacing. The results are presented in Table 4.9.

Table 4.9. Distributed Live Load Shear at Critical Section (Type IV Girder, Strand Dia. = 0.5 in.).

Girder Spacing (ft.)	Span (ft.)	STD Shear (kips)	LRFD							
			Skew 0°		Skew 15°		Skew 30°		Skew 60°	
			Shear (kips)	Diff. %	Shear (kips)	Diff. %	Shear (kips)	Diff. %	Shear (kips)	Diff. %
6	90	41.9	73.5	75.2	76.7	82.7	80.3	91.5	93.9	123.9
	100	42.2	76.5	81.1	79.9	89.2	83.8	98.5	98.5	133.1
	110	42.4	79.4	87.0	83.0	95.6	87.2	105.4	102.8	142.3
	120	42.6	82.1	92.9	86.0	101.9	90.4	112.4	107.0	151.4
	130	42.7	84.8	98.7	88.8	108.3	93.6	119.3	111.1	160.5
	133	-	85.5	-	89.7	-	94.5	-	-	-
	135	-	-	-	-	-	-	-	113.1	-
	136	43.5	-	-	-	-	-	-	-	-
8	90	55.9	89.3	59.6	93.1	66.5	97.5	74.4	114.1	104.0
	100	56.3	92.9	65.0	97.1	72.3	101.8	80.8	119.6	112.3
	110	56.6	96.4	70.3	100.8	78.1	105.9	87.1	124.9	120.7
	120	56.8	99.7	75.7	104.4	83.9	109.8	93.4	130.0	129.0
	124	56.8	-	-	-	-	-	-	-	-
	125	-	-	-	-	-	-	-	132.5	-
8.67	90	60.6	94.4	55.7	98.4	62.4	103.1	70.1	120.6	99.0
	100	61.0	98.3	61.0	102.6	68.1	107.7	76.4	126.5	107.2
	110	61.3	101.9	66.2	106.6	73.8	112.0	82.6	132.1	115.3
	116	-	104.1	-	108.9	-	-	-	-	-
	117	-	-	-	-	-	114.9	-	-	-
	119	61.5	-	-	-	-	-	-	-	-
	120	-	-	-	-	-	-	-	137.5	-
	121	-	-	-	-	-	-	-	138.0	-

4.3 SERVICE LOAD DESIGN

4.3.1 General

The impact of the LRFD Specifications on the service load design is discussed in this section, including the effect on prestress losses, required number of strands, and the required concrete strengths at service and at release. The increase in the live load moment and the change in equations for prestress loss calculations specified by the AASHTO LRFD Specifications results in different service load design requirements. The change in the service load combination and allowable stress limits also affects the design. Generally, the design requirements for the LRFD designs were found to be conservative as compared to the Standard designs.

4.3.2 Maximum Span Lengths

The maximum span lengths are limited by the maximum concrete strength at release of 6750 psi and the maximum concrete strength at service of 8750 psi. The maximum span is not governed by the maximum number of strands for any of the cases considered for the parametric study. The maximum allowable concrete strengths are reached when the number of strands is in the range of 70 to 74, whereas an AASHTO Type IV girder can hold up to 102 strands. Thus, by relaxing the limit on concrete strengths, longer spans can be achieved. The results for maximum span length are presented in Table 4.10. The LRFD Specifications tend to reduce the maximum span length for Type IV girders. This reduction is due to slightly higher required concrete strengths that reach the concrete strength limits for smaller spans than for the Standard Specifications. However, the difference between the maximum span lengths was relatively small, ranging from -5 ft. to 2 ft.

Table 4.10. Maximum Span Lengths (Type IV Girder).

Strand Dia. (in.)	Girder Spacing (ft.)	STD Max. Span (ft.)	LRFD							
			Skew 0°		Skew 15°		Skew 30°		Skew 60°	
			Max. Span (ft.)	Diff. (ft.)	Max. Span (ft.)	Diff. (%)	Max. Span (ft.)	Diff. (%)	Max. Span (ft.)	Diff. (%)
0.5	6	136	133	-3	133	-3	133	-3	135	-2
	8	124	120	-4	120	-4	120	-4	125	1
	8.67	119	116	-3	116	-3	117	-2	121	2
0.6	6	131	126	-5	126	-5	127	-4	130	-1
	8	119	116	-3	116	-3	116	-3	119	0
	8.67	115	113	-2	113	-2	114	-1	117	2

4.3.3 Required Number of Strands

The number of strands required depends on the allowable stress limits and the stresses caused by the dead and live loads. There is a change in the allowable stress limits in the LRFD Specifications, and the live load is also different. The Service III limit state that checks the bottom tensile stresses using a 0.8 factor for live load also impacts the prestressing strand requirements. The difference in the prestress losses is another factor that effects the final strand requirements. The strength limit state controls the number of strands for only one case when span length is 90 ft. with 6 ft. girder spacing.

The results for 0.5 in. diameter strands are presented in Table 4.11. Similar trends were found for 0.6 in. diameter strands, and the results are presented in Table 4.12. Figures 4.5 and 4.6 illustrate the comparison of strand requirements for the Standard and LRFD designs. The LRFD Specifications require a larger number of strands for most cases for 0.5 in. diameter strands. The difference in the required number of strands increases with an increase in span length and decreases with an increase in girder spacing and skew angle. For a few cases with a 60-degree skew angle, the number of strands required by the LRFD Specifications was found to be less than that of the Standard Specifications. The difference was found to range from a reduction of two strands to an increase of eight strands when comparing LRFD to Standard designs. This difference was smallest for a 60-degree skew angle.

Table 4.11. Required Number of Strands (Type IV Girder, Strand Dia. = 0.5 in.).

Girder Spacing (ft.)	Span (ft.)	No. of Strands	LRFD							
			Skew 0°		Skew 15°		Skew 30°		Skew 60°	
			No. of Strands	Diff.	No. of Strands	Diff.	No. of Strands	Diff.	No. of Strands	Diff.
6	90	24	26	2	26	2	26	2	24	0
	100	32	34	2	34	2	32	0	30	-2
	110	38	42	4	42	4	42	4	40	2
	120	48	54	6	54	6	52	4	50	2
	130	60	68	8	68	8	66	6	62	2
	133	-	74	-	74	-	74	-	-	-
	135	-	-	-	-	-	-	-	72	-
	136	70	-	-	-	-	-	-	-	-
8	90	30	32	2	32	2	32	2	28	-2
	100	40	42	2	42	2	40	0	38	-2
	110	50	54	4	54	4	52	2	50	0
	120	64	70	6	70	6	68	4	64	0
	124	74	-	-	-	-	-	-	-	-
	125	-	-	-	-	-	-	-	74	-
8.67	90	32	34	2	34	2	34	2	30	-2
	100	42	44	2	44	2	44	2	40	-2
	110	54	58	4	58	4	56	2	52	-2
	116	-	68	-	68	-	-	-	-	-
	117	-	-	-	-	-	68	-	-	-
	119	70	-	-	-	-	-	-	-	-
	120	-	-	-	-	-	-	-	68	-
	121	-	-	-	-	-	-	-	70	-

Table 4.12. Required Number of Strands (Type IV Girder, Strand Dia. = 0.6 in.).

Girder Spacing (ft.)	Span (ft.)	No. of Strands	LRFD							
			Skew 0°		Skew 15°		Skew 30°		Skew 60°	
			No. of Strands	Diff. %	No. of Strands	Diff. %	No. of Strands	Diff. %	No. of Strands	Diff. %
6	90	18	18	0	18	0	18	0	18	0
	100	22	24	2	24	2	22	0	22	0
	110	26	30	4	30	4	30	4	28	2
	120	34	36	2	36	2	36	2	34	0
	126	-	42	-	42	-	-	-	-	-
	127	-	-	-	-	-	42	-	-	-
	130	40	-	-	-	-	-	-	42	2
	131	42	-	-	-	-	-	-	-	-
8	90	22	22	0	22	0	22	0	20	-2
	100	28	30	2	30	2	28	0	26	-2
	110	34	36	2	36	2	36	2	34	0
	116	-	42	-	42	-	40	-	-	-
	119	42	-	-	-	-	-	-	42	0
8.67	90	22	24	2	24	2	24	2	22	0
	100	30	30	0	30	0	30	0	28	-2
	110	36	38	2	38	2	38	2	36	0
	113	-	42	-	42	-	-	-	-	-
	114	-	-	-	-	-	42	-	-	-
	115	42	-	-	-	-	-	-	-	-
	117	-	-	-	-	-	-	-	42	-

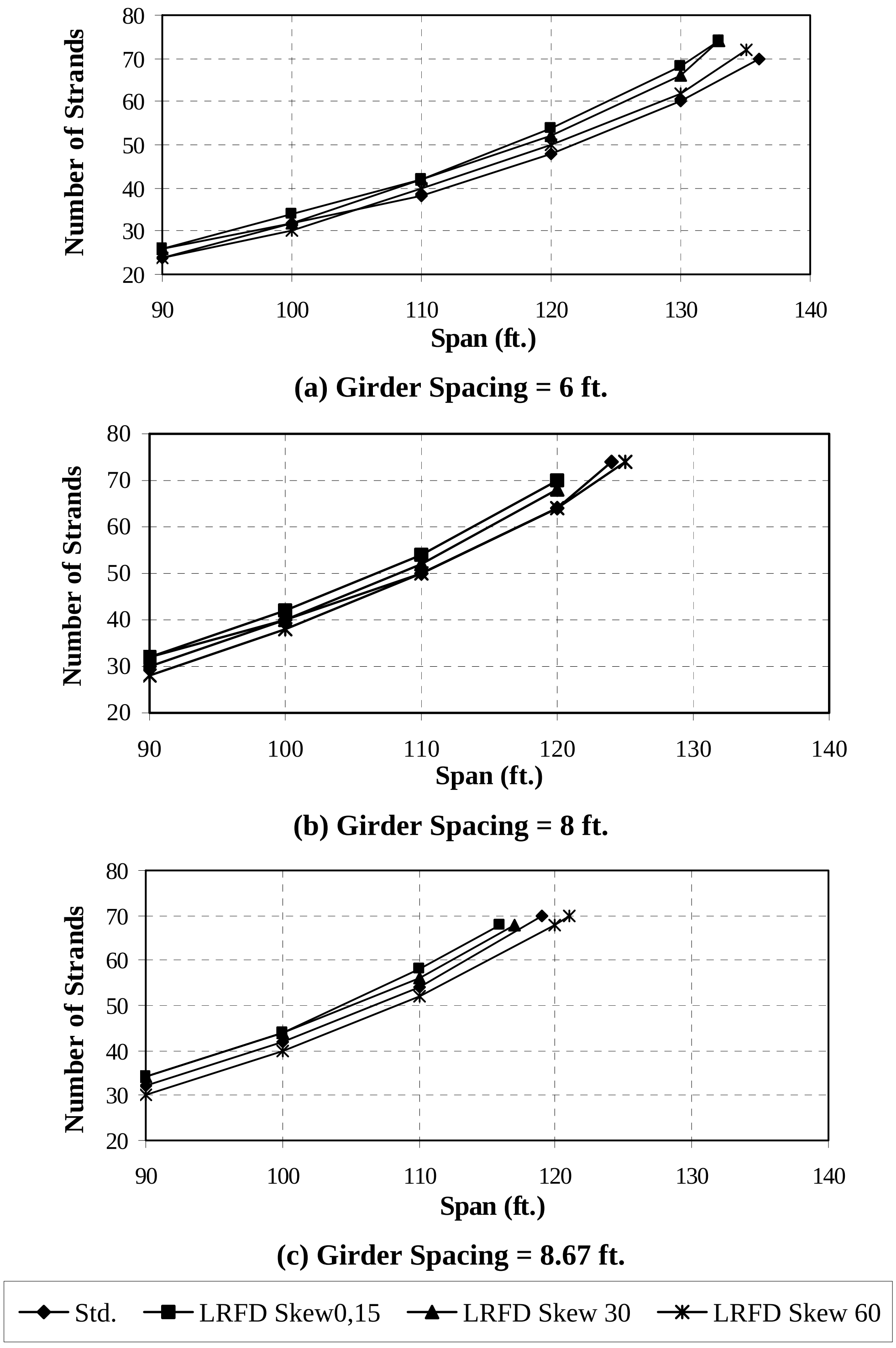

(a) Girder Spacing = 6 ft.

(b) Girder Spacing = 8 ft.

(c) Girder Spacing = 8.67 ft.

Figure 4.5. Comparison of Required Number of Strands (Type IV Girder, Strand Dia. = 0.5 in.).

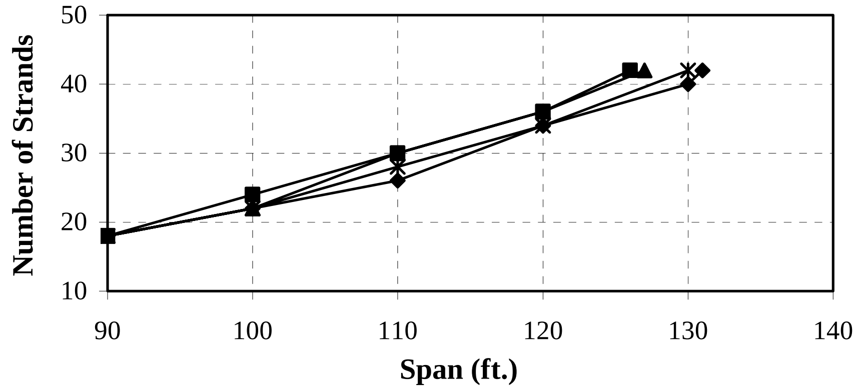

(a) Girder Spacing = 6 ft.

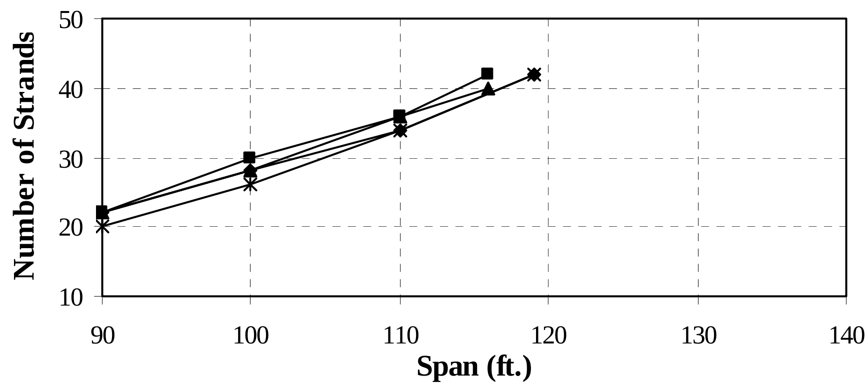

(b) Girder Spacing = 8 ft.

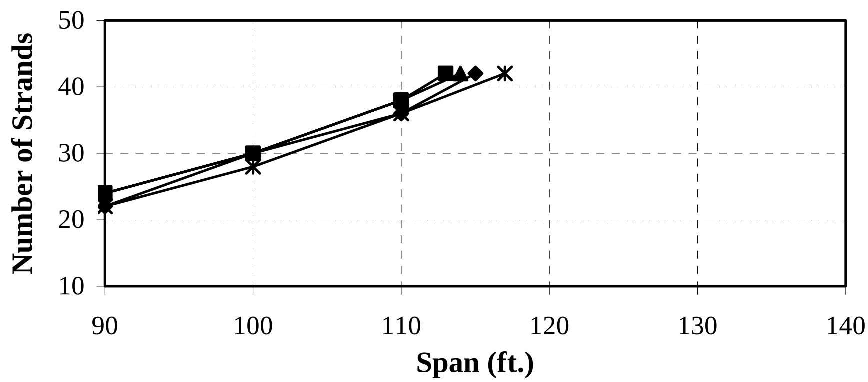

(c) Girder Spacing = 8.67 ft.

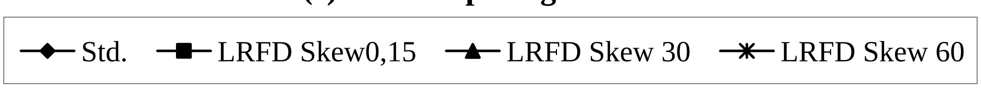

Figure 4.6. Comparison of Required Number of Strands (Type IV Girder, Strand Dia. = 0.6 in.).

4.3.4 Concrete Strengths Required at Release and at Service

4.3.4.1 Concrete Strength at Release

The optimized concrete strength at release depends on the stresses due to prestressing and the self-weight of the girder, along with the allowable stress limits at transfer. In general, there was a small increase in the number of strands required for some LRFD designs. As a result, an increase in the required concrete strength at release was observed. The results for 0.5 in. diameter strands are presented in Table 4.13.

Table 4.13. Concrete Strength at Release (f'_{ci}) (Type IV Girder, Strand Dia. = 0.5 in.).

Girder Spacing (ft.)	Span (ft.)	f'_{ci} (psi)	LRFD							
			Skew 0°		Skew 15°		Skew 30°		Skew 60°	
			f'_{ci} (psi)	Diff. %	f'_{ci} (psi)	Diff. %	f'_{ci} (psi)	Diff. %	f'_{ci} (psi)	Diff. %
6	90	4000.0	4000.0	0.0	4000.0	0.0	4000.0	0.0	4000.0	0.0
	100	4000.0	4009.7	0.2	4009.7	0.2	4000.0	0.0	4000.0	0.0
	110	4244.3	4739.7	11.7	4739.7	11.7	4739.8	11.7	4481.4	5.6
	120	5246.7	5930.6	13.0	5930.6	13.0	5692.1	8.5	5453.4	3.9
	130	6403.0	6510.0	1.7	6510.0	1.7	6506.0	1.6	6318.9	-1.3
	133	-	6655.0	-	6655.0	-	6655.0	-	-	-
	135	-	-	-	-	-	-	-	6598.7	-
	136	6613.4	-	-	-	-	-	-	-	-
8	90	4000.0	4000.0	0.0	4000.0	0.0	4000.0	0.0	4000.0	0.0
	100	4478.3	4707.7	5.1	4707.7	5.1	4450.0	-0.6	4191.4	-6.4
	110	5456.6	5893.2	8.0	5893.2	8.0	5655.3	3.6	5417.0	-0.7
	120	6538.4	6582.9	0.7	6582.9	0.7	6471.2	-1.0	6482.5	-0.9
	124	6750.8	-	-	-	-	-	-	-	-
	125	-	-	-	-	-	-	-	6624.7	-
8.67	90	4000.0	4000.0	0.0	4000.0	0.0	4000.0	0.0	4000.0	0.0
	100	4739.1	4964.5	4.8	4964.5	4.8	4964.6	4.8	4450.0	-6.1
	110	5939.6	6057.8	2.0	6057.8	2.0	5837.0	-1.7	5655.4	-4.8
	116	-	6603.4	-	6603.4	-	-	-	-	-
	117	-	-	-	-	-	6561.0	-	-	9-
	119	6716.0	-	-	-	-	-	-	-	-
	120	-	-	-	-	-	-	-	6471.2	-
	121	-	-	-	-	-	-	-	6538.9	-

The minimum strength at release was considered to be 4000 psi in this study, and this minimum value governed for a 90 ft. span length. The LRFD designs generally required a slightly higher concrete strength at release, with a maximum difference of 12 percent. The concrete strength at release is limited to 6750 psi and, in most cases, this governs the maximum span length.

4.3.4.2 Concrete Strength at Service

The concrete strength at service is affected by the stresses at midspan due to the prestressing force, dead loads, superimposed loads, and live loads, along with the allowable stress limits at service. The results for 0.5 in. diameter strands are presented in Table 4.14.

Table 4.14. Concrete Strength at Service (f'_c) (Type IV Girder, Strand Dia. = 0.5 in.).

Girder Spacing (ft.)	Span (ft.)	f'_c (psi)	LRFD							
			Skew 0°		Skew 15°		Skew 30°		Skew 60°	
			f'_c (psi)	Diff. %	f'_c (psi)	Diff. %	f'_c (psi)	Diff. %	f'_c (psi)	Diff. %
6	90	5000.0	5000.0	0.0	5000.0	0.0	5000.0	0.0	5000.0	0.0
6	100	5000.0	5000.0	0.0	5000.0	0.0	5000.0	0.0	5000.0	0.0
6	110	5000.0	5000.0	0.0	5000.0	0.0	5000.0	0.0	5000.0	0.0
6	120	5955.5	5930.6	-0.4	5930.6	-0.4	5692.1	-4.4	5453.4	-8.4
6	130	7384.6	6833.0	-7.5	6833.0	-7.5	7215.8	-2.3	6699.9	-9.3
6	133	-	8619.5	-	8619.5	-	7683.3	-	-	-
6	135	-	-	-	-	-	-	-	7937.6	-
6	136	8621.6	-	-	-	-	-	-	-	-
8	90	5000.0	5000.0	0.0	5000.0	0.0	5000.0	0.0	5000.0	0.0
8	100	5000.0	5000.0	0.0	5000.0	0.0	5000.0	0.0	5000.0	0.0
8	110	5583.9	5893.2	5.5	5893.2	5.5	5655.3	1.3	5417.0	-3.0
8	120	7164.7	7598.9	6.1	7598.9	6.1	7639.9	6.6	6482.5	-9.5
8	124	8306.4	-	-	-	-	-	-	-	-
8	125	-	-	-	-	-	-	-	8305.0	-
8.67	90	5000.0	5000.0	0.0	5000.0	0.0	5000.0	0.0	5000.0	0.0
8.67	100	5000.0	5000.0	0.0	5000.0	0.0	5000.0	0.0	5000.0	0.0
8.67	110	5939.6	6057.8	2.0	6057.8	2.0	5837.0	-1.7	5655.4	-4.8
8.67	116	-	6780.5	-	6780.5	-	-	-	-	-
8.67	117	-	-	-	-	-	7261.9	-	-	-
8.67	119	7602.4	-	-	-	-	-	-	-	-
8.67	120	-	-	-	-	-	-	-	7222.7	-
8.67	121	-	-	-	-	-	-	-	7806.4	-

The concrete strength at service is limited to 8750 psi in this study. However, this limitation does not affect the maximum span length because the initial concrete strength approaches its limit before maximizing the final concrete strength. The LRFD Specifications do not have a significant effect on the concrete strength at service. A small reduction in the required concrete strength was observed for most cases, with the maximum difference being nearly 10 percent. The minimum concrete strength at service was considered as 5000 psi. For span lengths less than 110 ft. it was observed that this limit controls. Also, the concrete strength at service cannot be smaller than the concrete strength at release. This limitation governs for a few cases for 0.5 in. diameter strands and most of the cases for 0.6 in. diameter strands.

4.3.5 Initial and Final Prestress Losses

The loss in prestress occurs mainly from four sources: elastic shortening and relaxation of the prestressing, and creep and shrinkage of concrete. These losses are categorized into initial prestress loss and final prestress loss. The initial prestress loss occurs due to initial relaxation of steel and elastic shortening of prestressing strands. The final loss occurs due to final steel relaxation and creep and shrinkage of concrete.

4.3.5.1 Prestress Loss Due to Elastic Shortening of Steel

The loss of prestress due to elastic shortening of steel is dependent on the modulus of the prestressing strands, modulus of concrete at release, and number of prestressing strands. The modulus of the elasticity of prestressing strands is specified in the Standard Specifications as 28,000 ksi and in the LRFD Specifications as 28,500 ksi. The modulus of the concrete depends on the concrete strength at release. The required concrete strength at release is different for Standard and LRFD Specifications. The combined effect of these parameters results in a non-uniform trend. The prestress loss due to elastic shortening was found to be increasing for LRFD Specifications based design, except for a few cases when skew angle was 60 degrees.

An increase in girder spacing corresponded to a decrease in the difference between the loss calculated using the two specifications. The skew angle does not have a well defined effect on the loss, but for skew angle of 60 degrees the loss decreases. This decrease can be attributed to the decrease in the live load moments, thereby decreasing the number of prestressing strands and consequently the stress in the concrete. Similar trends were observed for 0.5 in. and 0.6 in. diameter strands. The results for 0.5 in. diameter strands are presented in Table 4.15.

Table 4.15. Prestress Loss Due to Elastic Shortening (ES) (Type IV Girder, Strand Dia. = 0.5 in.).

Girder Spacing (ft.)	Span (ft.)	STD ES (ksi)	LRFD							
			Skew 0°		Skew 15°		Skew 30°		Skew 60°	
			ES (ksi)	Diff. %	ES (ksi)	Diff. %	ES (ksi)	Diff. %	ES (ksi)	Diff. %
6	90	11.33	12.95	14.3	12.95	14.3	12.95	14.3	11.49	1.4
	100	13.28	14.05	5.8	14.05	5.8	13.45	1.3	12.81	-3.5
	110	14.16	15.33	8.3	15.33	8.3	15.33	8.2	14.84	4.8
	120	15.62	16.97	8.6	16.97	8.6	16.60	6.2	16.20	3.7
	130	16.91	18.84	11.4	18.84	11.4	18.44	9.0	17.68	4.5
	133	-	19.28	-	19.28	-	19.28	-	-	-
	135	-	-	-	-	-	-	-	18.87	-
	136	18.31	-	-	-	-	-	-	-	-
8	90	14.02	14.78	5.4	14.78	5.4	14.80	5.6	13.59	-3.0
	100	15.95	16.58	4.0	16.58	4.0	16.14	1.2	15.68	-1.7
	110	17.24	18.13	5.2	18.13	5.2	17.79	3.2	17.43	1.1
	120	18.88	20.11	6.5	20.11	6.5	19.93	5.6	19.07	1.0
	124	19.91	-	-	-	-	-	-	-	-
	125	-	-	-	-	-	-	-	20.11	-
8.67	90	14.59	15.33	5.1	15.33	5.1	15.36	5.2	14.20	-2.7
	100	16.38	17.01	3.8	17.01	3.8	17.00	3.8	16.14	-1.5
	110	17.93	19.08	6.4	19.08	6.4	18.80	4.9	17.78	-0.8
	116	-	20.14	-	20.14	-	-	-	-	-
	117	-	-	-	-	-	20.10	-	-	-
	119	19.90	-	-	-	-	-	-	-	-
	120	-	-	-	-	-	-	-	19.93	-
	121	-	-	-	-	-	-	-	20.07	-

4.3.5.2 Prestress Loss Due to Initial Steel Relaxation

The loss in prestress due to initial relaxation of steel is specified by the LRFD Specifications as a function of time, along with the jacking stress and yield stress of the prestressing strands. The time for release of prestress is taken as 24 hours. This provides a constant estimate of initial relaxation loss as 1.98 ksi. The Standard Specifications do not specify a particular formula to evaluate the initial relaxation loss. Following TxDOT practices (TxDOT 2001), the initial relaxation loss is taken as half the total relaxation loss.

Tables 4.16 and 4.17 show the results for 0.5 in. and 0.6 in. diameter strands, respectively. The cases with a 0-degree skew angle are compared because the skew angle has no effect on the initial relaxation loss. It was observed that the prestress loss due to relaxation calculated in accordance with LRFD Specifications yields a conservative estimate. The increase in the loss estimate for the LRFD designs relative to the Standard design for 0.5 in. diameter strands is in the range of 36 to 148 percent for 6 ft., 62 to 223 percent for 8 ft., and 70 to 168 percent for 8.67 ft. girder spacing. The increase in the initial relaxation loss was found to be in the range of 48 to 116 percent for 6 ft., 78 to 143 percent for 8 ft., and 72 to 168 percent for 8.67 ft. girder spacing when 0.6 in. diameter strands were used. The increase in the loss estimate becomes larger with increasing span and also with an increase in girder spacing.

4.3.5.3 Initial Prestress Loss

The initial prestress loss is the combination of losses due to elastic shortening and initial steel relaxation. The initial loss estimates provided by the LRFD Specifications are found to be conservative as compared to the Standard Specifications. Table 4.18 presents the results for strand diameter of 0.5 in. Similar trends were observed for 0.6 in. diameter strands. For skew angles from 0 to 60 degrees, the LRFD initial losses were up to 18 percent larger than for the Standard designs, with the largest increases for the 6 ft. girder spacing. These results are compared graphically in Figure 4.7.

Table 4.16. Prestress Loss due to Initial Steel Relaxation (Type IV Girder, Strand Dia. = 0.5 in.).

Girder Spacing (ft.)	Span (ft.)	Initial Relaxation Loss (ksi)		Difference %
		Standard	LRFD	
6	90	1.45	1.98	36.1
	100	1.26	1.98	57.5
	110	1.17	1.98	69.3
	120	0.99	1.98	100.8
	130	0.80	1.98	147.5
	133	-	1.98	-
	136	0.65	-	-
8	90	1.22	1.98	61.6
	100	1.00	1.98	97.8
	110	0.83	1.98	137.4
	120	0.61	1.98	223.4
	124	0.48	-	-
8.67	90	1.16	1.98	70.4
	100	0.95	1.98	108.1
	110	0.74	1.98	167.4
	116	-	1.98	-
	119	0.49	-	-

Table 4.17. Prestress Loss due to Initial Steel Relaxation (Type IV Girder, Strand Dia. = 0.6 in.).

Girder Spacing (ft.)	Span (ft.)	Initial Relaxation Loss (ksi)		Difference %
		Standard	LRFD	
6	90	1.34	1.98	48.2
	100	1.25	1.98	58.1
	110	1.15	1.98	71.8
	120	0.91	1.98	116.4
	126	-	1.98	-
	130	0.78	-	-
	131	0.71	-	-
8	90	1.14	1.98	73.5
	100	0.94	1.98	109.7
	110	0.82	1.98	142.8
	116	-	1.98	-
	119	0.59	-	-
8.67	90	1.15	1.98	71.6
	100	0.86	1.98	130.4
	110	0.74	1.98	168.4
	113	-	1.98	-
	115	0.54	-	-

Table 4.18. Initial Prestress Loss
(Type IV Girder, Strand Dia. = 0.5 in.).

Girder Spacing (ft.)	Span (ft.)	STD Initial Loss (%)	Initial Loss Percent for LRFD							
			Skew 0°		Skew 15°		Skew 30°		Skew 60°	
			Init. Loss (%)	Diff. %	Init. Loss (%)	Diff. %	Init. Loss (%)	Diff. %	Init. Loss (%)	Diff. %
6	90	6.31	7.37	16.7	7.37	16.7	7.37	16.7	6.65	5.4
	100	7.18	7.92	10.3	7.92	10.3	7.62	6.2	7.30	1.8
	110	7.57	8.55	12.9	8.55	12.9	8.55	12.9	8.31	9.7
	120	8.20	9.36	14.1	9.36	14.1	9.17	11.8	8.98	9.5
	130	8.75	10.28	17.5	10.28	17.5	10.08	15.3	9.71	11.0
	133	-	10.50	-	10.50	-	10.50	-	-	-
	135	-	-	-	-	-	-	-	10.30	-
	136	9.36	-	-	-	-	-	-	-	-
8	90	7.53	8.28	9.9	8.28	9.9	8.29	10.1	7.69	2.2
	100	8.37	9.16	9.5	9.16	9.5	8.95	6.9	8.72	4.2
	110	8.93	9.93	11.3	9.93	11.3	9.76	9.4	9.59	7.4
	120	9.62	10.91	13.4	10.91	13.4	10.82	12.4	10.40	8.0
	124	10.07	-	-	-	-	-	-	-	-
	125	-	-	-	-	-	-	-	10.91	-
8.67	90	7.78	8.55	9.9	8.55	9.9	8.56	10.0	7.99	2.7
	100	8.56	9.38	9.5	9.38	9.5	9.37	9.5	8.95	4.5
	110	9.22	10.40	12.8	10.40	12.8	10.26	11.3	9.76	5.9
	116	-	10.92	-	10.92	-	-	-	-	-
	117	-	-	-	-	-	10.90	-	-	-
	119	10.07	-	-	-	-	-	-	-	-
	120	-	-	-	-	-	-	-	10.82	-
	121	-	-	-	-	-	-	-	10.89	-

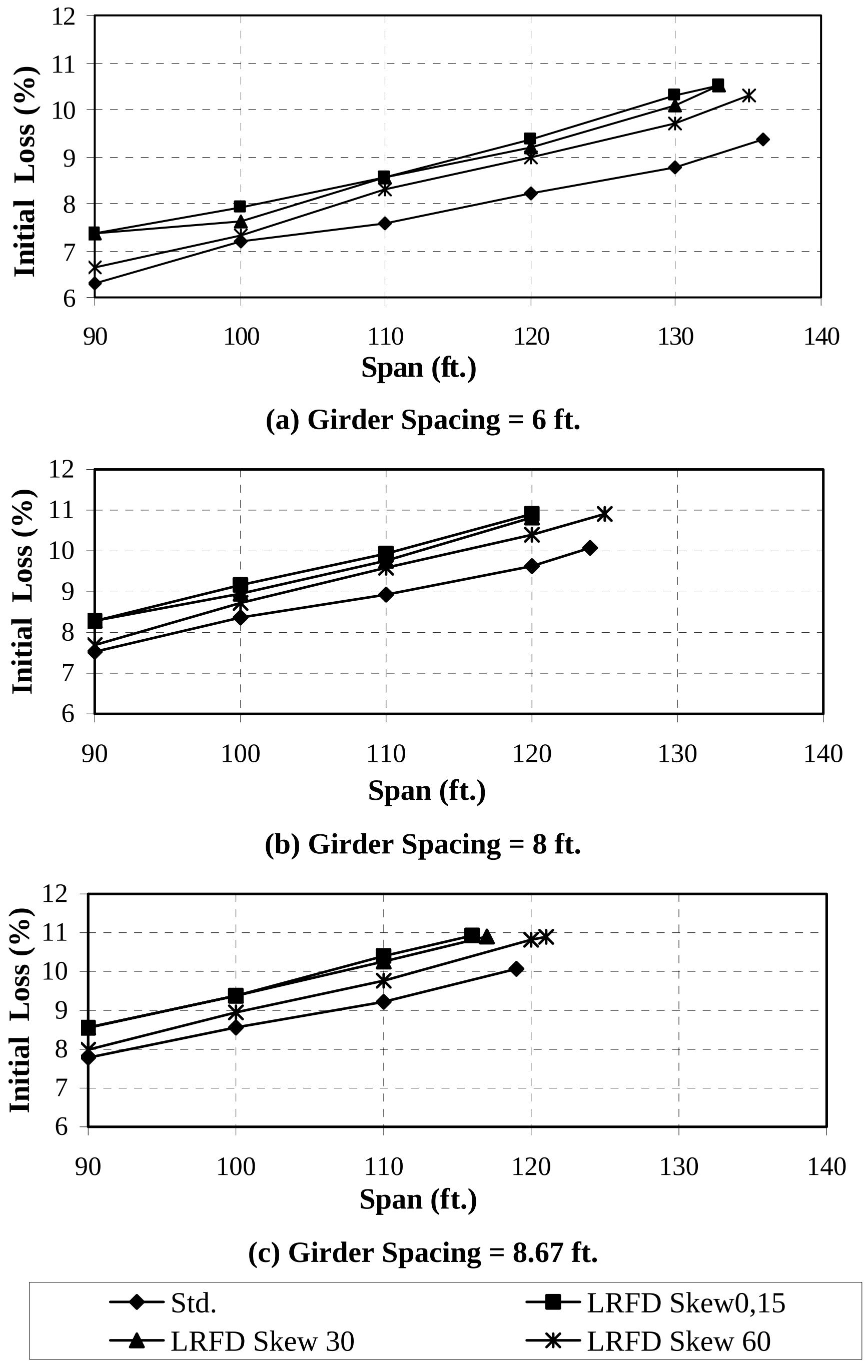

Figure 4.7. Initial Prestress Loss (Type IV Girder, Strand Dia. = 0.5 in.).

4.3.5.4 Total Prestress Loss Due to Steel Relaxation

The total prestress loss due to steel relaxation is a combination of loss due to initial relaxation and final relaxation of steel. The Standard Specifications specify empirical formulas to estimate the total loss due to steel relaxation, half of which is considered to be at initial conditions and the other half is considered in the final losses. This methodology is used by TxDOT Bridge Design Manual (TxDOT 2001). The LRFD Specifications specify an empirical formula to estimate the final prestress loss due to steel relaxation. The combined effect of the initial and final loss due to steel relaxation is presented in Table 4.19 for 0.5 in. diameter strand designs. Similar trends were observed for 0.6 in. diameter strands.

The estimate of total prestress loss due to steel relaxation provided by the LRFD Specifications is found to be significantly larger as compared to the Standard Specifications. The difference is in the range of 78 to 135 percent for 6 ft., 94 to 182 percent for 8 ft., and 98 to 164 percent for 8.67 ft. girder spacing when 0.5 in. strands are used. The difference increases with an increase in girder spacing, span length, and skew angle.

4.3.5.5 Prestress Loss Due to Shrinkage of Concrete

The Standard and LRFD Specifications prescribe the loss of prestress due to shrinkage of concrete as a function of relative humidity. For a relative humidity of 60 percent, the shrinkage loss was found to be 8 ksi for both Standard and LRFD Specifications for all design cases.

4.3.5.6 Prestress Loss Due to Creep of Concrete

The Standard and LRFD Specifications specify similar expressions for the estimation of prestress loss due to creep of concrete. The loss due to creep depends on the concrete stress at the center of gravity (c.g.) of prestressing strands due to dead loads before and after prestressing. The trends for 0.5 in. diameter are presented in Table 4.20 and the trends for 0.6 in. diameter strands were found to be similar. Small differences were observed in the estimates of the loss due to concrete creep for Standard and LRFD Specifications. The estimates for LRFD designs are slightly larger, except for cases with a skew angle of 60 degree. The difference decreases with an increase in span and girder spacing. The maximum difference was found to be 15 percent.

Table 4.19. Total Relaxation Loss (CR_S) (Type IV Girder, Strand Dia. = 0.5 in.).

Girder Spacing (ft.)	Span (ft.)	STD CR_S (ksi)	LRFD							
			Skew 0°		Skew 15°		Skew 30°		Skew 60°	
			CR_S (ksi)	Diff. %	CR_S (ksi)	Diff. %	CR_S (ksi)	Diff. %	CR_S (ksi)	Diff. %
6	90	2.91	5.18	78.0	5.18	78.0	5.18	78.0	5.46	87.6
	100	2.51	4.81	91.2	4.81	91.2	4.98	98.3	5.17	105.6
	110	2.34	4.46	90.7	4.46	90.7	4.46	90.8	4.62	97.4
	120	1.97	3.94	99.6	3.94	99.6	4.07	106.2	4.20	113.2
	130	1.60	3.42	113.8	3.42	113.8	3.53	120.5	3.76	135.0
	133	-	3.28	-	3.28	-	3.28	-	-	-
	135	-	-	-	-	-	-	-	3.41	-
	136	1.29	-	-	-	-	-	-	-	-
8	90	2.45	4.73	93.1	4.73	93.1	4.73	93.0	5.09	107.7
	100	2.00	4.22	111.0	4.22	111.0	4.37	118.5	4.53	126.1
	110	1.67	3.72	123.0	3.72	123.0	3.85	130.6	3.98	138.5
	120	1.22	3.15	157.4	3.15	157.4	3.23	163.7	3.45	182.1
	124	0.97	-	-	-	-	-	-	-	-
	125	-	-	-	-	-	-	-	3.17	-
8.67	90	2.32	4.58	97.3	4.58	97.3	4.58	97.1	4.93	112.3
	100	1.90	4.11	115.9	4.11	115.9	4.11	115.9	4.41	131.5
	110	1.48	3.49	135.5	3.49	135.5	3.60	143.1	3.88	162.4
	116	-	3.15	-	3.15	-	-	-	-	-
	117	-	-	-	-	-	3.18	-	-	-
	119	0.99	-	-	-	-	-	-	-	-
	120	-	-	-	-	-	-	-	3.27	-
	121	-	-	-	-	-	-	-	3.22	-

Table 4.20. Prestress Loss due to Creep of Concrete (CR_C) (Type IV Girder, Strand Dia. = 0.5 in.).

Girder Spacing (ft.)	Span (ft.)	STD CR_C (ksi)	LRFD							
			Skew 0°		Skew 15°		Skew 30°		Skew 60°	
			CR_C (ksi)	Diff. %	CR_C (ksi)	Diff. %	CR_C (ksi)	Diff. %	CR_C (ksi)	Diff. %
6	90	11.14	12.78	14.8	12.78	14.8	12.78	14.8	11.05	-0.8
	100	15.18	16.80	10.7	16.80	10.7	15.03	-1.0	13.23	-12.8
	110	16.90	19.99	18.3	19.99	18.3	19.98	18.2	18.35	8.6
	120	21.31	25.47	19.5	25.47	19.5	24.02	12.7	22.52	5.7
	130	26.18	30.31	15.8	30.31	15.8	29.32	12.0	26.99	3.1
	133	-	31.81	-	31.81	-	31.81	-	-	-
	135	-	-	-	-	-	-	-	30.33	-
	136	29.55	-	-	-	-	-	-	-	-
8	90	14.97	16.60	10.9	16.60	10.9	16.61	11.0	13.01	-13.1
	100	20.07	21.43	6.8	21.43	6.8	19.83	-1.2	18.19	-9.4
	110	24.16	26.75	10.7	26.75	10.7	25.30	4.7	23.83	-1.4
	120	29.76	32.24	8.3	32.24	8.3	31.33	5.3	29.29	-1.6
	124	32.86	-	-	-	-	-	-	-	-
	125	-	-	-	-	-	-	-	32.00	-
8.67	90	16.34	17.93	9.8	17.93	9.8	17.94	9.8	14.37	-12.0
	100	21.18	22.52	6.3	22.52	6.3	22.52	6.3	19.30	-8.9
	110	26.53	28.72	8.3	28.72	8.3	27.40	3.3	24.69	-6.9
	116	-	32.21	-	32.21	-	-	-	-	-
	117	-	-	-	-	-	31.83	-	-	-
	119	32.47	-	-	-	-	-	-	-	-
	120	-	-	-	-	-	-	-	30.67	-
	121	-	-	-	-	-	-	-	31.22	-

4.3.5.7 Total Prestress Loss

The total loss of prestress was estimated based on the Standard and LRFD Specifications. The results for 0.5 in. diameter strands are presented in Table 4.21 and Figure 4.8. The total losses for the LRFD designs are slightly larger as compared to those provided by the Standard Specifications. The difference was found to be in the range of 7 to 16 percent for 6 ft., 1 to 12 percent for 8 ft., and 1 to 11 percent for 8.67 ft. girder spacing. The conservatism was found to be decreasing with an increase in girder spacing, span length, and skew angle.

Table 4.21. Total Prestress Loss Percent (Type IV Girder, Strand Dia. = 0.5 in.).

Girder Spacing (ft.)	Span (ft.)	STD Tot. Loss (%)	LRFD Skew 0° Tot. Loss (%)	Skew 0° Diff. %	Skew 15° Tot. Loss (%)	Skew 15° Diff. %	Skew 30° Tot. Loss (%)	Skew 30° Diff. %	Skew 60° Tot. Loss (%)	Skew 60° Diff. %
6	90	16.48	19.22	16.6	19.22	16.6	19.22	16.6	17.78	7.8
	100	19.24	21.56	12.0	21.56	12.0	20.47	6.4	19.36	0.6
	110	20.44	23.60	15.4	23.60	15.4	23.59	15.4	22.62	10.6
	120	23.16	26.85	15.9	26.85	15.9	26.02	12.3	25.15	8.6
	130	26.02	29.91	15.0	29.91	15.0	29.28	12.5	27.87	7.1
	133	-	30.80	-	30.80	-	30.80	-	-	-
	135	-	-	-	-	-	-	-	29.94	-
	136	28.22	-	-	-	-	-	-	-	-
8	90	19.48	21.78	11.8	21.78	11.8	21.80	11.9	19.60	0.6
	100	22.72	24.81	9.2	24.81	9.2	23.87	5.1	22.91	0.8
	110	25.22	27.95	10.8	27.95	10.8	27.13	7.6	26.29	4.2
	120	28.57	31.36	9.8	31.36	9.8	30.86	8.0	29.54	3.4
	124	30.49	-	-	-	-	-	-	-	-
	125	-	-	-	-	-	-	-	31.25	-
8.67	90	20.37	22.64	11.1	22.64	11.1	22.66	11.2	20.50	0.6
	100	23.44	25.50	8.8	25.50	8.8	25.50	8.8	23.62	0.8
	110	26.64	29.28	9.9	29.28	9.9	28.54	7.2	26.84	0.8
	116	-	31.36	-	31.36	-	-	-	-	-
	117	-	-	-	-	-	31.16	-	-	-
	119	30.30	-	-	-	-	-	-	-	-
	120	-	-	-	-	-	-	-	30.55	-
	121	-	-	-	-	-	-	-	30.87	-

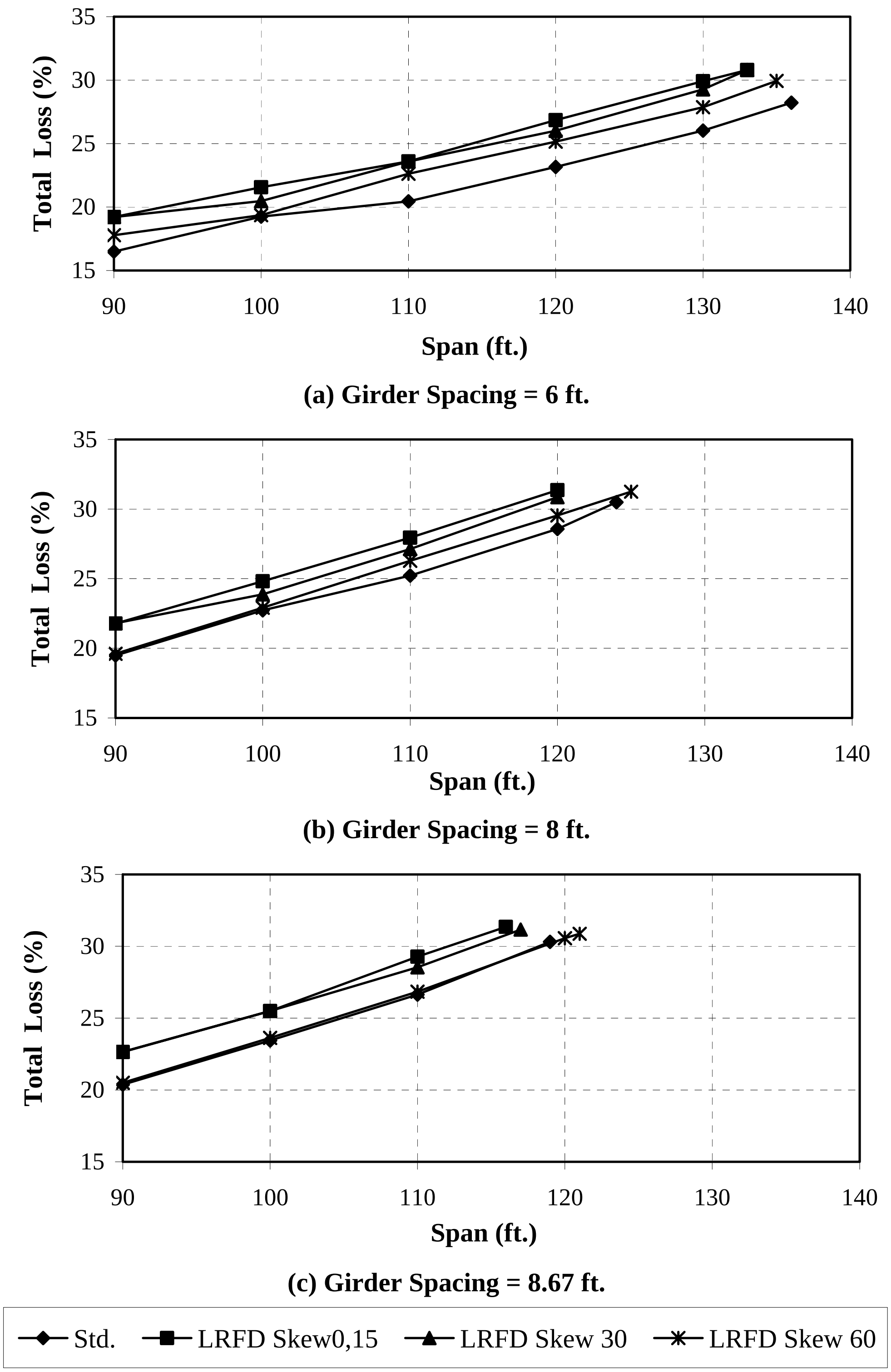

(a) Girder Spacing = 6 ft.

(b) Girder Spacing = 8 ft.

(c) Girder Spacing = 8.67 ft.

Figure 4.8. Total Prestress Loss (Type IV Girder, Strand Dia. = 0.5 in.).

4.4 ULTIMATE LIMIT STATE DESIGN

4.4.1 General

The impact of the LRFD Specifications on the requirements for the flexural and shear strength limit states is discussed in the following section. The decrease in the live load and live load factor, the required concrete strength at service, and the number of strands as determined for the service limit state, decreases the factored design moments and nominal moment capacities for the LRFD designs. The reinforcement limits are also different for both the Standard and LRFD designs. However, for all the design cases, the girder sections were found to be under-reinforced.

The LRFD Specifications employ a different methodology for the transverse and interface shear design as compared to the Standard Specifications. This change in the design procedures leads to a significant increase in the required shear reinforcement for LRFD designs.

4.4.2 Factored Design Moment

The load combinations for the ultimate limit state were significantly changed from the Standard to LRFD Specifications. The load factors for moments due to live load and dead loads except wearing surface load specified by the LRFD Specifications are smaller than the Standard Specifications. The load factor for moment due to wearing surface load is increased in the LRFD Specifications. The live load moments specified by the LRFD Specifications are larger than those of the Standard Specifications. The combined effect of these two changes results in design moments that are comparable.

A comparison of the design moments specified by the Standard and LRFD Specifications is presented in Table 4.22. The LRFD Specifications yield design moments for Type IV girders that are in general slightly larger than for the Standard Specifications. The difference is found to decrease with an increase in span length, girder spacing, and skew angle beyond 30 degrees. The LRFD design moments for a skew angle of 60 degrees are less conservative. The difference in the design moments was found to be in the range of -2 to 8 percent for 6 ft., -8 to 4 percent for 8 ft., and -10 to 3 percent for 8.67 ft. girder spacing.

Table 4.22. Factored Ultimate Moment (M_u) (Type IV Girder, Strand Dia. = 0.5 in.).

Girder Spacing (ft.)	Span (ft.)	STD M_u (k-ft.)	LRFD							
			Skew 0°		Skew 15°		Skew 30°		Skew 60°	
			M_u (k-ft.)	Diff. %	M_u (k-ft.)	Diff. %	M_u (k-ft.)	Diff. %	M_u (k-ft.)	Diff. %
6	90	3960.7	4278.7	8.0	4278.7	8.0	4200.0	6.0	3869.9	-2.3
	100	4690.2	5053.6	7.7	5053.6	7.7	4971.5	6.0	4626.8	-1.4
	110	5470.3	5884.6	7.6	5884.6	7.6	5799.2	6.0	5440.7	-0.5
	120	6299.9	6771.2	7.5	6771.2	7.5	6682.6	6.1	6310.9	0.2
	130	7179.5	7713.7	7.4	7713.7	7.4	7622.1	6.2	7237.7	0.8
	133	-	8007.3	-	8007.3	-	7914.9	-	-	-
	135	-	-	-	-	-	-	-	7722.4	-
	136	7731.2	-	-	-	-	-	-	-	-
8	90	4932.0	5117.6	3.8	5117.6	3.8	5006.4	1.5	4540.0	-7.9
	100	5821.5	6035.1	3.7	6035.1	3.7	5919.1	1.7	5432.5	-6.7
	110	6769.4	7017.9	3.7	7017.9	3.7	6897.3	1.9	6391.5	-5.6
	120	7774.6	8065.2	3.7	8065.2	3.7	7940.3	2.1	7416.3	-4.6
	124	8192.8	-	-	-	-	-	-	-	-
	125	-	-	-	-	-	-	-	7953.5	-
8.67	90	5232.1	5365.6	2.6	5365.6	2.6	5243.0	0.2	4728.9	-9.6
	100	6169.1	6323.7	2.5	6323.7	2.5	6195.8	0.4	5659.4	-8.3
	110	7166.6	7349.4	2.6	7349.4	2.6	7216.6	0.7	6659.1	-7.1
	116	-	7996.9	-	7996.9	-	-	-	-	-
	117	-	-	-	-	-	7971.0	-	-	-
	119	8114.9	-	-	-	-	-	-	-	-
	120	-	-	-	-	-	-	-	7727.0	-
	121	-	-	-	-	-	-	-	7837.6	-

4.4.3 Section Behavior in Flexure

The impact of the LRFD Specifications on the section behavior is discussed in this section. The Standard Specifications define a section to behave as a rectangular section if the depth of the equivalent stress block is less than the thickness of the compression flange (slab). The LRFD Specifications use the location of neutral axis to categorize the section behavior as rectangular or flanged. The section is defined to be rectangular if the neutral axis lies in the compression flange (slab). The expression specified by the LRFD Specifications for the determination of the neutral axis depth is different from the Standard Specifications.

Flanged section behavior is categorized into two cases in the Standard Specifications. The first case is when the depth of the stress block is less than the sum of the slab and girder flange thickness. The second case is when the depth of the stress block exceeds the sum of the thickness of the slab and girder flange. It was observed that for the Standard designs in this study, most of the sections have rectangular section behavior and for a few cases when the span length is larger than 120 ft. the stress block enters the girder flange. The stress block does not enter the web portion of the girder for any of the cases considered in the parametric study.

Flanged section behavior is divided into three categories in the LRFD Specifications based on the location of the neutral axis: (1) within the flange of the girder, (2) within the fillet portion of the girder, and (3) within the web of the girder. It was observed that for span lengths up to 110 ft. the compression zone is rectangular for most cases. For span lengths up to 120 ft. the neutral axis lies in the girder flange, and thereafter in the fillet portion of the girder. The neutral axis does not lie in the girder web for any of the cases considered for this study. Table 4.23 summarizes the type of section behavior observed in the parametric study when evaluating the nominal moment for Type IV beams. Figures 4.9 and 4.10 compare the depth of the equivalent stress block and neutral axis for the various design cases. Note that the slab (deck) thickness is 8 in.

Table 4.23. Section Behavior (Type IV Girder, Strand Dia. = 0.5 in.).

Girder Spacing (ft.)	Span (ft.)	Standard Section Behavior	LRFD Section Behavior			
			Skew 0°	Skew 15°	Skew 30°	Skew 60°
6	90	Rec.	Rec.	Rec.	Rec.	Rec.
	100	Rec.	Rec.	Rec.	Rec.	Rec.
	110	Rec.	Flanged*	Flanged*	Flanged*	Rec.
	120	Rec.	Flanged*	Flanged*	Flanged*	Flanged*
	130	Flanged*	Flanged**	Flanged**	Flanged**	Flanged**
	133	-	Flanged**	Flanged**	Flanged**	-
	135	-	-	-	-	Flanged**
	136	Flanged*	-	-	-	-
8	90	Rec.	Rec.	Rec.	Rec.	Rec.
	100	Rec.	Rec.	Rec.	Rec.	Rec.
	110	Rec.	Rec.	Rec.	Rec.	Rec.
	120	Rec.	Flanged*	Flanged*	Flanged*	Flanged*
	124	Flanged*	-	-	-	-
	125	-	-	-	-	Flanged*
8.67	90	Rec.	Rec.	Rec.	Rec.	Rec.
	100	Rec.	Rec.	Rec.	Rec.	Rec.
	110	Rec.	Rec.	Rec.	Rec.	Rec.
	116	-	Flanged*	Flanged*	-	-
	117	-	-	-	Flanged*	-
	119	Rec.	-	-	-	-
	120	-	-	-	-	Flanged*
	121	-	-	-	-	Flanged*

Notes:

1) Flanged*: The section behaves as a flanged section with neutral axis lying in the girder flange for LRFD Specifications and stress block lying in the girder flange for Standard Specifications.
2) Flanged**: The section behaves as a flanged section with neutral axis lying in the fillet area of the girder for LRFD Specifications and stress block lying in the fillet area of the girder for Standard Specifications.

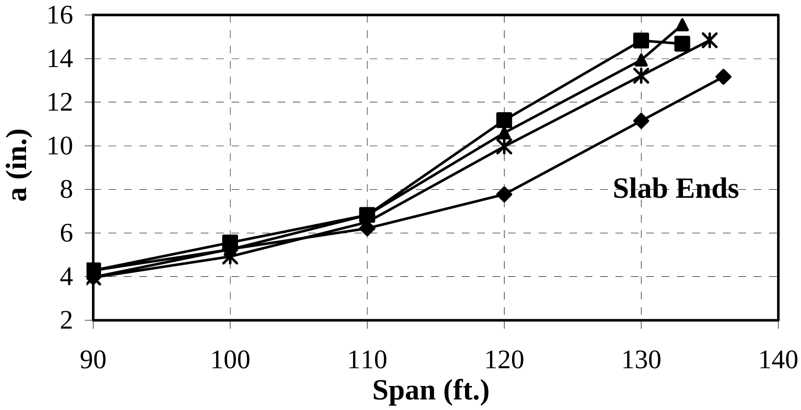

(a) Girder Spacing = 6 ft.

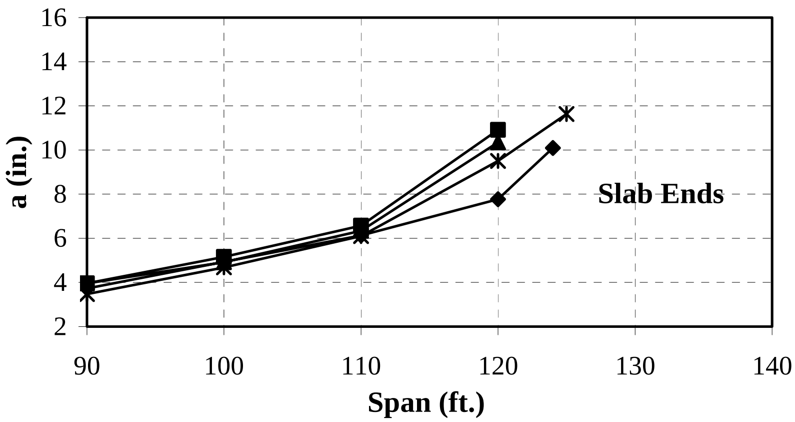

(b) Girder Spacing = 8 ft.

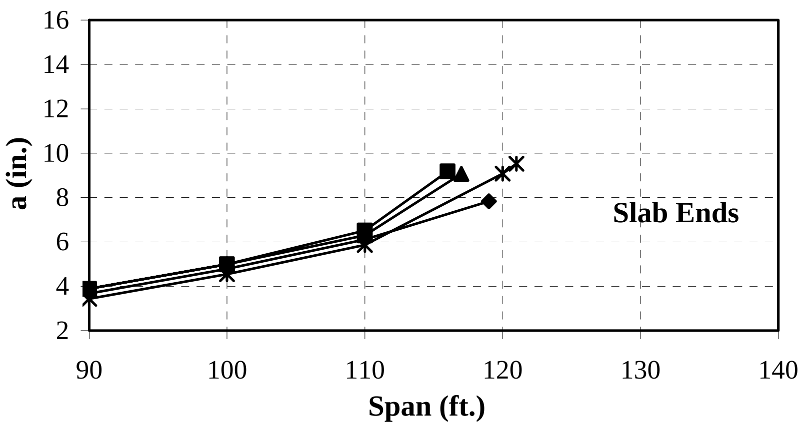

(c) Girder Spacing = 8.67 ft.

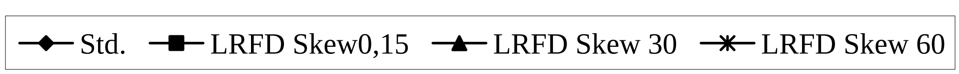

Figure 4.9. Comparison of Equivalent Stress Block Depth, *a*
(Type IV Girder, Strand Dia. = 0.5 in.).

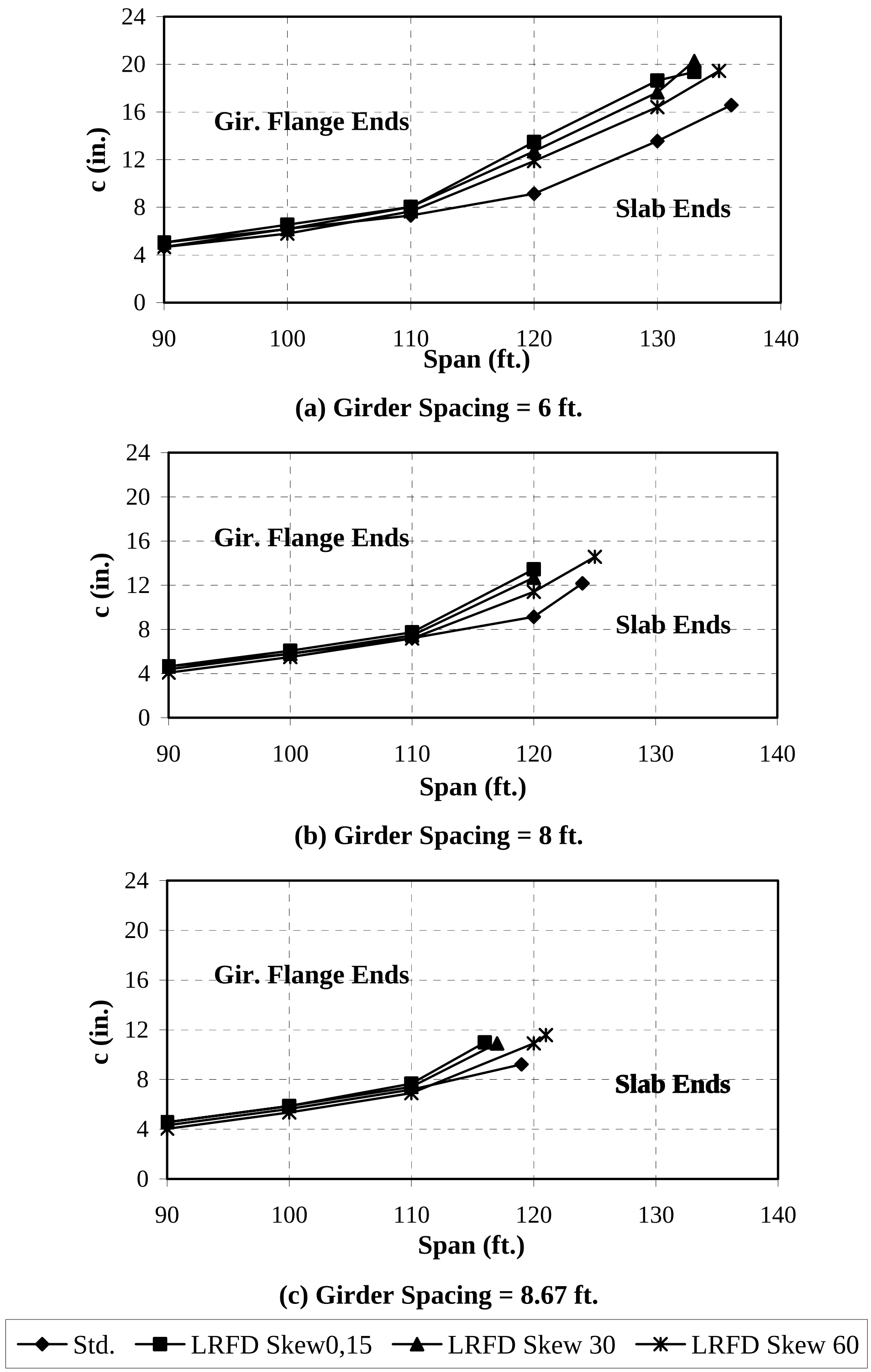

Figure 4.10. Comparison of Neutral Axis Depth, *c*
(Type IV Girder, Strand Dia. = 0.5 in.).

4.4.4 Nominal Moment Capacity

The changes in the concrete strength at service and the number of strands for LRFD designs, relative to Standard designs, affect the nominal moment resistance. The change in the expression for evaluation of effective prestress in the prestressing strands also has an impact. A comparison of the nominal moment capacities for the Type IV girder designs is presented in Table 4.24.

Table 4.24. Moment Resistance (M_r) (Type IV Girder, Strand Dia. = 0.5 in.).

Girder Spacing (ft.)	Span (ft.)	STD M_r (k-ft.)	LRFD Skew 0° M_r (k-ft.)	Skew 0° Diff. %	Skew 15° M_r (k-ft.)	Skew 15° Diff. %	Skew 30° M_r (k-ft.)	Skew 30° Diff. %	Skew 60° M_r (k-ft.)	Skew 60° Diff. %
6	90	4616.7	4946.8	7.2	4946.8	7.2	4946.8	7.2	4606.8	-0.2
	100	5962.4	6273.2	5.2	6273.2	5.2	5946.6	-0.3	5616.7	-5.8
	110	6923.2	7421.7	7.2	7421.7	7.2	7421.7	7.2	7205.9	4.1
	120	8400.9	8870.0	5.6	8870.0	5.6	8645.8	2.9	8416.9	0.2
	130	9959.0	10004.7	0.5	10004.7	0.5	9883.1	-0.8	9557.1	-4.0
	133	-	10391.0	-	10391.0	-	10303.4	-	-	-
	135	-	-	-	-	-	-	-	10242.8	-
	136	10964.0	-	-	-	-	-	-	-	-
8	90	5728.7	6059.9	5.8	6059.9	5.8	6059.9	5.8	5371.2	-6.2
	100	7398.1	7695.8	4.0	7695.8	4.0	7379.1	-0.3	7060.0	-4.6
	110	8936.6	9489.1	6.2	9489.1	6.2	9200.8	3.0	8910.2	-0.3
	120	10836.0	11018.7	1.7	11018.7	1.7	10872.3	0.3	10515.9	-3.0
	124	11857.1	-	-	-	-	-	-	-	-
	125	-	-	-	-	-	-	-	11278.7	-
8.67	90	6099.1	6430.4	5.4	6430.4	5.4	6430.4	5.4	5740.4	-5.9
	100	7760.2	8058.9	3.9	8058.9	3.9	8058.9	3.9	7420.0	-4.4
	110	9589.7	10113.7	5.5	10113.7	5.5	9838.6	2.6	9268.1	-3.4
	116	-	11078.3	-	11078.3	-	-	-	-	-
	117	-	-	-	-	-	11081.2	-	-	-
	119	11608.2	-	-	-	-	-	-	-	-
	120	-	-	-	-	-	-	-	11081.0	-
	121	-	-	-	-	-	-	-	11240.0	-

The nominal moment capacity for the LRFD designs tended to be slightly larger than for the parallel Standard designs for most cases. For a skew angle of 60 degrees, the LRFD nominal moment capacity values tend to be smaller compared to the Standard values. The difference between the moment resistance capacities predicted by the Standard and LRFD Specifications is found to be in the range of -6 to 7 percent for the cases considered.

The impact of the LRFD Specifications on the M_u/M_r ratio was also investigated. This ratio provides an assessment of the relative safety for flexure at ultimate. The comparison is presented in Table 4.25 and illustrated in Figure 4.11. A well-defined trend was not observed for this ratio. However, only a very small difference was observed between the M_u/M_r ratios when comparing the Standard and LRFD designs, and the maximum value was 0.86 for both specifications.

Table 4.25. M_u/M_r Ratio (Type IV Girder, Strand Dia. = 0.5 in.).

Girder Spacing (ft.)	Span (ft.)	STD M_u/M_r	LRFD							
			Skew 0°		Skew 15°		Skew 30°		Skew 60°	
			M_u/M_r	Diff. %	M_u/M_r	Diff. %	M_u/M_r	Diff. %	M_u/M_r	Diff. %
6	90	0.86	0.86	0.8	0.86	0.8	0.85	-1.0	0.84	-2.1
	100	0.79	0.81	2.4	0.81	2.4	0.84	6.3	0.82	4.7
	110	0.79	0.79	0.3	0.79	0.3	0.78	-1.1	0.76	-4.4
	120	0.75	0.76	1.8	0.76	1.8	0.77	3.1	0.75	0.0
	130	0.72	0.77	6.9	0.77	6.9	0.77	7.0	0.76	5.1
	133	-	0.77	-	0.77	-	0.77	-	-	-
	135	-	-	-	-	-	-	-	0.75	-
	136	0.71	-	-	-	-	-	-	-	-
8	90	0.86	0.84	-1.9	0.84	-1.9	0.83	-4.0	0.85	-1.8
	100	0.79	0.78	-0.3	0.78	-0.3	0.80	1.9	0.77	-2.2
	110	0.76	0.74	-2.4	0.74	-2.4	0.75	-1.0	0.72	-5.3
	120	0.72	0.73	2.0	0.73	2.0	0.73	1.8	0.71	-1.7
	124	0.69	-	-	-	-	-	-	-	-
	125	-	-	-	-	-	-	-	0.71	-
8.67	90	0.86	0.83	-2.7	0.83	-2.7	0.82	-5.0	0.82	-4.0
	100	0.79	0.78	-1.3	0.78	-1.3	0.77	-3.3	0.76	-4.1
	110	0.75	0.73	-2.8	0.73	-2.8	0.73	-1.9	0.72	-3.9
	116	-	0.72	-	0.72	-	-	-	-	-
	117	-	-	-	-	-	0.72	-	-	-
	119	0.70	-	-	-	-	-	-	-	-
	120	-	-	-	-	-	-	-	0.70	-
	121	-	-	-	-	-	-	-	0.70	-

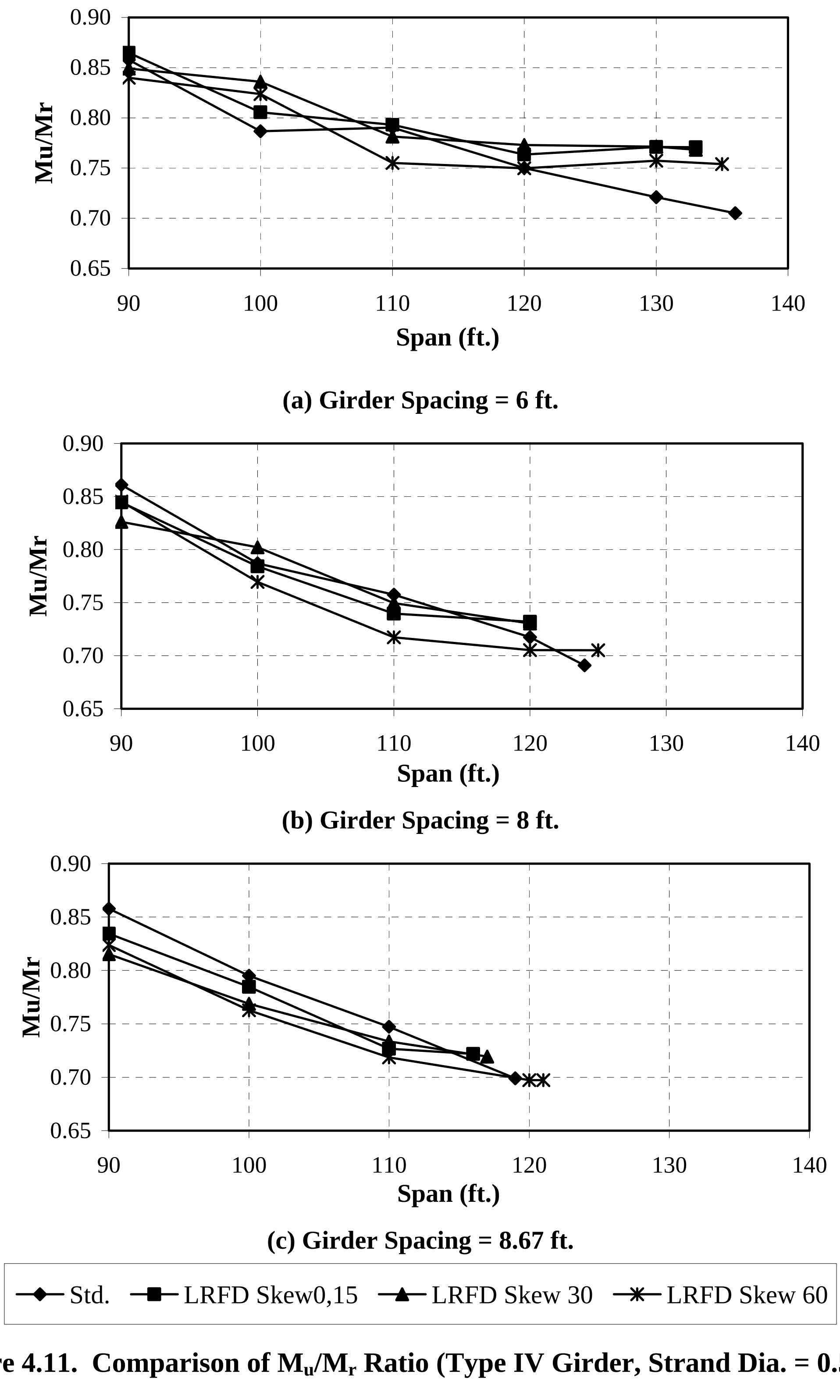

Figure 4.11. Comparison of M_u/M_r Ratio (Type IV Girder, Strand Dia. = 0.5 in.).

4.4.5 Shear Design

4.4.5.1 General

The transverse shear design and the interface shear design are two areas where significant differences between Standard and LRFD designs were observed in the parametric study results. These differences are caused due to a significant increase in the shear force specified by the LRFD Specifications. The increase in concrete strength and the new MCFT approach for transverse shear design in the LRFD Specifications also affect the transverse shear design.

Some basic background on the MCFT approach for transverse shear design use in the LRFD Specifications is provided in Chapter 3. The LRFD Specifications have provided an extensive background of the mechanics and development of the MCFT model, which can be very useful for bridge engineers to understand and implement the MCFT in shear designs. Transverse shear design using MCFT results in a relatively complex design process and, as such, may not be suitable for routine bridge design. Research is being carried out at the University of Illinois to develop simplified shear design procedures for use in practice. These formulas can be helpful for TxDOT engineers, if their applicability to the typical Texas bridges is verified. Similar research is being carried out at Purdue University to establish simplified design expressions for shear design.

4.4.5.2 Transverse Shear Reinforcement

A comparison of the transverse shear reinforcement area for Standard and LRFD designs is presented in Table 4.26. The transverse shear reinforcement area was found to increase significantly for LRFD designs for most of the Type IV cases studies. The transverse shear reinforcement increases in the range of -2.6 percent to 314 percent for a 6 ft. girder spacing. The difference increases with an increase in the span length, ranging from -29 percent to 423 percent for 8 ft. girder spacing and -40 percent to 66 percent for 8.67 ft. girder spacing.

Table 4.26. Comparison of Transverse Shear Reinforcement Area (Type IV Girder, Strand Diameter = 0.5 in.).

Girder Spacing (ft.)	Span (ft.)	STD A_v (in.^{2}/ft.)	LRFD							
			Skew = 0°		Skew = 15°		Skew = 30°		Skew = 60°	
			A_v (in.^{2}/ft.)	Diff. %	A_v (in.^{2}/ft.)	Diff. %	A_v (in.^{2}/ft.)	Diff. %	A_v (in.^{2}/ft.)	Diff. %
6	90	0.13	0.13	-2.6	0.14	7.0	0.16	17.7	0.21	60.7
	100	0.11	0.17	47.3	0.18	58.3	0.20	71.8	0.25	120.7
	110	0.09	0.20	113.0	0.21	128.5	0.23	146.4	0.29	213.0
	120	0.08	0.21	163.1	0.23	183.0	0.25	216.7	0.33	314.0
	130	0.08	0.21	167.5	0.23	188.4	0.23	190.4	0.32	301.7
	133	-	0.17	-	0.19	-	0.25	-	-	-
	135	-	-	-	-	-	-	-	0.32	-
	136	0.08	-	-	-	-	-	-	-	-
8	90	0.30	0.22	-28.5	0.23	-23.6	0.25	-18.1	0.31	3.4
	100	0.29	0.26	-10.4	0.27	-4.5	0.29	1.9	0.36	26.5
	110	0.22	0.26	16.4	0.28	24.8	0.31	39.3	0.40	79.4
	120	0.08	0.27	242.8	0.29	267.5	0.30	280.9	0.42	423.3
	124	0.08	-	-	-	-	-	-	-	-
	125	-	-	-	-	-	-	-	0.42	-
8.67	90	0.36	0.24	-33.7	0.26	-29.2	0.27	-24.1	0.34	-5.2
	100	0.34	0.28	-17.6	0.30	-12.6	0.32	-6.8	0.40	15.7
	110	0.26	0.28	6.6	0.30	14.3	0.33	26.1	0.42	62.4
	116	-	0.30	-	0.32	-	-	-	-	-
	117	-	-	-	-	-	0.33	-	-	-
	119	0.08	-	-	-	-	-	-	-	-
	120	-	-	-	-	-	-	-	0.44	-
	121	-	-	-	-	-	-	-	0.44	-

4.4.5.3 Interface Shear Reinforcement

This section includes the results for the interface shear design for Standard and LRFD designs. The LRFD Specifications provide the cohesion and friction factors for two cases: one when the interface is roughened and another when the interface is not roughened. Both these cases were evaluated for the Type IV girder cases and the results are summarized. The proposed provisions to be included in the LRFD Specifications are also investigated.

A comparison of the interface shear reinforcement area for Standard and LRFD designs is presented in Table 4.27. The interface shear reinforcement area was found to increase significantly for LRFD designs for the case when the interface is roughened. The interface shear reinforcement area increased in the range of 0 to 145 percent for a 6 ft. girder spacing. This difference was found to be in the range of 16 to 218 percent for an 8 ft. girder spacing and 40 to 192 percent for an 8.67 ft. girder spacing.

Table 4.27. Comparison of Interface Shear Reinforcement Area with Roughened Interface (Type IV Girder, Strand Diameter = 0.5 in.).

Girder Spacing (ft.)	Span (ft.)	STD A_{vh} (in.^{2}/ft.)	LRFD							
			Skew = 0°		Skew = 15°		Skew = 30°		Skew = 60°	
			A_{vh} (in.^{2}/ft.)	Diff. %	A_{vh} (in.^{2}/ft.)	Diff. %	A_{vh} (in.^{2}/ft.)	Diff. %	A_{vh} (in.^{2}/ft.)	Diff. %
6	90	0.20	0.20	0.0	0.20	0.0	0.20	0.0	0.24	21.4
	100	0.20	0.20	0.0	0.20	0.0	0.20	0.0	0.29	46.9
	110	0.20	0.20	0.0	0.22	9.2	0.25	23.9	0.35	76.2
	120	0.20	0.26	29.2	0.29	43.6	0.31	57.0	0.43	114.6
	130	0.20	0.31	55.3	0.34	71.2	0.37	84.8	0.49	145.6
	133	-	0.35	-	0.38	-	0.41	-	-	-
	135	-	-	-	-	-	-	-	0.55	-
	136	0.20	-	-	-	-	-	-	-	-
8	90	0.20	0.23	16.0	0.26	28.9	0.29	43.6	0.39	94.7
	100	0.20	0.28	41.8	0.31	56.1	0.34	70.2	0.46	128.6
	110	0.20	0.34	69.3	0.37	85.1	0.40	101.3	0.53	166.4
	120	0.20	0.45	124.0	0.48	142.3	0.51	155.5	0.64	217.9
	124	0.20	-	-	-	-	-	-	-	-
	125	-	-	-	-	-	-	-	0.74	-
8.67	90	0.20	0.27	33.8	0.30	47.5	0.33	63.2	0.44	118.1
	100	0.20	0.32	61.0	0.35	76.1	0.39	93.5	0.51	153.7
	110	0.20	0.38	90.7	0.42	107.5	0.45	124.1	0.58	192.4
	116	-	0.45	-	0.49	-	-	-	-	-
	117	-	-	-	-	-	0.54	-	-	-
	119	0.20	-	-	-	-	-	-	-	-
	120	-	-	-	-	-	-	-	0.71	-
	121	-	-	-	-	-	-	-	0.73	-

As expected, the interface shear reinforcement area shows even larger increases for LRFD designs for the case of the unroughened interface. A comparison of the interface shear reinforcement area for Standard and LRFD designs is presented in Table 4.28. The interface shear reinforcement area increases in the range of 75 to 392 percent for 6 ft. girder spacing. This difference is in the range of 180 to 513 percent for 8 ft. girder spacing and 200 to 470 percent for 8.67 ft. girder spacing.

Table 4.28. Comparison of Interface Shear Reinforcement Area without Roughened Interface (Type IV Girder, Strand Diameter = 0.5 in.).

Girder Spacing (ft.)	Span (ft.)	STD A_{vh} (in.^{2}/ft.)	LRFD							
			Skew = 0°		Skew = 15°		Skew = 30°		Skew = 60°	
			A_{vh} (in.^{2}/ft.)	Diff. %	A_{vh} (in.^{2}/ft.)	Diff. %	A_{vh} (in.^{2}/ft.)	Diff. %	A_{vh} (in.^{2}/ft.)	Diff. %
6	90	0.20	0.35	75.2	0.39	92.7	0.42	112.5	0.57	185.6
	100	0.20	0.42	110.1	0.46	129.4	0.50	149.0	0.66	228.2
	110	0.20	0.49	144.1	0.53	165.3	0.58	189.8	0.75	276.9
	120	0.20	0.60	198.7	0.65	222.7	0.69	245.0	0.88	341.0
	130	0.20	0.68	242.2	0.74	268.6	0.78	291.3	0.99	392.7
	133	-	0.75	-	0.80	-	0.86	-	-	-
	135	-	-	-	-	-	-	-	1.09	-
	136	0.20	-	-	-	-	-	-	-	-
8	90	0.20	0.55	176.7	0.60	198.1	0.65	222.7	0.82	307.9
	100	0.20	0.64	219.7	0.69	243.5	0.73	267.1	0.93	364.4
	110	0.20	0.73	265.5	0.78	291.8	0.84	318.8	1.05	427.3
	120	0.20	0.91	356.6	0.97	387.2	1.02	409.2	1.23	513.1
	124	0.20	-	-	-	-	-	-	-	-
	125	-	-	-	-	-	-	-	1.39	-
8.67	90	0.20	0.61	206.3	0.66	229.2	0.71	255.4	0.89	346.8
	100	0.20	0.70	251.6	0.75	276.8	0.81	305.9	1.01	406.2
	110	0.20	0.80	301.2	0.86	329.2	0.91	356.9	1.14	470.7
	116	-	0.92	-	0.98	-	-	-	-	-
	117	-	-	-	-	-	1.06	-	-	-
	119	0.20	-	-	-	-	-	-	-	-
	120	-	-	-	-	-	-	-	1.35	-
	121	-	-	-	-	-	-	-	1.39	-

4.5 CAMBER

The Standard Specifications do not provide guidelines for determining the camber of prestressed concrete members. The Hyperbolic Functions Method (Furr et al. 1968, Sinno 1968, Furr and Sinno 1970) for the calculation of maximum camber is used by TxDOT's prestressed concrete bridge design software, PSTRS14 (TxDOT 2004). The details of this method are described in the design examples provided in the second volume of this report. Because the camber is evaluated using the same methodology for both specifications, only a small difference is observed. The results for camber are summarized in Table 4.29. The camber values for LRFD designs are larger as compared to those for Standard designs. The maximum differences in the camber are 21 percent for 6 ft. girder spacing, 13 percent for 8 ft. girder spacing, and 12 percent for 8.67 ft. girder spacing.

Table 4.29. Comparison of Camber (Type IV Girder, Strand Dia. = 0.5 in.).

Girder Spacing (ft.)	**Span (ft.)**	**STD Camber (ft.)**	**LRFD**							
			Skew 0°		**Skew 15°**		**Skew 30°**		**Skew 60°**	
			Camber (ft.)	**Diff. %**	**Camber (ft.)**	**Diff. %**	**Camber (ft.)**	**Diff. %**	**Camber (ft.)**	**Diff. %**
6	90	0.12	0.12	3.1	0.12	3.1	0.12	3.1	0.11	-1.3
	100	0.17	0.19	11.5	0.19	11.5	0.17	-1.6	0.15	15.1
	110	0.21	0.25	20.3	0.25	20.3	0.25	20.3	0.23	9.3
	120	0.28	0.34	21.1	0.34	21.1	0.32	14.0	0.30	6.8
	130	0.36	0.36	2.3	0.36	2.3	0.36	2.2	0.35	-1.6
	133	-	0.33	-	0.33	-	0.34	-	-	-
	135	-	-	-	-	-	-	-	0.33	-
	136	0.34	-	-	-	-	-	-	-	-
8	90	0.16	0.18	10.0	0.18	10.0	0.18	10.0	0.14	13.3
	100	0.24	0.26	5.9	0.26	5.9	0.24	-1.8	0.22	-9.6
	110	0.32	0.35	8.3	0.35	8.3	0.33	3.4	0.32	-1.7
	120	0.40	0.38	-4.1	0.38	-4.1	0.38	-3.8	0.39	-1.3
	124	0.37	-	-	-	-	-	-	-	-
	125	-	-	-	-	-	-	-	0.36	-
8.67	90	0.18	0.19	8.5	0.19	8.5	0.19	8.5	0.16	11.8
	100	0.26	0.28	5.1	0.28	5.1	0.28	5.1	0.24	-8.9
	110	0.36	0.36	2.0	0.36	2.0	0.35	-1.6	0.33	-6.4
	116	-	0.39	-	0.39	-	-	-	-	-
	117	-	-	-	-	-	0.38	-	-	-
	119	0.39	-	-	-	-	-	-	-	-
	120	-	-	-	-	-	-	-	0.38	-
	121	-	-	-	-	-	-	-	0.38	-

5. PARAMETRIC STUDY - TYPE C GIRDERS

5.1 INTRODUCTION

A parametric study was conducted for Type C prestressed concrete bridge girders. A number of cases were considered based on the parameters summarized in Table 5.1. The procedure outlined in Chapter 3 was employed to evaluate the impact of the AASHTO LRFD Specifications on the design of Type C bridge girders. The results obtained from the design program for designs based on both the Standard and LRFD Specifications were validated using TxDOT's PRSTRS14 (TxDOT 2004) bridge design software. TxDOT's procedures were used for optimizing the number of strands and concrete strengths. This chapter provides a summary of results of the parametric study for Type C bridge girders. The impact of LRFD Specifications, as compared to the Standard Specifications, on various design results is discussed.

Table 5.1. Design Parameters for Type C Girders.

Parameter	**Description / Selected Values**
Design Codes	AASHTO Standard Specifications, 17th Edition (2002) AASHTO LRFD Specifications, 3rd Edition (2004)
Girder Spacing (ft.)	6'-0", 8'-0", and 8'-8"
Spans	40 ft. to maximum span at 10 ft. intervals
Strand Diameter (in.)	0.5 and 0.6
Concrete Strength at Release, f'_{ci}	Varied from 4000 to 6750 psi for design with optimum number of strands
Concrete Strength at Service, f'_c	Varied from 5000 to 8500 psi for design with optimum number of strands (f'_c may be increased up to 8750 psi for optimization on longer spans)
Skew Angle	0, 15, 30, and 60 degrees

The requirements for service load limit state design, flexural strength limit state design, transverse shear design, and interface shear design are evaluated in the parametric study. The following sections provide a summary of differences observed in parallel designs based on the Standard and LRFD Specifications. This summary includes differences occurring in the undistributed and distributed live load moments, the distribution factors, the number of strands, and the required concrete strengths at release and at service. The differences observed in the design for the flexural and shear strength limit states are provided in the following sections. The effect on camber is also evaluated and summarized.

5.2 LIVE LOAD MOMENTS AND SHEARS

5.2.1 General

The Standard Specifications stipulate the live load to be taken as an HS-20 truck load, tandem load, or lane load, whichever produces the maximum effect at the section considered. The LRFD Specifications specify a different live load model, HL-93, which is a combination of the HS-20 truck and lane load, or tandem load and lane load, whichever produces maximum effect at the section of interest. The live load governing the moments and shears at the sections of interest for the cases considered in the parametric study was determined and is summarized below. The undistributed live load moments at midspan and shears at critical section were calculated for each case and the differences are presented in this section.

There is a significant difference in the formulas for the distribution and impact factors specified by the Standard and the LRFD Specifications. The impact factors are applicable to truck, lane, and tandem loadings for designs based on Standard Specifications, whereas the LRFD Specifications do not require the lane load to be increased for the impact loading. The effect of the LRFD Specifications on the distribution and impact factors is evaluated and the results are summarized. The combined effect of the undistributed moments and shears and the distribution and impact factors on the distributed live load moments and shears was determined. The differences observed in the distributed live load moments at midspan and shears at the critical sections are presented below.

5.2.2 Governing Live Load for Moments and Shears

The live load producing the maximum moment at midspan and maximum shears at the critical section for shear was investigated. The critical section for shear in the designs based on the Standard Specifications is taken as $h/2$, where h is the depth of the composite section. For designs based on the LRFD Specifications, the critical section is calculated using an iterative process given by the specifications. The governing live loads are summarized in Tables 5.2 and 5.3. These tables also summarize the design cases considered using a Type C girder, along with the corresponding maximum span lengths. It was observed that for Standard designs, the HS-20 truck loading always governs the moments at midspan and shears at critical sections. For designs based on the LRFD Specifications, the combination of truck and lane loading governs for all cases, except for a 40 ft. span, where the combination of tandem and lane loading governs the live moments.

5.2.3 Undistributed Live Load Moments and Shears

The difference in the live loads specified by the Standard and LRFD Specifications affects the undistributed live load moments and shears. Skew and strand diameter have no effect on the undistributed live load moments or shears. Therefore, results for cases with a zero skew angle and 0.5 in. strand diameter are compared in Table 5.4. The undistributed live load moments are observed to increase in the range of 30 to 48 percent for 6 ft. girder spacing when live loads based on the LRFD Specifications are used as compared to the Standard Specifications. This increase ranges from 30 to 45 percent for an 8 ft. girder spacing and 30 to 44 percent for an 8.67 ft. girder spacing.

An increase was observed in the undistributed shears at the critical section. The increase was found to be in the range of 9 to 38 percent for a 6 ft. girder spacing for LRFD designs as compared to Standard designs. This increase was found to be in the range of 9 to 35 percent for an 8 ft. girder spacing and 9 to 33 percent for an 8.67 ft. girder spacing. This increase can be attributed to the change in live load and also the shifting of critical section. The critical section for shear is specified by the Standard Specifications as $h/2$, where h is the depth of the composite section. The LRFD Specifications requires the critical section to be calculated using an iterative process as discussed in Chapter 3. The difference between the undistributed moments and shears based on the Standard and LRFD Specifications increases with an increase in span length.

Table 5.2. Governing Live Load Moments at Midspan and Shears at Critical Section for Standard Specifications (Type C Girder).

Strand Diameter (in.)	Girder Spacing (ft.)	Span (ft.)	Governing Live Load for Moment	Governing Live Load for Shear
0.5	6	40	Truck Loading	Truck Loading
		50		
		60		
		70		
		80		
		90		
		96		
	8	40	Truck Loading	Truck Loading
		50		
		60		
		70		
		80		
		83		
	8.67	40	Truck Loading	Truck Loading
		50		
		60		
		70		
		80		
0.6	6	40	Truck Loading	Truck Loading
		50		
		60		
		70		
		80		
		90		
		95		
	8	40	Truck Loading	Truck Loading
		50		
		60		
		70		
		80		
		82		
	8.67	40	Truck Loading	Truck Loading
		50		
		60		
		70		
		79		

Table 5.3. Governing Live Load Moments at Midspan and Shears at Critical Section for LRFD Specifications (Type C Girder, Skew = 0°).

Strand Diameter (in.)	Girder Spacing (ft.)	Span (ft.)	Governing Live Load for Moment	Governing Live Load for Shear
0.5	6	40	Tandem+Lane Loading	Truck+Lane Loading
		50	Truck+Lane Loading	
		60		
		70		
		80		
		90		
		95		
	8	40	Tandem+Lane Loading	Truck+Lane Loading
		50	Truck+Lane Loading	
		60		
		70		
		80		
		83		
	8.67	40	Tandem+Lane Loading	Truck+Lane Loading
		50	Truck+Lane Loading	
		60		
		70		
		80		
0.6	6	40	Tandem+Lane Loading	Truck+Lane Loading
		50	Truck+Lane Loading	
		60		
		70		
		80		
		90		
		92		
	8	40	Tandem+Lane Loading	Truck+Lane Loading
		50	Truck+Lane Loading	
		60		
		70		
		80		
		82		
	8.67	40	Tandem+Lane Loading	Truck+Lane Loading
		50	Truck+Lane Loading	
		60		
		70		
		79		

Table 5.4. Undistributed Midspan Live Load Moments and Shears at Critical Section (Type C Girder, Skew = 0°, Strand Diameter = 0.5 in.).

Girder Spacing (ft.)	Span (ft.)	Undistributed Moment (k-ft.)			Undistributed Shear (kips)		
		Standard	LRFD	Difference k-ft. (%)	Standard	LRFD	Difference kips (%)
6	40	424.2	551.6	127.3 (30.0)	50.9	55.2	4.4 (8.6)
	50	602.4	791.3	188.8 (31.3)	55.2	63.8	8.6 (15.6)
	60	780.6	1055.2	274.6 (35.2)	58.1	70.7	12.7 (21.8)
	70	958.8	1335.1	376.3 (39.2)	60.1	76.6	16.5 (27.4)
	80	1137.0	1631.1	494.0 (43.4)	61.6	81.8	20.2 (32.8)
	90	1315.2	1943.0	627.8 (47.7)	62.8	86.7	23.9 (38.1)
	95	-	2105.0	-	-	89.2	-
	96	1422.4	-	-	63.4	-	-
8	40	424.2	551.6	127.3 (30.0)	50.9	55.2	4.4 (8.6)
	50	602.4	791.3	188.8 (31.3)	55.2	64.0	8.8 (15.9)
	60	780.6	1055.2	274.6 (35.2)	58.1	70.8	12.7 (21.9)
	70	958.8	1335.1	376.3 (39.2)	60.1	76.7	16.6 (27.6)
	80	1137.0	1631.1	494.0 (43.4)	61.6	81.9	20.3 (33.0)
	83	1190.5	1723.0	532.5 (44.7)	62.0	83.5	21.5 (34.7)
8.67	40	424.2	551.6	127.3 (30.0)	50.9	55.2	4.4 (8.6)
	50	602.4	791.3	188.8 (31.3)	55.2	64.0	8.7 (15.8)
	60	780.6	1055.2	274.6 (35.2)	58.1	70.8	12.7 (21.9)
	70	958.8	1335.1	376.3 (39.2)	60.1	76.7	16.6 (27.6)
	80	1137.0	1631.1	494.0 (43.4)	61.6	82.0	20.4 (33.1)

5.2.4 Impact Factors

The AASHTO Standard and LRFD Specifications require that live load moments and shears be increased for impact or dynamic loading. The Standard Specifications specify impact factors that decrease with an increase in span length, whereas the LRFD Specifications specify a constant value of dynamic loading as 33 percent of the undistributed live load moment or shear. The LRFD Specifications specify the impact loading to be 15 percent of the undistributed live load fatigue moment used to check the fatigue limit state required by the LRFD Specifications. The LRFD Specifications do not require the lane load moments and shears to be increased for impact loading. A summary of impact factors and the percent difference relative to Standard value is provided in Table 5.5. The skew angle and strand diameter do not affect the impact factor, hence only the cases with 0-degree skew angle and 0.5 in. strand diameter are presented.

Table 5.5. Live Load Impact Factors
(Type C Girder, Skew = 0°, Strand Diameter = 0.5 in.).

Girder Spacing (ft.)	Span (ft.)	Impact Factor		Difference (%)
		Standard	LRFD	
6	40	0.30	0.33	10.0
	50	0.29	0.33	15.5
	60	0.27	0.33	22.1
	70	0.26	0.33	28.7
	80	0.24	0.33	35.3
	90	0.23	0.33	41.9
	95	-	0.33	-
	96	0.23	-	-
8	40	0.30	0.33	10.0
	50	0.29	0.33	15.5
	60	0.27	0.33	22.1
	70	0.26	0.33	28.7
	80	0.24	0.33	35.3
	83	0.24	0.33	37.3
8.67	40	0.30	0.33	10.0
	50	0.29	0.33	15.5
	60	0.27	0.33	22.1
	70	0.26	0.33	28.7
	80	0.24	0.33	35.3

It was observed that the LRFD Specifications provide a larger estimate of dynamic loading as compared to the Standard Specifications. This difference increases with increasing span length. The increase in the impact factor is in the range of 10 to 42 percent of the impact factors specified by Standard Specifications. This essentially increases the distributed live load moments for the LRFD designs relative to the Standard designs. Figure 5.1 illustrates the effect of the LRFD Specifications on the dynamic load (impact) factors for a 6 ft. girder spacing. The same trend was observed for girder spacings of 8 ft. and 8.67 ft.

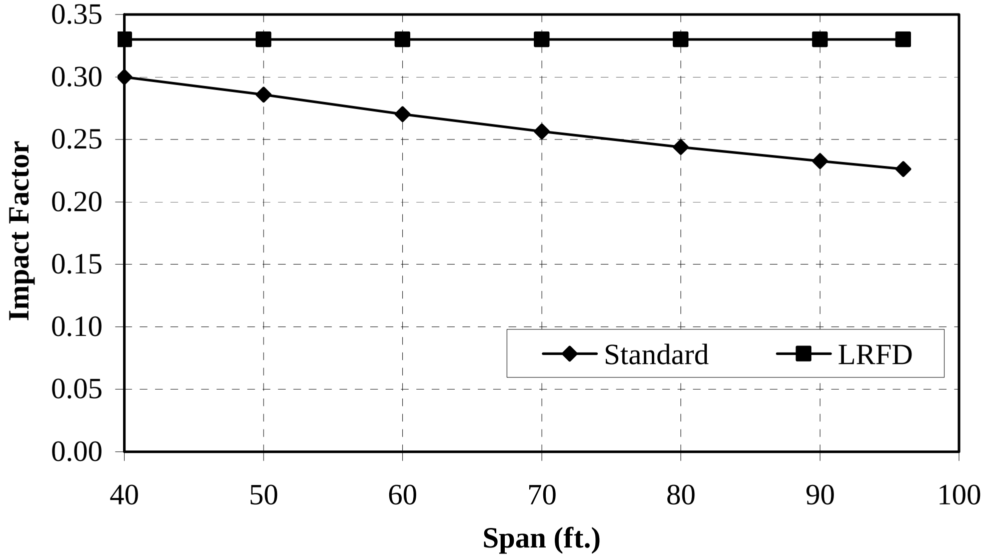

Figure 5.1. Comparison of Impact Factors (Type C Girder, Girder Spacing = 6 ft., Skew = 0°, Strand Diameter = 0.5 in.).

5.2.5 Live Load Distribution Factors

The live load moments and shears, including the dynamic (impact) load effect are distributed to the individual girders. The Standard Specifications provide a simple formula for moment DF as *S*/11 for prestressed concrete girder bridges, where *S* is the girder spacing in ft. The same DF is used for the distribution of live load shear to the girders. The LRFD Specifications provide more complex formulas for the distribution of live load moments and shears to individual girders. The effects of beam and slab stiffness are incorporated into these formulas. The LRFD Specifications require the DFs for moment to be reduced and DFs for shear to be corrected for skewed bridges. Table 5.6 compares the live load moment DFs for the Standard and LRFD Specifications.

Table 5.6. Live Load Moment DFs (DFM)
(Type C Girder, Strand Diameter = 0.5 in.).

Girder Spacing (ft.)	Span (ft.)	STD DFM	LRFD							
			Skew = 0°		Skew = 15°		Skew = 30°		Skew = 60°	
			DFM	Diff. %	DFM	Diff. %	DFM	Diff. %	DFM	Diff. %
6	40	0.545	0.632	15.8	0.632	15.8	0.600	9.9	0.466	-14.6
	50		0.594	9.0	0.594	9.0	0.569	4.4	0.463	-15.1
	60		0.566	3.8	0.566	3.8	0.545	0.0	0.457	-16.1
	70		0.543	-0.4	0.543	-0.4	0.526	-3.6	0.451	-17.4
	80		0.525	-3.8	0.525	-3.8	0.509	-6.7	0.444	-18.6
	90		0.509	-6.7	0.509	-6.7	0.495	-9.2	0.437	-19.8
	95		0.502	-	0.502	-	0.489	-	-	-
	96		-	-	-	-	-	-	-	-
	98		-	-	-	-	-	-	0.432	-
8	40	0.727	0.776	6.7	0.776	6.7	0.730	0.4	0.547	-24.8
	50		0.729	0.2	0.729	0.2	0.693	-4.7	0.543	-25.3
	60		0.693	-4.7	0.693	-4.7	0.664	-8.8	0.540	-25.8
	70		0.665	-8.6	0.665	-8.6	0.639	-12.1	0.534	-26.6
	80		0.641	-11.9	0.641	-11.9	0.619	-14.9	0.527	-27.5
	83		0.635	-12.7	0.635	-12.7	0.614	-15.6	-	-
	87		-	-	-	-	-	-	0.522	-
8.67	40	0.788	0.822	4.3	0.822	4.3	0.772	-2.0	0.573	-27.3
	50		0.772	-2.0	0.772	-2.0	0.733	-7.0	0.567	-28.0
	60		0.734	-6.8	0.734	-6.8	0.702	-11.0	0.565	-28.3
	70		0.704	-10.7	0.704	-10.7	0.676	-14.2	0.560	-29.0
	80		0.679	-13.9	0.679	-13.9	0.654	-17.0	0.553	-
	81		-	-	-	-	0.653	-	-	-
	85		-	-	-	-	-	-	0.550	-

It was observed that the live load moment DFs given by the LRFD Specifications are typically smaller as compared to those for the Standard Specifications. The difference increases with an increase in span length because the LRFD DFs decrease with an increase in the span while span length has no effect on the Standard DFs. The moment DFs increase with an increase in girder spacing for both the specifications. In addition, the difference between the DFs increased for larger girder spacings. The LRFD live load moment DFs are the same for 0- and 15-degree skews, but there is a significant change when the skew angles are 30 and 60 degrees. It was observed that an increase in skew angles beyond 30 degrees decreases the moment DFs significantly for Type C girder bridges. The maximum difference between the Standard and LRFD DFs was found to be 16 percent for 6 ft. girder spacing, and 14 percent for 8 ft and 8.67 ft. girder spacing for a 0-degree skew angle. This difference increased to 20 percent for 6 ft., 28 percent for 8 ft., and 30 percent for 8.67 ft. girder spacing for a skew angle of 60 degrees. Figure 5.2 illustrates the effect of skew on the moment DFs for the three girder spacings.

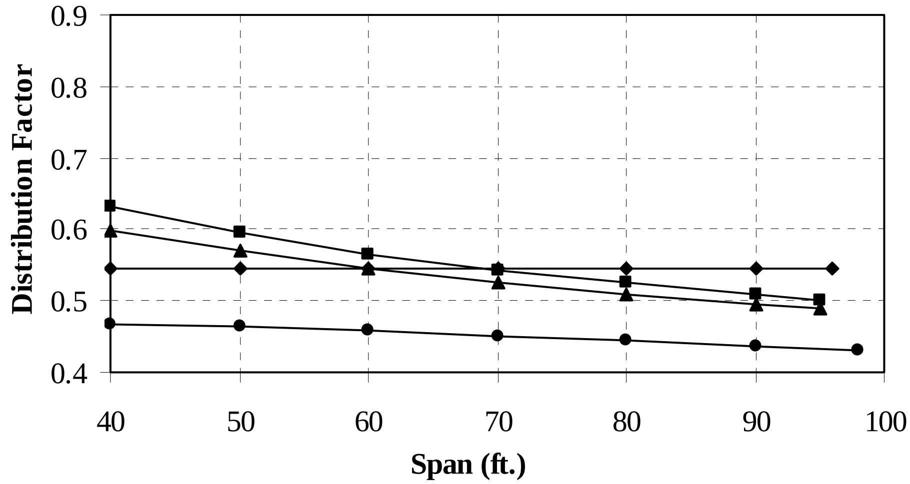

(a) Girder Spacing = 6 ft.

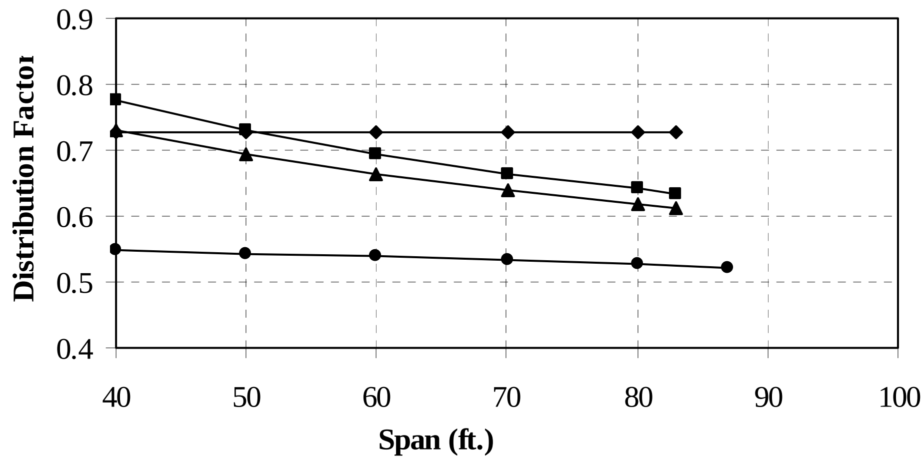

(b) Girder Spacing = 8 ft.

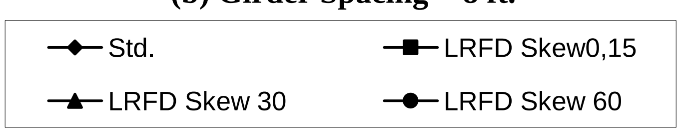

Figure 5.2. Live Load Moment DFs by Girder Spacing (Type C Girder, Strand Diameter = 0.5 in.).

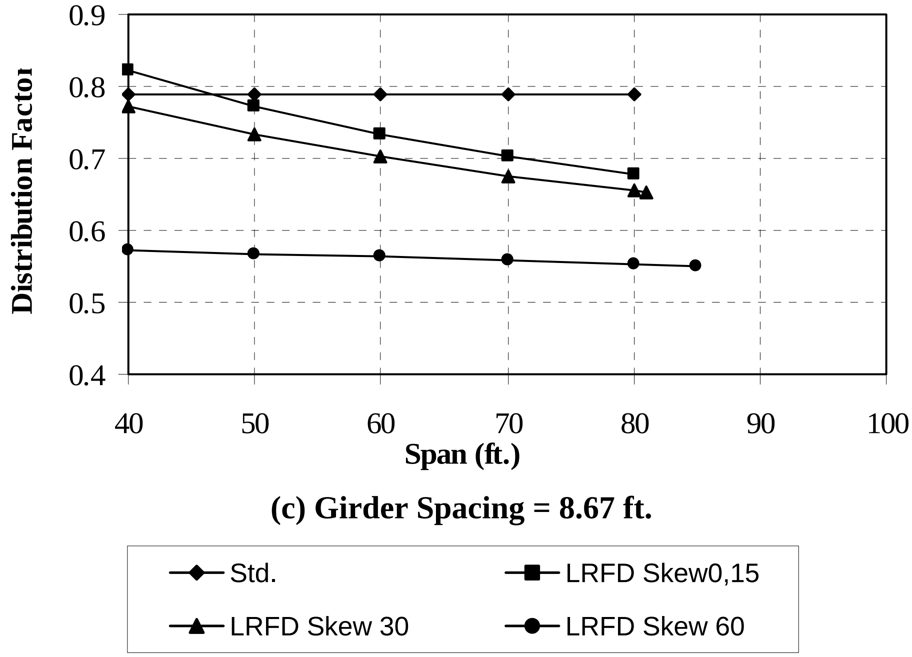

(c) Girder Spacing = 8.67 ft.

Figure 5.2. Live Load Moment DFs by Girder Spacing (Type C Girder, Strand Diameter = 0.5 in.) (cont.).

Table 5.7 and Figure 5.3 provide a summary of shear DFs for the parametric study with Type C girders. The strand diameter does not affect the DFs for shear. The LRFD live load shear DFs specified by the LRFD Specifications are larger as compared to the Standard Specifications. The DFs increase with an increase in girder spacing for both specifications, and the LRFD DFs approach Standard DFs as the girder spacing is increased. The span length and skew angle have no impact on the shear DFs for the Standard Specifications. The maximum difference in the shear DFs is 68 percent for 6 ft. spacing, 52 percent for 8 ft. spacing, and 47 percent for 8.67 ft. spacing.

Table 5.7. Live Load Shear DFs (DFV)
(Type C Girder, Strand Diameter = 0.5 in.).

Girder Spacing (ft.)	Span (ft.)	STD DFV	LRFD							
			Skew = 0°		Skew = 15°		Skew = 30°		Skew = 60°	
			DFV	Diff. %	DFV	Diff. %	DFV	Diff. %	DFV	Diff. %
6	40	0.545	0.671	22.9	0.700	28.4	0.735	34.7	0.863	58.3
	50	0.545	0.671	22.9	0.703	28.8	0.739	35.6	0.877	60.8
	60	0.545	0.671	22.9	0.704	29.1	0.743	36.3	0.889	63.0
	70	0.545	0.671	22.9	0.706	29.4	0.747	37.0	0.900	65.0
	80	0.545	0.671	22.9	0.708	29.7	0.750	37.5	0.909	66.7
	90	0.545	0.671	22.9	0.709	30.0	0.753	38.1	0.918	68.3
	95	-	0.671	-	0.710	-	0.754	-	-	-
	96	0.545	-	-	-	-	-	-	-	-
	98	-	-	-	-	-	-	-	0.925	-
8	40	0.727	0.814	12.0	0.851	17.0	0.892	22.7	1.049	44.2
	50	0.727	0.814	12.0	0.853	17.3	0.898	23.5	1.065	46.5
	60	0.727	0.814	12.0	0.855	17.6	0.903	24.1	1.080	48.5
	70	0.727	0.814	12.0	0.857	17.9	0.907	24.7	1.093	50.2
	80	0.727	0.814	12.0	0.859	18.2	0.911	25.3	1.104	51.8
	83	0.727	0.814	12.0	0.860	18.2	0.912	25.4	-	-
	87	-	-	-	-	-	-	-	1.112	-
8.67	40	0.788	0.861	9.3	0.899	14.1	0.944	19.7	1.109	40.7
	50	0.788	0.861	9.3	0.902	14.5	0.950	20.5	1.127	42.9
	60	0.788	0.861	9.3	0.905	14.8	0.955	21.1	1.142	44.9
	70	0.788	0.861	9.3	0.907	15.0	0.959	21.7	1.155	46.6
	80	0.788	0.861	9.3	0.909	15.3	0.963	22.2	1.168	-
	81	-	-	-	-	-	0.964	-	-	-
	85	-	-	-	-	-	-	-	1.173	-

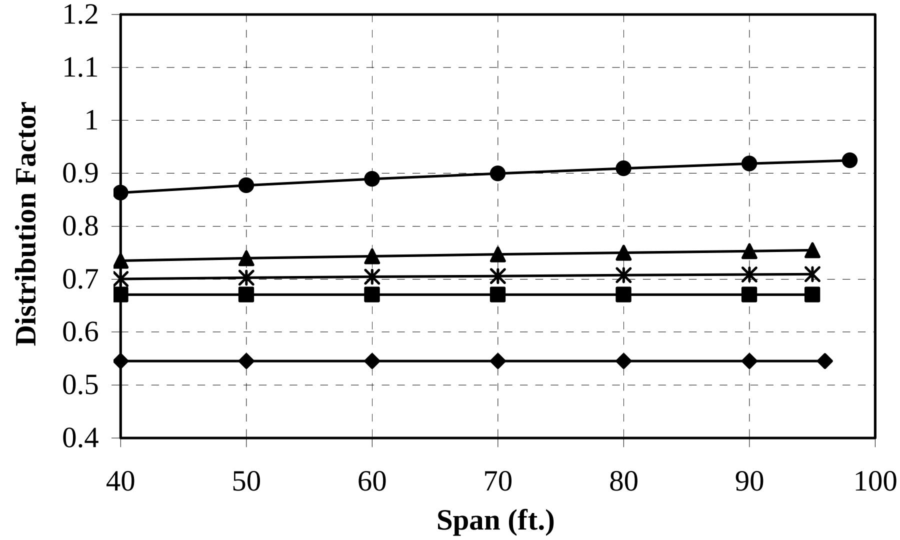

(a) Girder Spacing = 6 ft.

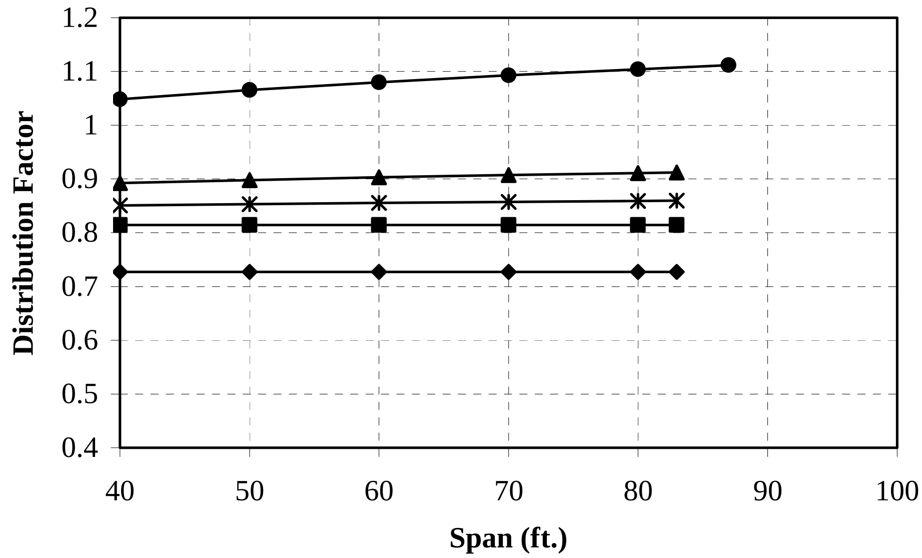

(b) Girder Spacing = 8 ft.

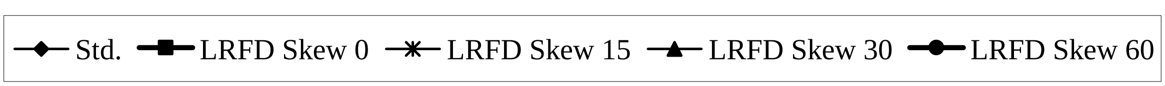

Figure 5.3. Live Load Shear DFs
(Type C Girder, Strand Dia. = 0.5 in.).

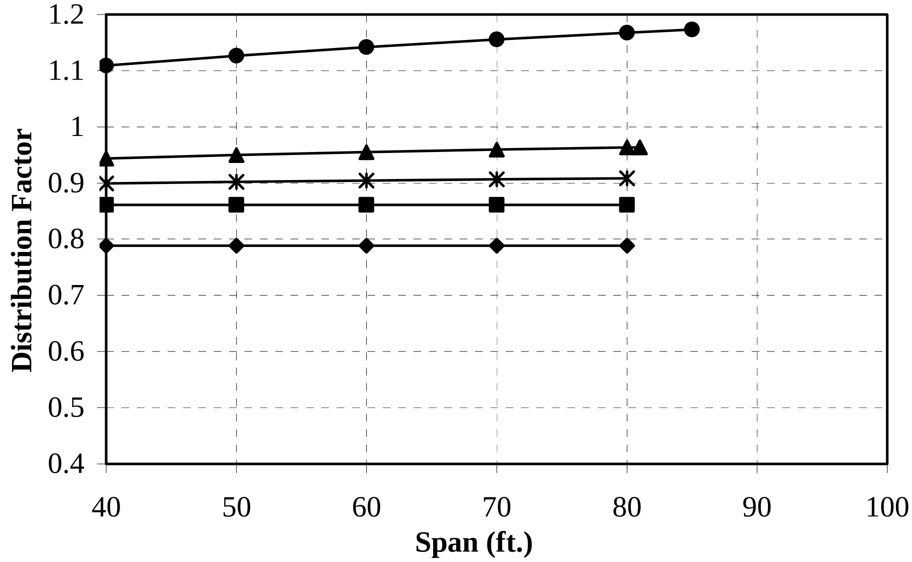

(c) Girder Spacing = 8.67 ft.

Figure 5.3. Live Load Shear DFs
(Type C Girder, Strand Dia. = 0.5 in.) (cont.).

5.2.6 Distributed Live Load Moments and Shears

The combined effect of the impact and DFs on the live load moment and shears is presented in this section. The distributed live load moments are compared in Table 5.8. The distributed live load moments are the same for 0- and 15-degree skew angles for the LRFD Specifications because the DFs for these skews are identical. The LRFD distributed live load moments are significantly larger than those for the Standard Specifications. The LRFD distributed live load moments increase in the range of 37 to 45 percent for 6 ft. girder spacing when the skew angle is 0 degrees. As the girder spacing increases, the difference between the distributed live load moments decreases. The LRFD moments were found to be in the range of 25 to 34 percent larger for 8 ft. spacing and 22 to 31 percent larger for 8.67 ft. girder spacing when the skew angle is 0 degrees.

An increase in the skew angle to 30 degrees and larger corresponds to a decrease in the DFs. This causes the live load moments to decrease. The difference between the live load moments for the Standard and LRFD Specifications was found to be in the range of 7 to 17 percent for 6 ft. girder spacing when the skew angle is 60 degrees. This difference reduces to the range of -7 to 2.5 percent and -11 to -3 percent for 8 ft. and 8.67 ft. girder spacings, respectively. An increase in span length tends to reduce the difference between the distributed live load moments from the two specifications.

Table 5.8. Distributed Midspan Live Load Moments (LL Mom.) (Type C Girder, Strand Dia. = 0.5 in.).

Girder Spacing (ft.)	Span (ft.)	STD LL Mom. (k-ft.)	LRFD							
			Skew = 0°		Skew = 15°		Skew = 30°		Skew = 60°	
			LL Mom. (k-ft.)	Diff. %	LL Mom. (k-ft.)	Diff. %	LL Mom. (k-ft.)	Diff. %	LL Mom. (k-ft.)	Diff. %
6	40	302.1	438.4	45.1	438.4	45.1	416.2	37.8	323.3	7.0
	50	423.3	587.4	38.8	587.4	38.8	562.5	32.9	457.7	8.1
	60	541.8	741.6	36.9	741.6	36.9	714.2	31.8	599.3	10.6
	70	658.1	895.4	36.1	895.4	36.1	866.0	31.6	742.8	12.9
	80	772.5	1050.8	36.0	1050.8	36.0	1019.6	32.0	889.0	15.1
	90	885.4	1208.8	36.5	1208.8	36.5	1176.1	32.8	1038.7	17.3
	95	-	1288.6	-	1288.6	-	1255.1	-	-	-
	96	952.5	-	-	-	-	-	-	-	-
	98	-	-	-	-	-	-	-	1160.4	-
8	40	402.9	538.3	33.6	538.3	33.6	507.0	25.8	375.2	-6.9
	50	564.3	720.3	27.6	720.3	27.6	684.9	21.4	536.6	-4.9
	60	722.4	908.1	25.7	908.1	25.7	869.4	20.4	706.9	-2.1
	70	877.5	1095.2	24.8	1095.2	24.8	1053.7	20.1	879.6	0.2
	80	1030.0	1283.8	24.6	1283.8	24.6	1239.9	20.4	1055.6	2.5
	83	1075.4	1341.1	24.7	1341.1	24.7	1296.5	20.6	-	-
	87	-	-	-	-	-	-	-	1181.4	-
8.67	40	436.6	570.7	30.7	570.7	30.7	536.0	22.8	390.6	-10.5
	50	611.6	763.2	24.8	763.2	24.8	724.2	18.4	560.6	-8.3
	60	782.9	961.9	22.9	961.9	22.9	919.2	17.4	740.0	-5.5
	70	950.9	1159.7	22.0	1159.7	22.0	1114.0	17.1	922.1	-3.0
	80	1116.3	1359.2	21.8	1359.2	21.8	1310.7	17.4	1107.6	-
	81	-	-	-	-	-	1330.7	-	-	-
	85	-	-	-	-	-	-	-	1202.2	-

The values for the distributed shear force at the critical section due to live load are presented in Table 5.9. The shear increases significantly when the LRFD Specifications are used. This increase can be attributed to a larger undistributed shear force due to HL-93 loading in combination with an increase in the shear DFs. The shear force at the critical section for the LRFD Specifications increases in the range of 53 to 140 percent for 6 ft. girder spacing relative to the Standard Specifications. The increase was found to be in the range of 33 to 110 percent for 8 ft. and 30 to 95 percent for 8.67 ft. girder spacing.

Table 5.9. Distributed Live Load Shear at Critical Section (Type C Girder, Strand Dia. = 0.5 in.).

Girder Spacing (ft.)	Span (ft.)	STD Shear (kips)	LRFD							
			Skew = 0°		Skew = 15°		Skew = 30°		Skew = 60°	
			Shear (kips)	Diff. %	Shear (kips)	Diff. %	Shear (kips)	Diff. %	Shear (kips)	Diff. %
6	40	36.2	52.8	45.8	55.2	52.3	57.9	59.8	68.0	87.7
	50	38.8	58.8	51.7	61.6	58.9	64.9	67.2	77.0	98.4
	60	40.3	63.5	57.6	66.7	65.6	70.4	74.7	84.2	109.0
	70	41.3	67.5	63.6	71.0	72.2	75.2	82.2	90.5	119.5
	80	41.9	71.0	69.5	74.9	78.9	79.4	89.6	96.2	129.9
	90	42.3	74.2	75.5	78.4	85.5	83.3	97.0	101.5	140.2
	95	-	75.7	-	80.1	-	85.1	-	-	-
	96	42.4	-	-	-	-	-	-	-	-
	98	-	-	-	-	-	-	-	105.6	-
8	40	48.3	64.1	32.8	67.0	38.7	70.3	45.5	82.6	71.0
	50	51.7	71.4	38.1	74.8	44.7	78.8	52.3	93.5	80.7
	60	53.7	77.1	43.6	81.0	50.8	85.5	59.2	102.3	90.4
	70	55.0	82.0	49.0	86.3	56.9	91.3	66.0	110.0	99.9
	80	55.8	86.2	54.4	90.9	62.9	96.4	72.7	116.9	109.4
	83	56.0	87.4	56.0	92.3	64.7	97.9	74.8	-	-
	87	-	-	-	-	-	-	-	121.4	-
8.67	40	52.3	67.8	29.6	70.8	35.3	74.3	42.0	87.3	66.8
	50	56.0	75.5	34.8	79.1	41.2	83.3	48.6	98.8	76.3
	60	58.2	81.6	40.1	85.7	47.1	90.4	55.3	108.2	85.7
	70	59.6	86.7	45.4	91.2	53.0	96.5	61.9	116.3	95.0
	80	60.5	91.1	50.7	96.2	59.0	102.0	68.5	123.6	-
	81	-	-	-	-	-	102.5	-	-	-
	85	-	-	-	-	-	-	-	127.0	-

5.3 SERVICE LOAD DESIGN

5.3.1 General

The impact of the LRFD Specifications on the service load design relative to the Standard Specifications is discussed in this section. The effect on prestress losses, required number of strands, and the required concrete strengths at service and release are discussed. The increase in the live load moment and the change in equations for prestress loss calculations specified by the

AASHTO LRFD Specifications result in different service load design requirements. The change in the service load combination and allowable stress limits also affects the design. Generally the design requirements for the LRFD Specifications were found to be conservative as compared to the Standard Specifications.

5.3.2 Maximum Span Lengths

The results for maximum span length are presented in Table 5.10. The maximum span lengths are limited by the maximum concrete strength at release of 6750 psi and maximum concrete strength at service of 8750 psi. The maximum span for Type C girders is not governed by the maximum number of strands for any of the cases considered for the parametric study. The maximum allowable concrete strengths were reached when the number of strands was in the range of 42 to 44, whereas a Type C girder can hold up to 74 strands. Thus, by relaxing the limit on concrete strengths, longer spans can be achieved. The LRFD Specifications have a reducing effect on the maximum span length in a few cases and no effect in others when the skew angle is less than 60 degrees. This is due to slightly higher required concrete strengths that reach the concrete strength limits for smaller spans than for the Standard Specifications. The maximum span length for a skew angle of 60 degrees is larger as compared to those possible by the Standard Specifications. However, the difference between the maximum span lengths was relatively small for all cases, ranging from -3 ft. to 5 ft.

Table 5.10. Maximum Span Lengths for Type C Girder.

Strand Dia. (in.)	Girder Spacing (ft.)	STD Max. Span (ft.)	LRFD							
			Skew 0°		Skew 15°		Skew 30°		Skew 60°	
			Max. Span (ft.)	Diff. (ft.)	Max. Span (ft.)	Diff. (ft.)	Max. Span (ft.)	Diff. (ft.)	Max. Span (ft.)	Diff. (ft.)
0.5	6	96	95	-1	95	-1	95	-1	98	2
	8	83	83	0	83	0	83	0	87	4
	8.67	80	80	0	80	0	81	1	85	5
0.6	6	95	92	-3	92	-3	93	-2	96	1
	8	82	82	0	82	0	83	1	87	5
	8.67	79	79	0	79	0	80	1	83	1

5.3.3 Impact on the Required Number of Prestressing Strands

The number of strands required depends on the allowable stress limits and the stresses caused by the dead and live loads. There is a change in the allowable stress limits in the LRFD Specifications, and the live load is also different. The Service III limit state that checks the bottom tensile stresses using a 0.8 factor for live load also impacts the prestressing strand requirements. The difference in the prestress losses is another factor that affects the final strand requirements. The strength limit state controls the number of strands for cases when span length is less than 60 ft.

A comparison of the number of strands required for the Type C girder designs is provided in Tables 5.11 and 5.12 for 0.5 in. and 0.6 in. diameter strands, respectively. The LRFD Specifications require the same number of strands as the Standard Specifications for most cases with 0.5 in. diameter strands. For cases with a skew angle of 60 degrees, the number of strands required for the LRFD designs was found to be less than for the corresponding Standard designs. The difference was found to be 2 to 4 strands. Similar trends were found for 0.6 in. diameter strands. Figure 5.4 compares the strand requirements for Type C girders with 0.5 in. strands.

Table 5.11. Required Number of Strands (Type C Girder, Strand Dia. = 0.5 in.).

Girder Spacing (ft.)	Span (ft.)	STD No. of Strands	LRFD							
			Skew = 0°		Skew = 15°		Skew = 30°		Skew = 60°	
			No. of Strands	Diff. %	No. of Strands	Diff. %	No. of Strands	Diff. %	No. of Strands	Diff. %
6	40	10	8	-2	8	-2	8	-2	8	-2
	50	10	10	0	10	0	10	0	10	0
	60	14	14	0	14	0	14	0	14	0
	70	20	20	0	20	0	20	0	18	-2
	80	26	28	2	28	2	28	2	26	0
	90	36	38	2	38	2	38	2	36	0
	95	-	46	-	46	-	44	-	-	-
	96	44	-	-	-	-	-	-	-	-
	98	-	-	-	-	-	-	-	46	-
8	40	12	10	-2	10	-2	10	-2	8	-4
	50	12	14	2	14	2	12	0	10	-2
	60	18	18	0	18	0	18	0	16	-2
	70	26	26	0	26	0	26	0	24	-2
	80	36	36	0	36	0	36	0	34	-2
	83	40	42	2	42	2	40	0	-	-
	87	-	-	-	-	-	-	-	42	-
8.67	40	12	10	-2	10	-2	10	-2	8	-4
	50	14	14	0	14	0	14	0	12	-2
	60	18	18	0	18	0	18	0	16	-2
	70	28	28	0	28	0	28	0	26	-2
	80	40	40	0	40	0	40	0	36	-4
	81	-	-	-	-	-	42	-	-	-
	85	-	-	-	-	-	-	-	44	-

Table 5.12. Required Number of Strands (Type C Girder, Strand Dia. = 0.6 in.).

Girder Spacing (ft.)	Span (ft.)	No. of Strands	LRFD							
			Skew 0°		Skew 15°		Skew 30°		Skew 60°	
			No. of Strands	Diff. %	No. of Strands	Diff. %	No. of Strands	Diff. %	No. of Strands	Diff. %
6	40	6	6	0	6	0	6	0	6	0
	50	10	8	-2	8	-2	8	-2	6	-4
	60	10	10	0	10	0	10	0	10	0
	70	14	14	0	14	0	14	0	14	0
	80	18	20	2	20	2	20	2	18	0
	90	24	26	2	26	2	26	2	24	0
	92	-	28	-	28	-	-	-	-	-
	93	-	-	-	-	-	28	-	-	-
	95	30	-	-	-	-	-	-	-	-
	96	-	-	-	-	-	-	-	30	-
8	40	6	6	0	6	0	6	0	6	0
	50	10	10	0	10	0	10	0	8	-2
	60	12	12	0	12	0	12	0	12	0
	70	18	18	0	18	0	18	0	16	-2
	80	24	26	2	26	2	24	0	22	-2
	82	26	28	2	28	2	-	-	-	-
	83	-	-	-	-	-	28	-	-	-
	87	-	-	-	-	-	-	-	30	-
8.67	40	10	8	-2	8	-2	6	-4	6	-4
	50	10	10	0	10	0	10	0	8	-2
	60	14	14	0	14	0	14	0	12	-2
	70	20	20	0	20	0	20	0	18	-2
	79	26	26	0	26	0	-	-	-	-
	80	-	-	-	-	-	28	-	24	-
	83	-	-	-	-	-	-	-	28	-

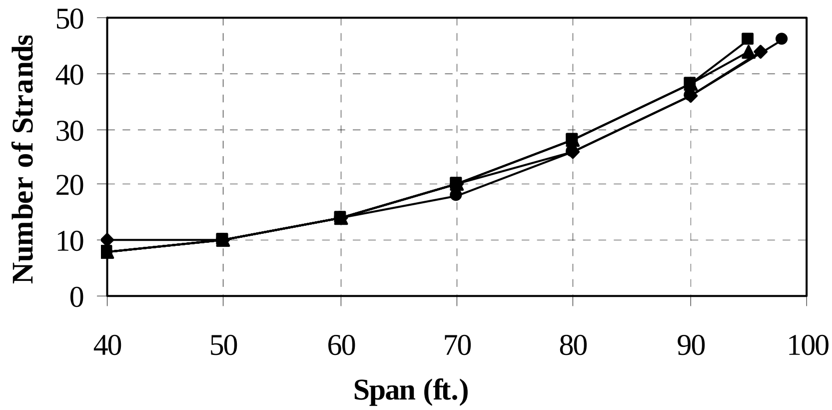

(a) Girder Spacing = 6 ft.

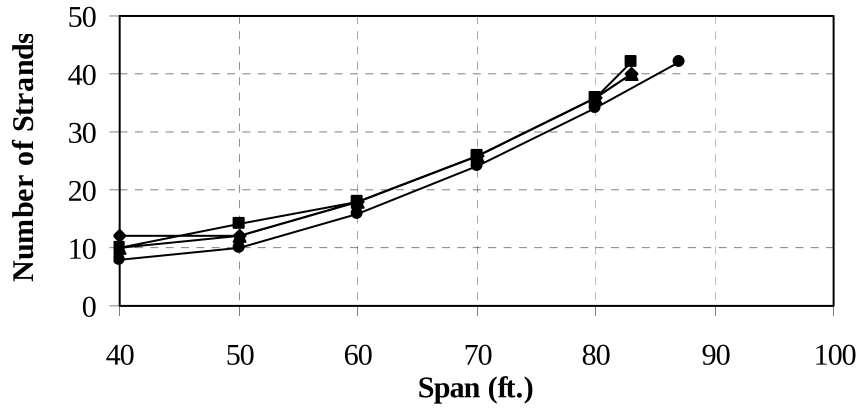

(b) Girder Spacing = 8 ft.

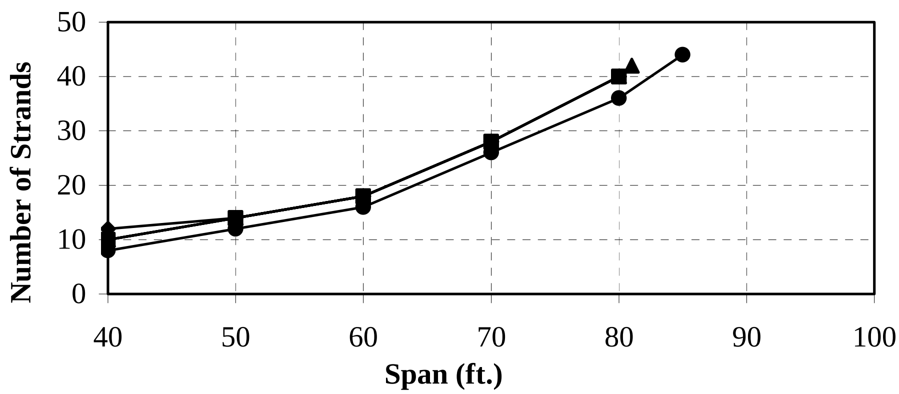

(c) Girder Spacing = 8.67 ft.

Std. LRFD Skew0,15 LRFD Skew 30 LRFD Skew 60

Figure 5.4. Required Number of Strands (Type C Girder, Strand Dia. = 0.5 in.).

5.3.4 Impact on Concrete Strengths

5.3.4.1 Concrete Strength at Release

The optimized concrete strength at release depends on the stresses due to prestressing and the self-weight of the girder, along with the allowable stress limits at transfer. The results for 0.5 in. diameter strands are presented in Table 5.13.

Table 5.13. Concrete Strength at Release (f'_{ci}) (Type C Girder, Strand Dia. = 0.5 in.).

Girder Spacing (ft.)	Span (ft.)	STD f'_{ci} (psi)	LRFD							
			Skew = 0°		Skew = 15°		Skew = 30°		Skew = 60°	
			f'_{ci} (psi)	Diff. %	f'_{ci} (psi)	Diff. %	f'_{ci} (psi)	Diff. %	f'_{ci} (psi)	Diff. %
6	40	4000.0	4000.0	0.0	4000.0	0.0	4000.0	0.0	4000.0	0.0
	50	4000.0	4000.0	0.0	4000.0	0.0	4000.0	0.0	4000.0	0.0
	60	4000.0	4000.0	0.0	4000.0	0.0	4000.0	0.0	4000.0	0.0
	70	4000.0	4000.0	0.0	4000.0	0.0	4000.0	0.0	4000.0	0.0
	80	4261.9	4606.2	8.1	4606.2	8.1	4606.2	8.1	4222.7	-0.9
	90	5658.0	5935.4	4.9	5935.4	4.9	5935.7	4.9	5593.8	-1.1
	95	-	6886.5	-	6886.5	-	6617.6	-	-	-
	96	6654.7	-	-	-	-	-	-	-	-
	98	-	-	-	-	-	-	-	6739.8	-
8	40	4000.0	4000.0	0.0	4000.0	0.0	4000.0	0.0	4000.0	0.0
	50	4000.0	4000.0	0.0	4000.0	0.0	4000.0	0.0	4000.0	0.0
	60	4000.0	4000.0	0.0	4000.0	0.0	4000.0	0.0	4000.0	0.0
	70	4640.5	4598.8	-0.9	4598.8	-0.9	4598.8	-0.9	4213.6	-9.2
	80	6088.5	6021.1	-1.1	6021.1	-1.1	6021.1	-1.1	5678.2	-6.7
	83	6624.5	6852.9	3.4	6852.9	3.4	6546.8	-1.2	-	-
	87	-	-	-	-	-	-	-	6681.0	-
8.67	40	4000.0	4000.0	0.0	4000.0	0.0	4000.0	0.0	4000.0	0.0
	50	4000.0	4000.0	0.0	4000.0	0.0	4000.0	0.0	4000.0	0.0
	60	4000.0	4000.0	0.0	4000.0	0.0	4000.0	0.0	4000.0	0.0
	70	5029.6	4982.2	-0.9	4982.2	-0.9	4982.3	-0.9	4598.8	-8.6
	80	6749.1	6669.9	-1.2	6669.9	-1.2	6670.2	-1.2	6021.4	-
	81	-	-	-	-	-	6935.6	-	-	-
	85	-	-	-	-	-	-	-	7073.0	-

Because there was a slight increase in the number of strands required for the LRFD designs, a subsequent small increase in the required concrete strength at release was observed for the Type C girders. The minimum strength at release was considered to be 4000 psi. For span lengths less than 70 ft., it was observed that minimum concrete strength governs and so no difference is found when comparing the two specifications. For larger spans, the difference in the required concrete strengths for LRFD designs relative to Standard designs ranged from -9 to 8 percent. The concrete strength at release is limited to 6750 psi and, in most of the cases, this limit governs the maximum span length.

5.3.4.2 Concrete Strength at Service

The concrete strength at service is affected by the stresses at the midspan due to the prestressing force, dead loads, superimposed loads, and live loads, along with the allowable stress limits at service. The results for 0.5 in. diameter strands are presented in Table 5.14.

Table 5.14. Concrete Strength at Service (f'_c) (Type C Girder, Strand Dia. = 0.5 in.).

Girder Spacing (ft.)	Span (ft.)	STD f'_c (psi)	LRFD							
			Skew = 0°		Skew = 15°		Skew = 30°		Skew = 60°	
			f'_c (psi)	Diff. %	f'_c (psi)	Diff. %	f'_c (psi)	Diff. %	f'_c (psi)	Diff. %
6	40	5000.0	5000.0	0.0	5000.0	0.0	5000.0	0.0	5000.0	0.0
	50	5000.0	5000.0	0.0	5000.0	0.0	5000.0	0.0	5000.0	0.0
	60	5000.0	5000.0	0.0	5000.0	0.0	5000.0	0.0	5000.0	0.0
	70	5000.0	5000.0	0.0	5000.0	0.0	5000.0	0.0	5000.0	0.0
	80	5000.0	5000.0	0.0	5000.0	0.0	5000.0	0.0	5000.0	0.0
	90	6375.5	6526.0	2.4	6526.0	2.4	5935.7	-6.9	5702.7	-10.6
	95	-	6886.5	-	6886.5	-	8012.2	-	-	-
	96	7754.7	-	-	-	-	-	-	-	-
	98	-	-	-	-	-	-	-	7877.3	-
8	40	5000.0	5000.0	0.0	5000.0	0.0	5000.0	0.0	5000.0	0.0
	50	5000.0	5000.0	0.0	5000.0	0.0	5000.0	0.0	5000.0	0.0
	60	5000.0	5000.0	0.0	5000.0	0.0	5000.0	0.0	5000.0	0.0
	70	5000.0	5000.0	0.0	5000.0	0.0	5000.0	0.0	5000.0	0.0
	80	6088.5	6804.5	11.8	6804.5	11.8	6021.1	-1.1	5678.2	-6.7
	83	6624.5	6852.9	3.4	6852.9	3.4	6546.8	-1.2	-	-
	87	-	-	-	-	-	-	-	7344.9	-
8.67	40	5000.0	5000.0	0.0	5000.0	0.0	5000.0	0.0	5000.0	0.0
	50	5000.0	5000.0	0.0	5000.0	0.0	5000.0	0.0	5000.0	0.0
	60	5000.0	5177.9	3.6	5177.9	3.6	5000.0	0.0	5000.0	0.0
	70	5029.6	5000.0	-0.6	5000.0	-0.6	5000.0	-0.6	5000.0	-0.6
	80	6749.1	6669.9	-1.2	6669.9	-1.2	6670.2	-1.2	6021.4	-
	81	-	-	-	-	-	6935.6	-	-	-
	85	-	-	-	-	-	-	-	7073.0	-

The concrete strength at service is limited to 8750 psi. However, this limitation does not affect the maximum span length as the initial concrete strength approaches its limits earlier than the final concrete strength. The minimum strength was considered as 5000 psi and for span lengths less than 80 ft. it was observed that this limit controls. Also, the concrete strength at service cannot be smaller than the concrete strength at release. This limitation governs for a few cases for 0.5 in. diameter strands and several cases for 0.6 in. diameter strands. The LRFD Specifications do not have a significant effect on the concrete strength at service. A small reduction in the required concrete strength was observed for a few cases, with the maximum difference being -11 percent and 12 percent for only a few cases.

5.3.5 Initial and Final Prestress Losses

The loss in prestress occurs mainly from four sources: elastic shortening and relaxation of the prestressing, and creep and shrinkage of concrete. These losses are categorized into initial prestress loss and final prestress loss. The initial prestress loss occurs due to initial relaxation of steel and elastic shortening of prestressing strands. The final loss occurs due to final steel relaxation and creep and shrinkage of concrete. The total prestress loss is a combination of initial and final losses.

5.3.5.1 Initial Prestress Loss

The initial prestress loss is the combination of losses due to elastic shortening and initial steel relaxation. The combined effect of these losses was computed for both the Standard and LRFD Type C girder designs. Table 5.15 presents the results for a strand diameter of 0.5 in. Similar trends were observed for 0.6 in. diameter strands. With a few exceptions, the initial loss estimates for the LRFD designs are larger than the values for the Standard designs. For 40 ft. spans and some 50 ft. spans, a reduction in the initial losses up to nearly 12 percent was observed for LRFD designs. For longer spans and skew angles from 0 to 60 degrees, the LRFD initial losses were up to 11 percent larger than for the Standard designs.

Table 5.15. Initial Prestress Loss (%) (Type C Girder, Strand Dia. = 0.5 in.).

Girder Spacing (ft.)	Span (ft.)	STD Initial Loss (%)	LRFD							
			Skew = 0°		Skew = 15°		Skew = 30°		Skew = 60°	
			Init. Loss (%)	Diff. %	Init. Loss (%)	Diff. %	Init. Loss (%)	Diff. %	Init. Loss (%)	Diff. %
6	40	6.5	6.2	-5.3	6.2	-5.3	6.2	-5.3	6.2	-5.3
	50	6.3	6.6	5.0	6.6	5.0	6.6	5.0	6.6	5.0
	60	7.0	7.4	6.0	7.4	6.0	7.4	5.7	7.4	5.7
	70	7.9	8.5	6.6	8.5	6.6	8.5	6.6	8.0	1.0
	80	8.6	9.5	10.7	9.5	10.7	9.5	10.7	9.2	7.1
	90	9.5	10.5	10.3	10.5	10.3	10.4	10.3	10.2	7.9
	95	-	11.0	-	11.0	-	10.9	-	-	-
	96	10.0	-	-	-	-	-	-	-	-
	98	-	-	-	-	-	-	-	11.0	-
8	40	7.0	6.9	-1.3	6.9	-1.3	6.9	-1.3	6.2	-11.6
	50	6.8	7.7	13.0	7.7	13.0	7.2	5.6	6.6	-2.8
	60	7.8	8.3	6.5	8.3	6.5	8.3	6.5	7.8	0.4
	70	8.8	9.4	7.4	9.4	7.4	9.4	7.4	9.1	3.9
	80	9.7	10.4	8.2	10.4	8.2	10.4	8.2	10.2	5.9
	83	9.9	10.9	10.0	10.9	10.0	10.8	8.4	-	-
	87	-	-	-	-	-	-	-	10.9	-
8.67	40	7.0	6.9	-1.3	6.9	-1.3	6.9	-1.3	6.2	-11.7
	50	7.2	7.7	6.1	7.7	6.1	7.7	6.1	7.2	-0.9
	60	7.8	8.3	6.4	8.3	6.4	8.3	6.4	7.9	0.7
	70	9.0	9.7	7.6	9.7	7.6	9.7	7.6	9.4	4.4
	80	10.0	10.8	8.6	10.8	8.6	10.8	8.5	10.4	-
	81	-	-	-	-	-	11.0	-	-	-
	85	-	-	-	-	-	-	-	11.0	-

5.3.5.2 Total Prestress Loss

The total loss of prestress was estimated based on the Standard and LRFD Specifications. The results for 0.5 in. diameter strands are presented in Table 5.16. The total prestress loss estimates provided by the LRFD Specifications tend to be slightly larger as compared to those provided by the Standard Specifications. The exceptions are for shorter spans (40 ft.) and for a skew angle of 60 degrees. The difference in total losses for LRFD designs relative to Standard designs was -5 to 11 percent for 6 ft. spacing, -14 to 18 percent for 8 ft. spacing, and -14 to 7 percent for 8.67 ft. girder spacing.

Table 5.16. Total Prestress Loss Percent (Type C Girder, Strand Dia. = 0.5 in.).

Girder Spacing (ft.)	Span (ft.)	STD Tot. Loss (%)	LRFD							
			Skew = 0°		Skew = 15°		Skew = 30°		Skew = 60°	
			Tot. Loss (%)	Diff. %	Tot. Loss (%)	Diff. %	Tot. Loss (%)	Diff. %	Tot. Loss (%)	Diff. %
6	40	17.1	16.3	-4.7	16.3	-4.7	16.3	-4.7	16.3	-4.7
	50	15.6	17.0	8.4	17.0	8.4	17.0	8.4	17.0	8.4
	60	17.5	18.8	7.4	18.8	7.4	18.8	7.3	18.8	7.3
	70	20.8	22.0	5.8	22.0	5.8	22.0	5.8	20.3	-2.2
	80	23.0	25.6	11.1	25.6	11.1	25.6	11.1	24.2	5.1
	90	27.2	29.5	8.1	29.5	8.1	29.4	8.1	28.3	3.9
	95	-	32.3	-	32.3	-	31.4	-	-	-
	96	30.2	-	-	-	-	-	-	-	-
	98	-	-	-	-	-	-	-	31.6	-
8	40	18.6	18.1	-2.6	18.1	-2.6	18.1	-2.6	16.0	-14.0
	50	17.0	20.1	17.9	20.1	17.9	18.3	7.7	16.5	-3.2
	60	20.4	21.6	6.0	21.6	6.0	21.6	6.1	19.9	-2.3
	70	24.2	25.3	4.7	25.3	4.7	25.3	4.7	24.0	-1.0
	80	28.3	29.3	3.7	29.3	3.7	29.3	3.7	28.2	-0.5
	83	29.8	31.8	6.5	31.8	6.5	30.8	3.3	-	-
	87	-	-	-	-	-	-	-	30.9	-
8.67	40	18.5	18.0	-2.6	18.0	-2.6	18.0	-2.6	15.9	-14.1
	50	18.7	19.9	6.8	19.9	6.8	19.9	6.8	18.2	-2.6
	60	20.2	21.4	6.1	21.4	6.1	21.4	6.1	19.7	-2.2
	70	25.3	26.5	4.4	26.5	4.4	26.5	4.4	25.1	-1.0
	80	30.2	31.2	3.3	31.2	3.3	31.1	3.2	29.0	-
	81	-	-	-	-	-	31.9	-	-	-
	85	-	-	-	-	-	-	-	32.0	-

5.4 ULTIMATE LIMIT STATE DESIGN

5.4.1 General

The impact of the LRFD Specifications with respect to the ultimate flexural strength limit state design is discussed in this section. The changes in the load combination, the required concrete strengths, and the number of strands from service limit state affect the ultimate flexural strength limit. The definition for rectangular and flanged section behavior and the reinforcement limits have also been changed in the LRFD Specifications. However, in all cases considered, the sections were found to be under-reinforced for both the Standard and LRFD designs.

5.4.2 Factored Design Moment

The load combinations for the ultimate limit state were significantly changed from the Standard to LRFD Specifications. The load factors for moments due to live load and dead loads except wearing surface load specified by the LRFD Specifications are smaller than the Standard Specifications. The load factor for moment due to wearing surface load is increased in the LRFD Specifications. The live load moments specified by the LRFD Specifications are larger than that of the Standard Specifications. The combined effect of these two changes results in design moments that are comparable.

A comparison of the design moments specified by the Standard and LRFD Specifications is presented in Table 5.17. The LRFD Specifications yield design moments for Type C girders that are in general slightly smaller as compared to the Standard Specifications. The difference is found to decrease with the increase in span length, girder spacing, and skew angle beyond 30 degrees. The difference in the design moments was found to be in the range of -25 to 7 percent for 6 ft., -25 to 2 percent for 8 ft., and -25 to 8 percent for 8.67 ft. girder spacing.

5.4.3 Nominal Moment Capacity

The change in the concrete strength at service and the number of strands, relative to Standard designs, affects the nominal moment capacity of the section. The change in expression for evaluation of effective prestress in the prestressing strands also has an impact on the ultimate moment resistance of the section.

A comparison of the nominal moment capacities for the Type C girder designs is presented in Table 5.18. The moment resistance determined for the LRFD designs tends to be lower compared to values determined for the Standard designs, with a few exceptions. The difference between the moment resistance capacities ranges from -9 to 6 percent for 6 ft., -22 to 15 percent for 8 ft., and -16 to 7 percent for 8.67 ft. girder spacing.

Table 5.17. Factored Ultimate Moment (M_u) (Type C Girder, Strand Dia. = 0.5 in.).

Girder Spacing (ft.)	Span (ft.)	STD M_u (k-ft.)	LRFD							
			Skew = 0°		Skew = 15°		Skew = 30°		Skew = 60°	
			M_u (k-ft.)	Diff. %	M_u (k-ft.)	Diff. %	M_u (k-ft.)	Diff. %	M_u (k-ft.)	Diff. %
6	40	1167.1	1072.3	-8.1	1072.3	-8.1	1033.6	-11.4	870.9	-25.4
	50	1415.1	1513.4	6.9	1513.4	6.9	1469.6	3.9	1286.0	-9.1
	60	1897.7	2003.5	5.6	2003.5	5.6	1955.4	3.0	1753.9	-7.6
	70	2417.6	2533.9	4.8	2533.9	4.8	2482.4	2.7	2266.2	-6.3
	80	2975.4	3106.9	4.4	3106.9	4.4	3052.3	2.6	2823.3	-5.1
	90	3571.8	3723.7	4.3	3723.7	4.3	3666.3	2.6	3425.8	-4.1
	95	-	4048.8	-	4048.8	-	3990.2	-	-	-
	96	3948.6	-	-	-	-	-	-	-	-
	98	-	-	-	-	-	-	-	3941.4	-
8	40	1360.7	1309.0	-3.8	1309.0	-3.8	1254.0	-7.8	1023.4	-24.8
	50	1820.9	1844.0	1.3	1844.0	1.3	1782.0	-2.1	1522.0	-16.4
	60	2434.4	2437.5	0.1	2437.5	0.1	2369.6	-2.7	2084.7	-14.4
	70	3092.0	3079.0	-0.4	3079.0	-0.4	3006.2	-2.8	2700.8	-12.7
	80	3794.6	3771.1	-0.6	3771.1	-0.6	3694.1	-2.6	3371.0	-11.2
	83	4014.3	3988.9	-0.6	3988.9	-0.6	3910.7	-2.6	-	-
	87	-	-	-	-	-	-	-	3872.5	-
8.67	40	1420.8	1381.1	-2.8	1381.1	-2.8	1320.5	-7.1	1065.9	-25.0
	50	1804.7	1944.0	7.7	1944.0	7.7	1875.7	3.9	1588.8	-12.0
	60	2603.1	2567.8	-1.4	2567.8	-1.4	2492.9	-4.2	2178.7	-16.3
	70	3302.7	3241.5	-1.9	3241.5	-1.9	3161.3	-4.3	2824.6	-14.5
	80	4049.2	3967.8	-2.0	3967.8	-2.0	3883.0	-4.1	3526.9	-
	81	-	-	-	-	-	3958.1	-	-	-
	85	-	-	-	-	-	-	-	3899.3	-

Table 5.18. Moment Resistance (M_r) (Type C Girder, Strand Dia. = 0.5 in.).

Girder Spacing (ft.)	Span (ft.)	STD M_r (k-ft.)	LRFD							
			Skew = 0°		Skew = 15°		Skew = 30°		Skew = 60°	
			M_r (k-ft.)	Diff. %	M_r (k-ft.)	Diff. %	M_r (k-ft.)	Diff. %	M_r (k-ft.)	Diff. %
6	40	1228.2	1236.5	0.7	1236.5	0.7	1236.5	0.7	1236.5	0.7
	50	1538.3	1536.3	-0.1	1536.3	-0.1	1536.3	-0.1	1536.3	-0.1
	60	2101.2	2097.5	-0.2	2097.5	-0.2	2097.5	-0.2	2097.5	-0.2
	70	2919.6	2912.9	-0.2	2912.9	-0.2	2912.9	-0.2	2644.6	-9.4
	80	3666.5	3897.5	6.3	3897.5	6.3	3897.5	6.3	3656.3	-0.3
	90	4805.1	5001.1	4.1	5001.1	4.1	5001.1	4.1	4789.3	-0.3
	95	-	5601.9	-	5601.9	-	5469.9	-	-	-
	96	5596.9	-	-	-	-	-	-	-	-
	98	-	-	-	-	-	-	-	5603.0	-
8	40	1587.0	1547.9	-2.5	1547.9	-2.5	1547.9	-2.5	1244.0	-21.6
	50	1837.5	2120.0	15.4	2120.0	15.4	1835.4	-0.1	1547.9	-15.8
	60	2685.8	2681.3	-0.2	2681.3	-0.2	2681.3	-0.2	2402.0	-10.6
	70	3739.3	3730.7	-0.2	3730.7	-0.2	3730.7	-0.2	3475.7	-7.0
	80	4940.9	4926.8	-0.3	4926.8	-0.3	4926.8	-0.3	4698.0	-4.9
	83	5379.7	5571.2	3.6	5571.2	3.6	5363.3	-0.3	-	-
	87	-	-	-	-	-	-	-	5571.2	-
8.67	40	1482.6	1550.6	4.6	1550.6	4.6	1550.6	4.6	1245.7	-16.0
	50	1984.8	2125.3	7.1	2125.3	7.1	2125.3	7.1	1839.2	-7.3
	60	2694.1	2689.9	-0.2	2689.9	-0.2	2689.9	-0.2	2408.8	-10.6
	70	4012.5	4003.4	-0.2	4003.4	-0.2	4003.4	-0.2	3748.3	-6.6
	80	5418.9	5403.0	-0.3	5403.0	-0.3	5403.0	-0.3	4959.4	-
	81	-	-	-	-	-	5614.7	-	-	-
	85	-	-	-	-	-	-	-	5824.1	-

5.4.4 Shear Design

5.4.4.1 General

The transverse shear design and the interface shear design are two areas where significant differences between Standard and LRFD designs were observed in the parametric study results. These differences are caused due to a significant increase in the shear force specified by LRFD Specifications. The increase in concrete strength and the new MCFT approach for transverse shear design in the LRFD Specifications also affect the transverse shear design.

Some basic background on the MCFT approach for transverse shear design used in the LRFD Specifications is provided in Chapter 3. The LRFD Specifications have provided an extensive background of the mechanics and development of the MCFT model, which can be very useful for bridge engineers to understand and implement the MCFT in shear designs. Transverse shear design using MCFT results in a relatively complex design process and, as such, may not be suitable for routine bridge design. Research is being carried out at the University of Illinois to develop simplified shear design procedures for use in practice. These formulas can be helpful for TxDOT engineers, if their applicability to the typical Texas bridges is verified. Similar research is being carried out at Purdue University to establish simplified design expressions for shear design.

5.4.4.2 Transverse Shear Reinforcement

The transverse shear reinforcement increased significantly for Type C LRFD designs for most cases. A comparison of the transverse shear reinforcement area for Standard and LRFD designs is presented in Table 5.19. The transverse shear reinforcement increases in the range of 15 to 475 percent for 6 ft. girder spacing. This difference is found to be in the range of -44 to 610 percent for 8 ft. girder spacing and -60 to 443 percent for 8.67 ft. girder spacing.

Table 5.19. Comparison of Transverse Shear Reinforcement Area (A_v) (Type C Girder, Strand Diameter = 0.5 in.).

Girder Spacing (ft.)	Span (ft.)	Std. A_v (in.^{2}/ft.)	LRFD							
			Skew = 0°		Skew = 15°		Skew = 30°		Skew = 60°	
			A_v (in.^{2}/ft.)	Diff. %	A_v (in.^{2}/ft.)	Diff. %	A_v (in.^{2}/ft.)	Diff. %	A_v (in.^{2}/ft.)	Diff. %
6	40	0.07	0.10	38.8	0.10	38.8	0.10	38.8	0.10	38.8
	50	0.15	0.23	50.8	0.26	69.5	0.28	84.0	0.36	136.2
	60	0.07	0.21	193.3	0.24	237.0	0.27	279.2	0.36	419.9
	70	0.17	0.19	15.2	0.21	25.8	0.23	38.0	0.31	85.9
	80	0.09	0.24	163.7	0.26	186.2	0.28	212.4	0.37	316.2
	90	0.07	0.22	209.2	0.24	241.9	0.29	312.7	0.40	475.0
	95	-	0.24	-	0.27	-	0.24	-	-	-
	96	0.07	-	-	-	-	-	-	-	-
	98	-	-	-	-	-	-	-	0.39	-
8	40	0.07	0.26	265.8	0.28	305.0	0.30	328.8	0.10	41.3
	50	0.18	0.30	70.1	0.33	89.2	0.10	-43.8	0.10	-43.8
	60	0.25	0.24	-5.5	0.26	2.3	0.28	10.9	0.50	98.9
	70	0.19	0.29	51.7	0.32	63.6	0.34	77.5	0.45	132.8
	80	0.07	0.28	298.6	0.30	335.6	0.36	419.3	0.50	610.1
	83	0.07	0.29	320.4	0.32	359.5	0.36	420.2	-	-
	87	-	-	-	-	-	-	-	0.48	-
8.67	40	0.12	0.10	-18.7	0.10	-18.7	0.10	-18.7	0.10	-18.7
	50	0.25	0.37	50.4	0.41	65.3	0.44	76.3	0.10	-60.1
	60	0.32	0.26	-18.1	0.28	-11.6	0.31	-2.2	0.60	87.4
	70	0.24	0.32	38.2	0.35	48.8	0.38	61.0	0.49	109.7
	80	0.07	0.32	361.0	0.35	399.3	0.38	443.5	0.53	-
	81	-	-	-	-	-	0.38	-	-	-
	85	-	-	-	-	-	-	-	0.52	-

5.4.4.3 Interface Shear Reinforcement

The interface shear reinforcement area is found to be increasing significantly for LRFD designs for the case when the interface is roughened. A comparison of the interface shear reinforcement area for Standard and LRFD designs is presented in Table 5.20. The interface shear reinforcement area increases in the range of 2 to 411 percent for 6 ft. girder spacing, 67 to 330 percent for 8 ft. girder spacing, and 87 to 284 percent for 8.67 ft. girder spacing.

Table 5.20. Comparison of Interface Shear Reinforcement Area with Roughened Interface (Type C Girder, Strand Diameter = 0.5 in.).

Girder Spacing (ft.)	Span (ft.)	Std. A_{vh} (in.^{2}/ft.)	LRFD							
			Skew = 0°		Skew = 15°		Skew = 30°		Skew = 60°	
			A_{vh} (in.^{2}/ft.)	Diff. %	A_{vh} (in.^{2}/ft.)	Diff. %	A_{vh} (in.^{2}/ft.)	Diff. %	A_{vh} (in.^{2}/ft.)	Diff. %
6	40	0.14	0.14	1.4	0.16	14.3	0.18	29.1	0.26	84.5
	50	0.14	0.21	49.7	0.23	65.6	0.26	83.9	0.35	152.3
	60	0.14	0.27	95.3	0.30	114.2	0.33	135.9	0.44	217.2
	70	0.14	0.33	136.9	0.36	158.6	0.40	183.7	0.52	273.3
	80	0.14	0.40	183.6	0.43	208.5	0.47	237.2	0.61	339.0
	90	0.14	0.47	234.8	0.51	263.1	0.55	295.8	0.72	411.6
	95	-	0.53	-	0.58	-	0.61	-	-	-
	96	0.17	-	-	-	-	-	-	-	-
	98	-	-	-	-	-	-	-	0.83	-
8	40	0.14	0.23	67.2	0.26	82.7	0.28	100.8	0.37	166.4
	50	0.14	0.33	133.4	0.35	153.0	0.38	171.2	0.49	248.4
	60	0.14	0.40	186.0	0.43	209.1	0.47	235.7	0.60	330.9
	70	0.20	0.48	145.5	0.52	164.7	0.56	186.9	0.71	265.5
	80	0.26	0.56	117.6	0.61	134.3	0.66	153.5	0.83	221.7
	83	0.29	0.60	110.3	0.65	126.2	0.69	141.4	-	-
	87	-	-	-	-	-	-	-	0.92	-
8.67	40	0.14	0.26	86.8	0.28	103.2	0.31	122.3	0.41	191.8
	50	0.14	0.36	156.2	0.39	176.8	0.42	200.7	0.54	284.5
	60	0.18	0.44	143.8	0.47	162.8	0.51	184.8	0.65	263.6
	70	0.25	0.52	109.0	0.56	124.9	0.61	143.2	0.77	208.7
	80	0.32	0.62	92.3	0.67	106.6	0.72	123.1	0.90	-
	81	-	-	-	-	-	0.73	-	-	-
	85	-	-	-	-	-	-	-	0.98	-

The interface shear reinforcement area is found to increase even more significantly for LRFD designs for the case of unroughened interface. A comparison of the interface shear reinforcement area for Standard and LRFD designs is presented in Table 5.21. The interface shear reinforcement area increases from 152 to 836 percent for 6 ft. girder spacing, 263 to 700 percent for 8 ft. girder spacing, and 294 to 624 percent for 8.67 ft. girder spacing.

Table 5.21. Comparison of Interface Shear Reinforcement Area without Roughened Interface (Type C Girder, Strand Diameter = 0.5 in.).

Girder Spacing (ft.)	Span (ft.)	Std. A_{vh} (in.^{2}/ft.)	LRFD							
			skew = 0°		skew = 15°		skew = 30°		skew = 60°	
			A_{vh} (in.^{2}/ft.)	Diff. %	A_{vh} (in.^{2}/ft.)	Diff. %	A_{vh} (in.^{2}/ft.)	Diff. %	A_{vh} (in.^{2}/ft.)	Diff. %
6	40	0.14	0.35	152.4	0.38	173.8	0.42	198.6	0.55	290.9
	50	0.14	0.47	232.8	0.50	259.3	0.55	289.8	0.71	403.8
	60	0.14	0.57	308.9	0.62	340.3	0.67	376.6	0.86	511.9
	70	0.14	0.67	378.2	0.72	414.4	0.78	456.1	0.99	605.4
	80	0.14	0.78	456.0	0.84	497.5	0.90	545.3	1.14	715.0
	90	0.14	0.90	541.3	0.96	588.5	1.04	643.0	1.31	836.1
	95	-	1.00	-	1.08	-	1.13	-	-	-
	96	0.17	-	-	-	-	-	-	-	-
	98	-	-	-	-	-	-	-	1.50	-
8	40	0.14	0.51	261.9	0.54	287.9	0.59	317.9	0.74	427.4
	50	0.14	0.66	372.3	0.71	404.9	0.75	435.3	0.93	564.0
	60	0.14	0.78	460.0	0.84	498.5	0.90	542.8	1.12	701.4
	70	0.20	0.92	368.9	0.98	400.9	1.05	437.8	1.31	568.9
	80	0.26	1.06	307.8	1.13	335.5	1.21	367.6	1.50	481.1
	83	0.29	1.12	291.4	1.19	317.8	1.27	343.1	-	-
	87	-	-	-	-	-	-	-	1.66	-
8.67	40	0.14	0.55	294.6	0.59	322.1	0.64	353.8	0.80	469.6
	50	0.14	0.71	410.3	0.76	444.7	0.82	484.5	1.01	624.1
	60	0.18	0.84	371.6	0.90	403.3	0.96	440.0	1.20	571.3
	70	0.25	0.99	294.9	1.06	321.3	1.13	351.9	1.41	461.1
	80	0.32	1.15	256.7	1.23	280.6	1.32	308.1	1.61	-
	81	-	-	-	-	-	1.34	-	-	-
	85	-	-	-	-	-	-	-	1.75	-

5.5 CAMBER

The Standard Specifications do not provide guidelines for determining the camber of prestressed concrete members. The Hyperbolic Functions Method (Furr et al. 1968, Sinno 1968, Furr and Sinno 1970) for the calculation of maximum camber is used by TxDOT's prestressed concrete bridge design software, PSTRS14 (TxDOT 2004). The details of this method are described in the design examples provided in the second volume of this report.

The cambers computed for the Type C girders are summarized in Table 5.22. Because the camber is evaluated using the same methodology for both specifications, only a small difference is observed. The cambers for LRFD designs were generally smaller as compared to those for Standard designs. The maximum difference in the camber is 22 percent for 6 ft. girder spacing and 35 percent for 8 ft. and 8.67 ft. girder spacings.

Table 5.22. Comparison of Camber (Type C Girder, Strand Dia. = 0.5 in.).

Girder Spacing (ft.)	Span (ft.)	STD Camber (ft.)	LRFD							
			Skew = 0°		Skew = 15°		Skew = 30°		Skew = 60°	
			Camber (ft.)	Diff. %	Camber (ft.)	Diff. %	Camber (ft.)	Diff. %	Camber (ft.)	Diff. %
6	40	0.041	0.032	-22.3	0.032	-22.3	0.032	-22.3	0.032	-22.3
	50	0.052	0.052	0.2	0.052	0.2	0.052	0.2	0.052	0.2
	60	0.090	0.087	-2.9	0.087	-2.9	0.089	-1.1	0.089	-1.1
	70	0.156	0.153	-1.4	0.153	-1.4	0.153	-1.4	0.129	-17.3
	80	0.220	0.241	9.4	0.241	9.4	0.241	9.4	0.216	-1.8
	90	0.312	0.327	4.5	0.327	4.5	0.331	5.9	0.310	-0.7
	95	-	0.372	-	0.372	-	0.355	-	-	-
	96	0.366	-	-	-	-	-	-	-	-
	98	-	-	-	-	-	-	-	0.365	-
8	40	0.049	0.041	-16.3	0.041	-16.3	0.041	-16.3	0.032	-35.3
	50	0.065	0.077	18.1	0.077	18.1	0.064	-0.9	0.051	-20.8
	60	0.124	0.123	-1.2	0.123	-1.2	0.123	-1.2	0.108	-13.4
	70	0.211	0.207	-1.6	0.207	-1.6	0.207	-1.6	0.192	-9.0
	80	0.313	0.302	-3.6	0.302	-3.6	0.308	-1.8	0.293	-6.4
	83	0.342	0.347	1.3	0.347	1.3	0.336	-1.9	-	-
	87	-	-	-	-	-	-	-	0.348	-
8.67	40	0.049	0.041	-16.2	0.041	-16.2	0.041	-16.2	0.032	-35.3
	50	0.076	0.077	0.3	0.077	0.3	0.077	0.3	0.064	-15.9
	60	0.124	0.122	-1.8	0.122	-1.8	0.123	-1.2	0.106	-14.6
	70	0.229	0.225	-1.5	0.225	-1.5	0.225	-1.5	0.207	-9.4
	80	0.337	0.330	-1.9	0.330	-1.9	0.330	-1.8	0.308	-
	81	-	-	-	-	-	0.345	-	-	-
	85	-	-	-	-	-	-	-	0.365	-

6. PARAMETRIC STUDY – TEXAS U54 GIRDERS

6.1 INTRODUCTION

A parametric study was conducted for Texas U54 prestressed concrete bridge girders. A number of cases were considered based on the parameters given in Table 6.1. The main objective was to investigate the effect of the provisions in the LRFD Specifications as compared to designs following the Standard Specifications. The procedure outlined in Chapter 3 was used to design the girders. The results obtained for designs based on both the Standard and LRFD Specifications were validated using TxDOT's bridge design software PSTRS14 (TxDOT 2004). TxDOT's procedures for optimizing the number of strands and concrete strength requirements were used.

Table 6.1. Design Parameters for Texas U54 Girders.

Parameter	Description / Selected Values
Design Codes	AASHTO Standard Specifications, 17th Edition (2002) AASHTO LRFD Specifications, 3rd Edition (2004)
Girder Spacing (ft.)	8'-6", 10'-0", 11'-6", 14'-0", and 16'-8"
Spans	90 ft. to maximum span at 10 ft. intervals
Strand Diameter (in.)	0.5 and 0.6
Concrete Strength at Release, f'_{ci}	Varied from 4000 to 6750 psi for design with optimum number of strands
Concrete Strength at Service, f'_c	Varied from 5000 to 8500 psi for design with optimum number of strands (f'_c may be increased up to 8750 psi for optimization on longer spans)
Skew Angle (degrees)	0, 15, 30, and 60

For the parametric study, the span lengths were increased from 90 ft. to the maximum possible span length at 10 ft. intervals. For the purpose of the discussion of results, the spans are categorized as "short spans," "long spans," and "maximum spans." A short span is considered to be in the range of 90 to 100 ft. length, and a long span is considered to be greater than 100 ft. up to, but not including, the maximum span length. The maximum span length is the length beyond which a particular limit state (e.g., service limit state) is exceeded or a particular set of parameters (e.g. f'_{ci}) reach their maximum value. The percent difference was calculated by the following equation.

$$\text{Diff. (percent)} = \left(\frac{\lambda_{LRFD} - \lambda_{STD}}{\lambda_{STD}}\right) \times 100 \tag{6.1}$$

where, λ_{LRFD} and λ_{STD} are the design values of interest based on the LRFD and Standard Specifications, respectively. Therefore, a negative difference indicates a decrease in the design value based on the LRFD Specifications with respect to the design value based on the Standard Specifications. The focus of this research was on the interior girders, so all results presented in this chapter relate to the interior girder calculations unless otherwise specified.

The requirements for service load limit state design, flexural strength limit state design, transverse shear design, and interface shear design are evaluated in the parametric study. The detailed design information for every U54 girder case studied is available in the tables and graphs provided in Appendix A of this report volume. Based on these results, the following sections summarize the findings with the help of tables and graphs that illustrate the overall trends. This summary includes differences occurring in the undistributed and distributed live load moments, the distribution factors, the number of strands required, and required concrete strengths at release and at service. The differences observed in the flexural and shear strength limit states design are also provided in the following sections.

6.2 LIVE LOAD MOMENTS AND SHEARS

6.2.1 General

The Standard Specifications specify the live load as the maximum effect produced by either HS-20 design truck load or a design lane load. The LRFD Specifications specify a different live load model (HL-93), which is the maximum effect produced by the combination of a design truck load or design tandem load with the design lane load. The formulas for load distribution and impact factors provided by the Standard Specifications differ significantly from those provided by the LRFD Specifications. The impact factors as given in the Standard Specifications vary with the span length and are applicable to both the truck and lane loading; whereas the LRFD Specifications require the impact factor, which is constant at 33 percent, to be applicable to only the design truck and design tandem loads.

The live load moments are calculated at the midspan location, whereas the live load shears are calculated at the critical section locations. The live load distribution factors and undistributed and distributed live load moments and shears are calculated for each case, and the comparisons between the Standard and LRFD Specifications are presented below.

6.2.2 Live Load Distribution Factors

A summary of the live load DFs for moment for all skew angles is provided in Table 6.2. The skew correction factors for skew angles of 0, 15, 30, and 60 degrees are 1, 0.983, 0.906, and 0.617. These skew correction factors, when applied to the live load DFs, do not change the DFs significantly for skew angles up to 30 degrees. However, they do have a significant effect for a skew angle of 60 degrees.

Table 6.3 presents the live load DFs for moment and shear calculated without applying the skew correction factor. In general, the LRFD live load DFs for moment, without the skew correction factor, decrease in the range of 23.8 to 40.8 percent. The skew does not affect shear live load DFs for the interior beams. In general, the LRFD shear DFs increase up to 3.9 percent and decrease up to 11.9 percent relative to the Standard values. Shear live load DFs for both specifications are drawn in Figure 6.2. For spacings of 10 ft. and 11.5 ft. the difference is negligible, but for the spacings of 8.5 ft., 14 ft., and 16.67 ft. the Standard Specifications' shear live load DFs are larger.

The live load DFs calculated in the Standard Specifications are larger than those calculated in the LRFD Specifications, but for moment live load DFs, when compared to shear live load DFs, this difference is more pronounced as can be seen in Figures 6.1 and 6.2. Figure 6.1 shows the live load DFs for moment, calculated by taking into account the skew correction factor, for all the spacings. It can be seen that for skew angles of 0, 15, and 30 degrees, the live load moment DFs decrease in the range of 23.8 to 46.4 percent, while for the skew angle of 60 degrees this decrease ranges from 57.8 to 63.5 percent. Detailed results for all skews are given in Appendix A.

Table 6.2. Live Load Moment Distribution Factors (DFM) for U54 Girders.

Girder Spacing (ft.)	Span (ft.)	STD DFM	LRFD							
			Skew = 0°		Skew = 15°		Skew = 30°		Skew = 60°	
			DFM	Diff. %	DFM	Diff. %	DFM	Diff. %	DFM	Diff. %
8.50	90	0.900	0.616	-31.6	0.605	-32.8	0.557	-38.1	0.380	-57.8
	100		0.599	-33.4	0.589	-34.5	0.543	-39.7	0.370	-58.9
	110		0.585	-35.0	0.575	-36.1	0.530	-41.1	0.361	-59.9
	120		0.572	-36.4	0.562	-37.5	0.518	-42.4	0.353	-60.8
	130		0.561	-37.7	0.551	-38.8	0.508	-43.6	0.346	-61.6
	140		0.550	-38.9	0.541	-39.9	0.498	-44.6	0.340	-62.3
10.00	90	0.909	0.692	-23.8	0.681	-25.1	0.627	-31.0	0.427	-53.0
	100		0.674	-25.8	0.663	-27.1	0.611	-32.8	0.416	-54.2
	110		0.658	-27.6	0.647	-28.8	0.596	-34.4	0.406	-55.3
	120		0.644	-29.2	0.633	-30.4	0.583	-35.9	0.397	-56.3
	130		0.631	-30.6	0.620	-31.8	0.571	-37.2	0.389	-57.2
	140		0.619	-31.9	0.609	-33.1	0.561	-38.3	0.382	-58.0
11.50	90	1.046	0.766	-26.7	0.753	-27.9	0.694	-33.6	0.473	-54.8
	100		0.746	-28.6	0.733	-29.9	0.676	-35.4	0.460	-56.0
	110		0.728	-30.3	0.716	-31.5	0.660	-36.9	0.449	-57.0
	120		0.712	-31.9	0.700	-33.0	0.645	-38.3	0.440	-58.0
	130		0.698	-33.2	0.686	-34.4	0.632	-39.5	0.431	-58.8
	140		0.685	-34.5	0.673	-35.6	0.620	-40.7	0.423	-59.6
14.00	90	1.273	0.884	-30.6	0.869	-31.7	0.800	-37.1	0.545	-57.2
	100		0.860	-32.4	0.846	-33.5	0.779	-38.8	0.531	-58.3
	110		0.840	-34.0	0.826	-35.1	0.761	-40.2	0.518	-59.3
	120		0.822	-35.4	0.808	-36.5	0.744	-41.5	0.507	-60.2
	130		0.805	-36.7	0.791	-37.8	0.729	-42.7	0.497	-61.0
	140		0.790	-37.9	0.777	-39.0	0.716	-43.8	0.487	-61.7
16.67	90	1.516	1.003	-33.8	0.986	-34.9	0.908	-40.1	0.619	-59.2
	100		0.977	-35.6	0.960	-36.7	0.884	-41.6	0.603	-60.2
	110		0.953	-37.1	0.937	-38.2	0.863	-43.0	0.588	-61.2
	120		0.932	-38.5	0.917	-39.5	0.844	-44.3	0.575	-62.0
	130		0.914	-39.7	0.898	-40.7	0.827	-45.4	0.564	-62.8
	140		0.897	-40.8	0.881	-41.8	0.812	-46.4	0.553	-63.5

Table 6.3. Live Load Distribution Factors (U54 Girder, Skew = 0°).

Spacing (ft.)	Span (ft.)	Moment DF		%diff. w.r.t STD	Shear DF		%diff. w.r.t STD
		LRFD	STD		LRFD	STD	
8.50	90	0.616	0.900	-31.6	0.830	0.900	-7.8
	100	0.599		-33.4	0.821		-8.8
	110	0.585		-35.0	0.813		-9.7
	120	0.572		-36.4	0.806		-10.5
	130	0.561		-37.7	0.799		-11.2
	140	0.550		-38.9	0.793		-11.9
10.00	90	0.692	0.909	-23.8	0.945	0.909	3.9
	100	0.674		-25.8	0.935		2.8
	110	0.658		-27.6	0.926		1.8
	120	0.644		-29.2	0.917		0.9
	130	0.631		-30.6	0.910		0.1
	140	0.619		-31.9	0.903		-0.6
11.50	90	0.766	1.046	-26.7	1.056	1.046	1.0
	100	0.746		-28.6	1.045		0.0
	110	0.728		-30.3	1.035		-1.0
	120	0.712		-31.9	1.026		-1.9
	130	0.698		-33.2	1.018		-2.7
	140	0.685		-34.5	1.010		-3.4
14.00	90	0.884	1.273	-30.6	1.237	1.273	-2.8
	100	0.860		-32.4	1.223		-3.9
	110	0.840		-34.0	1.212		-4.8
	120	0.822		-35.4	1.201		-5.6
	130	0.805		-36.7	1.191		-6.4
	140	0.790		-37.9	1.182		-7.1
16.67	90	1.003	1.516	-33.8	1.422	1.516	-6.2
	100	0.977		-35.6	1.407		-7.2
	110	0.953		-37.1	1.393		-8.1
	120	0.932		-38.5	1.381		-8.9
	130	0.914		-39.7	1.370		-9.6
	140	0.897		-40.8	1.360		-10.3

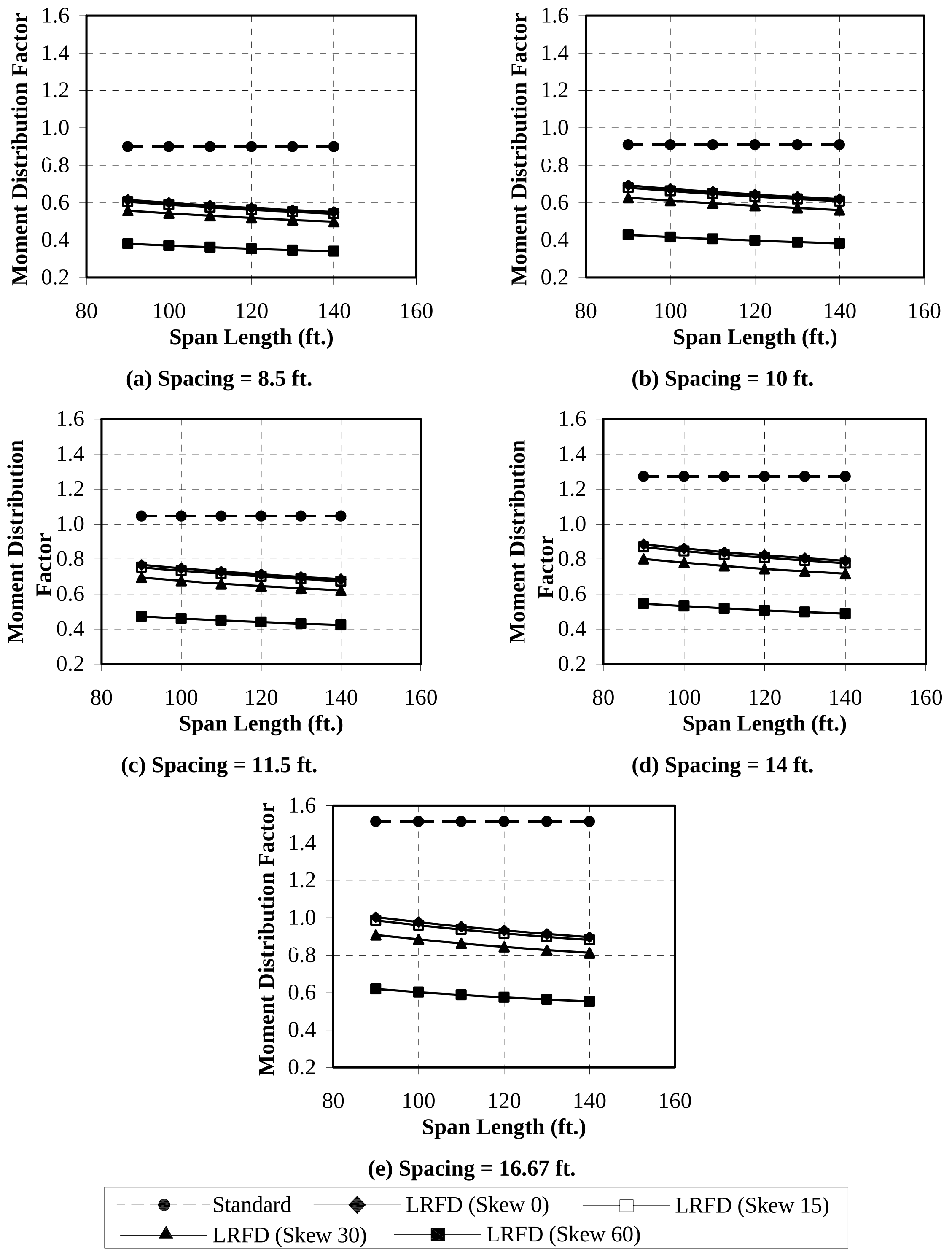

Figure 6.1. Comparison of Live Load Distribution Factor for Moment (U54 Girder).

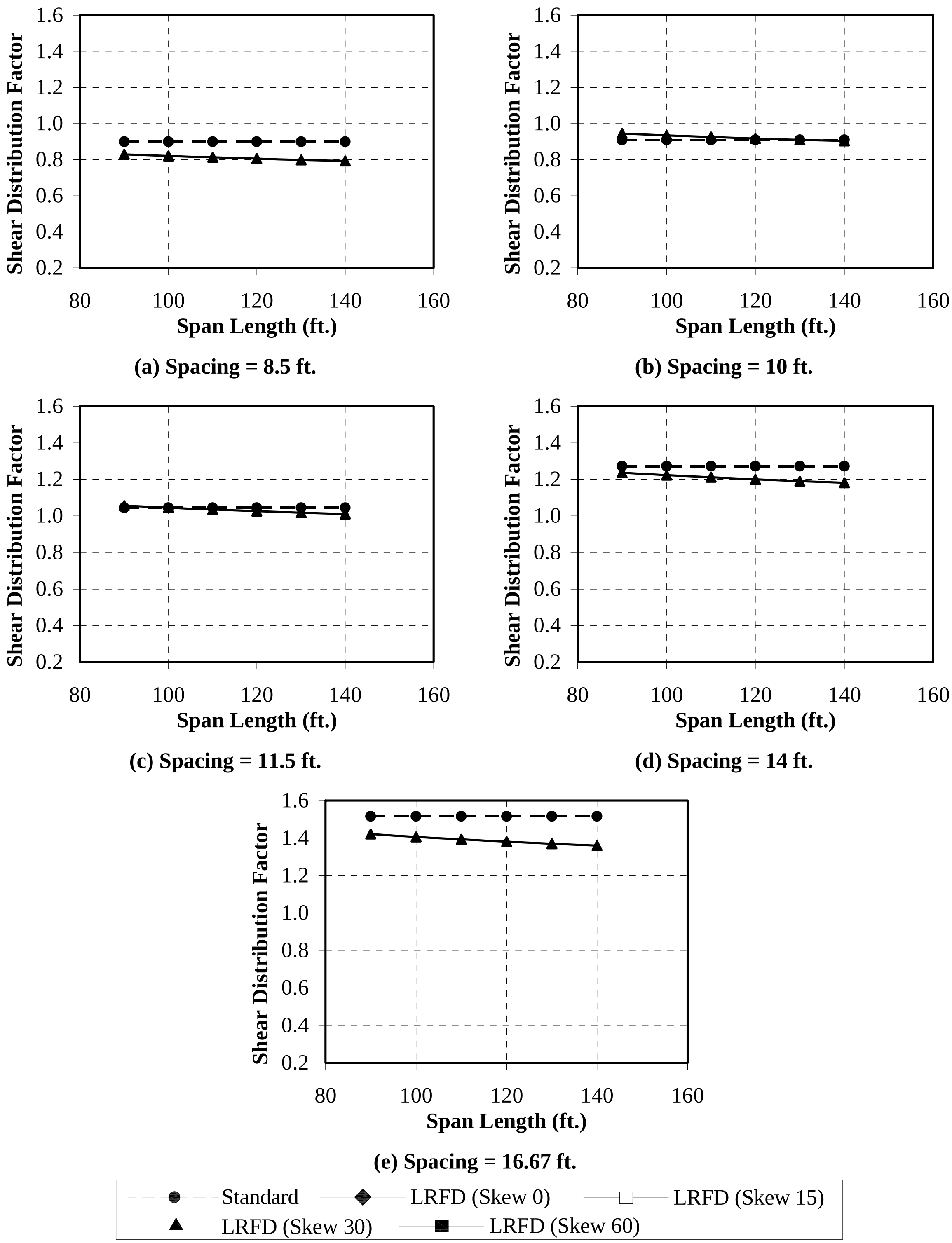

Figure 6.2. Comparison of Live Load Distribution Factor for Shear (U54 Girder).

6.2.3 Undistributed Live Load Moment and Shear

6.2.3.1 Undistributed Live Load Moment

For simply supported bridge superstructures, the undistributed live load moment is calculated by placing the vehicular live load on a simply supported beam, such that the maximum response is obtained. The LRFD Specifications introduced the new HL-93 live load model, which is heavier than its predecessor, HS-20, used in the Standard Specifications. The undistributed live load moment depends on the bridge span length and position of the live load. The LRFD Specifications give a larger design undistributed live load moment, as shown in Figure 6.3, when compared to that of the Standard Specifications. When the undistributed live load moment is calculated by the LRFD Specifications, it increases from 778.6 k-ft to 1884.5 k-ft (47.1 to 70.8 percent) relative to the Standard Specifications.

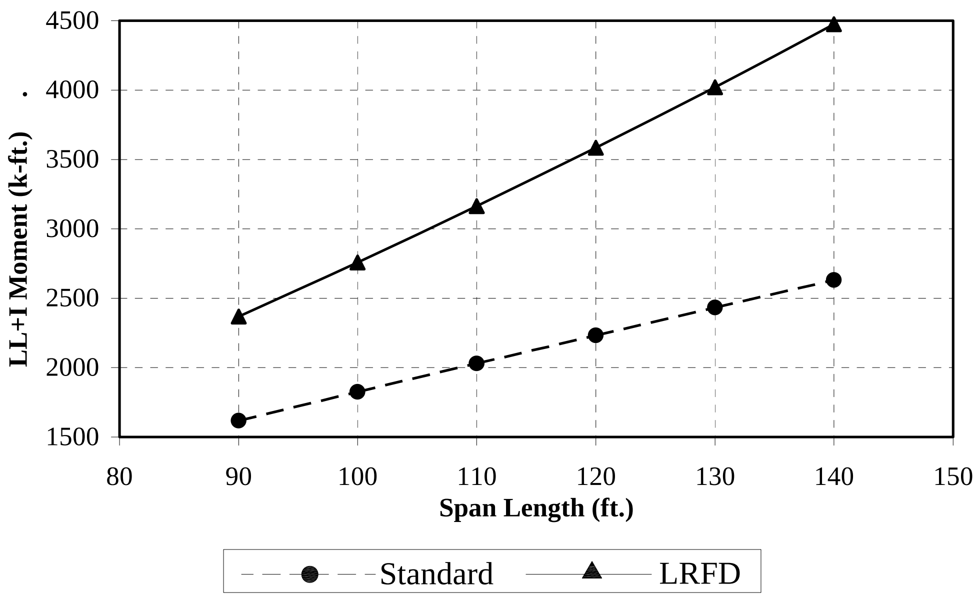

Figure 6.3. Comparison of Undistributed Live Load Moment (U54 Girder).

The HL-93 truck plus lane load combination, as compared to the tandem plus lane load combination, and the HS-20 truck load as compared to the lane load always control for the span range considered in this study. Detailed results are outlined in Appendix A.

6.2.3.2 Undistributed Live Load Shear and Critical Section Location

The critical section for shear varies significantly from the Standard to the LRFD Specifications. For the Standard Specifications the critical section is constant and is located at a distance *h*/2 (where *h* is the total height of the composite girder section) from the end of the beam. In the LRFD Specifications, the critical section is calculated by an iterative procedure. For all the bridges considered in this study, the critical section for Standard designs is 2.583 ft. from the end of the beam, whereas in the LRFD Specifications the critical section location varies from 5.03 ft. to 6.04 ft. from the beam end. The strand diameter has a very insignificant affect on the overall range of the critical section location. In general, the critical section location reduces with increased girder spacing.

Figure 6.4 shows the undistributed live load shear force at the critical section location versus the span length for various girder spacings. Detailed results are outlined in Appendix A. When the LRFD Specifications results are viewed alone, the variation in the undistributed live load shear force due to skew angle is negligible for the different spacings considered, as can be seen in Figure 6.4 where the shear force plots for all the skew angles are superimposed on each other. In addition, the undistributed live load shear force values change very insignificantly due to changes in girder spacing. The undistributed shear forces calculated for the LRFD designs increase by 27 to 43.5 kips (35 to 55.6 percent) relative to the Standard Specifications.

6.2.4 Distributed Live Load Moment and Shear

6.2.4.1 Distributed Live Load Moment

The distributed live load moment is determined by multiplying the undistributed live load moment by the corresponding distribution factor and skew correction factor to find the portion of the moment distributed to an individual bridge girder. Table 6.4 and Figure 6.5 provide the difference in the distributed live load moment for LRFD designs as compared to Standard designs. For skew angles of 0 and 15 degrees, the distributed live load moment comparison follows a similar trend and the LRFD moment increases up to 386.6 k-ft (16 percent) and decreases up to 117.5 k-ft (4.7 percent) relative to that of the Standard moment. For a 30-degree skew angle, the distributed live load moment increases up to 121.8 k-ft (5 percent) and decreases up to 358.3 k-ft (12.2 percent). For a 60-degree skew angle, the distributed live load moment decreases in the range of 467.7 to 1526.3 k-ft (28.4 to 40.2 percent).

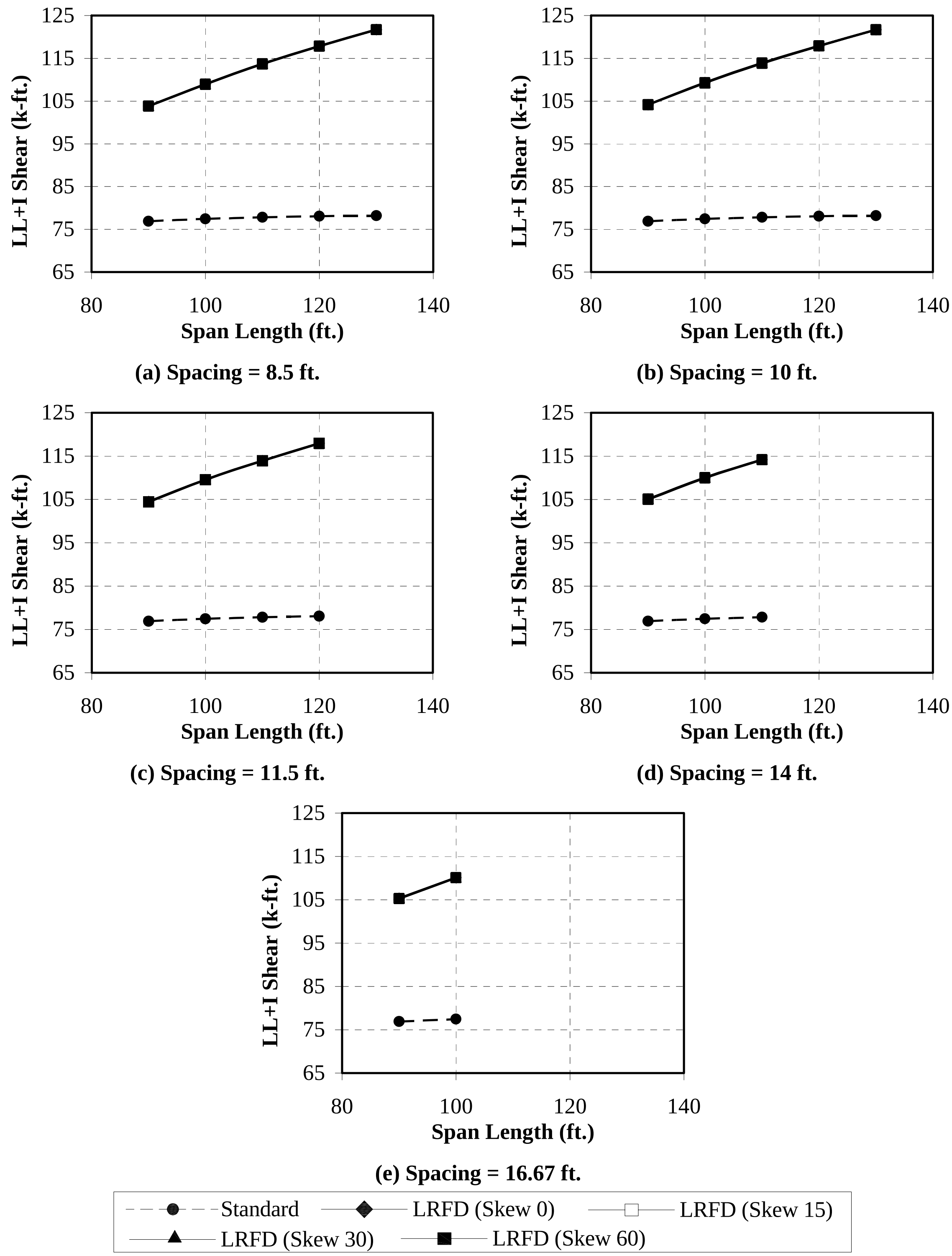

Figure 6.4. Undistributed Live Load Shear Force at Critical Section (U54 Girder).

Table 6.4. Distributed Live Load Moments (U54 Girder).

Girder Spacing (ft.)	Span (ft.)	STD LL Mom. (k-ft)	LRFD							
			Skew = 0°		Skew = 15°		Skew = 30°		Skew = 60°	
			LL Mom. (k-ft)	% Diff.	LL Mom. (k-ft)	% Diff.	LL Mom. (k-ft)	% Diff.	LL Mom. (k-ft)	% Diff.
8.50	90	1486.3	1489.1	0.2	1463.8	-1.5	1348.6	-9.3	918.8	-38.2
	100	1671.9	1684.0	0.7	1655.4	-1.0	1525.2	-8.8	1039.0	-37.9
	110	1855.4	1881.8	1.4	1849.8	-0.3	1704.3	-8.1	1161.0	-37.4
	120	2037.2	2082.8	2.2	2047.4	0.5	1886.3	-7.4	1285.0	-36.9
	130	2217.4	2287.1	3.1	2248.3	1.4	2071.4	-6.6	1411.1	-36.4
	140	2396.2	2495.0	4.1	2452.6	2.4	2259.6	-5.7	1539.4	-35.8
10.00	90	1501.3	1675.3	11.6	1646.9	9.7	1517.3	1.1	1033.7	-31.2
	100	1688.8	1894.6	12.2	1862.4	10.3	1715.9	1.6	1168.9	-30.8
	110	1874.1	2117.1	13.0	2081.2	11.0	1917.4	2.3	1306.2	-30.3
	120	2057.8	2343.2	13.9	2303.4	11.9	2122.2	3.1	1445.7	-29.7
	130	2239.8	2573.1	14.9	2529.4	12.9	2330.4	4.0	1587.6	-29.1
	140	2420.5	2807.0	16.0	2759.3	14.0	2542.2	5.0	1731.9	-28.4
11.50	90	1726.5	1854.0	7.4	1822.5	5.6	1679.1	-2.7	1143.9	-33.7
	100	1942.1	2096.6	8.0	2061.0	6.1	1898.8	-2.2	1293.6	-33.4
	110	2155.3	2342.9	8.7	2303.1	6.9	2121.9	-1.5	1445.5	-32.9
	120	2366.4	2593.1	9.6	2549.0	7.7	2348.5	-0.8	1599.9	-32.4
	130	2575.8	2847.5	10.5	2799.1	8.7	2578.9	0.1	1756.9	-31.8
	140	2783.5	3106.3	11.6	3053.6	9.7	2813.3	1.1	1916.6	-31.1
14.00	90	2101.9	2138.2	1.7	2101.9	0.0	1936.5	-7.9	1319.2	-37.2
	100	2364.3	2418.0	2.3	2377.0	0.5	2189.9	-7.4	1491.9	-36.9
	110	2623.8	2702.0	3.0	2656.1	1.2	2447.1	-6.7	1667.1	-36.5
	120	2880.9	2990.6	3.8	2939.8	2.0	2708.4	-6.0	1845.1	-36.0
	130	3135.7	3284.0	4.7	3228.2	2.9	2974.2	-5.2	2026.2	-35.4
	140	3388.6	3582.5	5.7	3521.6	3.9	3244.5	-4.3	2210.4	-34.8
16.67	90	2502.7	2426.6	-3.0	2385.4	-4.7	2197.7	-12.2	1497.2	-40.2
	100	2815.2	2744.2	-2.5	2697.6	-4.2	2485.4	-11.7	1693.2	-39.9
	110	3124.2	3066.5	-1.8	3014.5	-3.5	2777.3	-11.1	1892.0	-39.4
	120	3430.3	3394.0	-1.1	3336.4	-2.7	3073.8	-10.4	2094.1	-39.0
	130	3733.7	3727.0	-0.2	3663.7	-1.9	3375.4	-9.6	2299.5	-38.4
	140	4034.9	4065.8	0.8	3996.7	-0.9	3682.3	-8.7	2508.6	-37.8

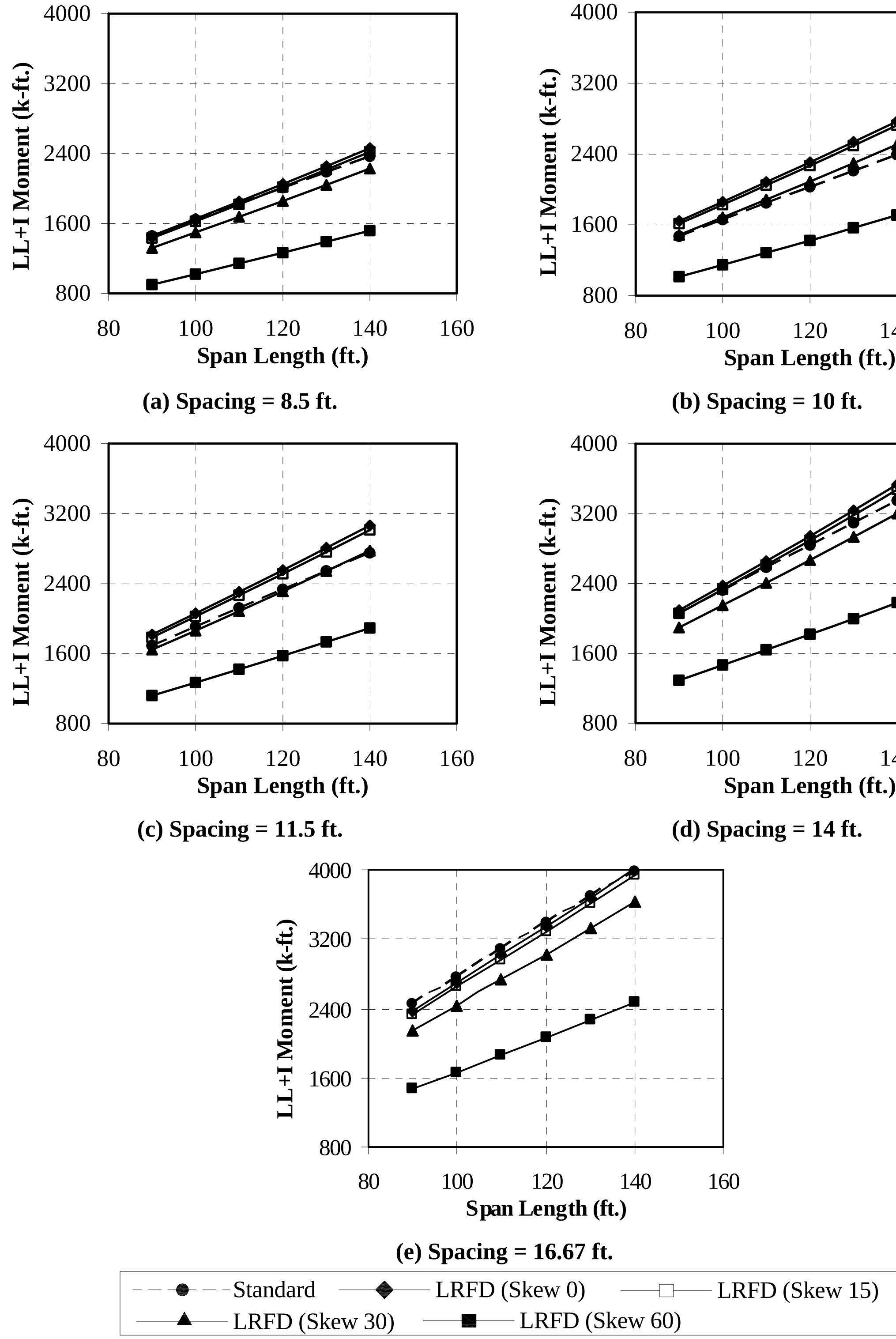

Figure 6.5. Distributed Live Load Moment (U54 Girder).

6.2.4.2 Distributed Live Load Shear

Table 6.5 shows the maximum and minimum range of difference in the distributed live load shear for LRFD designs relative to Standard designs. The distributed live load shear force was calculated at the critical section location for each specification and plotted versus the span lengths considered in Figure 6.6. As mentioned earlier, the LRFD Specifications provide a skew correction factor for shear only for the exterior girders, while this study focuses on the interior girders. Therefore, the skew does not affect the shear force in the girders. The distributed live load shear, as calculated in the LRFD Specifications, increases by 16.9 to 39.6 kips (24.5 to 55.7 percent) for all spacings considered.

Table 6.5. Difference in Distributed Live Load Shear (U54 Girder).

Girder Spacing (ft.)	Difference (kips)	Difference (%)
8.50	16.9 - 26.9	24.5 - 38.2
10.00	28.5 - 39.6	40.8 - 55.7
11.50	29.9 - 39.4	37.3 - 48.3
14.00	32.1 - 39.3	32.8 - 39.7
16.67	up to 37.6	up to 32

6.2.5 Comparison of Undistributed Dynamic Load Moment and Shear

The LRFD Specifications recommend the use of 33 percent of the total undistributed live load as the dynamic load. The Standard Specifications give a relationship to calculate the dynamic load allowance factor (known as the impact factor in the Standard Specifications), which is then multiplied with the total undistributed live load to get the dynamic load. The impact factor in the Standard Specifications ranges from 23.3 percent to 18.9 percent, and the variation in the dynamic load moments is shown in Table 6.6 and Figure 6.7.

There is a significant increase in the dynamic load moment from 125.5 to 310 k-ft. (40.8 to 73.9 percent) and the dynamic load shear force also increases in the range of 5.1 to 8.0 kips (34.9 to 62.1 percent). A trend in the change in dynamic load shear with respect to the span length can be observed in Figure 6.8. For the LRFD Specifications the dynamic load shear increases with respect to the span length, while for the Standard Specifications the dynamic load shear decreases with respect to the span length. The reason for this trend is that the impact factor in the Standard Specifications decreases with the span length, as compared to the LRFD Specifications where it is constant.

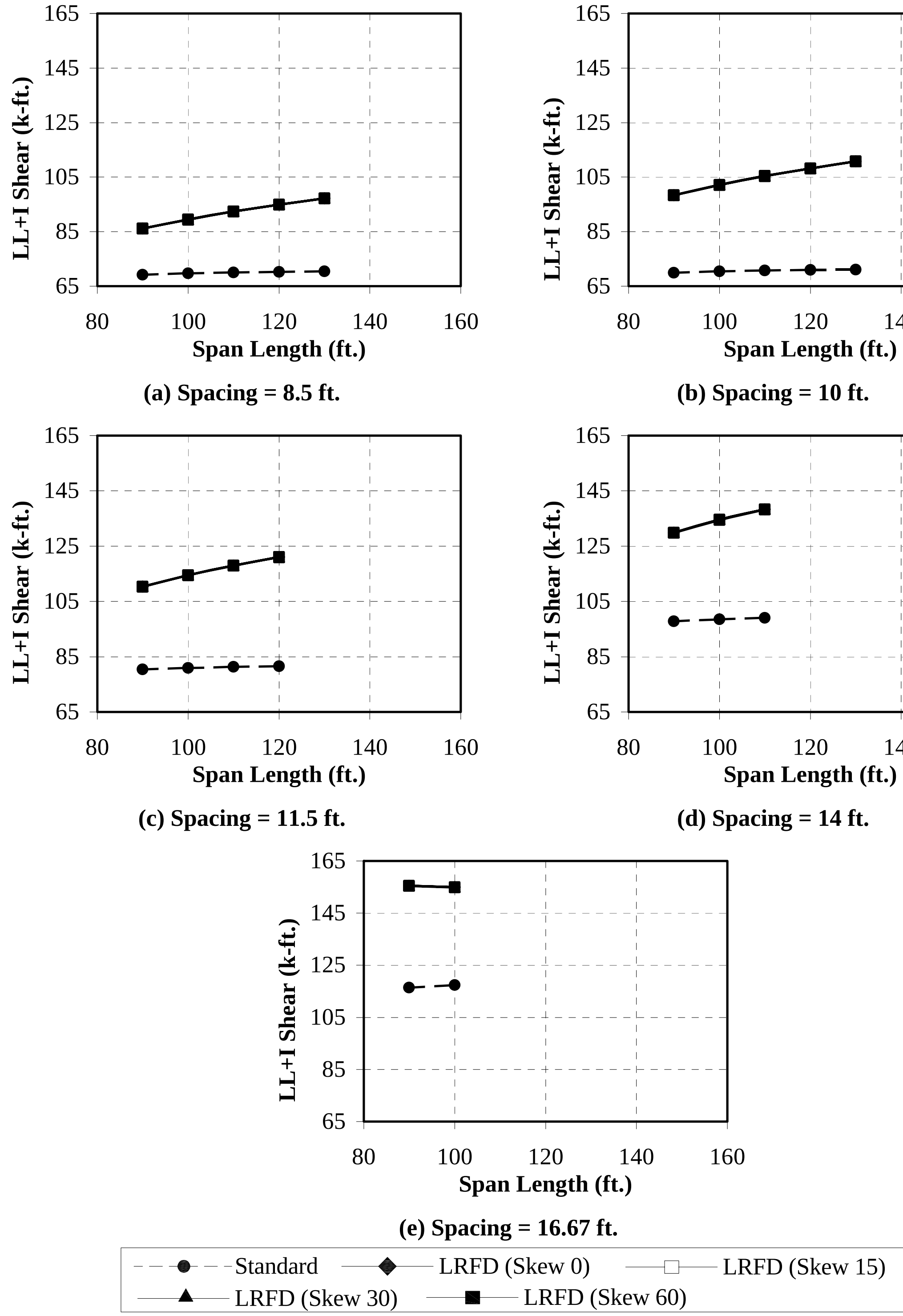

Figure 6.6. Distributed Live Load Shear Force at Critical Section (U54 Girder).

Table 6.6. Undistributed Dynamic Load Moment and Shear (U54 Girder).

Girder Spacing (ft.)	Shear		Moment	
	Difference (kips)	Difference (%)	Difference (kips)	Difference (%)
8.50	5.1 - 8.0	34.9 - 62.1	125.5 - 310.0	40.8 - 73.9
10.00				
11.50	5.2 - 7.4	35.6 - 55.6		
14.00	5.3 - 6.8	36.3 - 49.5		
16.67	5.3 - 6.1	36.6 - 43.1		

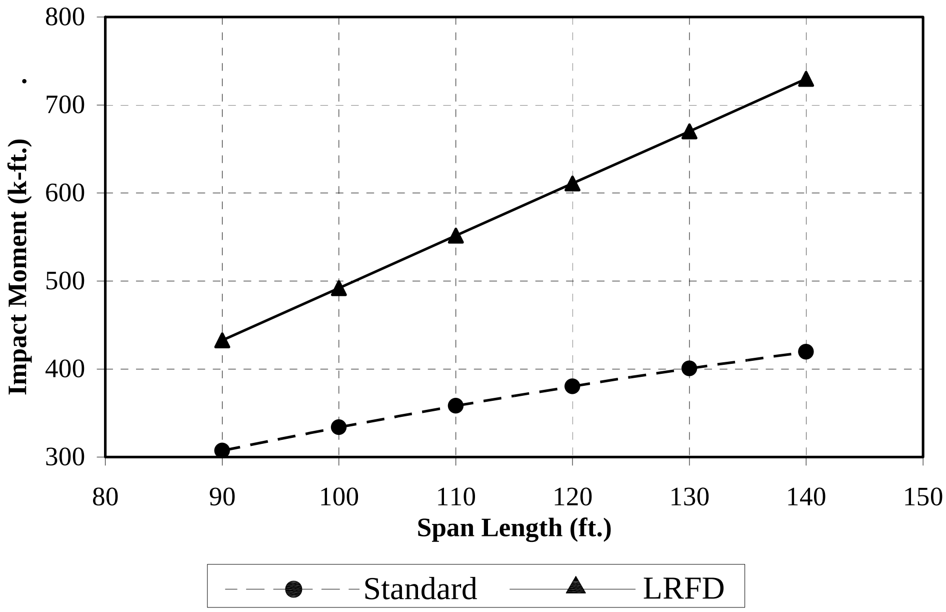

Figure 6.7. Undistributed Dynamic Load Moment at Midspan (U54 Girder).

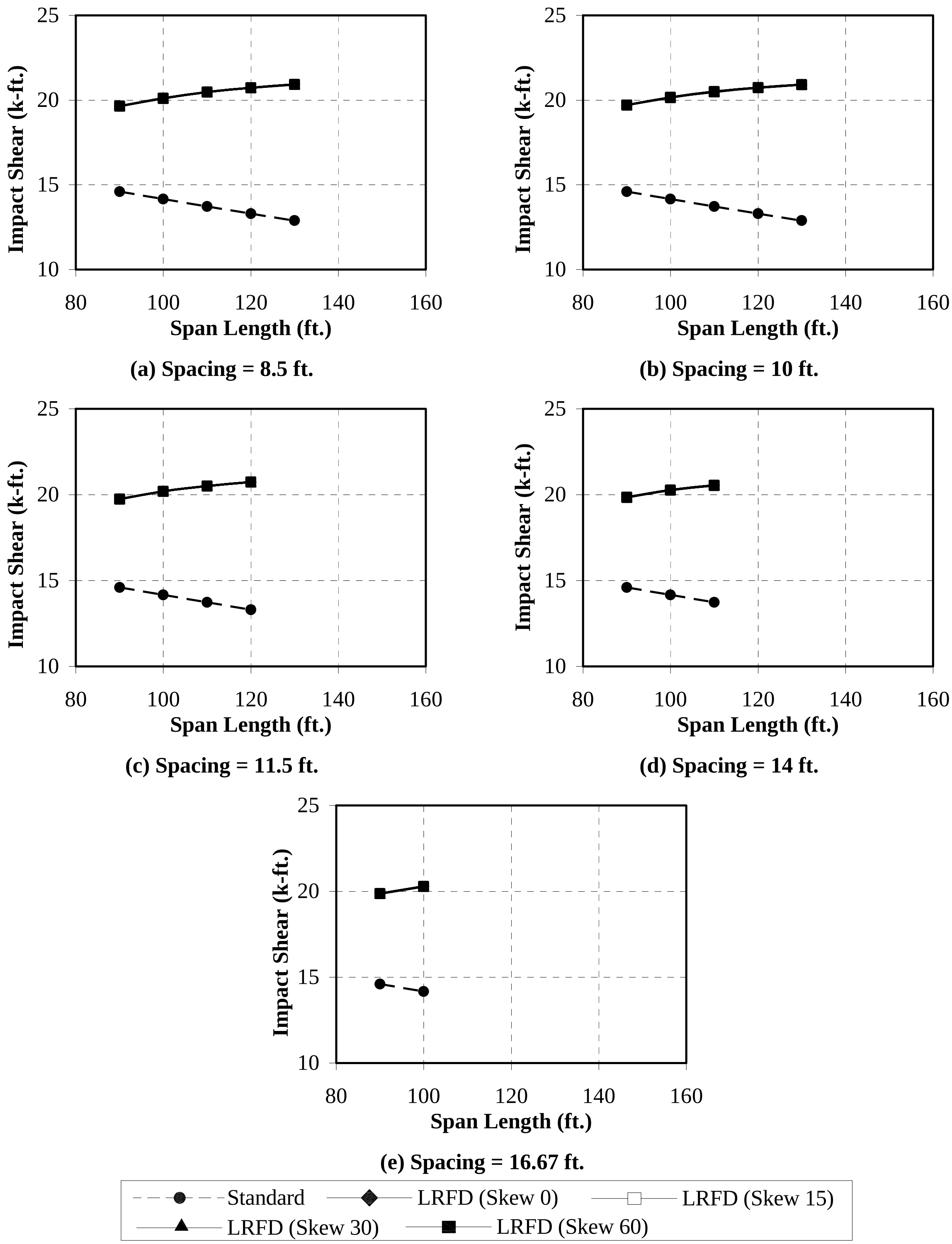

Figure 6.8. Undistributed Dynamic Load Shear Force at Critical Section (U54 Girder).

6.3 SERVICE LOAD DESIGN

6.3.1 General

The impact of the AASHTO LRFD Specifications on the service load design for flexure is discussed in this section. The effect on the maximum span length capability, required number of strands, initial and final prestress losses, and the required concrete strengths at service and at release is presented in graphical and tabular formats. In general, the LRFD designs achieved a longer span length with fewer strands, less prestress losses, and lower concrete strengths. A decrease in the live load moments and a different live load factor in the tension stress check at service help to explain this trend.

6.3.2 Maximum Span Lengths

Table 6.7 shows the overall comparison of maximum span lengths for the LRFD and Standard designs.

Table 6.7. Maximum Differences in Maximum Span Lengths – LRFD Designs Relative to Standard Designs (U54 Girder).

Girder Spacing (ft.)	Strand Diameter = 0.5 in.		Strand Diameter = 0.6 in.	
	Skew (degrees)		Skew (degrees)	
	0, 15, 30	60	0, 15, 30	60
8.5	1.5 - 3.5 ft.	10 ft.	2 - 4 ft.	10 ft.
	1.1 - 2.6%	7.4%	1.5 - 3%	7.4%
10.0	0.5 - 3 ft.	9 ft.	0 - 1.5 ft.	8.0 ft.
	0.4 - 2.3%	6.9%	0 - 1.2%	6.2%
11.5	1.5 - 3.5 ft.	10.0 ft.	0 - 2 ft.	9 ft.
	1.2 - 2.8%	8.1%	0 - 1.6%	7.3%
14.0	2.5 - 5 ft.	10.5 ft.	3.5 - 5 ft.	11.5 ft.
	2.2 - 4.4%	9.3%	3.1 - 4.5%	10.3%
16.67	4.5 - 6.5 ft.	12.5 ft.	7.5 - 11.5 ft.	18.5 ft.
	4.3 - 6.2%	12.0%	7.6 - 11.7%	18.8%

Tables 6.8 and 6.9 compare the maximum span lengths and required number of strands for the LRFD and the Standard designs, for 0.5 in. and 0.6 in. diameter strands, respectively. When a 0-degree skew is considered, it is observed that for an equal (or fewer, in some cases) number of strands the LRFD designs can span slightly longer, with an increase ranging from 1.5

to 7.5 ft. If the skew correction is taken into consideration and the comparison for maximum span length is made between the two specifications, then, based on Table 6.9 and Figure 6.9, it can be said that the overall increase in span capability ranges from 1.5 to 18.5 ft. (1.1 to 18.8 percent). The maximum span length increases with an increase in the skew.

Some of the maximum span lengths are greater than 140 ft., which is one of the limits for the use of the LRFD Specifications' live load distribution factor formulas. There are only two such cases, both for 8.5 ft. spacing and 60-degree skew, for strand diameters 0.5 and 0.6 in. For the purpose of the parametric study, this LRFD live load distribution factor limit is neglected and the distribution factor for moment and shear is calculated using the same formulas. The distribution factor for these two cases is checked by performing refined analysis (see Chapter 7).

Table 6.8. Comparison of Maximum Span Lengths (U54 Girder, Strand Diameter = 0.5 in.).

Skew (deg.)	Girder Spacing (ft.)	Standard		LRFD		Span Diff. ft. (%)
		Max. Span (ft.)	No. Strands	Max. Span (ft.)	No. Strands	
0	8.5	135.0	89	136.5	89	1.5 (1.1)
	10.0	130.0	87	130.5	89	0.5 (0.4)
	11.5	124.0	87	125.5	89	1.5 (1.2)
	14.0	113.0	87	115.5	87	2.5 (2.2)
	16.67	104.5	85	109.0	87	4.5 (4.3)
15	8.5	135.0	89	136.5	89	1.5 (1.1)
	10.0	130.0	87	131.0	89	1.0 (0.8)
	11.5	124.0	87	126.0	89	2.0 (1.6)
	14.0	113.0	87	116.0	87	3.0 (2.7)
	16.67	104.5	85	109.5	87	5.0 (4.8)
30	8.5	135.0	89	138.5	89	3.5 (2.6)
	10.0	130.0	87	133.0	91	3.0 (2.3)
	11.5	124.0	87	127.5	89	3.5 (2.8)
	14.0	113.0	87	118.0	89	5.0 (4.4)
	16.67	104.5	85	111.0	87	6.5 (6.2)
60	8.5	135.0	89	145.0	89	10.0 (7.4)
	10.0	130.0	87	139.0	89	9.0 (6.9)
	11.5	124.0	87	134.0	89	10.0 (8.1)
	14.0	113.0	87	123.5	87	10.5 (9.3)
	16.67	104.5	85	117.0	87	12.5 (12.0)

Table 6.9. Comparison of Maximum Span Lengths (U54 Girder, Strand Diameter = 0.6 in.)

Skew	Girder Spacing (ft.)	Standard		LRFD		Span Diff. ft. (%)
		Max. Span (ft.)	No. Strands	Max. Span (ft.)	No. Strands	
0	8.5	134.5	60	136.5	60	2.0 (1.5)
	10.0	130.0	60	130.0	60	0.0 (0.0)
	11.5	124.0	60	124.0	60	0.0 (0.0)
	14.0	112.0	58	115.5	60	3.5 (3.1)
	16.7	98.5	51	106.0	56	7.5 (7.6)
15	8.5	134.5	60	137.0	60	2.5 (1.9)
	10.0	130.0	60	130.0	60	0.0 (0.0)
	11.5	124.0	60	125.0	60	1.0 (0.8)
	14.0	112.0	58	116.0	60	4.0 (3.6)
	16.7	98.5	51	107.0	56	8.5 (8.6)
30	8.5	134.5	60	138.5	60	4.0 (3.0)
	10.0	130.0	60	131.5	60	1.5 (1.2)
	11.5	124.0	60	126.0	60	2.0 (1.6)
	14.0	112.0	58	117.0	60	5.0 (4.5)
	16.7	98.5	51	110.0	58	11.5 (11.7)
60	8.5	134.5	60	144.5	60	10.0 (7.4)
	10.0	130.0	60	138.0	60	8.0 (6.2)
	11.5	124.0	60	133.0	60	9.0 (7.3)
	14.0	112.0	58	123.5	60	11.5 (10.3)
	16.7	98.5	51	117.0	60	18.5 (18.8)

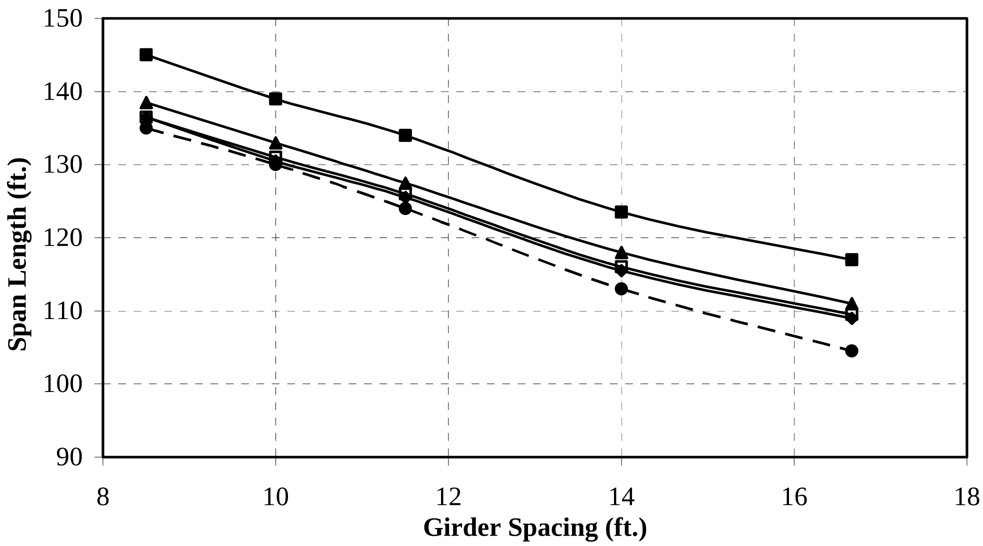

(a) Strand Diameter = 0.5 in.

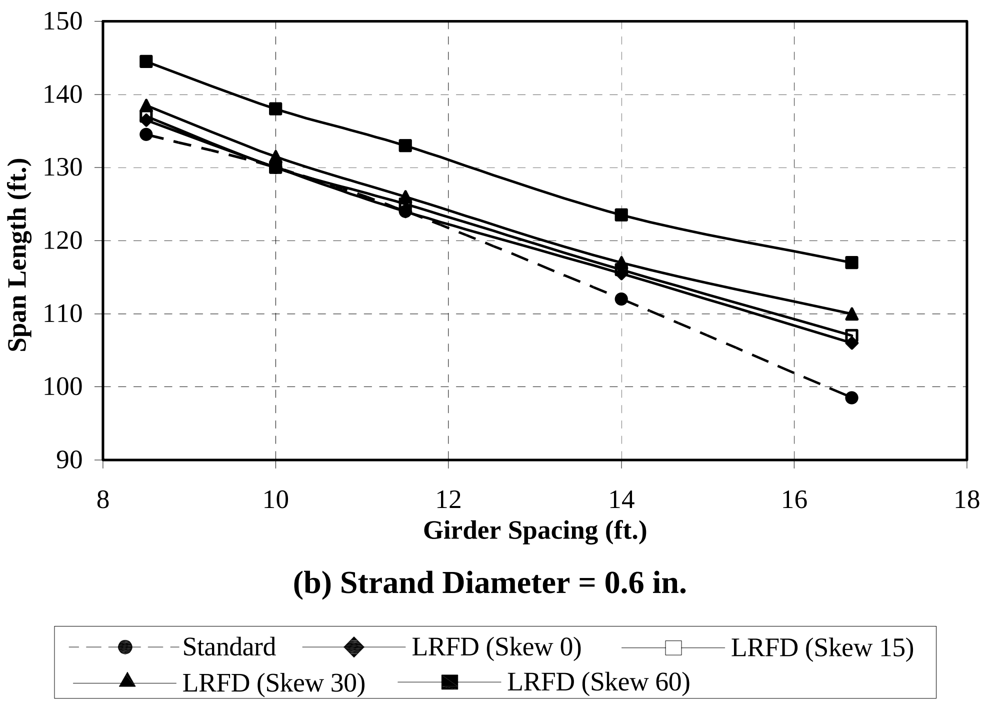

(b) Strand Diameter = 0.6 in.

Figure 6.9. Maximum Span Length versus Girder Spacing (U54 Girder).

6.3.3 Number of Strands

Tables 6.10 through 6.14 show the differences in the number of strands required for span lengths from 90 ft. to the maximum possible span lengths for the LRFD and Standard designs with 0.5 in. diameter strands. Similar tables are provided in Appendix A for 0.6 in. strand designs. The difference in the number of strands for maximum spans is not reported since the numbers for different spans are not directly comparable.

The general trend is that the LRFD designs required fewer strands than the Standard designs. The number of strands for LRFD designs decreases with an increase in spacing, span, or skew angle relative to the Standard designs. For the skew angles of 0, 15, and 30 degrees and for girder spacings less than or equal to 11.5 ft., the LRFD designs required between one to six fewer strands; and for girder spacings greater than 11.5 ft., the LRFD designs required between one to ten fewer strands. There is a significant drop in the number of strands required by the LRFD designs relative to those of the Standard designs for a 60-degree skew because the flexural demand reduces significantly in this case. For a 60-degree skew and for girder spacings less than or equal to 11.5 ft., the LRFD designs required between 4 to 14 fewer strands; and for girder spacings greater than 11.5 ft., the LRFD designs required between 12 to 18 fewer strands relative to the designs based on the Standard Specifications.

The effect of the 0.8 live load reduction factor included in the LRFD Service III limit state compared to the 1.0 live load reduction factor in the Standard Specifications should result in a reduction of strands required for the same load requirements. Although the LRFD Specifications provide for a heavier live load, the final distributed moment is less than that of the Standard Specifications, as explained in Section 6.2.4.

Table 6.10. Comparison of Number of Strands
(U54 Girder, Strand Diameter = 0.5 in., Girder Spacing = 8.5 ft.).

Skew	Standard		LRFD		Difference in No. of Strands
	Span Length (ft.)	No. of Strands	Span Length (ft.)	No. of Strands	
0	90	35	90	31	-4
	100	43	100	41	-2
	110	53	110	51	-2
	120	66	120	64	-2
	130	80	130	78	-2
	135	89	136.5	89	-
15	90	35	90	31	-4
	100	43	100	41	-2
	110	53	110	51	-2
	120	66	120	62	-4
	130	80	130	78	-2
	135	89	136.5	89	-
30	90	35	90	31	-4
	100	43	100	39	-4
	110	53	110	49	-4
	120	66	120	60	-6
	130	80	130	76	-4
	135	89	138.5	89	-
60	90	35	90	27	-8
	100	43	100	35	-8
	110	53	110	45	-8
	120	66	120	54	-12
	130	80	130	66	-14
	135	89	140	80	-
	-	-	145	89	-

Table 6.11. Comparison of Number of Strands (U54 Girder, Strand Diameter = 0.5 in., Girder Spacing = 10 ft.).

Skew	Standard		LRFD		Difference in No. of Strands
	Span Length (ft.)	No. of Strands	Span Length (ft.)	No. of Strands	
0	90	37	90	35	-2
	100	47	100	47	0
	110	58	110	58	0
	120	72	120	72	0
	130	87	130	87	0
	-	-	130.5	89	-
15	90	37	90	35	-2
	100	47	100	45	-2
	110	58	110	58	0
	120	72	120	70	-2
	130	87	130	87	0
	-	-	131	89	-
30	90	37	90	35	-2
	100	47	100	45	-2
	110	58	110	56	-2
	120	72	120	68	-4
	130	87	130	85	-2
	-	-	133	91	-
60	90	37	90	31	-6
	100	47	100	39	-8
	110	58	110	49	-9
	120	72	120	60	-12
	130	87	130	74	-13
	-	-	139	89	-

Table 6.12. Comparison of Number of Strands
(U54 Girder, Strand Diameter = 0.5 in., Girder Spacing = 11.5 ft.).

Skew	Standard		LRFD		Difference in No. of Strands
	Span Length (ft.)	No. of Strands	Span Length (ft.)	No. of Strands	
0	90	41	90	39	-2
	100	53	100	51	-2
	110	66	110	64	-2
	120	80	120	78	-2
	124	87	125.5	89	-
15	90	41	90	39	-2
	100	53	100	51	-2
	110	66	110	62	-4
	120	80	120	78	-2
	124	87	126	89	-
30	90	41	90	37	-4
	100	53	100	49	-4
	110	66	110	60	-6
	120	80	120	76	-4
	124	87	127.5	89	-
60	90	41	90	33	-8
	100	53	100	43	-10
	110	66	110	53	-13
	120	80	120	66	-14
	124	87	130	83	-4
	-	-	134	89	-

Table 6.13. Comparison of Number of Strands
(U54 Girder, Strand Diameter = 0.5 in., Girder Spacing = 14 ft.).

Skew	Standard		LRFD		Difference in No. of Strands
	Span Length (ft.)	No. of Strands	Span Length (ft.)	No. of Strands	
0	90	51	90	51	0
	100	64	100	60	-4
	110	81	110	76	-5
	113	87	115.5	87	-
15	90	51	90	49	-2
	100	64	100	60	-4
	110	81	110	76	-5
	113	87	116	87	-
30	90	51	90	45	-6
	100	64	100	58	-6
	110	81	110	74	-7
	113	87	118	89	-
60	90	51	90	39	-12
	100	64	100	51	-13
	110	81	110	64	-17
	113	87	120	81	-
	-	-	123.5	87	-

Table 6.14. Comparison of Number of Strands
(U54 Girder, Strand Diameter = 0.5 in., Girder Spacing = 16.67 ft.).

Skew	Standard		LRFD		Difference in No. of Strands
	Span Length (ft.)	No. of Strands	Span Length (ft.)	No. of Strands	
0	100	76	100	70	-6
	104.5	85	109	87	-
15	100	76	100	68	-8
	104.5	85	109.5	87	-
30	100	76	100	66	-10
	104.5	85	110	85	-
	-	-	111	87	-
60	100	76	100	58	-18
	104.5	85	110	74	-
	-	-	117	87	-

6.3.4 Concrete Strengths Required at Release and at Service

6.3.4.1 Concrete Strength at Release

Table 6.15 and Figure 6.10 compare required concrete strengths at release (f'_{ci}) for all the design cases considered in this study with 0.5 in. diameter strands. The comparison for 0.6 in. diameter strands is similar and can be found in Appendix A. In general, the U54 girder designs based on the Standard Specifications give a larger required f'_{ci} as compared to those based on the LRFD Specifications. This difference increases with increasing skew, as shown in Figure 6.10. For the 0-, 15-, and 30-degree skews, the difference in f'_{ci} decreases from 0 to 842 psi (0 to 14 percent) and for a 60-degree skew, the difference in f'_{ci} decreases from 0 to 1480 psi (0 to 24.6 percent).

Table 6.15. Comparison of Initial Concrete Strength (U54 Girder, Strand Diameter = 0.5 in.).

Spacing (ft.)	Span (ft.)	STD f'_{ci} (psi)	LRFD							
			Skew = 0		Skew = 15		Skew = 30		Skew = 60	
			f'_{ci} (psi)	% Diff.	f'_{ci} (psi)	% Diff.	f'_{ci} (psi)	% Diff.	f'_{ci} (psi)	% Diff.
8.50	90	4000	4000	0.0	4000	0.0	4000	0.0	4000	0.0
	100	4000	4000	0.0	4000	0.0	4000	0.0	4000	0.0
	110	4080	4000	-2.0	4000	-2.0	4000	-2.0	4000	-2.0
	120	5072	4879	-3.8	4719	-7.0	4559	-10.1	4077	-19.6
	130	6132	5929	-3.3	5929	-3.3	5771	-5.9	4977	-18.8
10.00	90	4000	4000	0.0	4000	0.0	4000	0.0	4000	0.0
	100	4000	4000	0.0	4000	0.0	4000	0.0	4000	0.0
	110	4491	4464	-0.6	4464	-0.6	4303	-4.2	4000	-10.9
	120	5555	5514	-0.7	5356	-3.6	5197	-6.4	4559	-17.9
	130	6653	6598	-0.8	6598	-0.8	6460	-2.9	5613	-15.6
11.50	90	4000	4000	0.0	4000	0.0	4000	0.0	4000	0.0
	100	4152	4000	-3.7	4000	-3.7	4000	-3.7	4000	-3.7
	110	5140	4944	-3.8	4784	-6.9	4624	-10.0	4058	-21.1
	120	6196	5988	-3.4	5988	-3.4	5830	-5.9	5038	-18.7
14.00	90	4055	4029	-0.6	4000	-1.4	4000	-1.4	4000	-1.4
	100	5050	4693	-7.1	4693	-7.1	4533	-10.2	4000	-20.8
	110	6342	5894	-7.1	5894	-7.1	5736	-9.6	4943	-22.1
16.67	90	4498	4200	-6.6	4200	-6.6	4029	-10.4	4000	-11.1
	100	6013	5488	-8.7	5329	-11.4	5171	-14.0	4533	-24.6

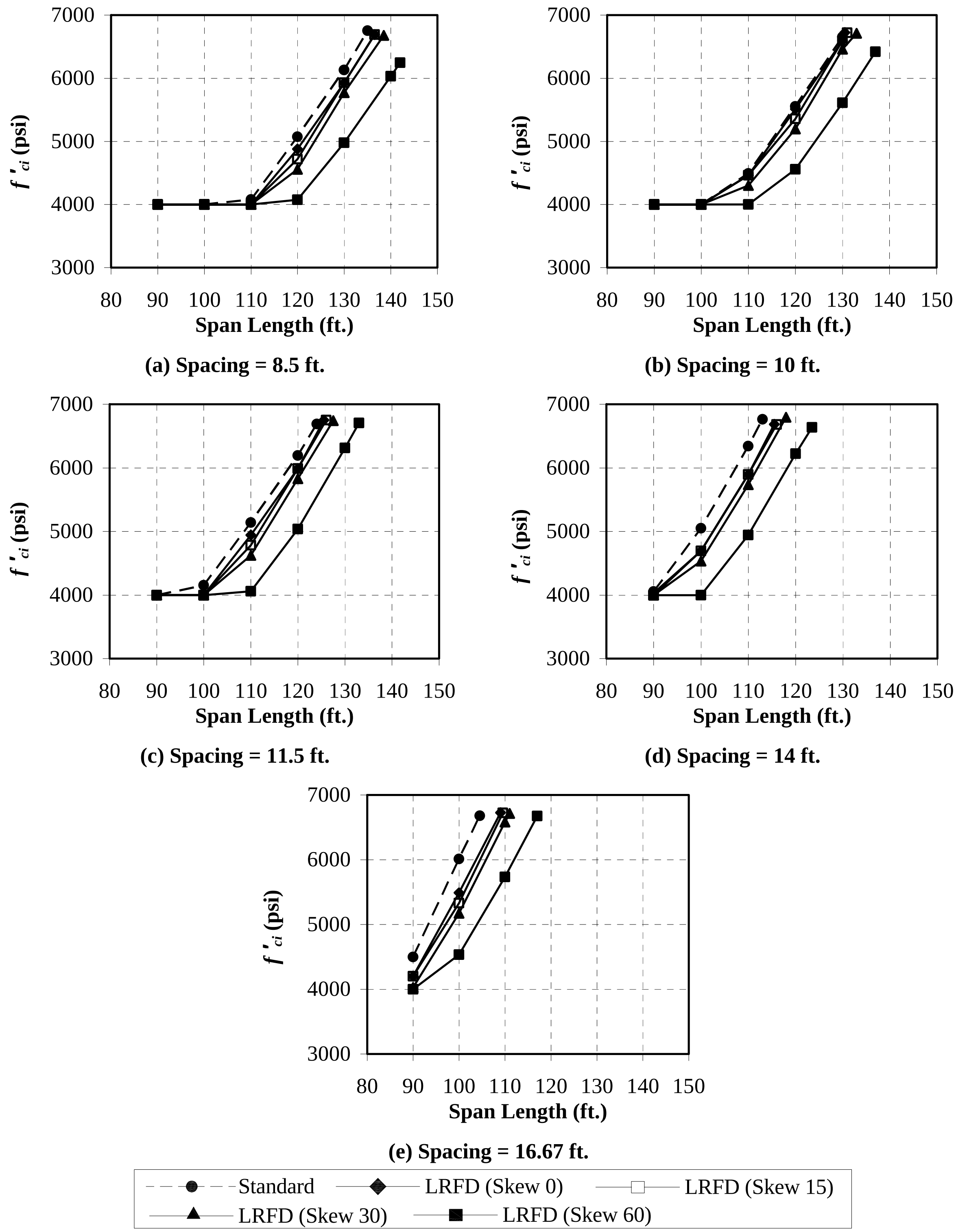

Figure 6.10. Comparison of Required Concrete Release Strength (U54 Girder, Strand Diameter = 0.5 in.).

6.3.4.2 *Concrete Strength at Service*

Table 6.16 and Figure 6.11 compare the concrete strength at service (f'_c), required for all design cases with a strand diameter of 0.5 in. The trends were the same for the cases using 0.6 in. strands, and details can be found in Appendix A. In general, the designs based on the Standard Specifications have a larger required f'_c as compared to those based on the LRFD Specifications. In addition, the skew angle does not affect the f'_c value significantly, as shown in Figure 6.11. For skew angles of 0, 15, and 30 degrees, the difference in f'_c decreases between 0 to 928 ksi (0 to 10.8 percent); and for a 60-degree skew, the difference in f'_c decreases between 0 to 837 ksi (0 to 9.8 percent).

Table 6.16. Comparison of Required Concrete Strength at Service (U54 Girder, Strand Diameter = 0.5 in.).

Spacing (ft.)	Span (ft.)	STD f'_c (psi)	LRFD							
			Skew = 0		Skew = 15		Skew = 30		Skew = 60	
			f'_c (psi)	% Diff.	f'_c (psi)	% Diff.	f'_c (psi)	% Diff.	f'_c (psi)	% Diff.
8.50	90	5000	5000	0.0	5000	0.0	5000	0.0	5000	0.0
	100	5000	5000	0.0	5000	0.0	5000	0.0	5000	0.0
	110	5431	5000	-7.9	5000	-7.9	5000	-7.9	5000	-7.9
	120	6598	5919	-10.3	5945	-9.9	5970	-9.5	6049	-8.3
	130	7893	7129	-9.7	7129	-9.7	7151	-9.4	7211	-8.6
10.00	90	5000	5000	0.0	5000	0.0	5000	0.0	5000	0.0
	100	5000	5000	0.0	5000	0.0	5000	0.0	5000	0.0
	110	5852	5231	-10.6	5231	-10.6	5257	-10.2	5391	-7.9
	120	7117	6358	-10.7	6381	-10.3	6405	-10.0	6505	-8.6
	130	8580	7660	-10.7	7660	-10.7	7652	-10.8	7743	-9.8
11.50	90	5000	5000	0.0	5000	0.0	5000	0.0	5000	0.0
	100	5000	5000	0.0	5000	0.0	5000	0.0	5000	0.0
	110	6223	5586	-10.2	5611	-9.8	5636	-9.4	5736	-7.8
	120	7593	6804	-10.4	6804	-10.4	6826	-10.1	6944	-8.5
14.00	90	5000	5000	0.0	5000	0.0	5000	0.0	5000	0.0
	100	5560	5022	-9.7	5022	-9.7	5047	-9.2	5165	-7.1
	110	6916	6233	-9.9	6233	-9.9	6255	-9.6	6374	-7.8
16.67	90	5000	5000	0.0	5000	0.0	5000	0.0	5000	0.0
	100	6119	5537	-9.5	5560	-9.1	5584	-8.7	5684	-7.1

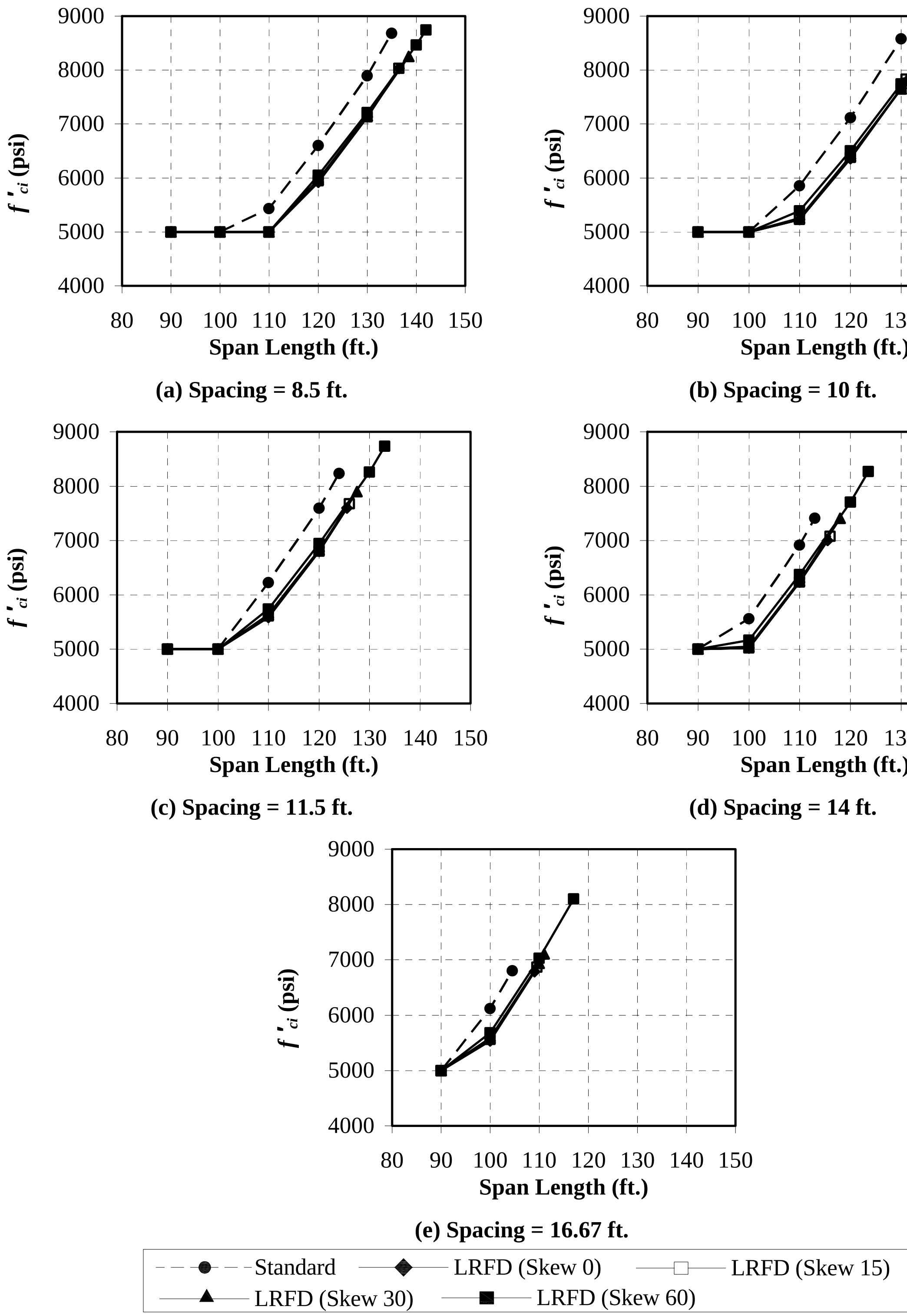

Figure 6.11. Comparison of Required Concrete Strength at Service (U54 Girder, Strand Diameter = 0.5 in.).

6.3.5 Initial and Final Prestress Losses

The loss in prestress occurs mainly from four sources: elastic shortening and relaxation of the prestressing, and creep and shrinkage of concrete. These losses are categorized into initial prestress loss and final prestress loss. The initial prestress loss occurs due to initial relaxation of steel and elastic shortening of prestressing strands. The final loss occurs due to final steel relaxation and creep and shrinkage of concrete.

6.3.5.1 Prestress Loss due to Elastic Shortening of Concrete

The loss of prestress due to elastic shortening is dependent on the elastic modulus of the prestressing strands, the elastic modulus of the concrete at release, and the total prestressing force at release. The modulus of elasticity of the prestressing strands is specified by the Standard Specifications as 28,000 ksi, while the LRFD Specifications specify this value to be 28,500 ksi. The elastic modulus of the concrete at release depends on the concrete strength at release based on the prediction formulas given in the specifications. As discussed in Section 6.3.4.1, the LRFD Specifications give a lower estimate of the concrete strength at release for the U54 girders considered in the parametric study.

A comparison of predicted elastic shortening losses for 0.5 in. diameter strands is presented in Table 6.17. A similar comparison for 0.6 in. diameter strands is presented in Appendix A. In general, relative to the designs based on the Standard Specifications, the elastic shortening loss decreases in the LRFD designs. For skew angles of 0, 15, and 30 degrees, the difference in the initial losses vary in the range of 0.2 to -1.3 ksi (1.3 to -13.3 percent) and for a 60-degree skew, the difference in the elastic shortening losses decrease from -1.5 to -2.5 ksi (-9.9 to -29.7 percent) relative to the Standard Specifications. These differences can be attributed to the combined effect of all the parameters discussed above. The effect of lower concrete strengths (reduced concrete modulus of elasticity) and a higher value of modulus of elasticity for prestressing strands provided in the LRFD Specifications should result in higher ES losses. On the contrary, the LRFD designs for the U54 girders tend to have fewer prestressing strands, which reduces the stress in the concrete and leads to lower ES losses.

Table 6.17. Comparison of Elastic Shortening Loss (U54 Girder, Strand Diameter = 0.5 in.).

Spacing (ft.)	Span (ft.)	STD ES (ksi)	LRFD							
			Skew = 0		Skew = 15		Skew = 30		Skew = 60	
			ES (ksi)	% Diff.	ES (ksi)	% Diff.	ES (ksi)	% Diff.	ES (ksi)	% Diff.
8.5	90	8.3	7.7	-7.3	7.7	-7.3	7.7	-7.3	5.9	-29.7
	100	10.8	10.2	-5.2	10.2	-5.2	9.5	-11.8	8.1	-25.0
	110	13.1	12.5	-4.8	12.5	-4.8	12.5	-4.8	10.4	-20.5
	120	14.2	14.0	-1.2	14.0	-1.2	13.7	-3.7	12.1	-14.6
	130	15.4	15.3	-0.8	14.9	-2.9	14.6	-5.0	13.2	-14.0
10	90	9.8	9.2	-5.9	9.2	-5.9	8.5	-13.3	7.7	-20.7
	100	12.1	11.6	-4.5	11.6	-4.5	11.6	-4.5	9.5	-21.7
	110	13.8	14.0	1.3	14.0	1.3	13.6	-1.3	11.8	-14.7
	120	15.1	15.3	1.2	15.0	-0.9	14.7	-3.0	13.7	-9.9
	130	16.3	16.5	1.2	16.5	1.2	16.0	-2.0	14.6	-10.4
11.5	90	11.2	10.6	-5.0	10.6	-5.0	9.9	-11.3	8.5	-24.1
	100	13.9	13.6	-2.1	13.0	-6.9	13.0	-6.9	10.9	-21.7
	110	15.2	15.0	-0.9	15.0	-0.9	14.7	-3.0	13.1	-13.8
	120	16.3	16.3	-0.6	16.3	-0.6	16.0	-2.4	14.4	-12.2
14	90	13.9	13.3	-3.7	13.3	-3.7	12.7	-8.6	10.6	-23.6
	100	15.7	15.3	-2.7	15.3	-2.7	15.0	-4.8	13.6	-13.4
	110	17.2	16.9	-2.0	16.9	-2.0	16.6	-3.7	15.0	-12.7
16.67	90	15.6	15.0	-4.1	15.0	-4.1	14.6	-6.4	12.7	-19.1
	100	17.5	16.8	-3.6	16.5	-5.2	16.2	-6.9	15.0	-14.2

6.3.5.2 Prestress Loss due to Initial Steel Relaxation

The loss in prestress due to the initial relaxation of steel is specified by the LRFD Specifications to be a function of time, jacking stress, and the yield stress of the prestressing strands. The time for release of prestress is taken as 12 hours in this study. This provides a constant estimate of initial steel relaxation loss of 1.975 ksi for the LRFD designs and is not affected by skew, strand diameter, or span length, as can be observed in Table 6.18. The Standard Specifications do not specify a particular formula to evaluate the initial relaxation loss. Based on the TxDOT Bridge Design Manual (TxDOT 2001) recommendation, the initial relaxation loss is taken as half of the total estimated relaxation loss. A comparison of predicted initial relaxation losses (IRL) for 0.5 in. diameter strands is presented in Table 6.18. A similar comparison for 0.6 in. diameter strands is presented in Appendix A.

Table 6.18. Comparison of Initial Relaxation Loss (U54 Girder, Strand Diameter = 0.5 in.).

Spacing (ft.)	Span (ft.)	STD IRL (ksi)	LRFD IRL (ksi)	% Diff.
8.5	90	1.65	1.97	19.3
	100	1.46	1.97	35.4
	110	1.26	1.97	56.5
	120	1.13	1.97	75.2
	130	0.97	1.97	104
	135	0.87	1.97	127
10	90	1.54	1.97	28.0
	100	1.35	1.97	45.9
	110	1.20	1.97	65.0
	120	1.03	1.97	92.0
	130	0.87	1.97	127
11.5	90	1.43	1.97	38.1
	100	1.20	1.97	64.8
	110	1.04	1.97	89.3
	120	0.89	1.97	122
	124	0.81	1.97	143
14	90	1.22	1.97	62.3
	100	1.00	1.97	97.0
	110	0.81	1.97	144
	113	0.72	1.97	173
16.67	90	1.03	1.97	92.0
	100	0.79	1.97	150
	104.5	0.68	1.97	191

While the percentage differences for the initial relaxation losses are significant, the magnitudes are only slightly more than 1.0 ksi. It was observed that the prestress loss due to initial steel relaxation for the LRFD designs were larger than for the Standard designs. For the designs based on the LRFD Specifications, the difference in the relaxation losses ranged from 0.32 to 1.3 ksi (19.3 to 191 percent) relative to the Standard designs.

6.3.5.3 Initial Prestress Loss

Table 6.19 and Figure 6.12 compare the initial prestress losses determined for all design cases with a strand diameter of 0.5 in. The comparison for the design cases with 0.6 in. strands shows similar trends and details can be found in Appendix A. Considering skew angles of 0, 15, and 30 degrees, the designs based on the Standard Specifications generally give a slightly lower estimate of initial losses as compared to those based on the LRFD Specifications. For the 60-degree skew, this difference is more significant, as shown in Figure 6.12. For skew angles of 0, 15, and 30 degrees, the difference in the initial losses vary from 7.7 to -12.5 percent; and for a 60-degree skew, the difference in the initial losses decrease -7.0 to -22.6 percent relative to the Standard Specifications.

Table 6.19. Comparison of Initial Prestress Loss (U54 Girder, Strand Diameter = 0.5 in.).

Spacing (ft.)	Span (ft.)	STD Init. Loss (ksi)	LRFD							
			Skew = 0		Skew = 15		Skew = 30		Skew = 60	
			Init. Loss (ksi)	% Diff.	Init. Loss (ksi)	% Diff.	Init. Loss (ksi)	% Diff.	Init. Loss (ksi)	% Diff.
8.50	90	10.6	9.7	-8.7	9.7	-8.7	9.7	-8.7	8.2	-22.6
	100	12.2	12.2	-0.2	12.2	-0.2	11.5	-6.0	10.1	-17.8
	110	14.2	14.4	1.9	14.4	1.9	13.8	-2.9	12.4	-12.5
	120	15.3	16.0	4.4	15.6	2.1	15.3	-0.3	14.1	-8.0
	130	16.4	17.3	5.4	17.3	5.4	16.9	3.4	15.2	-7.0
10.00	90	11.5	12.1	5.2	12.1	5.2	11.0	-4.2	9.9	-14.0
	100	13.7	14.5	5.7	14.5	5.7	13.5	-1.4	11.5	-15.9
	110	15.3	16.3	6.5	16.3	6.5	15.7	2.8	14.2	-6.8
	120	16.2	17.3	7.0	17.3	7.0	16.8	3.9	15.7	-2.8
	130	17.4	18.8	7.7	18.8	7.7	18.3	5.4	16.7	-3.9
11.50	90	12.6	12.6	0.0	12.6	0.0	11.9	-5.5	10.4	-17.0
	100	15.1	15.6	3.2	15.6	3.2	14.9	-1.4	12.9	-14.8
	110	16.2	17.0	5.0	16.7	2.9	16.3	0.8	15.0	-7.3
	120	17.2	18.2	5.9	18.2	5.9	17.9	4.2	16.3	-5.1
14.00	90	15.6	16.6	6.5	16.0	2.5	16.0	2.5	12.6	-19.4
	100	16.7	17.3	3.4	17.3	3.4	14.6	-12.5	15.6	-6.7
	110	18.1	18.9	3.9	18.9	3.9	18.6	2.3	17.0	-6.2
16.67	90	17.5	17.0	-2.9	17.0	-2.9	16.6	-5.1	14.6	-16.6
	100	18.3	18.8	3.2	18.5	1.6	18.2	-0.1	17.0	-7.0

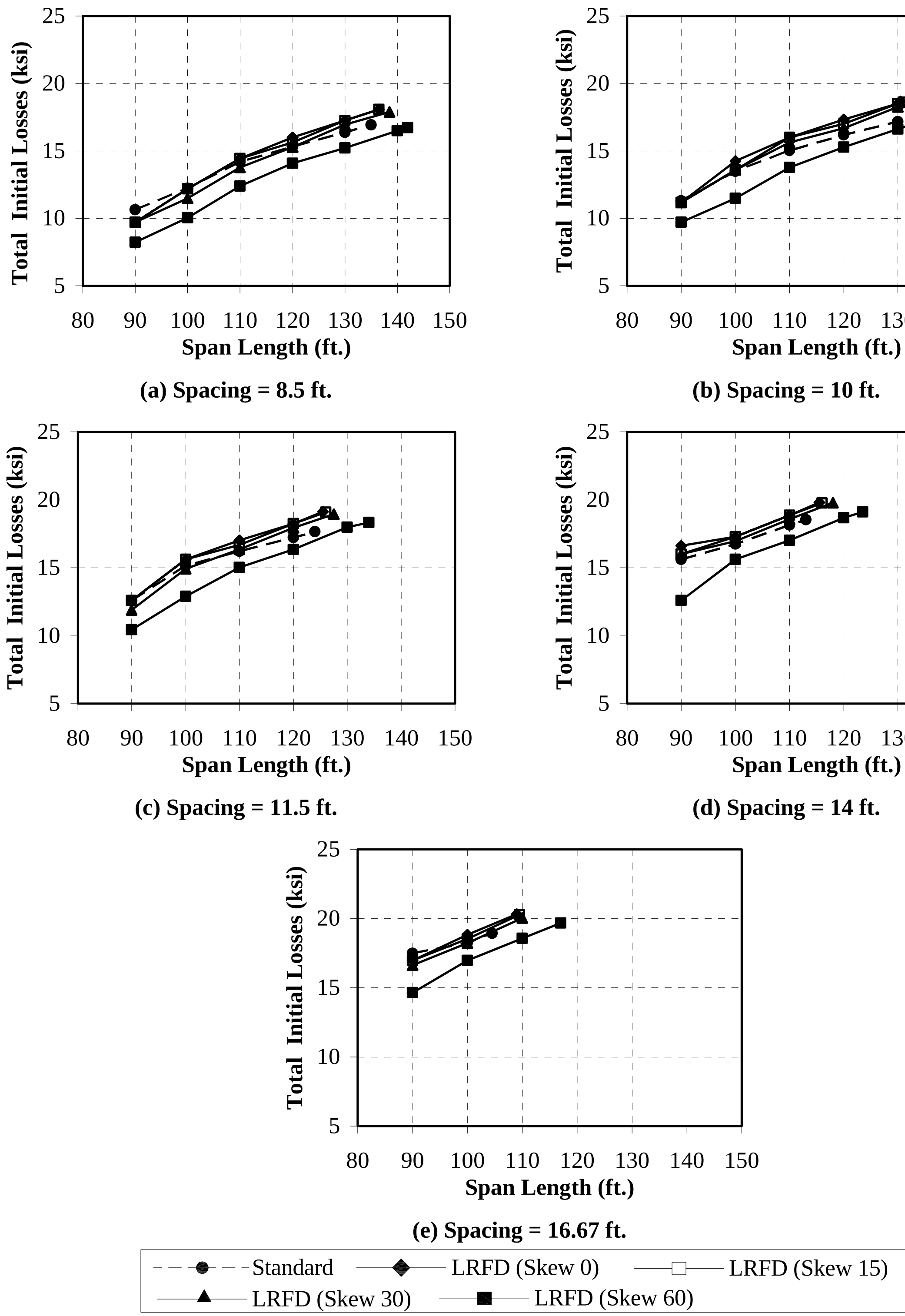

Figure 6.12. Comparison of Initial Prestress Loss (U54 Girder, Strand Diameter = 0.5 in.).

6.3.5.4 *Total Prestress Loss Due to Steel Relaxation*

The total prestress loss due to steel relaxation (CRs) is due to both the initial relaxation and final relaxation of the prestressing steel. The Standard and LRFD Specifications specify empirical formulas to estimate the loss due to steel relaxation at service. The formulas given in the two specifications are similar in form with only a slight difference in the coefficients. The steel relaxation depends upon the effects due to elastic shortening, creep of concrete, and shrinkage. Table 6.20 provides a comparison of estimated prestress loss due to steel relaxation for all U54 girder designs using 0.5 in. diameter strands. For U54 girders with a strand diameter of 0.6 in., a detailed comparison of each design case is included in Appendix A.

The estimate of prestress loss due to steel relaxation at service provided by the LRFD Specifications is larger as compared to the Standard Specifications, although the maximum difference is less than 2.0 ksi. For 0.5 in. diameter strands and skew angles of 0, 15, and 30 degrees, the percent increase for LRFD designs is less than 1.0 ksi. For 0.5 in. diameter strands and a skew angle of 60 degrees, the percent increase for the designs based on the LRFD Specifications is slightly greater (up to 1.2 ksi).

6.3.5.5 *Prestress Loss Due to Shrinkage of Concrete*

The LRFD and Standard Specifications prescribe the loss of prestress due to shrinkage of concrete as a function of relative humidity. For a relative humidity of 60 percent, the prestress loss due to shrinkage was found to be 8 ksi for both the Standard and LRFD Specifications for all the cases.

Table 6.20. Comparison of Steel Relaxation Loss (U54 Girder, Strand Diameter = 0.5 in.).

Spacing (ft.)	Span (ft.)	STD CRs (ksi)	LRFD							
			Skew = 0		Skew = 15		Skew = 30		Skew = 60	
			CRs (ksi)	% Diff.	CRs (ksi)	% Diff.	CRs (ksi)	% Diff.	CRs (ksi)	% Diff.
8.50	90	3.31	4.12	24.5	4.12	24.5	4.12	24.5	4.53	36.8
	100	2.92	3.64	24.9	3.64	24.9	3.80	30.1	4.11	40.9
	110	2.52	3.21	27.4	3.21	27.4	3.21	27.4	3.66	45.1
	120	2.25	2.80	24.3	2.80	24.3	2.91	29.0	3.35	48.8
	130	1.93	2.42	24.9	2.52	30.1	2.62	35.4	3.04	57.1
10.00	90	3.09	3.85	24.7	3.85	24.7	4.00	29.8	4.16	34.9
	100	2.71	3.39	25.2	3.39	25.2	3.39	25.2	3.85	42.0
	110	2.39	2.86	19.5	2.86	19.5	2.97	24.1	3.42	43.1
	120	2.06	2.46	19.7	2.56	24.6	2.66	29.6	2.98	44.9
	130	1.74	2.08	19.9	2.08	19.9	2.26	30.0	2.70	55.5
11.50	90	2.86	3.57	24.9	3.57	24.9	3.73	30.3	4.04	41.2
	100	2.40	2.99	24.7	3.13	30.8	3.13	30.8	3.58	49.6
	110	2.09	2.60	24.5	2.60	24.5	2.70	29.4	3.19	52.9
	120	1.78	2.22	25.2	2.22	25.2	2.32	30.7	2.83	59.3
14.00	90	2.43	3.06	25.6	3.06	25.6	3.21	31.7	3.66	50.3
	100	2.01	2.60	29.6	2.60	29.6	2.70	34.7	3.09	54.3
	110	1.62	2.13	31.5	2.13	31.5	2.22	37.5	2.72	68.3
16.67	90	2.06	2.72	32.2	2.72	32.2	2.83	37.7	3.27	58.9
	100	1.58	2.18	37.7	2.27	43.9	2.37	50.1	2.78	75.8

6.3.5.6 Prestress Loss Due to Creep of Concrete

The Standard and LRFD Specifications specify similar expressions for estimating the prestress loss due to creep of concrete. The loss due to creep depends on the concrete stress at the center of gravity (c.g.) of the prestressing strands due to dead loads before and after prestressing. Table 6.21 provides a comparison of estimated prestress loss due to creep of concrete for designs using 0.5 in. diameter strands in the parametric study. For designs using a strand diameter of 0.6 in., the detailed comparison of each design case is included in Appendix A.

Table 6.21. Comparison of Creep Loss (U54 Girder, Strand Diameter = 0.5 in.).

Spacing (ft.)	Span (ft.)	STD CRc (ksi)	LRFD							
			Skew = 0		Skew = 15		Skew = 30		Skew = 60	
			CRc (ksi)	% Diff.	CRc (ksi)	% Diff.	CRc (ksi)	% Diff.	CRc (ksi)	% Diff.
8.50	90	9.11	7.87	-13.6	7.87	-13.6	7.87	-13.6	4.79	-47.5
	100	12.13	10.90	-10.2	10.90	-10.2	9.74	-19.7	7.39	-39.1
	110	15.33	13.48	-12.0	13.48	-12.0	13.48	-12.0	10.11	-34.0
	120	18.56	17.28	-6.9	17.28	-6.9	16.21	-12.6	11.87	-36.1
	130	22.53	21.19	-5.9	20.15	-10.5	19.11	-15.2	14.87	-34.0
10.00	90	10.78	9.54	-11.5	9.54	-11.5	8.36	-22.4	7.16	-33.5
	100	13.56	12.32	-9.2	12.32	-9.2	12.32	-9.2	8.88	-34.5
	110	16.49	16.30	-1.1	16.30	-1.1	15.23	-7.6	11.34	-31.2
	120	20.57	20.31	-1.3	19.26	-6.4	18.21	-11.5	15.01	-27.0
	130	24.60	24.25	-1.4	24.25	-1.4	22.35	-9.1	17.72	-28.0
11.50	90	12.51	11.27	-9.9	11.27	-9.9	10.12	-19.1	7.76	-37.9
	100	16.23	14.93	-8.0	13.83	-14.8	13.83	-14.8	10.46	-35.5
	110	19.94	18.64	-6.5	18.64	-6.5	17.59	-11.8	12.70	-36.3
	120	23.78	22.43	-5.7	22.43	-5.7	21.39	-10.0	16.14	-32.1
14.00	90	15.59	14.34	-8.0	14.34	-8.0	13.23	-15.2	9.82	-37.0
	100	20.42	18.07	-11.5	18.07	-11.5	17.01	-16.7	13.16	-35.5
	110	25.21	22.81	-9.5	22.81	-9.5	21.78	-13.6	16.54	-34.4
16.67	90	19.55	16.65	-14.8	16.65	-14.8	15.51	-20.6	12.19	-37.6
	100	25.48	22.06	-13.4	21.02	-17.5	19.98	-21.6	15.75	-38.2

The estimate of prestress loss due to creep of concrete provided by the LRFD Specifications is found to be smaller as compared to the Standard Specifications. For 0.5 in. diameter strands and skew angles of 0, 15, and 30 degrees, the decrease for the designs based on the LRFD Specifications is in the range of 0.18 to 5.5 ksi. For 0.5 in. diameter strands and a skew angle of 60 degrees, the decrease for the designs based on the LRFD Specifications is in the range of 3.62 to 9.74 ksi. This difference increases with increasing skew angle, span length, and girder spacing.

6.3.5.7 Final Prestress Loss

Table 6.22 and Figure 6.13 summarize the comparison of final prestress losses for all U54 girder designs with 0.5 in. strands. For 0.6 in. strands, a detailed comparison of each design case along with figures is included in Appendix A. Except for 14 ft. and 16.67 ft. spacings, for the skew angles of 0 and 15 degrees, the designs based on the Standard Specifications give a slightly lower estimate of final losses as compared to those based on the LRFD Specifications. The difference increases with increasing skew, as shown in Figure 6.13. For 0-, 15-, and 30-degree skews, the difference in the final losses vary in the range of -3.9 to 2.5 ksi (-7.5 to 6.9 percent); and for a 60-degree skew, the difference in the final losses decreases from -2.6 to -9.0 ksi (-8.2 to -17.9 percent) relative to the Standard designs.

Table 6.22. Comparison of Final Prestress Loss (U54 Girder, Strand Diameter = 0.5 in.).

Spacing (ft.)	Span (ft.)	STD Tot. Loss (ksi)	LRFD							
			Skew = 0		Skew = 15		Skew = 30		Skew = 60	
			Tot. Loss (ksi)	% Diff.	Tot. Loss (ksi)	% Diff.	Tot. Loss (ksi)	% Diff.	Tot. Loss (ksi)	% Diff.
8.50	90	30.5	29.7	-2.7	29.7	-2.7	29.7	-2.7	26.1	-14.5
	100	33.8	34.7	2.8	34.7	2.8	33.0	-2.3	29.5	-12.6
	110	38.2	39.1	2.4	39.1	2.4	37.5	-1.9	34.2	-10.5
	120	43.0	44.1	2.4	42.8	-0.6	41.4	-3.7	37.3	-13.3
	130	47.9	48.8	1.9	48.8	1.9	47.6	-0.7	41.1	-14.1
10.00	90	31.6	32.6	3.0	32.6	3.0	32.6	3.0	29.0	-8.2
	100	36.4	38.9	6.9	37.3	2.4	37.3	2.4	32.2	-11.5
	110	40.7	43.2	6.0	43.2	6.0	41.8	2.7	36.5	-10.3
	120	45.8	48.1	5.1	46.8	2.3	45.6	-0.4	40.3	-11.9
	130	50.6	52.9	4.4	52.9	4.4	51.8	2.3	45.1	-11.0
11.50	90	34.5	35.4	2.6	35.4	2.6	33.7	-2.3	30.3	-12.4
	100	40.6	41.5	2.3	41.5	2.3	39.9	-1.7	35.0	-13.9
	110	45.2	46.3	2.4	45.0	-0.5	43.7	-3.4	38.9	-13.9
	120	49.9	50.9	2.1	50.9	2.1	49.7	-0.4	43.3	-13.2
14.00	90	41.5	40.7	-1.9	40.7	-1.9	39.1	-5.9	34.1	-17.9
	100	46.1	46.0	-0.4	46.0	-0.4	44.7	-3.2	39.9	-13.6
	110	52.7	51.8	-1.6	51.8	-1.6	50.6	-4.0	44.3	-15.9
16.67	90	45.1	44.4	-1.7	44.4	-1.7	43.0	-4.7	38.1	-15.5
	100	52.5	51.1	-2.8	49.9	-5.1	48.6	-7.5	43.5	-17.2

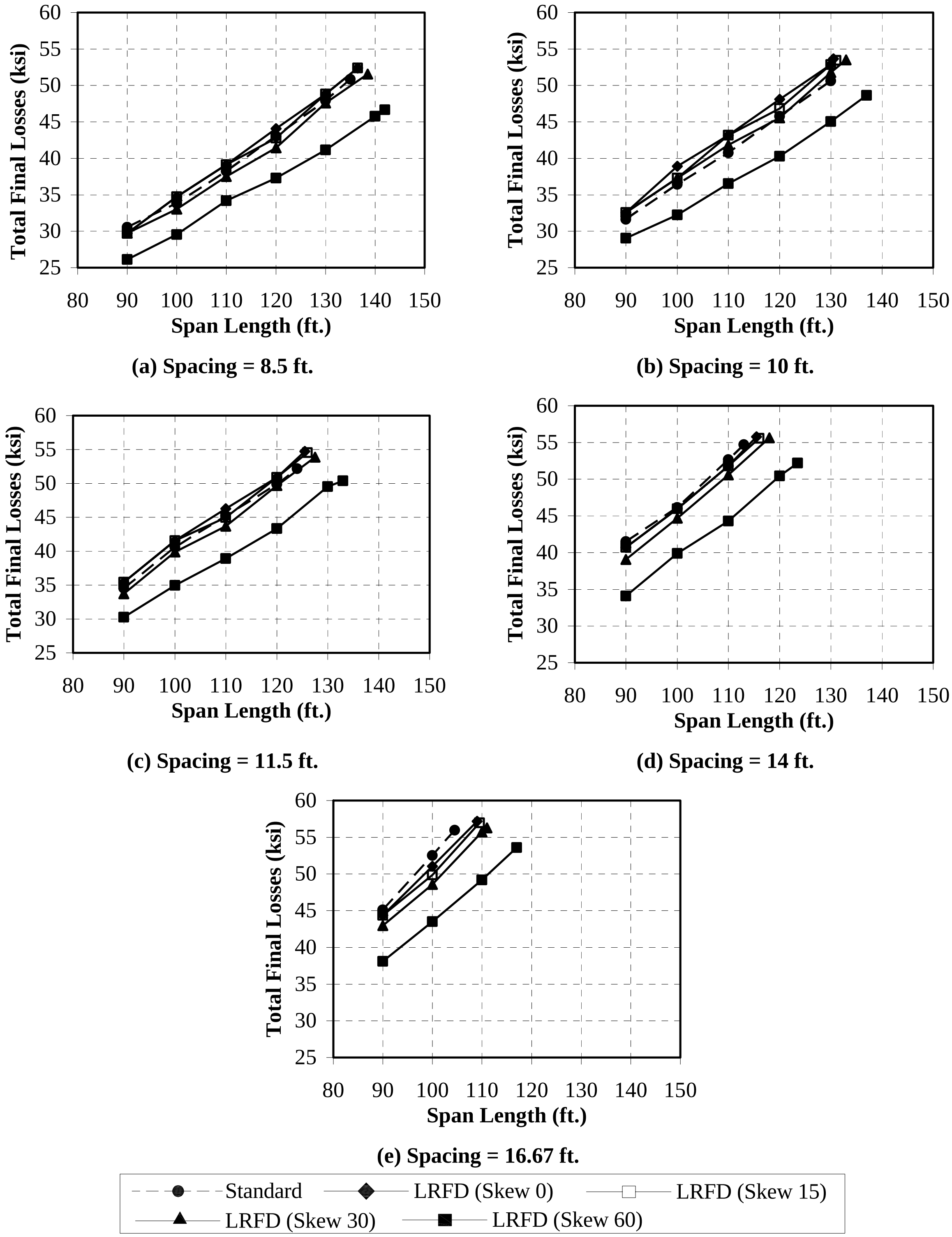

Figure 6.13. Comparison of Final Prestress Loss (U54 Girder, Strand Diameter = 0.5 in.).

6.4 ULTIMATE LIMIT STATE DESIGN

6.4.1 General

The impact of the LRFD Specifications on the requirements for the flexural and shear strength limit states is discussed in the following section. The decrease in the live load and live load factor, the required concrete strength at service, and the number of strands as determined for the service limit state, decreases the factored design moments and nominal moment capacities for the LRFD designs. The reinforcement limits are also different in the LRFD Specifications. However, for all the design cases, the girder sections were found to be under-reinforced.

The LRFD Specifications employ a different methodology for the transverse and interface shear design as compared to the Standard Specifications. This change in the design procedures significantly impacts the shear design results. In general, factored shear by the LRFD Specifications slightly increases with respect to the Standard Specifications. The interface shear reinforcement area requirement by the LRFD Specifications increases by a very large amount relative to the Standard Specifications, while the transverse shear reinforcement area decreased in the designs based on the LRFD Specifications.

6.4.2 Factored Design Moment and Shear

6.4.2.1 Factored Design Moment

Table 6.23 and Figure 6.14 show the differences in the factored design moments for the U54 girder LRFD designs relative to the Standard designs. Detailed results are reported in Appendix A. It can be observed in Figure 6.14 that the factored design moments based on the Standard Specifications are always larger relative to those of the LRFD Specifications, and the difference increases as the skew increases. However, the difference between the factored design moments for the two specifications does not tend to vary significantly with the changes in span length for a particular spacing. For the skew angles of 0, 15, and 30 degrees, the factored design moment of LRFD designs decreases -4.4 to -17.2 percent relative to the Standard designs. For a skew angle of 60 degrees, the design moment decreases -19.1 to -29.6 percent.

Table 6.23. Comparison of Factored Design Moment (U54 Girder).

Spacing (ft.)	Span (ft.)	STD Moment (k-ft.)	LRFD							
			Skew = 0		Skew = 15		Skew = 30		Skew = 60	
			Moment (k-ft.)	% Diff.	Moment (k-ft.)	% Diff.	Moment (k-ft.)	% Diff.	Moment (k-ft.)	% Diff.
8.50	90	6197	5511	-11.1	5466	-11.8	5266	-15.0	4530	-26.9
	100	7310	6541	-10.5	6492	-11.2	6270	-14.2	5433	-25.7
	110	8493	7653	-9.9	7597	-10.5	7348	-13.5	6410	-24.5
	120	9746	8839	-9.3	8776	-10.0	8500	-12.8	7463	-23.4
	130	11,070	10,108	-8.7	10,038	-9.3	9735	-12.1	8594	-22.4
10.00	90	6468	6067	-6.2	6021	-6.9	5797	-10.4	4965	-23.2
	100	7642	7201	-5.8	7147	-6.5	6896	-9.8	5953	-22.1
	110	8892	8418	-5.3	8357	-6.0	8074	-9.2	7020	-21.1
	120	10,219	9721	-4.9	9652	-5.5	9338	-8.6	8170	-20.1
	130	11,623	11,107	-4.4	11,029	-5.1	10,684	-8.1	9402	-19.1
11.50	90	7155	6559	-8.3	6505	-9.1	6259	-12.5	5340	-25.4
	100	8438	7777	-7.8	7714	-8.6	7438	-11.9	6393	-24.2
	110	9801	9082	-7.3	9016	-8.0	8705	-11.2	7536	-23.1
	120	11,245	10,478	-6.8	10,403	-7.5	10,057	-10.6	8770	-22.0
14.00	90	8466	7564	-10.7	7481	-11.6	7231	-14.6	6171	-27.1
	100	9975	8987	-9.9	8890	-10.9	8551	-14.3	7395	-25.9
	110	11,578	10,502	-9.3	10,392	-10.2	10,059	-13.1	8717	-24.7
16.67	90	9661	8391	-13.1	8320	-13.9	7999	-17.2	6798	-29.6
	100	11,387	9957	-12.6	9874	-13.3	9507	-16.5	8148	-28.4

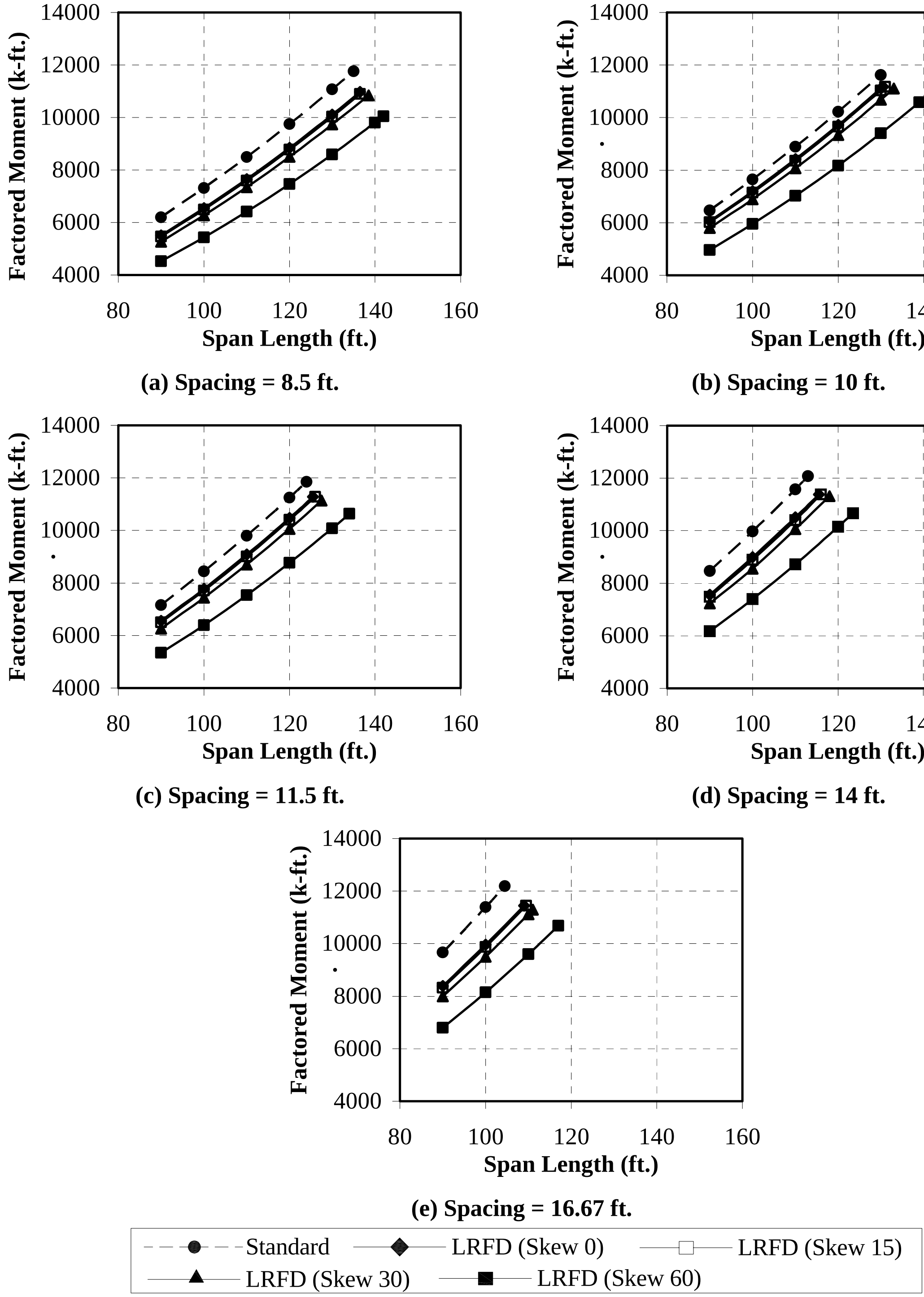

Figure 6.14. Comparison of Factored Design Moment (U54 Girder).

6.4.2.2 Factored Design Shear at Critical Section Location

Table 6.24 and Figure 6.15 compare the factored design shear for the LRFD designs relative to Standard designs for U54 girders with a strand diameter of 0.5 in. The detailed results for both 0.5 in. and 0.6 in. strands are reported in Appendix A. The factored design shear values are calculated at the critical section locations, which are determined based on the provisions of each specification. Except for the smaller spans with girder spacings of 8.5 ft. and 16.67 ft., the factored design shears for the LRFD designs increase relative to the Standard designs. Because only the interior girders were considered in this parametric study, the skew has a very insignificant effect on the factored design shear, as can be seen in Figure 6.15. The same trend is observed for the designs with 0.6 in. strands.

Table 6.24. Comparison of Factored Design Shear at Respective Critical Section Location (U54 Girder, Strand Diameter = 0.5 in.).

Spacing (ft.)	Span (ft.)	STD Shear (kips)	LRFD							
			Skew = 0		Skew = 15		Skew = 30		Skew = 60	
			Shear (kips)	% Diff.	Shear (kips)	% Diff.	Shear (kips)	% Diff.	Shear (kips)	% Diff.
8.50	90	277	265	-4.5	265	-4.5	265	-4.5	265	-4.5
	100	293	286	-2.6	286	-2.6	286	-2.7	286	-2.7
	110	309	306	-1.0	306	-1.0	306	-1.0	306	-1.1
	120	324	324	0.0	324	0.0	324	0.0	324	0.0
	130	339	342	0.8	342	0.8	342	0.8	342	0.8
10.00	90	289	297	2.5	297	2.5	296	2.5	296	2.5
	100	306	319	4.3	319	4.2	319	4.2	319	4.2
	110	323	341	5.5	341	5.5	341	5.4	340	5.3
	120	340	360	6.1	361	6.2	361	6.2	361	6.2
	130	356	380	6.7	380	6.7	380	6.7	380	6.7
11.50	90	320	325	1.6	325	1.6	325	1.6	325	1.5
	100	338	350	3.3	350	3.3	350	3.3	349	3.3
	110	356	372	4.4	372	4.4	372	4.4	372	4.4
	120	374	393	5.2	393	5.2	393	5.1	393	5.2
14.00	90	381	382	0.3	382	0.3	382	0.2	382	0.2
	100	402	410	1.9	410	1.9	410	1.9	409	1.8
	110	423	435	2.8	435	2.8	435	2.8	435	2.7
16.67	90	436	430	-1.2	430	-1.2	430	-1.2	430	-1.3
	100	459	460	0.3	460	0.2	460	0.2	460	0.2

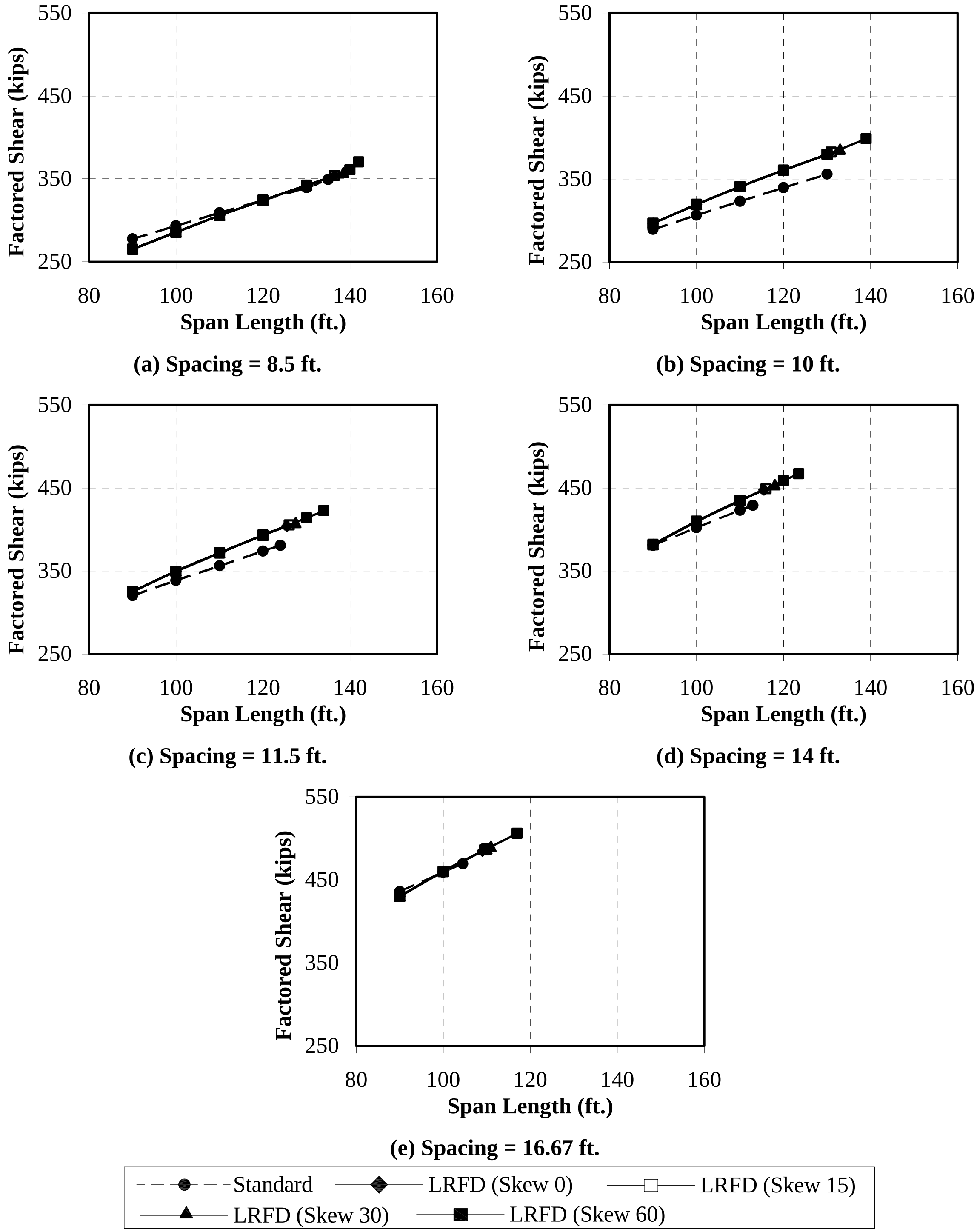

Figure 6.15. Comparison of Factored Design Shear at Respective Critical Section Location (U54 Girder, Strand Diameter = 0.5 in.).

6.4.3 Nominal Moment Capacity

Table 6.25 and Figures 6.16 and 6.17 show the comparison of nominal moment resistance for the LRFD designs relative to Standard designs for 0.5 in. and 0.6 in. strands. For a skew angle of zero degrees, the nominal moment capacity values calculated for the Standard designs are larger when compared to the LRFD designs. The difference increases for larger skew angles. In general, the difference increases with increasing girder spacing, while the increasing span length has a very insignificant effect. For skew angles of 0, 15, and 30 degrees, the nominal moment capacities for the LRFD designs vary relative to the Standard designs in the range of 1.9 to -13.3 percent, and for the skew angle of 60 degrees they decrease -10.4 to -22.9 percent.

Table 6.25. Comparison of Nominal Moment Resistance (U54 Girder, Strand Diameter = 0.5 in.).

Spacing (ft.)	Span (ft.)	STD Mn (k-ft)	LRFD							
			Skew = 0		Skew = 15		Skew = 30		Skew = 60	
			Mn (k-ft)	% Diff.	Mn (k-ft)	% Diff.	Mn (k-ft)	% Diff.	Mn (k-ft)	% Diff.
8.50	90.0	6707	6043	-9.9	6043	-9.9	6043	-9.9	5322	-20.7
	100.0	8077	7805	-3.4	7805	-3.4	7457	-7.7	6755	-16.4
	110.0	9729	9506	-2.3	9506	-2.3	9171	-5.7	8492	-12.7
	120.0	11,699	11608	-0.8	11,313	-3.3	11,013	-5.9	10,005	-14.5
	130.0	13,690	13624	-0.5	13,624	-0.5	13,354	-2.5	11,943	-12.8
10.00	90.0	7127	6814	-4.4	6814	-4.4	6814	-4.4	6090	-14.6
	100.0	8862	8936	0.8	8587	-3.1	8587	-3.1	7529	-15.0
	110.0	10,677	10789	1.0	10,789	1.0	10,465	-2.0	9282	-13.1
	120.0	12,830	13076	1.9	12,777	-0.4	12,380	-3.5	11,111	-13.4
	130.0	14,965	15203	1.6	15,203	1.6	14,955	-0.1	13,415	-10.4
11.50	90.0	7894	7583	-3.9	7583	-3.9	7221	-8.5	6492	-17.8
	100.0	9984	9717	-2.7	9717	-2.7	9365	-6.2	8301	-16.9
	110.0	12,086	11888	-1.6	11,562	-4.3	11,234	-7.0	10,066	-16.7
	120.0	14,250	14123	-0.9	14,123	-0.9	13,809	-3.1	12,212	-14.3
14.00	90.0	9763	9825	0.6	9466	-3.0	8743	-10.4	7648	-21.7
	100.0	11,958	11382	-4.8	11,382	-4.8	11,043	-7.7	9825	-17.8
	110.0	14,697	14042	-4.5	14,042	-4.5	13,714	-6.7	12,056	-18.0
16.67	90.0	11,422	10271	-10.1	10,271	-10.1	9907	-13.3	8807	-22.9
	100.0	14,100	13204	-6.4	12,864	-8.8	12,524	-11.2	11,147	-20.9

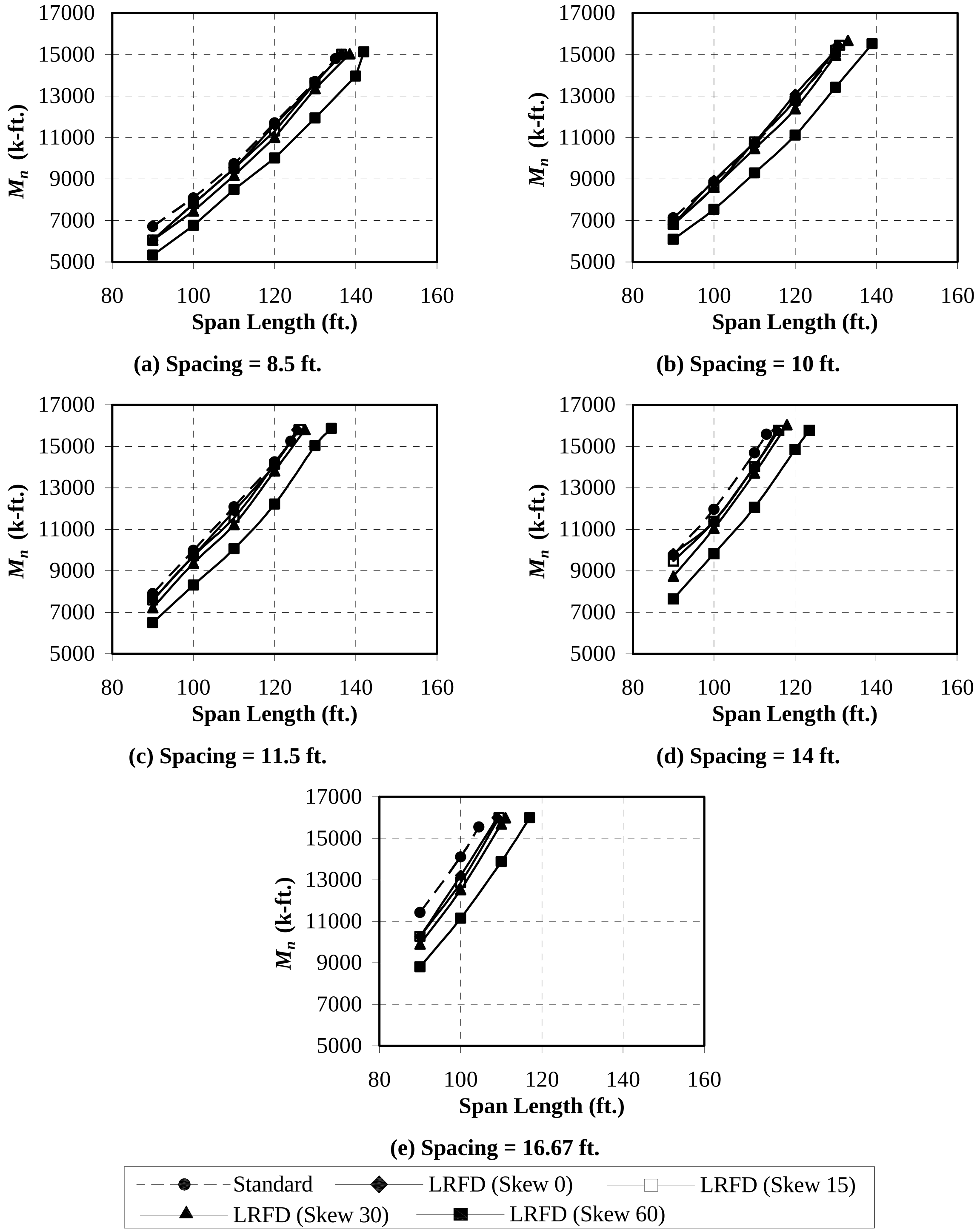

Figure 6.16. Comparison of Nominal Moment Resistance (U54 Girder, Strand Diameter = 0.5 in.).

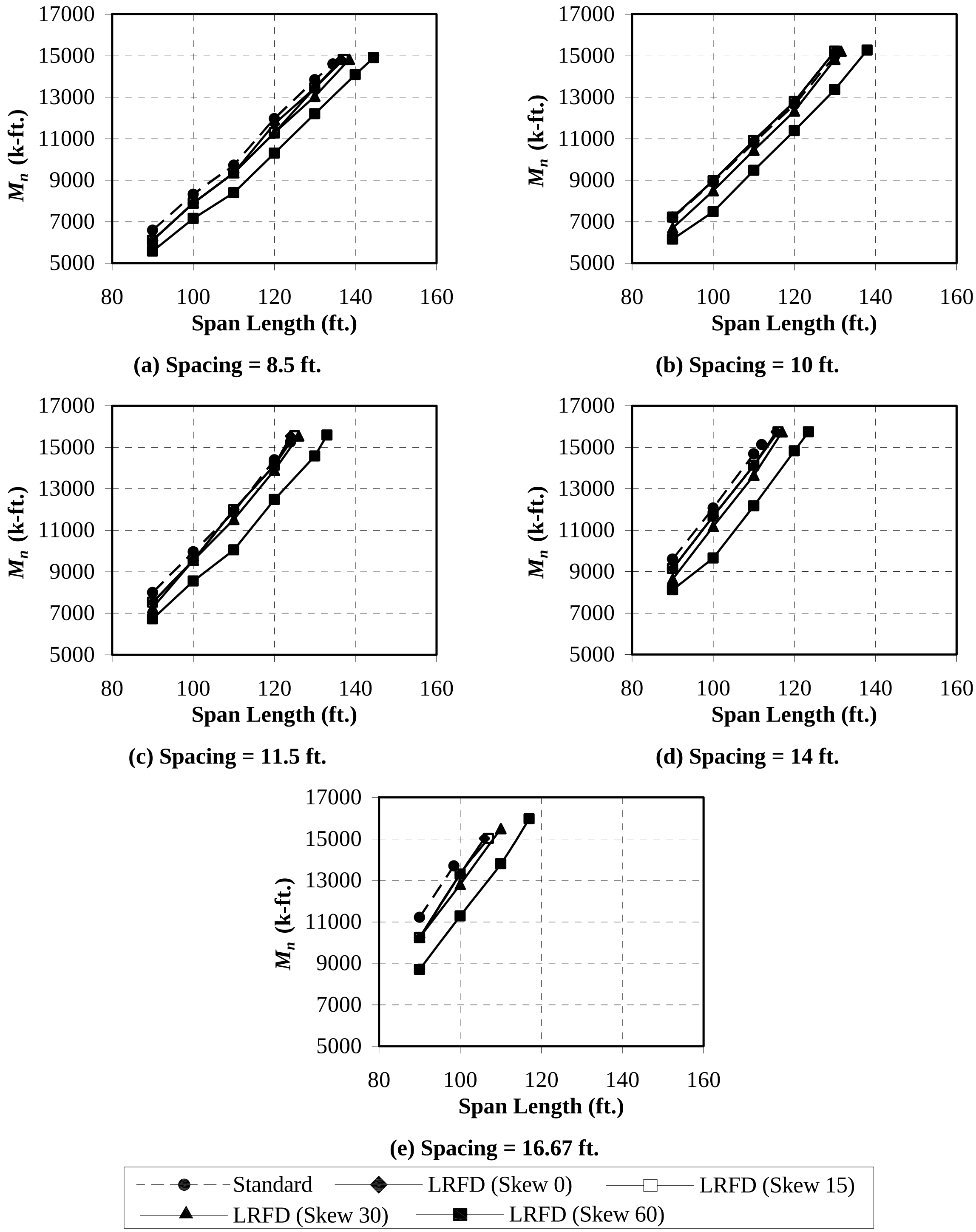

Figure 6.17. Comparison of Nominal Moment Resistance (U54 Girder, Strand Diameter = 0.6 in.).

6.4.4 Shear Design

6.4.4.1 Transverse Shear Reinforcement

Table 6.26 and Figure 6.18 show the comparison of the transverse shear reinforcement area (A_v) for LRFD U54 girder designs relative to Standard designs. The detailed results are reported in Appendix A. For all skews and strand diameters, the A_v values calculated for Standard designs are larger compared to the LRFD designs. In general, this difference increases with increasing girder spacing, while the increasing span length has a very insignificant effect on this comparison. Based on the summary of detailed results, the transverse shear reinforcement area for the LRFD designs decreases relative to the Standard designs from -26.1 to -46.6 percent.

Table 6.26. Comparison of Transverse Shear Reinforcement Area (U54 Girder, Strand Diameter = 0.5 in.).

Spacing (ft.)	Span (ft.)	STD A_v (in.^{2}/ft.)	LRFD Skew = 0 A_v (in.^{2}/ft.)	Skew = 0 % Diff.	Skew = 15 A_v (in.^{2}/ft.)	Skew = 15 % Diff.	Skew = 30 A_v (in.^{2}/ft.)	Skew = 30 % Diff.	Skew = 60 A_v (in.^{2}/ft.)	Skew = 60 % Diff.
8.5	90	0.42	0.23	-45.4	0.23	-45.4	0.23	-45.6	0.23	-46.6
	100	0.47	0.28	-39.8	0.28	-39.9	0.28	-40.6	0.27	-41.5
	110	0.50	0.33	-33.3	0.33	-33.3	0.33	-33.5	0.32	-35.2
	120	0.48	0.33	-30.7	0.33	-30.7	0.33	-31.1	0.32	-33.4
	130	0.46	0.32	-30.3	0.32	-30.5	0.32	-30.8	0.31	-33.7
10	90	0.48	0.30	-37.8	0.30	-37.8	0.29	-38.5	0.29	-39.0
	100	0.53	0.36	-33.3	0.36	-33.4	0.35	-33.5	0.35	-34.9
	110	0.55	0.40	-26.3	0.40	-26.4	0.40	-27.4	0.38	-30.1
	120	0.54	0.39	-27.1	0.39	-27.3	0.39	-27.6	0.38	-29.3
	130	0.52	0.38	-26.1	0.38	-26.2	0.38	-26.5	0.37	-28.3
11.5	90	0.61	0.36	-40.2	0.36	-40.3	0.36	-40.3	0.35	-41.7
	100	0.67	0.43	-36.0	0.43	-35.9	0.43	-36.0	0.42	-37.1
	110	0.66	0.45	-32.2	0.45	-32.2	0.45	-32.5	0.44	-34.5
	120	0.66	0.44	-32.7	0.44	-32.8	0.44	-33.5	0.43	-35.1
14	90	0.85	0.50	-41.5	0.50	-41.5	0.50	-41.5	0.49	-42.9
	100	0.90	0.57	-36.3	0.57	-36.3	0.57	-36.7	0.55	-38.7
	110	0.91	0.57	-37.9	0.57	-38.0	0.56	-38.6	0.54	-40.3
16.67	90	1.08	0.62	-42.5	0.62	-42.5	0.62	-42.5	0.61	-43.3
	100	1.11	0.67	-40.2	0.66	-40.6	0.66	-40.9	0.64	-42.3

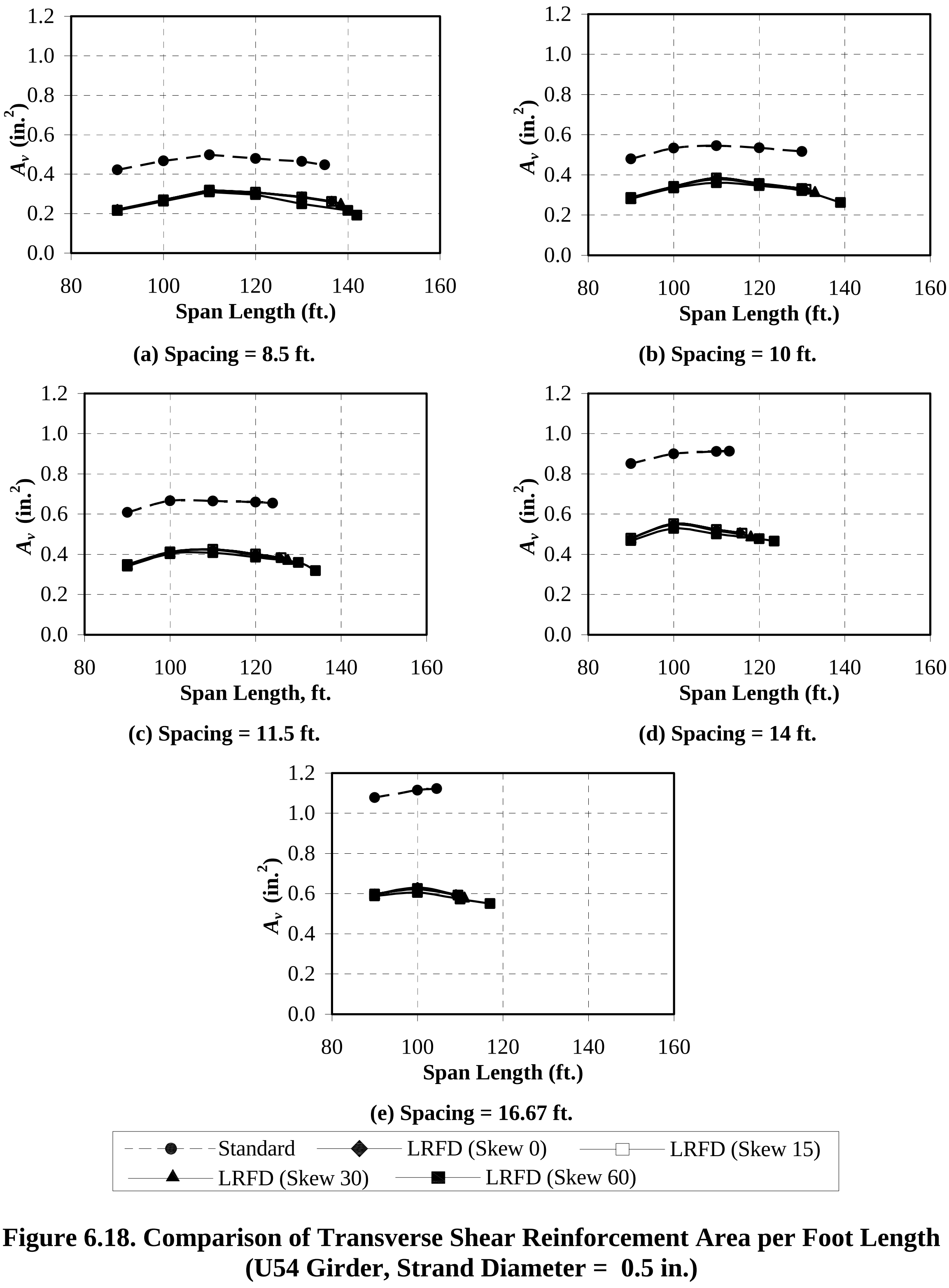

Figure 6.18. Comparison of Transverse Shear Reinforcement Area per Foot Length (U54 Girder, Strand Diameter = 0.5 in.)

6.4.4.2 Interface Shear Reinforcement

Table 6.27 and Figure 6.19 show the comparison of the interface shear reinforcement area (A_{vh}) for LRFD designs relative to Standard designs. The detailed results are reported in Appendix A. For all skews and both strand diameters, the A_{vh} calculated for designs based on the LRFD Specifications are larger when compared to those of the designs based on the Standard Specifications. In general, this difference increases with increased girder spacing and the span length. The interface shear reinforcement area A_{vh} for the LRFD designs increases relative to the Standard designs in the range of 0.47 to 1.39 in.^{2}/ft., which corresponds to a significant percentage difference of 148 to 443 percent.

Table 6.27. Comparison of Interface Shear Reinforcement Area (U54 Girder, Strand Diameter = 0.5 in.).

Spacing (ft.)	Span (ft.)	STD A_{vh} (in.^{2}/ft.)	LRFD							
			Skew = 0		Skew = 15		Skew = 30		Skew = 60	
			A_{vh} (in.^{2}/ft.)	% Diff.	A_{vh} (in.^{2}/ft.)	% Diff.	A_{vh} (in.^{2}/ft.)	% Diff.	A_{vh} (in.^{2}/ft.)	% Diff.
8.50	90.0	0.315	0.79	150.7	0.79	150.4	0.79	150.4	0.78	147.5
	100.0		0.86	172.2	0.86	172.1	0.85	170.9	0.85	168.4
	110.0		0.92	192.1	0.92	192.1	0.92	192.0	0.91	188.6
	120.0		0.98	211.1	0.98	211.1	0.98	209.8	0.96	204.1
	130.0		1.04	229.7	1.04	228.7	1.03	227.6	1.01	222.0
10.00	90.0		0.94	199.8	0.94	199.8	0.94	198.4	0.94	197.0
	100.0		1.02	223.1	1.02	223.1	1.02	223.1	1.01	219.5
	110.0		1.09	246.6	1.09	246.6	1.09	244.9	1.07	240.2
	120.0		1.16	267.3	1.15	266.1	1.15	264.9	1.14	260.7
	130.0		1.22	288.8	1.22	288.8	1.21	285.7	1.20	280.4
11.50	90.0		1.08	243.3	1.08	243.2	1.08	242.1	1.07	239.1
	100.0		1.16	268.9	1.16	268.0	1.16	267.9	1.15	264.5
	110.0		1.24	293.0	1.24	293.0	1.23	291.6	1.21	284.9
	120.0		1.31	314.5	1.31	314.5	1.30	313.1	1.28	307.0
14.00	90.0		1.37	333.5	1.37	333.5	1.36	332.5	1.35	328.4
	100.0		1.47	365.7	1.47	365.7	1.46	364.0	1.44	358.4
	110.0		1.56	393.7	1.56	393.7	1.55	392.2	1.53	385.0
16.67	90.0		1.59	406.0	1.59	406.0	1.59	405.0	1.58	401.5
	100.0		1.71	442.2	1.70	440.6	1.70	439.1	1.68	432.4

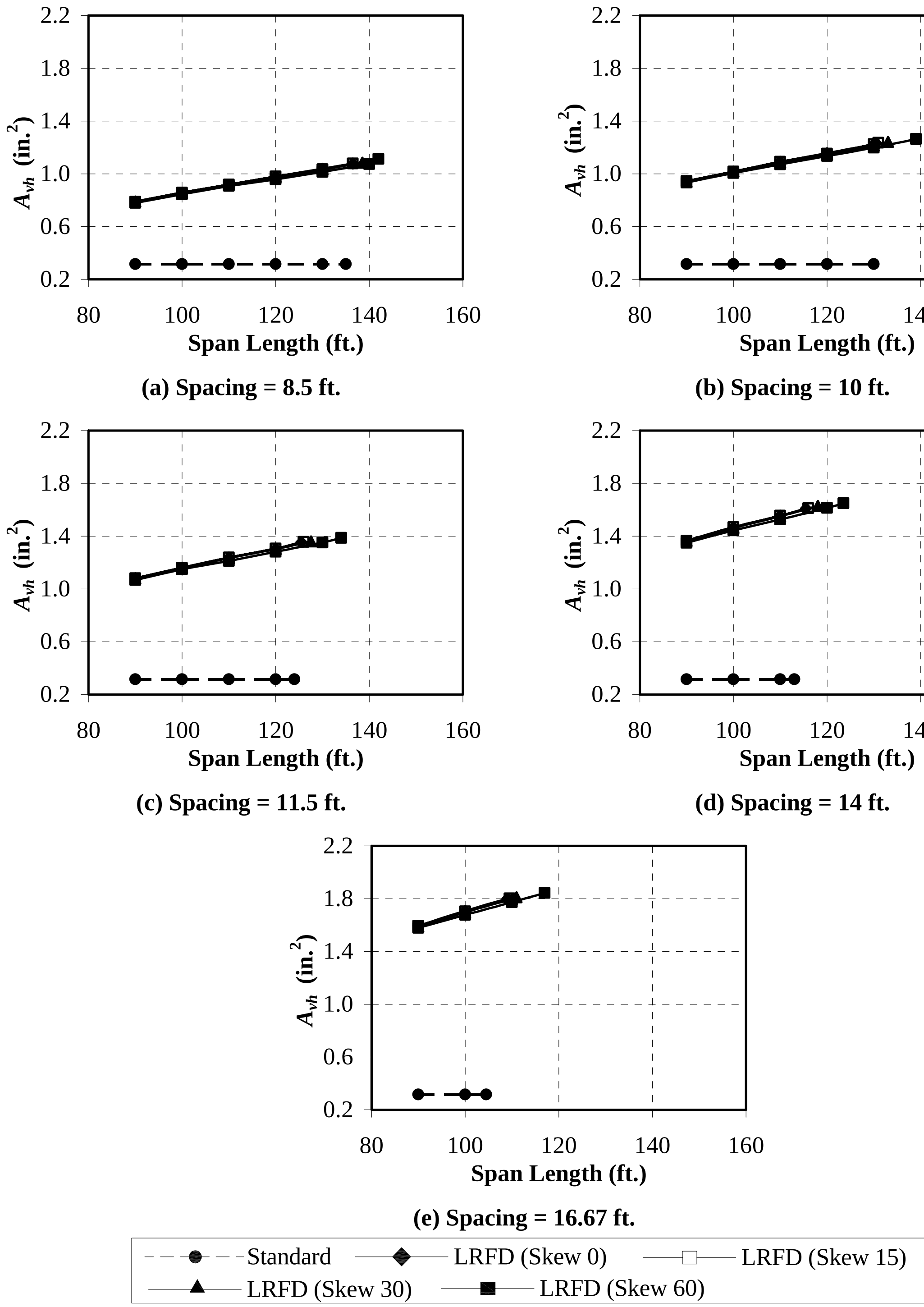

Figure 6.19. Comparison of Interface Shear Reinforcement Area per Foot Length (U54 Girder, Strand Diameter = 0.5 in.).

6.5 CAMBER

The Standard Specifications do not provide guidelines for determining the camber of prestressed concrete members. The Hyperbolic Functions Method (Furr et al. 1968, Sinno 1968, Furr and Sinno 1970) for the calculation of maximum camber is used by TxDOT's prestressed concrete bridge design software, PSTRS14 (TxDOT 2004). The details of this method are described in the design examples provided in the second volume of this report. Because the camber is evaluated using the same methodology for both specifications, only a small difference is observed. Table 6.28 and Figure 6.20 compare the camber values for LRFD designs to Standard designs for a strand diameter of 0.5 in. The comparison for 0.6 in. strands is reported in Appendix A.

For a skew angle of zero degrees, the camber calculated for designs based on the Standard Specifications are larger when compared to the LRFD designs. The difference becomes greater for larger skew angles. For skew angles of 0, 15, and 30 degrees and for a 0.5 in. strand diameter, the camber for the LRFD designs decrease -0.1 to -22.5 percent relative to the Standard designs; and for a skew angle of 60 degrees, the camber decreases in the range of -23.7 to -45.1 percent.

Table 6.28. Comparison of Camber (U54 Girder, Strand Diameter = 0.5 in.).

Spacing (ft.)	Span (ft.)	STD Camber (ft.)	LRFD							
			Skew = 0		Skew = 15		Skew = 30		Skew = 60	
			Camber (ft.)	% Diff.	Camber (ft.)	% Diff.	Camber (ft.)	% Diff.	Camber (ft.)	% Diff.
8.50	90.0	0.102	0.079	-22.5	0.079	-22.5	0.079	-22.5	0.056	-45.1
	100.0	0.145	0.131	-9.7	0.131	-9.7	0.118	-18.6	0.09	-37.9
	110.0	0.208	0.192	-7.7	0.192	-7.7	0.176	-15.4	0.144	-30.8
	120.0	0.293	0.276	-5.8	0.261	-10.9	0.245	-16.4	0.196	-33.1
	130.0	0.396	0.376	-5.1	0.376	-5.1	0.359	-9.3	0.268	-32.3
10.00	90.0	0.113	0.102	-9.7	0.102	-9.7	0.102	-9.7	0.079	-30.1
	100.0	0.171	0.17	-0.6	0.157	-8.2	0.157	-8.2	0.118	-31.0
	110.0	0.243	0.241	-0.8	0.241	-0.8	0.228	-6.2	0.176	-27.6
	120.0	0.339	0.338	-0.3	0.323	-4.7	0.307	-9.4	0.245	-27.7
	130.0	0.447	0.445	-0.4	0.445	-0.4	0.432	-3.4	0.341	-23.7
11.50	90.0	0.134	0.123	-8.2	0.123	-8.2	0.113	-15.7	0.091	-32.1
	100.0	0.209	0.196	-6.2	0.196	-6.2	0.183	-12.4	0.144	-31.1
	110.0	0.340	0.350	-0.1	0.268	-9.2	0.255	-13.6	0.207	-29.8
	120.0	0.399	0.382	-4.3	0.382	-4.3	0.367	-8.0	0.292	-26.8
14.00	90.0	0.186	0.185	-0.5	0.175	-5.9	0.155	-16.7	0.123	-33.9
	100.0	0.269	0.247	-8.2	0.247	-8.2	0.236	-12.3	0.196	-27.1
	110.0	0.388	0.356	-8.2	0.356	-8.2	0.344	-11.3	0.281	-27.6
16.67	90.0	0.227	0.195	-14.1	0.195	-14.1	0.185	-18.5	0.155	-31.7
	100.0	0.33	0.299	-9.4	0.289	-12.4	0.278	-15.8	0.236	-28.5

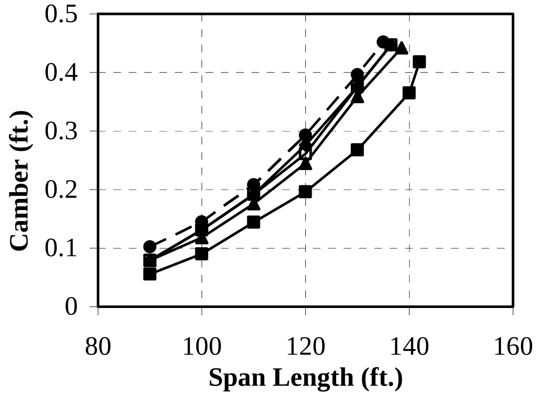

(a) Spacing = 8.5 ft.

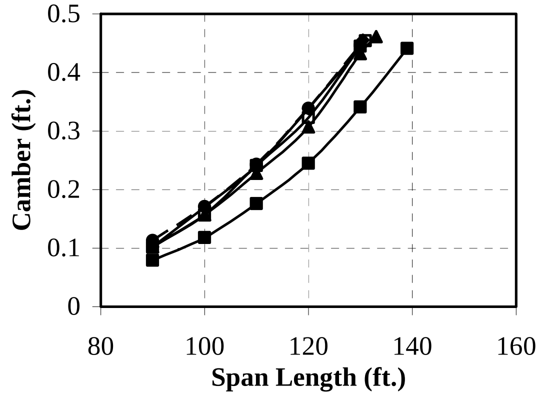

(b) Spacing = 10 ft.

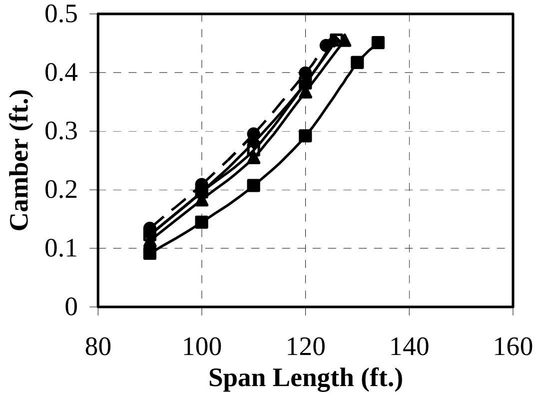

(c) Spacing = 11.5 ft.

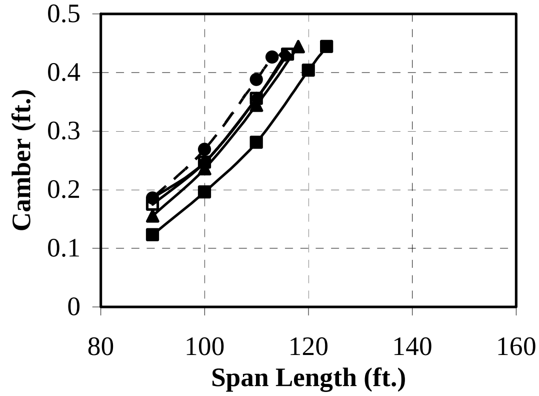

(d) Spacing = 14 ft.

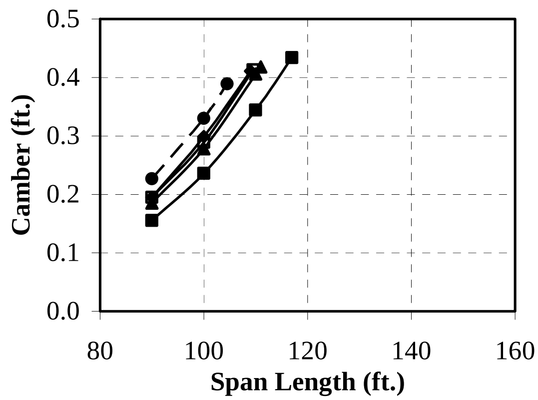

(e) Spacing = 16.67 ft.

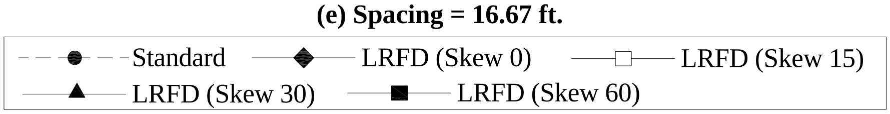

Figure 6.20. Comparison of Camber (U54 Girder, Strand Diameter = 0.5 in.).

7. DESIGN ISSUES

7.1 GENERAL

The following sections discuss several design issues that were identified when considering the transition from the AASHTO Standard Specifications to the AASHTO LRFD Specifications for typical prestressed concrete bridge girders designs. Some additional discussion on design issues and recommendations is provided in Section 8.3.

7.2 INTERFACE SHEAR DESIGN

For almost all girders in the parametric study designed according to the LRFD Specifications, the horizontal shear governed the design of the transverse shear reinforcement. As described in Chapters 4 through 6, designs following the current LRFD Specifications require a significant amount of interface shear reinforcement as compared to the Standard designs. Traditionally, TxDOT has extended the transverse shear reinforcement into the slab to resist the interface shear; and the interface shear requirements have not governed the required shear reinforcement area.

Revised interface shear design provisions have been approved by Committee T-10 and are proposed to be adopted by the LRFD Specifications in 2007. These provisions are based on a modified shear friction model, which takes into account the contribution of the cohesion between the precast girder and CIP slab to the interface shear strength. The cohesion factor (c) for the concrete placed against a clean, hardened, and intentionally roughened surface would increase from the present value of 0.100 ksi to 0.280 ksi (refer to Section 3.9.2).

The proposed design provisions were applied to the LRFD designs, and a significant reduction in the required A_{vh} was observed. The results for AASHTO Type IV and Type C girders are summarized in Tables 7.1 and 7.2. It was observed that the proposed LRFD interface shear provisions significantly reduce the interface shear reinforcement area requirement. The interface shear reinforcement requirement from the proposed provisions is the same as that required by the Standard Specifications for all the cases for Type IV girders and most of the cases for Type C girders.

The minimum requirement for interface shear reinforcement governs all the cases for Type IV girders when using the proposed provisions and was found to be the same as that required by the Standard Specifications. The minimum reinforcement requirement governed for most Type C girder cases and the required A_{vh} tended to be the same as that required by the Standard Specifications. However, for a few cases with 8 ft. and 8.67 ft. girder spacing, differences of -50 to 50 percent were observed.

Table 7.1. Comparison of Interface Shear Reinforcement Area using Proposed Provisions (Type IV Girder, Strand Diameter = 0.5 in.).

Girder Spacing (ft.)	Span (ft.)	STD A_{vh} (in.^{2}/ft.)	LRFD							
			Skew = 0°		Skew = 15°		Skew = 30°		Skew = 60°	
			A_{vh} (in.^{2}/ft.)	Diff. %	A_{vh} (in.^{2}/ft.)	Diff. %	A_{vh} (in.^{2}/ft.)	Diff. %	A_{vh} (in.^{2}/ft.)	Diff. %
6	90	0.20	0.20	0.0	0.20	0.0	0.20	0.0	0.20	0.0
	100	0.20	0.20	0.0	0.20	0.0	0.20	0.0	0.20	0.0
	110	0.20	0.20	0.0	0.20	0.0	0.20	0.0	0.20	0.0
	120	0.20	0.20	0.0	0.20	0.0	0.20	0.0	0.20	0.0
	130	0.20	0.20	0.0	0.20	0.0	0.20	0.0	0.20	0.0
	133	-	0.20	-	0.20	-	0.20	-	-	-
	135	-	-	-	-	-	-	-	0.20	-
	136	0.20	-	-	-	-	-	-	-	-
8	90	0.20	0.20	0.0	0.20	0.0	0.20	0.0	0.20	0.0
	100	0.20	0.20	0.0	0.20	0.0	0.20	0.0	0.20	0.0
	110	0.20	0.20	0.0	0.20	0.0	0.20	0.0	0.20	0.0
	120	0.20	0.20	0.0	0.20	0.0	0.20	0.0	0.20	0.0
	124	0.20	-	-	-	-	-	-	-	-
	125	-	-	-	-	-	-	-	0.20	-
8.67	90	0.20	0.20	0.0	0.20	0.0	0.20	0.0	0.20	0.0
	100	0.20	0.20	0.0	0.20	0.0	0.20	0.0	0.20	0.0
	110	0.20	0.20	0.0	0.20	0.0	0.20	0.0	0.20	0.0
	116	-	0.20	-	0.20	-	-	-	-	-
	117	-	-	-	-	-	0.20	-	-	-
	119	0.20	-	-	-	-	-	-	-	-
	120	-	-	-	-	-	-	-	0.20	-
	121	-	-	-	-	-	-	-	0.20	-

Table 7.2. Comparison of Interface Shear Reinforcement Area for Proposed Provisions (Type C Girder, Strand Diameter = 0.5 in.).

Girder Spacing (ft.)	Span (ft.)	Std. A_{vh} (in.^{2}/ft.)	LRFD							
			Skew = 0°		Skew = 15°		Skew = 30°		Skew = 60°	
			A_{vh} (in.^{2}/ft.)	Diff. %	A_{vh} (in.^{2}/ft.)	Diff. %	A_{vh} (in.^{2}/ft.)	Diff. %	A_{vh} (in.^{2}/ft.)	Diff. %
6	40	0.14	0.14	0.0	0.14	0.0	0.14	0.0	0.14	0.0
	50	0.14	0.14	0.0	0.14	0.0	0.14	0.0	0.14	0.0
	60	0.14	0.14	0.0	0.14	0.0	0.14	0.0	0.14	0.0
	70	0.14	0.14	0.0	0.14	0.0	0.14	0.0	0.14	0.0
	80	0.14	0.14	0.0	0.14	0.0	0.14	0.0	0.14	0.0
	90	0.14	0.14	0.0	0.14	0.0	0.14	0.0	0.21	51.6
	95	-	0.14	-	0.14	-	0.14	-	-	-
	96	0.17	-	-	-	-	-	-	-	-
	98	-	-	-	-	-	-	-	0.33	-
8	40	0.14	0.14	0.0	0.14	0.0	0.14	0.0	0.14	0.0
	50	0.14	0.14	0.0	0.14	0.0	0.14	0.0	0.14	0.0
	60	0.14	0.14	0.0	0.14	0.0	0.14	0.0	0.14	0.0
	70	0.20	0.14	-28.4	0.14	-28.4	0.14	-28.4	0.21	7.6
	80	0.26	0.14	-45.9	0.14	-45.9	0.15	-41.2	0.33	27.0
	83	0.29	0.14	-51.0	0.14	-50.0	0.19	-34.9	-	-
	87	-	-	-	-	-	-	-	0.42	-
8.67	40	0.14	0.14	0.0	0.14	0.0	0.14	0.0	0.14	0.0
	50	0.14	0.14	0.0	0.14	0.0	0.14	0.0	0.14	0.0
	60	0.18	0.14	-21.7	0.14	-21.7	0.14	-21.7	0.15	-18.4
	70	0.25	0.14	-44.1	0.14	-44.1	0.14	-44.1	0.27	7.6
	80	0.32	0.14	-56.6	0.16	-49.8	0.22	-33.3	0.39	-
	81	-	-	-	-	-	0.23	-	-	-
	85	-	-	-	-	-	-	-	0.47	-

7.3 PARTIAL DEBONDING OF PRESTRESSING STRANDS

A literature review was conducted to document the basis for the greater amounts of debonding used in TxDOT practice relative to the LRFD limits. The LRFD Specifications derive its debonding limits based on a Florida DOT study (Shahawy et al. 1992, 1993) where some specimen with 50 percent debonded strands (0.6 in. diameter) had inadequate shear capacity. Barnes, Burns, and Kreger (1999) recommended that up to 75 percent of the strands can be debonded if the following conditions are met: (1) cracking is prevented in or near the transfer length, and (2) the AASHTO LRFD (1998) rules for terminating the tensile reinforcement are applied to the bonded length of prestressing strands. Abdalla et al. (1993) recommended limiting debonding to 67 percent per section, while they did not consider a debonding limit per row to be necessary. In the aforementioned research studies, none of the specimens failed in a shear mode. All the specimens failed in pure flexure, flexure with slip, and bond failure mechanisms. Krishnamurthy (1971) observed that the shear resistance of the section increased by increasing the number of debonded strands in the upper flange, and it decreased when the number of debonded strands was increased in the bottom flange of the beam.

The current LRFD debonding provisions limit debonding of strands to 25 percent per section and 40 percent per row. These limits pose serious restrictions on the design of Texas U54 bridges relative to TxDOT's typical current practices and would restrict the span capability for U54 girder designs. Based on research by Barnes, Burns, and Kreger (1999) and successful past practice by TxDOT, it is suggested that up to 75 percent of the strands may be debonded, if the following conditions are met.

a) Cracking is prevented in or near the transfer length.
b) The AASHTO LRFD rules for terminating the tensile reinforcement are applied to the bonded length of prestressing strands.
c) The shear resistance at the regions where the strands are debonded is thoroughly investigated with due regard to the reduction in the horizontal force available, as recommended in the LRFD Commentary (Article C5.11.4.3).

7.4 LOAD DISTRIBUTION FACTORS

7.4.1 General

The approximate method of load distribution in the LRFD Specifications is convenient and gives conservative results, but it comes with certain limitations. The most restrictive limitations with respect to typical Texas U54 girder bridges include the limitation on span length, number of beams, edge distance parameter, and girder spacing. It becomes mandatory to apply refined analysis procedures recommended by the LRFD

Specifications in a case where these or other limitations are violated by any particular bridge design parameter. The limitations on the use of the distribution factor formulas are there because these formulas were developed based on a database of bridges that fell within these limitations. Therefore, it is possible that beyond these limitations the LRFD live load distribution factor (DF) formulas will continue to give conservative estimates for load distribution.

In the parametric study it was found that the span length limit for use of the LRFD live load DFs is violated for certain cases for the U54 girders. This section discusses the development of the equivalent grillage model of a typical Texas U54 beam bridge. Moreover, the results of the grillage analysis method and the results of the LRFD live load DF formulas are compared for the cases evaluated.

7.4.2 Grillage Analysis

7.4.2.1 General

Grillage analysis is one of the refined analysis methods that can be used to analyze bridge superstructures to determine appropriate DFs when the limitations for using the LRFD DF formulas are violated. A three-step procedure is followed to ensure that the grillage model developed represents the real bridge as correctly as possible. In the first step, a finite element model is verified against actual field measured results. In the second step, a grillage model is developed and calibrated against the finite element model. In the third step, the developed grillage model is used to evaluate the LRFD live load DF formulas. All steps and associated procedures are discussed in the following sections.

The use of the LRFD live load distribution factor formulas is limited to spans no longer than 140 ft. The parametric study indicated that this limitation is slightly violated for the U54 girder with 8.5 ft. girder spacing and a 60-degree skew (corresponding maximum span = 144 ft.). The two cases noted in Table 7.3 were investigated using grillage analysis to determine the applicability of the LRFD live load distribution factor for spread box beams spanning up to 150 ft.

Table 7.3. Parameters for Refined Analysis.

Span (ft.)	Spacing (ft.)	Skew (degrees)
140	8.5	60
150	8.5	60

7.4.2.2 Verification of the Finite Element Analysis

The FEM analysis results in this section are verified for their accuracy by comparing them with the results from field testing of an actual bridge. The purpose of this verification process is to ensure that the FEM model adequately represents the actual bridge structure by confirming that the response determined by FEM analysis closely estimate those measured experimentally for an actual bridge. This FEM model will then be used in the selection and calibration of the grillage model for the particular cases of interest for this study.

The Derhersville bridge in Pennsylvania, over Little Schuylkill River, was selected for the verification of the FEM analysis. It is a three-span, simply supported, spread box girder prestressed bridge with 0-degree skew as shown in Figures 7.1 and 7.2. The length of the test span was 61.5 ft. with a total roadway width of 30 ft. The specified minimum thickness of the bridge deck was 7.5 in. The bridge was supported by five prestressed spread box girders. The girder spacing and dimensions of girders, safety curb, and parapet are shown in Figure 7.2. Cast-in-place concrete diaphragms, 10 in. in thickness, are located between beams at the ends of the span and at the midspan. The joint between the slab and the curb was a construction joint with a raked finish and the vertical reinforcement for the curb section extended through the joint into the slab (Douglas and Vanhorn 1966).

Douglas and Vanhorn (1966) investigated the lateral distribution of static loads on the Derhersville bridge by loading it with vehicular live loads, and they determined the response quantities such as bending moments and deflections at sections M and N shown in the elevation view of the bridge in Figure 7.1.

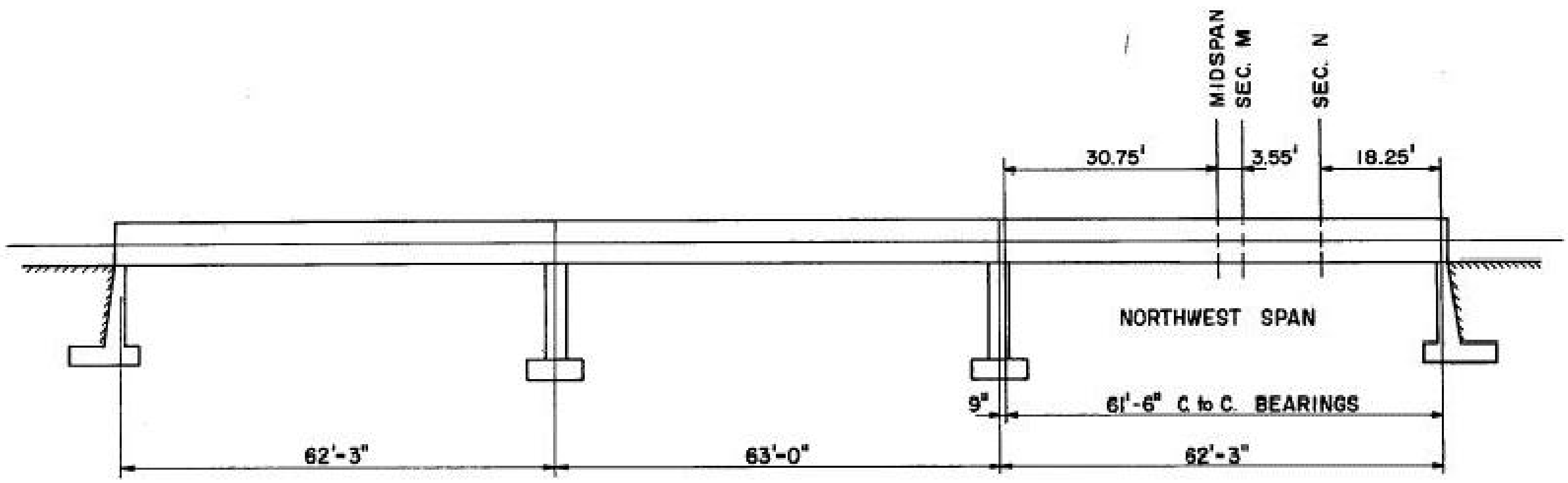

Figure 7.1. Elevation of Derhersville Bridge (Douglas 1966).

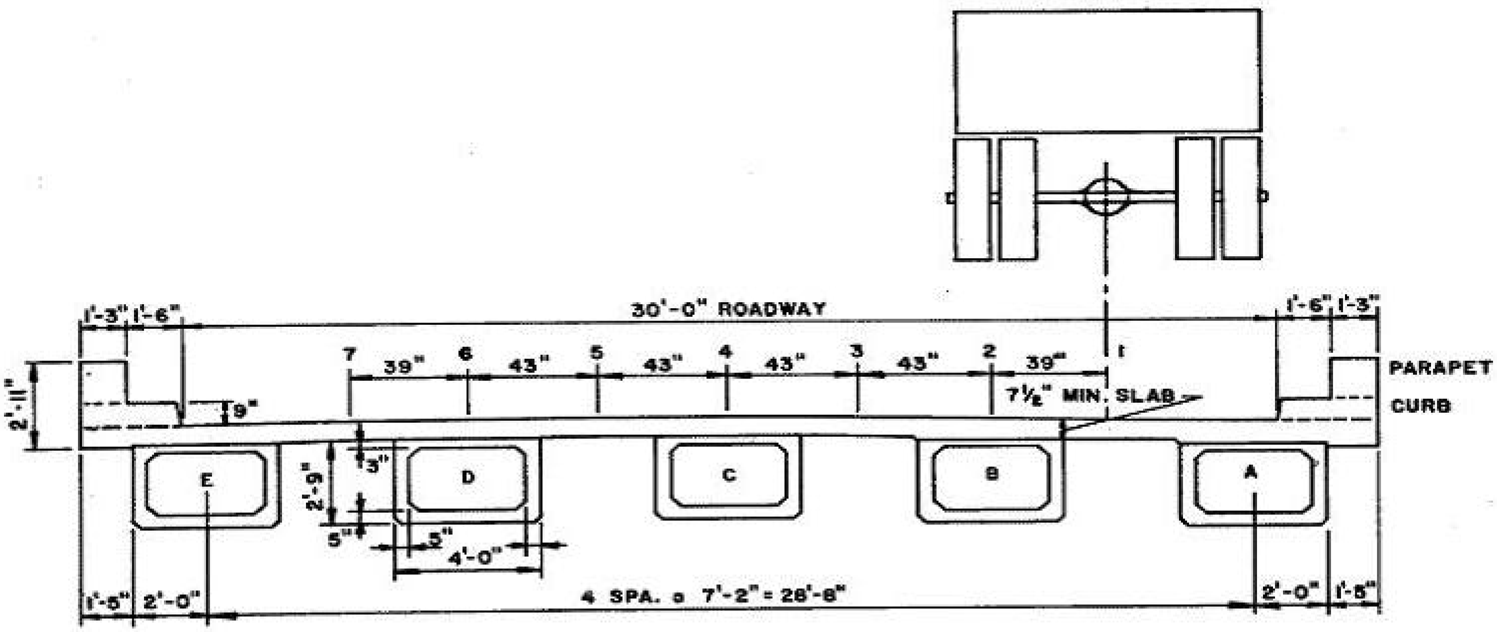

Figure 7.2. Cross-section of Derhersville Bridge and Centerlines of Loading Lanes (Douglas 1966).

A three-dimensional FEM model was developed for the test span of the Derhersville Bridge. Commercially available FEM analysis software, ANSYS version 8.0, was used for the analysis. The eccentricity of the centroids of the spread box girders, and curb and parapet was modeled with a rigid link element and assuming 100 percent composite action of these elements with the deck slab. The mesh was generated with all the nodes spaced at 6 in. from the adjacent nodes. The total count of nodes in the mesh representing the deck was 7564 and the beam elements were meshed into 124 nodes. The total number of nodes in the entire model was 8432. The idealized FEM model is superimposed on the actual bridge section in Figure 7.3. The truck axle load, as shown in Figure 7.4, was statically distributed to the closest nodes. Hinge support was considered at one end of the bridge and a roller support was considered at the other end of the bridge.

Based on the analyses conducted by Chen and Aswad (1996) for spread box girders, two elements from the ANSYS element library, BEAM44 and SHELL63, are appropriate for this study. BEAM44 element is a uniaxial element with tension, compression, torsion, and bending capabilities, while SHELL63 element has bending and membrane capabilities. Both the elements are three-dimensional elements with six degrees of freedom at each node (i.e., translation in nodal x, y, and z directions and rotations about nodal x, y, and z directions). The spread box beams were modeled with a BEAM44 element and the deck slab was modeled with a SHELL63 element. The parapet and curb were modeled with a BEAM44 element.

Figure 7.2 shows the location of seven loading lanes on the roadway. These lanes are selected such that the truck centerline closely corresponds to the girder centerline or to a line midway between girder centerlines. For the purpose of comparison only the results for the two cases of loading lanes are shown in this study: (1) Lane 4 loaded, (2) Lanes 1 and 4 loaded. The results are presented in Tables 7.4 and 7.5 and Figure 7.5. For interior girder C, the moment value of the FEM analysis is 8 and 18 percent higher than that of the moment values determined experimentally, while for the exterior girder A this difference is 41 and 25 percent less than that of the values determined experimentally.

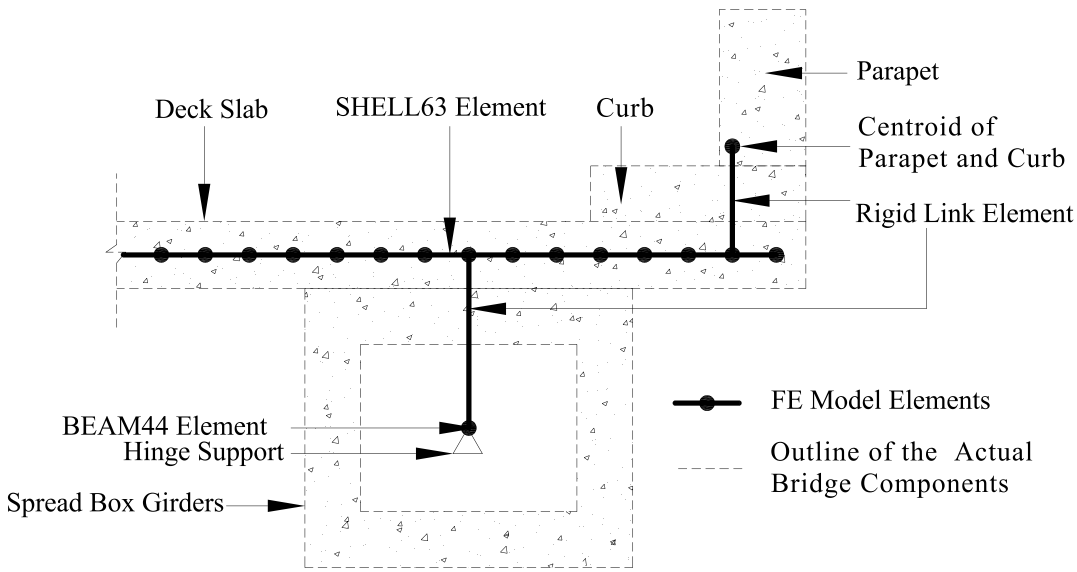

Figure 7.3. Illustration of the Finite Element Model Used for Verification.

Table 7.4. Comparison of Experimental Results and FEM Analysis Results (Lanes 1 and 4 Loaded).

Girder Location (See Fig. 7.2)	Experiment (k-ft.)	FEM (k-ft.)	Difference (%)
A	477.12	280.00	41
B	373.03	339.63	9
C	273.76	295.60	-8

Note: The comparison is made between respective bending moment values at section M as shown in Figure 7.1.

Table 7.5. Comparison of Experimental Results and FEM Analysis Results (Lane 4 Loaded).

Girder Location (See Fig. 7.2)	Experiment (k-ft.)	FEM (k-ft.)	Difference (%)
A	144.01	108.51	25
B	158.50	162.68	-3
C	178.35	210.93	-18
D	135.48	162.68	-20
E	131.96	108.51	18

Note: The comparison is made between respective bending moment values at section M as shown in Figure 7.1.

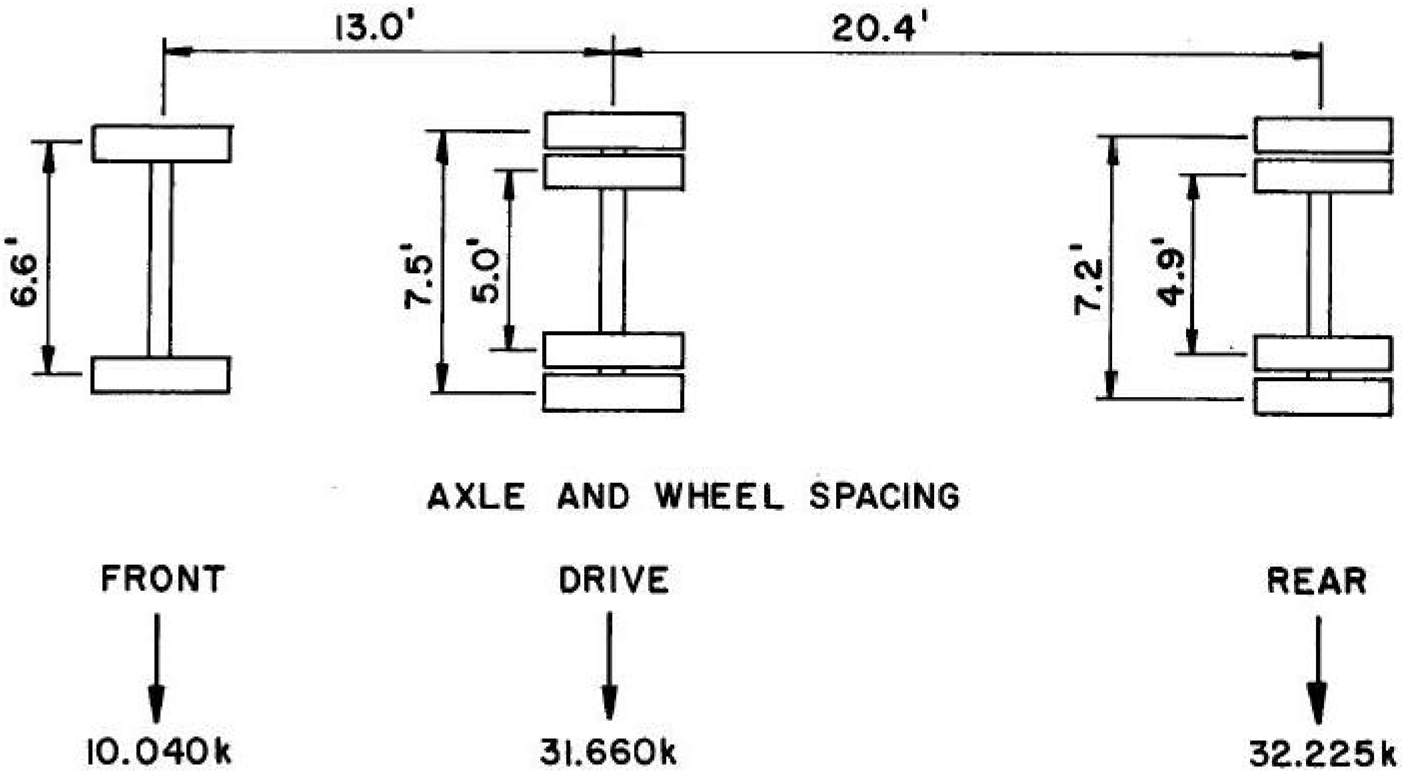

Figure 7.4. Axle Loads of the Test Vehicle Used in the Verification of Finite Element Model (Douglas 1966).

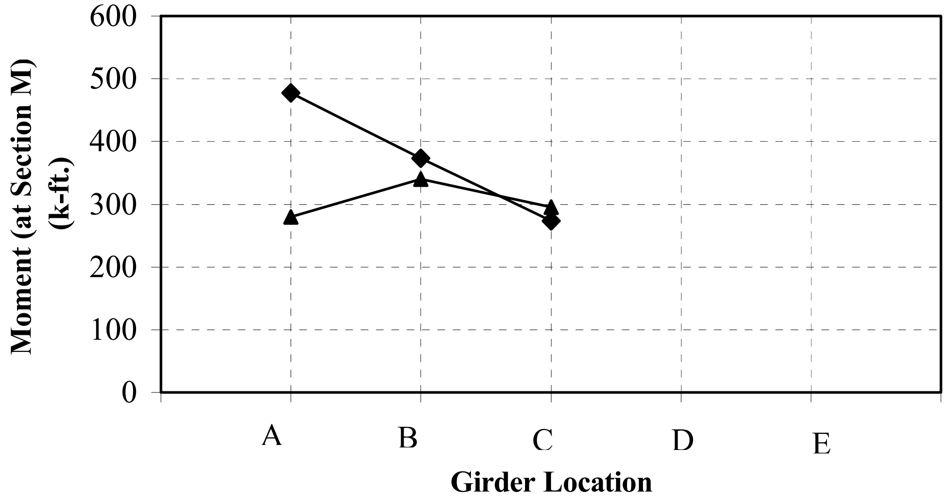

(a) Lanes 1 and 4 Loaded

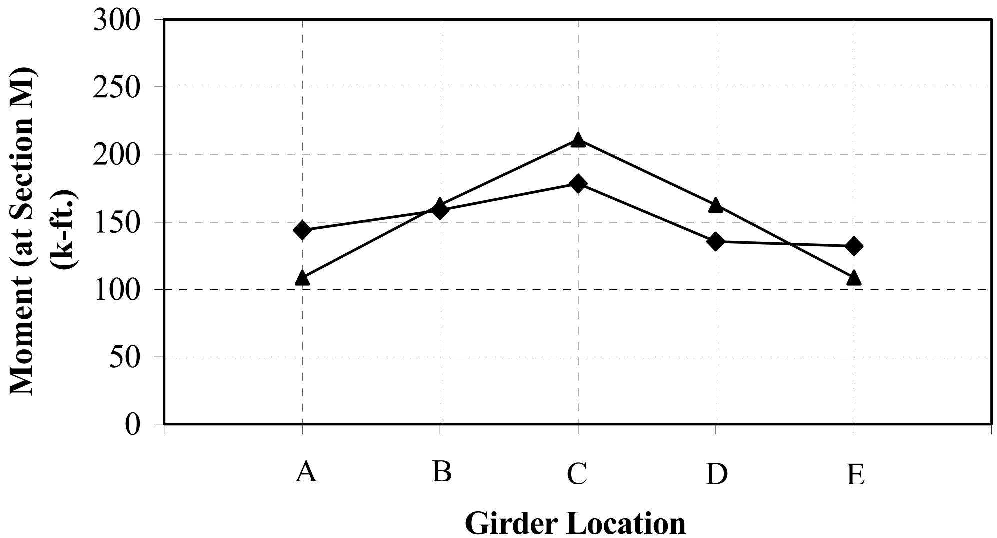

(b) Lane 4 Loaded

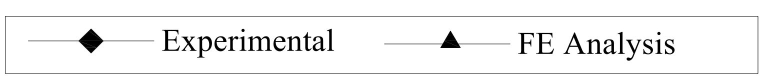

Figure 7.5. Comparison of Experimental Results versus FEM Results.

7.4.2.3 Calibration of Grillage Model

7.4.2.3.1 General. The grillage analogy is an approximate method of analysis in which a bridge superstructure is modeled as an equivalent grillage of rigidly connected beams at discrete nodes. The geometry and properties of the network of grillage beams, support conditions, and application of loads should be such that if the real bridge superstructure and the equivalent grillage are subjected to the same deflections and rotations at the grillage nodes, the resulting force response in both the structures should be equivalent. This section discusses the approach and results of calibration of the grillage model with respect to the results of the FEM analysis. The grillage model developed in this section is used to analyze the two cases described in Table 7.3. The FEM model of the U54 girder bridge shown in Figure 3.5 was developed based on the modeling approach discussed above.

7.4.2.3.2 Grillage Models. The development of the grillage model is discussed in detail below and is not repeated here. Only the differences are highlighted in this section. The calibration procedure was performed for a U54 girder bridge with 110 ft. span length and 8.5 ft. girder spacing with five U54 girders. Two grillage models were selected: the first model with one longitudinal grillage member representing each web of a U54 girder (see Figure 7.6), and the second model with one longitudinal grillage member representing a U54 girder (see Figure 7.7). Both of these models included supports with torsional restraint and edge longitudinal members. Moreover, the transverse grillage members that coincided with the end and intermediate diaphragm locations were assigned the section properties corresponding to the end and intermediate diaphragms described below. The transverse grillage members were spaced at 5 ft. center-to-center. The distance between the two longitudinal members, representing a U54 girder, was taken to be 65 in. for Grillage Model No. 1 (see Figure 7.8). For Grillage Model No. 2, the distance between adjacent longitudinal members was 102 in., corresponding to the girder spacing.

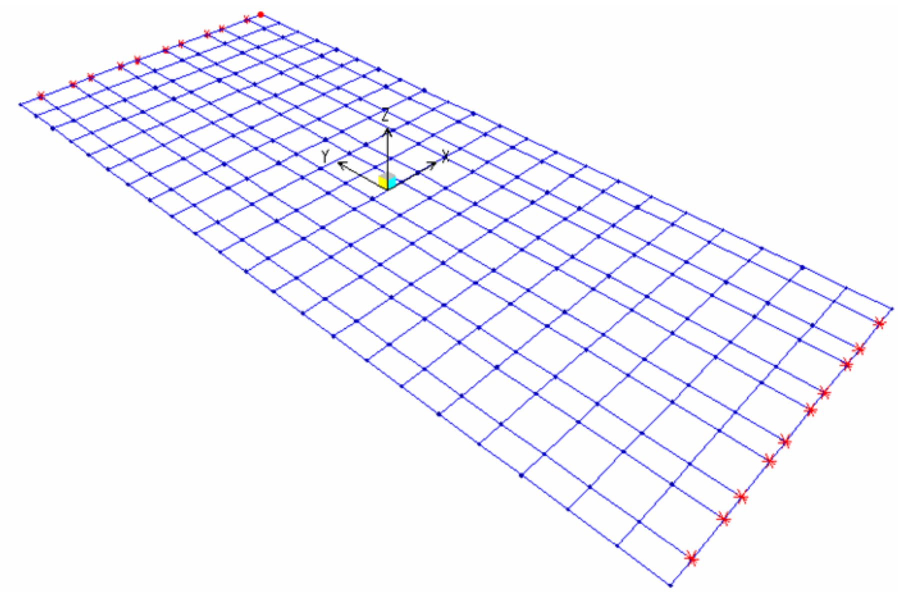

Figure 7.6. Grillage Model No. 1.

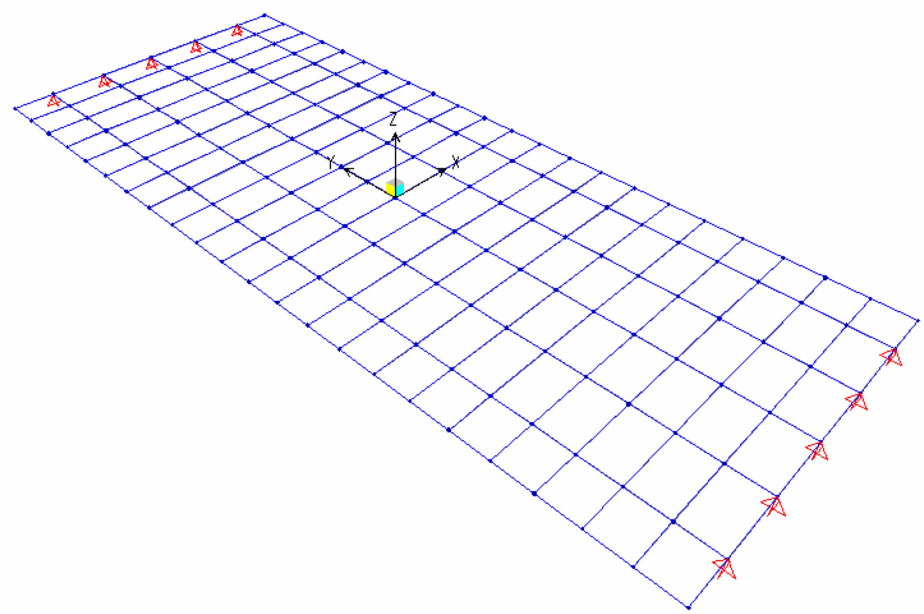

Figure 7.7. Grillage Model No. 2.

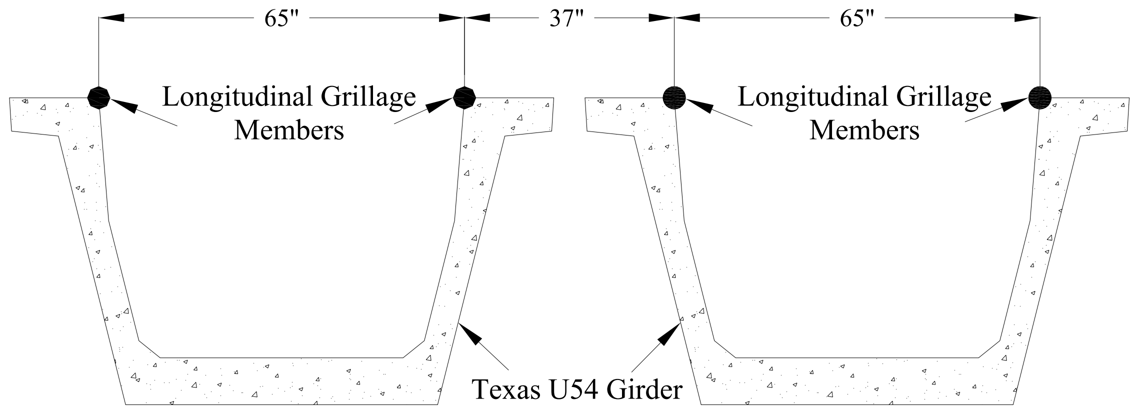

Figure 7.8. Location of Longitudinal Member for Grillage Model No. 1.

7.4.2.3.3 Comparison of Results. The analysis results from Grillage Models No. 1 and No. 2 were compared with those of the FEM analysis and are presented in Tables 7.6 and 7.7, respectively. It may be observed, that Grillage Model No. 1 yields results that are closer to the FEM analysis results. However, the difference is not large. For Grillage Model No. 1, the maximum difference is 4 percent for the interior girder and 8 percent for the exterior girder. For Grillage Model No. 2, the maximum difference is 8 percent and 11 percent for the interior and exterior girders, respectively.

Table 7.6. Comparison of FEM Analysis Results to Grillage Model No. 1.

No. of Lanes Loaded	Moment (k-ft.)			
	Interior Girder		Exterior Girder	
	FEM	Grillage	FEM	Grillage
One	381	396	557	513
Two or More	1116	1101	1246	1148

Table 7.7. Comparison of FEM Analysis Results to Grillage Model No. 2.

No. of Lanes Loaded	Moment (k-ft.)			
	Interior Girder		Exterior Girder	
	FEM	Grillage	FEM	Grillage
One	381	412	557	496
Two or More	1116	1080	1246	1114

Grillage Model No. 1 was further calibrated for several conditions and all the analysis cases are described in Table 7.8. The results of grillage analyses for cases 1 through 4 and their comparison with the FEM analysis results are presented in Table 7.9. Case 4 yields results closest to those of FEM analysis for the interior girder, and Case 1 yields results that are closest to the FEM analysis for the exterior girder. Case 4 is selected as the final grillage model, as the focus of this study is only on the interior girders.

Table 7.8. Cases for Further Calibration of Grillage Model No. 1.

Condition	Case 1	Case 2	Case 3	Case 4
Torsional Restraint Provided	no	yes	yes	Yes
Section Properties of Intermediate and End Diaphragm Provided	no	no	yes	Yes
Edge Longitudinal Members Provided	no	no	no	Yes

Table 7.9. Comparison of Results for Calibration of Grillage Model No. 1.

Case	No. of Lanes Loaded	Moment (k-ft.)			
		Interior Girder		Exterior Girder	
		FEM	Grillage	FEM	Grillage
1	One	381	441	557	567
	Two or More	1116	1152	1246	1218
2	One	381	431	557	548
	Two or More	1116	1140	1246	1195
3	One	381	429	557	513
	Two or More	1116	1101	1246	1148
4	One	381	419	557	529
	Two or More	1116	1127	1246	1182

7.4.2.4 Grillage Model Development

7.4.2.4.1 General. This section discusses the procedure of idealizing the physical bridge superstructure into an equivalent grillage model. The properties of longitudinal and transverse grid members are evaluated and support conditions are specified. The grillage model is developed based on the guidelines in the available literature such as Hambly (1991) and Zokaie et al. (1991). The grillage model was modeled and analyzed as a grid of beam elements by SAP2000, a program for structural analysis (SAP2000 Version 8).

7.4.2.4.2 Grillage Model Geometry. The bridge cross-section shown in Figure 3.5 was modeled with a set of longitudinal and transverse beam elements. Figure 7.9 shows the placement of transverse and longitudinal grillage members adopted in this study. The grillage members are placed in the direction of principle strengths. Two longitudinal grillage members were placed for each U54 girder, representing each web of the girder. The longitudinal grillage members are aligned in the direction of skew because the deck will tend to span in the skew direction. The longitudinal members are skewed at 60 degrees with the support centerline. The transverse grillage members are oriented perpendicular to the longitudinal grillage members as shown in Figure 7.9.

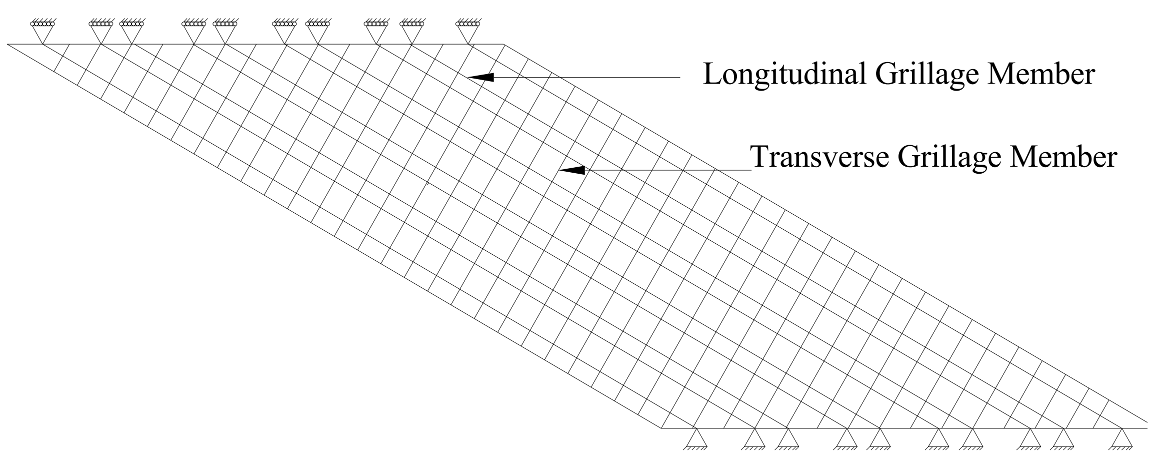

Figure 7.9. Grillage Model (for 60-Degree Skew).

7.4.2.4.3 Grillage Member Properties and Support Conditions. Grillage analysis requires the calculation of the moment of inertia, *I*, and torsional moment of inertia, *J,* for every grillage member. The LRFD commentary C.4.6.2.2.1 allows the use of the following relationships to determine the St. Venant's torsional inertia, J, instead of a more detailed evaluation.

1. For thin-walled open beams:

$$J = \frac{1}{3}\sum bt^3 \tag{7.1}$$

2. For stocky open sections (e.g., prestressed I-beams and T-beams) and solid sections:

$$J = \frac{A^4}{40.0 I_p} \tag{7.2}$$

3. For closed thin-walled shapes:

$$J = \frac{4A_o^2}{\sum \frac{s}{t}} \tag{7.3}$$

where:

b = Width of plate element, in.

t = Thickness of plate-like element, in.

A = Area of cross-section, in.^{2}

I_p = Polar moment of inertia, in.^{4}

A_o = Area enclosed by centerlines of elements, in.^{2}

s = Length of a side element, in.

Longitudinal grillage members distribute the live load in the longitudinal direction. Two longitudinal members are placed along each U54 beam, one along each web as recommended by Hambly (1991). The longitudinal girder moment of inertia is taken as the composite inertia of the girder with the contributing slab width for compositely designed U54 beams.

The St. Venant's torsional stiffness constant for a composite U54 beam bridge girder cross-section can be calculated by Equation 7.3 as it corresponds to a closed thin-walled shape. The quantities A_o and $\Sigma s/t$ for the composite section shown in Figure 7.10 are calculated and values are listed in Table 7.10. The torsional stiffness constant, J, and the moment of inertia, I, are also calculated and listed in Table 7.10. Because two longitudinal grillage members were used for each U54 beam, both inertia values are taken as half (i.e., I = 503,500 in.^{4} and J= 653,326.5 in.^{4}).

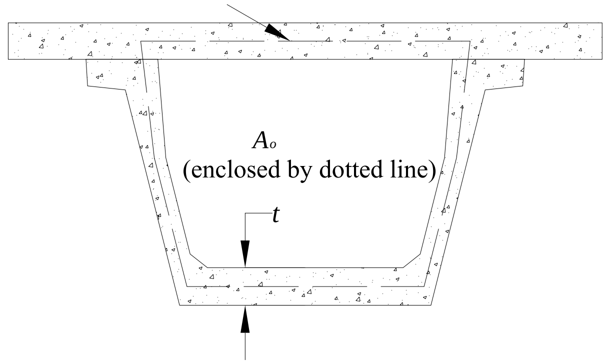

Figure 7.10. Calculation of St. Venant's Torsional Stiffness Constant for Composite U54 Girder.

Table 7.10. Composite Section Properties for U54 Girder.

A_o (in.^{2})	$\Sigma s/t$	J (in.^{4})	I (in.^{4})
3453	36.5	1,306,653	1,007,000

7.4.2.4.4 Edge Stiffening Elements. The edge stiffening elements represent the T501 rails that were used in this study as per TxDOT practice. To simplify the calculations, the T501 rail is approximated as a combination of two rectangular sections joined together as shown in Figure 7.11. The dimensions of the equivalent rectangular shape are selected such that the area is equal to the actual area of the T501 type barrier. Note that the effect of the edge stiffening elements was ignored during the development of the LRFD live load distribution factor formulas by Zokaie et al. (1991).

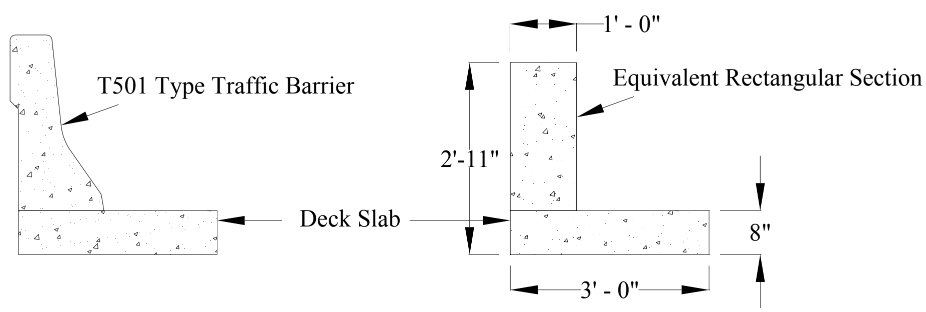

Figure 7.11. T501 Type Traffic Barrier and Equivalent Rectangular Section.

The St. Venant's torsional stiffness constant for the T501 rail or the equivalent rectangular section, which falls into the category of stocky open sections, was calculated by Equation 7.2. The torsional stiffness constant for the equivalent section is 28,088 in.^{4} and the moment of inertia for the equivalent section is 67,913 in.^{4}

7.4.2.4.5 Transverse Grillage Members. Transverse grillage members distribute the live load in the transverse direction. The number of transverse grillage members needed depends upon the type of results desired and the applied loading conditions. As the grillage mesh gets coarser, the load application becomes more approximate and a finer grillage mesh ensures not only a better result, but also the load application tends to be more exact. In this study, the grillage members are spaced 5 ft. center-to-center, so that errors introduced in applying the loads to the nodal locations is minimized. Zokaie et al. (1991) recommended that transverse grillage spacing should be less than 1/10 of the effective span length, and Hambly (1991) recommends less than 1/12 of the effective span length. The effective span length is the distance between the support centerlines, and transverse grillage spacing was taken as 1/28 of the effective span length for 140 ft. span length and 1/30 of the effective span length for 150 ft.

7.4.2.4.6 Bridge Deck in Transverse Direction. In the transverse direction where no diaphragms are present, the transverse grillage members are modeled as a rectangular section of the deck slab with a thickness of 8 in. and a tributary width of 60 in. The St. Venant's torsional stiffness constant for both diaphragm types, which can be treated as thin-walled open sections, is calculated by Equation 7.1. The resulting torsional stiffness constant and the moment of inertia for the general transverse grillage members is calculated to be 10,240 in.^{4} and 5120 in.^{4}, respectively.

7.4.2.4.7 End Diaphragms and Intermediate Diaphragms. The TxDOT Bridge Design Manual (TxDOT 2001) requires intermediate and end diaphragms in a Texas U54 beam type bridge. The idealized composite cross-sections considered for the end and intermediate diaphragms are shown in the Figure 7.12. The end diaphragm has a web thickness of 24 in., while the intermediate diaphragm has a web thickness of 13 in. Because the transverse grid members are spaced at 5 ft. center-to-center, the tributary width of the deck slab contributing to each diaphragm is taken to be 60 in. The St. Venant's torsional stiffness constant for both the diaphragm types, which can be treated as stocky open sections, is calculated by Equation 7.2. The torsional stiffness constant and the moment of inertia for the end diaphragm were calculated to be 194,347 in.^{4} and 1,073,566 in.^{4}, respectively. The torsional stiffness constant and the moment of inertia for the intermediate diaphragm is calculated to be 39,621 in.^{4} and 1,077,768 in.^{4}, respectively.

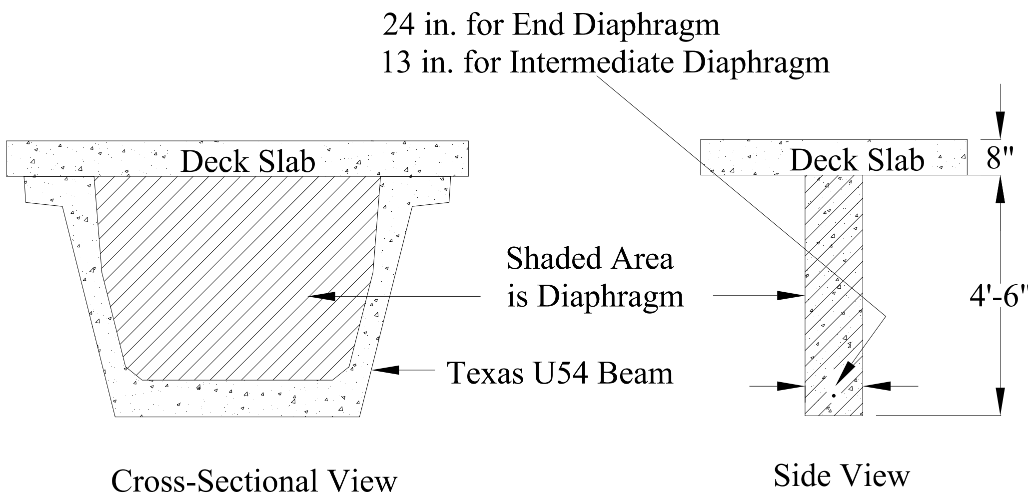

Figure 7.12. Cross-Sections of End and Intermediate Diaphragms.

7.4.2.4.8 Support Conditions. Because of the large transverse diaphragms at the supports, the torsional rotation of the longitudinal grillage members was fixed at the supports. Moreover, the translation was fixed in all three directions.

7.4.2.5 Application of HL-93 Design Truck Live Load

The HL-93 design live load truck was placed to produce the maximum response in the girders. In the case of bending moment, the resultant of the three axles of the HL-93 design truck was made coincident with the midspan location of the bridge. In the case of shear force calculations, the 32 kip axle of the HL-93 design truck was placed on the support location. In the transverse direction, first the HL-93 design truck is placed at 2 ft. from the edge of the barrier and all other trucks were placed at 4 ft. distance from each neighboring truck. The truck placement is shown in Figures 7.13 and 7.14. Several lanes were loaded with the design truck, and different combinations of the loaded lanes were considered and the maximum results were selected. After placement of the design truck, the wheel line load for each axle was distributed proportionally in the transverse direction to the adjacent longitudinal grillage members.

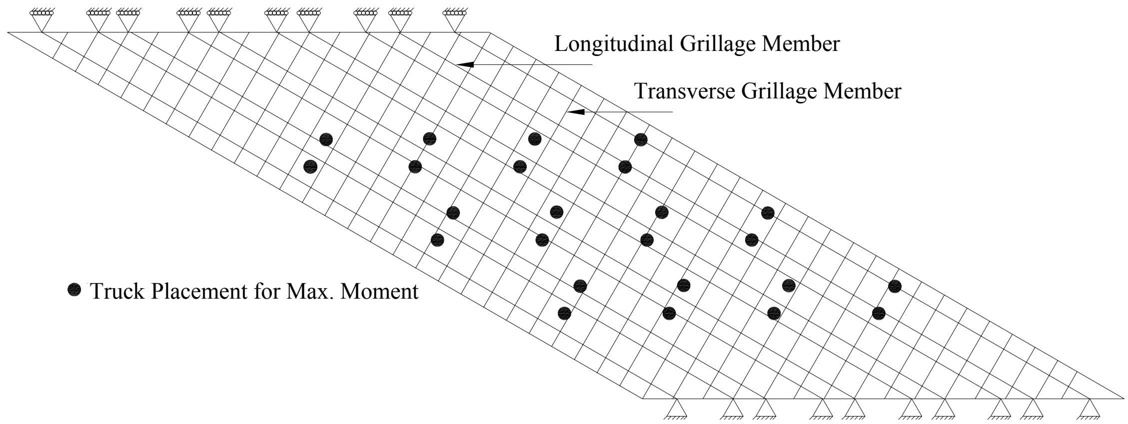

Figure 7.13. Application of Design Truck Live Load for Maximum Moment on Grillage Model.

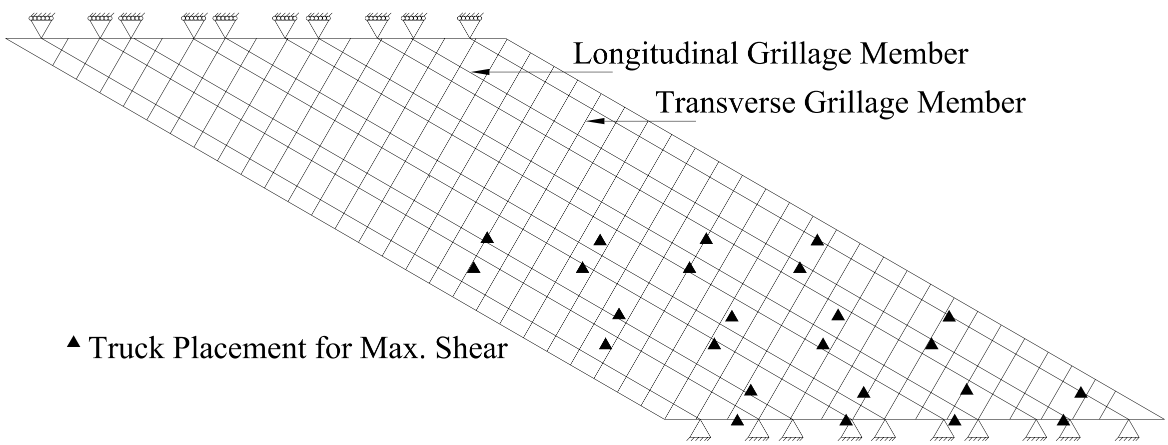

Figure 7.14. Application of Design Truck Live Load for Maximum Shear on Grillage Model.

7.4.2.6 Grillage Analysis and Results

The maximum girder moments and support shears were noted from the analysis of the grillage model for both the exterior and interior beams. After determining the moment and shear values from the grillage analysis, the moment and shear DFs were calculated to compare them with the LRFD DFs. The maximum distribution factor is the maximum force in a bridge girder divided by the maximum force produced by loading a simply supported beam with an axle load of the HL-93 design truck in the longitudinal location. The design truck placement on a simply supported beam for moment and shear is shown in Figure 7.15. The DFs from the grillage analysis results are calculated by the following equation.

$$DF = \frac{N_{grillage}}{N_{SS}} \tag{7.4}$$

where:

$N_{grillage}$ = Maximum moment or shear in a bridge girder calculated by the grillage analysis

N_{SS} = Maximum moment or shear calculated by loading a simply supported beam in the same longitudinal direction with the same load placement as the grillage analysis

The multiple presence factor is taken into account for cases of two or more lanes loaded by multiplying the DF, from Equation 7.4, by the appropriate multiple presence factor from Table 7.11, which provides the values recommended in LRFD Art. 3.6.1.1.2. Multiple presence factors are intended to account for the probability of simultaneous lane occupation by the full HL-93 design live load.

Table 7.11. LRFD Multiple Presence Factors.

No. of Lanes	Factors
One	1.20
Two	1.00
Three	0.85
More than Three	0.65

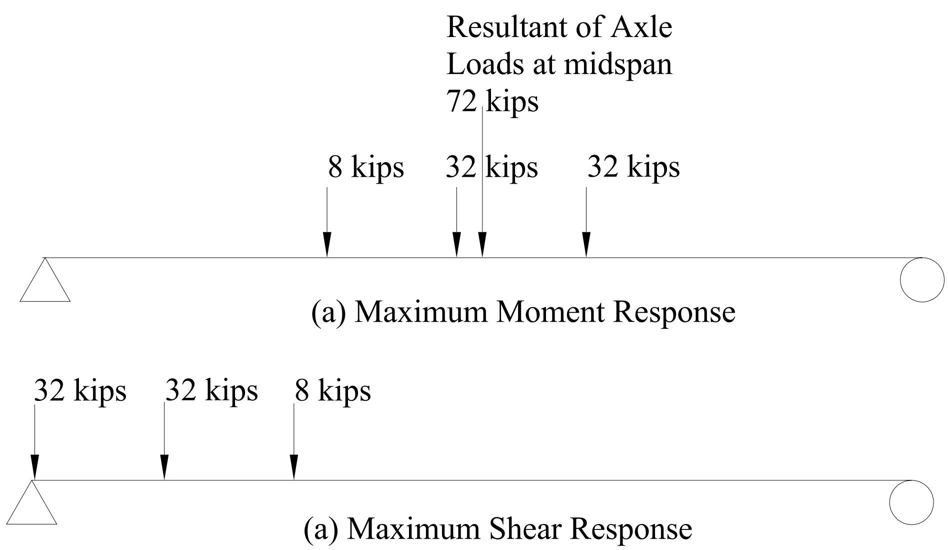

Figure 7.15. Design Truck Load Placement on a Simply Supported Beam for Maximum Response.

Based on the load placement shown in Figure 7.15, the maximum moments and shears for a simply supported beam are calculated for the two span lengths of 140 ft. and 150 ft., and are given in Table 7.12 below.

Table 7.12. Simply Support Beam Maximum Forces.

Span Length (ft.)	Moment (k-ft.)	Shear (kips)
140	2240	67.2
150	2420	67.5

The live load DFs based on LRFD Art. 4.6.2.2. were calculated for the purpose of comparison with those found by the grillage analysis method. The DFs for interior and exterior girders, for one lane and two or more lanes loaded, and for shear and moments are summarized in Table 7.13. As recommended in LRFD Table 4.6.2.2.3b-1 and LRFD Table 4.6.2.2.2d-1, the DFs for exterior girders and one lane loaded case are relatively large because these are calculated by the lever rule method as per LRFD Specifications, which gives very conservative results. For comparison, the DF computed using the LRFD approximations are provided in parentheses.

Table 7.13. LRFD Live Load Moment and Shear Distribution Factors.

Span Length (ft.)	No. of Lanes Loaded	Moment		Shear	
		Interior Girder	Exterior Girder	Interior Girder	Exterior Girder
140	One	0.187	1.200 (0.357)	0.643	2.220 (1.513)
	Two or More	0.340	0.357	0.792	1.513
150	One	0.180	0.740 (0.350)	0.639	2.260 (1.530)
	Two or More	0.333	0.350	0.787	1.530

Tables 7.14 and 7.15 summarize the findings of this section by comparing the live load DFs from the grillage analysis with those calculated by the LRFD Specifications for moment and shear, respectively. In general, the grillage analysis results are always conservative with respect to those of the LRFD Specifications. The difference for shear DFs for exterior girders is relatively large as compared to the difference for moment DFs and shear DFs for interior girders. This trend has two explanations: (1) for exterior girders with one lane loaded, the DFs are calculated by the lever rule method that gives very conservative results; and (2) for shear in exterior girders the LRFD Specifications specify large shear correction factors for skewed bridges. Thus, based on the results of the grillage analysis it can be concluded that the LRFD distribution factor formulas are conservative. However, a more refined analysis, such as a finite element analysis, may be beneficial in providing further validation of the results of the grillage analysis results presented in this section.

Table 7.14. Comparison of Moment DFs.

Span Length (ft.)	No. of Lanes Loaded	Moment			
		Interior Girder		Exterior Girder	
		LRFD DF	Grillage DF	LRFD DF	Grillage DF
140	One	0.187	0.152	1.200	0.200
	Two or More	0.340	0.250	0.357	0.293
150	One	0.180	0.178	0.740	0.212
	Two or More	0.333	0.280	0.350	0.310

Table 7.15. Comparison of Shear DFs.

Span Length (ft.)	No. of Lanes Loaded	Shear			
		Interior Girder		Exterior Girder	
		LRFD DF	Grillage DF	LRFD DF	Grillage DF
140	One	0.643	0.450	2.220 (1.513)	0.786
	Two or More	0.792	0.678	1.513	0.914
150	One	0.639	0.529	2.260 (1.530)	0.790
	Two or More	0.787	0.750	1.530	0.950

8. SUMMARY, CONCLUSIONS, AND RECOMMENDATIONS

8.1 SUMMARY

This report summarizes the results of a TxDOT sponsored research project conducted to evaluate the impact of the AASHTO LRFD Bridge Design Specifications (3rd edition) on the design of prestressed concrete bridge girders as compared to the AASHTO Standard Specifications for Highway Bridges (17th edition). The study was limited to single-span Type C, AASHTO Type IV, and Texas U54 bridge girders. The impact of the LRFD Specifications was evaluated for the flexural service, flexural strength, and shear strength limit states. When comparing the two specifications, differences were observed in the live load moments and shears, distribution factors, prestress losses, and flexural strength estimates. However, major differences were observed in the design requirements for transverse and interface shear. The impact of new interface shear provisions currently being considered for inclusion in the LRFD Specifications was assessed. The findings of this study provide information on how design parameters are affected by the transition to the LRFD Specifications.

Several tasks were completed as part of this research project. First, a review of the available literature on the development of AASHTO LRFD Specifications and related issues was carried out. A brief summary of the findings was documented. Second, detailed design examples were prepared as a reference for bridge engineers to follow step-by-step designs based on the Standard and LRFD Specifications (see Volume II of this report). Third, the simplification made by TxDOT in the bridge design by using the modular ratio between slab and girder concrete as unity was evaluated for its applicability when using the AASHTO LRFD Specifications. Fourth, a parametric study based on parameters representative of Texas bridges was conducted to investigate the impact of the AASHTO LRFD Specifications on the design as compared to the AASHTO Standard Specifications. The impact of the LRFD Specifications on service design, ultimate flexural design, shear design, and camber was evaluated. Fifth, based on the results from the parametric study, areas where major differences were occurring in the design were identified. Additional information and recommendations for these critical design issues have been provided to assist the implementation of the LRFD Specifications for TxDOT bridge designs.

The following major changes were found between the Standard and LRFD Specifications. Additional detail is provided in Chapters 2 and 3. Detailed design examples are provided in Volume II of this report.

1. The live load model has changed significantly. The Standard Specifications use the greater of an HS-20 truck or lane loading for live load. The LRFD Specifications use an HL-93 model, which is the greater of the combination of HS-20 truck and lane loading and tandem and lane loading.
2. The dynamic load (impact) factor has changed. The impact factor is specified as 33 percent of live load in the LRFD Specifications, which is significantly greater than the impact factors obtained in the Standard design.
3. The load combinations provided by the LRFD Specifications are different from those specified by the Standard Specifications. A new load combination, Service III, is specified by the LRFD Specifications for the tensile stress check in prestressed concrete members. A factor of 0.8 is applied to the live load moments in this load combination. This decreases the design tensile stress in the girder, neutralizing the effect of increased live load moments. The load factors for the ultimate flexural design load combination, Strength I are less than the ones provided by the Standard Specifications.
4. The Standard Specifications for transverse shear design are based on a constant 45-degree truss analogy, whereas LRFD adopted a variable truss analogy based on the Modified Compression Field Theory (MCFT).
5. New interface shear provisions were introduced in the LRFD Specifications that lead to significant increases in the required shear reinforcement.

The impact of the above modifications, along with other differences in the Standard and LRFD Specifications, on the design of typical Texas prestressed concrete bridge girder is discussed below.

8.2 CONCLUSIONS

8.2.1 Type C and Type IV Girders

The following conclusions were derived from the parametric study for Type C and AASHTO Type IV girders. The following observations compare the trends for LRFD designs versus Standard designs.

1. The HL-93 live load model used in the LRFD Specifications yields significantly larger moments and shears as compared to the HS-20 truck load in the Standard Specifications.
2. The distributed live load moments for LRFD designs are greater than for the Standard designs. The distributed shear increased significantly as compared to the Standard Specifications.
3. The required number of strands for LRFD designs is slightly larger as compared to Standard designs. This increase is due to an increase in live load moments.
4. The required concrete strengths at release and at service for LRFD designs are slightly greater than the ones obtained in the Standard designs. This increase is due to an increase in the number of strands, which increases the stresses in the girder, requiring larger concrete strengths.
5. The overall impact of the LRFD Specifications on the flexural service load design of Type IV and Type C prestressed concrete bridge girders is very small. The LRFD designs are generally slightly conservative as compared to the Standard designs.
6. The effect of the LRFD Specifications on the maximum span length is negligible. Slightly smaller span lengths were achieved using the LRFD Specifications for skew angles less than 30-degrees. However, slightly larger span lengths were obtained when a 60-degree skew angle was used. This is due to the significant decrease in live load moments for skew angles greater than 30-degrees.
7. A significant change was observed in the transverse shear design. The area of transverse reinforcement increased up to 300 percent in some cases. This increase is due to a significant increase in the live load shear and a different methodology for transverse shear design used in the LRFD Specifications.
8. The interface shear reinforcement area increased significantly for LRFD designs. The increase is up to 300 percent in some cases and 200 percent in most cases. This increase is

due to conservative cohesion and friction factors specified by the LRFD Specifications, based on a pure shear friction model. However, the interface shear provisions proposed to be included in the LRFD Specifications in 2007 yield shear reinforcement areas that are comparable to the Standard Specifications.

8.2.2 Texas U54 Girders

The following conclusions were derived based on the parametric study for Texas U54 girders. The following observations compare the trends for LRFD designs versus Standard designs. Note that the trends do not always follow the same trends observed for the Type C and AASHTO Type IV girders.

1. The HL-93 live load model used in the LRFD Specifications yields significantly larger moments and shears as compared to the HS-20 truck load in the Standard Specifications.
2. The LRFD distributed live load moments are greater than the Standard designs for a 0-degree skew and for all spacings except 16.67 ft. For all other skew angles, the LRFD values were smaller, and this difference increased with an increase in skew angle.
3. The effect of the LRFD Specifications on the maximum span length varies with support skew, strand diameter, and girder spacing. In general, for 0.6 in. strands and girder spacings less than 11.5 ft., LRFD designs resulted in longer span lengths compared to that of the Standard Specifications by up to a difference of 10 ft. The LRFD designs resulted in longer span lengths compared to that of the Standard Specifications for girder spacing less than 11.5 ft. by up to 18.5 ft. The same trends were found for 0.5 in. strand diameter; however, the differences are smaller.
4. The required number of strands for LRFD designs is smaller as compared to Standard designs. For 0-, 15-, and 30-degree skews, this difference is from 1 to 10 fewer strands. For a 60-degree skew, this difference increases from 4 to 18 fewer strands relative to Standard designs.
5. The required concrete strengths at release and at service for LRFD designs are slightly greater than the ones obtained in the Standard designs. This increase is due to an increase in the number of strands, which increases the stresses in the girder, requiring larger concrete strengths.

6. Relative to the Standard Specifications, the difference in the required concrete strength at transfer for LRFD designs decreased with an increase in skew, girder spacing, and span length. The maximum difference in f'_{ci} was a decrease of about 25 percent.
7. Designs based on the LRFD Specifications tend to give a smaller (up to about 10 percent) estimate of the required concrete strength at service as compared to Standard designs. This difference remained relatively constant for different skews, girder spacings, and span length.
8. The LRFD undistributed live load shears were much larger relative to that calculated by the Standard Specifications (35 to 55.6 percent). The LRFD distributed live load shears were significantly larger than that of the Standard designs (24.5 to 55.7 percent). Except for the shorter spans for 8.5 ft. and 16.67 ft. girder spacings, the factored design shear for LRFD designs slightly increased with respect to that for corresponding Standard designs.
9. For all skews and both strand diameters, the transverse shear reinforcement area values calculated for LRFD designs are smaller compared to the Standard designs. In general, the difference increases with increasing girder spacing, while increasing span length has a very insignificant affect on this comparison. The transverse shear reinforcement requirement for LRFD designs decreased relative to Standard designs up to 0.47 in.^{2}/ft. (46.6 percent).
10. For all skews and both strand diameters, the interface shear reinforcement area for LRFD designs are larger compared to the Standard designs. The difference increases with increasing girder spacing and span length. The reinforcement area for LRFD designs increases relative to the Standard designs from 0.47 to 1.39 in.^{2} (148 to 443 percent). This increase is due to conservative cohesion and friction factors specified by the LRFD Specifications, based on a pure shear friction model. However, the interface shear provisions proposed to be included in the LRFD Specifications in 2007 will lead to reduced interface shear reinforcement requirements.

8.3 DESIGN ISSUES AND RECOMMENDATIONS

8.3.1 General

The following design issues associated with transitioning to the AASHTO LRFD Specifications were identified through the literature review and parametric study.

Recommendations are provided based on available information and findings, as presented in this report.

8.3.2 Partial Debonding of Prestressing Strands

The current LRFD debonding provisions limit debonding of strands to 25 percent per section and 40 percent per row. These limits pose serious restrictions on the design of Texas U54 bridges relative to TxDOT's typical current practices and would restrict the span capability for U54 girder designs. Based on research by Barnes, Burns, and Kreger (1999) and successful past practice by TxDOT, it is suggested that up to 75 percent of the strands may be debonded, if the following conditions are satisfied.

a) Cracking is prevented in or near the transfer length.
b) The AASHTO LRFD rules for terminating the tensile reinforcement are applied to the bonded length of prestressing strands.
c) The shear resistance at the regions where the strands are debonded is thoroughly investigated with due regard to the reduction in the horizontal force available, as recommended in the LRFD Commentary (Article C5.11.4.3).

8.3.3 Limitations of LRFD Approximate Methods of Load Distribution

The formulas given in the LRFD Specifications for the approximate load distribution have certain limitations on the bridge geometry. The limitations come from the database of bridges used to develop these formulas. Thus, it may not be a necessary conclusion that beyond these limitations, the LRFD distribution factor (DF) formulas will cease to give conservative estimates. However, it is important for the engineer to understand these limitations and to be cautious if applying these formulas to cases falling outside the given range of applicability.

8.3.3.1 Span Length Limitation

The use of the LRFD live load DF formulas is limited to spans no longer than 140 ft. The parametric study for U54 girders indicated that this limitation is slightly violated for the 8.5 ft. girder spacing with a 60-degree skew (corresponding maximum span = 144 ft.). Therefore, two cases were investigated using grillage analysis (spans of 140 ft. and 150 ft. with 8.5 ft. girder spacing and 60-degree skew).

It was determined that the live load DF for moment in both interior and exterior U54 girders, the LRFD approximate method is applicable and the limiting span length can be increased up to a 150 ft. Also, a similar recommendation is made for the live load DFs for shear in interior girders only. However, based on the results, it was concluded that the LRFD approximate shear DFs are very conservative when used for exterior U54 girders. Further research is recommended using a more rigorous analysis method, such as finite element analysis, to validate the results of the grillage analysis.

8.3.3.2 Number of Beams Limitation

The selected U54 girder spacings of 14 ft. and 16.67 ft. violate the LRFD provisions for uniform distribution of permanent dead loads [LRFD Art. 4.6.2.2], which among other requirements, requires the number of beams to be equal to or greater than four. For U54 girder spacings of 14 ft. and 16.67 ft., the possible number of girders that the standard bridge width, used in this study, can accommodate is three.

The permanent dead loads include self-weight of the girder, deck slab, diaphragm, wearing surface, and the railing. According to design recommendations for Texas U54 beams in the TxDOT Bridge Design Manual (TxDOT 2001), two-thirds of the railing dead load should be distributed to the exterior girder and one-third to the adjacent interior girder. In the bridge superstructures, where there are only three girders, according to this TxDOT recommendation all the girders will be designed for two-thirds of the total rail dead load. As the railing is closer to the exterior girders, this TxDOT provision will cause the uniform distribution for permanent dead loads (especially considering the effect of barrier/rail load) to be unconservative for exterior beams and conservative for interior beams.

The implication of this violation of the number of beams limit is that to determine the actual distribution of the permanent dead loads the bridge designer will have to perform a refined analysis method to determine the appropriate distribution of permanent loads for the bridge (LRFD Art. 4.6.2.2.). The use of refined analysis methods such as the finite element method can be uneconomical, time consuming, and cumbersome relative to the application of the aforementioned provision of the LRFD Art. 4.6.2.2.

A parametric study could be conducted for typical Texas U54 girder bridges, where the uniform distribution of permanent dead loads is validated for bridges with the number of beams equal to three by more rigorous refined analysis methods. Alternatively, as a conservative approach the exterior girder can be assumed to carry the entire barrier/rail dead load.

8.3.3.3 Edge Distance Parameter Limitation

The edge distance parameter, d_e, is defined as the distance from the exterior web of the exterior beam to the interior edge of the curb or traffic barrier. The LRFD Specifications do not give any guidelines for the exact determination of d_e for the case where the girders have inclined webs, as is the case with Texas U54 beams. Thus, based on the engineering judgment, a particular definition of d_e was adopted as shown in Figure 8.1.

If the distribution of live load and permanent dead loads is to be determined according to the LRFD Art. 4.6.2.2, then among other requirements, the edge distance parameter, d_e, must be equal to or less than 3.0 ft. unless otherwise specified. For exterior girders that are spread box beams, such as Texas U54 girders, the edge distance parameter, d_e, is required to be equal to or less than 4.5 ft.

For Texas U54 girder design, the TxDOT Bridge Design Manual (TxDOT 2001) requires the standard overhang dimension to be equal to or less than 6 ft. 9 in. measured from the centerline of the bottom of the exterior U-beam to the edge of the slab. So, for this standard overhang dimension, the distance from the edge of the bridge to the nominal face of the barrier to be 1 ft., and the definition of the edge distance parameter, d_e, as adopted by the research team (see Figure 8.1), d_e will be 3.0 ft. This value is acceptable for using the LRFD Specifications approximate method for load distribution. If a greater overhang is desired, the aforementioned limit will be exceeded and the designer will have to perform the refined analysis procedure to determine the appropriate load distribution. A parametric study could be conducted for typical Texas U54 girder bridges, where the load distribution is validated for bridges with $d_e \geq 3.0$ ft. by more rigorous refined analysis methods.

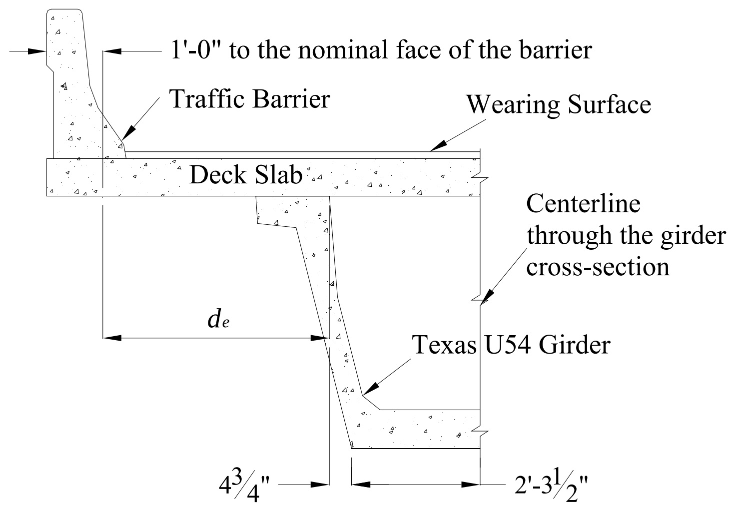

Figure 8.1. Definition of Edge Distance Parameter, d_e.

8.3.4 Modular Ratio

The evaluation of the impact of not updating the modular ratio was carried out for Type IV girder with 0-degree skew. The following are the findings from this evaluation. More information is provided in Section 3.10 and Adil (2005).

1. The impact of this practice is negligible in most of the cases evaluated. However, in a few cases a small difference was found, where the design using TxDOT methodology is on the unconservative side.
2. The LRFD live load moment and shear DFs were found to decrease by a small amount and consequently the live load moments and shears decreased slightly when the modular ratio was updated.
3. The service load design parameters, required number of strands, and required concrete strengths at service and at release were found to increase by a small amount in a few cases. There was no effect of updating the modular ratio for most of the cases.
4. The interface shear design is not affected by the process of updating the modular ratio. However, the transverse shear reinforcement area requirement decreased for a few cases due to increase in concrete strengths, which subsequently increases the shear capacity of concrete.
5. The camber decreased for a few cases, due to increase in the concrete strength which subsequently increases the elastic modulus of the concrete.

8.4 RECOMMENDATIONS FOR FUTURE RESEARCH

Based on the findings from this research project, the following recommendations are made for future studies.

1. Presently the LRFD Specifications are calibrated using a reliability approach for the ultimate design limit states. The service load design limit states need to be calibrated to obtain a more comprehensive reliability-based specification for prestressed concrete member design.
2. The use of the live load DFs specified by the LRFD Specifications is restricted to certain limits based on the bridge geometry. More research is needed to expand the approximate DFs specified by the LRFD Specifications, to a wider range of bridge configurations.
3. Transverse shear design using the MCFT is a relatively complex design process as compared to the approach in the Standard Specifications. Simplified approaches for implementing the MCFT design process for typical bridges would be helpful for routine design. Research is being carried out at the University of Illinois to arrive at simplified shear formulas. However, research is needed to determine the applicability of simplified formulas for typical Texas bridges.
4. The difference in the interface shear reinforcement area by the LRFD and Standard Specifications is very significant. New provisions currently under consideration for the 2007 LRFD Specifications should be considered when they are approved. In the interim, it is recommended that interface shear design criteria be based on successful past practices and research studies on typical Texas bridges.
5. The shear in exterior girders of a skewed bridge can significantly increase and, thus, it is strongly recommended that exterior girders should be designed for shear resistance based on the load distribution that takes into account the increased shear demand in obtuse corners of the bridge. Further study is also recommended to develop new, or verify the current formulas for, skew correction factors for shear in obtuse corners, for U54 girder spacings greater than 11.5 ft.

REFERENCES

AASHTO (1992), *Standard Specifications for Highway Bridges*, American Association of State Highway and Transportation Officials (AASHTO), Washington, D.C.

AASHTO (1994), *AASHTO LRFD Bridge Design Specifications*, 1st Ed., American Association of State Highway and Transportation Officials (AASHTO), Customary U.S. Units, Washington, D.C.

AASHTO (1998), *AASHTO LRFD Bridge Design Specifications*, 2nd Ed., American Association of State Highway and Transportation Officials (AASHTO), Customary U.S. Units, Washington, D.C.

AASHTO (2002), *Standard Specifications for Highway Bridges*, 17th Ed., American Association of State Highway and Transportation Officials (AASHTO), Inc., Washington, D.C.

AASHTO (2004), *AASHTO LRFD Bridge Design Specifications*, 3rd Ed., American Association of State Highway and Transportation Officials (AASHTO), Customary U.S. Units, Washington, D.C.

American Concrete Institute (ACI) (1989), "*Building Code Requirements for Reinforced Concrete and Commentary*," ACI 318-89 and ACI 318R-89, Detroit, Mich.

American Concrete Institute (ACI) (2002), "*Building Code Requirements for Structural Concrete and Commentary*," ACI 318-02 and ACI 318R-02, Farmington Hills, Mich.

Abdalla, O.A., J.A. Ramirez, and R.H. Lee (1993), "Strand Debonding in Pretensioned Beams: Precast Prestressed Concrete Bridges with Debonded Strands. Simply Supported Tests [PART 2]," *FHWA/INDOT/JHRP-92/25*, FHWA and Indiana Dept. of Transportation.

Adil, M. (2005), "Impact of AASHTO LRFD Bridge Design Specifications on the Design of Type C And AASHTO Type IV Girder Bridges," *M.S. Thesis*, Department of Civil Engineering, Texas A&M University, College Station.

Adnan, M. (2005), "Impact of AASHTO LRFD Specifications on the Design of Precast, Pretensioned U-Beam Bridges," *M.S. Thesis*, Department of Civil Engineering, Texas A&M University, College Station.

Aswad, A. and Y. Chen (1994), "Impact of LRFD Specification on Load Distribution of Prestressed Concrete Bridges," *PCI Journal*, 39(5), 78-89.

Bakht, B., and L.G. Jaeger (1982), "Simplified Methods of Bridge Analysis for the Third Edition of OHBDC," *Canadian Journal of Civil Engineering*, 19, 551-559.

Bakht, B., and L.G. Jaeger (1985), *Bridge Analysis Simplified*, McGraw Hill, Inc., New York, N.Y.

Barnes, R.W., N.H. Burns, and M.E. Kreger (1999), "Development Length of 0.6-inch Prestressing Strand in Standard I-Shaped Pretensioned Concrete Beams," *Research Report 1388-1*, Center for Transportation Research, The University of Texas at Austin.

Barr, J.P., O.M. Eberhard, and F.J. Stanton (2001), "Live-Load Distribution Factors in Prestressed Concrete Girder Bridges," ASCE *Journal of Bridge Engineering*, 6(5), 298-306.

Chen, Y., and A. Aswad (1996), "Stretching Span Capability of Prestressed Concrete Bridges under AASHTO LRFD," ASCE *Journal of Bridge Engineering*, 1(3), 112-120.

Cheung, M.S., B. Bakht, and L.G. Jaeger (1982), "Analysis of Box-Girder Bridges by Grillage and Orthotropic Plate Methods," *Canadian Journal of Civil Engineering*, 9, 595-601.

Computers & Structures, Inc. (CSI) (1998), SAP 2000 – Integrated Software for Structural Analysis and Design, Version 8, CSI, Berkeley, CA.

Crespo, M.C., and J.R. Casas (1998), "Fatigue Reliability Analysis of Prestressed Concrete Bridges," *Journal of Structural Engineering,* ASCE, 124(12), 1458-1466.

Cusens, A.R., and R.P. Pama (1975), *Bridge Deck Analysis*, John Wiley & Sons, Ltd., New York, N.Y.

Douglas, W.J., and D.A. Vanhorn (1966), "Lateral Distribution of Static Loads in Prestressed Concrete Box-Beam Bridge: Drehersville Bridge," *Fritz Engineering Laboratory Report No. 350.1*, Lehigh University, Bethlehem, Penn.

Eamon, C. D., and A.S. Nowak (2002), "Effects of Edge-Stiffening Elements and Diaphragms on Bridge Resistance and Load Distribution," ASCE *Journal of Bridge Engineering*, 7(5), 258-266.

Eby, C.C., J.M. Kulicki, and C.N. Kostem (1973), "The Evaluation of St. Venant Torsional Constants for Prestressed Concrete I-Beams," *Fritz Engineering Laboratory Report No. 400.12*, Lehigh University, Bethlehem, Penn.

Ellingwood, B., T.V. Galambos, J.G. MacGregor, and C.A. Cornell (1980), "Development of a Probability Based Load Criterion for American National Standard A58," *NBS Special Publication 577*, National Bureau of Standards, Washington, D.C.

Fu, G., and E.O. Hag (1996), "Bridge Live Load Model Including Overloads," *Proc. Specialty Conference on Probabilistic Mechanics and Structural and Geotechnical Reliability*, Worcester, Mass., 34-37.

Furr, H.L., R. Sinno and L.L. Ingram (1968), "Prestress Loss and Creep Camber in a Highway Bridge with Reinforced Concrete Slab on Prestressed Concrete Beams," *Texas Transportation Institute Report*, Texas A&M University, College Station.

Furr, H.L., and R. Sinno (1970) "Hyperbolic Functions for Prestress Loss and Camber," *Journal of the Structural Division*, 96 (4), pp. 803-821.

Hambly, E.C. and E. Pennells (1975), "Grillage Analysis Applied to Cellular Bridge Decks," *The Structural Engineer*, 53(7), 267-276.

Hambly, E.C. (1991), *Bridge Deck Behavior*, 2nd Ed., Chapman & Hall Inc., New York, N.Y.

Hueste, M.D., and G.G. Cuadros (2003), "Flexural Design of High Strength Concrete Prestressed Bridge Girders – Review of Current Practice and Parametric Study," *Report 2101-3*, Texas Transportation Institute and Texas Department of Transportation, 280 pages, College Station, Tex.

Huo, X.S., E.P. Wasserman, and P. Zhu (2004), "Simplified Method of Lateral Distribution of Live Load Moment," ASCE *Journal of Bridge Engineering*, 9(4), 382-390.

Hwang, E.S., and Nowak, A.S. (1991), "Simulation for Dynamic Load for Bridges," *Journal of Structural Engineering,* ASCE, 117(5), 1413-1434.

Jaeger, L.G. and B. Bakht (1982), "The Grillage Analogy in Bridge Analysis," *Canadian Journal of Civil Engineering*, 9, 224-235.

Khaloo, A.R., and H. Mirzabozorg (2003), "Load Distribution Factors in Simply Supported Skew Bridges," ASCE *Journal of Bridge Engineering*, 8(4), 241-244.

Kim, S.H., H.S. Park, and H.J. Hwang (1994), "Probabilistic Models of Bridge Live Loads," *Proc. 6th International Conference on Structural Safety and Reliability*, Balkema, Rotterdam, Vol. 2, 965.

Kocsis, P. (2004), "Evaluation of AASHTO Live Load and Line Load Distribution Factors for I-Girder Bridge Decks," ASCE Practice Periodical on Structural Design and Construction, 9(4), 211-215.

Krishnamurthy, D. (1971), "The Shear Strength of I-Beams with Debonded Tendons," *Materiaux et Constructions*, 4(22), 213-218.

Kulicki, J.M. (1994), "Development of Bridge Live Load Models," *Proceedings*, Structures Congress 94, Atlanta, Geor., 532-537.

Motarjemi, D., and Vanhorn, D.A. (1969), "Theoretical Analysis of Load Distribution in Prestressed Concrete Box-Beam Bridges," *Fritz Engineering Laboratory Report No. 315.9*, Lehigh University, Bethlehem, Penn.

Nowak, A.S., and Zhou, J.H. (1985), "Reliability Models for Bridge Analysis," *Report UMCE 85R3*, University of Michigan, Ann Arbor, Mich.

Nowak, A.S., J. Czernecki, J. Zhou, and R. Kayser (1987), "Design Loads for Future Bridges," *Report UMCE 87-1*, University of Michigan, Ann Arbor, Mich.

Nowak, A.S., and Y.K. Hong (1991), "Bridge Live Load Models," ASCE *Journal of Structural Engineering*, 117(9), 2757-2767.

Nowak A.S. (1993a), "Live Load Model for Highway Bridges," *Journal of Structural Safety*, 13 (1-2), 53-66.

Nowak, A.S. (1993b), "Calibration of LRFD Bridge Design Code," *Final Report*, National Cooperative Highway Research Program Project 12-33, December.

Nowak, A.S. (1993c), "Load Model for Highway Bridges," *IFIP Transactions B: Computer Applications in Technology*, n B-12, 1993, 17-30.

Nowak, A.S. (1993d), "Development of Bridge Load Model for LRFD Code," *Structural Engineering in Natural Hazards Mitigation, Proc. Structures Congress 93*, Irvine, Cal, 1041-1046.

Nowak, A.S. (1994), "Calibration of LRFD Bridge Design Code," *Proceedings*, 6th International Conference on Structural Safety and Reliability, 2, 927.

Nowak, A.S., A.S. Yamani, and S.W. Tabsh (1994), "Probabilistic Models for Resistance of Concrete Bridge Girders," *ACI Structural Journal*, 91(3), 269-276.

Nowak, A.S. (1995), "Calibration of LRFD Bridge Code," ASCE *Journal of Structural Engineering*, 121(8), 1245-1251.

Nowak, A.S. and V.K. Saraf (1996), "Target Safety Level for Bridges," Building an International Community of Structural Engineers, *Proceedings of Structures Congress*, 2, 696-703.

Nowak, A.S., and M.M. Szerszen (1996), "Bridge Load and Resistance Models," *Proceedings*, Conference on Structural Reliability in Bridge Engineering: Design and Workshop, D.M. Frangopol and G. Hearn (Editors), Boulder, Col., pp. 30-41.

Nowak, A.S. (1999), "Calibration of LRFD Bridge Design Code," *NCHRP Report No. 368*, National Research Council, Washington, D.C.

O'Brien, E.J., and D.L. Keogh (1999), *Bridge Deck Analysis*, Taylor & Francis Group, New York, N.Y.

PCI (2003), *Precast Prestressed Concrete Bridge Design Manual*, 2nd Ed., Precast/Prestressed Concrete Institute, Chicago, Ill.

Puckett, J.A. (2001), "Comparative Study of AASHTO Load and Resistance Factor Design Distribution Factors for Slab-Girder Bridges," *Transportation Research Record: Journal of the Transportation Research Board*, No. 1770.

Rackwitz, R., and B. Fiessler (1978), "Structural Reliability under Combined Random Load Sequences," *Computer and Structures*, 9, 489-494.

Ralls, M.L., L. Ybanez, and J.J. Panak (1993), "The Texas U-Beam Bridges: An Aesthetic and Economical Design Solution," *PCI Journal*, 38(5), pp. 20-29.

Richard, J.N., and E.R. Schmeckpeper (2002), "Single-Span Prestressed Girder Bridge: LRFD Design and Comparison," *Journal of Bridge Engineering*, ASCE, 7(1), 22-30.

Russell, B.W. and N.H. Burns (1993), "Design Guidelines for Transfer, Development and Debonding of Large Diameter Severn Wire Strands in Pretensioned Concrete Girders," *Research Report 1210-5F*, Center for Transportation Research, The University of Texas at Austin, Austin, TX, 286 pp.

Sanders, W.W., and H.A. Elleby (1970), "Distribution of Wheel Loads on Highway Bridges," *National Cooperative Highway Research Program Report 83*, Transportation Research Board, Washington, D.C.

Schwarz, M. and J.A. Laman (2001), Response of Prestressed Concrete I-Girder Bridges to Live Load, ASCE Journal of Bridge Engineering, 6(1), 1-8.

Shahawy, M.A., M. Issa, and B. deV Batchelor (1992), "Strand Transfer Lengths in Full Scale AASHTO Prestressed Concrete Girders," *PCI Journal*, 84-96.

Shahawy, M., and B. deV Batchelor (1992), "Bond and Shear Behavior of Prestressed AASHTO Type II Beams," *Progress Report*, Structural Research Center, Florida Department of Transportation, Tallahassee.

Shahawy, M., B. Robinson, and B. deV Batchelor (1993), "An Investigation of Shear Strength of Prestressed Concrete AASHTO Type II Girders," *Research Report*, Structures Research Center, Florida Department of Transportation, Tallahassee.

Shahawy, M.A., and B. deV Batchelor (1996), "Shear Behavior of Full-Scale Prestressed Concrete Girders: Comparison between AASHTO Specifications and LRFD Code," *PCI Journal*, 41(3), 48-62.

Sinno, R. (1968), "The Time-Dependent Deflections of Prestressed Concrete Bridge Beams," *Ph.D. Dissertation*, Texas A&M University, College Station.

Song, S.T., Y.H. Chai, and S.E. Hida (2003), "Live-Load Distribution Factors for Concrete Box-Girder Bridges," ASCE *Journal of Bridge Engineering*, 8(5), 273-280.

Tabsh, S.W. (1995), "Structural Safety of Post-Tensioned Concrete Slab Bridges with Unbonded Tendons," *ACI Materials Journal*, 92(4), 488-494.

Tobias, D.H., R.E. Anderson, S.Y. Khayyat, Z.B. Uzman, and K.L. Riechers (2004), "Simplified AASHTO Load and Resistance Factor Design Girder Live Load Distribution in Illinois," ASCE *Journal of Bridge Engineering*, 9(6), 606-613.

TxDOT (2001), *TxDOT Bridge Design Manual*, Bridge Division, Texas Department of Transportation, Austin, Tex.

TxDOT (2004), *Prestressed Concrete Beam Design/Analysis Program, User Guide*, Version 4.00, Bridge Division, Texas Department of Transportation, Austin, Tex.

Zokaie, T., T.A. Osterkamp, and R.A. Imbsen (1991), "Distribution of Wheel Loads on Highway Bridges," *NHCRP Project Report 12-26*, Transportation Research Board, Washington, D.C.

Zokaie, T., K.D. Mish, and R.A. Imbsen (1993), "Distribution of Wheel Loads on Highway Bridges, Phase III," *NCHRP Final Report 12-26(2)*, Transportation Research Board, Washington, D.C.

Zokaie, T. (2000), "AASHTO-LRFD Live Load Distribution Specifications," ASCE *Journal of Bridge Engineering*, 5(2), 131-138.

Zokaie, T., C. Harrington, and D.A. Tomley (2003), "Effect of the LRFD Specifications on the Design of Post-Tensioned Concrete Box Girder Bridges," *PTI Journal*, January, 72-77.

APPENDIX

ADDITIONAL PARAMETRIC STUDY RESULTS

FOR TEXAS U54 GIRDERS

Table A.1 Comparison of Distribution Factors (All Skews) for U54 Interior Beams.

Spacing (ft.)	Span (ft.)	All Skews	Skew = 0			Skew = 15			Skew = 30			Skew = 60		
		DF STD	DF LRFD	Diff.	% Diff. w.r.t STD	DF LRFD	Diff.	% Diff. w.r.t STD	DF LRFD	Diff.	% Diff. w.r.t STD	DF LRFD	Diff.	% Diff. w.r.t STD
8.50	90	0.900	0.616	-0.284	-31.6	0.605	-0.295	-32.8	0.557	-0.343	-38.1	0.380	-0.520	-57.8
	100		0.599	-0.301	-33.4	0.589	-0.311	-34.5	0.543	-0.357	-39.7	0.370	-0.530	-58.9
	110		0.585	-0.315	-35.0	0.575	-0.325	-36.1	0.530	-0.370	-41.1	0.361	-0.539	-59.9
	120		0.572	-0.328	-36.4	0.562	-0.338	-37.5	0.518	-0.382	-42.4	0.353	-0.547	-60.8
	130		0.561	-0.339	-37.7	0.551	-0.349	-38.8	0.508	-0.392	-43.6	0.346	-0.554	-61.6
	140		0.550	-0.350	-38.9	0.541	-0.359	-39.9	0.498	-0.402	-44.6	0.340	-0.560	-62.3
10.00	90	0.909	0.692	-0.217	-23.8	0.681	-0.228	-25.1	0.627	-0.282	-31.0	0.427	-0.482	-53.0
	100		0.674	-0.235	-25.8	0.663	-0.246	-27.1	0.611	-0.299	-32.8	0.416	-0.493	-54.2
	110		0.658	-0.251	-27.6	0.647	-0.262	-28.8	0.596	-0.313	-34.4	0.406	-0.503	-55.3
	120		0.644	-0.265	-29.2	0.633	-0.276	-30.4	0.583	-0.326	-35.9	0.397	-0.512	-56.3
	130		0.631	-0.278	-30.6	0.620	-0.289	-31.8	0.571	-0.338	-37.2	0.389	-0.520	-57.2
	140		0.619	-0.290	-31.9	0.609	-0.301	-33.1	0.561	-0.348	-38.3	0.382	-0.527	-58.0
11.50	90	1.046	0.766	-0.279	-26.7	0.753	-0.292	-27.9	0.694	-0.351	-33.6	0.473	-0.573	-54.8
	100		0.746	-0.299	-28.6	0.733	-0.312	-29.9	0.676	-0.370	-35.4	0.460	-0.585	-56.0
	110		0.728	-0.317	-30.3	0.716	-0.330	-31.5	0.660	-0.386	-36.9	0.449	-0.596	-57.0
	120		0.712	-0.333	-31.9	0.700	-0.345	-33.0	0.645	-0.400	-38.3	0.440	-0.606	-58.0
	130		0.698	-0.347	-33.2	0.686	-0.359	-34.4	0.632	-0.413	-39.5	0.431	-0.615	-58.8
	140		0.685	-0.360	-34.5	0.673	-0.372	-35.6	0.620	-0.425	-40.7	0.423	-0.623	-59.6
14.00	90	1.273	0.884	-0.389	-30.6	0.869	-0.404	-31.7	0.800	-0.472	-37.1	0.545	-0.727	-57.2
	100		0.860	-0.412	-32.4	0.846	-0.427	-33.5	0.779	-0.493	-38.8	0.531	-0.742	-58.3
	110		0.840	-0.433	-34.0	0.826	-0.447	-35.1	0.761	-0.512	-40.2	0.518	-0.755	-59.3
	120		0.822	-0.451	-35.4	0.808	-0.465	-36.5	0.744	-0.529	-41.5	0.507	-0.766	-60.2
	130		0.805	-0.468	-36.7	0.791	-0.481	-37.8	0.729	-0.544	-42.7	0.497	-0.776	-61.0
	140		0.790	-0.483	-37.9	0.777	-0.496	-39.0	0.716	-0.557	-43.8	0.487	-0.785	-61.7
16.67	90	1.516	1.003	-0.513	-33.8	0.986	-0.530	-34.9	0.908	-0.607	-40.1	0.619	-0.897	-59.2
	100		0.977	-0.539	-35.6	0.960	-0.556	-36.7	0.884	-0.631	-41.6	0.603	-0.913	-60.2
	110		0.953	-0.562	-37.1	0.937	-0.579	-38.2	0.863	-0.652	-43.0	0.588	-0.927	-61.2
	120		0.932	-0.583	-38.5	0.917	-0.599	-39.5	0.844	-0.671	-44.3	0.575	-0.940	-62.0
	130		0.914	-0.602	-39.7	0.898	-0.617	-40.7	0.827	-0.688	-45.4	0.564	-0.952	-62.8
	140		0.897	-0.619	-40.8	0.881	-0.634	-41.8	0.812	-0.703	-46.4	0.553	-0.962	-63.5

Table A.2 Comparison of Distribution Factors and Undistributed Live Load Moments for U54 Interior Beams.

Spacing (ft.)	Span (ft.)	Distribution Factors				% Diff. w.r.t STD	Moment (LL+I) per Lane (k-ft)				% Diff. w.r.t STD
		STD		LRFD			STD		LRFD		
		DF	Impact	DF	Impact		Truck (Controls)	Lane	Truck + Lane (Controls)	Tandem + Lane	
8.50	90	0.900	0.233	0.613	0.33	-26.5	1651.5	1053.0	2430.0	2077.8	47.1
	100		0.222	0.597		-27.8	1857.6	1250.0	2821.4	2396.0	51.9
	110		0.213	0.583		-29.0	2061.6	1463.0	3228.8	2730.3	56.6
	120		0.204	0.570		-30.0	2263.5	1692.0	3652.2	3080.5	61.4
	130		0.196	0.559		-30.9	2463.8	1937.0	4091.6	3446.8	66.1
	140		0.189	0.549		-31.8	2662.5	2198.0	4547.0	3829.0	70.8
10.00	90	0.909	0.233	0.689	0.33	-18.2	1651.5	1053.0	2430.0	2077.8	47.1
	100		0.222	0.672		-19.6	1857.6	1250.0	2821.4	2396.0	51.9
	110		0.213	0.656		-20.9	2061.6	1463.0	3228.8	2730.3	56.6
	120		0.204	0.642		-22.0	2263.5	1692.0	3652.2	3080.5	61.4
	130		0.196	0.629		-23.1	2463.8	1937.0	4091.6	3446.8	66.1
	140		0.189	0.617		-24.0	2662.5	2198.0	4547.0	3829.0	70.8
11.50	90	1.046	0.233	0.763	0.33	-21.3	1651.5	1053.0	2430.0	2077.8	47.1
	100		0.222	0.743		-22.7	1857.6	1250.0	2821.4	2396.0	51.9
	110		0.213	0.726		-23.9	2061.6	1463.0	3228.8	2730.3	56.6
	120		0.204	0.710		-25.0	2263.5	1692.0	3652.2	3080.5	61.4
	130		0.196	0.696		-26.0	2463.8	1937.0	4091.6	3446.8	66.1
	140		0.189	0.683		-26.9	2662.5	2198.0	4547.0	3829.0	70.8
14.00	90	1.273	0.233	0.880	0.33	-25.4	1651.5	1053.0	2430.0	2077.8	47.1
	100		0.222	0.857		-26.7	1857.6	1250.0	2821.4	2396.0	51.9
	110		0.213	0.837		-27.9	2061.6	1463.0	3228.8	2730.3	56.6
	120		0.204	0.819		-28.9	2263.5	1692.0	3652.2	3080.5	61.4
	130		0.196	0.803		-29.9	2463.8	1937.0	4091.6	3446.8	66.1
	140		0.189	0.788		-30.7	2662.5	2198.0	4547.0	3829.0	70.8
16.67	90	1.516	0.233	0.999	0.33	-28.9	1651.5	1053.0	2430.0	2077.8	47.1
	100		0.222	0.973		-30.2	1857.6	1250.0	2821.4	2396.0	51.9
	110		0.213	0.950		-31.3	2061.6	1463.0	3228.8	2730.3	56.6
	120		0.204	0.929		-32.3	2263.5	1692.0	3652.2	3080.5	61.4
	130		0.196	0.911		-33.2	2463.8	1937.0	4091.6	3446.8	66.1
	140		0.189	0.894		-34.0	2662.5	2198.0	4547.0	3829.0	70.8

Table A.3 Comparison of Distributed Live Load Moments for U54 Interior Beams.

Spacing (ft.)	Span (ft.)	All Skews Moment (k-ft) STD	Skew = 0 Skew Corr. Factor	Skew = 0 Moment (k-ft) LRFD	Skew = 0 % Diff. w.r.t STD	Skew = 15 Skew Corr. Factor	Skew = 15 Moment (k-ft) LRFD	Skew = 15 % Diff. w.r.t STD	Skew = 30 Skew Corr. Factor	Skew = 30 Moment (k-ft) LRFD	Skew = 30 % Diff. w.r.t STD	Skew = 60 Skew Corr. Factor	Skew = 60 Moment (k-ft) LRFD	Skew = 60 % Diff. w.r.t STD
8.50	90	1486.3	1	1489.1	0.2	0.983	1463.8	-1.5	0.906	1348.6	-9.3	0.617	918.8	-38.2
	100	1671.9		1684.0	0.7		1655.4	-1.0		1525.2	-8.8		1039.0	-37.9
	110	1855.4		1881.8	1.4		1849.8	-0.3		1704.3	-8.1		1161.0	-37.4
	120	2037.2		2082.8	2.2		2047.4	0.5		1886.3	-7.4		1285.0	-36.9
	130	2217.4		2287.1	3.1		2248.3	1.4		2071.4	-6.6		1411.1	-36.4
	140	2396.2		2495.0	4.1		2452.6	2.4		2259.6	-5.7		1539.4	-35.8
10.00	90	1501.3	1	1675.3	11.6	0.983	1646.9	9.7	0.906	1517.3	1.1	0.617	1033.7	-31.2
	100	1688.8		1894.6	12.2		1862.4	10.3		1715.9	1.6		1168.9	-30.8
	110	1874.1		2117.1	13.0		2081.2	11.0		1917.4	2.3		1306.2	-30.3
	120	2057.8		2343.2	13.9		2303.4	11.9		2122.2	3.1		1445.7	-29.7
	130	2239.8		2573.1	14.9		2529.4	12.9		2330.4	4.0		1587.6	-29.1
	140	2420.5		2807.0	16.0		2759.3	14.0		2542.2	5.0		1731.9	-28.4
11.50	90	1726.5	1	1854.0	7.4	0.983	1822.5	5.6	0.906	1679.1	-2.7	0.617	1143.9	-33.7
	100	1942.1		2096.6	8.0		2061.0	6.1		1898.8	-2.2		1293.6	-33.4
	110	2155.3		2342.9	8.7		2303.1	6.9		2121.9	-1.5		1445.5	-32.9
	120	2366.4		2593.1	9.6		2549.0	7.7		2348.5	-0.8		1599.9	-32.4
	130	2575.8		2847.5	10.5		2799.1	8.7		2578.9	0.1		1756.9	-31.8
	140	2783.5		3106.3	11.6		3053.6	9.7		2813.3	1.1		1916.6	-31.1
14.00	90	2101.9	1	2138.2	1.7	0.983	2101.9	0.0	0.906	1936.5	-7.9	0.617	1319.2	-37.2
	100	2364.3		2418.0	2.3		2377.0	0.5		2189.9	-7.4		1491.9	-36.9
	110	2623.8		2702.0	3.0		2656.1	1.2		2447.1	-6.7		1667.1	-36.5
	120	2880.9		2990.6	3.8		2939.8	2.0		2708.4	-6.0		1845.1	-36.0
	130	3135.7		3284.0	4.7		3228.2	2.9		2974.2	-5.2		2026.2	-35.4
	140	3388.6		3582.5	5.7		3521.6	3.9		3244.5	-4.3		2210.4	-34.8
16.67	90	2502.7	1	2426.6	-3.0	0.983	2385.4	-4.7	0.906	2197.7	-12.2	0.617	1497.2	-40.2
	100	2815.2		2744.2	-2.5		2697.6	-4.2		2485.4	-11.7		1693.2	-39.9
	110	3124.2		3066.5	-1.8		3014.5	-3.5		2777.3	-11.1		1892.0	-39.4
	120	3430.3		3394.0	-1.1		3336.4	-2.7		3073.8	-10.4		2094.1	-39.0
	130	3733.7		3727.0	-0.2		3663.7	-1.9		3375.4	-9.6		2299.5	-38.4
	140	4034.9		4065.8	0.8		3996.7	-0.9		3682.3	-8.7		2508.6	-37.8

Table A.4 Comparison of Undistributed and Distributed Shear Force at Respective Critical Sections (Strand Dia = 0.5 in. and Girder Spacing = 8.5 ft.).

Skew	Shear (LL+I) per lane, (kips)						% diff. w.r.t. STD	Shear (LL+I) per beam, (kips)				% diff. w.r.t. STD
	LRFD			Standard				LRFD		Standard		
	Span (ft.)	Truck + Lane (Controls)	Tandem + Lane	Span (ft.)	Truck (Controls)	Lane		Span (ft.)	Shear (kips)	Span (ft.)	Shear (kips)	
0	90.0	103.9	85.2	90	76.9	57.8	35.1	90.0	86.1	90	69.2	24.5
	100.0	109.0	89.2	100	77.4	60.8	40.7	100.0	89.5	100	69.7	28.3
	110.0	113.7	93.0	110	77.8	63.9	46.1	110.0	92.4	110	70.0	32.0
	120.0	117.9	96.4	120	78.1	66.9	51.0	120.0	94.9	120	70.3	35.1
	130.0	121.7	99.7	130	78.2	69.9	55.6	130.0	97.2	130	70.4	38.2
	136.5	124.2	101.9	135	78.3	71.5	-	136.5	98.8	135	71.5	-
15	90.0	103.9	85.2	90	76.9	57.8	35.1	90.0	86.1	90	69.2	24.5
	100.0	109.0	89.2	100	77.4	60.8	40.7	100.0	89.5	100	69.7	28.3
	110.0	113.7	93.0	110	77.8	63.9	46.1	110.0	92.4	110	70.0	32.0
	120.0	117.9	96.5	120	78.1	66.9	51.0	120.0	95.0	120	70.3	35.2
	130.0	121.7	99.7	130	78.2	69.9	55.6	130.0	97.2	130	70.4	38.2
	136.5	124.2	101.9	135	78.3	71.5	-	136.5	98.8	135	71.5	-
30	90.0	103.8	85.1	90	76.9	57.8	35.0	90.0	86.1	90	69.2	24.5
	100.0	108.9	89.1	100	77.4	60.8	40.6	100.0	89.4	100	69.7	28.2
	110.0	113.7	93.0	110	77.8	63.9	46.1	110.0	92.4	110	70.0	31.9
	120.0	117.9	96.4	120	78.1	66.9	51.0	120.0	94.9	120	70.3	35.1
	130.0	121.7	99.7	130	78.2	69.9	55.6	130.0	97.3	130	70.4	38.2
	138.5	125.1	102.6	135	78.3	71.5	-	138.5	99.3	135	71.5	-
60	90.0	103.8	85.1	90	76.9	57.8	35.0	90.0	86.1	90	69.2	24.4
	100.0	108.9	89.1	100	77.4	60.8	40.6	100.0	89.4	100	69.7	28.2
	110.0	113.7	93.0	110	77.8	63.9	46.1	110.0	92.4	110	70.0	31.9
	120.0	117.8	96.4	120	78.1	66.9	50.9	120.0	94.9	120	70.3	35.1
	130.0	121.7	99.7	130	78.2	69.9	55.6	130.0	97.2	130	70.4	38.1
	140.0	125.7	103.2	135	78.3	71.5	-	140.0	99.7	135	71.5	-
	145.0	127.8	105.0	-	-	-	-	145.0	101.0	-	-	-

Table A.5 Comparison of Undistributed and Distributed Shear Force at Respective Critical Sections (Strand Dia = 0.5 in. and Girder Spacing = 10 ft.).

Skew	Shear (LL+I) per lane, (kips)						% diff. w.r.t. STD	Shear (LL+I) per beam, (kips)				% diff. w.r.t. STD
	LRFD			Standard				LRFD		Standard		
	Span (ft.)	Truck + Lane (Controls)	Tandem + Lane	Span (ft.)	Truck (Controls)	Lane		Span (ft.)	Shear (kips)	Span (ft.)	Shear (kips)	
0	90.0	104.2	85.4	90	76.9	57.8	35.5	90.0	98.4	90	69.9	40.8
	100.0	109.3	89.5	100	77.4	60.8	41.2	100.0	102.2	100	70.4	45.1
	110.0	113.9	93.2	110	77.8	63.9	46.4	110.0	105.4	110	70.7	49.1
	120.0	117.9	96.5	120	78.1	66.9	51.0	120.0	108.1	120	71.0	52.4
	130.0	121.7	99.7	130	78.2	69.9	55.6	130.0	110.7	130	71.1	55.7
	130.5	121.9	99.9	-	-	-	-	130.5	110.9	-	-	-
15	90.0	104.2	85.4	90	76.9	57.8	35.5	90.0	98.4	90	69.9	40.8
	100.0	109.3	89.4	100	77.4	60.8	41.2	100.0	102.2	100	70.4	45.1
	110.0	113.9	93.2	110	77.8	63.9	46.4	110.0	105.4	110	70.7	49.1
	120.0	117.9	96.5	120	78.1	66.9	51.1	120.0	108.2	120	71.0	52.5
	130.0	121.7	99.7	130	78.2	69.9	55.6	130.0	110.7	130	71.1	55.7
	131.0	122.2	100.1	-	-	-	-	131.0	111.1	-	-	-
30	90.0	104.2	85.4	90	76.9	57.8	35.5	90.0	98.4	90	69.9	40.8
	100.0	109.3	89.4	100	77.4	60.8	41.1	100.0	102.1	100	70.4	45.0
	110.0	113.9	93.1	110	77.8	63.9	46.3	110.0	105.4	110	70.7	49.0
	120.0	117.9	96.5	120	78.1	66.9	51.1	120.0	108.2	120	71.0	52.5
	130.0	121.7	99.7	130	78.2	69.9	55.6	130.0	110.7	130	71.1	55.7
	133.0	122.9	100.7	-	-	-	-	133.0	111.6	-	-	-
60	90.0	104.2	85.4	90	76.9	57.8	35.5	90.0	98.4	90	69.9	40.8
	100.0	109.3	89.4	100	77.4	60.8	41.1	100.0	102.1	100	70.4	45.1
	110.0	113.8	93.0	110	77.8	63.9	46.2	110.0	105.3	110	70.7	48.9
	120.0	117.9	96.5	120	78.1	66.9	51.0	120.0	108.2	120	71.0	52.4
	130.0	121.7	99.7	130	78.2	69.9	55.6	130.0	110.7	130	71.1	55.8
	139.0	125.3	102.9	-	-	-	-	139.0	113.3	-	-	-

Table A.6 Comparison of Undistributed and Distributed Shear Force at Respective Critical Sections (Strand Dia = 0.5 in. and Girder Spacing = 11.5 ft.).

Skew	Shear (LL+I) per lane, (kips)						% diff. w.r.t. STD	Shear (LL+I) per beam, (kips)				% diff. w.r.t. STD
	LRFD			Standard				LRFD		Standard		
	Span (ft.)	Truck + Lane (Controls)	Tandem + Lane	Span (ft.)	Truck (Controls)	Lane		Span (ft.)	Shear (kips)	Span (ft.)	Shear (kips)	
0	90.0	104.4	85.6	90	76.9	57.8	35.8	90.0	110.3	90	80.4	37.3
	100.0	109.6	89.6	100	77.4	60.8	41.5	100.0	114.5	100	81.0	41.4
	110.0	113.9	93.2	110	77.8	63.9	46.4	110.0	117.9	110	81.4	45.0
	120.0	118.0	96.5	120	78.1	66.9	51.1	120.0	121.0	120	81.6	48.3
	125.5	119.9	98.2	124	78.1	68.1	-	125.5	122.5	124	81.7	-
15	90.0	104.4	85.6	90	76.9	57.8	35.8	90.0	110.3	90	80.4	37.3
	100.0	109.6	89.6	100	77.4	60.8	41.5	100.0	114.5	100	81.0	41.4
	110.0	113.9	93.2	110	77.8	63.9	46.4	110.0	117.9	110	81.4	45.0
	120.0	118.0	96.5	120	78.1	66.9	51.1	120.0	121.0	120	81.6	48.3
	126.0	120.1	98.4	124	78.1	68.1	-	126.0	122.7	124	81.7	-
30	90.0	104.5	85.7	90	76.9	57.8	35.9	90.0	110.4	90	80.4	37.3
	100.0	109.6	89.6	100	77.4	60.8	41.5	100.0	114.5	100	81.0	41.4
	110.0	114.0	93.2	110	77.8	63.9	46.5	110.0	118.0	110	81.4	45.0
	120.0	117.9	96.5	120	78.1	66.9	51.0	120.0	120.9	120	81.6	48.2
	127.5	120.7	98.9	124	78.1	68.1	-	127.5	123.1	124	81.7	-
60	90.0	104.4	85.6	90	76.9	57.8	35.8	90.0	110.3	90	80.4	37.2
	100.0	109.5	89.6	100	77.4	60.8	41.4	100.0	114.5	100	81.0	41.4
	110.0	113.9	93.2	110	77.8	63.9	46.4	110.0	117.9	110	81.4	44.9
	120.0	118.0	96.5	120	78.1	66.9	51.1	120.0	121.0	120	81.6	48.3
	130.0	121.7	99.7	124	78.1	68.1	-	130.0	123.8	124	81.7	-
	134.0	123.3	101.1	-	-	-	-	134.0	125.1	-	-	-

Table A.7 Comparison of Undistributed and Distributed Shear Force at Respective Critical Sections (Strand Dia = 0.5 in. and Girder Spacing = 14 ft.).

Skew	Shear (LL+I) per lane, (kips)						% diff. w.r.t. STD	Shear (LL+I) per beam, (kips)				% diff. w.r.t. STD
	LRFD			Standard				LRFD		Standard		
	Span (ft.)	Truck + Lane (Controls)	Tandem + Lane	Span (ft.)	Truck (Controls)	Lane		Span (ft.)	Shear (kips)	Span (ft.)	Shear (kips)	
0	90.0	105.1	86.2	90	76.9	57.8	36.7	90.0	130.0	90	97.9	32.8
	100.0	110.0	90.0	100	77.4	60.8	42.1	100.0	134.6	100	98.6	36.6
	110.0	114.2	93.4	110	77.8	63.9	46.7	110.0	138.3	110	99.0	39.7
	115.5	116.3	95.1	113	77.9	64.8	-	115.5	140.2	113	99.1	-
15	90.0	105.1	86.2	90	76.9	57.8	36.7	90.0	130.0	90	97.9	32.8
	100.0	110.0	90.0	100	77.4	60.8	42.1	100.0	134.6	100	98.6	36.6
	110.0	114.2	93.4	110	77.8	63.9	46.7	110.0	138.3	110	99.0	39.7
	116.0	116.5	95.3	113	77.9	64.8	-	116.0	140.3	113	99.1	-
30	90.0	105.1	86.1	90	76.9	57.8	36.6	90.0	129.9	90	97.9	32.7
	100.0	110.0	90.0	100	77.4	60.8	42.1	100.0	134.6	100	98.6	36.6
	110.0	114.2	93.4	110	77.8	63.9	46.7	110.0	138.3	110	99.0	39.7
	118.0	117.2	95.9	113	77.9	64.8	-	118.0	141.0	113	99.1	-
60	90.0	105.0	86.1	90	76.9	57.8	36.6	90.0	129.8	90	97.9	32.7
	100.0	109.9	89.9	100	77.4	60.8	41.9	100.0	134.5	100	98.6	36.4
	110.0	114.1	93.3	110	77.8	63.9	46.7	110.0	138.3	110	99.0	39.6
	120.0	118.0	96.6	113	77.9	64.8	-	120.0	141.7	113	99.1	-
	123.5	119.3	97.7	-	-	-	-	123.5	142.8	-	-	-

Table A.8 Comparison of Undistributed and Distributed Shear Force at Respective Critical Sections (Strand Dia = 0.5 in. and Girder Spacing = 16.67 ft.).

Skew	Shear (LL+I) per lane, (kips)						% diff. w.r.t. STD	Shear (LL+I) per beam, (kips)				% diff. w.r.t. STD
	LRFD			Standard				LRFD		Standard		
	Span (ft.)	Truck + Lane (Controls)	Tandem + Lane	Span (ft.)	Truck (Controls)	Lane		Span (ft.)	Shear (kips)	Span (ft.)	Shear (kips)	
0	100.0	110.1	90.1	100.0	77.4	60.8	42.2	100.0	154.9	100.0	117.4	32.0
	109.0	113.8	93.1	104.5	77.6	62.2	-	109.0	158.7	104.5	117.6	-
15	100.0	110.1	90.1	100.0	77.4	60.8	42.2	100.0	154.9	100.0	117.4	32.0
	109.5	114.0	93.2	104.5	77.6	62.2	-	109.5	158.9	104.5	117.6	-
30	100.0	110.1	90.1	100.0	77.4	60.8	42.2	100.0	154.9	100.0	117.4	32.0
	110.0	114.2	93.4	104.5	77.6	62.2	-	110.0	159.1	104.5	117.6	-
	111.0	114.6	93.7	-	-	-	-	111.0	159.5	-	-	-
60	100.0	110.1	90.0	100.0	77.4	60.8	42.1	100.0	154.8	100.0	117.4	31.9
	110.0	114.2	93.4	104.5	77.6	62.2	-	110.0	159.1	104.5	117.6	-
	117.0	116.9	95.6	-	-	-	-	117.0	161.8	-	-	-

Table A.9 Comparison of Undistributed and Distributed Shear Force at Respective Critical Sections (Strand Dia = 0.6 in. and Girder Spacing = 8.5 ft.).

Skew	Shear (LL+I) per lane, (kips)						% diff. w.r.t. STD	Shear (LL+I) per beam, (kips)				% diff. w.r.t. STD
	LRFD			Standard				LRFD		Standard		
	Span (ft.)	Truck + Lane (Controls)	Tandem + Lane	Span (ft.)	Truck (Controls)	Lane		Span (ft.)	Shear (kips)	Span (ft.)	Shear (kips)	
0	90.0	103.8	85.1	90.0	76.9	57.8	35.0	90.0	86.1	90.0	69.2	24.4
	100.0	108.9	89.1	100.0	77.4	60.8	40.6	100.0	89.4	100.0	69.7	28.2
	110.0	113.7	93.0	110.0	77.8	63.9	46.1	110.0	92.4	110.0	70.0	32.0
	120.0	117.9	96.5	120.0	78.1	66.9	51.0	120.0	95.0	120.0	70.3	35.2
	130.0	121.7	99.7	130.0	78.2	69.9	55.6	130.0	97.2	130.0	70.4	38.2
	136.5	124.3	102.0	134.5	78.3	71.3	-	136.5	98.8	134.5	71.3	-
15	90.0	103.8	85.1	90.0	76.9	57.8	35.0	90.0	86.1	90.0	69.2	24.4
	100.0	108.9	89.1	100.0	77.4	60.8	40.6	100.0	89.4	100.0	69.7	28.2
	110.0	113.7	93.0	110.0	77.8	63.9	46.1	110.0	92.4	110.0	70.0	32.0
	120.0	117.9	96.5	120.0	78.1	66.9	51.0	120.0	95.0	120.0	70.3	35.2
	130.0	121.7	99.7	130.0	78.2	69.9	55.6	130.0	97.2	130.0	70.4	38.2
	137.0	124.5	102.1	134.5	78.3	71.3	-	137.0	98.9	134.5	71.3	-
30	90.0	103.8	85.1	90.0	76.9	57.8	35.0	90.0	86.1	90.0	69.2	24.4
	100.0	108.9	89.1	100.0	77.4	60.8	40.6	100.0	89.4	100.0	69.7	28.2
	110.0	113.7	93.0	110.0	77.8	63.9	46.1	110.0	92.4	110.0	70.0	32.0
	120.0	117.9	96.5	120.0	78.1	66.9	51.0	120.0	95.0	120.0	70.3	35.2
	130.0	121.8	99.8	130.0	78.2	69.9	55.7	130.0	97.3	130.0	70.4	38.3
	138.5	125.1	102.6	134.5	78.3	71.3	-	138.5	99.3	134.5	71.3	-
60	90.0	103.8	85.1	90.0	76.9	57.8	35.0	90.0	86.1	90.0	69.2	24.4
	100.0	108.9	89.1	100.0	77.4	60.8	40.6	100.0	89.4	100.0	69.7	28.2
	110.0	113.6	92.9	110.0	77.8	63.9	46.0	110.0	92.4	110.0	70.0	31.9
	120.0	117.8	96.4	120.0	78.1	66.9	50.9	120.0	94.9	120.0	70.3	35.1
	130.0	121.7	99.7	130.0	78.2	69.9	55.6	130.0	97.3	130.0	70.4	38.2
	140.0	125.7	103.2	134.5	78.3	71.3	-	140.0	99.7	134.5	71.3	-
	144.5	127.5	104.8	-	-	-	-	144.5	100.8	-	-	-

Table A.10 Comparison of Undistributed and Distributed Shear Force at Respective Critical Sections (Strand Dia = 0.6 in. and Girder Spacing = 10 ft.).

Skew	Shear (LL+I) per lane, (kips)						% diff. w.r.t. STD	Shear (LL+I) per beam, (kips)				% diff. w.r.t. STD
	LRFD			Standard				LRFD		Standard		
	Span (ft.)	Truck + Lane (Controls)	Tandem + Lane	Span (ft.)	Truck (Controls)	Lane		Span (ft.)	Shear (kips)	Span (ft.)	Shear (kips)	
0	90.0	104.2	85.4	90	76.9	57.8	35.5	90.0	98.4	90	69.9	40.8
	100.0	109.2	89.4	100	77.4	60.8	41.1	100.0	102.1	100	70.4	45.0
	110.0	113.9	93.2	110	77.8	63.9	46.4	110.0	105.4	110	70.7	49.0
	120.0	118.0	96.5	120	78.1	66.9	51.1	120.0	108.2	120	71.0	52.5
	130.0	121.8	99.8	130	78.2	69.9	55.8	130.0	110.9	130	71.1	55.9
15	90.0	104.2	85.4	90	76.9	57.8	35.5	90.0	98.4	90	69.9	40.8
	100.0	109.2	89.4	100	77.4	60.8	41.1	100.0	102.1	100	70.4	45.0
	110.0	113.9	93.2	110	77.8	63.9	46.4	110.0	105.4	110	70.7	49.0
	120.0	118.0	96.5	120	78.1	66.9	51.1	120.0	108.2	120	71.0	52.5
	130.0	121.8	99.8	130	78.2	69.9	55.7	130.0	110.9	130	71.1	55.9
30	90.0	104.1	85.4	90	76.9	57.8	35.4	90.0	98.4	90	69.9	40.7
	100.0	109.3	89.4	100	77.4	60.8	41.1	100.0	102.1	100	70.4	45.0
	110.0	113.9	93.2	110	77.8	63.9	46.4	110.0	105.4	110	70.7	49.1
	120.0	118.0	96.5	120	78.1	66.9	51.1	120.0	108.2	120	71.0	52.5
	130.0	121.7	99.7	130	78.2	69.9	55.6	130.0	110.8	130	71.1	55.8
	131.5	122.3	100.2	-	-	-	-	131.5	111.2	-	-	-
60	90.0	104.1	85.4	90	76.9	57.8	35.4	90.0	98.4	90	69.9	40.7
	100.0	109.2	89.3	100	77.4	60.8	41.0	100.0	102.0	100	70.4	44.9
	110.0	113.9	93.1	110	77.8	63.9	46.3	110.0	105.4	110	70.7	49.0
	120.0	117.9	96.5	120	78.1	66.9	51.1	120.0	108.2	120	71.0	52.5
	130.0	121.8	99.8	130	78.2	69.9	55.7	130.0	110.8	130	71.1	55.8
	138.0	124.8	102.5	-	-	-	-	138.0	112.9	-	-	-

Table A.11 Comparison of Undistributed and Distributed Shear Force at Respective Critical Sections (Strand Dia = 0.6 in. and Girder Spacing = 11.5 ft.).

Skew	Shear (LL+I) per lane, (kips)						% diff. w.r.t. STD	Shear (LL+I) per beam, (kips)				% diff. w.r.t. STD
	LRFD			Standard				LRFD		Standard		
	Span (ft.)	Truck + Lane (Controls)	Tandem + Lane	Span (ft.)	Truck (Controls)	Lane		Span (ft.)	Shear (kips)	Span (ft.)	Shear (kips)	
0	90	104.4	85.6	90	76.9	57.8	35.7	90	110.3	90	80.4	37.2
	100	109.5	89.6	100	77.4	60.8	41.4	100	114.5	100	81.0	41.4
	110	114.1	93.3	110	77.8	63.9	46.6	110	118.1	110	81.4	45.1
	120	118.0	96.6	120	78.1	66.9	51.2	120	121.1	120	81.6	48.4
	124	119.6	97.9	124	78.1	68.1	53.0	124	122.3	124	81.7	49.7
15	90	104.4	85.6	90	76.9	57.8	35.7	90	110.3	90	80.4	37.2
	100	109.5	89.6	100	77.4	60.8	41.4	100	114.5	100	81.0	41.4
	110	114.1	93.3	110	77.8	63.9	46.6	110	118.1	110	81.4	45.1
	120	118.0	96.6	120	78.1	66.9	51.2	120	121.1	120	81.6	48.4
	125	119.9	98.2	124	78.1	68.1	-	125	122.6	124	81.7	-
30	90	104.4	85.6	90	76.9	57.8	35.8	90	110.3	90	80.4	37.2
	100	109.5	89.6	100	77.4	60.8	41.4	100	114.5	100	81.0	41.4
	110	114.0	93.2	110	77.8	63.9	46.5	110	118.0	110	81.4	45.0
	120	118.0	96.5	120	78.1	66.9	51.1	120	121.0	120	81.6	48.3
	126	120.2	98.5	124	78.1	68.1	-	126	122.8	124	81.7	-
60	90	104.4	85.6	90	76.9	57.8	35.8	90	110.3	90	80.4	37.2
	100	109.4	89.5	100	77.4	60.8	41.3	100	114.4	100	81.0	41.3
	110	113.9	93.2	110	77.8	63.9	46.4	110	117.9	110	81.4	44.9
	120	118.0	96.6	120	78.1	66.9	51.2	120	121.1	120	81.6	48.3
	130	121.8	99.8	124	78.1	68.1	-	130	123.9	124	81.7	-
	133	122.9	100.8	-	-	-	-	133	124.8	-	-	-

Table A.12 Comparison of Undistributed and Distributed Shear Force at Respective Critical Sections (Strand Dia = 0.6 in. and Girder Spacing = 14 ft.).

Skew	Shear (LL+I) per lane, (kips)						% diff. w.r.t. STD	Shear (LL+I) per beam, (kips)				% diff. w.r.t. STD
	LRFD			Standard				LRFD		Standard		
	Span (ft.)	Truck + Lane (Controls)	Tandem + Lane	Span (ft.)	Truck (Controls)	Lane		Span (ft.)	Shear (kips)	Span (ft.)	Shear (kips)	
0	90.0	105.0	86.1	90	76.9	57.8	36.6	90.0	129.8	90	97.9	32.7
	100.0	110.0	90.0	100	77.4	60.8	42.0	100.0	134.6	100	98.6	36.5
	110.0	114.2	93.4	110	77.8	63.9	46.8	110.0	138.4	110	99.0	39.7
	115.5	116.4	95.2	112	77.9	64.5	-	115.5	140.3	112	99.1	-
15	90.0	105.0	86.1	90	76.9	57.8	36.6	90.0	129.8	90	97.9	32.7
	100.0	110.0	90.0	100	77.4	60.8	42.0	100.0	134.6	100	98.6	36.5
	110.0	114.2	93.4	110	77.8	63.9	46.8	110.0	138.4	110	99.0	39.7
	116.0	116.6	95.4	112	77.9	64.5	-	116.0	140.5	112	99.1	-
30	90.0	105.0	86.1	90	76.9	57.8	36.6	90.0	129.9	90	97.9	32.7
	100.0	110.0	90.0	100	77.4	60.8	42.0	100.0	134.5	100	98.6	36.5
	110.0	114.3	93.4	110	77.8	63.9	46.8	110.0	138.4	110	99.0	39.8
	117.0	117.0	95.7	112	77.9	64.5	-	117.0	140.8	112	99.1	-
60	90.0	105.0	86.1	90	76.9	57.8	36.5	90.0	129.8	90	97.9	32.7
	100.0	109.9	89.9	100	77.4	60.8	41.9	100.0	134.5	100	98.6	36.4
	110.0	114.2	93.4	110	77.8	63.9	46.7	110.0	138.3	110	99.0	39.6
	120.0	118.1	96.7	112	77.9	64.5	-	120.0	141.8	112	99.1	-
	123.5	119.5	97.8	-	-	-	-	123.5	143.1	-	-	-

Table A.13 Comparison of Undistributed and Distributed Shear Force at Respective Critical Sections (Strand Dia = 0.6 in. and Girder Spacing = 16.67 ft.).

Skew	Shear (LL+I) per lane, (kips)						% diff. w.r.t. STD	Shear (LL+I) per beam, (kips)				% diff. w.r.t. STD
	LRFD			Standard				LRFD		Standard		
	Span (ft.)	Truck + Lane (Controls)	Tandem + Lane	Span (ft.)	Truck (Controls)	Lane		Span (ft.)	Shear (kips)	Span (ft.)	Shear (kips)	
0	100	110.0779	90.0549	98.5	77.378	60.37	-	100	154.838	98.5	117.2629	-
	106	112.3561	91.8836	-	-	-	-	106	157.1101	-	-	-
15	100	110.0779	90.0549	98.5	77.378	60.37	-	100	154.838	98.5	117.2629	-
	107	113.0154	92.4207	-	-	-	-	107	157.8814	-	-	-
30	100	110.1253	90.0934	98.5	77.378	60.37	-	100	154.9047	98.5	117.2629	-
	110	114.309	93.4799	-	-	-	-	110	159.2412	-	-	-
60	100	110.0305	90.0164	98.5	77.378	60.37	-	100	154.7714	98.5	117.2629	-
	110	114.2792	93.4555	-	-	-	-	110	159.1996	-	-	-
	117	117.0224	95.7352	-	-	-	-	117	162.0043	-	-	-

Table A.14 Comparison of Live Load Distribution Factors.

Spacing	Span	Moment DF		%diff. w.r.t STD	Shear DF		%diff. w.r.t STD
		LRFD	STD		LRFD	STD	
8.50	90	0.616	0.900	-31.6	0.830	0.900	-7.8
	100	0.599		-33.4	0.821		-8.8
	110	0.585		-35.0	0.813		-9.7
	120	0.572		-36.4	0.806		-10.5
	130	0.561		-37.7	0.799		-11.2
	140	0.550		-38.9	0.793		-11.9
10.00	90	0.692	0.909	-23.8	0.945	0.909	3.9
	100	0.674		-25.8	0.935		2.8
	110	0.658		-27.6	0.926		1.8
	120	0.644		-29.2	0.917		0.9
	130	0.631		-30.6	0.910		0.1
	140	0.619		-31.9	0.903		-0.6
11.50	90	0.766	1.046	-26.7	1.056	1.046	1.0
	100	0.746		-28.6	1.045		0.0
	110	0.728		-30.3	1.035		-1.0
	120	0.712		-31.9	1.026		-1.9
	130	0.698		-33.2	1.018		-2.7
	140	0.685		-34.5	1.010		-3.4
14.00	90	0.884	1.273	-30.6	1.237	1.273	-2.8
	100	0.860		-32.4	1.223		-3.9
	110	0.840		-34.0	1.212		-4.8
	120	0.822		-35.4	1.201		-5.6
	130	0.805		-36.7	1.191		-6.4
	140	0.790		-37.9	1.182		-7.1
16.67	90	1.003	1.516	-33.8	1.422	1.516	-6.2
	100	0.977		-35.6	1.407		-7.2
	110	0.953		-37.1	1.393		-8.1
	120	0.932		-38.5	1.381		-8.9
	130	0.914		-39.7	1.370		-9.6
	140	0.897		-40.8	1.360		-10.3

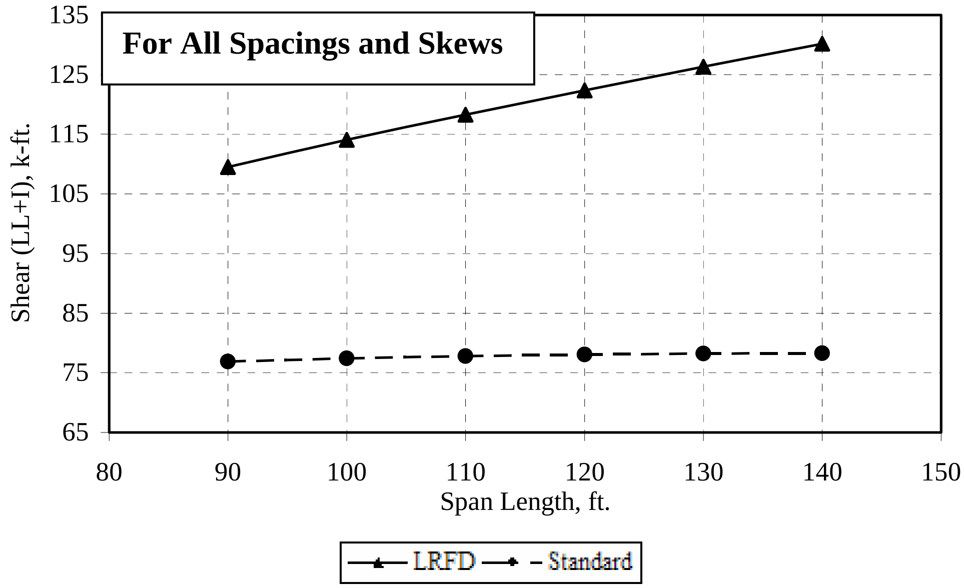

Figure A.1 Comparison of Undistributed Live Load Shear Force at *h*/2.

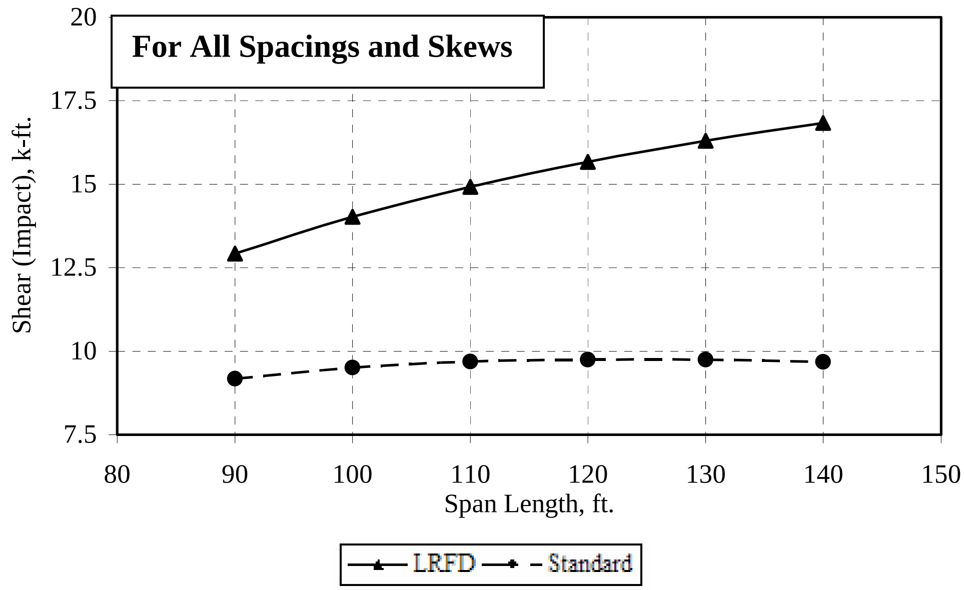

Figure A.2 Comparison of Undistributed Dynamic Load Shear Force at *h*/2.

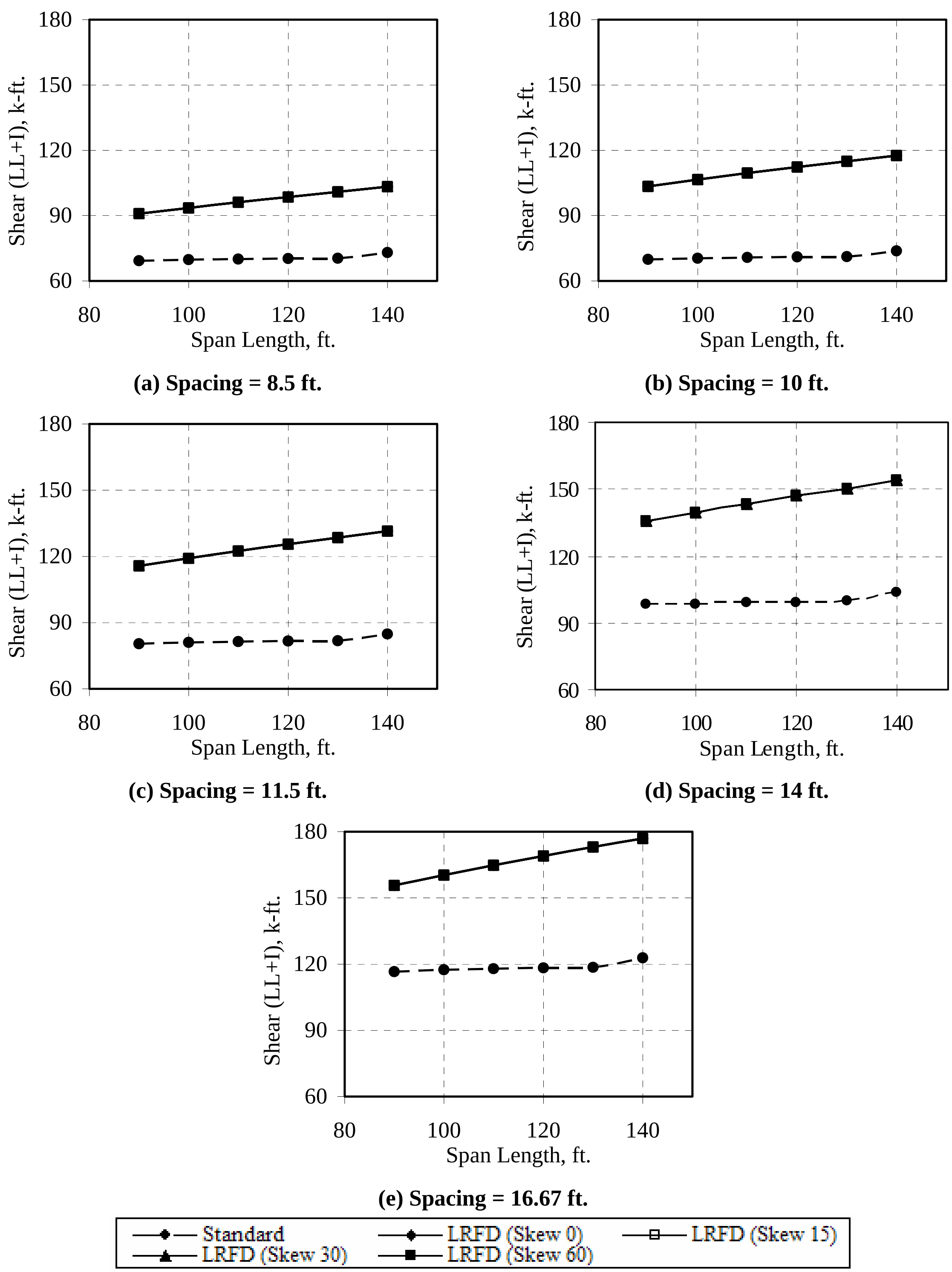

Figure A.3 Comparison of Distributed Live Load Shear Force at *h*/2.

Table A.15 Comparison of Initial Concrete Strength (Strand Dia = 0.5 in.).

Spacing (ft.)	Span (ft.)	All Skews f'_{ci} (psi) STD	Skew = 0 f'_{ci} (psi) LRFD	Skew = 0 Diff.	Skew = 0 % Diff. w.r.t STD	Skew = 15 f'_{ci} (psi) LRFD	Skew = 15 Diff.	Skew = 15 % Diff. w.r.t STD	Skew = 30 f'_{ci} (psi) LRFD	Skew = 30 Diff.	Skew = 30 % Diff. w.r.t STD	Skew = 60 f'_{ci} (psi) LRFD	Skew = 60 Diff.	Skew = 60 % Diff. w.r.t STD
8.50	90	4000	4000	0	0.0	4000	0	0.0	4000	0	0.0	4000	0	0.0
8.50	100	4000	4000	0	0.0	4000	0	0.0	4000	0	0.0	4000	0	0.0
8.50	110	4080	4000	-80	-2.0	4000	-80	-2.0	4000	-80	-2.0	4000	-80	-2.0
8.50	120	5072	4879	-193	-3.8	4719	-353	-7.0	4559	-513	-10.1	4077	-995	-19.6
8.50	130	6132	5929	-203	-3.3	5929	-203	-3.3	5771	-361	-5.9	4977	-1155	-18.8
10.00	90	4000	4000	0	0.0	4000	0	0.0	4000	0	0.0	4000	0	0.0
10.00	100	4000	4000	0	0.0	4000	0	0.0	4000	0	0.0	4000	0	0.0
10.00	110	4491	4464	-27	-0.6	4464	-27	-0.6	4303	-188	-4.2	4000	-491	-10.9
10.00	120	5555	5514	-41	-0.7	5356	-199	-3.6	5197	-358	-6.4	4559	-996	-17.9
10.00	130	6653	6598	-55	-0.8	6598	-55	-0.8	6460	-193	-2.9	5613	-1040	-15.6
11.50	90	4000	4000	0	0.0	4000	0	0.0	4000	0	0.0	4000	0	0.0
11.50	100	4152	4000	-152	-3.7	4000	-152	-3.7	4000	-152	-3.7	4000	-152	-3.7
11.50	110	5140	4944	-196	-3.8	4784	-356	-6.9	4624	-516	-10.0	4058	-1082	-21.1
11.50	120	6196	5988	-208	-3.4	5988	-208	-3.4	5830	-366	-5.9	5038	-1158	-18.7
14.00	90	4055	4029	-26	-0.6	4000	-55	-1.4	4000	-55	-1.4	4000	-55	-1.4
14.00	100	5050	4693	-357	-7.1	4693	-357	-7.1	4533	-517	-10.2	4000	-1050	-20.8
14.00	110	6342	5894	-448	-7.1	5894	-448	-7.1	5736	-606	-9.6	4943	-1399	-22.1
16.67	90	4498	4200	-298	-6.6	4200	-298	-6.6	4029	-469	-10.4	4000	-498	-11.1
16.67	100	6013	5488	-525	-8.7	5329	-684	-11.4	5171	-842	-14.0	4533	-1480	-24.6

Table A.16 Comparison of Initial Concrete Strength (Strand Dia = 0.6 in.).

Spacing (ft.)	Span (ft.)	All Skews f'_{ci} (psi) STD	Skew = 0 f'_{ci} (psi) LRFD	Skew = 0 Diff.	Skew = 0 % Diff. w.r.t STD	Skew = 15 f'_{ci} (psi) LRFD	Skew = 15 Diff.	Skew = 15 % Diff. w.r.t STD	Skew = 30 f'_{ci} (psi) LRFD	Skew = 30 Diff.	Skew = 30 % Diff. w.r.t STD	Skew = 60 f'_{ci} (psi) LRFD	Skew = 60 Diff.	Skew = 60 % Diff. w.r.t STD
8.50	90	4000	4000	0	0.0	4000	0	0.0	4000	0	0.0	4000	0	0.0
8.50	100	4000	4000	0	0.0	4000	0	0.0	4000	0	0.0	4000	0	0.0
8.50	110	4089	4000	-89	-2.2	4000	-89	-2.2	4000	-89	-2.2	4000	-89	-2.2
8.50	120	5240	4965	-275	-5.2	4725	-515	-9.8	4725	-515	-9.8	4243	-997	-19.0
8.50	130	6248	5857	-391	-6.3	5857	-391	-6.3	5620	-628	-10.1	5144	-1104	-17.7
10.00	90	4000	4000	0	0.0	4000	0	0.0	4000	0	0.0	4000	0	0.0
10.00	100	4000	4000	0	0.0	4000	0	0.0	4000	0	0.0	4000	0	0.0
10.00	110	4578	4549	-29	-0.6	4549	-29	-0.6	4308	-270	-5.9	4000	-578	-12.6
10.00	120	5481	5441	-40	-0.7	5441	-40	-0.7	5203	-278	-5.1	4725	-756	-13.8
10.00	130	6699	6642	-57	-0.9	6642	-57	-0.9	6420	-279	-4.2	5620	-1079	-16.1
11.50	90	4000	4000	0	0.0	4000	0	0.0	4000	0	0.0	4000	0	0.0
11.50	100	4161	4000	-161	-3.9	4000	-161	-3.9	4000	-161	-3.9	4000	-161	-3.9
11.50	110	5064	5028	-36	-0.7	5028	-36	-0.7	4789	-275	-5.4	4067	-997	-19.7
11.50	120	6309	6033	-276	-4.4	6033	-276	-4.4	5915	-394	-6.2	5203	-1106	-17.5
14.00	90	4000	4000	0	0.0	4000	0	0.0	4000	0	0.0	4000	0	0.0
14.00	100	5134	4856	-278	-5.4	4856	-278	-5.4	4617	-517	-10.1	4000	-1134	-22.1
14.00	110	6373	5976	-397	-6.2	5976	-397	-6.2	5740	-633	-9.9	5028	-1345	-21.1
16.67	90	4430	4207	-223	-5.0	4207	-223	-5.0	5000	570	12.9	5000	570	12.9

Table A.17 Comparison of Final Concrete Strength (Strand Dia = 0.5 in.).

Spacing (ft.)	Span (ft.)	All Skews	Skew = 0			Skew = 15			Skew = 30			Skew = 60		
		f'_c (psi)	f'_c (psi)	Diff.	% Diff. w.r.t STD	f'_c (psi)	Diff.	% Diff. w.r.t STD	f'_c (psi)	Diff.	% Diff. w.r.t STD	f'_c (psi)	Diff.	% Diff. w.r.t STD
		STD	LRFD			LRFD			LRFD			LRFD		
8.50	90	5000	5000	0	0.0	5000	0	0.0	5000	0	0.0	5000	0	0.0
8.50	100	5000	5000	0	0.0	5000	0	0.0	5000	0	0.0	5000	0	0.0
8.50	110	5431	5000	-431	-7.9	5000	-431	-7.9	5000	-431	-7.9	5000	-431	-7.9
8.50	120	6598	5919	-679	-10.3	5945	-653	-9.9	5970	-628	-9.5	6049	-549	-8.3
8.50	130	7893	7129	-764	-9.7	7129	-764	-9.7	7151	-742	-9.4	7211	-682	-8.6
10.00	90	5000	5000	0	0.0	5000	0	0.0	5000	0	0.0	5000	0	0.0
10.00	100	5000	5000	0	0.0	5000	0	0.0	5000	0	0.0	5000	0	0.0
10.00	110	5852	5231	-621	-10.6	5231	-621	-10.6	5257	-595	-10.2	5391	-461	-7.9
10.00	120	7117	6358	-759	-10.7	6381	-736	-10.3	6405	-712	-10.0	6505	-612	-8.6
10.00	130	8580	7660	-920	-10.7	7660	-920	-10.7	7652	-928	-10.8	7743	-837	-9.8
11.50	90	5000	5000	0	0.0	5000	0	0.0	5000	0	0.0	5000	0	0.0
11.50	100	5000	5000	0	0.0	5000	0	0.0	5000	0	0.0	5000	0	0.0
11.50	110	6223	5586	-637	-10.2	5611	-612	-9.8	5636	-587	-9.4	5736	-487	-7.8
11.50	120	7593	6804	-789	-10.4	6804	-789	-10.4	6826	-767	-10.1	6944	-649	-8.5
14.00	90	5000	5000	0	0.0	5000	0	0.0	5000	0	0.0	5000	0	0.0
14.00	100	5560	5022	-538	-9.7	5022	-538	-9.7	5047	-513	-9.2	5165	-395	-7.1
14.00	110	6916	6233	-683	-9.9	6233	-683	-9.9	6255	-661	-9.6	6374	-542	-7.8
16.67	90	5000	5000	0	0.0	5000	0	0.0	5000	0	0.0	5000	0	0.0
16.67	100	6119	5537	-582	-9.5	5560	-559	-9.1	5584	-535	-8.7	5684	-435	-7.1

Table A.18 Comparison of Final Concrete Strength (Strand Dia = 0.6 in.).

Spacing (ft.)	Span (ft.)	All Skews	Skew = 0			Skew = 15			Skew = 30			Skew = 60		
		f'_c (psi) STD	f'_c (psi) LRFD	Diff.	% Diff. w.r.t STD	f'_c (psi) LRFD	Diff.	% Diff. w.r.t STD	f'_c (psi) LRFD	Diff.	% Diff. w.r.t STD	f'_c (psi) LRFD	Diff.	% Diff. w.r.t STD
8.50	90	5000	5000	0	0.0	5000	0	0.0	5000	0	0.0	5000	0	0.0
8.50	100	5000	5000	0	0.0	5000	0	0.0	5000	0	0.0	5000	0	0.0
8.50	110	5340	5000	-340	-6.4	5000	-340	-6.4	5000	-340	-6.4	5000	-340	-6.4
8.50	120	6378	5756	-622	-9.8	5812	-566	-8.9	5812	-566	-8.9	5928	-450	-7.1
8.50	130	7611	6854	-757	-9.9	6854	-757	-9.9	6905	-706	-9.3	7011	-600	-7.9
10.00	90	5000	5000	0	0.0	5000	0	0.0	5000	0	0.0	5000	0	0.0
10.00	100	5000	5000	0	0.0	5000	0	0.0	5000	0	0.0	5000	0	0.0
10.00	110	5852	5231	-621	-10.6	5231	-621	-10.6	5257	-595	-10.2	5391	-461	-7.9
10.00	120	7117	6358	-759	-10.7	6381	-736	-10.3	6405	-712	-10.0	6505	-612	-8.6
10.00	130	8580	7660	-920	-10.7	7660	-920	-10.7	7652	-928	-10.8	7743	-837	-9.8
11.50	90	5000	5000	0	0.0	5000	0	0.0	5000	0	0.0	5000	0	0.0
11.50	100	5000	5000	0	0.0	5000	0	0.0	5000	0	0.0	5000	0	0.0
11.50	110	6223	5586	-637	-10.2	5611	-612	-9.8	5636	-587	-9.4	5736	-487	-7.8
11.50	120	7593	6804	-789	-10.4	6804	-789	-10.4	6826	-767	-10.1	6944	-649	-8.5
14.00	90	5000	5000	0	0.0	5000	0	0.0	5000	0	0.0	5000	0	0.0
14.00	100	5560	5022	-538	-9.7	5022	-538	-9.7	5047	-513	-9.2	5165	-395	-7.1
14.00	110	6916	6233	-683	-9.9	6233	-683	-9.9	6255	-661	-9.6	6374	-542	-7.8
16.67	90	5000	5000	0	0.0	5000	0	0.0	5000	0	0.0	5000	0	0.0

Table A.19 Comparison of Initial Prestress Loss (Strand Dia = 0.5 in.).

Spacing (ft.)	Span (ft.)	All Skews	Skew = 0			Skew = 15			Skew = 30			Skew = 60		
		TIL (ksi) STD	TIL (ksi) LRFD	Diff.	% Diff. w.r.t STD	TIL (ksi) LRFD	Diff.	% Diff. w.r.t STD	TIL (ksi) LRFD	Diff.	% Diff. w.r.t STD	TIL (ksi) LRFD	Diff.	% Diff. w.r.t STD
8.50	90	10.6	9.7	-0.9	-8.7	9.7	-0.9	-8.7	9.7	-0.9	-8.7	8.2	-2.4	-22.6
8.50	100	12.2	12.2	0.0	-0.2	12.2	0.0	-0.2	11.5	-0.7	-6.0	10.1	-2.2	-17.8
8.50	110	14.2	14.4	0.3	1.9	14.4	0.3	1.9	13.8	-0.4	-2.9	12.4	-1.8	-12.5
8.50	120	15.3	16.0	0.7	4.4	15.6	0.3	2.1	15.3	0.0	-0.3	14.1	-1.2	-8.0
8.50	130	16.4	17.3	0.9	5.4	17.3	0.9	5.4	16.9	0.6	3.4	15.2	-1.2	-7.0
10.00	90	11.5	12.1	0.6	5.2	12.1	0.6	5.2	11.0	-0.5	-4.2	9.9	-1.6	-14.0
10.00	100	13.7	14.5	0.8	5.7	14.5	0.8	5.7	13.5	-0.2	-1.4	11.5	-2.2	-15.9
10.00	110	15.3	16.3	1.0	6.5	16.3	1.0	6.5	15.7	0.4	2.8	14.2	-1.0	-6.8
10.00	120	16.2	17.3	1.1	7.0	17.3	1.1	7.0	16.8	0.6	3.9	15.7	-0.5	-2.8
10.00	130	17.4	18.8	1.3	7.7	18.8	1.3	7.7	18.3	0.9	5.4	16.7	-0.7	-3.9
11.50	90	12.6	12.6	0.0	0.0	12.6	0.0	0.0	11.9	-0.7	-5.5	10.4	-2.1	-17.0
11.50	100	15.1	15.6	0.5	3.2	15.6	0.5	3.2	14.9	-0.2	-1.4	12.9	-2.2	-14.8
11.50	110	16.2	17.0	0.8	5.0	16.7	0.5	2.9	16.3	0.1	0.8	15.0	-1.2	-7.3
11.50	120	17.2	18.2	1.0	5.9	18.2	1.0	5.9	17.9	0.7	4.2	16.3	-0.9	-5.1
14.00	90	15.6	16.6	1.0	6.5	16.0	0.4	2.5	16.0	0.4	2.5	12.6	-3.0	-19.4
14.00	100	16.7	17.3	0.6	3.4	17.3	0.6	3.4	14.6	-2.1	-12.5	15.6	-1.1	-6.7
14.00	110	18.1	18.9	0.7	3.9	18.9	0.7	3.9	18.6	0.4	2.3	17.0	-1.1	-6.2
16.67	90	17.5	17.0	-0.5	-2.9	17.0	-0.5	-2.9	16.6	-0.9	-5.1	14.6	-2.9	-16.6
16.67	100	18.3	18.8	0.6	3.2	18.5	0.3	1.6	18.2	0.0	-0.1	17.0	-1.3	-7.0

Table A.20 Comparison of Initial Prestress Loss (Strand Dia = 0.6 in.).

Spacing (ft.)	Span (ft.)	All Skews	Skew = 0			Skew = 15			Skew = 30			Skew = 60		
		TIL (ksi) STD	TIL (ksi) LRFD	Diff.	% Diff. w.r.t STD	TIL (ksi) LRFD	Diff.	% Diff. w.r.t STD	TIL (ksi) LRFD	Diff.	% Diff. w.r.t STD	TIL (ksi) LRFD	Diff.	% Diff. w.r.t STD
8.50	90	10.5	9.9	-0.6	-5.8	9.9	-0.6	-5.8	9.9	-0.6	-5.8	8.8	-1.7	-16.4
8.50	100	12.8	12.5	-0.3	-2.1	12.5	-0.3	-2.1	12.5	-0.3	-2.1	11.0	-1.8	-14.3
8.50	110	14.3	14.2	0.0	0.0	14.2	0.0	0.0	14.2	0.0	0.0	12.3	-2.0	-13.7
8.50	120	15.7	16.3	0.6	3.5	15.7	0.0	0.0	15.7	0.0	0.0	14.5	-1.2	-7.5
8.50	130	16.7	17.2	0.6	3.4	17.2	0.6	3.4	16.7	0.1	0.3	15.7	-1.0	-6.0
10.00	90	11.5	12.1	0.6	5.2	12.1	0.6	5.2	11.0	-0.5	-4.2	9.9	-1.6	-14.0
10.00	100	13.7	14.5	0.8	5.7	14.5	0.8	5.7	13.5	-0.2	-1.4	11.5	-2.2	-15.9
10.00	110	15.3	16.3	1.0	6.5	16.3	1.0	6.5	15.7	0.4	2.8	14.2	-1.0	-6.8
10.00	120	16.2	17.3	1.1	7.0	17.3	1.1	7.0	16.8	0.6	3.9	15.7	-0.5	-2.8
10.00	130	17.4	18.8	1.3	7.7	18.8	1.3	7.7	18.3	0.9	5.4	16.7	-0.7	-3.9
11.50	90	12.9	12.6	-0.3	-2.1	12.6	-0.3	-2.1	12.1	-0.8	-6.2	11.0	-1.9	-14.6
11.50	100	15.2	15.4	0.2	1.5	15.4	0.2	1.5	15.4	0.2	1.5	13.5	-1.7	-11.3
11.50	110	16.2	17.3	1.1	6.9	17.3	1.1	6.9	16.8	0.6	3.7	15.1	-1.1	-6.8
11.50	120	17.6	18.5	0.9	5.4	18.5	0.9	5.4	18.3	0.7	4.0	16.8	-0.8	-4.4
14.00	90	15.6	15.6	0.0	0.0	15.6	0.0	0.0	14.6	-1.0	-6.3	13.6	-1.9	-12.4
14.00	100	17.0	17.8	0.7	4.4	17.8	0.7	4.4	17.3	0.2	1.4	15.4	-1.6	-9.3
14.00	110	18.4	19.2	0.8	4.5	19.2	0.8	4.5	18.8	0.4	2.0	17.3	-1.1	-5.9
16.67	90	17.4	17.1	-0.3	-1.7	17.1	-0.3	-1.7	16.5	-0.9	-5.3	14.6	-2.8	-16.2

Table A.21 Comparison of Final Prestress Loss (Strand Dia = 0.5 in.).

Spacing (ft.)	Span (ft.)	All Skews	Skew = 0			Skew = 15			Skew = 30			Skew = 60		
		TFL (ksi) STD	TFL (ksi) LRFD	Diff.	% Diff. w.r.t STD	TFL (ksi) LRFD	Diff.	% Diff. w.r.t STD	TFL (ksi) LRFD	Diff.	% Diff. w.r.t STD	TFL (ksi) LRFD	Diff.	% Diff. w.r.t STD
8.50	90	30.5	29.7	-0.8	-2.7	29.7	-0.8	-2.7	29.7	-0.8	-2.7	26.1	-4.4	-14.5
8.50	100	33.8	34.7	0.9	2.8	34.7	0.9	2.8	33.0	-0.8	-2.3	29.5	-4.3	-12.6
8.50	110	38.2	39.1	0.9	2.4	39.1	0.9	2.4	37.5	-0.7	-1.9	34.2	-4.0	-10.5
8.50	120	43.0	44.1	1.1	2.4	42.8	-0.3	-0.6	41.4	-1.6	-3.7	37.3	-5.7	-13.3
8.50	130	47.9	48.8	0.9	1.9	48.8	0.9	1.9	47.6	-0.3	-0.7	41.1	-6.8	-14.1
10.00	90	31.6	32.6	1.0	3.0	32.6	1.0	3.0	32.6	1.0	3.0	29.0	-2.6	-8.2
10.00	100	36.4	38.9	2.5	6.9	37.3	0.9	2.4	37.3	0.9	2.4	32.2	-4.2	-11.5
10.00	110	40.7	43.2	2.4	6.0	43.2	2.4	6.0	41.8	1.1	2.7	36.5	-4.2	-10.3
10.00	120	45.8	48.1	2.3	5.1	46.8	1.1	2.3	45.6	-0.2	-0.4	40.3	-5.5	-11.9
10.00	130	50.6	52.9	2.2	4.4	52.9	2.2	4.4	51.8	1.2	2.3	45.1	-5.6	-11.0
11.50	90	34.5	35.4	0.9	2.6	35.4	0.9	2.6	33.7	-0.8	-2.3	30.3	-4.3	-12.4
11.50	100	40.6	41.5	1.0	2.3	41.5	1.0	2.3	39.9	-0.7	-1.7	35.0	-5.6	-13.9
11.50	110	45.2	46.3	1.1	2.4	45.0	-0.2	-0.5	43.7	-1.5	-3.4	38.9	-6.3	-13.9
11.50	120	49.9	50.9	1.0	2.1	50.9	1.0	2.1	49.7	-0.2	-0.4	43.3	-6.6	-13.2
14.00	90	41.5	40.7	-0.8	-1.9	40.7	-0.8	-1.9	39.1	-2.4	-5.9	34.1	-7.4	-17.9
14.00	100	46.1	46.0	-0.2	-0.4	46.0	-0.2	-0.4	44.7	-1.5	-3.2	39.9	-6.3	-13.6
14.00	110	52.7	51.8	-0.9	-1.6	51.8	-0.9	-1.6	50.6	-2.1	-4.0	44.3	-8.4	-15.9
16.67	90	45.1	44.4	-0.8	-1.7	44.4	-0.8	-1.7	43.0	-2.1	-4.7	38.1	-7.0	-15.5
16.67	100	52.5	51.1	-1.5	-2.8	49.9	-2.7	-5.1	48.6	-3.9	-7.5	43.5	-9.0	-17.2

Table A.22 Comparison of Final Prestress Loss (Strand Dia = 0.6 in.).

Spacing (ft.)	Span (ft.)	All Skews	Skew = 0			Skew = 15			Skew = 30			Skew = 60		
		TFL (ksi) STD	TFL (ksi) LRFD	Diff.	% Diff. w.r.t STD	TFL (ksi) LRFD	Diff.	% Diff. w.r.t STD	TFL (ksi) LRFD	Diff.	% Diff. w.r.t STD	TFL (ksi) LRFD	Diff.	% Diff. w.r.t STD
8.50	90	30.1	30.1	0.0	0.1	30.1	0.0	0.1	30.1	0.0	0.1	27.4	-2.6	-8.8
8.50	100	35.2	35.4	0.2	0.5	35.4	0.2	0.5	35.4	0.2	0.5	31.6	-3.6	-10.2
8.50	110	38.3	38.5	0.2	0.6	38.5	0.2	0.6	38.5	0.2	0.6	33.8	-4.5	-11.8
8.50	120	44.4	44.8	0.4	0.9	42.8	-1.6	-3.6	42.8	-1.6	-3.6	38.6	-5.8	-13.0
8.50	130	48.7	48.2	-0.5	-1.0	48.2	-0.5	-1.0	46.3	-2.4	-5.0	42.4	-6.4	-13.1
10.00	90	32.0	34.7	2.7	8.3	34.7	2.7	8.3	32.1	0.1	0.2	29.4	-2.6	-8.2
10.00	100	36.8	39.3	2.5	6.8	39.3	2.5	6.8	37.0	0.1	0.4	32.1	-4.7	-12.7
10.00	110	41.5	43.9	2.4	5.8	43.9	2.4	5.8	41.9	0.4	1.0	37.5	-3.9	-9.5
10.00	120	45.2	47.5	2.3	5.2	47.5	2.3	5.2	45.6	0.4	0.9	41.6	-3.6	-7.9
10.00	130	50.9	53.2	2.2	4.4	53.2	2.2	4.4	51.4	0.5	1.0	45.0	-6.0	-11.8
11.50	90	35.2	35.4	0.2	0.5	35.4	0.2	0.5	34.1	-1.1	-3.2	31.5	-3.7	-10.5
11.50	100	40.7	41.0	0.3	0.7	41.0	0.3	0.7	41.0	0.3	0.7	36.3	-4.4	-10.9
11.50	110	44.7	47.0	2.4	5.3	47.0	2.4	5.3	45.1	0.4	0.9	38.9	-5.7	-12.8
11.50	120	50.8	51.3	0.5	1.0	51.3	0.5	1.0	50.4	-0.4	-0.9	44.6	-6.2	-12.3
14.00	90	41.0	41.2	0.1	0.3	41.2	0.1	0.3	38.8	-2.3	-5.5	36.5	-4.6	-11.2
14.00	100	47.0	47.4	0.4	0.9	47.4	0.4	0.9	45.4	-1.5	-3.3	39.3	-7.7	-16.4
14.00	110	53.1	52.6	-0.5	-1.0	52.6	-0.5	-1.0	50.7	-2.4	-4.5	45.0	-8.2	-15.4
16.67	90	45.2	44.5	-0.7	-1.5	44.5	-0.7	-1.5	42.8	-2.4	-5.3	37.8	-7.4	-16.4

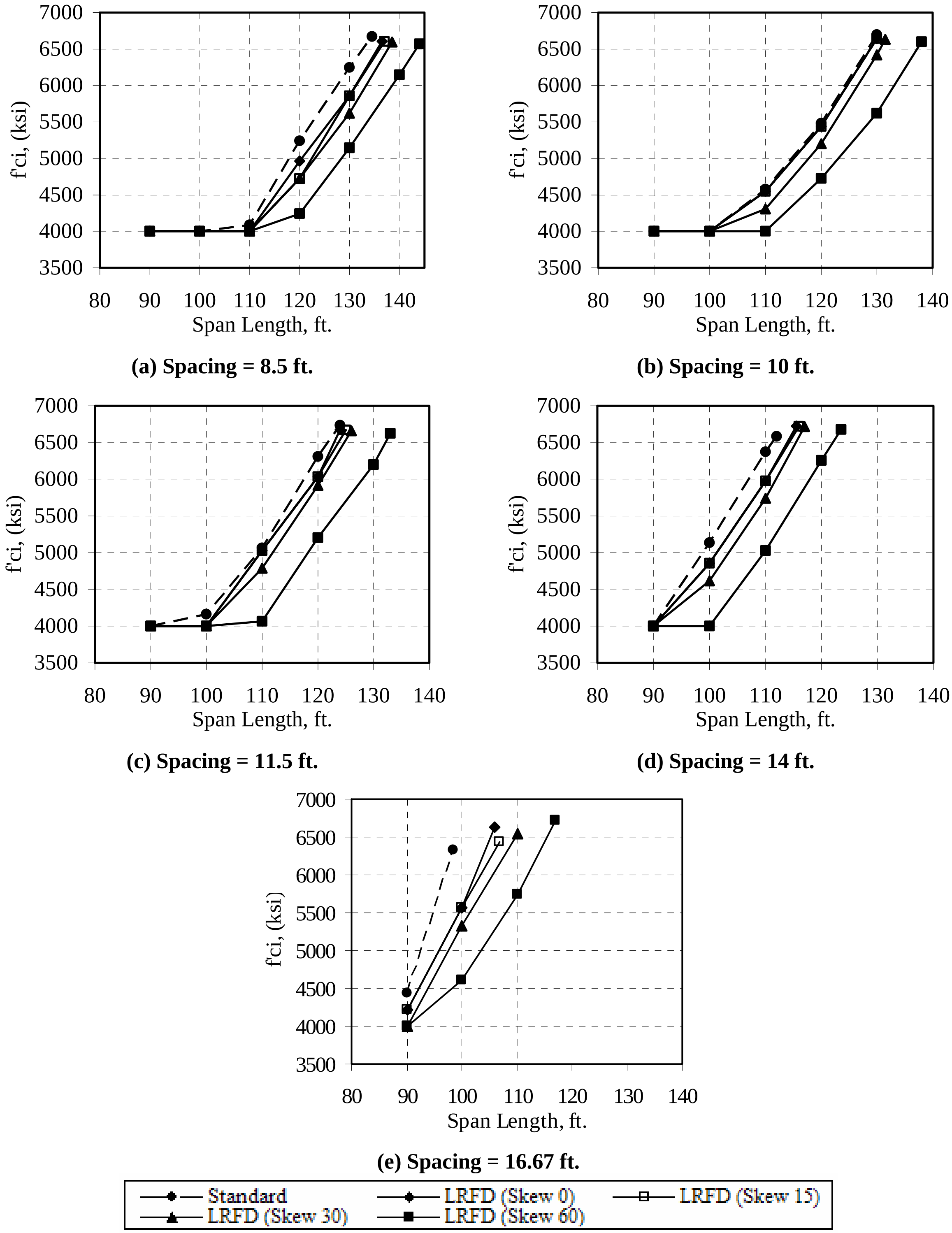

Figure A.4 Comparison of Initial Concrete Strength (Strand Diameter = 0.6 in.).

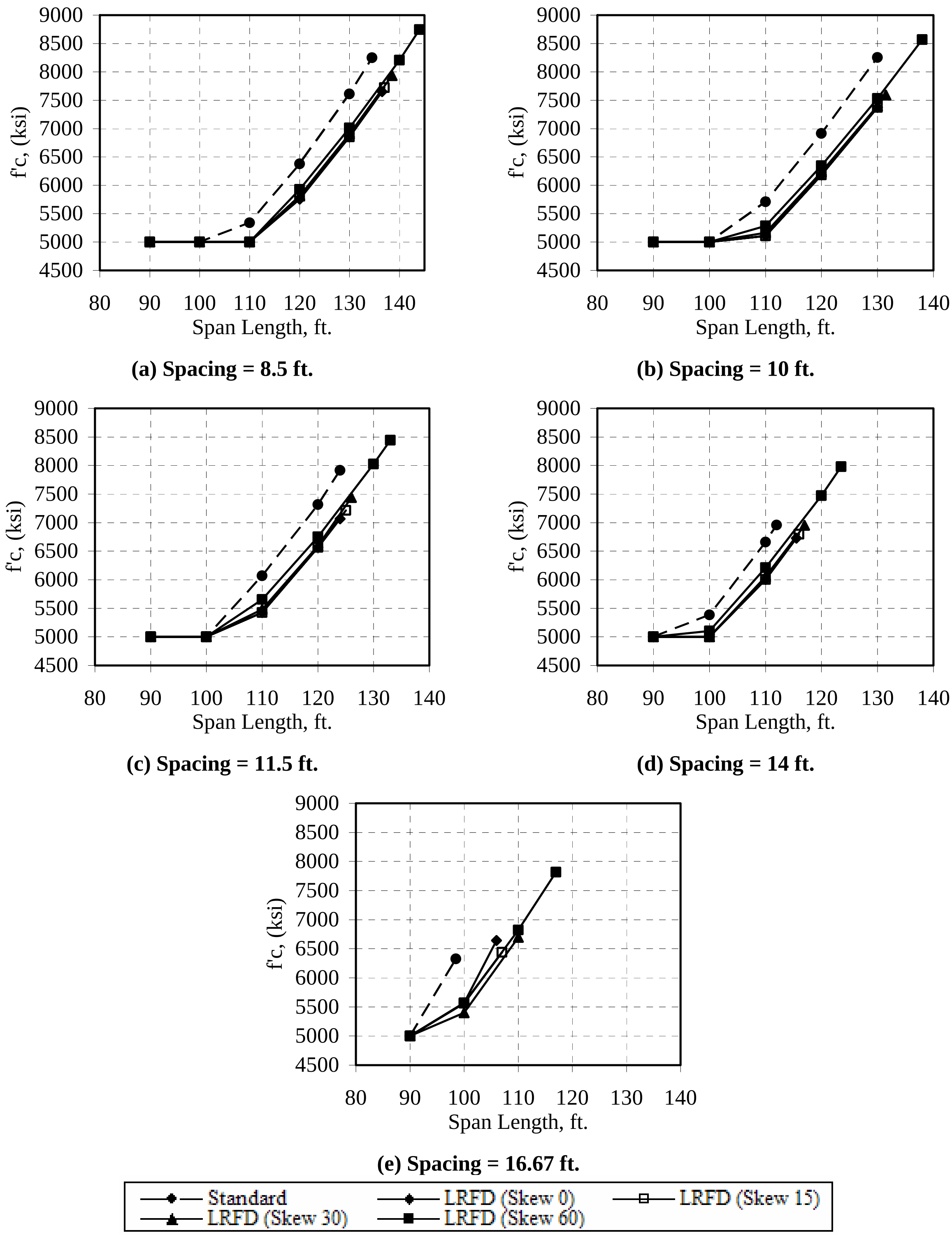

Figure A.5 Comparison of Final Concrete Strength (Strand Diameter = 0.6 in.).

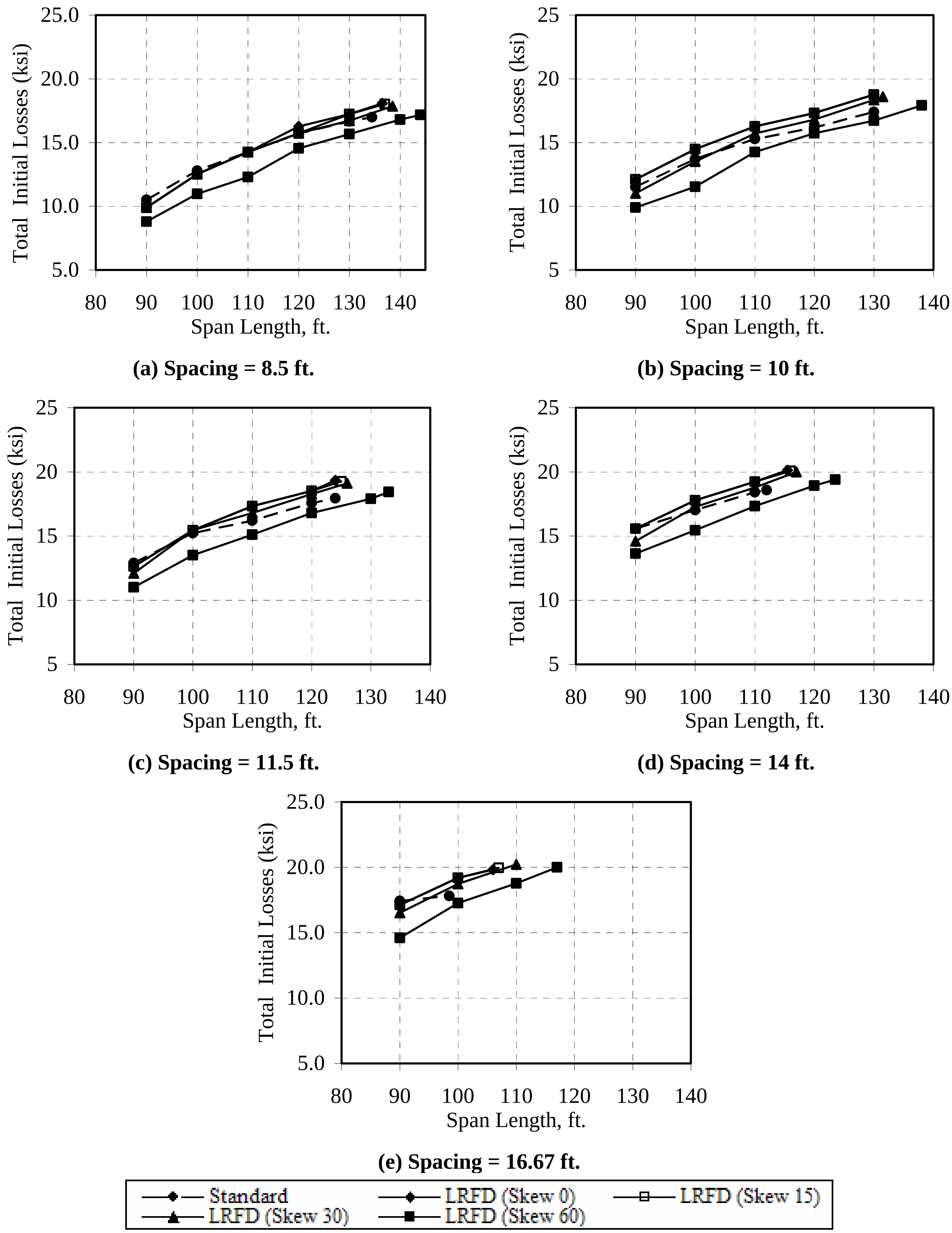

Figure A.6 Comparison of Initial Prestress Loss (Strand Diameter = 0.6 in.).

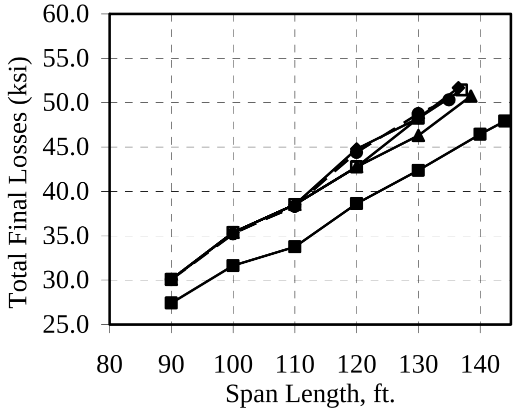

(a) Spacing = 8.5 ft.

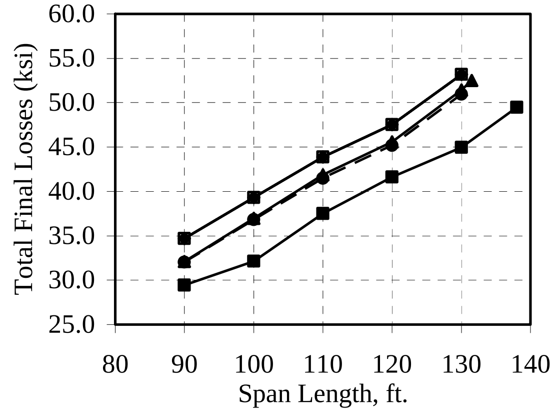

(b) Spacing = 10 ft.

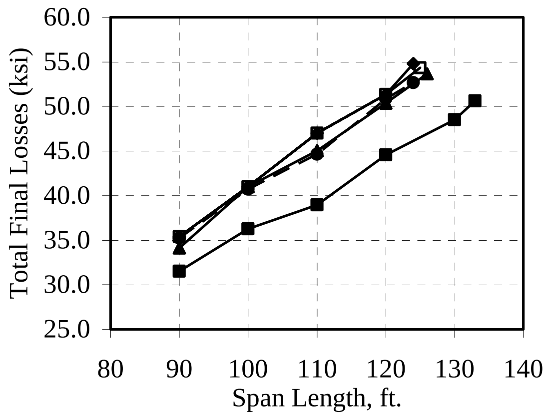

(c) Spacing = 11.5 ft.

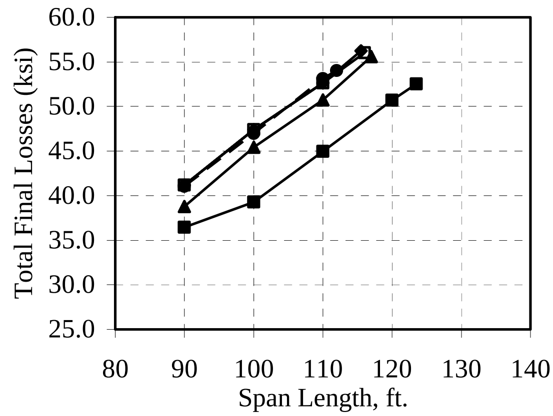

(d) Spacing = 14 ft.

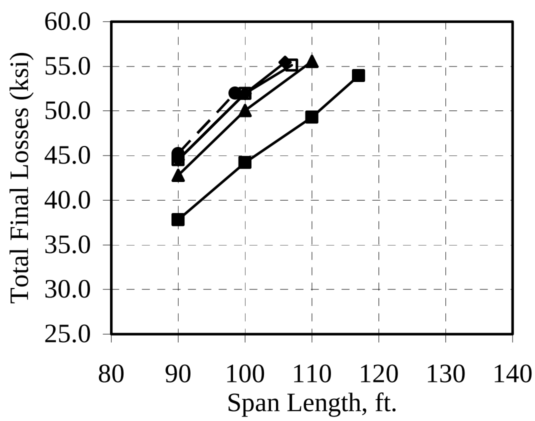

(e) Spacing = 16.67 ft.

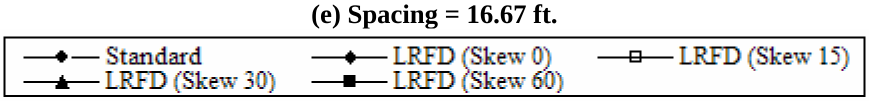

Figure A.7 Comparison of Final Prestress Loss (Strand Diameter = 0.6 in.).

Table A.23 Comparison of Number of Strands
(Strand Diameter = 0.6 in., Girder Spacing = 8.5 ft.).

Skew	Standard		LRFD		Difference in No. of Strands
	Span Length (ft.)	No. of Strands	Span Length (ft.)	No. of Strands	
0	90.0	24	90.0	22	-2
	100.0	31	100.0	29	-2
	110.0	37	110.0	35	-2
	120.0	47	120.0	45	-2
	130.0	56	130.0	53	-3
	134.5	60	136.5	60	-
15	90.0	24	90.0	22	-2
	100.0	31	100.0	29	-2
	110.0	37	110.0	35	-2
	120.0	47	120.0	43	-4
	130.0	56	130.0	53	-3
	134.5	60	137.0	60	-
30	90.0	24	90.0	22	-2
	100.0	31	100.0	29	-2
	110.0	37	110.0	35	-2
	120.0	47	120.0	43	-4
	130.0	56	130.0	51	-5
	134.5	60	138.5	60	-
60	90.0	24	90.0	20	-4
	100.0	31	100.0	26	-5
	110.0	37	110.0	31	-6
	120.0	47	120.0	39	-8
	130.0	56	130.0	47	-9
	134.5	60	140.0	56	-4
	-	-	144.5	60	-

Table A.24 Comparison of Number of Strands (Strand Diameter = 0.6 in., Girder Spacing = 10 ft.).

Skew	Standard		LRFD		Difference in No. of Strands
	Span Length (ft.)	No. of Strands	Span Length (ft.)	No. of Strands	
0	90.0	26	90.0	26	0
	100.0	33	100.0	33	0
	110.0	41	110.0	41	0
	120.0	49	120.0	49	0
	130.0	60	130.0	60	0
15	90.0	26	90.0	26	0
	100.0	33	100.0	33	0
	110.0	41	110.0	41	0
	120.0	49	120.0	49	0
	130.0	60	130.0	60	0
30	90.0	26	90.0	24	-2
	100.0	33	100.0	31	-2
	110.0	41	110.0	39	-2
	120.0	49	120.0	47	-2
	130.0	60	130.0	58	-2
	-	-	131.5	60	-
60	90.0	26	90.0	22	-4
	100.0	33	100.0	27	-6
	110.0	41	110.0	35	-6
	120.0	49	120.0	43	-6
	130.0	60	130.0	51	-9
	-	-	138.0	60	-

Table A.25 Comparison of Number of Strands (Strand Diameter = 0.6 in., Girder Spacing = 11.5 ft.).

Skew	Standard		LRFD		Difference in No. of Strands
	Span Length (ft.)	No. of Strands	Span Length (ft.)	No. of Strands	
0	90.0	29	90.0	27	-2
	100.0	37	100.0	35	-2
	110.0	45	110.0	45	0
	120.0	56	120.0	54	-2
	124.0	60	124.0	60	0
15	90.0	29	90.0	27	-2
	100.0	37	100.0	35	-2
	110.0	45	110.0	45	0
	120.0	56	120.0	54	-2
	124.0	60	125.0	60	-
30	90.0	29	90.0	26	-3
	100.0	37	100.0	35	-2
	110.0	45	110.0	43	-2
	120.0	56	120.0	53	-3
	124.0	60	126.0	60	-
60	90.0	29	90.0	24	-5
	100.0	37	100.0	31	-6
	110.0	45	110.0	37	-8
	120.0	56	120.0	47	-9
	124.0	60	130.0	56	-
	-	-	133.0	60	-

Table A.26 Comparison of Number of Strands (Strand Diameter = 0.6 in., Girder Spacing = 14 ft.).

Skew	Standard		LRFD		Difference in No. of Strands
	Span Length (ft.)	No. of Strands	Span Length (ft.)	No. of Strands	
0	90.0	35	90.0	33	-2
	100.0	45	100.0	43	-2
	110.0	56	110.0	53	-3
	112.0	58	115.5	60	-
15	90.0	35	90.0	33	-2
	100.0	45	100.0	43	-2
	110.0	56	110.0	53	-3
	112.0	58	116.0	60	-
30	90.0	35	90.0	31	-4
	100.0	45	100.0	41	-4
	110.0	56	110.0	51	-5
	112.0	58	117.0	60	-
60	90.0	35	90.0	29	-6
	100.0	45	100.0	35	-10
	110.0	56	110.0	45	-11
	112.0	58	120.0	56	-
	-	-	123.5	60	-

Table A.27 Comparison of Number of Strands (Strand Diameter = 0.6 in., Girder Spacing = 16.67 ft.).

Skew	Standard		LRFD		Difference in No. of Strands
	Span Length (ft.)	No. of Strands	Span Length (ft.)	No. of Strands	
0	90.0	41	90.0	37	-4
	98.5	51	100.0	49	-
	-	-	106.0	56	-
15	90.0	41	90.0	37	-4
	98.5	51	100.0	49	-
	-	-	107.0	56	-
30	90.0	41	90.0	35	-6
	98.5	51	100.0	47	-
	-	-	110.0	58	-
60	90.0	41	90.0	31	-10
	98.5	51	100.0	41	-
	-	-	110.0	51	-
	-	-	117.0	60	-

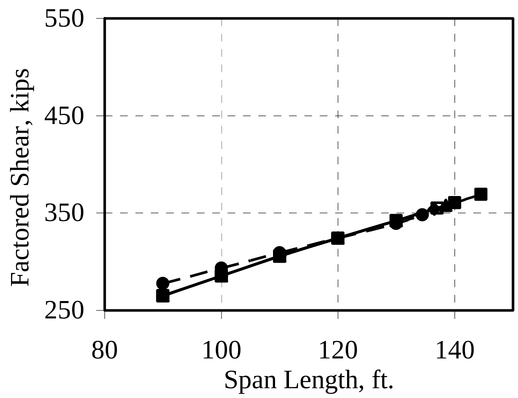

(a) Spacing = 8.5 ft.

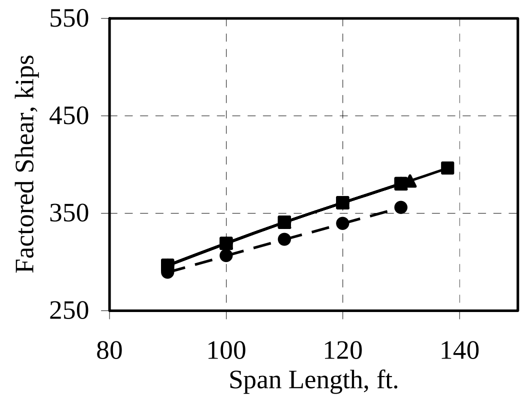

(b) Spacing = 10 ft.

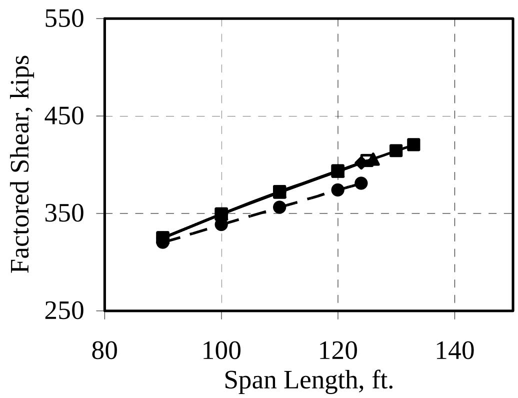

(c) Spacing = 11.5 ft.

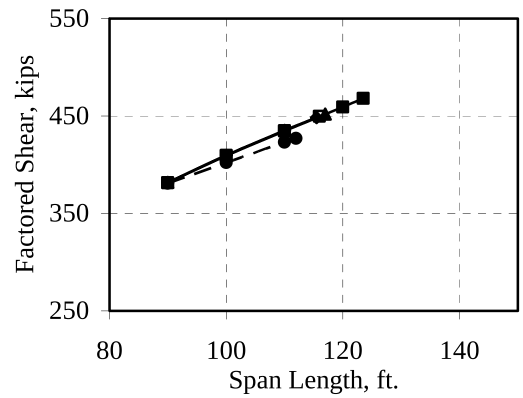

(d) Spacing = 14 ft.

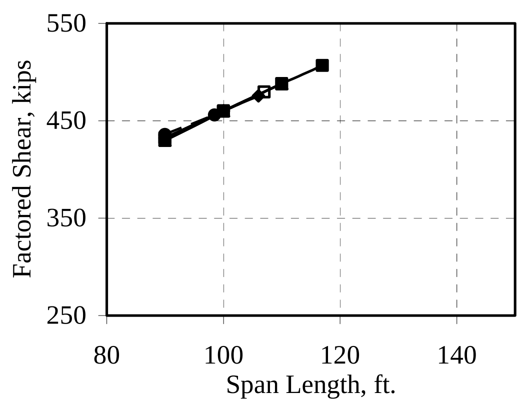

(e) Spacing = 16.67 ft.

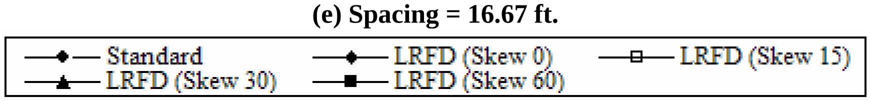

Figure A.8 Comparison of Factored Design Shear at Respective Critical Section Location (Strand Diameter = 0.6 in.).

Table A.28 Comparison of Factored Design Moment.

Spacing (ft.)	Span (ft.)	All Skews Moment (k-ft) STD	Skew = 0 Span (ft.) LRFD	Skew = 0 Moment (k-ft) LRFD	Skew = 0 % Diff. w.r.t STD	Skew = 15 Span (ft.) LRFD	Skew = 15 Moment (k-ft) LRFD	Skew = 15 % Diff. w.r.t STD	Skew = 30 Span (ft.) LRFD	Skew = 30 Moment (k-ft) LRFD	Skew = 30 % Diff. w.r.t STD	Skew = 60 Span (ft.) LRFD	Skew = 60 Moment (k-ft) LRFD	Skew = 60 % Diff. w.r.t STD
8.50	90.0	6197	90.0	5511	-11.1	90.0	5466	-11.8	90.0	5266	-15.0	90.0	4530	-26.9
8.50	100.0	7310	100.0	6541	-10.5	100.0	6492	-11.2	100.0	6270	-14.2	100.0	5433	-25.7
8.50	110.0	8493	110.0	7653	-9.9	110.0	7597	-10.5	110.0	7348	-13.5	110.0	6410	-24.5
8.50	120.0	9746	120.0	8839	-9.3	120.0	8776	-10.0	120.0	8500	-12.8	120.0	7463	-23.4
8.50	130.0	11070	130.0	10108	-8.7	130.0	10038	-9.3	130.0	9735	-12.1	130.0	8594	-22.4
8.50	135.0	11759	136.5	10972	-	136.5	10897	-	138.5	10844	-	140.0	9803	-
8.50	-	-	-	-	-	-	-	-	-	-	-	142.0	10047	-
10.00	90.0	6468	90.0	6067	-6.2	90.0	6021	-6.9	90.0	5797	-10.4	90.0	4965	-23.2
10.00	100.0	7642	100.0	7201	-5.8	100.0	7147	-6.5	100.0	6896	-9.8	100.0	5953	-22.1
10.00	110.0	8892	110.0	8418	-5.3	110.0	8357	-6.0	110.0	8074	-9.2	110.0	7020	-21.1
10.00	120.0	10219	120.0	9721	-4.9	120.0	9652	-5.5	120.0	9338	-8.6	120.0	8170	-20.1
10.00	130.0	11623	130.0	11107	-4.4	130.0	11029	-5.1	130.0	10684	-8.1	130.0	9402	-19.1
10.00	-	-	130.5	11176	-	131.0	11173	-	133.0	11107	-	139.0	10586	-
11.50	90.0	7155	90.0	6559	-8.3	90.0	6505	-9.1	90.0	6259	-12.5	90.0	5340	-25.4
11.50	100.0	8438	100.0	7777	-7.8	100.0	7714	-8.6	100.0	7438	-11.9	100.0	6393	-24.2
11.50	110.0	9801	110.0	9082	-7.3	110.0	9016	-8.0	110.0	8705	-11.2	110.0	7536	-23.1
11.50	120.0	11245	120.0	10478	-6.8	120.0	10403	-7.5	120.0	10057	-10.6	120.0	8770	-22.0
11.50	124.0	11846	125.5	11285	-	126.0	11283	-	127.5	11138	-	130.0	10086	-
11.50	-	-	-	-	-	-	-	-	-	-	-	134.0	10640	-
14.00	90.0	8466	90.0	7564	-10.7	90.0	7481	-11.6	90.0	7231	-14.6	90.0	6171	-27.1
14.00	100.0	9975	100.0	8987	-9.9	100.0	8890	-10.9	100.0	8551	-14.3	100.0	7395	-25.9
14.00	110.0	11578	110.0	10502	-9.3	110.0	10392	-10.2	110.0	10059	-13.1	110.0	8717	-24.7
14.00	113.0	12076	115.5	11381	-5.8	116.0	11378	-5.8	118.0	11309	-6.4	120.0	10144	-16.0
14.00	-	-	-	-	-	-	-	-	-	-	-	123.5	10664	-
16.67	90.0	9661	90.0	8391	-13.1	90.0	8320	-13.9	90.0	7999	-17.2	90.0	6798	-29.6
16.67	100.0	11387	100.0	9957	-12.6	100.0	9874	-13.3	100.0	9507	-16.5	100.0	8148	-28.4
16.67	104.5	12186	109.0	11446	-6.1	109.5	11445	-6.1	110.0	11120	-8.7	110.0	9596	-21.3
16.67	-	-	-	-	-	-	-	-	111.0	11293	-	117.0	10678	-

Table A.29 Comparison of Factored Design Shear at Respective Critical Section Location (Strand Diameter = 0.5 in.).

Spacing (ft.)	Span (ft.)	All Skews	Skew = 0			Skew = 15			Skew = 30			Skew = 60		
		Shear (k-ft) STD	Span (ft.) LRFD	Shear (k-ft) LRFD	% Diff. w.r.t STD	Span (ft.) LRFD	Shear (k-ft) LRFD	% Diff. w.r.t STD	Span (ft.) LRFD	Shear (k-ft) LRFD	% Diff. w.r.t STD	Span (ft.) LRFD	Shear (k-ft) LRFD	% Diff. w.r.t STD
8.50	90.0	277	90.0	265	-4.5	90.0	265	-4.5	90.0	265	-4.5	90.0	265	-4.5
8.50	100.0	293	100.0	286	-2.6	100.0	286	-2.6	100.0	286	-2.7	100.0	286	-2.7
8.50	110.0	309	110.0	306	-1.0	110.0	306	-1.0	110.0	306	-1.0	110.0	306	-1.1
8.50	120.0	324	120.0	324	0.0	120.0	324	0.0	120.0	324	0.0	120.0	324	0.0
8.50	130.0	339	130.0	342	0.8	130.0	342	0.8	130.0	342	0.8	130.0	342	0.8
8.50	135.0	349	136.5	354	-	136.5	354	-	138.5	358	-	140.0	361	-
8.50	-	-	-	-	-	-	-	-	-	-	-	142.0	371	-
10.00	90.0	289	90.0	297	2.5	90.0	297	2.5	90.0	296	2.5	90.0	296	2.5
10.00	100.0	306	100.0	319	4.3	100.0	319	4.2	100.0	319	4.2	100.0	319	4.2
10.00	110.0	323	110.0	341	5.5	110.0	341	5.5	110.0	341	5.4	110.0	340	5.3
10.00	120.0	340	120.0	360	6.1	120.0	361	6.2	120.0	361	6.2	120.0	361	6.2
10.00	130.0	356	130.0	380	6.7	130.0	380	6.7	130.0	380	6.7	130.0	380	6.7
10.00	-	-	130.5	381	-	131.0	382	-	133.0	386	-	139.0	398	-
11.50	90.0	320	90.0	325	1.6	90.0	325	1.6	90.0	325	1.6	90.0	325	1.5
11.50	100.0	338	100.0	350	3.3	100.0	350	3.3	100.0	350	3.3	100.0	349	3.3
11.50	110.0	356	110.0	372	4.4	110.0	372	4.4	110.0	372	4.4	110.0	372	4.4
11.50	120.0	374	120.0	393	5.2	120.0	393	5.2	120.0	393	5.1	120.0	393	5.2
11.50	124.0	381	125.5	404	-	126.0	405	-	127.5	408	-	130.0	414	-
11.50	-	-	-	-	-	-	-	-	-	-	-	134.0	423	-
14.00	90.0	381	90.0	382	0.3	90.0	382	0.3	90.0	382	0.2	90.0	382	0.2
14.00	100.0	402	100.0	410	1.9	100.0	410	1.9	100.0	410	1.9	100.0	409	1.8
14.00	110.0	423	110.0	435	2.8	110.0	435	2.8	110.0	435	2.8	110.0	435	2.7
14.00	113.0	429	115.5	448	4.3	116.0	449	4.6	118.0	454	5.8	120.0	459	6.9
14.00	-	-	-	-	-	-	-	-	-	-	-	123.5	467	-
16.67	90.0	436	90.0	430	-1.2	90.0	430	-1.2	90.0	430	-1.2	90.0	430	-1.3
16.67	100.0	459	100.0	460	0.3	100.0	460	0.2	100.0	460	0.2	100.0	460	0.2
16.67	104.5	469	109.0	485	3.3	109.5	486	3.5	110.0	487	3.8	110.0	487	3.8
16.67	-	-	-	-	-	-	-	-	111.0	490	-	117.0	506	-

Table A.30 Comparison of Factored Design Shear at Respective Critical Section Location (Strand Diameter = 0.6 in.).

Spacing (ft.)	Span (ft.)	All Skews	Skew = 0			Skew = 15			Skew = 30			Skew = 60		
		Shear (k-ft)	Span (ft.)	Shear (k-ft)	% Diff. w.r.t STD	Span (ft.)	Shear (k-ft)	% Diff. w.r.t STD	Span (ft.)	Shear (k-ft)	% Diff. w.r.t STD	Span (ft.)	Shear (k-ft)	% Diff. w.r.t STD
		STD	LRFD			LRFD			LRFD			LRFD		
8.50	90.0	277	90.0	265	-4.5	90.0	265	-4.5	90.0	265	-4.5	90.0	265	-4.5
8.50	100.0	293	100.0	286	-2.7	100.0	286	-2.7	100.0	285	-2.7	100.0	285	-2.7
8.50	110.0	309	110.0	306	-1.0	110.0	306	-1.0	110.0	306	-1.0	110.0	306	-1.1
8.50	120.0	324	120.0	324	0.0	120.0	324	0.0	120.0	324	0.0	120.0	324	0.0
8.50	130.0	339	130.0	342	0.8	130.0	342	0.8	130.0	342	0.9	130.0	342	0.8
8.50	134.5	348	136.5	354	-	137.0	355	-	138.5	358	-	140.0	361	-
8.50	-	-	-	-	-	-	-	-	-	-	-	144.5	369	-
10.00	90.0	289	90.0	296	2.5	90.0	296	2.5	90.0	296	2.5	90.0	296	2.5
10.00	100.0	306	100.0	319	4.1	100.0	319	4.1	100.0	319	4.2	100.0	319	4.1
10.00	110.0	323	110.0	341	5.5	110.0	341	5.5	110.0	341	5.5	110.0	341	5.4
10.00	120.0	340	120.0	361	6.2	120.0	361	6.2	120.0	361	6.3	120.0	361	6.2
10.00	130.0	356	130.0	380	6.9	130.0	380	6.9	130.0	380	6.8	130.0	380	6.8
10.00	-	-	-	-	-	-	-	-	131.5	383	-	138.0	396	-
11.50	90.0	320	90.0	325	1.5	90.0	325	1.5	90.0	325	1.5	90.0	325	1.5
11.50	100.0	338	100.0	349	3.3	100.0	349	3.3	100.0	349	3.3	100.0	349	3.2
11.50	110.0	356	110.0	372	4.5	110.0	372	4.5	110.0	372	4.5	110.0	372	4.4
11.50	120.0	374	120.0	394	5.3	120.0	394	5.3	120.0	393	5.2	120.0	393	5.3
11.50	124.0	381	124.0	402	-	125.0	404	-	126.0	406	-	130.0	414	-
11.50	-	-	-	-	-	-	-	-	-	-	-	133.0	420	-
14.00	90.0	381	90.0	382	0.2	90.0	382	0.2	90.0	382	0.2	90.0	382	0.2
14.00	100.0	402	100.0	410	1.8	100.0	410	1.8	100.0	410	1.8	100.0	409	1.8
14.00	110.0	423	110.0	435	2.8	110.0	435	2.8	110.0	435	2.9	110.0	435	2.8
14.00	112.0	427	115.5	448	5.0	116.0	450	5.3	117.0	452	5.9	120.0	459	7.5
14.00	-	-	-	-	-	-	-	-	-	-	-	123.5	468	-
16.67	90.0	436	90.0	432	-0.9	90.0	432	-0.9	90.0	430	-1.3	90.0	430	-1.4
16.67	98.5	456	100.0	460	0.9	100.0	460	0.9	100.0	460	1.0	100.0	460	0.9
16.67	-	-	106.0	475	-	107.0	479	-	110.0	488	-	110.0	488	-
16.67	-	-	-	-	-	-	-	-	-	-	-	117.0	507	-

Table A.31 Comparison of Nominal Moment Capacity (Strand Diameter = 0.5 in.).

Spacing (ft.)	Span (ft.)	All Skews	Skew = 0			Skew = 15			Skew = 30			Skew = 60		
		Mn (k-ft)	Span (ft.)	Mn (k-ft)	% Diff. w.r.t STD	Span (ft.)	Mn (k-ft)	% Diff. w.r.t STD	Span (ft.)	Mn (k-ft)	% Diff. w.r.t STD	Span (ft.)	Mn (k-ft)	% Diff. w.r.t STD
		STD	LRFD			LRFD			LRFD			LRFD		
8.50	90.0	6707	90.0	6043	-9.9	90.0	6043	-9.9	90.0	6043	-9.9	90.0	5322	-20.7
8.50	100.0	8077	100.0	7805	-3.4	100.0	7805	-3.4	100.0	7457	-7.7	100.0	6755	-16.4
8.50	110.0	9729	110.0	9506	-2.3	110.0	9506	-2.3	110.0	9171	-5.7	110.0	8492	-12.7
8.50	120.0	11699	120.0	11608	-0.8	120.0	11313	-3.3	120.0	11013	-5.9	120.0	10005	-14.5
8.50	130.0	13690	130.0	13624	-0.5	130.0	13624	-0.5	130.0	13354	-2.5	130.0	11943	-12.8
8.50	135.0	14802	136.5	15013	-	136.5	15013	-	138.5	15037	-	140.0	13962	-
8.50	-	-	-	-	-	-	-	-	-	-	-	142.0	15129	-
10.00	90.0	7127	90.0	6814	-4.4	90.0	6814	-4.4	90.0	6814	-4.4	90.0	6090	-14.6
10.00	100.0	8862	100.0	8936	0.8	100.0	8587	-3.1	100.0	8587	-3.1	100.0	7529	-15.0
10.00	110.0	10677	110.0	10789	1.0	110.0	10789	1.0	110.0	10465	-2.0	110.0	9282	-13.1
10.00	120.0	12830	120.0	13076	1.9	120.0	12777	-0.4	120.0	12380	-3.5	120.0	11111	-13.4
10.00	130.0	14965	130.0	15203	1.6	130.0	15203	1.6	130.0	14955	-0.1	130.0	13415	-10.4
10.00	-	-	130.5	15437	-	131.0	15439	-	133.0	15675	-	139.0	15524	-
11.50	90.0	7894	90.0	7583	-3.9	90.0	7583	-3.9	90.0	7221	-8.5	90.0	6492	-17.8
11.50	100.0	9984	100.0	9717	-2.7	100.0	9717	-2.7	100.0	9365	-6.2	100.0	8301	-16.9
11.50	110.0	12086	110.0	11888	-1.6	110.0	11562	-4.3	110.0	11234	-7.0	110.0	10066	-16.7
11.50	120.0	14250	120.0	14123	-0.9	120.0	14123	-0.9	120.0	13809	-3.1	120.0	12212	-14.3
11.50	124.0	15244	125.5	15793	-	126.0	15796	-	127.5	15802	-	130.0	15027	-
11.50	-	-	-	-	-	-	-	-	-	-	-	134.0	15859	-
14.00	90.0	9763	90.0	9825	0.6	90.0	9466	-3.0	90.0	8743	-10.4	90.0	7648	-21.7
14.00	100.0	11958	100.0	11382	-4.8	100.0	11382	-4.8	100.0	11043	-7.7	100.0	9825	-17.8
14.00	110.0	14697	110.0	14042	-4.5	110.0	14042	-4.5	110.0	13714	-6.7	110.0	12056	-18.0
14.00	113.0	15582	115.5	15763	1.2	116.0	15763	1.2	118.0	16041	2.9	120.0	14854	-4.7
14.00	-	-	-	-	-	-	-	-	-	-	-	123.5	15763	-
16.67	90.0	11422	90.0	10271	-10.1	90.0	10271	-10.1	90.0	9907	-13.3	90.0	8807	-22.9
16.67	100.0	14100	100.0	13204	-6.4	100.0	12864	-8.8	100.0	12524	-11.2	100.0	11147	-20.9
16.67	104.5	15541	109.0	15988	2.9	109.5	15988	2.9	110.0	15686	0.9	110.0	13880	-10.7
16.67	-	-	-	-	-	-	-	-	111.0	15988	-	117.0	15988	-

Table A.32 Comparison of Nominal Moment Capacity (Strand Diameter = 0.6 in.).

Spacing (ft.)	Span (ft.)	All Skews Mn (k-ft) STD	Skew = 0 Span (ft.) LRFD	Skew = 0 Mn (k-ft) LRFD	Skew = 0 % Diff. w.r.t STD	Skew = 15 Span (ft.) LRFD	Skew = 15 Mn (k-ft) LRFD	Skew = 15 % Diff. w.r.t STD	Skew = 30 Span (ft.) LRFD	Skew = 30 Mn (k-ft) LRFD	Skew = 30 % Diff. w.r.t STD	Skew = 60 Span (ft.) LRFD	Skew = 60 Mn (k-ft) LRFD	Skew = 60 % Diff. w.r.t STD
8.50	90.0	6587	90.0	6108	-7.3	90.0	6108	-7.3	90.0	6108	-7.3	90.0	5579	-15.3
8.50	100.0	8316	100.0	7904	-5.0	100.0	7904	-5.0	100.0	7904	-5.0	100.0	7153	-14.0
8.50	110.0	9721	110.0	9355	-3.8	110.0	9355	-3.8	110.0	9355	-3.8	110.0	8392	-13.7
8.50	120.0	11958	120.0	11717	-2.0	120.0	11279	-5.7	120.0	11279	-5.7	120.0	10299	-13.9
8.50	130.0	13837	130.0	13446	-2.8	130.0	13446	-2.8	130.0	13037	-5.8	130.0	12195	-11.9
8.50	134.5	14606	136.5	14811	-	137.0	14815	-	138.5	14824	-	140.0	14092	-
8.50	-	-	-	-	-	-	-	-	-	-	-	144.5	14901	-
10.00	90.0	7172	90.0	7217	0.6	90.0	7217	0.6	90.0	6688	-6.7	90.0	6155	-14.2
10.00	100.0	8905	100.0	8978	0.8	100.0	8978	0.8	100.0	8483	-4.7	100.0	7480	-16.0
10.00	110.0	10805	110.0	10918	1.0	110.0	10918	1.0	110.0	10439	-3.4	110.0	9469	-12.4
10.00	120.0	12633	120.0	12794	1.3	120.0	12794	1.3	120.0	12331	-2.4	120.0	11393	-9.8
10.00	130.0	14976	130.0	15213	1.6	130.0	15213	1.6	130.0	14821	-1.0	130.0	13362	-10.8
10.00	-	-	-	-	-	-	-	-	131.5	15221	-	138.0	15273	-
11.50	90.0	7994	90.0	7532	-5.8	90.0	7532	-5.8	90.0	7265	-9.1	90.0	6729	-15.8
11.50	100.0	9971	100.0	9554	-4.2	100.0	9554	-4.2	100.0	9554	-4.2	100.0	8551	-14.2
11.50	110.0	11884	110.0	12002	1.0	110.0	12002	1.0	110.0	11520	-3.1	110.0	10051	-15.4
11.50	120.0	14392	120.0	14130	-1.8	120.0	14130	-1.8	120.0	13897	-3.4	120.0	12481	-13.3
11.50	124.0	15244	124.0	15536	-	125.0	15541	-	126.0	15548	-	130.0	14575	-
11.50	-	-	-	-	-	-	-	-	-	-	-	133.0	15588	-
14.00	90.0	9599	90.0	9146	-4.7	90.0	9146	-4.7	90.0	8632	-10.1	90.0	8115	-15.5
14.00	100.0	12072	100.0	11673	-3.3	100.0	11673	-3.3	100.0	11173	-7.4	100.0	9658	-20.0
14.00	110.0	14677	110.0	14125	-3.8	110.0	14125	-3.8	110.0	13641	-7.1	110.0	12169	-17.1
14.00	112.0	15125	115.5	15742	4.1	116.0	15742	4.1	117.0	15742	4.1	120.0	14828	-2.0
14.00	-	-	-	-	-	-	-	-	-	-	-	123.5	15742	-
16.67	90.0	11211	90.0	10252	-8.6	90.0	10252	-8.6	90.0	10252	-8.6	90.0	8693	-22.5
16.67	98.5	13694	100.0	13300	-2.9	100.0	13300	-2.9	100.0	12798	-6.5	100.0	11278	-17.6
16.67	-	-	106.0	15018	-	107.0	15018	-	110.0	15489	-	110.0	13799	-
16.67	-	-	-	-	-	-	-	-	-	-	-	117.0	15958	-

Table A.33 Comparison of Camber (Strand Diameter = 0.5 in.).

Spacing (ft.)	Span (ft.)	All Skews	Skew = 0			Skew = 15			Skew = 30			Skew = 60		
		Camber (ft.)	Span (ft.)	Camber (ft.)	% Diff. w.r.t STD	Span (ft.)	Camber (ft.)	% Diff. w.r.t STD	Span (ft.)	Camber (ft.)	% Diff. w.r.t STD	Span (ft.)	Camber (ft.)	% Diff. w.r.t STD
		STD	LRFD			LRFD			LRFD			LRFD		
8.50	90.0	0.102	90.0	0.079	-22.5	90.0	0.079	-22.5	90.0	0.079	-22.5	90.0	0.056	-45.1
8.50	100.0	0.145	100.0	0.131	-9.7	100.0	0.131	-9.7	100.0	0.118	-18.6	100.0	0.09	-37.9
8.50	110.0	0.208	110.0	0.192	-7.7	110.0	0.192	-7.7	110.0	0.176	-15.4	110.0	0.144	-30.8
8.50	120.0	0.293	120.0	0.276	-5.8	120.0	0.261	-10.9	120.0	0.245	-16.4	120.0	0.196	-33.1
8.50	130.0	0.396	130.0	0.376	-5.1	130.0	0.376	-5.1	130.0	0.359	-9.3	130.0	0.268	-32.3
8.50	135.0	0.452	136.5	0.447	-	136.5	0.447	-	138.5	0.442	-	140.0	0.365	-
8.50	-	-	-	-	-	-	-	-	-	-	-	142.0	0.418	-
10.00	90.0	0.113	90.0	0.102	-9.7	90.0	0.102	-9.7	90.0	0.102	-9.7	90.0	0.079	-30.1
10.00	100.0	0.171	100.0	0.17	-0.6	100.0	0.157	-8.2	100.0	0.157	-8.2	100.0	0.118	-31.0
10.00	110.0	0.243	110.0	0.241	-0.8	110.0	0.241	-0.8	110.0	0.228	-6.2	110.0	0.176	-27.6
10.00	120.0	0.339	120.0	0.338	-0.3	120.0	0.323	-4.7	120.0	0.307	-9.4	120.0	0.245	-27.7
10.00	130.0	0.447	130.0	0.445	-0.4	130.0	0.445	-0.4	130.0	0.432	-3.4	130.0	0.341	-23.7
10.00	-	-	130.5	0.455	-	131.0	0.454	-	133.0	0.461	-	139.0	0.441	-
11.50	90.0	0.134	90.0	0.123	-8.2	90.0	0.123	-8.2	90.0	0.113	-15.7	90.0	0.091	-32.1
11.50	100.0	0.209	100.0	0.196	-6.2	100.0	0.196	-6.2	100.0	0.183	-12.4	100.0	0.144	-31.1
11.50	110.0	0.295	110.0	0.281	-4.7	110.0	0.268	-9.2	110.0	0.255	-13.6	110.0	0.207	-29.8
11.50	120.0	0.399	120.0	0.382	-4.3	120.0	0.382	-4.3	120.0	0.367	-8.0	120.0	0.292	-26.8
11.50	124.0	0.446	125.5	0.454	-	126.0	0.455	-	127.5	0.455	-	130.0	0.417	-
11.50	-	-	-	-	-	-	-	-	-	-	-	134.0	0.451	-
14.00	90.0	0.186	90.0	0.185	-0.5	90.0	0.175	-5.9	90.0	0.155	-16.7	90.0	0.123	-33.9
14.00	100.0	0.269	100.0	0.247	-8.2	100.0	0.247	-8.2	100.0	0.236	-12.3	100.0	0.196	-27.1
14.00	110.0	0.388	110.0	0.356	-8.2	110.0	0.356	-8.2	110.0	0.344	-11.3	110.0	0.281	-27.6
14.00	113.0	0.426	115.5	0.43	0.9	116.0	0.431	1.2	118.0	0.444	4.2	120.0	0.404	-5.2
14.00	-	-	-	-	-	-	-	-	-	-	-	123.5	0.444	-
16.67	90.0	0.227	90.0	0.195	-14.1	90.0	0.195	-14.1	90.0	0.185	-18.5	90.0	0.155	-31.7
16.67	100.0	0.33	100.0	0.299	-9.4	100.0	0.289	-12.4	100.0	0.278	-15.8	100.0	0.236	-28.5
16.67	104.5	0.389	109.0	0.411	5.7	109.5	0.413	6.2	110.0	0.406	4.4	110.0	0.344	-11.6
16.67	-	-	-	-	-	-	-	-	111.0	0.418	-	117.0	0.434	-

Table A.34 Comparison of Camber (Strand Diameter = 0.6 in.).

Spacing (ft.)	Span (ft.)	All Skews	Skew = 0			Skew = 15			Skew = 30			Skew = 60		
		Camber (ft.)	Span (ft.)	Camber (ft.)	% Diff. w.r.t STD	Span (ft.)	Camber (ft.)	% Diff. w.r.t STD	Span (ft.)	Camber (ft.)	% Diff. w.r.t STD	Span (ft.)	Camber (ft.)	% Diff. w.r.t STD
		STD	LRFD			LRFD			LRFD			LRFD		
8.50	90.0	0.101	90.0	0.083	-17.8	90.0	0.083	-17.8	90.0	0.083	-17.8	90.0	0.065	-35.6
8.50	100.0	0.160	100.0	0.140	-12.5	100.0	0.140	-12.5	100.0	0.140	-12.5	100.0	0.111	-30.6
8.50	110.0	0.214	110.0	0.191	-10.7	110.0	0.191	-10.7	110.0	0.191	-10.7	110.0	0.146	-31.8
8.50	120.0	0.322	120.0	0.296	-8.1	120.0	0.271	-15.8	120.0	0.271	-15.8	120.0	0.220	-31.7
8.50	130.0	0.429	130.0	0.389	-9.3	130.0	0.389	-9.3	130.0	0.361	-15.9	130.0	0.303	-29.4
8.50	134.5	0.475	136.5	0.469	-	137.0	0.469	-	138.5	0.465	-	140.0	0.405	-
8.50	-	-	-	-	-	-	-	-	-	-	-	144.5	0.446	-
10.00	90.0	0.118	90.0	0.118	0.0	90.0	0.118	0.0	90.0	0.101	-14.4	90.0	0.083	-29.7
10.00	100.0	0.178	100.0	0.177	-0.6	100.0	0.177	-0.6	100.0	0.159	-10.7	100.0	0.121	-32.0
10.00	110.0	0.257	110.0	0.255	-0.8	110.0	0.255	-0.8	110.0	0.234	-8.9	110.0	0.191	-25.7
10.00	120.0	0.347	120.0	0.345	-0.6	120.0	0.345	-0.6	120.0	0.321	-7.5	120.0	0.271	-21.9
10.00	130.0	0.478	130.0	0.475	-0.6	130.0	0.475	-0.6	130.0	0.451	-5.6	130.0	0.361	-24.5
10.00	-	-	-	-	-	-	-	-	131.5	0.475	-	138.0	0.467	-
11.50	90.0	0.142	90.0	0.126	-11.3	90.0	0.126	-11.3	90.0	0.118	-16.9	90.0	0.101	-28.9
11.50	100.0	0.214	100.0	0.195	-8.9	100.0	0.195	-8.9	100.0	0.195	-8.9	100.0	0.159	-25.7
11.50	110.0	0.298	110.0	0.297	-0.3	110.0	0.297	-0.3	110.0	0.276	-7.4	110.0	0.213	-28.5
11.50	120.0	0.427	120.0	0.404	-5.4	120.0	0.404	-5.4	120.0	0.392	-8.2	120.0	0.321	-24.8
11.50	124.0	0.474	124.0	0.471	-	125.0	0.472	-	126.0	0.474	-	130.0	0.427	-
11.50	-	-	-	-	-	-	-	-	-	-	-	133.0	0.474	-
14.00	90.0	0.186	90.0	0.171	-8.1	90.0	0.171	-8.1	90.0	0.156	-16.1	90.0	0.141	-24.2
14.00	100.0	0.282	100.0	0.264	-6.4	100.0	0.264	-6.4	100.0	0.247	-12.4	100.0	0.195	-30.9
14.00	110.0	0.405	110.0	0.376	-7.2	110.0	0.376	-7.2	110.0	0.357	-11.9	110.0	0.297	-26.7
14.00	112.0	0.428	115.5	0.453	5.8	116.0	0.455	6.3	117.0	0.457	6.8	120.0	0.424	-0.9
14.00	-	-	-	-	-	-	-	-	-	-	-	123.5	0.470	-
16.67	90.0	0.227	90.0	0.199	-12.3	90.0	0.199	-12.3	90.0	0.199	-12.3	90.0	0.156	-31.3
16.67	98.5	0.324	100.0	0.314	-3.1	100.0	0.314	-3.1	100.0	0.297	-8.3	100.0	0.247	-23.8
16.67	-	-	106.0	0.390	-	107.0	0.393	-	110.0	0.419	-	110.0	0.357	-
16.67	-	-	-	-	-	-	-	-	-	-	-	117.0	0.457	-

Table A.35 Comparison of Transverse Shear Reinforcement Area (Strand Diameter 0.5 in.)

Spacing (ft.)	Span (ft.)	All Skews	Skew = 0			Skew = 15			Skew = 30			Skew = 60		
		A_v (in^2)	Span (ft.)	A_v (in^2)	% Diff. w.r.t STD	Span (ft.)	A_v (in^2)	% Diff. w.r.t STD	Span (ft.)	A_v (in^2)	% Diff. w.r.t STD	Span (ft.)	A_v (in^2)	% Diff. w.r.t STD
		STD	LRFD			LRFD			LRFD			LRFD		
8.50	90.0	0.101	90.0	0.083	-17.8	90.0	0.083	-17.8	90.0	0.083	-17.8	90.0	0.065	-35.6
8.50	100.0	0.160	100.0	0.140	-12.5	100.0	0.140	-12.5	100.0	0.140	-12.5	100.0	0.111	-30.6
8.50	110.0	0.214	110.0	0.191	-10.7	110.0	0.191	-10.7	110.0	0.191	-10.7	110.0	0.146	-31.8
8.50	120.0	0.322	120.0	0.296	-8.1	120.0	0.271	-15.8	120.0	0.271	-15.8	120.0	0.220	-31.7
8.50	130.0	0.429	130.0	0.389	-9.3	130.0	0.389	-9.3	130.0	0.361	-15.9	130.0	0.303	-29.4
8.50	134.5	0.475	136.5	0.469	-	137.0	0.469	-	138.5	0.465	-	140.0	0.405	-
8.50	-	-	-	-	-	-	-	-	-	-	-	144.5	0.446	-
10.00	90.0	0.118	90.0	0.118	0.0	90.0	0.118	0.0	90.0	0.101	-14.4	90.0	0.083	-29.7
10.00	100.0	0.178	100.0	0.177	-0.6	100.0	0.177	-0.6	100.0	0.159	-10.7	100.0	0.121	-32.0
10.00	110.0	0.257	110.0	0.255	-0.8	110.0	0.255	-0.8	110.0	0.234	-8.9	110.0	0.191	-25.7
10.00	120.0	0.347	120.0	0.345	-0.6	120.0	0.345	-0.6	120.0	0.321	-7.5	120.0	0.271	-21.9
10.00	130.0	0.478	130.0	0.475	-0.6	130.0	0.475	-0.6	130.0	0.451	-5.6	130.0	0.361	-24.5
10.00	-	-	-	-	-	-	-	-	131.5	0.475	-	138.0	0.467	-
11.50	90.0	0.142	90.0	0.126	-11.3	90.0	0.126	-11.3	90.0	0.118	-16.9	90.0	0.101	-28.9
11.50	100.0	0.214	100.0	0.195	-8.9	100.0	0.195	-8.9	100.0	0.195	-8.9	100.0	0.159	-25.7
11.50	110.0	0.298	110.0	0.297	-0.3	110.0	0.297	-0.3	110.0	0.276	-7.4	110.0	0.213	-28.5
11.50	120.0	0.427	120.0	0.404	-5.4	120.0	0.404	-5.4	120.0	0.392	-8.2	120.0	0.321	-24.8
11.50	124.0	0.474	124.0	0.471	-	125.0	0.472	-	126.0	0.474	-	130.0	0.427	-
11.50	-	-	-	-	-	-	-	-	-	-	-	133.0	0.474	-
14.00	90.0	0.186	90.0	0.171	-8.1	90.0	0.171	-8.1	90.0	0.156	-16.1	90.0	0.141	-24.2
14.00	100.0	0.282	100.0	0.264	-6.4	100.0	0.264	-6.4	100.0	0.247	-12.4	100.0	0.195	-30.9
14.00	110.0	0.405	110.0	0.376	-7.2	110.0	0.376	-7.2	110.0	0.357	-11.9	110.0	0.297	-26.7
14.00	112.0	0.428	115.5	0.453	5.8	116.0	0.455	6.3	117.0	0.457	6.8	120.0	0.424	-0.9
14.00	-	-	-	-	-	-	-	-	-	-	-	123.5	0.470	-
16.67	90.0	0.227	90.0	0.199	-12.3	90.0	0.199	-12.3	90.0	0.199	-12.3	90.0	0.156	-31.3
16.67	98.5	0.324	100.0	0.314	-3.1	100.0	0.314	-3.1	100.0	0.297	-8.3	100.0	0.247	-23.8
16.67	-	-	106.0	0.390	-	107.0	0.393	-	110.0	0.419	-	110.0	0.357	-
16.67	-	-	-	-	-	-	-	-	-	-	-	117.0	0.457	-

Table A.36 Comparison of Transverse Shear Reinforcement Area (Strand Diameter = 0.6 in.).

Spacing (ft.)	Span (ft.)	All Skews	Skew = 0			Skew = 15			Skew = 30			Skew = 60		
		A_v (in^2)	Span (ft.)	A_v (in^2)	% Diff. w.r.t STD	Span (ft.)	A_v (in^2)	% Diff. w.r.t STD	Span (ft.)	A_v (in^2)	% Diff. w.r.t STD	Span (ft.)	A_v (in^2)	% Diff. w.r.t STD
		STD	LRFD			LRFD			LRFD			LRFD		
8.50	90.0	0.42	90.0	0.22	-49.2	90.0	0.22	-49.2	90.0	0.21	-49.3	90.0	0.21	-49.4
8.50	100.0	0.47	100.0	0.27	-43.3	100.0	0.27	-43.3	100.0	0.26	-44.2	100.0	0.26	-45.0
8.50	110.0	0.51	110.0	0.32	-37.3	110.0	0.32	-37.3	110.0	0.32	-37.3	110.0	0.31	-39.3
8.50	120.0	0.50	120.0	0.32	-36.8	120.0	0.32	-36.9	120.0	0.31	-37.4	120.0	0.30	-39.7
8.50	130.0	0.49	130.0	0.30	-39.5	130.0	0.30	-39.6	130.0	0.29	-40.1	130.0	0.28	-42.3
8.50	134.5	0.49	136.5	0.28	-	137.0	0.28	-	138.5	0.27	-	140.0	0.26	-
8.50	-	-	-	-	-	-	-	-	-	-	-	144.5	0.22	-
10.00	90.0	0.48	90.0	0.29	-40.4	90.0	0.28	-40.9	90.0	0.28	-41.1	90.0	0.28	-42.1
10.00	100.0	0.54	100.0	0.34	-36.4	100.0	0.34	-36.4	100.0	0.34	-37.2	100.0	0.33	-38.4
10.00	110.0	0.55	110.0	0.39	-29.7	110.0	0.39	-29.8	110.0	0.38	-30.4	110.0	0.37	-33.0
10.00	120.0	0.55	120.0	0.37	-33.6	120.0	0.37	-33.7	120.0	0.37	-33.8	120.0	0.35	-36.2
10.00	130.0	0.54	130.0	0.35	-35.3	130.0	0.35	-35.3	130.0	0.34	-36.5	130.0	0.33	-38.5
10.00	-	-	-	-	-	-		-	131.5	0.34	-	138.0	0.29	-
11.50	90.0	0.61	90.0	0.35	-43.1	90.0	0.35	-43.2	90.0	0.35	-43.1	90.0	0.34	-43.9
11.50	100.0	0.67	100.0	0.41	-38.6	100.0	0.41	-38.6	100.0	0.41	-38.7	100.0	0.40	-40.3
11.50	110.0	0.67	110.0	0.43	-35.5	110.0	0.43	-35.5	110.0	0.43	-36.1	110.0	0.42	-38.0
11.50	120.0	0.67	120.0	0.41	-38.6	120.0	0.41	-38.7	120.0	0.41	-39.6	120.0	0.40	-41.4
11.50	124.0	0.67	124.0	0.41	-	125.0	0.40	-	126.0	0.40	-	130.0	0.37	-
11.50	-	-	-	-	-	-	-	-	-	-	-	133.0	0.37	-
14.00	90.0	0.85	90.0	0.48	-43.8	90.0	0.48	-43.8	90.0	0.48	-43.9	90.0	0.46	-45.3
14.00	100.0	0.90	100.0	0.55	-38.9	100.0	0.55	-39.0	100.0	0.55	-39.5	100.0	0.54	-40.6
14.00	110.0	0.92	110.0	0.53	-41.9	110.0	0.53	-41.9	110.0	0.53	-42.3	110.0	0.51	-44.5
14.00	112.0	0.91	115.5	0.52	-43.0	116.0	0.52	-43.2	117.0	0.51	-43.8	120.0	0.49	-46.5
14.00	-	-	-	-	-	-	-	-	-	-	-	123.5	0.48	-
16.67	90.0	1.07	90.0	0.60	-44.2	90.0	0.60	-44.2	90.0	0.59	-44.8	90.0	0.58	-45.5
16.67	98.5	1.09	100.0	0.62	-	100.0	0.64	-	100.0	0.63	-	100.0	0.61	-
16.67	-	-	106.0	0.58	-	107.0	0.60	-	110.0	0.60	-	110.0	0.58	-
16.67	-	-	-	-	-	-	-	-	-	-	-	117.0	0.56	-

Table A.37 Comparison of Interface Shear Reinforcement Area (Strand Diameter = 0.5 in.).

Spacing (ft.)	Span (ft.)	All Skews	Skew = 0			Skew = 15			Skew = 30			Skew = 60		
		A_{vh} (in^2) STD	Span (ft.) LRFD	A_{vh} (in^2) LRFD	% Diff. w.r.t STD	Span (ft.) LRFD	A_{vh} (in^2) LRFD	% Diff. w.r.t STD	Span (ft.) LRFD	A_{vh} (in^2) LRFD	% Diff. w.r.t STD	Span (ft.) LRFD	A_{vh} (in^2) LRFD	% Diff. w.r.t STD
8.50	90.0	0.315	90.0	0.79	150.7	90.0	0.79	150.4	90.0	0.79	150.4	90.0	0.78	147.5
8.50	100.0	0.315	100.0	0.86	172.2	100.0	0.86	172.1	100.0	0.85	170.9	100.0	0.85	168.4
8.50	110.0	0.315	110.0	0.92	192.1	110.0	0.92	192.1	110.0	0.92	192.0	110.0	0.91	188.6
8.50	120.0	0.315	120.0	0.98	211.1	120.0	0.98	211.1	120.0	0.98	209.8	120.0	0.96	204.1
8.50	130.0	0.315	130.0	1.04	229.7	130.0	1.04	228.7	130.0	1.03	227.6	130.0	1.01	222.0
8.50	135.0	0.315	136.5	1.08	-	136.5	1.08	-	138.5	1.09	-	140.0	1.07	-
8.50	-	-	-	-	-	-	-	-	-	-	-	142.0	1.11	-
10.00	90.0	0.315	90.0	0.94	199.8	90.0	0.94	199.8	90.0	0.94	198.4	90.0	0.94	197.0
10.00	100.0	0.315	100.0	1.02	223.1	100.0	1.02	223.1	100.0	1.02	223.1	100.0	1.01	219.5
10.00	110.0	0.315	110.0	1.09	246.6	110.0	1.09	246.6	110.0	1.09	244.9	110.0	1.07	240.2
10.00	120.0	0.315	120.0	1.16	267.3	120.0	1.15	266.1	120.0	1.15	264.9	120.0	1.14	260.7
10.00	130.0	0.315	130.0	1.22	288.8	130.0	1.22	288.8	130.0	1.21	285.7	130.0	1.20	280.4
10.00	-	-	130.5	1.23	-	131.0	1.24	-	133.0	1.24	-	139.0	1.26	-
11.50	90.0	0.315	90.0	1.08	243.3	90.0	1.08	243.2	90.0	1.08	242.1	90.0	1.07	239.1
11.50	100.0	0.315	100.0	1.16	268.9	100.0	1.16	268.0	100.0	1.16	267.9	100.0	1.15	264.5
11.50	110.0	0.315	110.0	1.24	293.0	110.0	1.24	293.0	110.0	1.23	291.6	110.0	1.21	284.9
11.50	120.0	0.315	120.0	1.31	314.5	120.0	1.31	314.5	120.0	1.30	313.1	120.0	1.28	307.0
11.50	124.0	0.315	125.5	1.35	-	126.0	1.36	-	127.5	1.36	-	130.0	1.35	-
11.50	-	-	-	-	-	-	-	-	-	-	-	134.0	1.39	-
14.00	90.0	0.315	90.0	1.37	333.5	90.0	1.37	333.5	90.0	1.36	332.5	90.0	1.35	328.4
14.00	100.0	0.315	100.0	1.47	365.7	100.0	1.47	365.7	100.0	1.46	364.0	100.0	1.44	358.4
14.00	110.0	0.315	110.0	1.56	393.7	110.0	1.56	393.7	110.0	1.55	392.2	110.0	1.53	385.0
14.00	113.0	0.315	115.5	1.61	410.9	116.0	1.61	411.7	118.0	1.63	417.1	120.0	1.61	412.2
14.00	-	-	-	-	-	-	-	-	-	-	-	123.5	1.65	-
16.67	90.0	0.315	90.0	1.59	406.0	90.0	1.59	406.0	90.0	1.59	405.0	90.0	1.58	401.5
16.67	100.0	0.315	100.0	1.71	442.2	100.0	1.70	440.6	100.0	1.70	439.1	100.0	1.68	432.4
16.67	104.5	0.315	109.0	1.80	-	109.5	1.80	-	110.0	1.80	-	110.0	1.77	-
16.67	-	-	-	-	-	-	-	-	-	-	-	117.0	0.457	-

Table A.38 Comparison of Interface Shear Reinforcement Area (Strand Diameter = 0.6 in.).

Spacing (ft.)	Span (ft.)	All Skews	Skew = 0			Skew = 15			Skew = 30			Skew = 60		
		A_{vh} (in^2)	Span (ft.)	A_{vh} (in^2)	% Diff. w.r.t STD	Span (ft.)	A_{vh} (in^2)	% Diff. w.r.t STD	Span (ft.)	A_{vh} (in^2)	% Diff. w.r.t STD	Span (ft.)	A_{vh} (in^2)	% Diff. w.r.t STD
		STD	LRFD			LRFD			LRFD			LRFD		
8.50	90.0	0.315	90.0	0.78	148.9	90.0	0.78	148.9	90.0	0.78	148.8	90.0	0.78	148.0
8.50	100.0	0.315	100.0	0.85	168.9	100.0	0.85	168.9	100.0	0.84	166.9	100.0	0.84	165.3
8.50	110.0	0.315	110.0	0.91	189.9	110.0	0.91	189.9	110.0	0.91	188.4	110.0	0.90	184.8
8.50	120.0	0.315	120.0	0.97	207.0	120.0	0.97	207.0	120.0	0.96	205.5	120.0	0.95	202.3
8.50	130.0	0.315	130.0	1.02	222.5	130.0	1.02	222.5	130.0	1.01	221.3	130.0	1.00	218.5
8.50	134.5	0.315	136.5	1.05	-	137.0	1.06	-	138.5	1.06	-	140.0	1.06	-
8.50	-	-	-	-	-	-	-	-	-	-	-	144.5	1.08	-
10.00	90.0	0.315	90.0	0.94	197.5	90.0	0.93	196.5	90.0	0.93	196.5	90.0	0.93	195.3
10.00	100.0	0.315	100.0	1.01	220.7	100.0	1.01	220.7	100.0	1.00	218.8	100.0	0.99	215.0
10.00	110.0	0.315	110.0	1.08	243.0	110.0	1.08	243.0	110.0	1.08	241.4	110.0	1.06	237.7
10.00	120.0	0.315	120.0	1.14	260.4	120.0	1.14	260.4	120.0	1.14	260.3	120.0	1.12	255.9
10.00	130.0	0.315	130.0	1.20	280.6	130.0	1.20	280.6	130.0	1.19	278.7	130.0	1.18	274.5
10.00	-	-	-	-	-	-	-	-	131.5	1.20	-	138.0	1.23	-
11.50	90.0	0.315	90.0	1.07	238.4	90.0	1.07	238.4	90.0	1.06	238.1	90.0	1.06	236.9
11.50	100.0	0.315	100.0	1.15	264.7	100.0	1.15	264.7	100.0	1.15	264.6	100.0	1.14	260.8
11.50	110.0	0.315	110.0	1.22	288.0	110.0	1.22	288.0	110.0	1.22	286.5	110.0	1.21	283.1
11.50	120.0	0.315	120.0	1.28	306.9	120.0	1.28	306.9	120.0	1.28	305.9	120.0	1.27	301.8
11.50	124.0	0.315	124.0	1.31	-	125.0	1.32	-	126.0	1.32	-	130.0	1.33	-
11.50	-	-	-	-	-	-	-	-	-	-	-	133.0	1.35	-
14.00	90.0	0.315	90.0	1.35	328.9	90.0	1.35	328.9	90.0	1.35	327.2	90.0	1.33	322.6
14.00	100.0	0.315	100.0	1.45	360.7	100.0	1.45	360.7	100.0	1.45	359.1	100.0	1.43	355.5
14.00	110.0	0.315	110.0	1.53	385.1	110.0	1.53	385.1	110.0	1.52	383.8	110.0	1.51	378.9
14.00	112.0	0.315	115.5	1.58	400.7	116.0	1.58	401.5	117.0	1.58	403.0	120.0	1.59	403.8
14.00	-	-	-	-	-	-	-	-	-	-	-	123.5	1.62	-
16.67	90.0	0.315	90.0	1.59	403.4	90.0	1.59	403.4	90.0	1.57	399.5	90.0	1.56	395.6
16.67	98.5	0.315	100.0	1.68	-	100.0	1.68	-	100.0	1.68	-	100.0	1.66	-
16.67			106.0	1.73	-	107.0	1.74	-	110.0	1.76	-	110.0	1.74	-
16.67	-	-	-	-	-	-	-	-	-	-	-	117.0	1.81	-

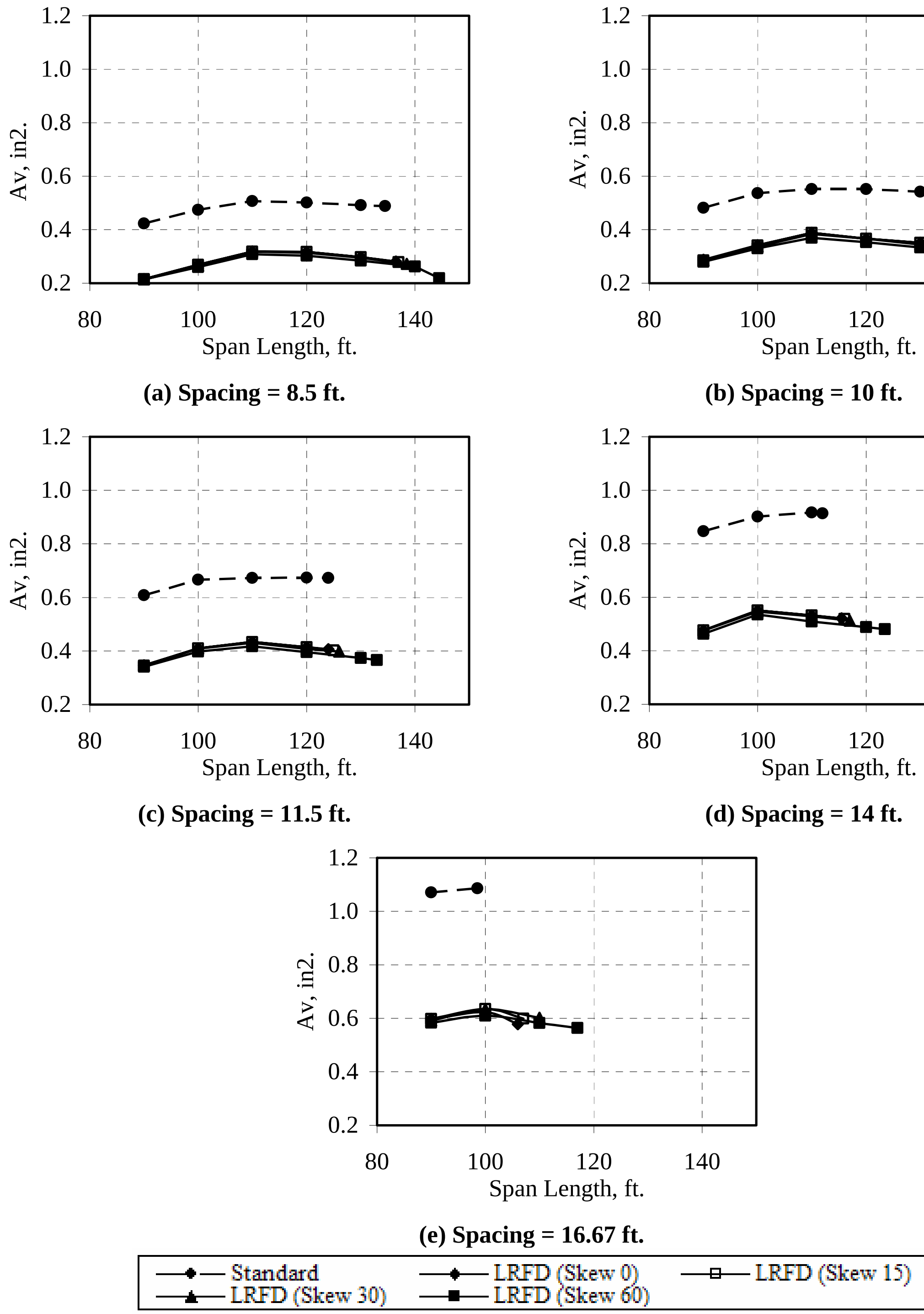

Figure A.9 Comparison of Transverse Shear Reinforcement Area (Strand Diameter = 0.6 in.).

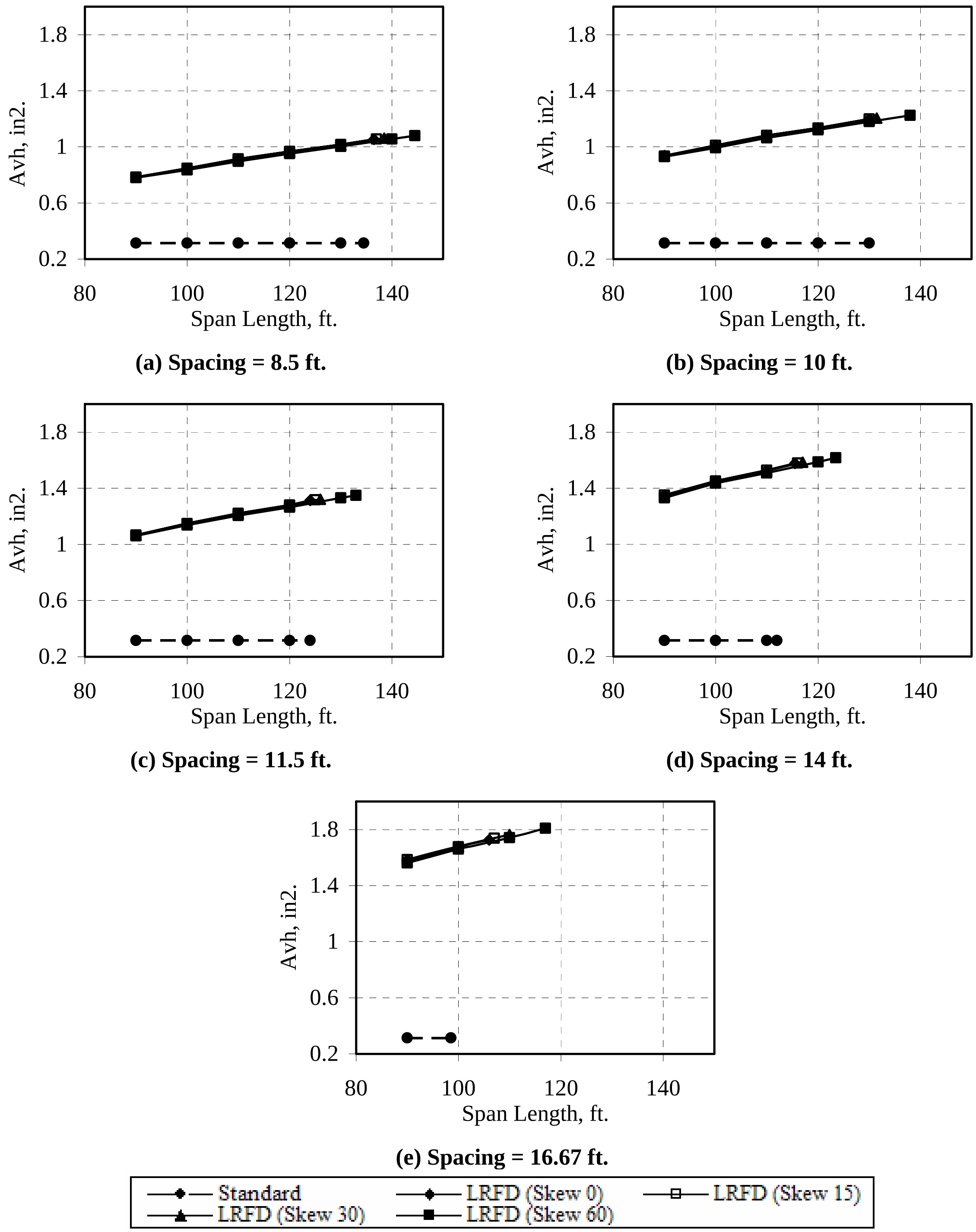

Figure A.10 Comparison of Interface Shear Reinforcement Area (Strand Diameter = 0.6 in.).

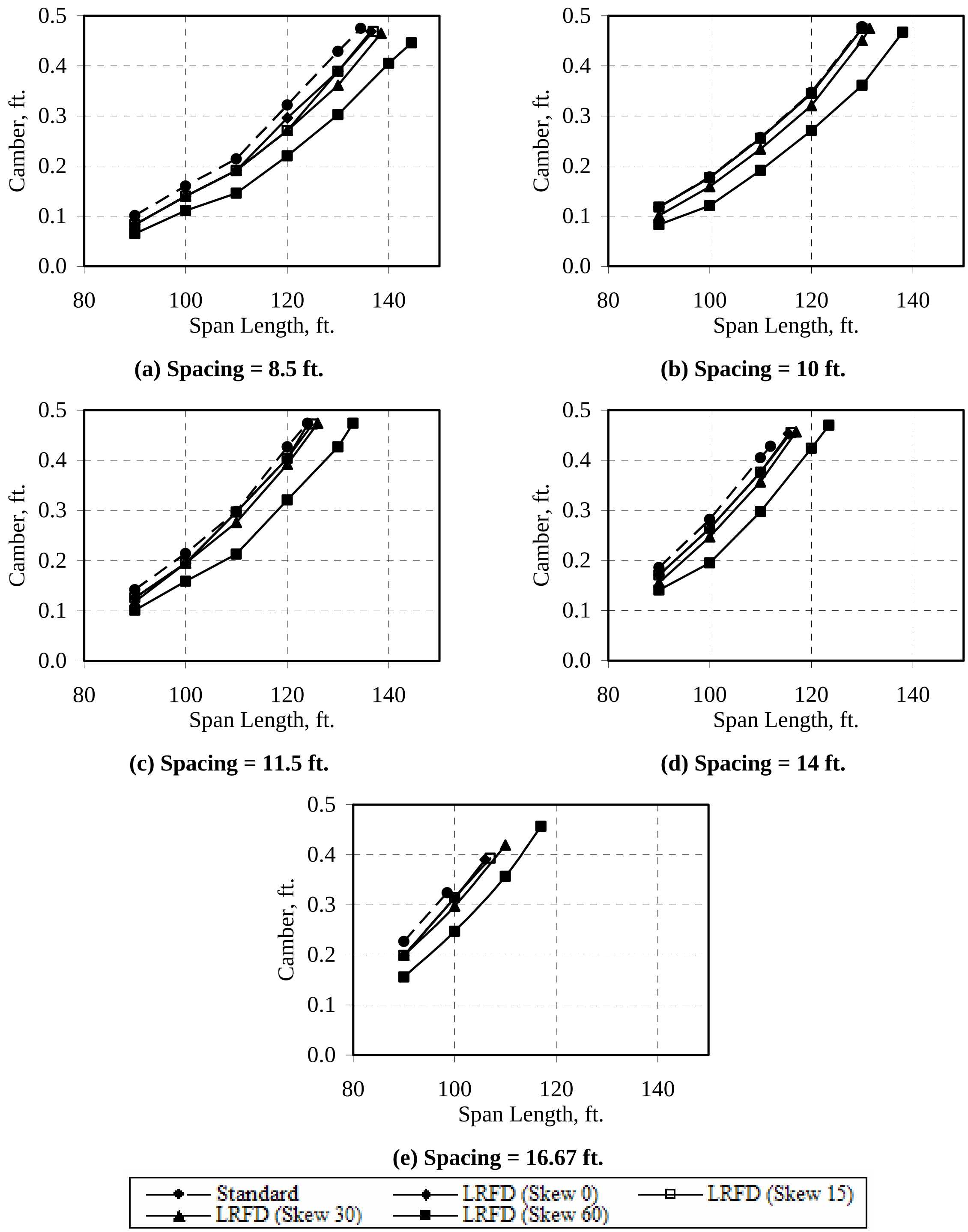

Figure A.11 Comparison of Camber (Strand Diameter = 0.6 in.).